

Gels Horizons: From Science to Smart Materials

Vijay Kumar Thakur
Manju Kumari Thakur *Editors*

Polymer Gels

Science and Fundamentals

 Springer

Gels Horizons: From Science to Smart Materials

Series editor

Vijay Kumar Thakur, School of Aerospace, Transport and Manufacturing,
Cranfield University, Cranfield, Bedfordshire, UK

This series aims at providing a comprehensive collection of works on the recent advances and developments in the domain of *Gels*, particularly as applied to the various research fields of sciences and engineering disciplines. It covers a broad range of topics related to *Gels* ranging from *Polymer Gels*, *Protein Gels*, *Self-Healing Gels*, *Colloidal Gels*, *Composites/Nanocomposites Gels*, *Organogels*, *Aerogels*, *Metallogels & Hydrogels* to *Micro/Nano gels*. The series provides timely and detailed information on advanced synthesis methods, characterization and their application in a broad range of interrelated fields such as chemistry, physics, polymer science & engineering, biomedical & biochemical engineering, chemical engineering, molecular biology, mechanical engineering and materials science & engineering.

This Series accepts both edited and authored works, including textbooks, monographs, reference works, and professional books. The books in this series will provide a deep insight into the state-of-art of *Gels* and serve researchers and professionals, practitioners, and students alike.

More information about this series at <http://www.springer.com/series/15205>

Vijay Kumar Thakur · Manju Kumari Thakur
Editors

Polymer Gels

Science and Fundamentals

 Springer

Editors

Vijay Kumar Thakur
Faculty in Manufacturing, Enhanced
Composites and Structures Centre,
School of Aerospace, Transport
and Manufacturing
Cranfield University
Cranfield
UK

Manju Kumari Thakur
Division of Chemistry
Government Degree College Bhoranj,
Himachal Pradesh University
Shimla, Himachal Pradesh
India

ISSN 2367-0061

ISSN 2367-007X (electronic)

Gels Horizons: From Science to Smart Materials

ISBN 978-981-10-6085-4

ISBN 978-981-10-6086-1 (eBook)

<https://doi.org/10.1007/978-981-10-6086-1>

Library of Congress Control Number: 2018939938

© Springer Nature Singapore Pte Ltd. 2018

This work is subject to copyright. All rights are reserved by the Publisher, whether the whole or part of the material is concerned, specifically the rights of translation, reprinting, reuse of illustrations, recitation, broadcasting, reproduction on microfilms or in any other physical way, and transmission or information storage and retrieval, electronic adaptation, computer software, or by similar or dissimilar methodology now known or hereafter developed.

The use of general descriptive names, registered names, trademarks, service marks, etc. in this publication does not imply, even in the absence of a specific statement, that such names are exempt from the relevant protective laws and regulations and therefore free for general use.

The publisher, the authors and the editors are safe to assume that the advice and information in this book are believed to be true and accurate at the date of publication. Neither the publisher nor the authors or the editors give a warranty, express or implied, with respect to the material contained herein or for any errors or omissions that may have been made. The publisher remains neutral with regard to jurisdictional claims in published maps and institutional affiliations.

This Springer imprint is published by the registered company Springer Nature Singapore Pte Ltd. The registered company address is: 152 Beach Road, #21-01/04 Gateway East, Singapore 189721, Singapore

Preface

A gel is described as a soft, solid- or liquid-like unique condensed material that has a three-dimensional network composed of several components such as long polymers, species of small molecules and a large amount of solvent. These 3D network condensed materials usually form through chemical, physical or supramolecular crosslinking. The weight and size of gels are more like a liquid, but they are treated like a solid. Two important characteristics of gels are phase state and their rheological properties. On the other hand, a polymer is defined a large molecule (macromolecules) composed of repeating structural units that comprise of multiple assemblies of simple structural units. In gels, the polymer network can be physically or chemically crosslinked. In case of physical gels, the network formation occurs due to various weak interactions, like the entanglement of the polymer chains, hydrogen bonds or van der Waals interactions. Such structures are usually not permanent and they dissolve over the time when immersed in their solvents. However, the polymer chains can also be crosslinked through chemical reactions, leading to strong covalent bonds. The chemically crosslinked network is much more stable and cannot be dissolved without the degradation of the polymer. Therefore, chemical gels are usually preferable in the majority of the application fields. Polymer gels comprise a great variety of different polymeric components that present innumerable industrial applications. Polymers can be naturally produced (some time referred as bio-based polymers), in which case the most representative group is polysaccharides. Natural polymers' demand is expected to grow 7.1% every year. Moreover, their low toxicity and excellent biodegradability have also attracted researchers to pay attention towards the widespread application of natural polymers. Polymer obtained from natural sources such as chitosan, alginate, dextran, starch, pectin, cellulose and lignin has shown excellent potential for biomedical and other applications in the form of microsphere, nanoparticles, crosslinked hydrogels, beads, membranes and granules. On the other hand, a wide variety of synthetic polymers capable of forming gels present different industrial applications, such as polyacrylamide and polyvinyl alcohol-based gels. Both synthetic and natural polymer-based gels find applications from health sciences such as

agents for controlled drug delivery, sustained drug delivery, targeted drug delivery and various other types of novel drug delivery systems to water purification.

Polymer gels due to their several unique characteristics have become an indispensable part of new advanced and smart materials in the twenty-first century for numerous applications including but not limited to biological, biomedical, electronic and environmental. Keeping in mind the immense advantages of polymer gel-based materials, this volume of the series is solely focused on the science and fundamental of polymer gels. It provides a comprehensive collection of works on the recent advances and developments in science and fundamentals of both synthetic and natural polymer-based gels particularly as applied to the various research fields of sciences and engineering disciplines. Some of the important topics include but not limited to: polysaccharide-based gels and their fundamentals; stimuli-responsive polymer gels; polymer gels applied to enzyme and cell immobilization; chitosan-based gels for cancer therapy; natural polymeric and gelling agents; radiation dosimetry—a different prospective of polymer gel; polymeric gels as vehicles for enhanced drug delivery across skin; transport in and through gel; graphene oxide—polymer gels; polymer gel nanocomposites; and functional gels to name a few.

In editing and organising this volume *Polymer Gels: Science and Fundamentals* of the book series *Gels Horizons: From Science to Smart Materials*, we have made our best efforts to cover the growing field of polymer gels and related technologies. It reflects the recent theoretical advances and experimental results and opens new avenues for researchers as well as readers working in the fields of polymer and functional materials. In addition, several critical issues and suggestions for future work are comprehensively discussed in this book with the hope that the book will provide a deep insight into the state of the art of *Polymer Gels*. We express our sincere thanks to all the authors, who have contributed their extensive experience through their work for the success of this book. We would also like to thank Swati Meherishi and the rest of the team at Springer for invaluable help in the organisation of the editing process.

Cranfield, UK
Shimla, India

Vijay Kumar Thakur, Ph.D.
Manju Kumari Thakur, M.Sc., M.Phil., Ph.D.

Contents

1	Polymer Hydrogel-Clay (Nano)Composites	1
	Piotr Kuśtrowski, Piotr Natkański, Anna Rokicińska and Ewa Witek	
2	An Overview on Polymer Gels Applied to Enzyme and Cell Immobilization	63
	Gustavo Pagotto Borin, Ricardo Rodrigues de Melo, Elaine Crespim, Helia Harumi Sato and Fabiano Jares Contesini	
3	Hemicellulose-Based Hydrogels and Their Potential Application	87
	Weiqing Kong, Qingqing Dai, Cundian Gao, Junli Ren, Chuanfu Liu and Runcang Sun	
4	Updates on Stimuli-Responsive Polymers: Synthesis Approaches and Features	129
	Ibrahim M. El-Sherbiny, Islam A. Khalil and Isra H. Ali	
5	Polysaccharide-Based Polymer Gels	147
	Tamás Fekete and Judit Borsa	
6	Polysaccharide Containing Gels for Pharmaceutical Applications	231
	Catalina Natalia Cheaburu-Yilmaz, Sakine Tuncay Tanriverdi, Ozgen Ozer and Cornelia Vasile	
7	Design of Multifunctional Nanogels with Intelligent Behavior	279
	G. Rimondino, C. Biglione, M. Martinelli, C. Alvarez Igarzábal and M. Strumia	
8	Radiation Dosimetry—A Different Perspective of Polymer Gel	309
	Deena Titus, E. James Jebaseelan Samuel and Selvaraj Mohana Roopan	

9	Polymeric Gels: Vehicles for Enhanced Drug Delivery Across Skin	343
	Rachna Prasad and Veena Koul	
10	Graphene Oxide–Polymer Gels	377
	Abbas Dadkhah Tehrani, Mohsen Adeli, Sh. Sattari and Kh. Soleimani	
11	Transport in and Through Gel	413
	Masayuki Tokita	
12	Incorporation of Filler/Additives in Polymer Gel for Advanced Application	445
	Ida Idayu Muhamad, Eraricar Salleh, Shahrulzaman Shahrudin, Norhayatie Pa'e, Suguna Selvakumaran and Mohd. Harfiz Salehudin	

About the Editors



Dr. Vijay Kumar Thakur, Ph.D. Prior to commencing in the School of Aerospace, Transport and Manufacturing at Cranfield University, Dr. Vijay Kumar Thakur was working as a Staff Scientist in the School of Mechanical and Materials Engineering at Washington State University, USA (2013–2016). Some of his other prior significant appointments include being a Research Scientist in Temasek Laboratories at Nanyang Technological University, Singapore (2009–2012) and a Visiting Research Fellow in the Department of Chemical and Materials Engineering at LHM—Taiwan. He did his post-doctoral study in Materials Science and Engineering at Iowa State University and received Ph.D. in Polymer Chemistry (2009).

In his academic career, he has published more than 100 SCI journal research articles in the field of chemical sciences/materials science and holds one US patent. He has also published 33 books and 35 chapters on the advanced state-of-the-art of polymer science/materials science/nanotechnology with numerous publishers. His research interests include the synthesis and processing of bio-based polymers, composites, nanostructured materials, hydrogels, polymer micro/nanocomposites, nanoelectronic materials, novel high dielectric constant materials, engineering nanomaterials, electrochromic materials, green synthesis of nanomaterials and surface functionalization of polymers/nanomaterials. Application aspects range from automotive to aerospace, energy storage, water purification and biomedical fields.

He is an editorial board member of several international journals, as well as a member of scientific bodies around the globe. Some of his significant appointments include Associate Editor for *Materials Express* (SCI); Advisory Editor for *SpringerPlus* (SCI); Editor for *Energies* (SCI); Editor for *Cogent Chemistry* (SCI); Associate Editor for *Current Smart Materials*; Associate Editor for *Current Applied Polymer Science*; Regional Editor for *Recent Patents on Materials Science* (Scopus); and Regional Editor for *Current Biochemical Engineering* (CAS). He also serves on the Editorial Advisory Board of *Polymers for Advanced Technologies* (SCI) and is on the Editorial Board of *Journal of Macromolecular Science, Part A: Pure and Applied Chemistry* (SCI), *International Journal of Industrial Chemistry* (SCI), *Biointerface Research in Applied Chemistry* (SCI) and *Advances in Natural Sciences: Nanoscience and Nanotechnology* (SCI). e-mail: Vijay.Kumar@cranfield.ac.uk



Dr. Manju Kumar Thakur, M.Sc., M.Phil., Ph.D. has been working as an Assistant Professor of Chemistry at the Division of Chemistry, Government Degree College, Sarkaghat, Himachal Pradesh University, Shimla, India, since June 2010. She received her B.Sc. in Chemistry, Botany and Zoology; M.Sc., M. Phil. in Organic Chemistry; and Ph.D. in Polymer Chemistry from the Chemistry Department at Himachal Pradesh University, Shimla, India. She has rich experience in the fields of organic chemistry, biopolymers, composites/nanocomposites, hydrogels, applications of hydrogels in the removal of toxic heavy metal ions, drug delivery, etc. She has published more than 30 research papers in several international journals, co-authored five books and also published 25 chapters in the field of polymeric materials. e-mail: chauhanmanjuchem@gmail.com

Chapter 1

Polymer Hydrogel-Clay (Nano)Composites



Piotr Kuśtrowski, Piotr Natkański, Anna Rokicińska and Ewa Witek

Abstract Among various (nano)composites containing hydrogels, materials based on clays are emphasized. We show features of clays, which are beneficial in the formation of (nano)composites with hydrogels. Methods used in the synthesis of these materials and the resulting structures are demonstrated. Physicochemical techniques being valuable tools for characterization of this type of materials are also presented. Furthermore, the most important properties of hydrogel-clay (nano)-composites are shown. Beside typically improved features like thermal stability, mechanical, rheological, and optical properties, as well as swelling and adsorption capacity are discussed. Finally, a wide range of possible applications of hydrogel-clay (nano)composites is outlined.

Keywords Hydrogel-clay (nano)composites · Synthesis · Physicochemical characterization · Applications

1 Introduction

Organic polymers, next to minerals, belong to the most widespread materials on the earth. From the 20s of the twentieth century, when the era of synthetic polymers was born, these materials have been introduced into each area of human life replacing traditional feedstock (e.g., metals, alloys, glass, ceramics, or wood) due to relatively low cost, low weight, anti-corrosion properties, easy forming and processing, etc. On the other hand, some unrewarding properties of polymers preclude them from many applications. To improve mechanical and rheological properties, to enhance thermal stability as well as to reduce permeability and production costs, polymers are often filled with various inorganic particles (Sinha Ray and Okamoto 2003; Okada and Usuki 2006; Kotal and Bhowmick 2015). Multiphasic solid

P. Kuśtrowski (✉) · P. Natkański · A. Rokicińska · E. Witek
Department of Chemical Technology, Faculty of Chemistry, Jagiellonian University,
Ingardena 3, 30-060 Krakow, Poland
e-mail: piotr.kustrowski@uj.edu.pl

© Springer Nature Singapore Pte Ltd. 2018
V. K. Thakur and M. K. Thakur (eds.), *Polymer Gels*, Gels Horizons: From Science to Smart Materials, https://doi.org/10.1007/978-981-10-6086-1_1

materials with the matrix reinforced by randomly and homogeneously dispersed particles are so-called composites or nanocomposite in the case if at least one of the phases shows dimension within the nanometer range. Layered aluminosilicates, known as clays, have been recognized as good candidates to be the effective fillers for the polymer matrices due to the ability of their particles to disperse into highly dispersed individual layers (exfoliation) and the relatively easy introduction of ionic forms into the structure (ion exchange) (Silvestre et al. 2016). The formation of stable composite sometimes demands the suitable modification of clay to become compatible with the chosen polymer, and, therefore, strongly depends on the type of polymer matrix and reinforcement. Four different kinds of (nano)composites are possible to obtain: (i) immiscible (nano)composites (with the filler particles simply entrapped in the polymer matrix), (ii) intercalated (nano)composites (with the polymer chains introduced between the clay layers), (iii) flocculated (nano)composites (with the partially intercalated structure, but with some clay layers flocculated due to the edge-edge hydroxyl interactions), and (iv) exfoliated (nano)composites (with the separate clay layers dispersed in the polymer matrix) (Alexandre and Dubois 2000; Pavlidou and Papaspyrides 2008; Paul and Robeson 2008; Silvestre et al. 2016).

From the synthetic point of view, the formation of (nano)composites is especially facile in the case of the in situ free-radical polymerization of water-soluble monomer performed in an aqueous slurry of clay particles. Such procedure is most frequently used for the production of (nano)composites containing synthetic and natural hydrogels with homogeneously dispersed platelets of clay (usually montmorillonite or synthetic laponite belonging to the smectite group), which play a role of crosslinker stabilizing the structure of formed (nano)composite (Haraguchi 2007b, 2011b; Schexnailder and Schmidt 2009; Haraguchi and Takehisa 2002; Janovák et al. 2009a; Kabiri et al. 2011). For the formation of hydrogel network, monomers containing amide (e.g., acrylamide, *N*-isopropylacrylamide, *N,N*-dimethylacrylamide) or carboxyl groups (e.g., acrylic acid) are most often chosen as effectively interacting with the clay surface. Nevertheless, cheap and widely available natural gelatin or polysaccharide gels, composed of monosaccharide units linked by glycosidic bonds (cf. Fig. 1), are also used as individual components or grafted additives in the studied (nano)composites. The resulting hydrogel-clay materials are capable of reversible volume change, induced by swelling in a water solvent under various conditions, without discernible deterioration of properties. In the presented chapter, we have discussed the structure of various layered aluminosilicates, which had been demonstrated in the literature as useful for the formation of hydrogel-clay (nano)composites. The more popular methods applied for their synthesis have been discussed. A special emphasis has been placed on the presentation of fundamental properties (e.g., swelling, mechanical, rheological, thermal, optical), which characterize the hydrogel networks filled with clays. Furthermore, their main possible applications, including biomedicine, drug delivery and adsorption, have been discussed.

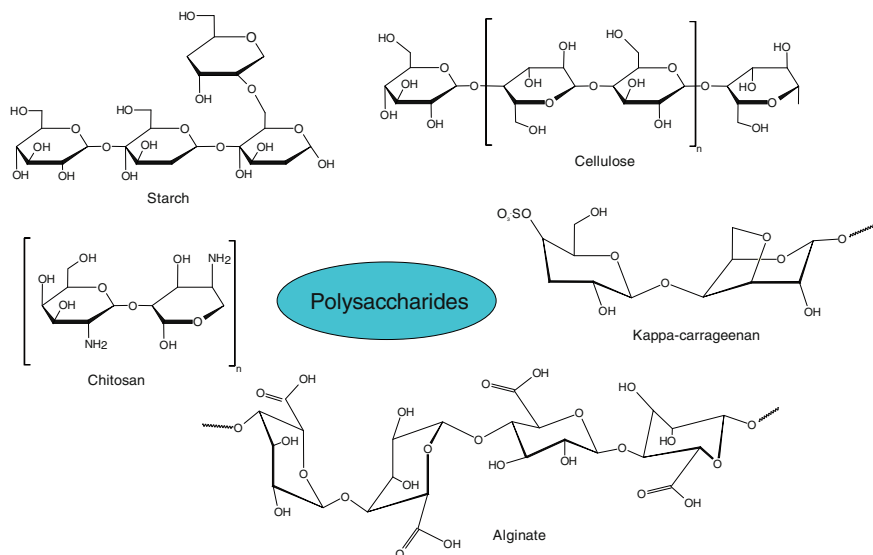


Fig. 1 Polysaccharides most frequently introduced into hydrogel-clay composites

2 Clay Materials

The layered minerals incorporated into polymers, even at small amounts (1–5 wt%), play a crucial role in the formation of desirable structures of polymeric or composite materials, acting not only as fillers, but also as crosslinking agents and stabilizers (Haraguchi 2007a; Sinha Ray and Okamoto 2003; Haraguchi and Takehisa 2002). Being highly dispersed within polymer, they enhance its thermal stability, permeability, biodegradability, biocompatibility, rheological, and mechanical properties (Oliveira et al. 2014; Haraguchi 2011a; Nistor et al. 2013). Moreover, in the case of hydrophilic polymers, forming hydrogels, the addition of layered aluminosilicates can significantly improve adsorption properties in relation to metal cations (Natkański et al. 2012, 2013b; Güçlü et al. 2010; Kundakci et al. 2011), dyes (Yi and Zhang 2008; Zhang et al. 2013; Bhattacharyya and Ray 2014), and drugs (Nistor et al. 2013; Kevadiya et al. 2011; Dadkhah et al. 2014), as well as swelling ability in polar solvents (Kamoun and Menzel 2012; Li et al. 2009a; Nair et al. 2007). These features depend on the clay type (the charge of layer), its form (e.g., organophilized, acid activated), concentration and dispersion degree in the polymer matrix.

The units building layered aluminosilicates are tetrahedral and octahedral sheets (sublayers) composed of $[\text{SiO}_4]^{4-}$ tetrahedrons or $[\text{AlO}_6]^{9-}$ octahedrons, respectively. The sheets are parallelly arranged to each other and connected to each other by common oxygen atoms located in one layer (package) (Brindley and Brown 1980; Schulze 2005; Brigatti et al. 2006). The tetrahedral and octahedral sheets can

be grouped into two-sublayer (1:1 type) or three-sublayer packages (2:1 type), that are separated by a interlayer space (so-called gallery), which most often contains metal cations (mainly alkali and alkaline earth metal) and/or water molecules or remains empty (Brindley and Brown 1980; Schulze 2005; Brigatti et al. 2006; Murray 2007b). The presence of hydrated cations in the gallery is closely related to the net layer charge, that is generated by isomorphic substitution of cations in tetrahedral (e.g., Si^{4+} by Al^{3+}) and/or octahedral (e.g., Al^{3+} by Mg^{2+}) positions. Depending on the occupation of sites in the octahedral sheet by metal cations, dioctahedral (gibbsitic, gibbsite-like) or trioctahedral (brucitic, brucite-like) type of clays are distinguished. In the dioctahedral clays, one site is vacant and two others are occupied by Me^{3+} , while in the trioctahedral minerals all sites of brucite-like layer are filled by Me^{2+} cations (Brigatti et al. 2006; Guggenheim et al. 2006).

In 2006, the international organization AIPEA (Association Internationale pour l'Etude des Argil), clustering scientists and institutions dealing with the clay minerals, proposed an actual classification of layered aluminosilicates (Table 1) (Guggenheim et al. 2006). The layered aluminosilicates were classified in terms of various arrangement of octahedral and tetrahedral sheets, types of octahedral sublayer (e.g., trioctahedral, dioctahedral, di, trioctahedral), types of interactions between adjacent layers, as well as a layer charge attributed to the structure unit (x).

In the literature, the hydrogel-clay materials synthesized based on various types of clay minerals (e.g., montmorillonite, hectorite (laponite), saponite, kaolinite,

Table 1 Classification of layered aluminosilicates according to AIPEA Nomenclature Committee (Guggenheim et al. 2006)

Layer type (tetrahedral: octahedral)	Groups of minerals (x is the net layer charge)	Interlayer material	Type of octahedral sublayer	Examples of species
1:1	Serpentine-kaolin	None or water ($x \approx 0$)	Trioctahedral	Lizardite, amesite, cronstedtite
			Dioctahedral	Kaolinite, dickite, halloysite
			Di, trioctahedral	Odinite
2:1	Talc–pyrophyllite	None ($x \approx 0$)	Trioctahedral	Talc, kerolite, willemsite
			Dioctahedral	Pyrophyllite, ferripyrophyllite
	Smectite	Hydrated exchangeable cations ($x \approx 0.2$ – 0.6)	Trioctahedral	Saponite, hectorite, sauconite
			Dioctahedral	Montmorillonite, beidellite, nontronite

(continued)

Table 1 (continued)

Layer type (tetrahedral: octahedral)	Groups of minerals (x is the net layer charge)	Interlayer material	Type of octahedral sublayer	Examples of species
	Vermiculite	Hydrated exchangeable cations ($x \approx 0.6-0.9$)	Trioctahedral	Trioctahedral vermiculite
			Diocahedral	Diocahedral vermiculite
	True (flexible) mica	Non-hydrated monovalent cations ($x \approx 0.85-1.0$)	Trioctahedral	Phlogopite, annie, lepidolite
			Diocahedral	Muscovite, celadonite, paragonite
	Interlayer-deficient mica	Non-hydrated monovalent or divalent cations ($x \approx 0.6-0.85$)	Trioctahedral	Illite, glauconite, brammalite
			Diocahedral	Wonesite ($x < 0.6$)
	Brittle mica	Non-hydrated divalent cations ($x \approx 1.8-2.0$)	Trioctahedral	Clintonite, bityit, anandite
			Diocahedral	Margarite, chernykhite
2:1:1	Chlorite	Hydroxide sheet ($x = \text{variable}$)	Trioctahedral	Clinochlore, chamosite, nimite
			Diocahedral	Donbassite
			Di, triocahedral	Cookeite, sudoite
			Tri, diocahedral	None
1:1	Regularly interstratified	Variable	Trioctahedral	Corrensite, kulkeite, hydrobiotite
			Diocahedral	Rectorite, tosudite, brinrobertsite
1:1, 2:1			Trioctahedral	Dozyite

halloysite, attapulgite, illite, and vermiculite) are described. Most of them occur naturally as components of rocks (e.g., kaolinite in the kaolin rock, montmorillonite and small amount of hectorite in the bentonite minerals), however they can be also synthesized.

The minerals from serpentine-kaolin (1:1) group belong to less often used clays in the synthesis of hydrogel-clay (nano)composites. The general crystal structure of the 1:1 minerals is shown in Fig. 2. In the serpentine-kaolin family of clay minerals, the single layer with a thickness of about 0.7 nm, consists of one tetrahedral and one octahedral sheet, joined each other by common oxygen anions. The unit cell

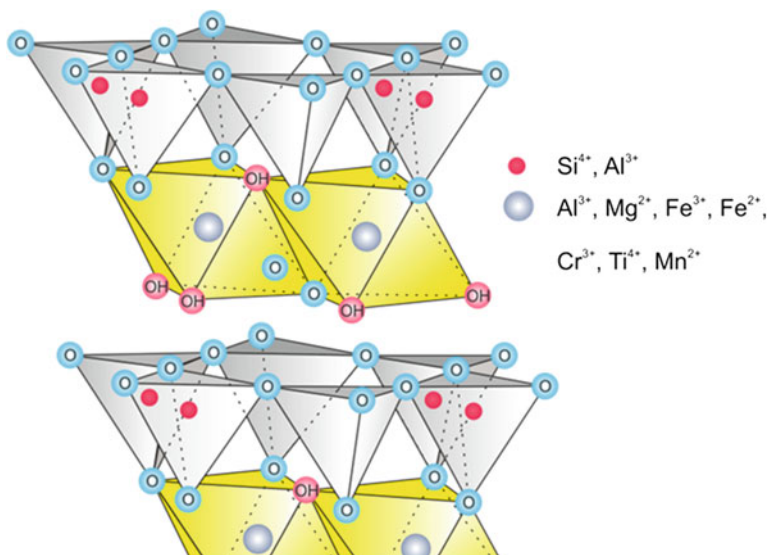


Fig. 2 General structure of minerals from serpentine-kaolin group (1:1)

includes six octahedral sites and four tetrahedral sites (Brindley and Brown 1980; Brigatti et al. 2006; Murray 2007b). The $[\text{SiO}_4]^{4-}$ tetrahedrons are connected into rings of hexagonal symmetry, however in the real crystal, the orientation of tetrahedral units is disturbed and they are turned toward each other, giving the ditrigonal (pseudo-hexagonal) arrangement. A part of Si^{4+} cations may be isomorphically substituted by cations with lower valence (e.g., Al^{3+} or Fe^{3+}) (Wang and Siu 2006). The second, gibbsite sheet, contains metal cations (Al^{3+} , Fe^{3+} , Mg^{2+}) in the central position of octahedrons, which are coordinated with O^{2-} and OH^- ions, located in the corners of the polyhedron. The clay layers interact with each other via van der Waals forces and hydrogen bonds formed between O^{2-} anions in the tetrahedral layer and the octahedral hydroxyl groups and/or water molecules (e.g., in halloysite) (Murray 2007b; Wang and Siu 2006). In the group of 1:1 phyllosilicates, the octahedral sites in the metal–oxygen sheet are entirely or nearly completely filled with Me^{2+} or Me^{3+} cations. In the case of dioctahedral clays of this group (e.g., kaolinite, halloysite), the substitution of central Al^{3+} ions by other cations (e.g., Mg^{2+} , Fe^{3+} , Cr^{3+} , or Ti^{4+}) almost does not occur. The total charge of layer, resulting mainly from the substitutions in the tetrahedral sheet is close to zero (Brigatti et al. 2006; Wang and Siu 2006). On the other hand, in the minerals from the serpentine group (trioctahedral), the octahedral sites are fully occupied by cations Mg^{2+} (most commonly), Fe^{2+} , Fe^{3+} , and/or Mn^{2+} (rarely) (Murray 2007b). The layered structure of clay is stable only when a very large number of layers is overlaid and in some cases can form tubes (e.g., halloysite) (Schulze 2005; Murray 2007b). The most known member of the 1:1 clay minerals, used in the hydrogel-clay (nano)composites synthesis, is kaolinite. Due to the absence of interlayer cations, kaolinite does not exhibit a natural ability to swelling. However,

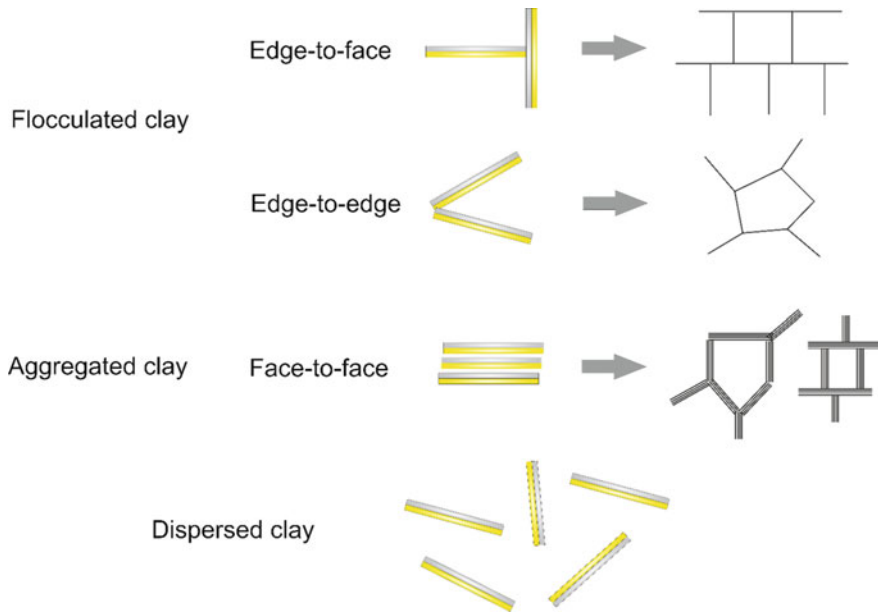


Fig. 3 Particle associations in kaolinite (Wang and Siu 2006)

because of the presence of octahedral hydroxyl groups, isomorphous substitutions of Si^{4+} by Al^{3+} or Fe^{3+} in the tetrahedral sheet, as well as charges on the edge sites, the particles of kaolinite form various associations in the solution influenced by pH changes and electrolyte concentration (e.g., NaCl). It should be noted that the overall surface charge of the basal planes is always considered as negative regardless of pH (only magnitude is pH dependent), but the edge charge may be converted from positive to negative and reversely by pH changes (Wang and Siu 2006). Depending on this parameter in relation to the isoelectric point of edge sites (IEP) kaolinite particles may form flocculated forms (edge-to-edge, edge-to-face arrangement) or aggregates (face-to-face arrangement) as well as be dispersed or deflocculated (Fig. 3) (Wang and Siu 2006). The described relationship between pH and the arrangement of clay layers is remarkably significant for the dispersion of filler in the synthesized hydrogel-clay (nano)composites, affecting their mechanical and swelling properties.

The layered aluminosilicates of 2:1 type are also often used as inorganic fillers in polymer-inorganic (nano)composite materials. They are represented by six groups of minerals, which differ mainly in the content of the interlayer spaces and the charge value of packages (x) (cf. Table 1). The general structure of the 2:1 clay minerals is presented in Fig. 4. The single package of the 2:1 clay the internal octahedral sublayer is sandwiched between two tetrahedral sheets surrounding. The neighboring octahedrons of the internal sheet are connected by common planes, while the whole octahedral sheet is bounded with adjacent tetrahedral sublayers by

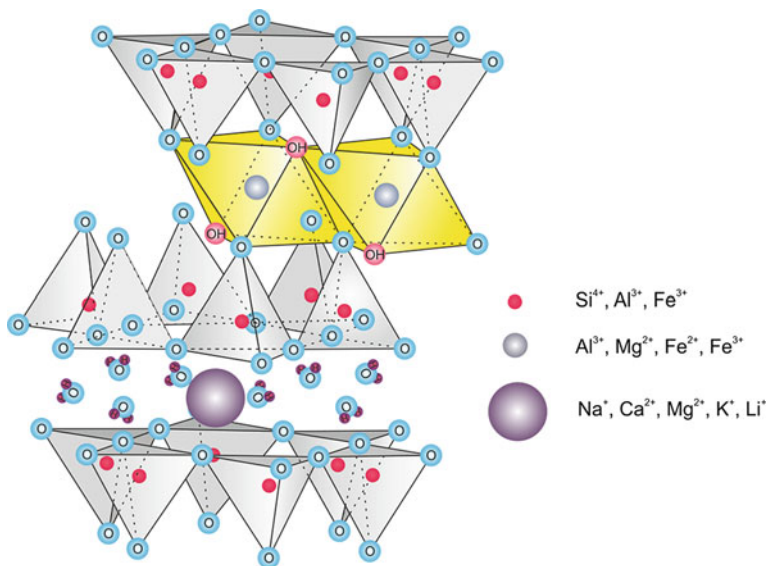


Fig. 4 General structure of 2:1-type clay minerals

corners, sharing oxyanions. In most cases (except for the minerals from talc–pyrophyllite group), the layers are negatively charged, that is a result of isomorphic substitution of Al^{3+} cations for Si^{4+} ions in the tetrahedral sheet and substitutions occurring in the octahedral sublayer (Brindley and Brown 1980; Brigatti et al. 2006; Murray 2007b; Klopogge 1998). Excluding the minerals from the talc–pyrophyllite and chlorite groups, the aluminosilicates of 2:1 type contain metal cations in the interlayer spaces, which counterbalance the negative charge of the layer and play a role in a stabilization of the layered structure. The $d_{(001)}$ -spacing for these materials is equal to ca. 0.96 nm and includes both the thickness of the layer and interlayer space (Brigatti et al. 2006; Murray 2007b).

Regarding the structure, chlorites belong to the most distinctive layered minerals of 2:1 type. In this group of clays, the interlayer spaces contain an additional single positively charged octahedral sheet, linked with the 2:1 layer by hydrogen bonds. The thickness of such formed chlorite package (described as 2:1:1) is about 1.4 nm (Schulze 2005; Brigatti et al. 2006). Due to the wide range of substitutions in both tetrahedral and octahedral sublayers, the charge of basal structure unit, as well as the composition of chlorites are variable. The tetrahedral sheets contain mainly Si^{4+} and Al^{3+} , while the octahedral sites are occupied most frequently by Al^{3+} , Mg^{2+} , Fe^{2+} , and Fe^{3+} . However, the presence of other cations, such as Cr^{3+} , Mn^{3+} , Ni^{2+} , V^{3+} , Cu^{2+} , Zn^{2+} , and Li^+ , is also possible (Schulze 2005; Brigatti et al. 2006; Murray 2007b).

The characteristic feature of the 2:1 clay minerals belonging to talc–pyrophyllite family is a neutral charge of layers, that results from only limited substitutions of Si^{4+} for Al^{3+} and minor amounts of Fe^{2+} , Fe^{3+} , Mg^{2+} , or Ti^{4+} (Schulze 2005;

Guggenheim et al. 2006). Although, the interlayer spaces do not contain cations and/or water molecules, the layered structure of clay is stable due to the presence of van der Waals forces. The weak interactions between the layers cause a very low hardness of crystals (1-2 according to Mohs scale) (Schulze 2005; Murray 2007b; Guggenheim et al. 2006).

In the family of mica minerals, the clay gallery is filled with non-hydrated metal mono- and/or divalent cations (e.g., K^+ , Na^+ , Ca^{2+}). Depending on the type of interlayer cations, true micas ($\geq 50\%$ monovalent cations), brittle ($\geq 50\%$ divalent cations), and interlayer-deficient micas (mono- and divalent cations at various amounts) can be distinguished. The overall net layer charge, equal to approx. -1.0 (in true micas) or -2.0 (for brittle micas), is a result of a substitution of Si^{4+} by Al^{3+} (or Fe^{3+}) cations in the tetrahedral layers (Murray 2007b; Guggenheim et al. 2006; Rieder et al. 1998). The exception is the interlayer-deficient micas, in which the charge is within the range from -0.6 to -0.85 . A strong interaction between the strongly negatively charged clay layers and cations located between them maintaining the layered structure in micas, as well as a lack of hydration shell around the interlayer ions cause a non-expandable character of layers, that is a distinctive feature of this group of aluminosilicates. The $d_{(001)}$ -spacing of these materials is usually approx. 1 nm and depends only on the type of cations present in the clay gallery (Schulze 2005). Similarly to other above mentioned layered minerals, micas can be classified as di- and trioctahedral types. In the case of dioctahedral type, the internal sheet is occupied by trivalent ions (e.g., Al^{3+} , Fe^{3+}), whereas in the trioctahedral micas, these positions may be filled by Mg^{2+} , Fe^{2+} , Mn^{2+} , or Li^+ (Schulze 2005; Guggenheim et al. 2006). Due to the specific layered structure, the mica minerals are characterized by a lamellar crystal shape and an excellent cleavage parallel to the basal plane. They also reveal high dielectric resistance, high thermal stability, resistance to fire and chemical agents, whereby are widely used in industry (Brigatti et al. 2006; Murray 2007b; Rieder et al. 1998).

The vermiculite group concentrates minerals also characterized by relatively high negative net charge (in the range from -0.6 to -0.9), however containing hydrated, exchangeable interlayer cations (Schulze 2005; Murray 2007b; Guggenheim et al. 2006). In contrast to the smectites, interlayer ions are regularly arranged (ordered) at specific positions in relation to oxygen anions of tetrahedral layers, resulting in "permanent" value of $d_{(001)}$ -spacing of ca. 1.4 nm (Schulze 2005; Murray 2007b). The negative charge of clay surface is generated mainly by the substitutions in the tetrahedral sheet (e.g., Si^{4+} by Al^{3+}). Trioctahedral vermiculites usually contain Mg^{2+} cations in the metal-oxygen layer, that may be partly replaced by Fe^{2+} , Ni^{2+} , Fe^{3+} , Al^{3+} , while in the interlayer spaces hydrated Ca^{2+} and Mg^{2+} cations are located (Brindley and Brown 1980; Schulze 2005; Klopogge et al. 1999). In the dioctahedral vermiculites, the internal sheet is mostly occupied by aluminum cations, which are also present in the interlayer spaces. Due to high thermal insulation properties, they are used as additives for concrete and refractory elements. Moreover, due to the ion-exchange abilities, vermiculites are tested as sorbent materials (Brigatti et al. 2006; Murray 2007b; Klopogge et al. 1999).

Smectites are the most popular family of clay minerals, used in many fields of science and technology. Among the best-known materials of this group, montmorillonite, saponite, and hectorite (laponite) should be highlighted. The reason of wide range of application of these minerals is their specific layered structure, characterized by the presence of hydrated cations in the interlayer spaces. The general chemical formulas of the main smectite representatives are shown in Table 2 (Kloprogge 1998). In the layered aluminosilicates of this group, the substitutions are present both in the tetrahedral and octahedral sublayers. The isomorphic substitution in the tetrahedral sheets involves mainly the replacement of Si^{4+} by Al^{3+} (Fe^{3+}), while Al^{3+} cations in the octahedral sublayer can be exchanged by mono-, di-, and/or trivalent cations (Li^+ , Mg^{2+} , Fe^{2+} , Ni^{2+} , Zn^{2+} , and Fe^{3+}) (Brindley and Brown 1980; Schulze 2005; Brigatti et al. 2006; Murray 2007b; Guggenheim et al. 2006). Due to the nature of the octahedral sheet, di- and trioctahedral-type smectites can be distinguished (cf. Table 1). Trioctahedral smectites (e.g., saponite, hectorite), being rather rare silicates and usually appearing as soil-forming minerals, are most often synthesized. In this case, the structure of octahedral sheet is similar to that of talc. In saponite, the octahedral sites are usually occupied by magnesium cations, while in hectorite a part of Mg^{2+} ions is substituted by Li^+ (Brindley and Brown 1980; Schulze 2005; Kloprogge et al. 1999).

Diocahedral smectites (e.g., montmorillonite, beidellite, and nontronite), being main constituents of sedimentary rocks (clays) (e.g., bentonite), belong to the most common group of the 2:1 type minerals. The low, negative charge of the surface (in the range from -0.2 to -0.6) is a result of the partial substitution of Al^{3+} by Mg^{2+} cations in the octahedral sublayer (e.g., in montmorillonite) or substitution of Si^{4+} by Al^{3+} ions in the tetrahedral sheet (e.g., in beidellite). In the octahedral layer, small amounts of iron and other metal cations may be present (Schulze 2005; Brigatti et al. 2006; Murray 2007b). In the smectites, the negative charge of the layers is compensated by hydrated cations of alkali and alkaline earth metals (Na^+ , K^+ , Li^+ , Ca^{2+} , and Mg^{2+}) located on the outer surface of the layers and in the interlayer spaces. The small content of interlayer ions causes a weak interaction between clay layers, which results in high cation-exchange capacity (Brigatti et al. 2006; Murray 2007b; Kloprogge 1998). Therefore, the originally occurring interlayer cations can be relatively easily replaced by other cations (e.g., Sr^{2+} , Ba^{2+} , H_3O^+ , or NH_4^+) or larger positively charged molecules, such as metal oligomers, surfactants, monomers, or polymer chains (Sinha Ray and Okamoto 2003; Kloprogge 1998; Lagaly et al. 2007; Murray 2007a). Moreover, due to the specific structure, smectites reveal an excellent ability to swelling in polar solvents, which

Table 2 General chemical formulas of the best known smectite minerals

Montmorillonite	$\text{Mn}^{n+}_{x/n} [\text{Al}_{4-x}\text{Mg}_x][\text{Si}_8]\text{O}_{20}(\text{OH})_4 \cdot m\text{H}_2\text{O}$
Beidellite	$\text{Mn}^{n+}_{x/n} [\text{Al}_4][\text{Si}_{8-x}\text{Al}_x]\text{O}_{20}(\text{OH})_4 \cdot m\text{H}_2\text{O}$
Nontronite	$\text{Mn}^{n+}_{x/n} [\text{Fe}_4][\text{Si}_{8-x}\text{Al}_x]\text{O}_{20}(\text{OH})_4 \cdot m\text{H}_2\text{O}$
Saponite	$\text{Mn}^{n+}_{x/n} [\text{Mg}_6][\text{Si}_{8-x}\text{Al}_x]\text{O}_{20}(\text{OH})_4 \cdot m\text{H}_2\text{O}$
(F-)hectorite	$\text{Mn}^{n+}_{x/n} [\text{Mg}_{6-x}\text{Li}_x][\text{Si}_8]\text{O}_{20}(\text{OH}, \text{F})_4 \cdot m\text{H}_2\text{O}$

facilitates their further modification and layers rearrangement (Anderson et al. 2010). Thus, the introduction of larger molecules into the clay gallery results mostly in an increase in the $d_{(001)}$ distance and usually leads to the change of ordered-layered structure into the three possible forms: intercalated, pillared, or exfoliated. In the case of the intercalated form, the clay mineral maintains the layered arrangement with a simultaneous increase in the $d_{(001)}$ -spacing. Furthermore, the intercalation of certain modifiers (e.g., metal oligocations or organosilanes) combined with a suitable treatment leads to the formation of “pillars” between aluminosilicate layers, which results in obtaining the mineral with 3D structure (Kloprogge 1998). On the other hand, for many applications (e.g., synthesis of clay-polymer (nano)composites) the transformation of pristine clay mineral into the exfoliated form is required. This process may be carried out both on mechanical modification (e.g., ultrasound treatment) and with use of chemical agents (e.g., polymers).

A low availability of sufficient quantities of some layered aluminosilicates in their natural form, as well as a presence of large variation of impurities, forced a development of many methods of synthesis of clay minerals. Due to the synthesis conditions, these preparation techniques can be divided into four groups, namely: (i) synthesis at low temperature and pressure (<100 °C, 1 bar), (ii) hydrothermal synthesis (100–1000 °C, P_{H_2O} or high pressure), (iii) synthesis above 1000 °C and at very high pressure, as well as (iv) synthesis in the presence of fluoride (Kloprogge et al. 1999). Briefly, the layered minerals syntheses involve the preparation of aqueous solution of metal salts (e.g., chlorides and nitrates of Fe, Mg, Al, and Li) and/or hydroxides [e.g., $Al(OH)_3$, $Mg(OH)_2$, $Na(OH)$, and $Li(OH)$] with silica precursors (e.g., TEOS, Na_2SiO_3 , silica gel, or sol) at defined stoichiometric ratios and pH followed by thermal or hydrothermal treatment at various conditions of temperature, pressure, and time (Kloprogge 1998; Kloprogge et al. 1999). One of the best-known commercial synthetic clay is hectorite from Laporte Industries Ltd., known by the trade name Laponite (Kloprogge 1998; Kloprogge et al. 1999). The first patented method of laponite synthesis involved the formation of aqueous slurry composed of water-soluble salt of Mg^{2+} , Na^+ , and Li^+ and their hydrothermal treatment at increased pressure (10–50 bar) and temperature (185–265 °C) (Kloprogge et al. 1999).

The clay minerals, exhibiting ion-exchange ability, are a subject of many modifications based mostly on the replacement of interlayer cations by other cations or molecules. The ion-exchange reaction may be carried out in an aqueous environment, organic solvents, and molten salts. In the case of aluminosilicates characterized by a small layer charge (montmorillonite, vermiculite), the substitution of interlayer cations in aqueous solutions is very fast and reversible (in contrast to the highly charged micas layers). Moreover, the efficiency of ion exchange increases for higher valency cations or greater ionic radius (for cations of the same valency). In the case of smectites, the series of convertibility of alkali and alkaline earth metal cations are as follows: $Li^+ < Na^+ < K^+ < Rb^+ < Cs^+$ and $Mg^{2+} < Ca^{2+} < Sr^{2+} < Ba^{2+}$ (Li et al. 2012). The parameter characterizing the clay minerals in terms of their ion-exchange properties is cation-exchange capacity

(CEC), expressed in meq/100 g of clay. The type of interlayer cations determines the material properties, such as ion-exchange capacity, water absorption (swelling), thermal stability, and other functional features (e.g., thixotropic properties) (Murray 2007a). The examples of commercial clays containing the specified type of interlayer ions are Cloisite[®]Na⁺ and Cloisite[®]Ca⁺⁺.

A particular example of cation exchange in layered aluminosilicates is an acid activation, involving a treatment of clay mineral with a strong acid (e.g., H₂SO₄, HCl, H₃PO₄) (Komadel and Madejova 2006). During this process, both the interlayer cations (e.g., Na⁺, Ca²⁺) and ions within the framework positions (e.g., Al³⁺ and Mg²⁺) are replaced by protons, while the cations removed from the internal sheet are located in gaps between the layers. Acid-activated aluminosilicates are characterized by an increased specific surface area and porosity, as well as an improved acidity of the surface. The most important parameters of acid modification of smectites, determining their physicochemical properties are the type and concentration of acid, chemical composition of the modified aluminosilicate, temperature, and activation time (Komadel and Madejova 2006; Adams and McCabe 2006; Breen and Watson 1998; Chitnis and Sharma 1997; Vaccari 1999). Examples of acid-treated montmorillonites are commercially available K10, K30, and KSF materials (Flessner et al. 2001).

Smectites and vermiculites can be also modified by the intercalation of surfactants (e.g., alkylammonium salts). This process, called sometimes as organophilization, can be done by mixing an aqueous slurry of clay mineral with a solution of organoammonium salt. In the case of solid-state reaction, the intercalation of organic compound in dried clay minerals without any solvent using high shear mixer can be performed (Lagaly et al. 2007; Ganguly et al. 2011). Alkylammonium cations, with general formula R₄N⁺, maintain a positive charge, independent of pH of solution in which they are present. The examples of most often, commercially used surfactants for the clay modifications are: dimethyl dihydrogenated tallow quaternary ammonium chloride (e.g., organofilized montmorillonites: Cloisite 6A, Cloisite 15A, Cloisite 20A), dimethyl benzyl hydrogenated tallow quaternary ammonium chloride (Cloisite 10A organoclay), methyl tallow bis(2-hydroxyethyl) quaternary ammonium chloride (Cloisite 30B organoclay). The introduction of surfactant molecules into the clay gallery results in a significant increase in the d₍₀₀₁₎-spacing, and ordering of layers, as well as facilitates the intercalation of larger particles (e.g., polymeric chains) and exfoliation of clay layers. Thus, modified silicates are often used as the starting form for further processing (e.g., in synthesis of polymer-clay (nano)composites).

3 Methods of Hydrogel-Clay (Nano)Composites Synthesis

Conventional hydrogels are three-dimensional networks consisting of synthetic or natural hydrophilic polymeric chains crosslinked together (i) chemically by covalent bonds, (ii) physically by noncovalent interactions or (iii) by a combination of

both. The presence of functional hydrophilic pendant groups causes that hydrogels show water swelling. Furthermore, the crosslinked structure makes hydrogels insoluble in water. Depending on the nature of functional groups, the polymeric chains of hydrogels may be polycations, polyanions, polyampholytes, polybetaines, or may be nonionic.

The chemically crosslinked hydrogels are prepared by two different methods: (i) three-dimensional free-radical polymerization of water-soluble monomers in the presence of multifunctional monomer (crosslinker), (ii) chemical crosslinking of water-soluble polymers by a reaction between functional groups of polymers and bifunctional crosslinking agent. Copolymerization of the water-soluble vinyl monomers and multifunctional monomers (crosslinkers) is a preferable route of hydrogels synthesis in three-dimensional free-radical polymerization (TFRP) (Thakur and Thakur 2014a, b, 2015). The commercially available monomers used as crosslinkers are shown in Fig. 5.

Using this method, interpenetrating (IPN) and semi-interpenetrating (sIPN) hydrogel networks are synthesized (Shivashankar and Mandal 2012; Dinu et al. 2011). The polymerization can be carried out in solution, suspension/inverse-suspension, emulsion/inverse-emulsion, or as bulk polymerization (Oadian 1991; Choudhary 2009; Hussain et al. 2012). The solution polymerization is used for the synthesis of large amounts of the hydrogel. The process is most frequently proceeded in water, but a variety of polar solvents can be applied. Moreover, they can be exchanged for water in the hydration step. The polymerization is usually initiated by the presence of free-radical initiators [such as 2,2-azo-isobutyronitrile

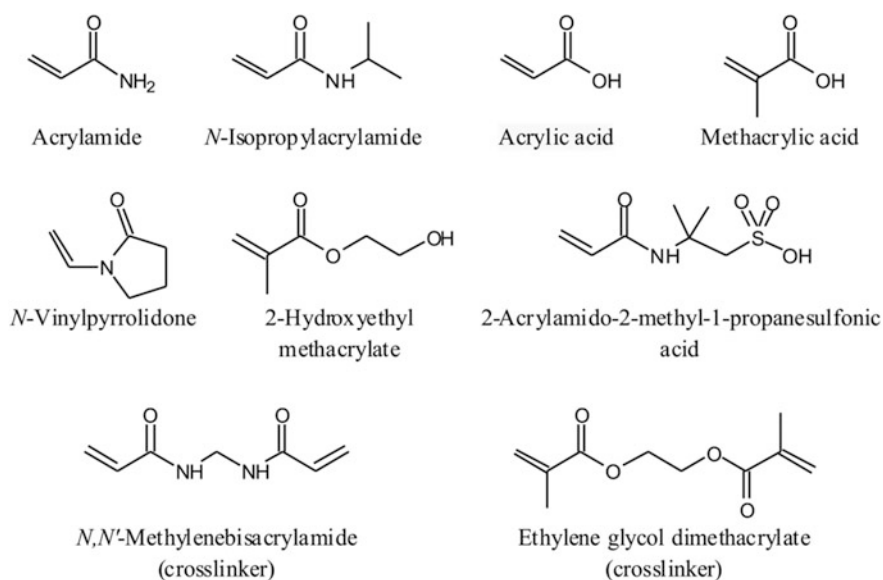


Fig. 5 Typical monomers used for the preparation of hydrogels

(AIBN), 2,2'-azobis(2-methylpropionamide)dihydrochloride (AIBA), ammonium persulfate (APS), potassium persulfate (KPS)] or redox systems (such as persulfates activated by *N,N,N',N'*-tetramethylethylenediamine (TMEDA)), heating or UV radiation. Gamma-, electron beam-, or microwave-radiations are also used to initiate the radical polymerization instead of chemical free-radical initiators.

Chemical crosslinking of polymer chains is another method commonly applied in the preparation of synthetic hydrogels, which is performed in dilute solutions of hydrophilic polymers. In this approach, a bifunctional crosslinking agent added to the solution reacts with functional groups of the polymer and forms covalent bonds with polymer chains. Epichlorohydrin (ECH), glutaraldehyde (GA), and diepoxides react readily with hydroxyl, amine, and carboxylic pendant group of synthetic or natural polymeric chains, thus they are widely used as the crosslinking agents (Varma et al. 2004; Wan Ngah et al. 2011).

Chemically crosslinked hydrogels of synthetic and natural polymers are also obtained using an electron beam or γ radiation. The radiation generates macro-radicals on polymeric chains by the homolytic scission of C–H bonds and additionally, induces radiolysis of water molecules. The hydroxyl radicals can attack the polymer chains forming the macroradicals, which being present on different chains can subsequently recombine giving the polymer network (Hennink and Van Nostrum 2012).

Other important hydrogels are physically crosslinked hydrophilic polymers. These hydrogels are formed by different physical interactions, such as hydrogen bonding, ionic interactions, and hydrophobic association. The water-soluble polymeric chains have ionic or polar pendant groups that interact with each other forming noncovalent intermolecular bonds and finally the crosslinked structure. The appropriate methods of preparation physically crosslinked hydrogels are solvent techniques (Hennink and Van Nostrum 2012; Song et al. 2013). Physically crosslinked hydrogels are also prepared in the freezing-thawing process. During several cycles of freezing-thawing, the crystalline domains are formed being junctions of the polymer network (Hoffman 2002). Stability of physically crosslinked hydrogels depends on many factors, such as pH, ionic strength, temperature, polymer concentration. For example, swelling of poly(acrylic acid) and poly(ethylene glycol) strongly depends on pH because hydrogen bonds are only formed when the carboxylic acid groups are protonated (Hennink and Van Nostrum 2012).

Grafting polymerization involves anchoring of hydrophilic monomers on supports (e.g., polymer chains). There are two variants of such synthesis: (i) grafting through when the polymerizable functional groups are located on the support and participate in propagation, and (ii) grafting from when the centers initiating polymerization (e.g., free radicals) are present on the surface of support (Hennink and Van Nostrum 2012).

The above-presented synthesis methods are sometimes adopted for the processes, which are used to obtain hydrogel-clay (nano)composite taking into consideration specific interactions of monomers or polymers with layered silicate. The simplest method of synthesis of hydrogel-clay (nano)composite is the in situ free-radical polymerization of hydrophilic vinyl monomers in an aqueous medium

in the presence of dispersed clay. The degree of dispersion of layered silicate determines the way of conducting the process, and also the structure of the obtained composite, namely microcomposite, intercalated nanocomposite, and exfoliated nanocomposite. When the clay is not exfoliated in the aqueous medium, polymerization can undergo in the clay gallery as the in situ intercalation polymerization. In the case of homogeneous dispersion of the clay particles, they act as multifunctional crosslinking agents, and form the stable crosslinked structure, which does not use the crosslinking monomers (Haraguchi and Tekehisa 2002). The hydrogel-clay (nano)composites obtained by this method are characterized by a unique structure significantly different from that of typical exfoliated (nano)composite, because the clay platelets are not dispersed in the polymer network, but take part in its formation as shown in Fig. 6 (Haraguchi 2011b).

A typical procedure of synthesis of hydrogel-clay (nano)composite consists of two crucial steps: (i) preparation of initial reaction solution and (ii) appropriate free-radical polymerization. The initial reaction solution is usually prepared in freezing temperature by mixing homogeneous dispersion of clay with a solution of monomers and free-radical initiator. Typically, mechanical stirring is sufficient for

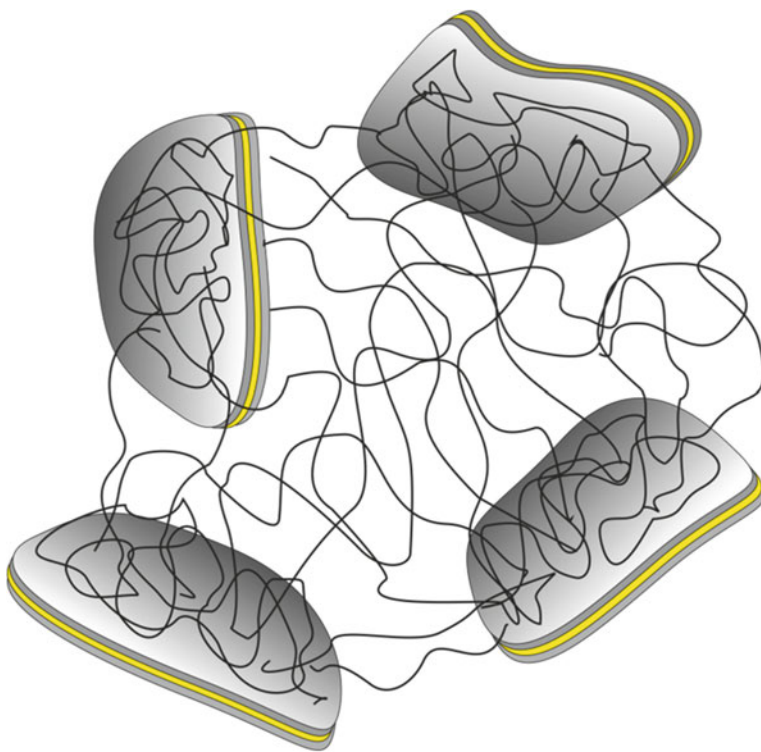


Fig. 6 Schematic representation of structural model of organic (polymer)/inorganic (clay) networks in (nano)composite gels

effective exfoliation of clays in water, but also sonication is often applied at this stage. The appropriate radical polymerization is usually carried out at ambient temperature for 24–72 h in an inert atmosphere and does not require stirring, which makes the method relatively simple. However, not all of the vinyl monomers can form (nano)composites in the presence of exfoliated clay in such a simple way, because the effective stabilization of clay dispersion by the monomer molecules is required to prepare hydrogels crosslinked by the clay platelets. The nonionic vinyl monomers having amide groups such as acrylamide, *N*-isopropylacrylamide, and *N,N*-dimethylacrylamide effectively stabilize clay platelets in aqueous media as a result of mild interaction between the ionic clay and the dipolar molecules, and so largely prevent the gel formation of clay itself. The ionic monomers, such as acrylic acid, form strong hydrogen bonds with hydroxyl and silane groups present on the clay surface, and consequently, inhomogeneous hydrogel-clay aggregates are formed. Thus, obtaining the homogeneous initial reaction solution by simple mixing of the solution of acrylic acid and clay dispersion is impossible (Song et al. 2008).

Contrary to other ionic monomers, 2-acrylamido-2-methylpropanesulfonic acid (AMPS), which is a commonly used vinyl monomer for the synthesis of conventional hydrogels, can successfully avoid the aggregation and gelation of laponite even in the presence of acrylic acid. The stabilization of clay suspension by AMPS is the result of synergistic interaction of acrylamido and sulfonic acid groups with the laponite platelets (Chen et al. 2013; Du et al. 2014).

The chemical redox systems (e.g., APS or KPS) in combination with TMEDA are used to initiate the process as well as UV irradiation in the presence of photoinitiators (Haraguchi and Takada 2010).

The mechanism of hydrogel-clay (nano)composite formation is determined by specific interactions between clay platelets and monomer as well as initiator molecules. Haraguchi et al. revealed that in the polymerization of *N*-isopropylacrylamide initialized by the KPS/TMEDA system, the ionic groups of initiator more intensively interact with the clay platelets by strong ionic interactions than the polar monomer molecules, and therefore, on the surface of clay platelet centers of radical polymerization are located. Hence, the formed polymer chains are grafted on the clay surface (Haraguchi et al. 2005).

All layered silicates in their pristine state are of good water swellability and obtaining homogeneously dispersed clay platelets in aqueous media does not cause any problem at low clay concentrations. Nevertheless, the clay suspensions are characterized by high viscosity, which makes the polymerization extremely difficult. Due to this fact, the clay concentration in the initial reaction solution usually does not exceed 6 wt%. At high concentrations of nonmodified clays, the preparation of aqueous dispersion is hard, even under strong agitation. The commercially modified clay (laponite), which is mixed with the sodium salt of pyrophosphate as an inorganic modifying agent, is much easier dispersible in water and gives less viscous solutions (Liu et al. 2007). Another way to the lower viscosity of initial reaction solution is an addition of poly(ethylene glycol) to suspension, which easily adsorbs on the clay platelets and acts as a dispersing agent (Hu et al. 2010).

The synthesis of hydrogel-clay (nano)composites by the in situ free-radical polymerization can be also done according to other modified procedures described in the literature. Shirsath et al. reported the preparation of hydrogel-clay (nano)-composites based on acrylic acid and modified bentonite by the in situ free-radical polymerization using ultrasound irradiation (Shirsath et al. 2015). In turn, Zhu et al. described the synthesis of poly(acrylic acid)-based (nano)composite using chemically modified attapulgite, which played the role of initiator and crosslinking agent (Zhu et al. 2014). The attapulgite nanorods modified by aminopropyltriethoxysilane acted as the surface-initiated redox system, whereas introduced 3-methacryloxypropyltrimethoxysilane was the crosslinker. The presented method is an example of both variants of grafting polymerization, i.e., grafting through and grafting from.

The in situ intercalation polymerization is free radical polymerization of water-soluble monomers in the presence (or not) of the multifunctional monomer (crosslinker) in an aqueous dispersion of not exfoliated clay. Owing to the hydrophilic nature of clay, intercalation by water-soluble monomers into the interlayer space is relatively simple and does not require an initial modification of silicate with cationic surfactants. The methodology of preparation of initial reaction solution and conducting the polymerization process does not differ in principle from the above-described procedures. The product of such polymerization can be hydrogel-clay (nano)composite with the structure of intercalated or exfoliated (nano)composite (Natkański et al. 2012; Nie et al. 2014).

The synthesis of homogeneous hydrogel-clay (nano)composites by the in situ free-radical polymerization in dispersion containing exfoliated clay mixed with a solution of hydrophilic polymer is relatively simple, but is simultaneously time-consuming and needs particular skills. Zhu et al. used for that purpose the dendrimeric polymers, in which dendron units with the guanidinium ion groups are located at both termini of a long, hydrophilic poly(ethylene glycol) (Zhu et al. 2014). It was observed that transparent hydrogel in the aqueous dispersion of clay was formed after 3 min as a result of polymer crosslinking by the clay platelets. The hydrogelation was observed in the presence of poly(sodium acrylate), but also without taking part of the last one. The presented synthesis method of hydrogel-clay (nano)composite is easy, but obtaining the dendrimeric polymers in the multistage process is a relatively difficult challenge. Tamesue et al. prepared linear polymers with the guanidinium ion groups located at both termini of linear poly(ethylene glycol) and obtained the hydrogel-clay (nano)composite under conditions identical to those using the dendritic polymers (Tamesue et al. 2013). The key importance, in this case, had the structure of used polymers, in which the guanidinium ion groups played an important role in interactions with the clay platelets.

The layered silicates are fairly well-miscible with nonionic hydrophilic polymers [e.g., poly(vinyl alcohol) and poly(ethylene oxide)], but an addition of this polymer to a clay dispersion does not guarantee the formation of hydrogel-clay (nano)-composite. Thus, the freezing-thawing process, based on the formation of physical network nodes of crystalline polymer domains, is sometimes used (Ibrahim and El-Naggar 2013).

4 Main Techniques Used for Characterization of Hydrogel-Clay (Nano)Composites

Due to the complex framework, the characterization of structure, composition and functional properties of composite materials requires an involvement of many methods, including more sophisticated ones. The applied methods are dedicated to recognize features of either one of component (hydrogel or clay) or both of them as well as the determination of interactions between both phases.

The most significant and basic method used in the characterization of hydrogel-clay composites, enabling studies of ordering and dispersion of clay particles in a polymer matrix, is X-ray diffractometry (XRD) (Chen et al. 2008). The XRD patterns observed for the polymer-clay composites in relation to types of their structure are schematically presented in Fig. 7. The diffraction lines found in the XRD patterns of these materials are usually attributed only to the crystallographic planes in the ordered clay. Generally, the most intensive reflections, assigned to the family of (001) planes, are used to describe the structural changes of aluminosilicate filler and determination of composite type. The position of (001) diffraction line corresponds to the distance between adjacent clay layers ($d_{(001)}$ -spacing). In turn, the appearance of other additional reflections from the (001) group reveals the higher ordering of layered structure (Merinska et al. 2002). As can be seen in Fig. 7, a broadening and gradually disappearing of (001) reflection is a result of increasing disorder of clay layers in the hydrogel matrix (Chen et al. 2008).

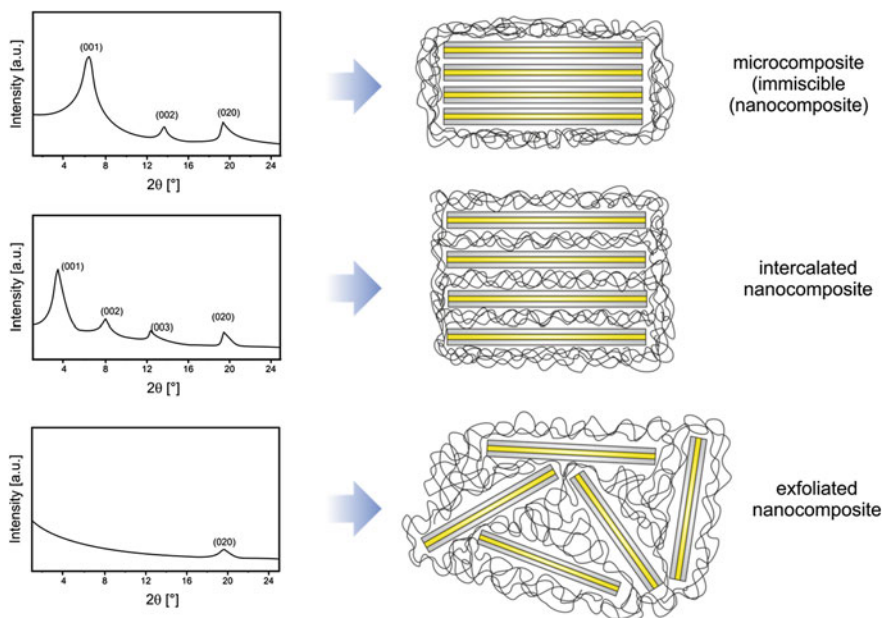


Fig. 7 XRD patterns recorded dependently on types of structure of polymer-clay composites

In view of various electron densities of polymer and clay components, the examination of the structure of hydrogel-clay composites can be carried out by means of small angle-(SAXS) and wide-angle X-ray scattering (WAXS) (Mauroy et al. 2013; Paranhos et al. 2007). These methods enable the determination of shape, thickness, dispersion, volume fraction, and orientation of the clay layers to each other, as well as the thickness of the transition layer between the clay particles. The SAXS and WAXS techniques are especially useful for the studies on the behavior of clay particles during the in situ polymerization (Mauroy et al. 2013), as well as the response of composite to tensile stress (Takeno and Nakamura 2013; Nishida et al. 2012) or temperature changes (Agrawal et al. 2010).

In the characterization of hydrogel-clay systems, the hydrodynamic diameter and the distribution of clay, polymer, and their mixture in an aqueous solution can be acquired with dynamic light scattering (DLS) (Lian et al. 2015). The results obtained by this technique, combined with those from the SAXS method, enable to determine the network structure, gelation mechanism, and crosslinking effect (Beisebekov et al. 2014). The DLS analyses are very often supported by complementary measurements of zeta potential (ζ), which corresponds to the surface charge of filler and polymer particles in the solution.

Especially convenient methods for the examination of clay dispersion in the hydrogel and composite morphology are transition electron microscopy (TEM) and scanning electron microscopy (SEM). However, the precise observations of single aluminosilicate particles are only possible by use of the former technique. Moreover, both SEM and TEM techniques are usually coupled with EDS (Energy-Dispersive X-ray Spectroscopy) detector, which enables an analysis of chemical composition on the surface and in bulk of composite material in the micro- and nanometric scale, respectively (Haraguchi and Varade 2014; Natkański et al. 2013a). In the case of the SEM method, due to the lack of conductivity and the nature of polymeric hydrogels, the analysis of hydrogel-clay composites most often requires an application of special SEM techniques (modes), such as VP-SEM (Variable Pressure SEM), Cryo-SEM (cryo-scanning electron microscopy), or ESEM (Environmental SEM), as well as low beam energies (5–20 kV) and a special sample preparation (i.e., freeze-drying, sputtering of conductive gold, platinum, palladium or gold-palladium film) (Liu et al. 2012b, 2013; Chen et al. 2014b; Helvacioğlu et al. 2011; Beisebekov et al. 2014; Guilherme et al. 2010; Ma et al. 2008; Irani et al. 2013; Bhattacharyya and Ray 2014). The examples of SEM and TEM images collected for the hydrogel-clay nanocomposites are shown in Fig. 8.

The studies of the morphology of hydrogel-clay composites are also performed by means of atomic force microscopy (AFM), which allows to observe surface roughness and dispersion of clay particles in the surface layer. The surface roughness determination is of interest due to potential applications of the hybrid hydrogels in tissue engineering, for example, in the treatment of skin burns, where slightly rough surface of dressing provides a better contact with the burned tissue (Silva et al. 2008).

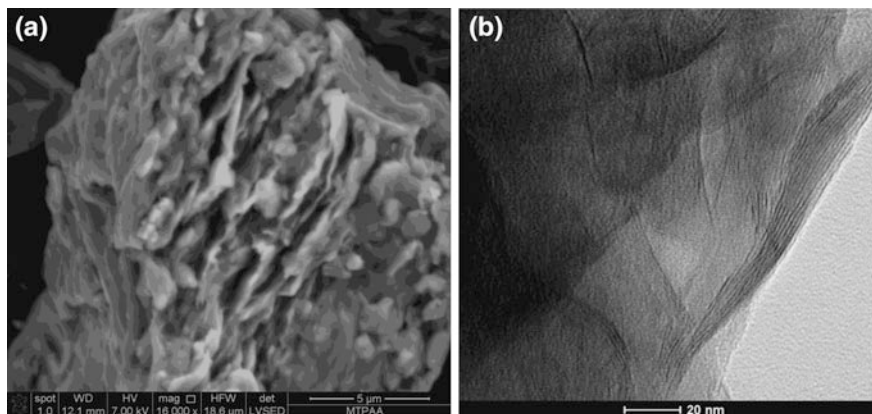


Fig. 8 SEM (a) and TEM (b) images of poly(acrylic acid)-montmorillonite nanocomposite

The interaction between the hydrogel and clay surface are very often studied by Fourier transform infrared spectroscopy (FTIR). The negative charge of clay surface (electronegative oxygen), as well as the presence of hydroxyl groups, results in the interaction with functional groups of the polymer by van der Waals forces or hydrogen bonds (Xiang et al. 2006). For instance, the interaction of hydroxyl groups of clay mineral with carboxylic groups of poly(acrylic acid) is identified in the FTIR spectrum as a shift of band attributed to C=O groups toward lower wavenumbers in relation to unmodified polymer (Fig. 9a), while the absorption band attributed to the Si–O bond is shifted toward lower frequencies ($1007\text{ cm}^{-1} \rightarrow 1037\text{ cm}^{-1}$) (Janovák et al. 2008). Similar effects are found during the formation of hydrogen bonds between N–H groups of poly(acrylamide) and hydroxyl groups of halloysite (Fig. 9b) (Liu et al. 2012b).

In the case of adsorption studies of dyes or heavy metal cations on hydrogel-clay composites, the FTIR technique is applied to determine the type of complex, which forms between hydrogel functional groups and adsorbed species, and thus indirectly to study the adsorption mechanism (Nakamoto 1986).

Furthermore, certain effects accompanying the presence of clay particles in the hydrogel matrix may be studied by means of Raman spectroscopy. Namely, based on the analysis of wavenumber shifts of the band attributed to the CH₃ stretching vibrations, the hydration degree of the polymer chains in the aqueous solution in the function of clay content can be estimated (Lian et al. 2015).

The changes of thermal and swelling properties of the polymer after the introduction of small amounts of clay filler are examined with the use of thermal methods, namely thermogravimetry analysis (TGA) and differential scanning calorimetry (DSC). Basically, the TGA technique is used to determine the clay content in the composite, as well as the decomposition mechanism of polymer part. However, in order to study the thermal decomposition process precisely, an additional analysis of gaseous products (evolved during the sample heating) by

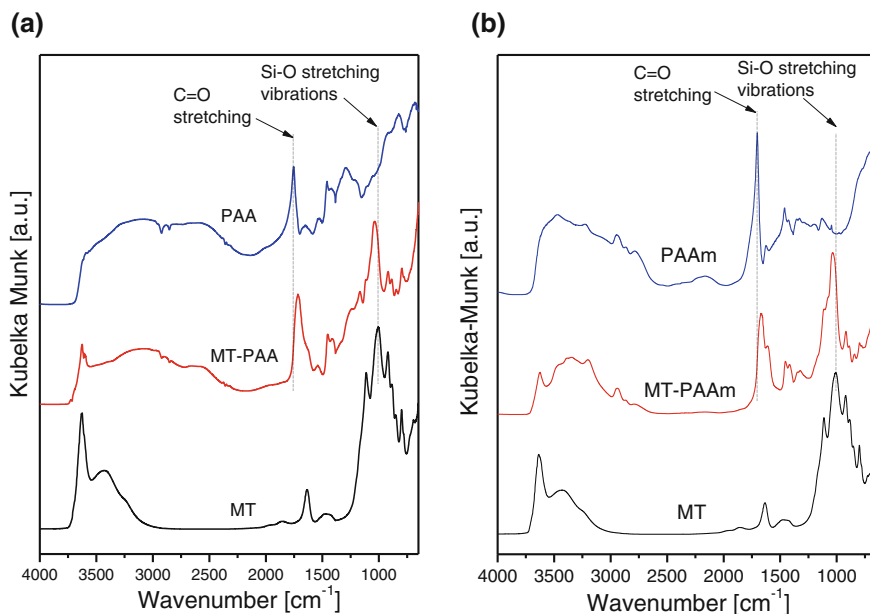


Fig. 9 Interactions between functional groups of montmorillonite (MT) and hydrogels (poly (acrylic acid)—PAA (a) and poly(acrylamide)—PAAm (b)) observed in FTIR spectra

mass spectroscopy (TGA-MS) or infrared spectroscopy (TGA-FTIR) is required (Natkański et al. 2013b, 2016). Moreover, the hydration properties of hydrogels and hydrogel-clay composites, in terms of different states of water (free, bound, loosely bound water, or crystallized and uncrystallized water) existing in the material are also examined by the TGA method (Panagopoulou et al. 2013). A unique feature of temperature-responsive polymers (e.g., poly(*N*-isopropylacrylamide)) is the presence of volume phase transition temperature, in which polymer undergoes a reversible coil-to-globule transition (Shen et al. 2015). At this temperature, determined by means of the DSC method, dramatic changes in the swelling and deswelling behavior are observed (Xiang et al. 2006). Glass transition temperature, attributed to the increase in free volume caused by thermal expansion of the system, can be also determined by the DSC measurements (Paranhos et al. 2007). In the case of hydrogel-clay composites, the changes of this parameter can be a result of crosslinking effect of clay, which influences functional properties of the discussed materials (e.g., swelling, mechanical properties) (Vanamudan et al. 2014; Urbano and Rivas 2011; Wang and Chen 2012).

One of the most frequently studied characteristics of hydrogel-clay composites is their swelling capacity. Due to the high affinity of such systems to water molecules, these materials are especially applied as superabsorbents, which are able to absorb, swell, and retain a large volume of water or other biological fluids. In the typical approach, a dried and pre-weighted sample is immersed in a specified solution, kept

to achieve absorption equilibrium and weighted again after sorption. According to Eq. 1, the swelling capacity (S_{eq}) is calculated (Natkański et al. 2012).

$$S_{eq} = \frac{(\text{mass of swollen sample}) - (\text{mass of dried sample})}{\text{mass of dried sample}} = \frac{\text{mass of water}}{\text{mass of dried sample}} \quad (1)$$

Depending on the intended application of hydrogel-clay composites, a sample is subjected to the swelling experiments in various aqueous media, such as distilled water (most often), solutions of various salts (buffer solutions) and acids with different pHs (Dadkhah et al. 2014; Aalaie et al. 2008; Wan et al. 2015a; Zheng et al. 2012). Moreover, for determining the response rate of the composite hydrogels upon temperature stimuli, the swelling–shrinking kinetics of the composite hydrogels at various temperature are studied (Zhang et al. 2013).

The hydrophilic/hydrophobic nature of hydrogel-clay composites is examined by the measurements of contact angle (θ_w) for water with the use of laser-scanning confocal microscope (Haraguchi and Li 2010). It was shown that the composition of hydrogel-clay material (i.e., water content and clay loading) as well as contact time with water influenced significantly hydrophilicity/hydrophobicity of the composite surface (Haraguchi and Li 2010).

Many hydrogels exhibit excellent adsorption properties in relation to heavy metal cations, dyes, drugs, or fertilizers. Additionally, the incorporation of clay particles into hydrogels can improve their adsorption properties (Natkański et al. 2012; Dalaran et al. 2009; Bortolin et al. 2013; Shi et al. 2013; Bhattacharyya and Ray 2014; Zhang et al. 2014a; Kundakci et al. 2011; Kevadiya et al. 2011; Bortolin et al. 2013). The general procedure of determination of adsorption capacity of the composite material involves an exposure of pre-weighed sample in a specified amount of solution of appropriate adsorbate (with a known concentration), at adjusted pH and temperature for time sufficient to achieve the equilibrium sorption capacity. In the case of application of hydrogel-clay composites as drug deliveries, the desorption tests are also performed. The measurement of the amount of adsorbed/desorbed compound is usually carried out by chemical quantitative analysis of remaining solution after the adsorption process by ICP-OES, ICP-AES, and UV-VIS methods (Zheng et al. 2014; Haraguchi and Varade 2014; Bhattacharyya and Ray 2014; Bortolin et al. 2013).

Many reports, devoted to the studies on hydrogel-clay composites, concern on stimuli-sensitive hydrogels (characterized by volume or phase transition in response to external environmental changes, such as temperature, pH, ionic strength, pressure, electronic and magnetic field) as materials widely applied in tissue engineering, pharmaceutical systems, medical treatment, artificial organs, physiology, and environmental protection (Xiang et al. 2006; Wang and Chen 2012). The mechanical properties of hydrogel-clay composites (e.g., toughness, fracture strength, tensile elongation, tensile strength, tensile modulus, tensile strain, and compression) are estimated analogously to metals or polymers, however relative

humidity and temperature have a greater influence on the material function, therefore during tensile testing these conditions must be precisely controlled. In the case of rheological studies, an experimental method allowing the examination of mechanical properties of gels under appropriately chosen loads is oscillation rheometry. In this method, sample is placed between two elements, one of them is rotating and the other is fixed. During the test, the torque of rotating part is measured at a known rotating frequency, which subsequently allows to calculate the shear rate and the corresponding shear stress present in the analyzed sample. The final obtained viscoelastic parameters of the material at the time of dynamic loading are storage modulus (G'), elastic component of rheological behavior, and loss modulus (G''), a viscous component of rheological behavior (Janovák et al. 2008). Rheometry allows to examine an effect of clay content on the elastic properties (Kamoun and Menzel 2012), as well as an effect of clay on the polymerization rate (Lungu et al. 2012) and crosslinking of polymer.

5 Beneficial Features of Hydrogel-Clay (Nano)Composites

5.1 *Mechanical and Rheological Properties*

Hydrogels as soft polymeric networks show inherent poor mechanical properties, which significantly restrict their practical applications. The homogeneous dispersion of clay in the polymer matrix improves its mechanical and rheological parameters due to the energy dissipating effect of rigid clay in the hydrogel (hydrogel-clay (nano)composites are much more viscous than conventional cross-linked hydrogels) and strong interactions between functional groups present on the polymer chains and the clay surface. Generally, the hydrogel-clay (nano)composites, being prepared in various shapes including films, rods, spheres, hollow tubes, etc., with different thicknesses or diameters (Haraguchi 2007a), exhibit striking mechanical toughness, which allows them to be deformed to large extent without significant signs of damage under various stresses, including elongation, compression, bending, tearing, twisting, or even knotting. For example, Zhu et al. (2006) compared the mechanical properties of pure and laponite-modified poly (acrylamide) crosslinked with N,N' -methylenebisacrylamide. The tensile strength increased after the introduction of inorganic filler from 14 to 270 kPa (an almost 20-fold improvement) at the increase of elongation at break from 35% to even 2500% (a 70-fold improvement). Moreover, the increase in the clay content usually results in the better storage modulus G' (elastic response) and loss modulus G'' (viscous behavior), which determine the rheological properties of the materials (Okay and Oppermann 2007; Li et al. 2009a; Song et al. 2010; Shen et al. 2014). The hydrogel-clay (nano)composites are very often characterized by a higher value of glass transition temperature (T_g), defined as the temperature at which the mechanical properties of a hydrogel radically change due to the internal movement

of the polymer chains. This effect observed for many (nano)composites can be explained by the restriction of movement of hydrogel chains in the presence of well-dispersed clay nanoparticles (Wang and Chen 2012; Mansoori and Salemi 2015; Kamoun and Menzel 2012; Nair et al. 2007).

It was observed that no linear correlation between the clay content and the mechanical properties of the formed (nano)composite exists. The highest strength of the composite is usually achieved at the critical concentration of clay, and a further increase in its loading leads to the formation of disordered organic–inorganic network and does not improve the expected properties (Lungu et al. 2012; Haraguchi 2008). Nevertheless, at the high clay contents, a steep increase in initial modulus can be found due to the appearance of rigid structures involving clay–clay interactions, similar to house-of-card or nematic-like structures (Haraguchi 2011b).

The mechanical properties of hydrogel-clay (nano)composites depend also strongly on many other factors such as a type of clay and polymer, their initial functionalization and modification, a clay dispersion, and a synthesis method. The post-synthesis treatment of (nano)composite materials can have also a crucial influence on their mechanical strength. For example, drying procedure can result in additional crosslinking by irreversible rearrangement of polymer-clay system proceeding at more concentrated state. On the other hand, a lower water content in the (nano)composite promotes its plastic-like deformations (Haraguchi and Li 2009).

The details of mechanical and rheological properties determined for the (nano)composites containing various more common synthetic hydrogels as well as clays can be found in the scientific papers listed in Table 3, which summarizes other properties of the studied materials as well.

5.2 Swelling Properties

An incorporation of small amounts of hydrophilic clay nanoparticles as additives into a polymer hydrogel can contribute to increase in water absorption capacity, depending on the dispersion level. Furthermore, the tortuosity effect, attributed to the disposition of nanostructures inside the polymer matrix, is another important feature that may directly affect on the loading of solutes onto and their release process (Guilherme et al. 2010). Nevertheless, the swelling properties of hydrogel-clay (nano)composites decline with increasing the clay content due to the fact that the clay nanoparticles act as effective crosslinkers giving stiffer materials (Yi and Zhang 2007). In the chosen cases, high swelling capacities were found even at high clay loadings, especially for the (nano)composites prepared at a high monomer concentration, when the presence of clay during polymerization reduces the degree of chemical crosslinking (Li and Wang 2005; Harini and Deshpande 2009). Generally, to construct efficient superadsorbents, more hydrophilic (co) polymers [e.g., poly(acrylic acid) or poly(acrylamide)] and lower loadings of clay (rather below 5 wt%) should be however applied (Janovák et al. 2009a).

Table 3 The main properties of basic hydrogel-clay nanocomposites described in the literature

Hydrogel	Clay	Properties			References
		Mechanical/rheological	Swelling	Optical	
Poly(acrylamide)	Attapulgite		Water absorbency, saline solution absorbency, swelling rate, water retention capacity	Thermal	Zhang et al. (2005b)
	Halloysite	Tensile modulus, tensile strength, elongation at break, permanent deformation, compression strength	Water absorbency		Liu et al. (2012b)
	Kaolinite (kaolin)	Tensile strength, Young modulus, elongation at break, storage modulus, loss modulus	Water absorbency, swelling rate		Ibraeva and El-Naggar (2015), Salimi et al. (2014), Shirsath et al. (2015)
	Laponite (hectorite)	Tensile strength, stress relaxation, elongation at break, shear modulus, tensile modulus, storage modulus, loss modulus	Water absorbency, swelling rate, water diffusion	Transparency	Can et al. (2007), Li et al. (2008, 2009a, b), Okay and Oppermann (2007), Xtong et al. (2008), Zhu et al. (2006)
	Montmorillonite (bentonite)	Compressive strength, tensile strength, Young modulus, elongation at break, storage modulus, loss modulus	Water absorbency, swelling rate		Helvacloğlu et al. (2011), Ibraeva et al. (2015), Pereira et al. (2015), Salimi et al. (2014)
	Septolite		Water absorbency, swelling rate, water diffusion		Ekici et al. (2006)

(continued)

Table 3 (continued)

Hydrogel	Clay	Properties				References
		Mechanical/rheological	Swelling	Optical	Thermal	
Poly (acrylamide-co-2-(dimethylamino)ethyl methacrylate)	Laponite (hectorite)	Tensile strength, tensile strain, elongation at break	Water absorbency	Transparency		Zhu et al. (2010)
Poly (acrylamide-co-2-acrylamido-2-methylpropane sulfonic acid)	Montmorillonite (bentonite)	Storage modulus, loss modulus, shear stress	Water absorbency, swelling rate, Water diffusion, saline solution absorbency			Aalae et al. (2008), Kasgöz and Durmus (2008), Yavari-Gohar et al. (2010)
	Laponite (hectorite)	Tensile strength, storage modulus, loss modulus				Du et al. (2014)
Poly (acrylamide-co-2-hydroxyethyl acrylate)	Montmorillonite (bentonite)		Surface tension of water			Beisebekov et al. (2014)
Poly(acrylamide-co-itaconic acid)	Laponite (hectorite)	Gel strength, shear resistance	Water absorbency, water retention capacity, saline solution absorbency, swelling rate		Thermal analysis	Marandi et al. (2015), Wan et al. (2015a, b)
	Montmorillonite (bentonite)		Water absorbency, swelling rate			Kaplan and Kasgoz (2011)
Poly(acrylamide-co-maleic acid)	Montmorillonite (bentonite)		Water absorbency			Dadkhah et al. (2014)

(continued)

Table 3 (continued)

Hydrogel	Clay	Properties			References	
		Mechanical/rheological	Swelling	Optical	Thermal	
Poly (acrylamide-co- <i>N</i> -isopropylacrylamide)	Montmorillonite (bentonite)	Storage modulus, loss modulus	Water absorbency		Thermal analysis	Janovák et al. (2008, 2009b)
Poly (acrylamide-co-sodium acrylate)	Montmorillonite (bentonite)		Water absorbency		Thermal analysis	Natkański et al. (2013a)
Poly (acrylamide-co-vinyl alcohol)	Montmorillonite (bentonite)		Water absorbency, water retention capacity, swelling rate			Swain et al. (2013)
Poly(acrylic acid)	Kaolinite (kaolin)	Compression strength, Young modulus, storage modulus, loss modulus	Water absorbency, swelling rate		Thermal analysis	Lungu et al. (2012), Shirsath et al. (2013)
	Laponite (hectorite)	Young modulus, tensile strength, peel strength, storage modulus, loss modulus	Water absorbency, swelling rate	Transparency		Li et al. (2009a, 2014), Shen et al. (2014)
	Montmorillonite (bentonite)	Gel strength, storage modulus	Water absorbency, swelling rate		Thermal analysis	Mansoori and Salemi (2015), Molu et al. (2010), Natkański et al. (2012, 2013b, 2016), Shirsath et al. (2011), Weian et al. (2005), Xu et al. (2007b)
	Sepiolite		Water absorbency swelling rate, water diffusion			Santiago et al. (2006)

(continued)

Table 3 (continued)

Hydrogel	Clay	Properties			References	
		Mechanical/rheological	Swelling	Optical	Thermal	
Poly(acrylic acid-co-2-ethyl methacrylate)	Montmorillonite (bentonite)	Shear modulus	Water absorbency, swelling rate			Dalaran et al. (2011)
Poly(acrylic acid-co-2-acrylamido-2-methylpropane sulfonic acid)	Laponite (hectorite)	Tensile strength, elongation at break	Water absorbency	Transparency		Chen et al. (2013)
	Montmorillonite (bentonite)	Compressive modulus, storage modulus	Water absorbency, saline solution absorbency, water retention capacity			Zhang et al. (2014b)
Poly(acrylic acid-co-acrylamide)	Kaolinite (kaolin)		Water absorbency			Hussien et al. (2012)
	Montmorillonite (bentonite)		Water absorbency, saline solution absorbency, water retention capacity			Zhang et al. (2014c)
	Sepiolite		Water absorbency, saline solution absorbency			Zhang et al. (2005a)
Poly(acrylic acid-co-ethylene glycol)	Montmorillonite (bentonite)		Water absorbency, swelling rate, water diffusion		Thermal analysis, DSC analysis	Bhattacharyya and Ray (2014)
Poly(acrylic acid-co-N-isopropylacrylamide)	Laponite (hectorite)	Tensile strength, tensile modulus, elongation at break, compressive strength, storage modulus, loss modulus	Water absorbency, swelling rate, water retention capacity	Transparency	Thermal analysis, DSC analysis	Shen et al. (2015), Huang (2012), Song et al. (2008)

(continued)

Table 3 (continued)

Hydrogel	Clay	Properties			References
		Mechanical/rheological	Swelling	Optical	
	Montmorillonite (bentonite)	Storage modulus, loss modulus	Water absorbency		Janovák et al. (2008)
Poly(acrylic acid-co-vinyl alcohol)	Montmorillonite (bentonite)		Water absorbency, swelling rate		Bornuah et al. (2015)
Poly (N-isopropyl acrylamide)	Laponite (hectorite)	Tensile strength, tensile strain, tensile modulus, elongation at break, stress relaxation, shear modulus, storage modulus, loss modulus	Water absorbency, swelling rate, water retention capacity	Transparency	Can et al. (2007), Chen et al. (2014a), Erika et al. (2016), Haraguchi et al. (2006, 2010, 2011), Haraguchi (2007a), Haraguchi and Takada (2010), Haraguchi and Xu (2012), Lian et al. (2014, 2015), Liu et al. (2007), Ma et al. (2008), Maury et al. (2013), Wang et al. (2013a, b), Zhang et al. (2009, 2014a), Zhu et al. (2006)
	Montmorillonite (bentonite)	Storage modulus	Water absorbency, swelling rate, shrinking rate		Zhang et al. (2009)
Poly(N,N-dimethyl acrylamide)	Laponite (hectorite)	Tensile strength, storage modulus, loss modulus, tensile stress, tensile strain, tensile modulus, elongation at break	Water absorbency, swelling rate, water retention capacity	Transparency	Can et al. (2007), Haraguchi (2007a), Haraguchi et al. (2006, 2010, 2011), Haraguchi and Takada (2010), Wang et al. (2011a, b)
Poly(ammonium acrylate)	Montmorillonite (bentonite)		Water absorbency		Natkański et al. (2012)

(continued)

Table 3 (continued)

Hydrogel	Clay	Properties				References
		Mechanical/rheological	Swelling	Optical	Thermal	
Poly(sodium acrylate)	Laponite (hectorite)	Tensile strength, storage modulus			Thermal	Takeno and Nakamura (2013)
	Vermiculite		Water absorbency, saline solution absorbency		Thermal analysis	Zheng et al. (2007)
	Montmorillonite (bentonite)		Water absorbency		Thermal analysis	Natkański et al. (2012)
Poly(vinyl alcohol)	Laponite (hectorite)		Water absorbency, swelling rate		Thermal analysis	Oliveira et al. (2012)
	Montmorillonite (bentonite)	Tensile modulus, compressive modulus, hardness, tensile strength, elongation at break	Water absorbency, vapor transmission rate, dehydration kinetics		Thermal analysis	Chen et al. (2014b), Ibrahim and El-Naggar (2013), Kokabi et al. (2007), Sirousazar et al. (2011a, b)

The rate of swelling ($\varepsilon(t)$) is usually well described by the Voigt model (Eq. 2), which consists of two parameters—spring parameter (corresponding to the resistance to expansion of the polymer network— σ_0/E) and dashpot parameter (corresponding to the resistance to permeation— τ_0) (Santiago et al. 2006):

$$\varepsilon(t) = \frac{\sigma_0}{E} \left(1 - e^{-\frac{(t_0-t)}{\tau_0}} \right) \quad (2)$$

It was found that the values of τ_0 become rather independent of the external solution, whereas the values of σ_0/E decrease with an increase in ionic strength. It means that the water absorbency in the saline solutions is slower than in deionized water mainly due to (i) the osmotic pressure difference between the hydrogel composite and the saline solution, and (ii) possible complexation. The effect of salt is more distinct if the salt contains multivalent ions (Zhang et al. 2014b, c; Li et al. 2007) and is used at a higher concentration (Xu et al. 2007a). At the elevated saline solution concentration, the solute ions migrate to the (nano)composite structure shielding a part of charged functionalities (e.g., carboxylic) located in the hydrogel bulk (Zhang et al. 2005a). Furthermore, Zheng et al. (2007) demonstrated that the water absorbency of vermiculite-filled poly(acrylic acid) was also affected by the kind of anions and was the highest in a trivalent anion (PO_4^{3-}) salt solution.

The initial water uptake process of hydrogel-clay (nano)composites corresponds to the diffusion of water molecules into the structure, which can be analyzed using a simple power law equation (Eq. 3):

$$\frac{M_t}{M_e} = kt^n \quad (3)$$

where M_t and M_e are the weight of the swollen (nano)composite at time t and equilibrium swollen state. The constant n is often used to determine the swelling mechanism. In the case of disk-shaped samples, if $n \leq 0.5$ swelling proceeds by the Fickian diffusion (the swelling process is controlled by solvent diffusion). For $n \geq 1$ swelling is limited by the relaxation of hydrogel chains. Finally, if $0.5 < n < 1$ non-Fickian diffusion is prominent and is meant as the synergistic effect of solvent diffusion and polymer chains relaxation (Kaşgöz and Durmus 2008; Yi and Zhang 2007; Boruah et al. 2015). The analysis of various systems indicates that the physical and chemical interactions between the water molecules and the (nano)composite lead to diffusion of H_2O toward the inside dry material. At the beginning, the water molecules react with more exposed polar moieties located on the surface of hydrogel and dispersed clay platelets, initializing the hydration process. The macromolecular rearrangement of the hydrogel is subsequently continued resulting in the accommodation of absorbed H_2O (Guilherme et al. 2010). Such mechanism was confirmed by the swelling measurements combined with the elasticity tests, which showed that the effective crosslink density (ν_e) of hydrogel first decreased, but then increased with increasing time of swelling (Can et al. 2007).

The swelling rate depends strongly on size of particles and their porosity. For the large grains, more void is available to absorb water, but the quick absorption requires rather smaller particles. This effect was demonstrated for poly (acrylamide-co-itaconic acid)-laponite (nano)composite crosslinked by different amounts of *N*-methylene-bis-acrylamide resulting in the average particle size ranging from 0.12 to 4.6 μm and consequently a prolonged swelling time from 30 to 300 min, respectively (Wan et al. 2015a, b). Nevertheless, the (nano)composite particles cannot be too fine, because the adverse gel blocking effect occurs (Kabiri et al. 2011). The porosity of hydrogel-clay (nano)composites can be improved by using of various porogens (such as acetone or sodium dicarbonate) during the synthesis. The kind of clay filler and its modification are also important factors influencing the swelling capacity and swelling rate (Swain et al. 2013; Zhang et al. 2014c).

5.3 Thermal Properties

The crosslinking of polymeric materials usually contributes to their thermal stability. It should not be, therefore, surprising that the presence of crosslinking clay platelets dispersed in the hydrogel matrix improves its thermal resistance. Additionally, polymer chains intercalated between the clay layers show restricted molecular mobility and inhibit diffusion of the gaseous products of decomposition.

The thermogravimetric measurements revealed that the onset temperature of degradation of poly(acrylamide) increased by almost 40 °C after adding organophilized montmorillonite (0.1–1.0 wt%) (Helvacioğlu et al. 2011). The similar effect was observed for Na^+ -montmorillonite- or kaolinite-containing poly(acrylamide) (Salimi et al. 2014; Ibraeva et al. 2015). Even higher stabilization effect was found for poly(sodium acrylate) modified with montmorillonite (11.8 wt%), which showed the shift in the beginning of main weight loss effect from 368 °C (clay-free hydrogel) to 424 °C (the hydrogel-clay (nano)composite) (Su et al. 2008). In turn, poly(acrylic acid-co-*N*-isopropylacrylamide) filled with laponite exhibited higher thermal stability at the increasing amount of clay and the decreasing content of poly(acrylic acid) (Shen et al. 2015). On the other hand, transition metal cations introduced into the structure of hydrogel-clay (nano)composites promote the burning of organic matter, and the decomposition of the hydrogel is observed at relatively low temperatures (Natkański et al. 2016; Rokicińska et al. 2016).

5.4 Optical Properties

Deterioration of optical transparency of hydrogel after its modification with a clay filler, manifested by obtaining translucent or opaque (nano)composite, can originate from the spatial inhomogeneity observed in the case of insufficient exfoliation of

layered aluminosilicate or aggregation of composite components. Obviously, the higher content of clay favors the formation of opaque materials, but transparent (nano)composites within a broad range of hydrogel and clay contents were successfully synthesized and demonstrated in the literature (Haraguchi 2011b; Zhang et al. 2013). On the other hand, the characteristic changes observed in optical transmittance during the formation of (nano)composite of poly(*N*-isopropylacrylamide) and synthetic laponite were used to account for the gelation mechanism studied by dynamic light scattering (DLS) and contrast variation small-angle neutron scattering (SANS) (Miyazaki et al. 2007).

6 Applications of Hydrogel-Clay (Nano)Composites

The above-discussed properties of hydrogel-clay (nano)composites make them very useful in a wide variety of applications, which include biomedicine and pharmacy (e.g., tissue engineering, drug and gene delivery system, ocular devices, wound healing materials, and artificial extracellular matrices), agriculture and horticulture (e.g., controlled release of moisture, fertilizers, pesticides), chemical sensors, enhanced oil recovery, ceramic and building materials, water purification and separation processes. Some more important examples of application studies are presented in the following sections.

6.1 Adsorption

Adsorption can be considered as the accumulation of various species at the surface of solid (known as an adsorbent) due to the excess of unsaturated surface forces. The occurring interactions can have both physical and chemical nature. In the case of physical adsorption, bonding to the surface, based on van der Waals or dispersion forces, is relatively weak. On the contrary, in chemical adsorption (so-called chemisorption) ionic and/or covalent bonding are formed, which give significantly stronger interaction. The adsorption processes are very often used for the elimination of various contaminants from aqueous solutions. In such a case, the progress of the process is monitored as the adsorption capacity (q_t),

$$q_t = \frac{(C_0 - C_t)V}{m} \quad (4)$$

where q_t is an amount adsorbed at time t , V is a volume of solution, C_0 and C_t are concentrations of the solution at the beginning of the process and after time t , m is a mass of adsorbent.

Three main kinetic models, pseudo-first-order (Eq. 5), pseudo-second-order (Eq. 6) and intra-particle diffusion model (Eq. 7), are usually chosen to evaluate the adsorption processes in solid/liquid systems,

$$\ln(q_e - q_t) = \ln q_e - k_1 t \quad (5)$$

$$\frac{t}{q_t} = \frac{1}{k_2 q_e^2} + \frac{t}{q_e} \quad (6)$$

$$q_t = k_3 t^{0.5} + A \quad (7)$$

where q_e is an amount adsorbed at equilibrium, k_1 , k_2 , k_3 , are rate constants for pseudo-first-order, pseudo-second-order and intra-particle diffusion, A is the thickness of boundary layer.

Furthermore, the adsorption equilibrium concentrations of the solution are fitted by different isotherms including the most appropriate Langmuir (Eq. 8) and Freundlich models (Eq. 9),

$$q_e = \frac{q_m k_L C_e}{1 + k_L C_e} \quad (8)$$

$$q_e = k_F C_e^{1/n} \quad (9)$$

where C_e is a concentration of a solution at equilibrium, q_m is a monolayer capacity of an adsorbent, k_L and k_F are Langmuir and Freundlich constants, respectively.

6.1.1 Dyes

Dyes have been commonly used from ancient times for coloring textiles and production of paints and pigments. They have been recognized as dangerous organic pollutants, which escape conventional wastewater treatment processes and persist in the environment being highly stable during treatment with light, temperature, or various chemicals. Bioaccumulation of dyes causes chemical and biological changes in the aquatic system resulting in environmental damage and human disease. Therefore, new, effective technologies for the purification of water from redundant dyes have been still developed. Beside some known techniques (such as coagulation-flocculation, aerobic or anaerobic treatment, electrochemical treatment, membrane filtration), cheap, simple, and efficient adsorption process seems to be a reasonable way to achieve this target (Mahdavinia et al. 2012; Mahdavinia and Asgari 2013; Hosseinzadeh et al. 2015; Dalaran et al. 2009, 2011; Wan Ngah et al. 2011). Usually, activated carbons are applied as solid adsorbents, but this role can be also played by other materials including polymer-clay (nano)composites (Tan et al. 2015; Mahdavinia et al. 2013). Especially, the hydrogel-clay

(nano)composites combining elasticity and permeability of polymer with high ability of clays in the dye adsorption show superior adsorption properties.

Dyes can be classified by their chemical nature as ionic (anionic and cationic) and nonionic (vat and disperse dyes). The cationic dyes interact electrostatically with negatively charged sites of hydrogel-clay (nano)composites forming a neutral complex, which can subsequently adsorb another organic cation by hydrophobic interactions. Furthermore, a monovalent complex can form by the interaction of one dye cation with a neutral site of composite (Li et al. 2008). Some more popular cationic dyes, tested in the adsorption involving polymer hydrogels, are shown in Fig. 10. Most of the applied (nano)composites contained montmorillonite (Kundakci et al. 2008, 2009; Karadağ et al 2014; Dalaran et al. 2009, 2011; Kaplan and Kasgoz 2011; Mahdavinia et al. 2013; Shirsath et al. 2011; Bhattacharyya and Ray 2014; Shi et al. 2013; El-Sigeny et al. 2014), laponite (Marandi et al. 2015; Haraguchi and Li 2010; Li et al. 2008, 2009a, b; Yi and Zhang 2008; Zhang et al. 2006; Mahdavinia et al. 2012), kaolinite (Shirsath et al 2013, 2015) and sepiolite (Ekici et al. 2006; Mahdavinia and Asgari 2013) as a clay component, and poly (acrylamide) (Kundakci et al. 2008, 2009; Karadağ et al 2014; Nakamura and

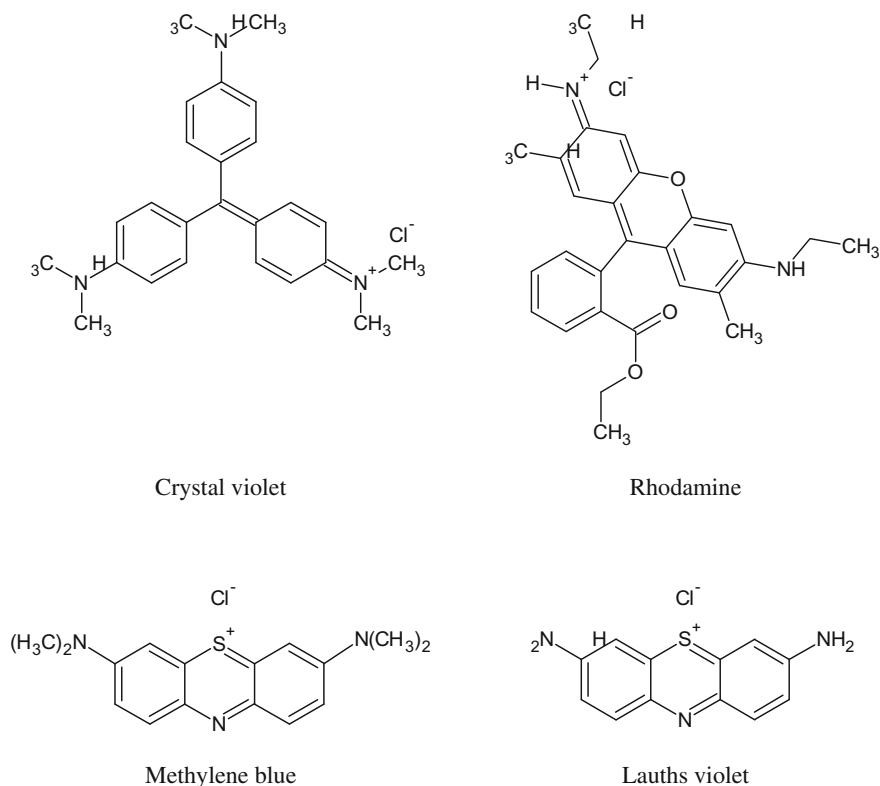


Fig. 10 Structure of chosen cationic dyes

Ogawa 2013; Kaplan and Kasgoz 2011; Marandi et al. 2015; Haraguchi and Li 2010; Ekici et al. 2006; Yi and Zhang 2008; Mahdavinia et al. 2012, 2013; Mahdavinia and Asgari 2013; Shirsath et al. 2015) and poly(acrylic acid)-based (co) polymers (Li et al. 2008; Shirsath et al. 2011, 2013; Dalaran et al. 2011; Zhang et al. 2006; Bhattacharyya and Ray 2014; Shi et al. 2013; El-Sigeny et al. 2014) as a hydrogel part.

The adsorption capacity of crystal violet was examined for (nano)composites containing poly(acrylic acid-co-*N*-vinyl-2-pyrrolodine)-laponite (Zhang et al. 2006), poly(acrylic acid)-FeCo-bentonite (Shirsath et al. 2011), kappa-carrageenan-g-alginate-g-poly(acrylamide)-montmorillonite (Mahdavinia et al. 2013), poly(acrylamide)-g-carrageenan-laponite (Mahdavinia et al. 2012), poly(*N*-isopropylacrylamide) crosslinked by lithium magnesium silicate hydrate (Zhang et al. 2014a), kappa-carrageenan-g-poly(acrylamide)-sepiolite (Mahdavinia and Asgari 2013), kappa-carrageenan-g-poly(vinyl alcohol)-montmorillonite (Hosseinzadeh et al. 2015), poly(acrylamide)-laponite (Li et al. 2008), poly(acrylamide)-kaolin (Shirsath et al. 2015), poly(acrylamide-co-itaconic acid)-laponite (Marandi et al. 2015). The kinetics of adsorption of crystal violet on the presented materials was well described by the pseudo-second-order model. Moreover, the Langmuir model was found as the best one for the description of equilibrium adsorption of this dye (Zhang et al. 2006; Shirsath et al. 2011; Mahdavinia et al. 2012, 2013; Hosseinzadeh et al. 2015; Mahdavinia and Asgari 2013). Basing on the Langmuir isotherm, the maximum dye adsorption capacity of about 151 mg/g was achieved for kappa-carrageenan-g-poly(vinyl alcohol)-montmorillonite (Hosseinzadeh et al. 2015). Calculations of thermodynamic parameters confirmed the spontaneity, feasibility and endothermic nature of the adsorption process (Shirsath et al. 2011; Hosseinzadeh et al. 2015).

The adsorption capacity of crystal violet strongly influenced the adsorbent composition (especially the clay loading) and content, pH, and temperature used during the adsorption process, as well as the initial concentration of dye solution (Hosseinzadeh et al. 2015). More dye was adsorbed by the materials containing higher amounts of clay due to enhanced negative charge density related mainly to the negative clay surface (Zhang et al. 2006; Mahdavinia et al. 2012, 2013; Hosseinzadeh et al. 2015; Mahdavinia and Asgari 2013; Shirsath et al. 2011; Dalaran et al. 2011; Zhang et al. 2014a). For example, the incorporation of nonionic poly(acrylamide) into the laponite clay gave a material characterized by the presence of high amount of ionizable groups, which exhibited the dye adsorption corresponding to type S adsorption isotherms in the Giles classification (Li et al. 2008). Such isotherm type is typical of the so-called cooperative adsorption promoted by increasing adsorbate concentration. It should, therefore, be assumed that a part of the surface was covered by multilayers of adsorbed dye, whereas its monolayer was still incomplete on remaining fragments of the surface. On the other hand, the rate of dye removal increased with raising clay loading in the (nano)-composite. The partition coefficient (K_d) is defined as (Eq. 10), which is as follows:

$$K_d = \frac{(C_0 - C_e)}{C_e} \quad (10)$$

where K_d is an empirical partition coefficient at equilibrium, and C_0 and C_e —an initial and equilibrium concentration of the dye solution, which expresses relation between the concentration of dissolved species and the adsorbed ones, increased from 0.8 for the composite with the clay content of 14 wt% to 21.6 for the material containing 40 wt% of laponite. The adsorption capacity of the studied composites could be additionally improved by a heat treatment at 60 °C. This beneficial effect was explained by the changes in the composite structure into more homogeneous and loose form, favoring easier migration of cationic dye molecules into the network and interaction with the adsorption sites.

It was found that the adsorption of crystal violet was strongly affected by pH, which tuned the ionization of adsorbent and its surface charge (Hosseinzadeh et al. 2015; Mahdavinia et al. 2013; Mahdavinia and Asgari 2013; Zhang et al. 2014a). At low pH, the reduction in dye adsorption capacity was observed, attributed to: (i) competition between protons and cationic dye molecules in adsorption on anionic sites present on the (nano)composite surface, (ii) a high degree of protonation of surface groups. When pH increased, the concentration of H^+ was reduced and higher number of dissociated anionic surface species appeared, which could electrostatically attract the positively charged dye-forming ionic surface complex. Moreover, the absence of organic crosslinker in a (nano)composite resulted in flexible polymer chains so that the cationic dye molecules could easily enter into the hydrogel network and interact with the adsorption sites (Li et al. 2008; Shirsath et al. 2011).

The behavior of poly(acrylamide)-containing composites in the adsorption of crystal violet at varied pH was studied on poly(acrylamide)-kaolin (3.4 wt%) material synthesized by the ultrasound-assisted route (Shirsath et al. 2015). The highest adsorption capacities were observed in the pH range of 8–11. At lower pH values, strong protonation of the amino groups and the positive charge of kaolin surface limited the dye adsorption. In turn, above the pH = 10 the structure of crystal violet changed influencing the adsorption capacity. Moreover, an increase in temperature promoted mobility of dye molecules and consequently enhanced their adsorption. An increase in the initial dye concentration, as well as the amount of adsorbent, improved the dye uptake. The positive effect on the adsorption behavior was also observed for an increase in the content of kaolin in the studied composite and using of ultrasound assistance during the dye removal.

Marandi et al. (2015) compared the efficiency of poly(acrylamide-co-itaconic acid) hydrogel (with the AAm:IA molar ratio of 1.74:0.26) filled with laponite (46–76 wt%) in the removal of three different water-soluble cationic dyes (crystal violet, methylene green, and methylene blue). At lower laponite contents, the clay could be highly dispersed in the polymer matrix favoring the adsorption of cationic dyes. The prepared adsorbents appeared to be the most efficient in the elimination of

methylene green due to the presence of $-\text{NO}_2$ functionalities forming hydrogen bonds with $-\text{CO}_2\text{H}$ and $-\text{NH}_2$ groups of the hydrogel.

Comparing to crystal violet, significantly higher adsorption capacities were achieved for cationic methylene blue, which was removed using poly(acrylic acid)-functionalized attapulgite nanorods (Zhu et al. 2014), chitosan-g-poly(acrylic acid)-biotite (Liu et al. 2011), sodium alginate-g-poly(acrylic acid-co-styrene)-illite (smectite) (Wang et al. 2013a, b), lignocellulose-g-poly(acrylic acid)-montmorillonite (Shi et al. 2013), chitosan-g-poly(acrylic acid)-montmorillonite (vermiculite) (Wang et al. 2008a; Liu et al. 2010) and sodium humate-g-poly(acrylamide)-laponite (Yi and Zhang 2008). The adsorption, which occurred according to the pseudo-second-order (kinetics) and Langmuir (equilibrium) models, allowed to obtain the dye loading even higher than 2000 mg/g (Liu et al. 2011). In the case of the highest efficient chitosan-g-poly(acrylic acid)-biotite composite, mainly carboxyl groups within the hydrogel network played an active role in the adsorption, because of a majority of amine groups of chitosan took part in the copolymerization process. Therefore, $\text{pH} \geq 5$ was necessary to improve the adsorption kinetics by the formation of COO^- groups increasing the electrostatic force between adsorbent and dye. The additional improvement of adsorption capacity of clay-containing (nano)composites was found after partial exfoliation of aluminosilicate by its organofilization (Wang et al. 2013a, b). Nevertheless, the excess of cationic surfactant (e.g., cetyltrimethylammonium cations) reduced the negative charge of the (nano)composite and blocked diffusion of dye molecules into the polymer network decreasing the adsorption capacity. The used (nano)composite adsorbents with attached methylene blue could be regenerated by desorption at lower pH, which was demanded to remove the strongly bonded dye. It was shown that about 70% of methylene blue could be desorbed from the surface of chitosan-g-poly(acrylic acid)-montmorillonite at $\text{pH} = 2.0$ (Wang et al. 2008a).

Rhodamine 6G was another model cationic dye studied in the adsorption on chitosan-g-poly(*N*-vinyl pyrrolidone)-montmorillonite (Vanamudan et al. 2014) and poly(*N*-isopropylacrylamide)-saponite (Nakamura and Ogawa 2013) (nano)composites. The adsorption of this dye clearly depended on pH, temperature, initial dye concentration and its composition, and was well fitted by the Freundlich (Vanamudan et al. 2014) or Langmuir (Nakamura and Ogawa 2013) isotherm and the pseudo-second-order rate model. What was surprising, the adsorption capacity increased with temperature suggesting the endothermic nature of process, explained by an increase in kinetic energy of dye molecules and enhanced rate of diffusion of adsorbate. The best results were obtained at $\text{pH} = 10$, which favored deprotonation of positively charged groups and electrostatic attraction between negatively charged sites on the adsorbent and cationic dye. In turn, the adsorption of Lauth's violet dye was tested on poly(acrylamide-co-2-acrylamido-2-methyl-1-propanesulfonic acid)-bentonite (Kundakci et al. 2008, 2009). Apart from electrostatic repulsion, additional interactions between the composite and cationic dye were revealed. They were related to: (i) hydrogen bonding involving amine groups and nitrogen atoms of the dye molecules and the amine and carbonyl groups of the monomer unit of crosslinked polymer, (ii) hydrophobic effects between aromatic ring on the dye

molecules and the methine and methyl groups on the composite, as well as (iii) dipole–dipole and dipole-induced dipole interactions between the dye molecules and the hydrogel chains.

In the open literature, some examples of adsorption process of other cationic dyes can be also identified, including Safranin T (ST) on poly(acrylamide)-poly (sodium methacrylate)-kappa-carrageenan-montmorillonite and starch-g-poly (acrylic acid)-montmorillonite (Karadağ et al. 2014; Al et al. 2008), brilliant cresyl blue on poly(acrylamide-co-itaconic acid)-montmorillonite (Kaplan and Kasgoz 2011), Basic Blue 12 (BB-12) Basic Blue 9 (BB-9), and Basic Violet 1 (BV-1) on poly(acrylamide)-laponite (hectorite) (Li et al. 2009b; Ekici et al. 2006), Brilliant Green on poly(acrylic acid)-kaolin (Shirsath et al 2013), Janus Green B on poly (acrylamide-co-zinc acrylate)-g-xanthan gum-sepiolite (Karadağ et al. 2015), as well as Acid Green B and Maxilon C.I. Basic on poly(styrene-co-acrylic acid)-organophilic montmorillonite (El-Sigeny et al. 2014).

In some exceptional cases, the adsorption of dyes containing negatively charged functional groups (e.g., indigo carmine (Dalaran et al. 2009, 2011) and congo red (Bhattacharyya and Ray 2014) presented in Fig. 11) on hydrogel-clay (nano)-composites was also examined. Both poly(acrylic acid-co-2-(*N,N*-dimethylamino) ethyl methacrylate)-montmorillonite (Dalaran et al. 2011) and poly(2-(*N,N*-dimethylamino)ethyl methacrylate-co-2-acrylamido-2-methylpropane sulfonic acid-co-2-hydroxyethyl methacrylate)-montmorillonite (Dalaran et al. 2009) with enhanced mechanical properties showed a high adsorption performance in the elimination of indigo carmine (up to 320 mg/g). On the other hand, (nano)composites synthesized from crosslinked poly(acrylic acid), poly(ethylene glycol) and a bentonite nanofiller appeared to be efficient adsorbents of congo red (Bhattacharyya and Ray 2014). The ionization and polarization of various functional groups of hydrogel and filler (such as amide, hydroxyl, or carboxylic ones) changed with pH. The abrupt

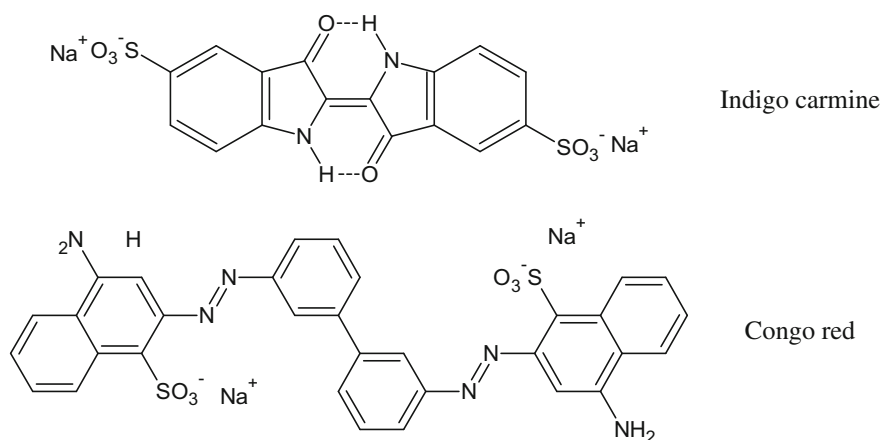


Fig. 11 Structure of chosen anionic dyes

increase in ionization of carboxylate ions observed in the pH range of 4–7 caused a rise in the dye adsorption. However, above pH = 9 deprotonation of amine groups resulted in the decrease in the adsorption capacity. The adsorption of congo red was recognized to be an exothermic process, which was strongly controlled by diffusion of the dye molecules within the composite structure.

6.1.2 Inorganic Cations

Heavy metals (e.g., Pb, Cr, Cd, Hg, As, Ni, Cu, and Zn) are pollutants discharged from industrial, domestic, and agricultural wastewater that can enter the drinking water system through groundwater. These components are non-biodegradable and accumulate in the natural ecosystem with a harmful influence on the human health (toxic effects on various systems and organs, including nervous system, cardiovascular system, or kidneys) (Ihsanullah et al. 2016; Zhao et al. 2016; Fu and Wang 2011). In spite of a few disadvantages (related mainly to production of waste products and low selectivity), adsorption, being relatively simple, cheap, and highly effective, is considered as a powerful method used for the removal of heavy metal cations (Zhang et al. 2006; Ihsanullah et al. 2016; Zhao et al. 2016; Beisebekov et al. 2014). Various activated carbons, biomaterials, metal oxides, and zeolite, as well as natural and modified clays, are applied adsorbents of heavy metal cations, which can operate in a wide pH range and be easily recovered/regenerated after the adsorption process.

A possible application of hydrogel-clay (nano)composites in adsorption of metal cations was preliminarily verified using Fe^{3+} as a model ion (Natkański et al. 2013a, b). The studied (nano)composites contained montmorillonite (20–50 wt%) dispersed in matrix of poly(acrylamide), poly(acrylic acid), poly(sodium acrylate), poly(ammonium acrylate), or poly(acrylamide-co-sodium acrylate) copolymers. For the poly(acrylic acid)-based (nano)composites, an increase in the hydrogel content had a positive effect on the adsorption capacity of Fe^{3+} ions, which were removed from a solution by ion exchange with protons of carboxyl groups. The adsorption kinetic was well described by the model of pseudo-second order (Natkański et al. 2013b). The adsorption properties of hydrogel-clay (nano)composites is strongly influenced by chemical content and distribution of polymer part. This issue was deeply recognized for the (nano)composites containing poly(acrylic acid) and its salts (sodium and ammonium). During the synthesis, poly(ammonium acrylate) was preferentially deposited on the external surface of clay particles, and therefore exhibited the superior adsorption capacity of Fe^{3+} cations. It was shown that the Langmuir model better described the adsorption on the poly(acrylic acid)-containing material, whereas the Freundlich model was more adequate for the description of process occurring on the polyacrylate-based samples, suggesting unspecific adsorption of Fe^{3+} ions in the composite structure (Natkański et al. 2012). In the case of materials based on poly(acrylamide-co-sodium acrylate) copolymers, higher adsorption capacities were observed for those containing free

carboxylate moieties originating from poly(sodium acrylate), which attract Fe^{3+} cations electrostatically (Natkański et al. 2013a).

The adsorption capacity of inorganic cations was also tested using NH_4^+ , representing a group of nitrogen-containing compounds, on chitosan-grafted poly (acrylic acid)-clay [vermiculite (Zheng et al. 2012) or rectorite (Zheng and Wang 2009)]. It was found that the adsorption equilibrium was achieved within a few minutes, and the amount of adsorbed species depended strongly on the number of COO^- groups available in the composite structure. When the studied (nano)composite was immersed in an aqueous solution, H_2O molecules penetrated the composite structure resulting in a dimensional increase of polymeric networks due to the repulsion between negatively charged dissociated carboxylate groups. The electrostatic attraction between these species and positively charged NH_4^+ was responsible for the quick adsorption process. Moreover, the addition of clay improved hydrogel strength and enhanced its thermal stability, which are important features from the application point of view.

Güçlü et al. (2010) and Irani et al. (2015) reported on the uptake of Cu^{2+} and Pb^{2+} ions from aqueous solutions using starch-g-poly(acrylic acid)-montmorillonite and polyethylene-g-poly(acrylic acid)-g-starch-organo-montmorillonite (nano)-composites, respectively. The adsorption process was modeled by pseudo-second-order kinetic equation and both Freundlich and Langmuir isotherms. At low pH level, the COO^- groups were greatly protonated, and the formed COOH species showed the reduced ability of metal cations adsorption. With an increase in the pH value, H^+ cations were outcompeted, and higher amounts of metal cations could be eliminated on both carboxyl and hydroxyl groups. The adsorption capacities of the studied (nano)composites followed in order: $\text{Cu}^{2+} > \text{Pb}^{2+}$, in spite of more electropositive character of Pb^{2+} ions. This surprising effect was explained by straitened diffusion of bigger Pb^{2+} ions in the crosslinked hydrogel network containing the clay particles.

The removal of uranyl ions (UO_2^{2+}) on poly(acrylamide-co-2-acrylamido-2-methyl-1-propanesulfonic acid)-bentonite was also studied (Kundakci et al. 2011). It was verified that poly(acrylamide) did not sorb any uranyl ions. Comparing the adsorption capacity of poly(acrylamide-co-2-acrylamido-2-methyl-1-propanesulfonic acid) hydrogel to poly(acrylamide-co-2-acrylamido-2-methyl-1-propanesulfonic acid)-bentonite composite, an increase from 0.67×10^{-3} to 2.11×10^{-3} mol of uranyl ions per gram was observed. The addition of hydrophilic 2-acrylamido-2-methylpropane sulfonic acid and bentonite enhanced the observed uranyl ion sorption capability due to the increasing number of ionic units.

Adsorption of transition metal cations in the structure of poly(acrylic acid)-montmorillonite (nano)composites was recently applied by Natkański et al. (2016) for the production of clay-based catalysts with a metal-oxide active phase highly dispersed on a surface of the partially delaminated clay. The (nano)composite containing 50 wt% of Wyoming montmorillonite was synthesized by the intercalation copolymerization of acrylic acid and N,N' -methylenebisacrylamide. In the subsequent step, the controlled amount of Fe^{3+} was introduced into the structure of

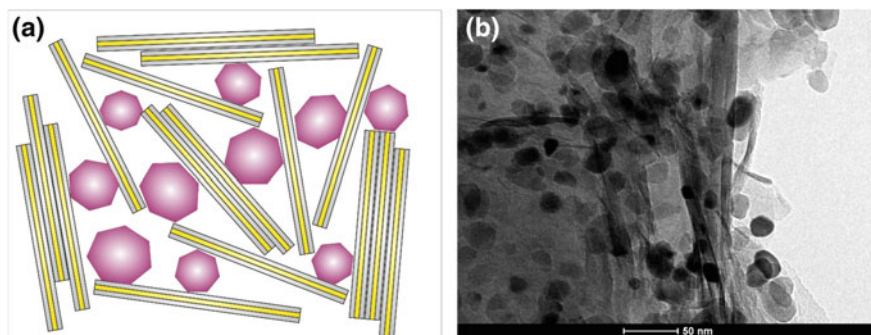


Fig. 12 Model (a) and TEM images (b) of structure of metal-oxide particles-pillared montmorillonite after elimination of hydrogel template

composite at constant pH (from 2.0 to 4.0) and temperature (30 °C). The intercalation of hydrogel into the gallery of montmorillonite followed by the Fe^{3+} adsorption resulted in the layer disordering (Fig. 12a) which was preserved after calcination at 600 °C. High dispersion of $\alpha\text{-Fe}_2\text{O}_3$ nanoparticles was confirmed by TEM images (Fig. 12b). The presented synthesis strategy was used by Rokicińska et al. (2016) to obtain the Co_3O_4 containing catalysts for the total oxidation of volatile organic compounds. The highest dispersion and Co loading were achieved for the poly(acrylic acid)-montmorillonite (nano)composite modified by adsorption of Co^{2+} cations at pH = 6–8. For these materials, the highest conversions in the toluene combustion were observed. The catalytic activity was additionally correlated to the reducibility of active phase suggesting that the process undergoes according to the Mars–van Krevelen mechanism.

6.2 Drug Delivery

Hydrogels filled with selected clays have good potential to be used as functional soft materials in biological applications, because of their excellent mechanical and rheological properties, high water content, and good biocompatibility. Based upon properties such as swelling, film-forming ability, bioadhesion, and cell capture capacity, the hydrogel-clay (nano)composites have been considered as platforms to construct new forms of drug release systems with highly specific dosage and an improvement of technological and biopharmaceutical properties (Tu et al. 2013; Rodrigues et al. 2013; Pongjanyakul and Puttipipatkachorn 2007). The hydrogel-clay (nano)composites were sometimes used as tablet-coating materials for modifying drug release from tablets, which present good stability towards enzymatic degradation in simulated intestinal fluid (Khunawattanakul et al. 2011). However, a majority of studies was concerned on the active role of these composites in a drug storage and its subsequent delivery. It was found that the drug

release largely depends on the clay content, its dispersion in the polymer matrix, the presence of intercalated agents, the charge of drug, the interaction between the gel and the drug, and ionic strength of the medium. The swelling capacity is also the crucial parameter influencing the drug release from the composite structure. As revealed for poly(*N*-2-vinyl pyrrolidone) (PVP) hydrogels containing chitosan and laponite (Oliveira et al. 2014), the minor release of glucantime was presented by the PVP/chitosan/clay (nano)composite, which was associated to the crosslinking between PVP and chitosan, compared to the more loosely bonded clay-free hydrogel. Similarly, the release of sulfamethoxazole and diclofenac sodium from polyester-polyol-acrylate-bentonite (nano)composites was controlled by the physical or chemical crosslinking density (Thatiparti et al. 2010). Chemically crosslinked hydrogels degraded due to hydrolysis or enzymatic digestion, and the rate of polymer degradation decided mostly on the drug delivery from these systems.

The stimuli-responsive materials containing pH-sensitive hydrogels, exhibiting phase transitions (i.e., volume change) in response to changes in pH, have been very often studied. Such systems could allow to deliver desired drugs introduced into a human body directly to the small and large intestines (pH = 5–8), while avoiding release in the stomach (pH = 1–3), because of hydrogels containing ionizable weakly acidic groups swell in the acidic medium of stomach much lesser than in the basic medium of intestines, resulting in the release of loaded drug mainly in the latter (Dadkhah et al. 2014).

Wang et al. (2009) studied pH-sensitive (nano)composites containing chitosan-g-poly(acrylic acid), attapulgite and sodium alginate as diclofenac sodium delivery matrices crosslinked by Ca^{2+} owing to the ionic gelation of sodium alginate. It was shown that at pH = 6.8 the drug release was slower than at pH = 7.4, and additionally decreased with an increase in the attapulgite content. The drug release mechanism based on the swelling-controlled mode was proposed. At low pH and in the presence of attapulgite and sodium alginate crosslinked by Ca^{2+} , a longer path for diclofenac sodium to migrate from the composite structure promoted the prolongation of its release time. The entrapment efficiency of hydrogel materials, especially under basic conditions, can be improved by the intercalation of drug molecules between the positively charged layers of clay, used as an inorganic filler. This effect was revealed for alginate modified with montmorillonite intercalated with bovine serum albumin (Kaygusuz and Erim 2013), procainamide hydrochloride (Kevadiya et al. 2010) or lidocaine hydrochloride (Kevadiya et al. 2011), magnesium aluminum silicate intercalated with complexes of propranolol HCl (Pongjanyakul and Rongthong 2010), and chitosan crosslinked with sodium tripolyphosphate containing montmorillonite pillared with ofloxacin (Hua et al. 2010). The mechanism of drug release can be studied based on the kinetic exponent (n) calculated from the Ritger and Peppas model (Ritger and Peppas 1987) describing the process kinetics as follows:

$$F = k_p \cdot t^n \quad (11)$$

where F is the fraction of drug released at time t , k_p —the rate constant and n —the release exponent. For spherical matrices (such as alginate beads), $n \leq 0.43$ indicates a Fickian diffusion, $0.43 \leq n \leq 0.85$ —a non-Fickian transport (involving both Fickian diffusion and polymer chain relaxation), whereas $n \geq 0.85$ —a zero-order release mechanism (swelling or erosion controlled). It was shown that the introduction of bovine serum albumin-intercalated montmorillonite into alginate gel resulted in the decrease of the n value from 1.05 to 0.60–0.63 showing the change in the release mechanism from the surface erosion to the swelling/erosion combined with diffusion (Kaygusuz and Erim 2013).

Another mechanism of drug release from hydrogel-clay (nano)composites is based on thermally induced volume phase transition phenomenon characteristic of ionic temperature-sensitive hydrogels. Such polymers, for example, poly(*N*-isopropylacrylamide), exhibit critical gel transition temperature which defines changes in their swelling capacity. Below this point, the functional groups of hydrogel form strong hydrogen bonds with water molecules. When critical gel transition temperature is reached, the hydrophobic force of the gel increases, it collapses, and the bound water together with entrapped substances are released from the gel. The destruction of the hydrogel structure was clearly evidenced by a sudden drop in generalized diffusion coefficient (K_z) determined from the following Eq. 12 describing 2D anomalous diffusion (Stempfle et al. 2014):

$$\langle \Delta r^2(\tau) \rangle = 4K_z \tau^\alpha \quad (12)$$

where $\langle \Delta r^2(\tau) \rangle$ is the mean square displacement at time t , and α —anomaly parameter, which is 1 for normal diffusion and below 1 for anomalous subdiffusion. At increasing temperature from 31 to 38 °C, the value of K_z dropped from 4.7×10^{-15} to 0.4×10^{-15} m²/s ^{α} , whereas the α parameter changed the value from 0.65 to 0.41.

The release of caffeine (uncharged), phenol red (anionic), and crystal violet (cationic) was studied for the gels composed of poly(*N*-isopropylacrylamide-co-sodium acrylate) and (3-acrylamidopropyl)trimethyl ammonium chloride-intercalated montmorillonite at the deionized water or saline solution at 37 °C (Lee and Jou 2004). The collected results confirmed that the drug release behavior was strongly affected by the charge of drug solute and ionic strength of surroundings. The fractional release of caffeine was not affected by ionicity of hydrogels. Since negative charges on the surface of montmorillonite were partially neutralized by cations, the crystal violet release increased with an increase of the content of the intercalation agent. On the other hand, phenol red gave the opposite results of release kinetics compared to crystal violet.

The drug release rate can be easily controlled by modulating the electric field for electro-sensitive hydrogel-containing (nano)composites. Unfortunately, pure hydrogels lose the responsiveness and reversibility after several on-off switching

operations. In order to overcome this fatigue problem, the incorporation of an inorganic nanophase (e.g., clay) was proposed. The presence of inorganic filler has a significant effect on the electrical deformation and relaxation behaviors. The excellent anti-fatigue performance and better pulsatile release of vitamin B₁₂ were demonstrated by Liu et al. (2008) for chitosan modified with montmorillonite. In the presence of the clay-doped materials, the release process proceeded constantly during repeated on-off switching operations according to pseudo-zero-order kinetics at the swelling-controlled mode.

Drug delivery hydrogel-based formulations should be often characterized by mucoadhesion properties with the ability to be attached to a mucosal surface and release a drug directly to the mucus. Both the nature of polymer (including possible physical and chemical interactions) and the environment (including mucus physiology and pH) influence on the extent of mucoadhesion. It is important that hydrogel contains numerous hydrogen bond forming groups (i.e., carboxyl and hydroxyl groups), which are considered to be main interactions between the mucus and hydrophilic polymers apart from physical entanglement (Pongjanyakul and Suksri 2009; Salcedo et al. 2012; Yuan et al. 2010; Wang et al. 2008b). Furthermore, the mucoadhesive capability of hydrogels can be promoted by the addition of clays, which interact with mucin being the main component of mucus gel (Salcedo et al. 2012). It was revealed (Güler et al. 2015) that the mucoadhesion properties of gelatinized wheat starch grafted with poly(methacrylic acid), measured as work of adhesion [mJ/cm^2] and maximal detachment force [N] using ewe vaginal mucosa, could be enhanced by the addition of montmorillonite. Exfoliated clay particles dispersed in the hydrogel matrix were found to interact with mucin, due to the London-van der Waals forces and hydrogen bonding. This resulted in a synergistic effect to that of the polymer, which entrapped mucin chains as well as interacted with the mucosal substrate chemically and physically. The opposite tendency was observed in the case of (nano)composites synthesized by photopolymerization of acrylic acid, poly(ethylene glycol) methyl ether acrylate, and bentonite. The adhesive force measured as the force required to break the adhesive surface between the substrate (PET film) and the gels was not affected by the addition of clay, and mainly depended on the content of acrylic acid (Lee and Chen 2004).

As confirmed by fluorescence spectroscopy, during oral delivery the addition of montmorillonite to poly(D,L-lactide-co-glycolide) significantly enhanced the cellular uptake of the formed nanoparticles containing anticancer paclitaxel drug by Caco-2 and HT-29 cells (Dong and Feng 2005). This behavior was explained by the strong interactions between the composite nanoparticles and the gastrointestinal tract mucus/epithelial cells prolonging the residence time and enhancing the absorption of the drug-loaded nanoparticles. On the other hand, the genotoxicity evaluation of 5-fluorouracil (used in effectual chemotherapy) in lymphocyte cell culture by comet assay indicated significant retardation in DNA damage at an unchanged efficacy toward cancer cells, when this drug was introduced into the structure of chitosan/montmorillonite (nano)composite (Kevadiya et al. 2012). Additionally, for such delivery system reduced side effects, such as hepatotoxicity and pathological symptoms, were observed.

6.3 Biomedicine

6.3.1 Cell Culturing

Hydrogel-clay (nano)composites, especially based on poly(*N*-isopropylacrylamide) being a well-known thermo-responsive polymer, were found to be very efficient substrates for the cell culture. Poly(*N*-isopropylacrylamide) has optimal hydrophobic properties and electric charge to adsorb proteins of cell adhesion, such as collagen, fibronectin, and vitronectin, which enhance the cell attachment. Additionally, this hydrogel is characterized by suitable roughness and stiffness affecting the surface accumulation and growth of cells.

Haraguchi et al. (2006) revealed that the adhesion and proliferation of different human cells (HepG2, dermal fibroblast and HUVEC) on the surface of poly(*N*-isopropylacrylamide)-laponite strongly depended on the clay content, which was recognized as a crucial component responsible of the gel bioactivity. It was shown that similar cell cultures were hardly developed on the pure or crosslinked hydrogel without the clay admixture. Furthermore, using of the composite substrate played the beneficial role regardless to the water content and the thicknesses of gel sheet. The observed effect was explained by the balanced hydrophobic (due to the presence of hydrogel chains) and hydrophilic properties (related to the clay) enhanced by the negative charge of surface, which were required to sustain adhesion and proliferation of cells. The charge of gel surface was controlled by Liu et al. (2014) using copolymerization with small quantities of 2-(dimethylamino)ethyl methacrylate (resulting in positive charge) or 2-acrylamido-2-methylpropane sulfonic acid (giving negative charge). The proliferation of mouse fibroblast L929 cells was promoted on the (nano)composites containing less than 5 mol% of 2-(dimethylamino)ethyl methacrylate. At higher concentrations, the presence of 2-(dimethylamino)ethyl methacrylate admixture hindered the cell adhesion. On the other hand, the negative charge of the 2-acrylamido-2-methylpropane sulfonic acid-containing gels caused the electrostatic repulsion of L929 cells, and the proliferation process proceeded very slowly.

Poly(*N*-isopropylacrylamide) exhibits a clear coil-to-globule transition at its lower critical solution temperature of about 32 °C and, therefore, the cultured cells could be easily detached from the surface as an intact sheet by decreasing temperature from that of used during cultivation (~37 °C) to slightly lower one without treatment by trypsin. During the decrease in temperature, hydration of hydrogel chains occurs at the cell–substrate interface. Due to the cytoskeletal tensile force, the cells change their shape from a spread to a round form from the sheet edge, and finally detached completely from the surface. To accelerate the cell sheet detachment, some hydrophilic components (e.g., alginate (Wang et al. 2011a, b) or poly(ethylene glycol) (Liu et al. 2012a) were added to the poly(*N*-isopropylacrylamide)-clay gel).

6.3.2 Wound Healing

Biodegradable, biocompatible, cost-effective, and antimicrobial hydrogel-clay (nano)composites are very promising materials for tissue engineering, including the production of wound dressings, which should minimize infection and pain, prevent excessive fluid loss, maintain a moist healing environment, and promote epithelial restoration (Sirousazar et al. 2011b; Kokabi et al. 2007; Nistor et al. 2013).

Ghadiri et al. (2014) reported wound dressing tests using alginate and mafenide-intercalated laponite (nano)composite hydrogel. The eluted mafenide showed active antibacterial effects against tested bacteria (*Escherichia coli*, *Staphylococcus aureus*, and *Pseudomonas aeruginosa*), whereas the composite matrix formed a breathable dressing with the capacity to absorb wound exudates. The clay, which stabilized gel structure, had a soothing effect on skin and released Mg^{2+} ions during the wound healing process reducing the cytotoxic effect of mafenide on fibroblast cells.

Polyurethane foam combined with protein drug-loaded pH-sensitive alginate-bentonite (nano)composite was also tested in the wound dressings (Oh et al. 2011). The release of protein (bovine serum albumin) from this nontoxic and biocompatible material increased with pH and reached the highest equilibrium value at pH = 8.2. In acidic conditions, the alginate hydrogel shrank and the drug release was hindered, whereas at higher pH the crosslinking of the hydrogel was disrupted exposing the drug. On the other hand, increasing content of clay decreased the rate of drug release, which was the highest in the case of pure alginate hydrogel. The addition of clay can be, therefore, considered as very useful in controlling the release rate and amount of protein drug delivered in order to bring about the maximal treatment affect.

Three-dimensional (nano)composite hydrogel-containing bone-derived gelatin and ciprofloxacin-intercalated montmorillonite was applied as an ideal biomaterial for tissue engineering by Kevadiya et al. (2014). The results of in vitro migration and proliferation of lung cancer cells (A549) in the presence of gel composite confirmed a significant increase in the cell density near the wound edges probably due to cell proliferation promoted by gelatin. It was found that the composite gel acted as a barrier biomaterial against microbes protecting wounds from infection, and hence accelerating the healing process. The presence of montmorillonite reduced the rate of composite degradation, which plays an important role in new cell regeneration process. Furthermore, the drug molecules located in the interlayer space of clay dispersed in the hydrogel matrix was effectively sheltered from the aqueous environment delaying their dissolution and in consequence diffusion out of the formulation.

6.4 Others

6.4.1 Ceramic Materials

Gelcasting is presently considered as the most promising process of ceramic production, which can replace conventional technologies due to an achievement of high solids contents and high green densities without pressure. Basically, a slurry of ceramic powder is dispersed in a solution of organic monomers, poured into a mold and polymerized to form green body composites. However, the suitable monomers providing the gel a high mechanical strength have to be selected. Therefore, acrylamide, methacrylamide, hydroxymethylacrylamide, *N*-vinyl pyrrolidone, and poly(ethylene glycol) sometimes in combination with bifunctional monomers, such as methylene bisacrylamide and poly(ethylene glycol) dimethacrylate, have been most commonly studied (Potoczek and Zawadzak 2004). Lungu et al. (2012) proposed to adopt a low toxic and cost-effective poly(acrylic acid)-kaolin (nano)-composite to develop kaolin porous ceramics for separation purposes. Acrylic acid monomer served both as a network component and as a sacrificial porogen compound, without adding any other porogens. Highly porous (>60%) kaolin ceramics with interconnected pores were obtained by burning out the hydrogel, which gave a very interesting material for filtration applications.

6.4.2 Building Materials

In spite of autoclaved-aerated concrete and polyurethane or polystyrene foams are commonly applied lightweight-insulating materials in the building industry, significant flammability of polymer foams and relatively high cost of production of an aerated concrete cause that alternative routes for fabrication of novel lightweight porous materials have been still developed. Rutkevičius et al. (2012) showed a nonconventional way of preparation of lightweight porous materials by templating hydrogels (poly(acrylamide) and gellan gum) with a range of hydrophilic and hydrophobic scaffolding materials (cement, gypsum, and clay-cement mixtures, alternatively dispersed in curable polydimethylsiloxane). After the solidification of the scaffolding material, the evaporation of structured hydrogel produced the porous composite material whose pores mimic the hydrogel mesostructure.

6.4.3 Agriculture and Horticulture

The hydrogel-clay (nano)composites can play a role of controlled-release systems delivering bioactive agents (such as pesticides or fertilizers) slowly and continuously for a longer duration to a specified target. By the incorporation of these chemicals into the (nano)composite structure, the negative impact on the environment is minimized, which could be caused by losses due to leaching, volatilization,

or degradation. The controlled-release materials based on polysaccharides have received a great attention in the agriculture applications (Campos et al. 2014). However, in spite of benefits for the use of polysaccharides, the final price of the product ends up making its application unfeasible. This problem can be solved by the formation of (nano)composites from hydrogels with high content of clay, which drastically reduces the production costs and often improves some very important properties of the final product, such as ion-exchange capacity, water absorption rate, and mechanical resistance (Ni et al. 2011).

Bortolin et al. (2013) showed that the materials composed of poly(acrylamide), methylcellulose, and montmorillonite released the nitrogenated fertilizer (namely urea) about 72 times more slowly in the hydrogel without the hydrolysis treatment and up to 192 times more slowly for the hydrolyzed hydrogels, compared to urea in the absence of (nano)composite. What is especially noteworthy the developed material showed the extremely high quantity of urea released per the hydrogel content (about 90 g per g of dry hydrolyzed hydrogel). The urea-containing poly(acrylamide)-montmorillonite (nano)composites appeared to substantially reduce the emission of N_2O during the utilization of fertilizer when applied to soil planted with wheat (Pereira et al. 2015). Probably, the montmorillonite layers act as a physical barrier, preventing exposure of urea molecules, thereby reducing the rate of their hydrolysis. Additionally, the evolved NH_4^+ cations are incorporated into the interlayer galleries of clay by ion exchange with naturally occurring cations (e.g., Na^+ , Ca^{2+}) and consequently are not transformed into other nitrogenous compounds like N_2O .

Clays (especially sepiolite) incorporated into the hydrogel matrix (commercial Stockosorb[®] K-400) were also considered to be components of formulations for improving the stock quality of seedlings destined for forest restoration in dryland ecosystems (Chirino et al. 2011).

6.4.4 Chemical Sensors

Some smart hydrogels possess tunable stimuli-responsive properties, which enable them to undergo substantial and abrupt changes in volume in response to changes in external stimuli, such as pH, light, electric or magnetic field, and temperature (Liu and Urban 2010). This phenomenon can be applied in the construction of sensors and actuators after the suitable improvement of mechanical strength of hydrogels by their modification with clay fillers (Lian et al. 2014; Gao et al. 2015). The introduction of clay into hydrogel also results in micro-phase separation of polymer chains, which, in consequence, favors evacuation of water during shrinking. The detailed properties of stimuli-responsive hydrogel-clay systems are elaborated in the reviews by Haraguchi (2011a, b).

As mentioned in Sect. 6.2, poly(*N*-isopropylacrylamide), characterized by the facile phase transition temperature about 32 °C, is a well-known thermo-sensitive hydrogel. Nevertheless, this phase transition temperature can be adjusted within the range from 25 to 90 °C by an exploitation of poly(2-(2-methoxyethoxy)ethyl

methacrylate) copolymerized with oligo(ethylene glycol) methacrylate monomers instead of poly(*N*-isopropylacrylamide) (Xia et al. 2015). Moreover, the introduction of laponite into such hydrogel allowed to obtain the (nano)composite with reversible double-volume phase transition temperatures, the upper critical solution temperature (UCST) and the lower critical solution temperature (LCST), which can be controlled by varying the fraction of oligo(ethylene glycol) methacrylate and the clay content. This double thermosensitivity was attributed to the consecutive changes of the clay/copolymer aggregation from loose microaggregation ($T < UCST$), over homogeneous network structure ($UCST < T < LCST$), to dense macroaggregation ($T > LCST$).

A majority of pH-responsive hydrogel-clay (nano)composites is anionic and swells at $pH > 5$. Nevertheless, some examples of other materials, based mainly on positively charged poly(2-(dimethylamino)ethyl methacrylate), which swells at $pH < 4$ and shrinks at $pH > 4$, can be also found in the literature (Zhu et al. 2010). Furthermore, Xiang et al. (2006) revealed that the introduction of fibrillary attapulgite into the poly(2-hydroxyethyl methacrylate-co-poly(ethylene glycol) methyl ether methacrylate-co-methacrylic acid) network allowed to synthesize organic/inorganic nanocomposite characterized by much greater equilibrium-swelling ratio, much faster response rate to pH and significantly improved tensile mechanical properties compared to the unmodified hydrogel.

In addition, the hydrogel can contain both pH-sensitive units (or network) and thermo-sensitive units (or network) forming double-responsive system (Wang and Chen 2012). Extraordinary swelling/deswelling and mechanical properties were obtained for the double network-based (nano)composite consisting of poly(*N*-isopropylacrylamide), poly(acrylic acid) and laponite as an effective crosslinker (Shen et al. 2015). Instead of poly(acrylic acid), natural carboxymethyl chitosan or sodium carboxymethylcellulose could be also used resulting in pH- and temperature-responsive semi-interpenetrating polymer network (nano)composite with the volume phase transition temperature around 33 °C and the minimum swelling capacities near the isoelectric point of carboxymethyl chitosan (Ma et al. 2007a, b).

6.4.5 Enhanced Oil Recovery

Sulfonated poly(acrylamide) crosslinked with Cr^{3+} is commercially used in the enhanced oil recovery for the control of excess water production (Moradi-Araghi 2000). It was found that the introduction of montmorillonite into such hydrogel results in an increase of its storage modulus and ion resistance, presenting it as a potentially good candidate for application in the enhanced oil recovery (Aalaie et al. 2008).

7 Conclusion and Future Perspective

Hydrogels, being crosslinked hydrophilic polymer networks characterized by extremely high swelling capacity, are widely used in many applications. Furthermore, the modification of their properties by the controlled introduction of clay filler improves some features of these polymer matrices and diversifies their applicability. It was shown that layered aluminosilicates dispersed in the hydrogel networks have, in chosen cases, a beneficial effect on their mechanical, rheological, swelling, and thermal parameters. The results demonstrated in the literature evidence that the properly modified hydrogels forming (nano)composites can have a powerful impact in many fields. Especially, they can become materials commonly used in a wide variety of biomedical, pharmaceutical, and agriculture applications. In these cases, the improvement of mechanical toughness of hydrogels by filling with a clay allows to construct stable, valuable materials characterized by long-term biocompatibility, and controlled biodegradability. Nevertheless, a large effort is still needed to develop the commercial methods of production of hydrogel-clay (nano)composites, in which the content of the unreacted monomer(s) would be minimized as well as the particles size and phase distribution would be sufficiently controlled. In this respect, designing more sophisticated multicomponent and complex (nano)composites, being tailored to specific applications, can be also expected.

References

- Aalaie J, Vasheghani-Farahani E, Rahmatpour A, Semsarzadeh MA (2008) Effect of montmorillonite on gelation and swelling behavior of sulfonated polyacrylamide nanocomposite hydrogels in electrolyte solutions. *Eur Polym J* 44:2024–2031
- Adams JM, McCabe RW (2006) Handbook of clay science: developments in clay science, vol 1. Chapter 10.2: clay minerals as catalysts. Elsevier, USA
- Agrawal SK, Sanabria-Delong N, Bhatia SK, Tew GN, Bhatia SR (2010) Energetics of association in poly(lactic acid)-based hydrogels with crystalline and nanoparticle—polymer junctions. *Langmuir* 26:17330–17338
- Al E, Güçlü G, İyim TB, Emik S, Özgümüş S (2008) Synthesis and properties of starch-graft-acrylic acid/Na-montmorillonite superabsorbent nanocomposite hydrogels. *J Appl Polym Sci* 109:16–22
- Alexandre M, Dubois P (2000) Polymer-layered silicate nanocomposites: preparation, properties and uses of a new class of materials. *Mater Sci Eng* 28:1–63
- Anderson RL, Ratcliffe I, Greenwell HC, Williams PA, Cliffe S, Coveney PV (2010) Clay swelling—a challenge in the oilfield. *Earth Sci Rev* 98:201–216
- Beisebekov MM, Serikpayeva SB, Zhumagalieva SN, Beisebekov MK, Abilov ZA, Kosmella S, Koetz J (2014) Interactions of bentonite clay in composite gels of non-ionic polymers with cationic surfactants and heavy metal ions. *Colloid Polym Sci* 293:633–639
- Bhattacharyya R, Ray SK (2014) Removal of congo red and methyl violet from water using nano clay filled composite hydrogels of poly acrylic acid and polyethylene glycol. *Chem Eng J* 260:269–283

- Bortolin A, Aouada FA, Mattoso LHC, Ribeiro C (2013) Nanocomposite PAAm/methyl cellulose/montmorillonite hydrogel: evidence of synergistic effects for the slow release of fertilizers. *J Agric Food Chem* 61:7431–7439
- Boruah M, Mili M, Sharma S, Gogoi B, Dolui SK (2015) Synthesis and evaluation of swelling kinetics of electric field responsive poly(vinyl alcohol)-g-polyacrylic acid/OMNT nanocomposite hydrogels. *Polym Compos* 36:34–41
- Breen Ch, Watson R (1998) Acid activated organoclays: preparation, characterization and catalytic activity of polycation-treated bentonites. *Appl Clay Sci* 12:479–494
- Brigatti MF, Galan E, Theng BKG (2006) Handbook of clay science: developments in clay science, vol 1. Chapter 2: structures and mineralogy of clay minerals. Elsevier, USA
- Brindley GW, Brown G (eds) (1980) Crystal structures of clay minerals and their X-ray identification. Mineralogical Society, London
- Campos EVR, de Oliveira JL, Fraceto LF, Singh B (2014) Polysaccharides as safer release systems for agrochemicals. *Agron Sustain Dev* 35:47–66
- Can V, Abdurrahmanoglu S, Okay O (2007) Unusual swelling behavior of polymer-clay nanocomposite hydrogels. *Polymer* 48:5016–5023
- Chen B, Evans JRG, Greenwell HC, Boulet P, Coveney PV, Bowden AA, Whiting A (2008) A critical appraisal of polymer-clay nanocomposites. *Chem Soc Rev* 37:568–594
- Chen P, Xu S, Wu R, Wang J, Gu R, Du J (2013) A transparent Laponite polymer nanocomposite hydrogel synthesis via in-situ copolymerization of two ionic monomers. *Appl Clay Sci* 72:196–200
- Chen Y, Xu W, Zeng G (2014a) The preparation and characteristic of robust inorganic/organic IPN nanocomposite hydrogels with fast response rate. *J Mater Sci* 49:7360–7370
- Chen HB, Hollinger E, Wang YZ, Schiraldi DA (2014b) Facile fabrication of poly(vinyl alcohol) gels and derivative aerogels. *Polymer* 55:380–384
- Chirino E, Vilagrosa A, Vallejo VR (2011) Using hydrogel and clay to improve the water status of seedlings for dryland restoration. *Plant Soil* 344:99–110
- Chitnis SD, Sharma MM (1997) Industrial applications of acid-treated clays as catalysts. *React Funct Polym* 32:93–115
- Choudhary MS (2009) Inverse suspension polymerization of partially neutralized and lightly cross-linked acrylic acid: effect of reaction parameters. *Macromol Symp* 277:171–176
- Dadkhah D, Navarchian AH, Aref L, Tavakoli N (2014) Application of taguchi method to investigate the drug release behavior of poly(acrylamide-co-maleic acid)/montmorillonite nanocomposite hydrogels. *Adv Polym Tech* 33:21426
- Dalaran M, Emik S, Güçlü G, Iyim TB, Özgümüş S (2009) Removal of acidic dye from aqueous solutions using poly(DMAEMA-AMPS-HEMA) terpolymer/MMT nanocomposite hydrogels. *Polym Bull* 63:159–171
- Dalaran M, Emik S, Güçlü G, Iyim TB, Özgümüş S (2011) Study on a novel polyampholyte nanocomposite superabsorbent hydrogels: synthesis, characterization and investigation of removal of indigo carmine from aqueous solution. *Desalination* 279:170–182
- Dinu MV, Perju MM, Drăgan ES (2011) Porous semi-interpenetrating hydrogel networks based on dextran and polyacrylamide with superfast responsiveness. *Macromol Chem Phys* 212:240–251
- Dong Y, Feng SS (2005) Poly(D, L-lactide-co-glycolide)/montmorillonite nanoparticles for oral delivery of anticancer drugs. *Biomaterials* 26:6068–6076
- Du J, Chen P, Adalati A, Xu S, Wu R, Wang J, Zhang C (2014) Preparation and mechanical properties of a transparent ionic nanocomposite hydrogel. *J Polym Res* 21:541
- Ekici S, Işıkver Y, Saraydm D (2006) Poly (acrylamide-sepiolite) composite hydrogels: preparation, swelling and dye adsorption properties. *Polym Bull* 57:231–241
- El-Sigeny S, Mohamed SK, Abou Taleb MF (2014) Radiation synthesis and characterization of styrene/acrylic acid/organophilic montmorillonite hybrid nanocomposite for sorption of dyes from aqueous solutions. *Polym Compos* 35:2353–2364
- Etika KC, Liu L, Cox MA, Grunlan JC (2016) Clay-mediated carbon nanotube dispersion in poly (N-Isopropylacrylamide). *Colloid Surf A* 489:19–26

- Flessner U, Jones DJ, Rozière J, Zajac J, Storaro L, Lenarda M, Pavan M, Jiménez-López A, Rodríguez-Castellón E, Trombetta M, Busca G (2001) A study of the surface acidity of acid-treated montmorillonite clay catalysts. *J Mol Catal A Chem* 168:247–256
- Fu F, Wang Q (2011) Removal of heavy metal ions from wastewaters: a review. *J Environ Manag* 92:407–418
- Ganguly S, Dana K, Mukhopadhyay TK, Parya TK, Ghatak S (2011) Organophilic nano clay: a comprehensive review. *Trans Ind Ceram Soc* 70:189–206
- Gao L, Sun Y, Zhang W, Li D, Hou C, Liu Y (2015) Mechanical behavior of a terpolymer-based pH- and temperature-responsive hydrogel. *J Polym Res* 22:221–230
- Ghadiri M, Chrzanowski W, Rohanzadeh R (2014) Antibiotic eluting clay mineral (Laponite®) for wound healing application: an in vitro study. *J Mater Sci Mater Med* 25:2513–2526
- Güçlü G, Al E, Emik S, Iyim TB, Özgümüş S, Özyürek M (2010) Removal of Cu²⁺ and Pb²⁺ ions from aqueous solutions by starch-graft-acrylic acid/montmorillonite superabsorbent nanocomposite hydrogels. *Polym Bull* 65:333–346
- Guggenheim S, Adams JM, Bain DC, Bergaya F, Brigatti MF, Drits VA, Formoso ML, Galan E, Kogure T, Stanjek H (2006) Summary of recommendations of nomenclature committees relevant to clay mineralogy: report of the Association Internationale Pour L'étude Des Argiles (AIPEA) nomenclature committee for 2006. *Clays Clay Miner* 54:761–772
- Guilherme MR, Fajardo AR, Moia TA, Kunita MH, Gonçalves MDC, Rubira AF, Tambourgi EB (2010) Porous nanocomposite hydrogel of vinylated montmorillonite-crosslinked maltodextrin-co-dimethylacrylamide as a highly stable polymer carrier for controlled release systems. *Eur Polym J* 46:1465–1474
- Güler MA, Gök MK, Figen AK, Özgümüş S (2015) Swelling, mechanical and mucoadhesion properties of Mt/starch-g-PMAA nanocomposite hydrogels. *Appl Clay Sci* 112–113:44–52
- Haraguchi K (2007a) Nanocomposite gels: new advanced functional soft materials. *Macromol Symp* 256:120–130
- Haraguchi K (2007b) Nanocomposite hydrogels. *Curr Opin Solid State Mater Sci* 11:47–54
- Haraguchi K (2008) Nanocomposite gels—fundamental significance and new functions. *Kobunshi Ronbunshu* 65:619–633
- Haraguchi K (2011a) Stimuli-responsive nanocomposite gels. *Colloid Polym Sci* 289:455–473
- Haraguchi K (2011b) Synthesis and properties of soft nanocomposite materials with novel organic/inorganic network structures. *Polym J* 43:223–241
- Haraguchi K, Li HJ (2009) The effect of water content on the ultimate properties of rubbery nanocomposite gels. *J Polym Sci Part B Polym Phys* 47:2328–2340
- Haraguchi K, Li HJ (2010) Hydrophobic surface characteristics of nanocomposite hydrogels. *Macromol Symp* 291–292:159–167
- Haraguchi K, Takada T (2010) Synthesis and characteristics of nanocomposite gels prepared by in situ photopolymerization in an aqueous system. *Macromolecules* 43:4294–4299
- Haraguchi K, Takehisa T (2002) Nanocomposite hydrogels: a unique organic–inorganic network structure with extraordinary mechanical, optical, and swelling/de-swelling properties. *Adv Mater* 14:1120–1124
- Haraguchi K, Varade D (2014) Platinum-polymer-clay nanocomposite hydrogels via exfoliated clay-mediated in situ reduction. *Polymer (UK)* 55:2496–2500
- Haraguchi K, Xu Y (2012) Thermal analyses of poly(*N*-isopropylacrylamide) in aqueous solutions and in nanocomposite gels. *Colloid Polym Sci* 290:1627–1636
- Haraguchi K, Li H-J, Matsuda K, Takehisa T, Elliott E (2005) Mechanism of forming organic/inorganic network structures during in-situ free-radical polymerization in PNIPAA-clay nanocomposite hydrogels. *Macromolecules* 2005(38):3482–3490
- Haraguchi K, Takehisa T, Ebato M (2006) Control of cell cultivation and cell sheet detachment on the surface of polymer/clay nanocomposite hydrogels. *Biomacromol* 7:3267–3275
- Haraguchi K, Li HJ, Ren HY, Zhu M (2010) Modification of nanocomposite gels by irreversible rearrangement of polymer/clay network structure through drying. *Macromolecules* 43:9848–9853

- Haraguchi K, Uyama K, Tanimoto H (2011) Self-healing in nanocomposite hydrogels. *Macromol Rapid Commun* 32:1253–1258
- Harini M, Deshpande AP (2009) Rheology of poly(sodium acrylate) hydrogels during cross-linking with and without cellulose microfibrils. *J Rheol* 53:31–47
- Helvacioğlu E, Aydın V, Nugay T, Nugay N, Uluocak BG, Şen S (2011) High strength poly (acrylamide)-clay hydrogels. *J Polym Res* 18:2341–2350
- Hennink WE, Van Nostrum C (2012) Novel crosslinking methods to design hydrogels. *Adv Drug Deliv Rev* 64:223–236
- Hoffman AS (2002) Hydrogels for biomedical applications. *Adv Drug Deliv Rev* 43:3–12
- Hosseinzadeh H, Zoroufi S, Mahdavinia GR (2015) Study on adsorption of cationic dye on novel kappa-carrageenan/poly(vinyl alcohol)/montmorillonite nanocomposite hydrogels. *Polym Bull* 72:1339–1363
- Hu X, Wang T, Xiong L, Wang C, Liu X, Tong Z (2010) Preferential adsorption of poly(ethylene glycol) on hectorite clay and effects on poly(*N*-isopropylacrylamide)/hectorite nanocomposite hydrogels. *Langmuir* 26:4233–4238
- Hua S, Yang H, Wang W, Wang A (2010) Controlled release of ofloxacin from chitosan-montmorillonite hydrogel. *Appl Clay Sci* 50:112–117
- Huang T (2012) P(NIPAM-co-AA)/clay nanocomposite hydrogels exhibiting high swelling ratio accompanied by excellent mechanical strength. *Appl Phys A Mater Sci Process* 107:905–909
- Hussain YA, Liu T, Roberts GW (2012) Synthesis of cross-linked, partially neutralized poly (acrylic acid) by suspension polymerization in supercritical carbon dioxide. *Ind Eng Chem Res* 51:11401–11408
- Hussien RA, Donia AM, Atia AA, El-Sedfy OF, El-Hamid ARA, Rashad RT (2012) Studying some hydro-physical properties of two soils amended with kaolinite-modified cross-linked poly-acrylamides. *Catena* 92:172–178
- Ibraeva ZE, Zhumaly AA, Blagih E, Kudaibergenov SE (2015) Preparation and characterization of organic-inorganic composite materials based on poly(acrylamide) hydrogels and clay minerals. *Macromol Symp* 351:97–111
- Ibrahim SM, El-Naggar AA (2013) Preparation of poly(vinyl alcohol)/clay hydrogel through freezing and thawing followed by electron beam irradiation for the treatment of wastewater. *J Thermoplast Compos Mater* 26:1332–1348
- Ihsanullah AA, Al-Amer AM, Laoui T, Al-Marri MJ, Nasser MS, Khraisheh M, Atieh MA (2016) Heavy metal removal from aqueous solution by advanced carbon nanotubes: critical review of adsorption applications. *Sep Purif Technol* 157:141–161
- Irani M, Ismail H, Ahmad Z (2013) Preparation and properties of linear low-density polyethylene-g-poly(acrylic acid)/organo-montmorillonite superabsorbent hydrogel composites. *Polym Test* 32:502–512
- Irani M, Ismail H, Ahmad Z, Fan M (2015) Synthesis of linear low-density polyethylene-g-poly (acrylic acid)-co-starch/organo-montmorillonite hydrogel composite as an adsorbent for removal of Pb(II) from aqueous solutions. *J Environ Sci* 27:9–20
- Janovák L, Varga J, Kemény L, Dékány I (2008) Investigation of the structure and swelling of poly(*N*-isopropyl-acrylamide-acrylamide) and poly(*N*-isopropyl-acrylamide-acrylic acid) based copolymer and composite hydrogels. *Colloid Polym Sci* 286:1575–1585
- Janovák L, Varga J, Kemény L, Dékány I (2009a) Swelling properties of copolymer hydrogels in the presence of montmorillonite and alkylammonium montmorillonite. *Appl Clay Sci* 43:260–270
- Janovák L, Varga J, Kemény L, Dékány I (2009b) The effect of surface modification of layer silicates on the thermoanalytical properties of poly(NIPAAm-co-AAm) based composite hydrogels. *J Therm Anal Calorim* 98:485–493
- Kabiri K, Omidian H, Zohuriaan-Mehr MJ, Doroudiani S (2011) Superabsorbent hydrogel composites and nanocomposites: a review. *Polym Compos* 32:277–289
- Kamoun EA, Menzel H (2012) HES-HEMA nanocomposite polymer hydrogels: swelling behavior and characterization. *J Polym Res* 19:1–14

- Kaplan M, Kaşgoz H (2011) Hydrogel nanocomposite sorbents for removal of basic dyes. *Polym Bull* 67:1153–1168
- Karadağ E, Hasgül B, Kundakci S, Üzümlü ÖB (2014) A study of polymer/clay hybrid composite sorbent-based AAm/SMA hydrogels and semi-IPNs composed of 1-carrageenan and montmorillonite for water and dye sorption. *Adv Polym Tech* 33:21432
- Karadağ E, Ödemiş H, Kundakci S, Üzümlü ÖB (2015) Swelling characterization of acrylamide/zinc acrylate/xanthan gum/sepilolite hybrid hydrogels and its application in sorption of Janus Green B from aqueous solutions. *Adv Polym Tech* 35:248–259
- Kaşgöz H, Durmus A (2008) Dye removal by a novel hydrogel-clay nanocomposite with enhanced swelling properties. *Polym Adv Technol* 19:838–845
- Kaygusuz H, Erim FB (2013) Alginate/BSA/montmorillonite composites with enhanced protein entrapment and controlled release efficiency. *React Funct Polym* 73:1420–1425
- Kevadiya BD, Joshi GV, Bajaj HC (2010) Layered bionanocomposites as carrier for procainamide. *Int J Pharm* 388:280–286
- Kevadiya BD, Joshi GV, Mody HM, Bajaj HC (2011) Biopolymer-clay hydrogel composites as drug carrier: host-guest intercalation and in vitro release study of lidocaine hydrochloride. *Appl Clay Sci* 52:364–367
- Kevadiya BD, Patel TA, Jhala DD, Thumbar RP, Brambhath H, Pandya MP, Rajkumar S, Jena PK, Joshi GV, Gadhia PK, Tripathi CB, Bajaj HC (2012) Layered inorganic nanocomposites: a promising carrier for 5-fluorouracil (5-FU). *Eur J Pharm Biopharm* 81:91–101
- Kevadiya BD, Rajkumar S, Bajaj HC, Chettiar SS, Gosai K, Brahmabhath H, Bhatt AS, Barvaliya YK, Dave GS, Kothari RK (2014) Biodegradable gelatin-ciprofloxacin-montmorillonite composite hydrogels for controlled drug release and wound dressing application. *Colloids Surf B* 122:175–183
- Khunawattanakul W, Puttipipatkachorn S, Rades T, Pongjanyakul T (2011) Novel chitosan-magnesium aluminum silicate nanocomposite film coatings for modified-release tablets. *Int J Pharm* 407:132–141
- Kloppogge JT (1998) Synthesis of smectites and porous pillared clay catalysts: a review. *J Porous Mater* 5:5–41
- Kloppogge JT, Komarneni S, Amonette JE (1999) Synthesis of smectite clay minerals: a critical review. *Clays Clay Miner* 47:529–554
- Kokabi M, Sirousazar M, Hassan ZM (2007) PVA-clay nanocomposite hydrogels for wound dressing. *Eur Polym J* 43:773–781
- Komadel P, Madejova J (2006) Handbook of clay science: developments in clay science, vol 1. Chapter 7.1: Acid activation of clay minerals. Elsevier, USA
- Kotal M, Bhowmick AK (2015) Polymer nanocomposites from modified clays: recent advances and challenges. Review article. *Prog Polym Sci* 51:127–187
- Kundakci S, Üzümlü ÖB, Karadağ E (2008) Swelling and dye sorption studies of acrylamide/2-acrylamido-2-methyl-1-propanesulfonic acid/bentonite highly swollen composite hydrogels. *React Funct Polym* 68:458–473
- Kundakci S, Üzümlü ÖB, Karadağ E (2009) A new composite sorbent for water and dye uptake: highly swollen acrylamide/2-acrylamido-2-methyl-1-propanesulfonic acid/clay hydrogels crosslinked by 1,4-butanediol dimethacrylate. *Polym Compos* 30:29–37
- Kundakci S, Üzümlü ÖB, Karadağ E (2011) Behaviors of polyelectrolyte AAm/AMPS/bentonite composite hydrogels in uptake of uranyl ions from aqueous solutions. *Polym Compos* 32:994–1001
- Lagaly G, Ogawa M, Dekany I (2007) Applied clay mineralogy: developments in clay science 2, Chapter 7.3: Clay mineral organic interactions. Elsevier, USA
- Lee WF, Chen JC (2004) Effect of bentonite on the physical properties and drug-release behavior of poly(AA-co-PEGMEA)/bentonite nanocomposite hydrogels for mucoadhesive. *J Appl Polym Sci* 91:2934–2941
- Lee WF, Jou LL (2004) Effect of the intercalation agent content of montmorillonite on the swelling behavior and drug release behavior of nanocomposite hydrogels. *J Appl Polym Sci* 94:74–82

- Li A, Wang A (2005) Synthesis and properties of clay-based superabsorbent composite. *Eur Polym J* 41:1630–1637
- Li A, Zhang J, Wang A (2007) Utilization of starch and clay for the preparation of superabsorbent composite. *Bioresour Technol* 98:327–332
- Li P, Siddaramaiah Kim NH, Heo SB, Lee JH (2008) Novel PAAm/Laponite clay nanocomposite hydrogels with improved cationic dye adsorption behavior. *Compos B* 39:756–763
- Li P, Kim NH, Hui D, Rhee KY, Lee JH (2009a) Improved mechanical and swelling behavior of the composite hydrogels prepared by ionic monomer and acid-activated Laponite. *Appl Clay Sci* 46:414–417
- Li P, Siddaramaiah Kim NH, Yoo GH, Lee JH (2009b) Poly(acrylamide/laponite) nanocomposite hydrogels: swelling and cationic dye adsorption properties. *J Appl Polym Sci* 111:1786–1798
- Li Y, Wang X, Wang J (2012) Cation exchange, interlayer spacing, and thermal analysis of Na/Ca-montmorillonite modified with alkaline and alkaline earth metal ions. *J Therm Anal Calorim* 110:1199–1206
- Li H, Gu R, Xu S, Abudurman A, Wang J (2014) Surfactant-assisted synthesis of a transparent ionic nanocomposite hydrogel. *Appl Clay Sci* 101:335–338
- Lian C, Yang Y, Wang T, Sun W, Liu X, Tong Z (2014) A facile method for reinforcing poly(*N*-isopropylacrylamide)-hectorite clay nanocomposite hydrogels by heat treatment. *Polym Compos* 37:1557–1563
- Lian C, Zhang E, Wang T, Sun W, Liu X, Tong Z (2015) Binding interaction and gelation in aqueous mixtures of poly(*N*-isopropylacrylamide) and hectorite clay. *J Phys Chem B* 119:612–619
- Liu F, Urban MW (2010) Recent advances and challenges in designing stimuli-responsive polymers. *Prog Polym Sci* 35:3–23
- Liu Y, Zhu M, Liu X, Jiang YM, Ma Y, Qin ZY, Kuckling D, Adler HJP (2007) Mechanical properties and phase transition of high clay content clay/poly(*N*-isopropylacrylamide) nanocomposite hydrogel. *Macromol Symp* 254:353–360
- Liu KH, Liu TY, Chen SY, Liu DM (2008) Drug release behavior of chitosan–montmorillonite, nanocomposite hydrogels following electrostimulation. *Acta Biomater* 4:1038–1045
- Liu Y, Zheng Y, Wang A (2010) Enhanced adsorption of methylene blue from aqueous solution by chitosan-g-poly (acrylic acid)/vermiculite hydrogel composites. *J Environ Sci* 22:486–493
- Liu Y, Zheng Y, Wang A (2011) Effect of biotite content of hydrogels on enhanced removal of methylene blue from aqueous solution. *Ionics* 17:535–543
- Liu D, Wang T, Liu X, Tong Z (2012a) Accelerated cell sheet detachment by copolymerizing hydrophilic PEG side chains into PNIPAm nanocomposite hydrogels. *Biomed Mater* 7:055008
- Liu M, Li W, Rong J, Zhou C (2012b) Novel polymer nanocomposite hydrogel with natural clay nanotubes. *Colloid Polym Sci* 290:895–905
- Liu M, Zhang Y, Li J, Zhou C (2013) Chitin-natural clay nanotubes hybrid hydrogel. *Int J Biol Macromol* 58:23–30
- Liu D, Wang T, Liu X, Tong Z (2014) Cell proliferation and cell sheet detachment from the positively and negatively charged nanocomposite hydrogels. *Biopolymers* 101:58–65
- Lungu A, Perrin FX, Belec L, Sarbu A, Teodorescu M (2012) Kaolin/poly(acrylic acid) composites as precursors for porous kaolin ceramics. *Appl Clay Sci* 62–63:63–69
- Ma J, Xu Y, Fan B, Liang B (2007a) Preparation and characterization of sodium carboxymethylcellulose/poly(*N*-isopropylacrylamide)/clay semi-IPN nanocomposite hydrogels. *Eur Polym J* 43:2221–2228
- Ma J, Xu Y, Zhang Q, Zha L, Liang B (2007b) Preparation and characterization of pH- and temperature-responsive semi-IPN hydrogels of carboxymethyl chitosan with poly(*N*-isopropyl acrylamide) crosslinked by clay. *Colloid Polym Sci* 285:479–484
- Ma J, Zhang L, Li Z, Liang B (2008) Preparation and characterization of porous poly (*N*-isopropylacrylamide)/clay nanocomposite hydrogels. *Polym Bull* 61:593–602
- Mahdavinia GR, Asgari A (2013) Synthesis of kappa-carrageenan-g-poly(acrylamide)/sepiolite nanocomposite hydrogels and adsorption of cationic dye. *Polym Bull* 70:2451–2470

- Mahdavinia GR, Massoudi A, Baghban A, Massoumi B (2012) Novel carrageenan-based hydrogel nanocomposites containing laponite RD and their application to remove cationic dye. *Iran Polym J* 21:609–619
- Mahdavinia GR, Aghaie H, Sheykhoie H, Vardini MT, Etemadi H (2013) Synthesis of CarAlg/MMt nanocomposite hydrogels and adsorption of cationic crystal violet. *Carbohydr Polym* 98:358–365
- Mansoori Y, Salemi H (2015) Nanocomposite hydrogels composed of cloisite 30B-graft-poly (acrylic acid)/poly(acrylic acid): synthesis and characterization. *Polym Sci Ser B* 57:167–179
- Marandi GB, Baharloui M, Kurdtabar M, Sharabian LM, Mojarad MA (2015) Hydrogel with high laponite content as nanoclay: swelling and cationic dye adsorption properties. *Res Chem Intermed* 41:7043–7058
- Mauroy H, Rozynek Z, Plivelic TS, Fossum JO, Helgesen G, Knudsen KD (2013) Oxygen-controlled phase segregation in poly(*N*-isopropylacrylamide)/laponite nanocomposite hydrogels. *Langmuir* 29:371–379
- Merinska D, Malac Z, Pospisil M, Weiss Z, Chmielova M, Capkova P, Simonik J (2002) Polymer/clay nanocomposites based on MMT/ODA intercalates. *Compos Interf* 9:529–541
- Miyazaki S, Endo H, Karino T, Haraguchi K, Shibayama M (2007) Gelation mechanism of poly (*N*-isopropylacrylamide)–clay nanocomposite gels. *Macromolecules* 40:4287–4295
- Molu ZB, Seki Y, Yurdaoç K (2010) Preparation and characterization of poly(acrylic acid)/pillared clay superabsorbent composite. *Polym Bull* 64:171–183
- Moradi-Araghi A (2000) A review of thermally stable gels for fluid diversion in petroleum production. *J Petrol Sci Eng* 26:1–10
- Murray HH (2007a) Handbook of clay science: developments in clay science, vol 2. Chapter 6: bentonite applications. Elsevier, USA
- Murray HH (2007b) Handbook of clay science: developments in clay science, vol 2. Chapter 2: applied clay mineralogy occurrences, processing and application of kaolins, bentonites, palygorskite-sepiolite, and common clays. Elsevier, USA
- Nair SH, Pawar KC, Jog JP, Badiger MV (2007) Swelling and mechanical behavior of modified poly(vinyl alcohol)/laponite nanocomposite membranes. *J Appl Polym Sci* 103:2896–2903
- Nakamoto K (1986) Infrared and Raman spectra of inorganic and coordination compounds. Part III, 4th edn. Wiley, New York
- Nakamura T, Ogawa M (2013) Adsorption of cationic dyes within spherical particles of poly(*N*-isopropylacrylamide) hydrogel containing smectite. *Appl Clay Sci* 83–84:469–473
- Natkański P, Kuśtrowski P, Białas A, Piwowarska Z, Michalik M (2012) Controlled swelling and adsorption properties of polyacrylate/ montmorillonite composites. *Mater Chem Phys* 136:1109–1115
- Natkański P, Kuśtrowski P, Białas A, Piwowarska Z, Michalik M (2013a) Thermal stability of montmorillonite polyacrylamide and polyacrylate nanocomposites and adsorption of Fe(III) ions. *Appl Clay Sci* 75–76:153–157
- Natkański P, Kuśtrowski P, Białas A, Surman J (2013b) Effect of Fe³⁺ ions present in the structure of poly(acrylic acid)/montmorillonite composites on their thermal decomposition. *J Therm Anal Calorim* 113:335–342
- Natkański P, Kuśtrowski P, Białas A, Wach A, Rokicińska A, Kozak M, Lityńska-Dobrzyńska L (2016) Hydrogel template-assisted synthesis of nanometric Fe₂O₃ supported on exfoliated clay. *Microporous Mesoporous Mater* 221:212–219
- Ni B, Liu M, Lü S, Xie L, Wang Y (2011) Environmentally friendly slow-release nitrogen fertilizer. *J Agric Food Chem* 59:10169–10175
- Nie X, Adalati A, Du J, Liu H, Xu S, Wang J (2014) Preparation of amphoteric nanocomposite hydrogels based on exfoliation of montmorillonite via in-situ intercalative polymerization of hydrophilic cationic and anionic monomers. *Appl Clay Sci* 97–98:132–137
- Nishida T, Obayashi A, Haraguchi K, Shibayama M (2012) Stress relaxation and hysteresis of nanocomposite gel investigated by SAXS and SANS measurement. *Polymer* 53:4533–4538

- Nistor MT, Vasile C, Chiriac AP, Tarțau L (2013) Biocompatibility, biodegradability, and drug carrier ability of hybrid collagen-based hydrogel nanocomposites. *J Bioact Compat Polym* 28:540–556
- Odian G (1991) Principles of polymerization, 3rd edn. Wiley, New York
- Oh ST, Kim WR, Kim SH, Chung YC, Park JS (2011) The preparation of polyurethane foam combined with pH-sensitive alginate/bentonite hydrogel for wound dressings. *Fiber Polym* 12:159–165
- Okada A, Usuki A (2006) Twenty years of polymer-clay nanocomposites. *Macromol Mater Eng* 291:1449–1476
- Okay O, Oppermann W (2007) Polyacrylamide-clay nanocomposite hydrogels: rheological and light scattering characterization. *Macromolecules* 40:3378–3387
- Oliveira MJA, Amato VS, Lugão AB, Parra DF (2012) Hybrid hydrogels produced by ionizing radiation technique. *Radiat Phys Chem* 81:1471–1474
- Oliveira MJA, Estefânia OS, Braz LMA, Regina M, Amato VS, Lugão AB, Parra DF (2014) Influence of chitosan/clay in drug delivery of glucantime from PVP membranes. *Radiat Phys Chem* 94:194–198
- Panagopoulou A, Vázquez Molina J, Kyritsis A, Monleón Pradas M, Vallés Lluch A, Gallego Ferrer G, Pissis P (2013) Glass transition and water dynamics in hyaluronic acid. *Food Biophys* 8:192–202
- Paranhos CM, Soares BG, Machado JC, Windmüller D, Pessan LA (2007) Microstructure and free volume evaluation of poly(vinyl alcohol) nanocomposite hydrogels. *Eur Polym J* 43:4882–4890
- Paul DR, Robeson LM (2008) Polymer nanotechnology: nanocomposites. *Polymer* 49:3187–3204
- Pavlidou S, Papaspyrides CD (2008) A review on polymer-layered silicate nanocomposites. *Prog Polym Sci* 33:1119–1198
- Pereira EI, Da Cruz CCT, Solomon A, Le A, Cavigelli MA, Ribeiro C (2015) Novel slow-release nanocomposite nitrogen fertilizers: the impact of polymers on nanocomposite properties and function. *Ind Eng Chem Res* 54:3717–3725
- Pongjanyakul T, Puttipipatkachorn S (2007) Alginate-magnesium aluminum silicate films: effect of plasticizers on film properties, drug permeation and drug release from coated tablets. *Int J Pharm* 333:34–44
- Pongjanyakul T, Rongthong T (2010) Enhanced entrapment efficiency and modulated drug release of alginate beads loaded with drug-clay intercalated complexes as microreservoirs. *Carbohydr Polym* 81:409–419
- Pongjanyakul T, Suksri H (2009) Alginate-magnesium aluminum silicate films for buccal delivery of nicotine. *Colloids Surf B* 74:103–113
- Potoczek M, Zawadzak E (2004) Initiator effect on the gelcasting properties of alumina in a system involving low-toxic monomers. *Ceram Int* 30:793–799
- Rieder M, Cavazzini G, D'yakonov YS, Frank-Kamenetskii VA, Gottardi G, Guggenheim S, Koval PV, Muller G, Neiva AMR, Radoslovich EW, Robert JL, Sassi FP, Takeda H, Weiss Z, Wones DR (1998) Nomenclature of the micas. *Canad Miner* 36:1366–1374
- Ritger PL, Peppas NA (1987) A simple equation for description of solute release II. Fickian and anomalous release from swellable devices. *Control Release* 5:37–42
- Rodrigues LADS, Figueiras A, Veiga F, de Freitas RM, Nunes LCC, da Silva Filho EC, da Silva Leite CM (2013) The systems containing clays and clay minerals from modified drug release: a review. *Colloids Surf B* 103:642–651
- Rokicińska A, Natkański P, Dudek B, Drozdek M, Lityńska-Dobrzyńska L, Kuśtrowski P (2016) Co_3O_4 -pillared montmorillonite catalysts synthesized by hydrogel-assisted route for total oxidation of toluene. *Appl Catal B Environ* 195:59–68
- Rutkevicius M, Munusami SK, Watson Z, Field AD, Salt M, Stoyanov SD, Petkov J, Mehl GH, Paunov VN (2012) Fabrication of novel lightweight composites by a hydrogel templating technique. *Mater Res Bulletin* 47 (4):980–986

- Salcedo I, Aguzzi C, Sandri G, Bonferoni MC, Mori M, Cerezo P, Sanchez R, Viseras C, Caramella C (2012) In vitro biocompatibility and mucoadhesion of montmorillonite chitosan nanocomposite: a new drug delivery. *Appl Clay Sci* 55:131–137
- Salimi F, Sefti MV, Jarrahan K, Rafipoor M, Ghorashi SS (2014) Preparation and investigation of the physical and chemical properties of clay-based polyacrylamide/Cr (III) hydrogels as a water shut-off agent in oil reservoirs. *Korean J Chem Eng* 31:986–993
- Santiago F, Mucientes AE, Osorio M, Poblete FJ (2006) Synthesis and swelling behaviour of poly (sodium acrylate)/sepiolite superabsorbent composites and nanocomposites. *Polym Int* 55:843–848
- Schexnailder P, Schmidt G (2009) Nanocomposite polymer hydrogels. *Colloid Polym Sci* 287:1–11
- Schulze DG (2005) Clay minerals, vol 1. In: Hillel D (ed) *Encyclopedia of soils in the environment*. Elsevier, Academic Press, Boston, pp 246–254
- Shen M, Sun Y, Xu J, Guo X, Prud'homme RK (2014) Rheology and adhesion of poly(acrylic acid)/Laponite nanocomposite hydrogels as biocompatible adhesives. *Langmuir* 30:1636–1642
- Shen J, Li N, Ye M (2015) Preparation and characterization of dual-sensitive double network hydrogels with clay as a physical crosslinker. *Appl Clay Sci* 103:40–45
- Shi Y, Xue Z, Wang X, Wang L, Wang A (2013) Removal of methylene blue from aqueous solution by sorption on lignocellulose-g-poly(acrylic acid)/montmorillonite three-dimensional cross-linked polymeric network hydrogels. *Polym Bull* 70:1163–1179
- Shirsath SR, Hage AP, Zhou M, Sonawane SH, Ashokkumar M (2011) Ultrasound assisted preparation of nanoclay Bentonite-FeCo nanocomposite hybrid hydrogel: a potential responsive sorbent for removal of organic pollutant from water. *Desalination* 281:429–437
- Shirsath SR, Patil AP, Patil R, Naik JB, Gogate PR, Sonawane SH (2013) Removal of Brilliant Green from wastewater using conventional and ultrasonically prepared poly(acrylic acid) hydrogel loaded with kaolin clay: a comparative study. *Ultrason Sonochem* 20:914–923
- Shirsath SR, Patil AP, Bhanvase BA, Sonawane SH (2015) Ultrasonically prepared poly (acrylamide)-kaolin composite hydrogel for removal of crystal violet dye from wastewater. *J Environ Chem Eng* 3:1152–1162
- Shivashankar M, Mandal BK (2012) A review on interpenetrating polymer network. *Int J Pharm Pharm Sci* 4:1–7
- Silva SS, Luna SM, Gomes ME, Benesch J, Pashkuleva I, Mano JF, Reis RL (2008) Plasma surface modification of chitosan membranes: characterization and preliminary cell response studies. *Macromol Biosci* 8:568–576
- Silvestre J, Silvestre N, de Brito J (2016) Polymer nanocomposites for structural applications: recent trends and new perspectives. *Mech Adv Mater Struct* 23:1263–1277
- Sinha Ray S, Okamoto M (2003) Polymer/layered silicate nanocomposite: a review from preparation to processing. *Prog Polym Sci* 28:1539–1641
- Sirousazar M, Kokabi M, Hassan ZM, Bahramian AR (2011a) Dehydration kinetics of polyvinyl alcohol nanocomposite hydrogels containing Na-montmorillonite nanoclay. *Sci Iran* 18:780–784
- Sirousazar M, Kokabi M, Zuhair MH (2011b) In vivo and cytotoxic assays of a poly(vinyl alcohol)/clay nanocomposite hydrogel wound dressing. *J Biomater Sci Polym Ed* 22:1023–1033
- Song L, Zhu M, Chen Y, Haraguchi K (2008) Temperature- and pH-sensitive nanocomposite gels with semi-interpenetrating organic/inorganic networks. *Macromol Chem Phys* 209:1564–1575
- Song F, Zhang LM, Shi JF, Li NN (2010) Viscoelastic and fractal characteristics of a supramolecular hydrogel hybridized with clay nanoparticles. *Colloids Surf B* 81:486–491
- Song G, Zhang L, He C, Fang D-C, Whitten PG, Wang H (2013) Facile fabrication of tough hydrogels physically cross-linked by strong cooperative hydrogen bonding. *Macromolecules* 46:7423–7435
- Stempfle B, Große A, Ferse B, Arndt KF, Wöll D (2014) Anomalous diffusion in thermoresponsive polymer-clay composite hydrogels probed by wide-field fluorescence microscopy. *Langmuir* 30:14056–14061

- Su X, Zhang G, Xu K, Wang J, Song C, Wang P (2008) The effect of MMT/modified MMT on the structure and performance of the superabsorbent compos. *Polym Bull* 60:69–78
- Swain SK, Shur B, Patra SK (2013) Poly(acrylamide-co-vinyl alcohol)-superabsorbent materials reinforced by modified clay. *Polym Compos* 34:1794–1800
- Takeho H, Nakamura W (2013) Structural and mechanical properties of composite hydrogels composed of clay and a polyelectrolyte prepared by mixing. *Colloid Polym Sci* 291:1393–1399
- Tamesue S, Ohtani M, Yamada K, Ishida Y, Spruell JM, Lynd NA, Hawker CJ, Aida T (2013) Linear versus dendritic molecular binders for hydrogel network formation with clay nanosheets: studies with ABA triblock copolyethers carrying guanidinium ion pendants. *J Am Chem Soc* 135:15650–15655
- Tan KB, Vakili M, Horri BA, Poh PE, Abdullah AZ, Salamatinia B (2015) Adsorption of dyes by nanomaterials: recent developments and adsorption mechanism. *Sep Purif Technol* 150:229–242
- Thakur VK, Thakur MK (2014a) Recent trends in hydrogels based on psyllium polysaccharide: a review. *J Clean Prod* 82:1–15
- Thakur VK, Thakur MK (2014b) Recent advances in graft copolymerization and applications of chitosan: a review. *ACS Sustain Chem Eng* 2(12):2637–2652
- Thakur VK, Thakur MK (2015) Recent advances in green hydrogels from lignin: a review. *Int J Biol Macromol* 72:834–847
- Thatiparti TR, Tammishetti S, Nivasu MV (2010) UV curable polyester polyol acrylate)/bentonite nanocomposites: synthesis, characterization, and drug release. *J Biomed Mater Res B* 92:111–119
- Tu J, Cao Z, Jing Y, Fan C, Zhang C, Liao L, Liu L (2013) Halloysite nanotube nanocomposite hydrogels with tunable mechanical properties and drug release behavior. *Compos Sci Technol* 85:126–130
- Urbano B, Rivas BL (2011) Poly(sodium 4-styrene sulfonate) and poly(2-acrylamidoglycolic acid) nanocomposite hydrogels: montmorillonite effect on water absorption, thermal, and rheological properties. *Polym Bull* 67:1823–1836
- Vaccari A (1999) Clays and catalysis: a promising future. *Appl Clay Sci* 14:161–198
- Vanamudan A, Bandwala K, Pamidimukkala P (2014) Adsorption property of Rhodamine 6G onto chitosan-g-(*N*-vinyl pyrrolidone)/montmorillonite composite. *Int J Biol Macromol* 69:506–513
- Varma AJ, Deshpande SV, Kennedy JF (2004) Metal complexation by chitosan and its derivatives: a review. *Carbohydr Polym* 55:77–93
- Wan T, Cheng W, Zhou Z, Xu M, Zou C, Li R (2015a) Influence of crosslinker amount on swelling and gel properties of hectorite/poly(acrylamide/itaconic acid) nanocomposite hydrogels. *Korean J Chem Eng* 32:1434–1439
- Wan T, Zou C, Wang L, Wu D, Cheng W, Li R, Xu M (2015b) Hectorite effects on swelling and gel properties of hectorite/poly(AM/IA) nanocomposite hydrogels. *Polym Bull* 72:1113–1125
- Wan Ngah WS, Teong LC, Hanafiah MAKM (2011) Adsorption of dyes and heavy metal ions by chitosan composites: a review. *Carbohydr Polym* 83:1446–1456
- Wang Y, Chen D (2012) Preparation and characterization of a novel stimuli-responsive nanocomposite hydrogel with improved mechanical properties. *J Colloid Interface Sci* 372:245–251
- Wang YH, Siu WK (2006) Structure characteristics and mechanical properties of kaolinite soils. I. Surface charges and structural characterizations. *Can Geotech J* 43:587–600
- Wang L, Zhang JP, Wang AQ (2008a) Removal of methylene blue from aqueous solution using chitosan-g-poly (acrylic acid)/montmorillonite superadsorbent nanocomposite. *Colloids Surf A* 322:47–53
- Wang X, Du Y, Luo J (2008b) Biopolymer/montmorillonite nanocomposite: preparation, drug-controlled release property and cytotoxicity. *Nanotechnology* 19:1–7
- Wang Q, Zhang J, Wang A (2009) Preparation and characterization of a novel pH-sensitive chitosan-g-poly (acrylic acid)/attapulgite/sodium alginate composite hydrogel bead for controlled release of diclofenac sodium. *Carbohydr Polym* 78:731–737

- Wang T, Liu D, Lian C, Zheng S, Liu X, Wang C, Tong Z (2011a) Rapid cell sheet detachment from alginate semi-interpenetrating nanocomposite hydrogels of PNIPAm and hectorite clay. *React Funct Polym* 71:447–454
- Wang Y, Ma J, Yang S, Xu J (2011b) PDMAA/clay nanocomposite hydrogels based on two different initiations. *Colloids Surf A* 390:20–24
- Wang T, Sun W, Liu X, Wang C, Fu S, Tong Z (2013a) Promoted cell proliferation and mechanical relaxation of nanocomposite hydrogels prepared in cell culture medium. *React Funct Polym* 73:683–689
- Wang Y, Wang W, Wang A (2013b) Efficient adsorption of methylene blue on an alginate-based nanocomposite hydrogel enhanced by organo-illite/smectite clay. *Chem Eng J* 228:132–139
- Weian Z, Wei L, Yue EF (2005) Synthesis and properties of a novel hydrogel nanocomposites. *Mater Lett* 59:2876–2880
- Xia M, Cheng Y, Meng Z, Jiang X, Chen Z, Theato P, Zhu M (2015) A novel nanocomposite hydrogel with precisely tunable UCST and LCST. *Macromol Rapid Commun* 36:477–482
- Xiang Y, Peng Z, Chen D (2006) A new polymer/clay nano-composite hydrogel with improved response rate and tensile mechanical properties. *Eur Polym J* 42:2125–2132
- Xiong L, Hu X, Liu X, Tong Z (2008) Network chain density and relaxation of in situ synthesized polyacrylamide/hectorite clay nanocomposite hydrogels with ultrahigh tensibility. *Polymer* 49:5064–5071
- Xu K, Wang J, Xiang S, Chen Q, Yue Y, Su X, Song C, Wang P (2007a) Polyampholytes superabsorbent nanocomposites with excellent gel strength. *Compos Sci Technol* 67:3480–3486
- Xu K, Wang J, Xiang S, Chen Q, Zhang W, Wang P (2007b) Study on the synthesis and performance of hydrogels with ionic monomers and montmorillonite. *Appl Clay Sci* 38:139–145
- Yavari-Gohar MR, Kabiri K, Zohuriaan-Mehr MJ, Hashemi SA (2010) Thermo-hydrolytic stability of swelling capacity of superabsorbing composite hydrogels based on AMPS and acrylamide. *J Polym Res* 17:151–159
- Yi JZ, Zhang LM (2007) Studies of sodium humate/polyacrylamide/clay hybrid hydrogels. I. Swelling and rheological properties of hydrogels. *Eur Polym J* 43:3215–3221
- Yi JZ, Zhang LM (2008) Removal of methylene blue dye from aqueous solution by adsorption onto sodium humate/polyacrylamide/clay hybrid hydrogels. *Bioresour Technol* 99:2182–2186
- Yuan Q, Shah J, Hein S, Misra RDK (2010) Controlled and extended drug release behavior of chitosan-based nanoparticle carrier. *Acta Biomater* 6:1140–1148
- Zhang FQ, Guo ZJ, Gao H, Li YC, Ren L, Shi L, Wang LX (2005a) Synthesis and properties of sepiolite/poly(acrylic acid-co-acrylamide) nanocomposites. *Polym Bull* 55:419–428
- Zhang J, Chen H, Wang A (2005b) Study on superabsorbent composite. III. Swelling behaviors of polyacrylamide/attapulgitic composite based on acidified attapulgitic and organo-attapulgitic. *Eur Polym J* 41:2434–2442
- Zhang LM, Zhou YJ, Wang Y (2006) Novel hydrogel composite for the removal of water-soluble cationic dye. *J Chem Technol Biotechnol* 81:799–804
- Zhang Q, Li X, Zhao Y, Chen L (2009) Preparation and performance of nanocomposite hydrogels based on different clay. *Appl Clay Sci* 46:346–350
- Zhang Q, Chen L, Dong Y, Lu S (2013) Temperature-sensitivity and cell biocompatibility of freeze-dried nanocomposite hydrogels incorporated with biodegradable PHBV. *Mater Sci Eng C* 33:1616–1622
- Zhang Q, Zhang T, He T, Chen L (2014a) Removal of crystal violet by clay/PNIPAm nanocomposite hydrogels with various clay contents. *Appl Clay Sci* 90:1–5
- Zhang S, Guan Y, Fu GQ, Chen BY, Peng F, Yao CL, Sun RC (2014b) Organic/inorganic superabsorbent hydrogels based on xylan and montmorillonite. *J Nanomater*. Article ID 675035
- Zhang Y, Gu Q, Yin J, Wang Z, He P (2014c) Effect of organic montmorillonite type on the swelling behavior of superabsorbent nanocomposites. *Adv Polym Technol* 33:21400

- Zhao M, Xu Y, Zhang C, Rong H, Zeng G (2016) New trends in removing heavy metals from wastewater. *Appl Microbiol Biotechnol* 100:6509–6518
- Zheng Y, Wang A (2009) Evaluation of ammonium removal using a chitosan-g-poly (acrylic acid)/rectorite hydrogel composite. *J Hazard Mater* 171:671–677
- Zheng Y, Li P, Zhang J, Wang A (2007) Study on superabsorbent composite XVI. Synthesis, characterization and swelling behaviors of poly(sodium acrylate)/vermiculite superabsorbent composites. *Eur Polym J* 43:1691–1698
- Zheng Y, Xie Y, Wang A (2012) Rapid and wide pH-independent ammonium-nitrogen removal using a composite hydrogel with three-dimensional networks. *Chem Eng J* 179:90–98
- Zheng X, Wu D, Su T, Bao S, Liao C, Wang Q (2014) Magnetic nanocomposite hydrogel prepared by ZnO-initiated photopolymerization for La (III) adsorption. *ACS Appl Mater Inter* 6:19840–19849
- Zhu M, Liu Y, Sun B, Zhang W, Liu X, Yu H, Zhang Y, Kuckling D, Adler HJP (2006) A novel highly resilient nanocomposite hydrogel with low hysteresis and ultrahigh elongation. *Macromol Rapid Commun* 27:1023–1028
- Zhu M, Xiong L, Wang T, Liu X, Wang C, Tong Z (2010) High tensibility and pH-responsive swelling of nanocomposite hydrogels containing the positively chargeable 2-(dimethylamino) ethyl methacrylate monomer. *React Funct Polym* 70:267–271
- Zhu L, Liu P, Wang A (2014) High clay-content attapulgite/poly(acrylic acid) nanocomposite hydrogel via surface-initiated redox radical polymerization with modified attapulgite nanorods as initiator and cross-linker. *Ind Eng Chem Res* 53:2067–2071

Chapter 2

An Overview on Polymer Gels Applied to Enzyme and Cell Immobilization



Gustavo Pagotto Borin, Ricardo Rodrigues de Melo, Elaine Crespim, Helia Harumi Sato and Fabiano Jares Contesini

Abstract Immobilization of enzymes and cells is crucial in several industrial areas. This is mainly due to the possibility to improve enzyme properties including thermal stability, substrate selectivity, and biocatalyst reuse. These modifications allow for a considerable decrease in the cost of many commercial applications. The use of polymer gels for cell and enzyme immobilization presents numerous advantages over other immobilization supports, since they allow the protein or cell entrapment to be performed in a more efficient and simpler way. The polymers used here include polysaccharides and synthetic polymers in which several industrially relevant enzymes were immobilized with positive results. In addition to the immobilization of enzymes, there are many studies reporting the immobilization of microbial cells in polymers for enzyme production. Enzyme and cell immobilization in polymer gels show potential to deliver useful and efficient strategies to make use of microbial enzymes from an industrial point of view. However, further efforts must be made to better understand and apply immobilization of biocatalysts and to develop new technologies. This chapter focuses on general aspects of polymer gels, particularly regarding the immobilization of enzymes and microbial cells in different industrial fields.

Keywords Polymer gel · Immobilization · Microbial enzymes
Whole-cells

G. P. Borin · R. R. de Melo · E. Crespim · F. J. Contesini (✉)
Laboratório Nacional de Ciência E Tecnologia Do Bioetanol (CTBE), Centro Nacional de Pesquisa Em Energia E Materiais (CNPEM), Campinas, Brazil
e-mail: fabiano.contesini@gmail.com

G. P. Borin · F. J. Contesini
Institute of Biology, University of Campinas, Unicamp, Brazil

R. R. de Melo · H. H. Sato
College of Food Engineering, University of Campinas, Campinas, Brazil

1 Introduction

Polymer gels comprise a great variety of different polymeric compounds that present innumerable industrial applications. Polymers can be naturally produced, in which case the most representative group is polysaccharides (Thakur and Thakur 2014a, b). This includes alginate, chitosan, and agar-agar. Some polysaccharides form gels through ionic gelation in the presence of ions like calcium (Ca^{2+}), such as alginate or pectin, while other gels solidify in high temperatures. In addition to polysaccharides, lignin based hydrogels have recently been studied and reviewed (Thakur and Thakur 2015). On the other hand, a wide variety of synthetic polymers capable of forming gels presents different industrial applications, such as polyacrylamide and polyvinyl alcohol.

An extremely important use of polymer gels is for biocatalyst immobilization, fixing in place microbial enzymes or cells (Lahiri 2015; Wilkowska et al. 2015). In the latter case, the cells can be entrapped and used for biotransformation or they can be used for the production of enzymes with industrial interest (Kamble and Banoth 2013; Hemachander et al. 2001). Immobilization of biocatalysts takes place via the fixation of the protein or cells to a support medium through any of various means including adsorption, covalent bonding, or entrapment inside a polymeric matrix. The last technique is the main focus of this review, as several polymer gels can be used for enzyme or cell entrapment and is a method in which activity loss is low when compared to other techniques.

Enzyme or cell immobilization allows the reuse of the biocatalyst and reduces cost if the catalytic activity is maintained. Furthermore, the enzyme immobilization process is able to allow for an improvement in the stability of the enzyme (Milessi et al. 2015). Lastly, both the advantages and disadvantages of immobilizing enzymes as well as comparing this to microbial cells will be discussed.

In this chapter, various aspects of polymer gels applied to enzyme and cell immobilization will be discussed. Initially, polymer gels used for biocatalyst immobilization will be introduced, followed by a more detailed discussion on enzyme immobilization. Afterwards, the results of cell entrapment in gels will be reported.

2 Supports for Entrapment Techniques

Determining the appropriate immobilization support is an important step in the development of feasible and efficient processes. The choice of polymeric matrix determines the rigidity, absorption capacity, mechanical strength, and porosity characteristics of the beads used in immobilization. Physical entrapment of cells and enzymes within a polymeric matrix is recognized as being one of the most used immobilization techniques. The entrapment method utilizes a simple and single-step procedure for both cell and enzyme immobilization within a polymeric

network. Typically, entrapment techniques utilize any of several natural and synthetic supports for efficient immobilization. The use of natural polymers such as chitosan, chitin, alginate, and many others have been applied as important matrices for immobilization (Table 1) (Hsuanyu 2004; Taylor et al. 2010; Zajkoska et al. 2013). Natural polymeric materials used in entrapment processes demonstrate important characteristics, such as their ability to be gathered from many sources, ease of modification, and lack of pollutants. Furthermore, they have a range of functional groups and good biocompatible properties such as being non-toxic and inert to organisms that are often necessary for applications in the pharmaceutical and food industries (Zhang et al. 2013).

In other science sectors, synthetic polymeric matrices are also efficiently applied for the immobilization of cells and enzymes. Synthetic polymers present several advantages: good mechanical rigidity, high specific surface area, easy alteration of their surface characteristics, and their potential for providing specific functional groups that match the individual needs of each bioprocess. Other advantages offered by synthetic polymers are that they can be synthesized in larger amounts more easily than most natural polymers, and do not suffer batch-to-batch variations like natural polymers (Zhang et al. 2013; De Vos et al. 2014). In general, polyvinyl alcohol, polyacrylamide, and polyacrylonitrile are often the most suitable synthetic matrices for gel immobilization (Table 1).

Table 1 Commonly used materials for entrapment techniques

	Compounds carriers	Formation principle	Gel geometry
Natural polymers	Alginate	Ionotropic gelation	Gel cylinder/ beads
	Cellulose	Ionotropic gelation	Beads
	Chitosan	Ionotropic gelation	Beads
	Chitin	Ionotropic gelation	Beads
	Pectin	Ionotropic gelation	Beads
	Pectate	Ionotropic gelation	Beads
	Carrageenan	Ionotropic/thermal gelation	Gel cylinder
	Gelatin	Thermal gelation	Gel cylinder
	Agar	Thermal gelation	Gel cylinder/ beads
Agarose	Thermal gelation	Gel cylinder	
Synthetic polymers	Polyvinyl alcohol— PVA	Thermal gelation	Lentikats/gel
	Polyacrylamide	Chemical gelation	Gel cylinders/ beads
	Polyacrylonitrile	Thermal gelation	Beads

2.1 Natural Polymers

2.1.1 Immobilization in Ionic Hydrogels

A wide variety of ionic hydrogels are used as supports for cell and enzyme entrapment. Normally, ionic hydrogels used in immobilization are alginate, cellulose, chitosan, chitin, pectin, and pectate. Ionic hydrogels contain ionizable groups in their structures such as amino groups, carboxylates, sulfates, and hydroxyls that possess varying degrees of affinity with water molecules. In addition, several anionic polymers are also utilized with their own benefits and drawbacks.

Alginate is a natural anionic biomaterial formed by β -D-mannuronic acid and α -L-glucuronic acid chains. The L-glucuronic acid content present in the alginate's structure has great importance on its mechanical rigidity and can influence the stability of the gels in the presence of anti-gelling ions and calcium ion sequesters. Structurally, alginates rich in glucuronic acid exhibit high porosity and low shrinkage capacity during gel formation and do not swell when dried. In contrast, alginates showing higher mannuronic acid levels make the gels softer and more elastic (Thu et al. 1996). Alginate gels can be constructed by an ionic network in the presence of cations such as Ca^{2+} or other multivalent counterions (Orive et al. 2006).

Cellulose is a natural, semi-crystalline polysaccharide that is very abundant on earth, typically composed of 1,4-linked β -D-glucopyranosyl chains. Cellulose is a very useful matrix for enzyme immobilization due to its low cost and commercial availability both in fibrous and granular forms. However, this support is accompanied by some drawbacks, such as susceptibility to hydrolysis by microbial enzymes (cellulases) and low particle size, which impairs their use in rapid high-pressure applications (Hsuanyu 2004; Agbor et al. 2011).

Chitosan is a polymer obtained from deacetylated chitin chains, and is the second most abundant support compound that can be obtained from nature after cellulose. It is a natural product, non-toxic, biocompatible, biodegradable, and inexpensive, making it very important, both economically and environmentally. Chitosan is a polymer that has a molecular structure similar to cellulose, only differing in a few specific functional groups. The main difference between these biopolymers is the presence of amino groups ($-\text{NH}_2$) in the chitosan structure. Chitosan is recognized for its solubility in dilute acid media, forming a polymer with cationic characteristics due to the protonation of the amino group, generating an ammonium ($-\text{NH}_3^+$) ion, which gives special properties to this biomaterial (Berger et al. 2004; Mendes et al. 2011).

Carrageenans are described as a family of linear, sulfated polysaccharides and are isolated from certain species of red seaweed. These polysaccharides are inexpensive and possess distinct, flexible helical structures that give them the capacity to form a variety of distinct gels. The formation of carrageenan gels can be carried out either by cooling or by interacting with an aqueous solution containing cations (i.e. K^+ ,

Cu^{2+} , Fe^{3+} , Mg^{2+} , NH_4^+ , Ca^{2+} , and Mn^{2+}), amine-containing compounds, and/or water-miscible organic solvents (Van De Velde et al. 2002; Zajkoska et al. 2013).

Pectins are one of the main water-soluble structural polysaccharides present in plant cell walls. Structurally, pectins are formed by biopolymers of 1,4- α -D-galacturonic acid partially linked by methyl esterification. The process of pectin gelation is carried out by connection between the divalent cations and polygalacturonate structure. The gelling reaction is depicted using the egg-box model where the divalent cations form non-covalent interpolymer associations with clusters of two or sometimes four adjacent polygalacturonate structures (Braccini and Pérez 2001; Müller-Maatsch et al. 2016).

2.1.2 Immobilization in Thermogels

Gelatin consists of proteins and peptides derived from the partial hydrolysis of collagen extracted from skin and bones. The proteins found in gelatin are applicable in various sectors in the food industry due to their physical properties, such as a melting point similar to physiological temperatures. The gelatin-based immobilization process has already been developed for the immobilization of different cells and enzymes. The gelation process of gelatin can occur reversibly with temperature; however, when solutions are cooled to 30–35 °C, more efficient immobilization occurs. However, some techniques have been described as achieving an irreversible gelation process, for example, using cross-linking compounds (Tanriseven and Doğan 2002; Yang and Ou 2005; Górecka and Jastrzębska 2011).

Agar and agarose are polysaccharides used as entrapment supports for cells and enzymes. Agar is an inert polymer composed of two principal components: agarose and agaropectin. Agarose is a heteropolysaccharide with neutral properties that has a strong ability for gelation. Agar and agarose are both advantageous in their price, availability, acid tolerance, and low reactivity with other biomolecules (Duckworth and Yaphe 1971). However, their use is limited by their low melting points (Zajkoska et al. 2013).

2.2 Synthetic Polymers

Among synthetic gels, polyacrylamide was the first matrix used for cell immobilization and is currently the most used matrix for enzyme entrapment. The polyacrylamide matrix has the advantage of being nonionic and the properties of immobilized enzymes are only minimally altered when in its gel matrix. However, the initiator of the polymerization process, dimethylaminopropionitrile, is highly toxic and requires great care (Hsuanyu 2004).

An alternative is polyvinyl alcohol (PVA), a non-toxic thermoplastic polymer, and is biodegradable, water-soluble, and biocompatible. Polyvinyl alcohol is commercially obtained from polyvinyl acetate, in which the vinyl acetate is

hydrolyzed to form vinyl alcohol groups. PVA is completely insoluble in organic solvents with the exception of ethanol, in which it exhibits low solubility. As a thermoplastic polymer, it can be converted to different structures by freeze-thawing processes and as such, the gelation of PVA is performed through repeated freeze-thawing cycles (Qi et al. 2004; Vrana et al. 2009).

Polyacrylonitrile is a synthetic polymer that has attracted considerable attention due to some important features, such as chemical resistance, abrasion resistance, and thermal stability. However, a major obstacle to the long-term use of a polyacrylonitrile matrix is its biodegradability and low hydrophilicity (Stoilova et al. 2010; Potvorova et al. 2012; Feng et al. 2013).

3 Enzyme Immobilization in Polymer Gels

Polymer gels, whether natural or synthetic, can be used for entrapment by utilizing the porous matrix of the gel. In this context, biocatalyst immobilization is rising as a useful and robust technology to facilitate and improve many bioconversion processes based on whole cells or enzymes. Among the many advantages of this technology are the following: (i) increase of the robustness of the biocatalyst, (ii) possibility of reuse, (iii) improvement of the product yield, and (iv) reduction or even elimination of hazardous and toxic substances from the process (Zajkoska et al. 2013; Kras et al. 2016).

According to IUPAC (1997), biocatalyst immobilization is the fixation of a cell or its derivatives (e.g. organelles and proteins) into or onto a support to increase their stability and prolong their use. In other words, the immobilized structure may be inside or alongside a support depending on the desired purpose and type of immobilization method applied. Likewise, the cells and their derivatives may be retained by a membrane (Kras et al. 2016). In choosing the best method of immobilization, four criteria must be considered: (1) the substrates that will be used for biotransformation or production and the type of biocatalyst used (enzyme or whole-cell); (2) the equipment to be used for the biocatalysis reaction; (3) the downstream-process technology necessary for the purification of the product(s); and (4) how to avoid the release of compounds toxic to humans or the environment (Bianchini et al. 2015).

In this section, different studies on enzyme immobilization using various polymer gels are discussed.

3.1 Enzyme Immobilization Using Alginate

For a more efficient and feasible process, the immobilization conditions using calcium alginate must be optimized. Alginate concentration is a very important parameter, since higher concentrations of sodium alginate may result in a decrease

of pore size which can limit the ability of compounds to reach the enzymes (Kumar et al. 2009). Another important parameter is CaCl_2 concentration, since high concentrations of this compound can modify the pH of the system and affect enzyme activity (Rehman et al. 2014).

It is possible that some of an enzyme's characteristics can suffer alterations after immobilization in gels, such as an increase of the optimum temperature of its reaction (likely due to physical limitations of enzymes within the interior of the gel). This results in a higher activation energy needed for the substrate to easily diffuse into the beads and bind to the biocatalyst (Kara et al. 2006). In addition, thermal stability of a confined protein can be altered compared to the free form, often likely due to the restriction in conformational changes allowed, directly caused by the support matrix (Shah et al. 2008).

Abdulla and Ravindra (2013) described the immobilization of a microbial lipase using glutaraldehyde and gel confinement into a hybrid matrix of equal amounts of κ -carrageenan and alginate. The immobilization of the lipase improved certain properties of the enzyme, including its thermal stability and hydrolysis performance. The immobilized enzyme showed an activity yield of 89.26%, and maintained 84.02% of its activity after being stored at 4 °C for 14 days. And subsequently, after being run for 10 cycles, it was still possible to observe 75.54% of enzymatic activity. As for the evaluation of the influence of immobilization on the enzyme properties, both enzyme preparations were characterized, showing that V_{\max} values remained approximately similar, while K_m values changed considerably between the free and immobilized lipase.

Awad et al. (2015) studied the immobilization of phytase from *Penicillium purpurogenum* GE1 on grafted alginate/carrageenan beads. The authors observed maximum loading capacity after 20 h at the enzyme: acetate buffer dilution ratio of 1:2. Some properties of the confined enzyme were different from those observed in the free form. The optimal temperature and pH of the immobilized preparation were greater than the soluble one. The immobilized biocatalyst was more stable in higher temperatures (50 °C for 1 h) and acidic pH conditions (pH 4 for 45 min). In addition, the immobilization allowed 100% activity retention when the enzyme was incubated at 4 °C for 3 months, while the free form preparation completely lost activity after 4 weeks when incubated at the same temperature. Regarding the reusability of the immobilized enzyme, the gel beads containing the enzyme maintained 100% activity for more than 12 repeated batch reutilizations.

The immobilization of a pectinase from *Bacillus licheniformis* KIBGE-IB21 into calcium alginate has been studied by Rehman et al. (2014). These enzymes are particularly important since they catalyze the hydrolysis of pectin and are industrially applied such as in the clarification of fruit juices. The authors optimized the concentration of calcium chloride and sodium alginate, 0.2 M and 3.0%, respectively. The immobilized enzyme showed increased optimal reaction time for the degradation of pectin, showing an increased optimal activity. In addition, the entrapped enzyme showed increased thermal stability.

In another experiment, a commercial α -amylase (Diastase) was entrapped in calcium alginate beads. The best conditions for immobilization were 4% (wt/v)

sodium alginate, 1 M calcium chloride, and 2 h of curing time and as a result, 85% of immobilization yield was obtained. Immobilized enzymes showed a higher K_m than the free enzyme, indicating that the substrate affinity of α -amylase was decreased after immobilization (Lahiri 2015).

3.2 Enzyme Immobilization Using Agar

An important gel for the immobilization of enzymes is agar, since it is biocompatible, non-toxic, and has strong solidifying properties. As in the case of other gels, the concentration of agar is very important for protein immobilization, since the porosity of the agar matrix is dependent on the concentration of agar used. And once again, the optimal pH and temperature of the enzyme can be altered after immobilization in agar (Rehman et al. 2014).

Xylooligosaccharides are important, small oligosaccharides (2–10 units) that present interesting functional properties. These compounds are produced through hydrolysis of xylan, catalyzed by endoxylanases. As such, the use of immobilization for the entrapment of xylanase can be of great interest, since it can reduce the cost of the industrial process. In the study by Milesi et al. (2015), a recombinant endoxylanase from *Bacillus subtilis* was immobilized in different gel-based supports, with immobilization yields above 80%. A remarkable increase was observed in the stability of the proteins immobilized in chitosan or agarose activated by glyoxal groups. The authors explained that the thermal stability observed for the agarose-glyoxal derivative was probably due to lysine residues present in unstable sites.

Bibi et al. (2015) studied an endoxylanase that hydrolyzes xylan, presenting several applications, including in the pulp and paper industry. The authors immobilized this xylanase from *Geobacillus stearothermophilus* KIBGE-IB29 in agar-agar gel beads and the best results were found using 2.5% of the polymer. The optimum temperature increased by 10 °C (from 50 to 60 °C) for the immobilized biocatalyst. In addition, the immobilization led to an increase in thermal stability, retaining 79.0% of activity at 80 °C while the free enzyme completely lost activity at this temperature. The immobilized enzyme was successfully reused for up to six reaction cycles.

3.3 Enzyme Immobilization Using Chitosan

Chitosan is a well-studied support for the immobilization of enzymes because of the availability of various chitosan products with different N-deacetylation grades (Betigeri and Neau 2002). It is frequently studied for the immobilization of enzymes in combination with other gels. This is based on the intense electrostatic interactions of the carboxyl groups of supports like alginate with the amine groups

of chitosan, resulting in chitosan–alginate hybrid gels. Frequently, these hybrid gels are stronger than pure chitosan and is what makes them have a longer activity span under intense conditions of temperature and mechanical agitation (Mi et al. 2002). Finally, chitosan has low cost and a lack of toxicity and biological reactivity.

In one experiment, the purified α -amylase from *Exiguobacterium* sp. DAU5 was immobilized in chitosan beads, utilizing glutaraldehyde (Fang et al. 2016). The immobilized enzyme displayed higher organic-solvent tolerance than free enzymes. The specific activity of the enzyme immobilized in chitosan beads and chitosan-carbon beads was 2240 and 2320 U/g, respectively. The optimal conditions for the immobilized protein were 50 °C and pH 8.5.

In a study by Xie and Wang (2011), the commercial lipase from *Candida rugosa* was immobilized in magnetic chitosan microspheres using glutaraldehyde. The esterification of soybean oil had a maximum yield of 87% using the ratio of methanol:oil of 4:1, at 35 °C, after a 30 h reaction time. Furthermore, the immobilized protein was used 4 times without a significant decrease in performance.

In a different experiment, a *C. rugosa* lipase was covalently immobilized in magnetic Fe₃O₄–chitosan nanoparticles. The best results obtained were 20 U/g of Fe₃O₄–chitosan. The immobilized preparation was utilized in twenty repeated uses, retaining more than 83% of its initial activity. In addition, lipases after immobilization remained stable over wide ranges of pH and temperature (Kuo et al. 2012).

3.4 Enzyme Immobilization in Synthetic Polymers

Non-natural polymers have also been studied for enzyme immobilization. These matrices allow the obtention of particles with good mechanical and chemical stability and appear to be promising alternatives to natural polymers to overcome the disadvantages of some polysaccharides (Lozinsky et al. 2003; Schlieker and Vorlop 2006).

A commercial invertase was immobilized in a system composed of polyacrylamide and gelatin (Emregul 2006). The authors observed that the K_m values were 166 and 86 mM for immobilized and free enzymes, respectively. All immobilized preparations were successfully utilized twenty times within 60 days approximately, still showing good activity.

Fernandes et al. (2009) studied the immobilization of an inulinase with invertase activity in particles composed of PVA. After immobilization, the enzyme showed a broadened optimal pH towards lower values, as well as good mechanical stability of the particles when the temperature was above 55 °C. The authors observed a 1.8-fold increase in K_m , probably due to diffusion limitations. In addition, a 10% decrease in the reaction yield was observed at a reaction temperature of 50 °C, after 20 repeated, consecutive batches.

4 Immobilization of Whole Cells Using Polymer Gels Applied to Biocatalysis and Biotransformation

Immobilized cells in gelatinous and porous matrices have been extensively employed in the last decades, with reports dating back to before the 1960s. In 1960, Hattori and Furusaka published a work evaluating cells of the bacterium *Escherichia coli* in relation to the changes in its chemical activity after immobilization in a resin. They observed a decrease in substrate oxidation activity that persisted even after the detachment of the adsorbed cells. In 1974, a strategy was announced for the use of immobilized cells for the continuous fermentation of L-aspartic acid (Chibata et al. 1974a, b; Ramakrishna and Prakasham 1999; Martins et al. 2013).

The ability to immobilize microorganisms like bacteria, yeasts, and fungi (Meunier et al. 2010) combined with their capacity to display the functional properties of their proteins on the cell surface or at the intracellular microenvironment has made it possible for many species to be used for cell immobilization. In addition, this has been accomplished in diverse types of natural (agar, agarose, and pectin), synthetic (PVA and polyacrylamide), and hybrid supports (derived from the incorporation of organic and inorganic materials) (Ramakrishna and Prakasham 1999; Fukuda et al. 2008; Desimone et al. 2009; Léonard et al. 2011). For immobilization, filamentous fungi and yeasts have often been chosen as some of the most resistant cell biocatalyst systems for industrial purposes, such as the filamentous fungi *Rhizopus niveous*, *Rhizopus chinensis*, *Mucor circinelloides*, *Rhizomucor miehei*, *Trichoderma reesei*, *Aspergillus niger*, and the yeasts *Saccharomyces cerevisiae* and *Yarrowia lipolytica* (Kumakura et al. 1989; Ramakrishna and Prakasham 1999; Fukuda et al. 2008; Robles-Medina et al. 2009; Andrade 2012).

In this section, special attention will be given to whole-cell immobilization. Basically, an immobilization process consists of the attachment of cells to a solid phase (matrix or membrane support), enabling the exchange of nutrients and gases between the cells and the broth medium (Ramakrishna and Prakasham 1999).

Cell immobilization techniques have been described for many plant and mammalian cells (Seifert and Phillips 1997; Uludag et al. 2000; Murthy et al. 2014), as well as bacterial and fungal strains, with positive results for both natural and genetically modified types (Shriver-Lake et al. 2002; Prasad et al. 2005; Mrudula and Shyam 2012; Bisht et al. 2013). As previously mentioned, the main methods used are adsorption, covalent bonding/cross-linking, entrapment, and encapsulation (Fig. 1). Cell-matrix interaction, biocompatibility of the carrier, mass transfer, and aeration of the cells are some of the factors that affect whole-cell immobilization (Nedovic and Willaert 2004; Liu and Wang 2010) and thus influence the parameters for an experiment. Each method has its pros and cons, making one more suited for a specific application than another (Desimone et al. 2009; Pajic-Ilijakovic et al. 2015), but entrapment is the most used cell immobilization method (Trelles and Rivero 2013).

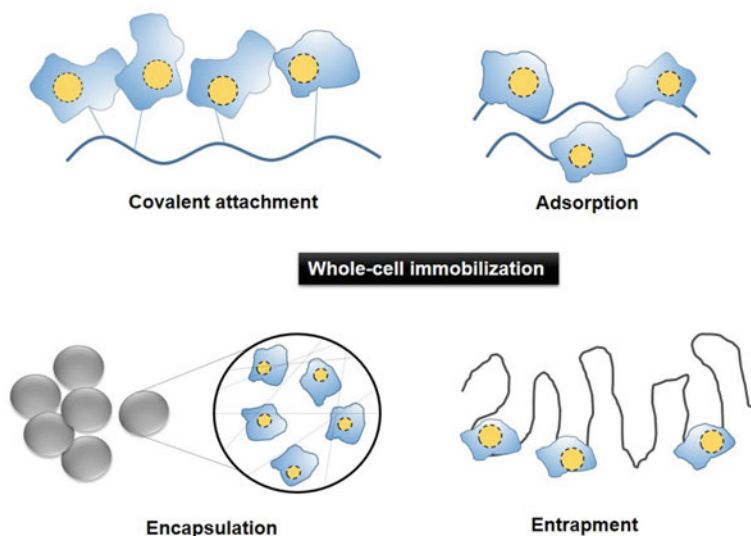


Fig. 1 Different strategies for whole-cell immobilization

Some studies have been carried out to understand the physiological and morphological changes that cells may undergo when they are immobilized (Omar et al. 1992; Niu et al. 2013). Due to various physical characteristics of supports, the choice of polymer may also influence cell productivity, seemingly even differing across microorganisms (Bisht et al. 2013; Chandorkar et al. 2014). Further building upon that data, attempts to attain the optimal conditions for a particular product's production or bioconversion (Chen et al. 2012) as well as studies focusing on the development of new polymer gels with different characteristics (Niu et al. 2013) were also carried out.

4.1 Whole-Cell Immobilization Versus Enzyme Immobilization

In contrast with individual enzymes, whole-cell immobilization is preferred for having all the needed catalysts and cofactor regeneration for a specific reaction (Bianchini et al. 2015). This technology is cheaper than enzyme immobilization and has excellent operational stability, providing a valid alternative to improve industrial processes (Fukuda et al. 2008). Likewise, immobilization is exceptionally useful for certain microorganisms that exhibit different morphologies throughout their life cycles, as is the case of fungi (Prasad et al. 2005). These cells can be immobilized in a morphological state that allows their highest catalytic activity, therefore assuring the maintenance of their highest productivity form for a longer

period (Covizzi et al. 2007). In addition, immobilized cells can work in a higher concentration than free cells, which increases fermentation speed and throughput, guarantees the synthesis of the metabolites, and protects the living cells from environmental stress factors that might arise from the process such as pH changes, high concentrations of the end-products, or phenols and other toxic compounds (Bisht et al. 2013; Martins et al. 2013; Vilela et al. 2013; Lin et al. 2015).

Still, the major advantage of cell immobilization, often cited in literature, is that they are easily recovered and can be reused for many cycles, remaining nearly just as effective as in the first use for a long period (Pradella 2001). Additionally, continuous systems can be operated above the usual μ_{\max} (maximum specific growth rate) observed for free cells. In this sense, Chandorkar et al. (2014) observed that lipase production by *A. niger* entrapped in sodium alginate remained almost the same after 4 cycles, whereas Bisht et al. (2013) described the maintenance of lipase activity by *Pseudomonas aeruginosa* for 7 cycles in a bioreactor. In another study (Duarte et al. 2013), *S. cerevisiae* cells were evaluated for ethanol production through the fermentation of glucose and sucrose after immobilization using two different substrates, calcium alginate and calcium alginate covered with chitosan. In both cases, the immobilized cells could withstand 8 fermentation cycles of 10 h each, with no observed contamination.

In contrast with the easier whole-cell recovery, enzyme immobilization is an expensive technology due to the enzyme recovery and purification steps that are required to obtain the desired products from the fermentation broth. Furthermore, there may be losses during the enzyme purification process, as well as catalytic activity reduction (Sührer et al. 2015). Conversely, some disadvantages of whole-cell immobilization must be considered, namely: (1) it can generate undesired byproducts and/or toxic metabolites which might damage the cell biocatalyst; (2) possibility of cell leakage from the carrier; and (3) alteration in the physiology and growth kinetics of the cells (Hattori and Furusaka 1959; Mattiasson and Hahn-Hägerdal 1982; Robles-Medina et al. 2009; Martins et al. 2013; Sührer et al. 2015). Mattiasson and Hahn-Hägerdal (1982) discussed that many studies had demonstrated that immobilized cells have alterations in metabolism in comparison to the same free cells. According to these authors, while in some cases growth rates might be reduced, specific metabolites can become highly produced, of which industrial processes take advantage. They propose that the microenvironment of entrapped cells might be responsible for such changes, more specifically due to a decreased water activity and/or oxygen deficiency. Vilela et al. (2013) also discuss that the interior of the polymer beads, having a limited access to the substrate, does not promote cellular growth. The authors point to other studies that suggest it is the microenvironment inside the gelatinous bead—and not the polymer itself—that causes changes in the entrapped microbial cell physiology.

The advances in the understanding of the metabolism and physiology of microorganisms and cells and the development of new matrices allowed the use of cell immobilization for various applications, predominantly the production of ethanol, biodiesel and alcohols, organic acids, antibiotics and enzymes; aroma formation; the bioremediation of waste residues; and biosensors. Some of these

practical applications are described below, concretely showing the vast potential of this technology.

4.2 Applications of Whole-Cell Immobilization

4.2.1 Biodiesel Production

Biodiesel fuel (BDF) is composed of fatty acid alkyl esters or methyl esters (MEs) derived from vegetable oil or animal fats and may be produced from any of three different reactions: (i) pyrolysis (or cracking), (ii) microemulsion, or (iii) transesterification. The first two options are considered too expensive for industrialization and yield low-quality biodiesel. The transesterification (i.e. acidolysis, alcoholysis, or interesterification, depending on the acyl group acceptor) is the most common reaction used to produce biodiesel (Robles-Medina et al. 2009). It consists of a reaction between triglycerides (TAGs) from an oil or fat along with an acyl-acceptor, such as alcohols like methanol and ethanol. As products of this reaction, methyl esters (MEs or biodiesel) and glycerol (via alcoholysis) can be formed, as well as another triacylglycerol (via interesterification) (Fig. 2) (Huang et al. 2012).

Transesterification can be catalyzed by acids such as sulfuric acid (H_2SO_4) or phosphoric acid (H_3PO_4), bases such as potassium hydroxide (KOH) or sodium hydroxide (NaOH), enzymatically, or through lipases attached to the surface of immobilized cells or overexpressed in the intracellular environment (Fig. 2) (Fukuda et al. 2008; Robles-Medina et al. 2009). An alkaline biocatalyst is the most used process worldwide for transesterification catalysis, contributing to almost 100% of the biodiesel production process as of 2008 (Demirbas 2008; Robles-Medina et al. 2009).

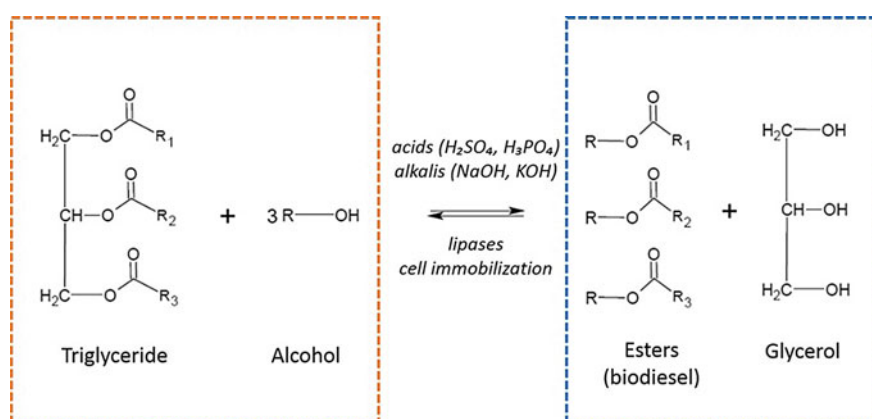


Fig. 2 Example of transesterification reactions (alcoholysis) and types of catalysts used for biodiesel production

Facing the need to discover another low-cost and more environmentally friendly way to produce biodiesel than by an alkaline biocatalyst or enzymatic process, cell immobilization recently appeared as an attractive substitute due its aforementioned advantages. The first project with this type of technology aimed at BDF production was described by Ban et al. (2001). In this work, the 1,3-specific fungal lipase (ROL) of *Rhizopus oryzae* cells was immobilized within biomass support particles (BSPs). They were then used for the catalysis of the transesterification reactions and ME production. Interestingly, ME content reached 90% yield, the same percentage obtained by extracellular lipases (Ban et al. 2001), and these results supported further research regarding cell immobilization as a good alternative to produce biodiesel.

Since then, many other studies have been conducted to discover the most appropriate culture conditions and microorganisms for whole-cell immobilization systems and to attain the same—or higher—levels of biodiesel production obtained through the enzymatic process. Table 2 shows a small bibliographic survey with some promising studies of biodiesel production.

Table 2 Whole-cell immobilization of microorganisms, culture conditions, and biodiesel yield (ME %)

Microorganism	Support	Carbon source	Oil	Alcohol	ME** (%)	References
<i>R. oryzae</i>	BSP*	Olive oil and glucose	Soybean oil	Methanol	90	Ban et al. (2001, 2002), Hama et al. (2007), Hama et al. (2015)
<i>R. oryzae</i>	BSP*	Fatty acids	Soybean oil	Methanol	80	Hama et al. (2004)
<i>R. oryzae</i>	BSP*	Olive oil or glucose	Jatropha oil	Different alcohols	89	Tamalampudi et al. (2008)
<i>R. oryzae</i>	BSP*	Soybean oil	Soybean oil	Methanol	70	Li et al. (2007a)
<i>R. oryzae</i>	BSP*	Soybean oil	Rapeseed oil	Methanol	72	Li et al. (2007b)
<i>R. oryzae</i>	BSP*	Soybean oil	Oleic acid	Methanol	90	Li et al. (2008)
<i>R. oryzae</i>	BSP*	Olive oil	Soybean oil	Methanol	73	Chen and Lin (2010)
<i>R. oryzae</i>	Sodium alginate	Olive oil	Jatropha oil	Methanol	80.5	Ganesan et al. (2011)
<i>A. niger</i>	BSP*	Olive oil	Palm oil	Methanol	87	Xiao et al. (2010)
<i>S. cerevisiae</i> (intracellular ROL)	–	Glucose	Soybean oil	Methanol	71	Matsumoto et al. (2001)
<i>S. cerevisiae</i> (cell surface ROL)	–	Glucose	Soybean oil	Methanol	78	Matsumoto et al. (2002)

Hama et al. (2007) studied the methanolysis of soybean oils for the production of biodiesel using *R. oryzae* biomass immobilized in polyurethane foam. The repeated methanolysis reaction was carried out in a 20-L air-lift bioreactor (also named packed-bed reactor (PBR) system) for 20 batch cycles and a ME content of 65–80% was reached and maintained during the entire process. In addition, when methanol (four molar equivalents to oil) was added in the first cycle, 90% of the ME conversion was achieved. The disadvantages observed in the PBR system, however, included cellular exfoliation when the reaction flow rate was high (near 55 L/h) and a decrease in the conversion rate at a flow of 5 L/h because of the inefficiency of the mixture inside the reactor (Hama et al. 2007). One of the reasonable explanations for exfoliation is the shear stress at high flow rates that damages the cells and causes loss of lipase activity (Hama et al. 2007; Andrade 2012).

Ban et al. (2001; 2002) investigated the immobilization of *R. oryzae*, the effects of pretreatments on the cell biomass, the effect of water on the transesterification reaction, and also studied vegetable oils used for biodiesel production. The researchers found that in the presence of 15% water, methanolysis increased up to 90%, a conversion rate similar to that reached with extracellular lipases. They used a discontinuous mode process and after six cycles, the biocatalyst cells retained a yield of 70–80% of ME.

Comparing the enzymatic transesterification of fungal lipases with cell immobilization, the latter is still disadvantageous because it does not attain the high ME mixture content and has a lower reaction rate than the former. However, the results observed so far point to a hopeful future, where cell immobilization can be as efficient as free enzymes, overcoming the current major bottlenecks and increasing economic viability.

4.2.2 Enzyme Production

Immobilized cells are showing great potential for the production of enzymes, particularly those of industrial interest. There are already a myriad of examples in published literature. Siddiqui et al. (2016) used *A. niger* cells immobilized by entrapment in calcium-alginate beads for the production of native cellulolytic enzymes, achieving up to 0.37 IU/mL of enzymatic activity on glucose after 48 h of incubation. In comparison, the same *A. niger* free cells took twice the time to obtain enzymatic activity close to this value. Bacterial cells immobilized in calcium alginate beads were also successfully employed by Darah et al. (2015) for polygalacturonase production. Entrapped *Enterobacter aerogenes* NBO2 cells produced 23.48 U/mL of the enzyme, while 18.54 U/mL were obtained using the free cells. In these two studies, there is a clear observation that, given the appropriate optimization, cell immobilization can significantly enhance enzyme production.

4.2.3 Aroma Formation

Another industrial application for cell immobilization is aroma formation. The flavor industry has a huge market around the world, having dealt with about US \$20.3 billion in 2009 (Markets andMarkets 2015). The compounds produced by fungi, yeasts, and bacteria that confer aromas are metabolites resulting from the catabolism of sugars and nitrogenous and sulfur compounds, as well as from the synthesis of essential molecules for the growth of microorganisms like nucleic acids, amino acids, and lipids (Nedovi et al. 2015). These metabolites include alcohols (ethanol), esters (phenylethyl acetate, ethyl hexanoate), carbonyls (acetaldehyde, diketones), organic acids, and sulfur compounds (hydrogen sulfide, sulfur dioxide) and their use in the industrial field has high added value, mainly because flavor is an important ally for the acceptance of many available food products (Lalou et al. 2013).

Aroma compounds have been studied since the 1960s and 1970s with jasmonates and lenthionin production by the fungi ascomycete *Lasiodiplodia theobromae* (synonym *Botryodiplodia theobromae*) and basidiomycete *Lentinus edodes*, respectively (Yasumoto et al. 1974; Krings and Berger 1998). However, only a few years ago cell immobilization started to be employed for aroma production as an advantageous biocatalyst. Some works have showed positive results with this technology for beer and wine making (Tataridis et al. 2005; Willaert and Nedovic 2006; Vilela et al. 2013).

Wilkowska et al. (2015) observed abundant production of volatiles when using apple/cranberry and apple/chokeberry pomaces with the yeast *Kluyveromyces marxianus* cells immobilized in foamed alginate. It was possible to identify 11 aroma compounds, esters and alcohols, with fruity and floral aromas (e.g. ethyl acetate, isoamyl alcohol, and ethyl butyrate). Thus, depending on the desired flavor compounds, the fermentation of fruit pomaces using immobilized cells can be an effective method of producing commercially valuable volatiles (Wilkowska et al. 2015).

4.2.4 Bioremediation of Wastewater and Organophosphates, and Biosensors

Whole-cell immobilization has also been used in wastewater treatment, as one of the most widely used uses for immobilized cells (Pradella 2001). Usually, wastewater has to undergo two separate processes to avoid the proliferation of nitrogen compound-consuming cyanobacteria in the water: nitrification and denitrification. Nitrification is the oxidation of ammonia to nitrites and subsequently nitrites to nitrates by the action of bacteria, such as *Nitrosomonas* and *Nitrobacter*, respectively. Denitrification must then be carried out under anoxic conditions and can be performed by other bacterial genera, i.e. *Micrococcus* and *Pseudomonas*. These two reactions occur in treatment plants and require a high flow rate to degrade the nitrogen contaminants. In this system, the active sludge formed by free

bacteria is responsible for both reactions. However, the sludge needs additional organic compounds, such as acetic acid, glucose, or methanol, because the organic molecules existing in the wastewater are not sufficient for bacterial growth and proliferation, the addition of which increases wastewater treatment costs. Hence, there are some disadvantages in the conventional process that can be overcome by bacterial cell immobilization (Kras et al. 2016).

One example of this is the LentiKats® technology developed, patented, and improved in recent years by a group from the Czech Republic. The last update of this technology initiative consisted of two tanks: the first one is filled with immobilized bacteria of nitrifiers *N. europaea* and *N. winogradskyi*, while the second has immobilized denitrifiers *P. denitrificans* and *P. fluorescens*. These strains are immobilized on a porous hydrogel matrix made of polyvinyl alcohol (PVA), being non-toxic and non-biodegradable. The manufacturer states that this technology can treat waste residues containing 800 mg/L of N-NH^{4+} or 1000 mg/L of N-NO_3^- with an efficiency of 98% (Cechovská et al. 2009; Bousková 2010). Several different waste sources have been treated with LentiKats®, from industrial wastewater to groundwater from uranium mining sites (Kras et al. 2016). LentiKats® still remains an expensive investment for wastewater treatment, but it can be used for other applications, like ethanol production, bioconversion of malic to lactic acid present in apple juices, and even could potentially be used for xylitol production from sugarcane bagasse (lignocellulosic residue, abundant in Brazil). Thus, despite being costly, this technology may be a good long-term alternative for various applications.

Another application for whole-cell immobilization is the bioremediation of organophosphates (OPs). These neurotoxic compounds are found in pesticides and insecticides and their removal or decomposition is currently done by chemical treatment, incineration, or deposition in landfills. It is of paramount importance that these OPs be detoxified and converted in new, non-harmful compounds in order to not damage the environment and human health (Kim et al. 2014). Organophosphorus hydrolases (OPHs) are enzymes produced by soil microorganisms and are able to degrade the OPs. Many attempts have been made to improve OP degradation efficiency by immobilizing these metalloenzymes in different supports (Kim et al. 2014); however whole-cell immobilization has also attracted attention because of its many advantages already cited, including higher enzyme stability and lower cost.

Bacteria and yeasts have been used as OP degradation biocatalysts, such as *E. coli*, *Moraxella* sp., *Pseudomonas putida*, *Stenotrophomonas* sp., and *Y. lipolytica*. Their OPHs were attached on the cell surface through fusion systems (like lipoprotein and outer membrane protein A, Lpp-OmpA system; protein InaV from *Pseudomonas syringae*; GPI-based; or Flo1p-based) or were located inside the periplasm. Different enzymatic activities were found against each class of OP (paraoxon, parathion, diazinon, fenitrothion) and the whole-cell immobilization stability lasted up to weeks (Kim et al. 2014).

Besides the ability to detoxify OPs, whole-cell immobilization also can be applied to construct biosensors to detect different compounds such as heavy metals

(Shing et al. 2013), pesticides (Anu Prathap et al. 2012), sugar (Kitova et al. 2010), urea (Jha et al. 2009), lactate (Smutok et al. 2007), and even carry out quorum sensing related to N-acylhomoserine lactones (Struss et al. 2010). Notably, a cell-based system was developed by Grosh et al. (2008) to measure the levels of cytokines in the sera of cancer patients. For this, a cellulose triacetate (CTA) membrane of an ion-selective electrode was used to immobilize human umbilical vein endothelial cells (HUVEC). The electrode was exposed to the serum of healthy and cancer patients and after one hour, it was possible to note differences between cytokine (β -FGF, HGF, TNF- α , etc.) levels of the two patient groups and to correctly correlate the response of the biosensor with the stage of cancer (Ghosh et al. 2008). Despite promising results, the hype created from the use of biosensors for medical applications remains in the numerous research reports instead of transitioning to the commercialization of practical biosensors. In addition to the initial studies, it would be more than reasonable to expect the development of new biosensor technologies (D'Orazio 2011).

5 Conclusions and Future Perspectives

As described in this chapter, polymer gels show tremendous potential for the immobilization of industrially relevant enzymes, such as lipases, amylases, and xylanases. In general, it can be expected that enzyme immobilization results in increased enzyme stability, reaction efficiency, and reusability. All of these factors are involved in the cost reduction of enzyme-related industrial processes. To achieve the best results, the enzyme immobilization must be individually optimized, using simple and low-cost supports and processes.

In addition, depending on the conditions and goal, whole-cell immobilization appears to be an effective and less expensive strategy, while remaining just as efficient as other methods. Different types of cells can be immobilized in several matrices for biocatalytic reactions. Their applicability ranges from environmental issues, like heavy metal and pesticide contamination of the soil, to more industrial and clinical uses, like complex chemical production and biosensors for medical tests.

Despite many efforts to better understand and optimize whole-cell immobilization, including better understanding cell physiology and metabolism, selecting the type of matrix, dealing with inhibitory compounds released during biocatalysis steps, and optimizing cell growth conditions, a lot has yet to be done to best benefit from this technology and promote more efficient applications in all fields. Genetic improvement of microorganisms, development of new materials for support, and perfecting growth conditions are just some of the details that deserve more attention to translate the preliminary results into industrial reality.

References

- Abdulla R, Ravindra P (2013) Characterization of cross linked *Burkholderia cepacia* lipase in alginate and k-carrageenan hybrid matrix. *J Taiwan Inst Chem Eng* 44:545–551. <https://doi.org/10.1016/j.jtice.2013.01.003>
- Agbor VB, Cicek N, Sparling R et al (2011) Biomass pretreatment: fundamentals toward application. *Biotechnol Adv* 29:675–685. <https://doi.org/10.1016/j.biotechadv.2011.05.005>
- Andrade GSS (2012) Produção de Biodiesel a partir de Óleos Vegetais usando Células Íntegras Imobilizadas de Fungos Filamentosos com Elevada Atividade Lipolítica. Universidade de São Paulo
- Anu Prathap MU, Chaurasia AK, Sawant SN, Apte SK (2012) Polyaniline-based highly sensitive microbial biosensor for selective detection of lindane. *Anal Chem* 84:6672–6678. <https://doi.org/10.1021/ac301077d>
- Awad GEA, Esawy MA, El-gammal EW et al (2015) Comparative studies of free and immobilized phytase, produced by *P. Purpurogenu* GE1, using grafted alginate/carrageenan beads. *Egypt Pharm J* 14:87–93. <https://doi.org/10.4103/1687-4315.161268>
- Ban K, Hama S, Nishizuka K et al (2002) Repeated use of whole-cell biocatalysts immobilized within biomass support particles for biodiesel fuel production. *J Mol Catal B Enzym* 17:157–165. [https://doi.org/10.1016/S1381-1177\(02\)00023-1](https://doi.org/10.1016/S1381-1177(02)00023-1)
- Ban K, Kaieda M, Matsumoto T et al (2001) Whole cell biocatalyst for biodiesel fuel production utilizing *R. oryzae* cells immobilized within biomass support particles. *Biochem Eng J* 8:39–43
- Berger J, Reist M, Mayer JM et al (2004) Structure and interactions in covalently and ionically crosslinked chitosan hydrogels for biomedical applications. *Eur J Pharm Biopharm* 57:19–34. [https://doi.org/10.1016/S0939-6411\(03\)00161-9](https://doi.org/10.1016/S0939-6411(03)00161-9)
- Betigeri SS, Neau SH (2002) Immobilization of lipase using hydrophilic polymers in the form of hydrogel beads. *Biomaterials* 23:3627–3636. [https://doi.org/10.1016/S0142-9612\(02\)00095-9](https://doi.org/10.1016/S0142-9612(02)00095-9)
- Bianchini LF, Arruda MFC, Vieira SR, Campelo PMS (2015) Microbial biotransformation to obtain new antifungals. *Front Microbiol* 6:1–12. <https://doi.org/10.3389/fmicb.2015.01433>
- Bibi Z, Shahid F, Ali S et al (2015) Agar-agar entrapment increases the stability of endo- β -1,4-xylanase for repeated biodegradation of xylan. *Int J Biol Macromol* 75:121–127. <https://doi.org/10.1016/j.ijbiomac.2014.12.051>
- Bisht D, Yadav SK, Darmwal NS et al (2013) Optimization of immobilization conditions by conventional and statistical strategies for alkaline lipase production by *P. aeruginosa* mutant cells: scale-up at bench-scale bioreactor level. *Turkish J Biol* 37:392–404. <https://doi.org/10.3906/biy-1209-19>
- Bousková A (2010) Solve your nitrogen problems with LentiKats. *Pollut Solut* 3:4–5
- Braccini I, Pérez S (2001) Molecular basis of Ca^{2+} -induced gelation in alginates and pectins: The egg-box model revisited. *Biomacromol* 2:1089–1096. <https://doi.org/10.1021/bm010008g>
- Cechovská L, Mrátkota J, Bousková A, Stlou (2009) Intenzifikace cistíren pomocí biotechnologie Lentikats—provozní výsledky. *Ekotechnika*, pp 38–40
- Chandorkar V, Gomashe AV, Parlewar S (2014) Production of lipase by immobilized cells of *A. niger*. *Int J Curr Microbiol Appl Sci* 3:703–707
- Chen J-P, Lin G-H (2010) Optimization of biodiesel production catalyzed by fungus cells immobilized in fibrous supports. *Appl Biochem Biotechnol* 161:181–194. <https://doi.org/10.1007/s12010-009-8776-8>
- Chen X-H, Wang X-T, Lou W-Y et al (2012) Immobilization of *Acetobacter* sp. CCTCC M209061 for efficient asymmetric reduction of ketones and biocatalyst recycling. *Microb Cell Fact* 11:119. <https://doi.org/10.1186/1475-2859-11-119>
- Chibata I, Tosa T, Sato T (1974a) Japan Kokai. p 189
- Chibata I, Tosa T, Sato T (1974b) Immobilized aspartase-containing microbial cells: preparation and enzymatic properties. *Appl Microbiol* 27:878–885

- Covizzi LG, Giese EC, Gomes E et al (2007) Imobilização de células microbianas e suas aplicações biotecnológicas Immobilization of microbial cells and their biotechnological applications. *Semin Ciências Exatas e Tecnológicas* 28:143–160
- D’Orazio P (2011) Biosensors in clinical chemistry—2011 update. *Clin Chim Acta* 412:1749–1761. <https://doi.org/10.1016/j.cca.2011.06.025>
- Darah I, Nisha M, Lim S-H (2015) Polygalacturonase production by calcium alginate immobilized *Enterobacter aerogenes* NBO₂ cells. *Appl Biochem Biotechnol* 175:2629–2636. <https://doi.org/10.1007/s12010-014-1447-4>
- De Vos P, Lazarjani HA, Poncelet D, Faas MM (2014) Polymers in cell encapsulation from an enveloped cell perspective. *Adv Drug Deliv Rev* 67–68:15–34. <https://doi.org/10.1016/j.addr.2013.11.005>
- Demirbas A (2008) Comparison of transesterification methods for production of biodiesel from vegetable oils and fats. *Energy Convers Manag* 49:125–130. <https://doi.org/10.1016/j.enconman.2007.05.002>
- Desimone MF, Alvarez GS, Foglia ML, Diaz LE (2009) Development of sol-gel hybrid materials for whole cell immobilization. *Recent Pat Biotechnol* 3:55–60. <https://doi.org/10.2174/187220809787172605>
- Duarte JC, Rodrigues JAR, Moran PJS et al (2013) Effect of immobilized cells in calcium alginate beads in alcoholic fermentation. *AMB Express* 3:31. <https://doi.org/10.1186/2191-0855-3-31>
- Duckworth M, Yaphe W (1971) The structure of agar: Part I. Fractionation of a complex mixture of polysaccharides. *Carbohydr Res* 16:189–197. [https://doi.org/10.1016/S0008-6215\(00\)86113-3](https://doi.org/10.1016/S0008-6215(00)86113-3)
- Emregul E (2006) Polyacrylamide—gelatine carrier system used for invertase immobilization. *Food Chem* 97:591–597. <https://doi.org/10.1016/j.foodchem.2005.05.017>
- Fang S, Chang J, Hwang YLE et al (2016) Immobilization of α -amylase from *Exiguobacterium* sp. DAU5 on chitosan and chitosan-carbon bead: its properties. *J Appl Biol Chem* 59:75–81. <https://doi.org/10.3839/jabc.2016.014>
- Feng Q, Wang Q, Tang B et al (2013) Immobilization of catalases on amidoxime polyacrylonitrile nanofibrous membranes. *Polym Int* 62:251–256. <https://doi.org/10.1002/pi.4293>
- Fernandes P, Marques MPC, Carvalho F, Cabral JMS (2009) A simple method for biocatalyst immobilization using PVA-based hydrogel particles. *J Chem Technol Biotechnol* 561–564. <https://doi.org/10.1002/jctb.2080>
- Fukuda H, Hama S, Tamalampudi S, Noda H (2008) Whole-cell biocatalysts for biodiesel fuel production. *Trends Biotechnol* 26:668–673. <https://doi.org/10.1016/j.tibtech.2008.08.001>
- Ganesan D, Thangavelu V, Rajendran A (2011) Statistical optimisation of methanolysis of jatropha oil using immobilised *R. oryzae* cells in n-hexane system. *Int J Environ Stud* 68:31–42. <https://doi.org/10.1080/00207233.2010.539422>
- Ghosh G, Bachas LG, Anderson KW (2008) Biosensor incorporating cell barrier architectures on ion selective electrodes for early screening of cancer. *Anal Bioanal Chem* 391:2783–2791. <https://doi.org/10.1007/s00216-008-2192-8>
- Górecka E, Jastrzębska M (2011) Immobilization techniques and biopolymer carriers—a review. *Biotechnol Food Sci* 75:27–34
- Hama S, Ogino C, Kondo A (2015) Enzymatic synthesis and modification of structured phospholipids: recent advances in enzyme preparation and biocatalytic processes. *Appl Microbiol Biotechnol* 99:7879–7891. <https://doi.org/10.1007/s00253-015-6845-1>
- Hama S, Yamaji H, Fukumizu T et al (2007) Biodiesel-fuel production in a packed-bed reactor using lipase-producing *Rhizopus oryzae* cells immobilized within biomass support particles. *Biochem Eng J* 34:273–278. <https://doi.org/10.1016/j.bej.2006.12.013>
- Hama S, Yamaji H, Kaieda M et al (2004) Effect of fatty acid membrane composition on whole-cell biocatalysts for biodiesel-fuel production. *Biochem Eng J* 21:155–160. <https://doi.org/10.1016/j.bej.2004.05.009>
- Hattori T, Furusaka C (1959) Chemical Activities of *E. coli* Adsorbed on a Resin, Dowex-I. *Nature* 184:1566–1567. <https://doi.org/10.1038/1841566a0>

- Hemachander C, Bose N, Puvanakrishnan R (2001) Whole cell immobilization of *R. pickettii* for lipase production. *Process Biochem* 36:629–633. [https://doi.org/10.1016/S0032-9592\(00\)00256-9](https://doi.org/10.1016/S0032-9592(00)00256-9)
- Hsuanyu Y (2004) Enzyme immobilization. In: Bisen PS (ed) *Laboratory protocols in applied life sciences*
- Huang D, Zhou H, Lin L (2012) Biodiesel: an alternative to conventional fuel. *Energy Procedia* 16:1874–1885. <https://doi.org/10.1016/j.egypro.2012.01.287>
- IUPAC (1997) *Compendium of Chemical Terminology*, 2nd edn. Blackwell Scientific Publications
- Jha SK, Kanungo M, Nath A, D'Souza SF (2009) Entrapment of live microbial cells in electropolymerized polyaniline and their use as urea biosensor. *Biosens Bioelectron* 24:2637–2642. <https://doi.org/10.1016/j.bios.2009.01.024>
- Kamble AL, Banoth L (2013) Nitrile hydratase of *Rhodococcus erythropolis*: characterization of the enzyme and the use of whole cells for biotransformation of nitriles. *Biotech* 3:319–330. <https://doi.org/10.1007/s13205-012-0104-2>
- Kara F, Demirel G, Tümtürk H (2006) Applications of chitosan-alginate polyelectrolyte complexes and interpenetrating polymer networks of poly (acrylamide-co-acrylic acid)/kappa-carrageenan as immobilization supports of enzyme. *Bioprocess Biosyst Eng* 29:207–211
- Kim C, Seo J, Kang D, Cha H (2014) Engineered whole-cell biocatalyst-based detoxification and detection of neurotoxic organophosphate compounds. *Biotechnol Adv* 32:652–662. <https://doi.org/10.1016/j.biotechadv.2014.04.010>
- Kitova A, Reshetilov A, Ponamoreva O, Leathers T (2010) *Microbial Biosensors for Selective Detection of Disaccharides*
- Kras V, Stloukal R, Rosenberg M, Rebro M (2016) Immobilization of cells and enzymes to LentiKats®. *Appl Microbiol Biotechnol* 100:2535–2553. <https://doi.org/10.1007/s00253-016-7283-4>
- Krings U, Berger RG (1998) Biotechnological production of flavours and fragrances. *Appl Microbiol Biotechnol* 49:1–8. <https://doi.org/10.1007/s002530051129>
- Kumakura M, Tamada M, Kasai N, Kaestu I (1989) Enhancement of cellulase production by immobilization of *Trichoderma reesei* cells 33:1358–1362. <https://doi.org/10.1002/bit.260331021>
- Kumar S, Dwevedi A, Kayastha AM (2009) Immobilization of soybean (*Glycine max*) urease on alginate and chitosan beads showing improved stability: analytical applications. *J Mol Catal B Enzym* 58:138–145. <https://doi.org/10.1016/j.molcatb.2008.12.006>
- Kuo C, Liu Y, Chang CJ et al (2012) Optimum conditions for lipase immobilization on chitosan-coated Fe₃O₄ nanoparticles. *Carbohydr Polym* 87:2538–2545. <https://doi.org/10.1016/j.carbpol.2011.11.026>
- Lahiri P (2015) Development of the optimal conditions for alpha-amylase immobilization. *Int J Sci Res* 4:500–502
- Lalou S, Mantzouridou F, Paraskevopoulou A et al (2013) Bioflavour production from orange peel hydrolysate using immobilized *S. cerevisiae*. *Appl Microbiol Biotechnol* 97:9397–9407. <https://doi.org/10.1007/s00253-013-5181-6>
- Léonard A, Dandoy P, Danloy E et al (2011) Whole-cell based hybrid materials for green energy production, environmental remediation and smart cell-therapy. *Chem Soc Rev* 40:860–885. <https://doi.org/10.1039/c0cs00024h>
- Li W, Du W, Liu D (2007a) Optimization of whole cell-catalyzed methanolysis of soybean oil for biodiesel production using response surface methodology. *J Mol Catal B Enzym* 45:122–127. <https://doi.org/10.1016/j.molcatb.2007.01.002>
- Li W, Du W, Liu D (2007b) *R. oryzae* IFO 4697 whole cell catalyzed methanolysis of crude and acidified rapeseed oils for biodiesel production in tert-butanol system. *Process Biochem* 42:1481–1485. <https://doi.org/10.1016/j.procbio.2007.05.015>
- Li W, Du W, Liu D (2008) *Rhizopus oryzae* Whole-cell-catalyzed biodiesel production from oleic acid in tert-butanol medium. *Energy Fuels* 22:155–158. <https://doi.org/10.1021/ef700624v>

- Lin CW, Wu CH, Huang WT, Tsai SL (2015) Evaluation of different cell-immobilization strategies for simultaneous distillery wastewater treatment and electricity generation in microbial fuel cells. *Fuel* 144:1–8. <https://doi.org/10.1016/j.fuel.2014.12.009>
- Liu Q, Wang P (2010) Cell-based biosensors: principles and applications. Artech House
- Lozinsky VI, Galaev IY, Plieva FM et al (2003) Polymeric cryogels as promising materials of biotechnological interest. *Trends Biotechnol* 21:445–451. <https://doi.org/10.1016/j.tibtech.2003.08.002>
- Markets and Markets (2015) Natural food colors & flavors market by food color type, food flavor type, application & by region—global forecast to 2020
- Martins SCS, Martins CM, Fiúza LMCG, Santaella ST (2013) Immobilization of microbial cells: a promising tool for treatment of toxic pollutants in industrial wastewater. *African J Biotechnol* 12:4412–4418. <https://doi.org/10.5897/AJB12.2677>
- Matsumoto T, Fukuda H, Ueda M et al (2002) Construction of yeast strains with high cell surface lipase activity by using novel display systems based on the Flo1p flocculation functional domain. *Appl Environ Microbiol* 68:4517–4522. <https://doi.org/10.1128/AEM.68.9.4517-4522.2002>
- Matsumoto T, Takahashi S, Kaieda M et al (2001) Yeast whole-cell biocatalyst constructed by intracellular overproduction of *R. oryzae* lipase is applicable to biodiesel fuel production. *Appl Microbiol Biotechnol* 57:515–520. <https://doi.org/10.1007/s002530100733>
- Mattiasson B, Hahn-Hägerdal B (1982) Microenvironmental effects on metabolic behaviour of immobilized cells a hypothesis. *Eur J Appl Microbiol Biotechnol* 16:52–55. <https://doi.org/10.1007/BF01008243>
- Mendes AA, De Oliveira PC, De Castro HF, Giordano RDLC (2011) Aplicação de quitosana como suporte para a imobilização de enzimas de interesse industrial. *Quim Nova* 34:831–840. <https://doi.org/10.1590/S0100-40422011000500019>
- Meunier CF, Le A, Le A (2010) Living hybrid materials capable of energy conversion and CO₂ assimilation. *Chem Commun* 46:3843–3859. <https://doi.org/10.1039/c001799j>
- Mi F, Sung HW, Shyu SS (2002) Drug release from chitosan–alginate complex beads reinforced by a naturally occurring cross-linking agent. *Carbohydr Polym* 48:61–72. [https://doi.org/10.1016/S0144-8617\(01\)00212-0](https://doi.org/10.1016/S0144-8617(01)00212-0)
- Milessi TSS, Kopp W, Rojas MJ et al (2015) Immobilization and stabilization of an endoxylanase from *Bacillus subtilis* (XynA) for xylooligosaccharides (XOs) production. *Catal Today* 259:130–139. <https://doi.org/10.1016/j.cattod.2015.05.032>
- Mrudula S, Shyam N (2012) Immobilization of bacillus megaterium mtcc 2444 by caalginate entrapment method for enhanced alkaline protease production. *Brazilian Arch Biol Technol* 55:135–144. <https://doi.org/10.1590/S1516-89132012000100017>
- Müller-Maatsch J, Bencivenni M, Caligiani A et al (2016) Pectin content and composition from different food waste streams. *Food Chem* 201:37–45. <https://doi.org/10.1016/j.foodchem.2016.01.012>
- Murthy HN, Lee EJ, Paek KY (2014) Production of secondary metabolites from cell and organ cultures: strategies and approaches for biomass improvement and metabolite accumulation. *Plant Cell, Tissue Organ Cult* 118:1–16. <https://doi.org/10.1007/s11240-014-0467-7>
- Nedovi V, Gibson B, Mantzouridou TF et al (2015) Aroma formation by immobilized yeast cells in fermentation processes. *Yeast* 32:173–216. <https://doi.org/10.1002/yea>
- Nedovic V, Willaert R (eds) (2004) Fundamentals of cell immobilisation biotechnology, 1st edn. Springer Science & Business Media
- Niu X, Wang Z, Li Y et al (2013) “Fish-in-net”, a novel method for cell immobilization of *Z. mobilis*. *PLoS ONE* 8:e79569. <https://doi.org/10.1371/journal.pone.0079569>
- Omar SH, Honecker S, Rehm H-J (1992) A comparative study on the formation of citric acid and polyols and on morphological changes of three strains of free and immobilized *A. niger*. *Appl Microbiol Biotechnol* 36:518–524. <https://doi.org/10.1007/BF00170195>
- Orive G, Hernández RM, Gascón AR, Pedraz JL (2006) Immobilization of enzymes and cells. In: Guisan JM (ed) Humana Press. Totowa, NJ, pp 345–355

- Pajic-lijakovic I, Levic S, Nedovic V, Bugarski B (2015) Biointerface dynamics—multi scale modeling considerations. *Colloids Surf B Biointerfaces* 132:236–245. <https://doi.org/10.1016/j.colsurfb.2015.05.013>
- Potvorova N, Vakuliuk P, Furtat I, Burban A (2012) Polyacrylonitrile membranes with antibacterial properties. *Procedia Eng* 44:1594–1595. <https://doi.org/10.1016/j.proeng.2012.08.879>
- Pradella JGDC (2001) Reatores com células imobilizadas. In: Schmidell W, Lima U de A, Aquirone E, Borzani W (eds) *Biocologia Industrial*. Edgard Blücher LTDA
- Prasad KK, Mohan SV, Bhaskar YV et al (2005) Laccase production using *P. ostreatus* 1804 immobilized on PUF cubes in batch and packed bed reactors: influence of culture conditions. *J Microbiol* 43:301–307
- Qi M, Gu Y, Sakata N et al (2004) PVA hydrogel sheet macroencapsulation for the bioartificial pancreas. *Biomater* 25:5885–5892. <https://doi.org/10.1016/j.biomaterials.2004.01.050>
- Ramakrishna SV, Prakasham RS (1999) Microbial fermentations with immobilized cells. *Curr Sci* 77:1–22
- Rehman HU, Aman A, Zohra RR et al (2014) Immobilization of pectin degrading enzyme from *B. licheniformis* KIBGE IB-21 using agar-agar as a support. *Carbohydr Polym* 102:622–626. <https://doi.org/10.1016/j.carbpol.2013.11.073>
- Robles-Medina A, González-Moreno PA, Esteban-Cerdán L, Molina-Grima E (2009) Biocatalysis: Towards ever greener biodiesel production. *Biotechnol Adv* 27:398–408. <https://doi.org/10.1016/j.biotechadv.2008.10.008>
- Schlieker M, Vorlop K (2006) A novel immobilization method for entrapment Lentikats. In: Guisan J (ed) *Immobilization of enzymes and cells*, 2nd edn. Humana Press, pp 333–343
- Seifert DB, Phillips JA (1997) Production of small, monodispersed alginate beads for cell immobilization. *Biotechnol Prog* 13:562–568. <https://doi.org/10.1021/bp9700723>
- Shah P, Sridevi N, Prabhune A, Ramaswamy V (2008) Structural features of Penicillin acylase adsorption on APTES functionalized SBA-15. *Microporous Mesoporous Mater* 116:157–165. <https://doi.org/10.1016/j.micromeso.2008.03.030>
- Shing WL, Heng LY, Surif S (2013) Performance of a cyanobacteria whole cell-based fluorescence biosensor for heavy metal and pesticide detection. *Sens* 13:6394–6404. <https://doi.org/10.3390/s130506394>
- Shriver-Lake LC, Gammeter WB, Bang SS, Pazirandeh M (2002) Covalent binding of genetically engineered microorganisms to porous glass beads. *Anal Chim Acta* 470:71–78. [https://doi.org/10.1016/S0003-2670\(02\)00540-8](https://doi.org/10.1016/S0003-2670(02)00540-8)
- Siddiqui M, Siddiqui N, Varma R (2016) Enhanced production of cellulolytic enzymes from immobilized cells of *A. niger*. *Int J Pure Appl Biosci* 4:109–114. <https://doi.org/10.18782/2320-7051.2185>
- Smutok O, Dmytruk K, Gonchar M et al (2007) Permeabilized cells of flavocytochrome b2 over-producing recombinant yeast *hansenula polymorpha* as biological recognition element in amperometric lactate biosensors. *Biosens Bioelectron* 23:599–605. <https://doi.org/10.1016/j.bios.2007.06.021>
- Stoilova O, Manolova N, Gabrovska K et al (2010) Electrospun polyacrylonitrile nanofibrous membranes tailored for acetylcholinesterase immobilization. *J Bioact Compat Polym* 25:40–57. <https://doi.org/10.1177/0883911509353680>
- Struss A, Pasini P, Ensor CM et al (2010) Paper strip whole cell biosensors: a portable test for the semiquantitative detection of bacterial quorum signaling molecules. *Anal Chem* 82:4457–4463. <https://doi.org/10.1021/ac100231a>
- Sührer I, Langemann T, Lubitz W et al (2015) A novel one-step expression and immobilization method for the production of biocatalytic preparations. *Microb Cell Fact* 14:1–9. <https://doi.org/10.1186/s12934-015-0371-9>
- Tamalampudi S, Talukder MR, Hama S et al (2008) Enzymatic production of biodiesel from *Jatropha* oil: a comparative study of immobilized-whole cell and commercial lipases as a biocatalyst. *Biochem Eng J* 39:185–189. <https://doi.org/10.1016/j.bej.2007.09.002>

- Tanriseven A, Doğan Ş (2002) A novel method for the immobilization of β -galactosidase. *Process Biochem* 38:27–30. [https://doi.org/10.1016/S0032-9592\(02\)00049-3](https://doi.org/10.1016/S0032-9592(02)00049-3)
- Tataridis P, Ntagas P, Voulgaris I, Nerantzis E (2005) Production of sparkling wine with immobilized yeast fermentation. *Electron J Sci Technol* 1:1–21
- Taylor P, Lai Y, Thirumavalavan M, Lee J (2010) Effective adsorption of heavy metal ions (Cu, Pb, Zn) from aqueous solution by immobilization of adsorbents on Ca-alginate beads. *Toxicol Environ Chem* 2248:37–41. <https://doi.org/10.1080/02772240903057382>
- Thakur VK, Thakur MK (2014a) Recent trends in hydrogels based on psyllium polysaccharide: a review. *J Clean Prod* 82:1–15
- Thakur VK, Thakur MK (2014b) Recent advances in graft copolymerization and applications of Chitosan: a review. *ACS Sustain Chem Eng* 2(12):2637–2652
- Thakur VK, Thakur MK (2015) Recent advances in green hydrogels from lignin: a review. *Macromolecules* 72:834–847. <https://doi.org/10.1016/j.ijbiomac.2014.09.044>
- Thu B, Smidsrød O, Skjak-Brk G (1996) Alginate gels—some structure-function correlations relevant to their use as immobilization matrix for cells. *Prog Biotechnol* 11:19–30. [https://doi.org/10.1016/S0921-0423\(96\)80004-9](https://doi.org/10.1016/S0921-0423(96)80004-9)
- Trelles JA, Rivero CW (2013) Whole cell entrapment techniques. *Methods Mol Biol* 1051:365–374. https://doi.org/10.1007/978-1-62703-550-7_24
- Uludag H, De Vos P, Tresco PA (2000) Technology of mammalian cell encapsulation. *Adv Drug Deliv Rev* 42:29–64. [https://doi.org/10.1016/S0169-409X\(00\)00053-3](https://doi.org/10.1016/S0169-409X(00)00053-3)
- Van De Velde F, Lourenço ND, Pinheiro HM, Bakker M (2002) Carrageenan: a food-grade and biocompatible support for immobilisation techniques. *Adv Synth Catal* 344:815–835. [https://doi.org/10.1002/1615-4169\(200209\)344:8<815:AID-ADSC815>3.0.CO;2-H](https://doi.org/10.1002/1615-4169(200209)344:8<815:AID-ADSC815>3.0.CO;2-H)
- Vilela A, Schuller D, Mendes-Faia A, Côte-Real M (2013) Reduction of volatile acidity of acidic wines by immobilized *S. cerevisiae* cells. *Appl Microbiol Biotechnol* 97:4991–5000. <https://doi.org/10.1007/s00253-013-4719-y>
- Vrana NE, O'Grady A, Kay E et al (2009) Cell encapsulation within PVA-based hydrogels via freeze-thawing: a one-step scaffold formation and cell storage technique. *J Tissue Eng Regen Med* 3:524–531. <https://doi.org/10.1002/term.193>
- Wilkowska A, Kregiel D, Guneser O, Karagul Yuceer Y (2015) Growth and by-product profiles of *K. marxianus* cells immobilized in foamed alginate. *Yeast* 32:217–225. <https://doi.org/10.1002/yea.3044>
- Willaert R, Nedovic VA (2006) Primary beer fermentation by immobilised yeast—a review on flavour formation and control strategies. *J Chem Technol Biotechnol* 81:1353–1367. <https://doi.org/10.1002/jctb.1582>
- Xiao M, Mathew S, Obbard JP (2010) A newly isolated fungal strain used as whole-cell biocatalyst for biodiesel production from palm oil. *GCB Bioenergy* 2:45–51. <https://doi.org/10.1111/j.1757-1707.2010.01038.x>
- Xie W, Wang J (2011) Immobilized lipase on magnetic chitosan microspheres for trans esterification of soybean oil. *Biomass Bioenergy* 36:373–380. <https://doi.org/10.1016/j.biombioe.2011.11.006>
- Yang LJ, Ou YC (2005) The micro patterning of glutaraldehyde (GA)-crosslinked gelatin and its application to cell-culture. *Lab Chip* 5:979–984. <https://doi.org/10.1039/b505193b>
- Yasumoto K, Iwami K, Mitsuda H (1974) Enzymatic formation of Shi-Ta-ke aroma from non-volatile precursor(s)—lenthionine from lenticic acid. In: *Proceedings of the 9th international scientific congress on the cultivation of E. Fungi*. Tokyo, pp 371–383
- Zajkoska P, Rebore M, Rosenberg M (2013) Biocatalysis with immobilized *E. coli*. *Appl Environ Microbiol* 97:1441–1455. <https://doi.org/10.1007/s00253-012-4651-6>
- Zhang D, Yuwen L, Peng L (2013) Parameters affecting the performance of immobilized enzyme. *J Chem* 2013:1–7. <https://doi.org/10.1155/2013/946248>

Chapter 3

Hemicellulose-Based Hydrogels and Their Potential Application



Weiqing Kong, Qingqing Dai, Cundian Gao, Junli Ren,
Chuanfu Liu and Runcang Sun

Abstract The hydrogels obtained from renewable resources have aroused great interests because they are nontoxic, economical, biodegradable, and biocompatible. Hemicellulose is the second most abundant polysaccharides after cellulose in lignocellulosic biomass. In recent years, hemicellulose-based hydrogels as biomaterials have received ever-increasing attention and they have a wide range of the promising applications in drug delivery and release, waste treatment, dye adsorption, and tissue engineering because of their peculiar physicochemical properties. This paper described the structure of hemicellulose in plant and its physical-chemical prosperities, and summarized the type of hemicellulose-based hydrogels and their potential application, which provide useful information for the utilization of hemicellulose polymers.

Keywords Hemicellulose · Structure · Physical-chemical prosperities
Hydrogels preparation · Application

1 Introduction

Hydrogels are typical soft-solid materials with 3D network structures (Vermonden et al. 2012). Due to their high stretchability, responsiveness, swelling and deswelling abilities, hydrogels have a wide range of applications in drug delivery and release (Gao et al. 2015a; Kong et al. 2016; Lin and Gitsov 2010; Thakur and Thakur 2014, 2015), waste treatment (Albertsson et al. 2010; Kong et al. 2014; Lin and Gitsov 2010; Okazaki et al. 1995; Ren et al. 2014), dye adsorption (Zhou et al. 2014), biological medicine and tissue engineering (Cheng et al. 2012; Lai et al. 2012), agriculture and food chemistry (Mv et al. 2000), etc. However, most of the traditional hydrogels generally suffer from the poor biodegradability and the bio-

W. Kong · Q. Dai · C. Gao · J. Ren (✉) · C. Liu · R. Sun
State Key Laboratory of Pulp and Paper Engineering, South China University
of Technology, Guangzhou 510640, China
e-mail: renjunli@scut.edu.cn

© Springer Nature Singapore Pte Ltd. 2018
V. K. Thakur and M. K. Thakur (eds.), *Polymer Gels*, Gels Horizons: From Science
to Smart Materials, https://doi.org/10.1007/978-981-10-6086-1_3

compatibility, which significantly limits their application range such as biomaterials and bioengineering. In recent years, natural polymers based hydrogels have aroused broad interests with the low cost, good biodegradability, and biocompatibility (Gao et al. 2015a; Bhattarai et al. 2010). The natural polymers based intelligent hydrogels have been extensively applied in biomedical fields, such as biological scaffolds for tissue engineering, biosensors, immunization barriers for the cells encapsulation, absorbent materials for heavy metal, and controlled drug delivery systems because of their special properties (Lee and Mooney 2001; Sefton et al. 2000; Dai et al. 2015; Lin and Metters 2006; Qiu and Park 2012; Gao et al. 2015a).

With the deterioration of the environment and the depletion of conventional resource, the exploration of natural renewable resource has been increasingly emphasized. Lignocellulosic biomass is an abundant resource on the earth and can be generated through photosynthesis worldwide. But the vast majority of lignocellulosic biomass has not been used effectively, leading to an enormous waste of resources (Ayoub et al. 2013; Trache et al. 2017; Corobea et al. 2016; Voicu et al. 2016; Miculescu et al. 2016). Therefore, it is still a challenge to convert lignocellulosic biomass into bioenergy and biomaterials as alternative energy sources during the last few decades.

Hemicellulose is a renewable plant polysaccharide next to cellulose in lignocellulosic biomass and they account for 1/4–1/3 in agriculture residues (Sun et al. 2015a). Recently, more and more researchers have focused on the high value-added utilization of hemicellulose (Nghiem et al. 2011). Hemicellulose has the unique physiological properties, such as inhibiting cell mutation, promoting cell adhesion and proliferation, innate immunological defense, and anticancer effect which make it suitable for preparation of hydrogels used in drug release and biomedical engineering (Barbat et al. 2008; Noaman et al. 2008; Oliveira et al. 2010). Moreover, the presence of hydroxyl and carboxylic groups on the hemicellulosic chains provides more opportunity for chemical or enzymatic modifications while keeping their native structure, biodegradability, and biocompatibility. Many studies have introduced functional groups such as carboxyl groups, acetyl groups, etc., onto the hemicellulose structure to improve the subsequent reactivity in preparing cross-linked hemicellulose-based hydrogels (Albertsson et al. 2010; Edlund and Albertsson 2008; Gao et al. 2015a; Yang et al. 2011). Especially, the introduction of carboxyl groups improves the pH or salts response performance of hemicellulose-based hydrogels, thereby extending their application in drug release. It is known that the variations in pH occur at several body sites, such as the gastrointestinal tract, blood vessels, and vagina, and the pH sensitivity hemicellulose-based hydrogels can provide a suitable pH-responsive for drug release. Furthermore, the incorporation of carboxyl groups into hydrogels also could improve the adsorptive properties of metal ions and dye. Therefore, the preparation of hemicellulose and hemicellulose derivatives based hydrogels not only provides an important approach to achieve the high-value utilization of hemicellulose but also expands the application range of the hydrogel.

This article provides a brief introduction to the structure and the physical and chemical properties of hemicellulose. The preparation methods and the application

of hemicellulose and hemicellulose derivatives based hydrogels are importantly emphasized. They possessing good biodegradability and biocompatibility which will make advantages in the industry and medical system in the future.

2 Hemicellulose

2.1 The Structure of Hemicellulose

Hemicellulose is a kind of regenerate energy source which is only second to cellulose in abundance in plant cell walls. Decomposition and utilization of hemicellulose are significant to solve the energy crisis and environmental problems. The content of hemicellulose in plants is associated with the plant species, such as the content of hemicellulose in maize stems, wheat straw, barley straw, and rye straw is 28.0, 38.8, 34.9, and 36.9%, respectively. Different from cellulose, hemicellulose represents a type of hetero-polysaccharides with complex structures, which comprise arabinose, xylose, D-glucuronic acid, glucose, mannose, fucose, rhamnose, galactose, galacturonic acid and 4-O-methyl glucuronic acid, and so on. Moreover, hemicellulose is branched polymer of low molecular weight with a degree of polymerization in the range of 80–450 (Bai et al. 2012) (Table 1). Figure 1 shows the monosaccharide composition of hemicellulose.

Hemicellulose usually consists of various monosaccharides. According to the monosaccharide composition, hemicellulose can be divided into mannosan, xylan, galactosan, xyloglucanase, and arabinan (Ebringerová 2005).

Mannan is the main component of hemicellulose in the coniferous wood. Two types of mannans exist, namely, galactomannans consisting of $\beta(1 \rightarrow 4)$ linked D-mannopyranoses and glucomannans comprised of D-mannopyranose and D-glucopyranose with $\beta(1 \rightarrow 4)$ linkages (Capek et al. 2002). Both types of mannoglycans have the various branching degrees with D-galactopyranose residues in the 6-position of the mannose backbone (Ebringerová et al. 2005). Most of them exist in softwoods, while minor amounts of them exist in hardwoods, seeds and coffee beans.

Xylan is the most common hemicellulose of the cell walls of herbaceous and hardwoods plants and thus can be acquired from agriculture, wood, and industrial by-product (Stephen 1983). It can be speculated that the chemical structure of xylan depends on their functionality in plants. Moreover, the chemical structure of xylan varies among different plants, including the molecular architecture and the degree of substitution. (Samuelsen 2000; Sandhu et al. 1981). Generally, xylan is classified into the subgroups of heteroxylan (HX) and homoxylan (X), and they have the different chemical structure. HX is common in the cell wall of higher plants (Table 2). In hardwoods, glucuronoxylan (GX) consists of a backbone of (1 \rightarrow 4)-linked β -D-xylopyranosyl (Xylp) and is substituted with glucuronosyl and 4-O-methylglucuronosyl by α -(1 \rightarrow 2) linkages. In addition, most of the xylose residues

Table 1 The main types of polysaccharides of hemicellulose (Buranov and Mazza 2010; Sun et al. 2004a, 2005)

Polysaccharide	Biological units origin	Amount ^a	Units		Side chains	Linkages		DP ^b
			Backbone					
Arabinogalactan	Softwoods	5–35	β -D-Galp		β -D-Galp α -L-Araf β -L-Arap		β -(1 \rightarrow 6) α -(1 \rightarrow 3) β -(1 \rightarrow 3)	100–600
Xyloglucan	Hardwoods, softwoods, and grasses	2–25	β -D-Glep β -D-Xylp		β -D-Xylp β -D-Galp α -L-Araf α -L-Fucp Acetyl		β -(1 \rightarrow 4) α -(1 \rightarrow 3) β -(1 \rightarrow 2) α -(1 \rightarrow 2) α -(1 \rightarrow 6)	
Galactoglucomannan	Softwoods	10–25	β -D-Manp β -D-Glep		β -D-Galp Acetyl		α -(1 \rightarrow 6)	40–100
Glucomannan	Hardwoods	2–5	β -D-Manp β -D-Glep					40–70
Glucuronoxylan	Hardwoods	15–30	β -DXylp		4-OMe- α -D-GlcpA Acetyl		α -(1 \rightarrow 2)	100–200
Arabinoglucuronoxylan	Grasses And softwoods	5–10	β -D-Xylp		4-OMe- α -D-GlcpA α -Laraf		α -(1 \rightarrow 2) α -(1 \rightarrow 3)	50–185
Glucuronarabinoxylans	Grasses	0.15–30	β -D-Xylp		α -LArarf 4-OMe- α -D-GlcpA Acetyl		α -(1 \rightarrow 2) α -(1 \rightarrow 3)	
Homoxylans β -DXylpc β -(1 \rightarrow 3, 1 \rightarrow 4)-glucan	Algae Grasses	2–15	β -D-Xylp ^c β -D-Glep				β -(1 \rightarrow 3) β -(1 \rightarrow 4)	

^a%, dry biomass. ^bDegree of polymerization. ^cMay also present β -(1 \rightarrow 3) linkages on the backbone

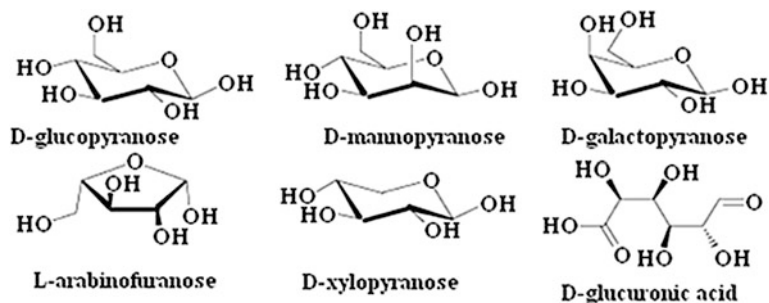


Fig. 1 The monosaccharide composition of hemicellulose

contain acetyl groups at C-2 or C-3. In softwoods, the β -(1 \rightarrow 4)-D-xylopyranose backbone of arabinoglucuronoxylan (AGX) is substituted with single 4-*O*-methyl-D-glucuronic acid (MeGlcA) and α -L-arabinofuranosyl (α -L-Araf) units at position 2 and 3. And arabinoxylan (AX) in Gramineae has the linear β -(1 \rightarrow 4)-D-Xylp as backbone and is substituted by α -L-Araf units in the positions 2-*O* and/or 3-*O* (Ebringerová and Heinze 2000).

Galactosan contains a backbone of β (1 \rightarrow 4) linked galactose residues and side chains linked by galactose substituted at in *O*-6 (Habibi et al. 2004). Arabinogalactan is the main representative of this kind of hemicellulose. They exist widely in larch.

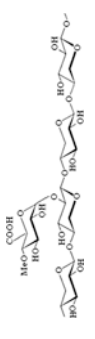
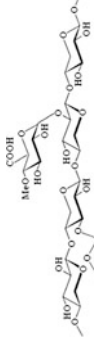
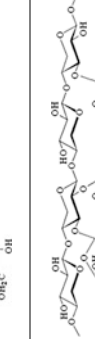
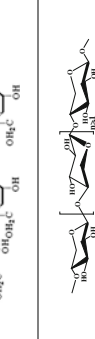
Xyloglucan (XG) consists of a backbone of β (1 \rightarrow 4) linked D-glycopyranose residues with a distribution of D-xylopyranose in position 6 (Kiefer et al. 1990). Xyloglucan can be divided into two categories depending on the distribution of the side chains: one with two xylopyranose units followed by two glucopyranose units (termed XXGG) and one with three xylopyranose units followed by a single glucopyranose unit (termed XXXG). Furthermore, there are many side chains in xyloglucans, including α -L-arabinofuranose leading to the characterization of this group of hemicellulose especially challenging (Ebringerová et al. 2005). XG is a hemicellulosic polysaccharide in all higher plants, such as grass, onion, dicotyledonous angiosperms, fir tress, soybean, olive fruit, and so on.

Arabinan is composed of α -L-arabinofuranose (α -L-Araf) residues linked at position C-5 as backbone. Moreover, many side chains exist in araban, including both arabinose side chain linked at position *O*-2/*O*-3 or both *O*-2 and *O*-3 and arabiligosaccharide side chains (Stevens and Selvendran 1980). Araban in the primary cell wall is composed essentially of arabinose.

2.2 The Physical and Chemical Properties of Hemicellulose

Because of the excellent nontoxicity, low price, biocompatibility, and biodegradation of hemicellulose, the development and application of hemicellulose-based

Table 2 Categories of xylan (Ebringerová and Heinze 2000)

Plant type	Xylan-type	Biological origin	Structure
Higher plants	heteroxylan	Hardwoods	
	glucuronoxylan	Softwoods	
	Arabinoglucuronoxylan	Gramineae	
Others	Homoxylan		

products have caused wide public concern over the recent years (Ebringerová et al. 2005; Oliveira et al. 2010). More importantly, the biological activity is one of the most important features of hemicellulose for the promising application in medicine and biology fields. Some studies have reported that xylan-type hemicellulose has unique physiological properties (inhibiting cell mutation) and some functions (anti-inflammatory, detoxification and anticancer) (Oliveira et al. 2010). Additionally, xylan-type hemicellulose is digested little in the stomach and intestine of the body, but can be degraded by anaerobic bacteria in the colon (Ebringerová and Heinze 2000; Sinha and Kumria 2001; Sinha et al. 2004; Yang et al. 2002). Those striking features of xylan-type hemicellulose have greatly broadened the application of xylan in medicinal materials and biological engineering.

There are large amounts of active hydroxyl groups on the main chain and side chain of hemicellulose, which offers the chance of the chemical or enzymatic modification. The chemical modification endows hemicellulose with specific properties depending on the functional groups, the substitution pattern, and the degree of substitution. There are many hemicellulose derivatives that have been synthesized including carboxymethyl hemicellulose (Gulati et al. 2014; Peng et al. 2010a; Petzold et al. 2005), cationic hemicellulose (Kong et al. 2014; Petzold et al. 2005; Ren et al. 2008a, 2011, 2007b, 2006; Schwikal and Heinze 2007; Schwikal et al. 2005), acetylated hemicellulose (Fang et al. 2000; Ren et al. 2007a), laurylated hemicellulose (Ren et al. 2008b), oleoylated hemicellulose (Sun et al. 2004b), Σ -caprolactone-grafted hemicellulose (Zhang et al. 2014a, b), etc. Those hemicellulose derivatives with different functional groups can be used to prepare functional polymers (Petzold et al. 2006; Ren et al. 2007a, b 2008a, b; Schwikal et al. 2005) and materials (Hansen and Plackett 2008; Hartman et al. 2006; Liu et al. 2001) to expand the application of hemicellulose. Among them, hemicellulose and hemicellulose derivatives based hydrogels containing environmental multi-responsive sensitivity to temperature, pH, salt, light, etc., have aroused broad interests due to the special physical and chemical properties such as biodegradability and biocompatibility (Gao et al. 2015a; Bhattarai et al. 2010).

2.3 Hemicellulose-Based Hydrogels

In recent years, the synthesis of hemicellulose and hemicellulose derivatives based hydrogels has attracted much attention because it can reduce the cost, improve the biocompatibility of hydrogels, and broaden the application of hydrogels in various industrial and biomedical fields. For example, xylan and glycidyl methacrylate-modified xylan (GMAX) based hydrogels were synthesized and their properties in drug controlled release and biocompatibility were studied in detail (Gao et al. 2015a). The results showed that GMAX-gels had higher drug cumulative release and longer release time in the intestine fluids. Furthermore, the NIH3T3 cell viabilities of both xylan-gels and GMAX-gels were higher than the

control group, which showed that the incorporation of xylan or GMAX in hydrogels could improve the biocompatibility of hydrogels. Hydrogels based on the acetylated galactoglucomannan (AcGGM) were prepared and their properties in drug release were studied (Voepel et al. 2009, 2010; Edlund and Albertsson 2008; Liu et al. 2004; Roos et al. 2008). It was found that ACGGM-based hydrogels had the great performance for the drug release. In addition, hemicellulose-based hydrogels were also prepared as novel bioadsorbents for the removal of heavy metal ions and dye from the wastewater. For example, xylan-type hemicellulose-based hydrogel was synthesized by the graft copolymerization of acrylic acid (AA) and xylan for adsorption of Cd^{2+} , Pd^{2+} , and Zn^{2+} from aqueous solutions (Peng et al. 2012b). The maximum adsorption capacities of Cd^{2+} , Pd^{2+} , and Zn^{2+} were 495, 859, and 274 mg/g, respectively. The xylan/poly(acrylic acid) magnetic nanocomposite hydrogel adsorbent was synthesized from wheat straw xylan and Fe_3O_4 nanoparticles, and its adsorption property was studied on the methylene blue removal and the maximum adsorption capacity was estimated to be 438.60 mg/g (Sun et al. 2015c). Therefore, hemicellulose and hemicellulose derivatives based hydrogels have a promising application in drug release, water absorption and storage, metal ion absorption and dye absorption, etc. (Gabrielii and Gatenholm 1998; Xu et al. 2007). The preparation methods and the applications of hemicellulose and hemicellulose derivatives based hydrogels will be described in detail in the following sections.

3 Preparation of Hemicellulose-Based Hydrogels

The preparation methods of hemicellulose-based hydrogels are similar to the polymeric hydrogels. Based on the difference of formation mechanism or cross-linking agents, hydrogels can be divided into physically cross-linking hydrogel and chemically cross-linking hydrogels as shown in Fig. 2. Chemically, cross-linking methods include cross-linking by the radical polymerization, cross-linking by the high energy irradiation, cross-linking using enzymes, and cross-linking by the chemical reaction with complementary groups. Physically cross-linking methods include cross-linking by ion interactions, physically cross-linked hydrogels from amphiphilic block and graft copolymers, and cross-linking by crystallization.

3.1 Chemically Cross-linking Hydrogel

Chemical cross-linking hydrogel has three-dimensional network structure which is irreversible cross-linking formed by chemical reactions between covalent bonds or electrovalent bonds. The hydroxyls on the hemicellulose chain could react with monomers and cross-linking agents, and it can be easily modified, which make them suitable for the formation of three-dimensional networks.

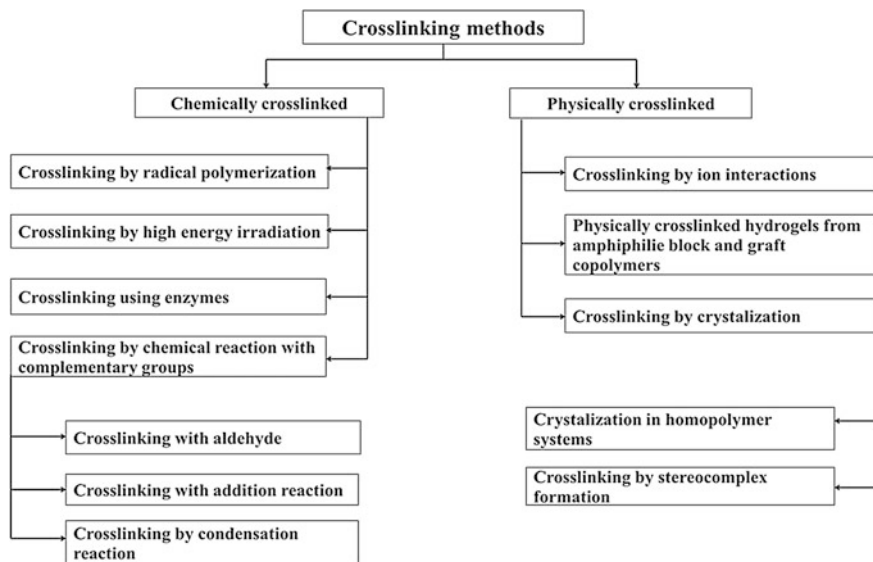


Fig. 2 Cross-linking methods used in hydrogels

3.1.1 Monomers Cross-linking Copolymerization

Monomers cross-linking polymerization mainly includes free radical homopolymerization and copolymerization monomer polymerization. Monomers used for preparing hydrogel are mainly acrylic acid series, acrylamide series, vinyl acetate series, etc. (Pourjavadi et al. 2004; Gao et al. 2015a). The cross-linking agents such as *N,N*-methylenebis-acrylamide (MBA), vinyl ethyl benzene (DVB), and ethyldiol methacrylate (EGDMA) (Kopecek and Yang 2007) are used to make polymers cross-linked. Common monomers and cross-linking agents used in preparing hydrogels are presented in Table 3. The polymerization reaction could occur under the trigger of initiator or radiation (Gao et al. 2015a). By controlling the polymerization methods, monomers, cross-linking agent, and the properties of hydrogel can be controlled. Figure 3 demonstrates the formation of chemically cross-linking hydrogels based on the radical polymerization.

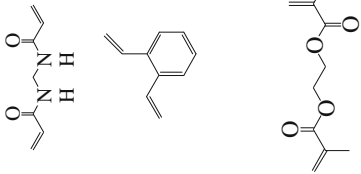
Karaaslan et al. (2011) prepared biocompatible hydrogels based wood cellulose whiskers and hemicellulose by in situ radical polymerization of the methacrylic groups of the absorbed coating to form a network of poly (2-hydroxyethylmethacrylate) (PHEMA) matrix reinforced with cellulose whiskers which showed a great biocompatibility. Hemicellulose was modified with 2-hydroxyethylmethacrylate prior to adsorption onto the cellulose whiskers in aqueous medium.

Table 3 Common monomers that used for the preparation of hemicellulose-based hydrogel (R represent for the alkyl groups in the table)

Properties	Structure	Name
Graft monomers	$\begin{array}{c} \text{CH}_3 \\ \\ \text{H}_2\text{C}=\text{C}-\text{CO}-\text{O}-\text{C}-\text{C}-\text{OH} \\ \quad \\ \text{H}_2 \quad \text{H}_2 \end{array}$ $\begin{array}{c} \text{CH}_3 \\ \\ \text{H}_2\text{C}=\text{C}-\text{CO}-\text{NH}-\text{R} \end{array}$	Hydroxyethyl methacrylate
	Neutral	<i>N</i> -alkyl methyl acrylamide
	$\begin{array}{c} \text{H}_2\text{C}=\text{C}-\text{CO}-\text{NH}-\text{R} \\ \\ \text{H} \end{array}$	<i>N</i> -alkyl acrylamide
	$\begin{array}{c} \text{H}_2\text{C}=\text{C}-\text{CO}-\text{N}(\text{R})_2 \\ \quad \\ \text{H} \quad \text{R} \end{array}$	<i>N,N</i> -alkyl acrylamide
	$\begin{array}{c} \text{H}_2\text{C}=\text{C}-\text{COOH} \\ \\ \text{H} \end{array}$	acrylic acid (AA)
Acidity	$\begin{array}{c} \text{CH}_3 \\ \\ \text{H}_2\text{C}=\text{C}-\text{COOH} \end{array}$ $\begin{array}{c} \text{CH}_3 \\ \\ \text{H}_2\text{C}=\text{C}-\text{CO}-\text{N}-\text{C}-\text{CH}_2\text{SO}_3\text{H} \\ \quad \quad \\ \text{H} \quad \text{H} \quad \text{CH}_3 \end{array}$	methacrylic acid (MAA)
		2-acrylamido 2-methylpropane sulfonic acid

(continued)

Table 3 (continued)

Properties	Structure	Name
	$\begin{array}{c} \text{CH}_3 \\ \\ \text{H}_2\text{C}=\text{C}-\text{CO}-\text{O}-\text{C}-\text{C}-\text{N}(\text{R})_2 \\ \quad \\ \text{H}_2 \quad \text{H}_2 \end{array}$ $\begin{array}{c} \text{R} \\ \\ \text{H}_2\text{C}=\text{C}-\text{CO}-\text{O}-\text{C}-\text{C}-\text{N}^{\oplus}(\text{R})_2 \text{Br}^{\ominus} \\ \quad \\ \text{H}_2 \quad \text{H}_2 \end{array}$ Alkaline	2-Diethylaminoethyl methacrylate Oxygen ethyl methyl acryloyl trialkyl ammonium bromide
Cross-linking agent	$\begin{array}{c} \text{CH}_3 \\ \\ \text{H}_2\text{C}=\text{C}-\text{CO}-\text{O}-\text{C}-\text{O}-\text{C}-\text{CO}-\text{C}=\text{CH} \\ \quad \\ \text{H}_2 \quad \text{H}_2 \quad \text{CH}_3 \end{array}$ 	Ethylene glycol dimethyl acrylic ester <i>N,N</i> -methylenebis-acrylamide (MBA) Vinyltoluene (DVB) Ethyldiol methacrylate (EGDMA)

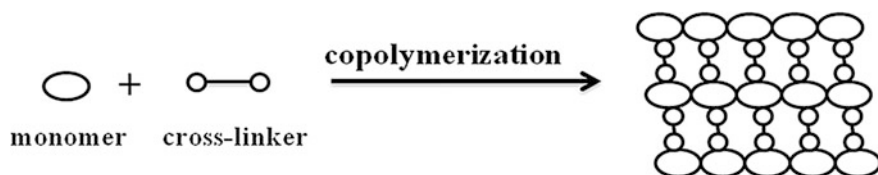


Fig. 3 Formation of chemically cross-linking hydrogels based on the radical polymerization

3.1.2 Graft Copolymerization

Graft copolymerization, as a method of preparing hydrogels, connected α -alkene monomers onto the polymer. Generally, polymeric carriers are hemicellulose, starch, methyl cellulose, polyvinyl alcohol and chitosan, and sodium alginate. Vinyl groups are the major polymerizable groups which are commonly used in grafting for specific application and purpose (Thakur et al 2016; Singha et al 2008). The existence of vinyl groups in the polymer backbone or side chain contributes to themselves participating in the polymerization with polymerizable monomers or macromonomers containing carbon-carbon double bonds (Frechet et al.1995; Hawker et al. 2001; Ishizu et al. 2000; Li and Armes 2005). Hydroxyl groups on the chain of hemicellulose can be easily modified by enzymatic or chemical functionalization (Lindblad et al. 2001). The presence of the OH groups provides more reactive sites for the grafting reaction of hemicellulose. Therefore, introducing vinyl groups to the backbone of hemicellulose is an essential way to further prepare novel hemicellulose-based hydrogels by the graft polymerization.

Peng et al. (2011) synthesized novel ionic hydrogels based on the free radical graft copolymerization between xylan and acrylic acid (AA), which could respond to multiple stimuli. Synthetic mechanism of xylan-graft-acrylic acid hydrogels is shown in Fig. 4. AA is a common monomer for the synthesis of functional hydrogels. The introduce of AA into hydrogels gives a lot of carboxylic groups in the network of hydrogels. The functional hydrogels with amounts of carboxylic groups have potential applications in the removal of heavy metal ions or dyes from the wastewater. Moreover, glycidyl methacrylate (GMA) is another important approach to prepare the polymers containing vinyl groups (Guilherme et al. 2005; Hebeish et al. 1997; Ishizu and Mori 2000; Morimoto et al. 2005; Nagasaki et al. 1997; Ohsedo et al. 2004). A novel maleic anhydrided hemicellulose containing carbon-carbon double bonds were prepared by further polymerized with *N*-isopropylacrylamide (Peng et al. 2010b; Yang et al. 2011).

AcGGM is a common hemicellulose. Because of the properties of abundance, cheap and renewable, it is an ideal candidate for the design of AcGGM-based hydrogels. Acetylated galactoglucomannan (AcGGM) based hydrogels were prepared using ammonium peroxodisulfate (APS) and $\text{Na}_2\text{S}_2\text{O}_5$ by radical polymerization showed in Fig. 5 (Voepel et al. 2009). When maleic anhydride was added to the M-AcGGM producing a “double-modified” hemicellulose, ionic poly (CM-AcGGMco-HEMA) hydrogels could be achieved.

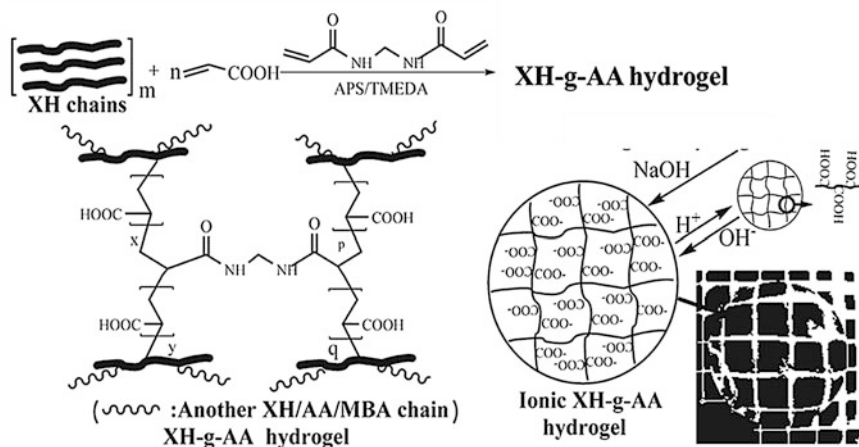


Fig. 4 Synthetic mechanism of xylan-graft-acrylic acid hydrogels (Peng et al. 2011)

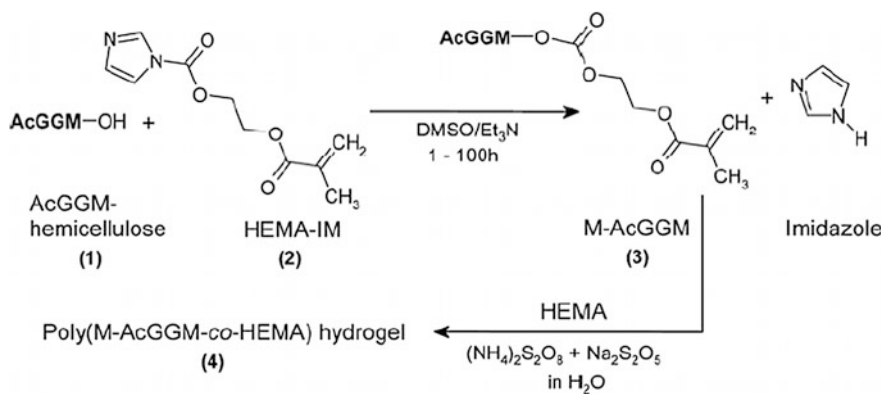


Fig. 5 Synthesis mechanism of poly(M-AcGGM-co-HEMA) hydrogels (Voepel et al. 2009)

Jens Voepel et al. (2010) designed AcGGM-based hydrogels and studied its release properties of different model drugs (Voepel et al. 2010). The synthesis route consists of the following three steps: (1) the carbonyldiimidazole activation of primary hydroxylated vinylic molecules such as acrylates, vinyl alcohols, and vinyl ethers (2) the covalent coupling of the alkenyl precursors to the polysaccharide backbone hydroxyls (3) the radical cross-linking of pendant vinyl functionalities affording a hydrophilic network (Fig. 6). The results showed that the properties of hydrogels are affected by the different functionalization strategies.

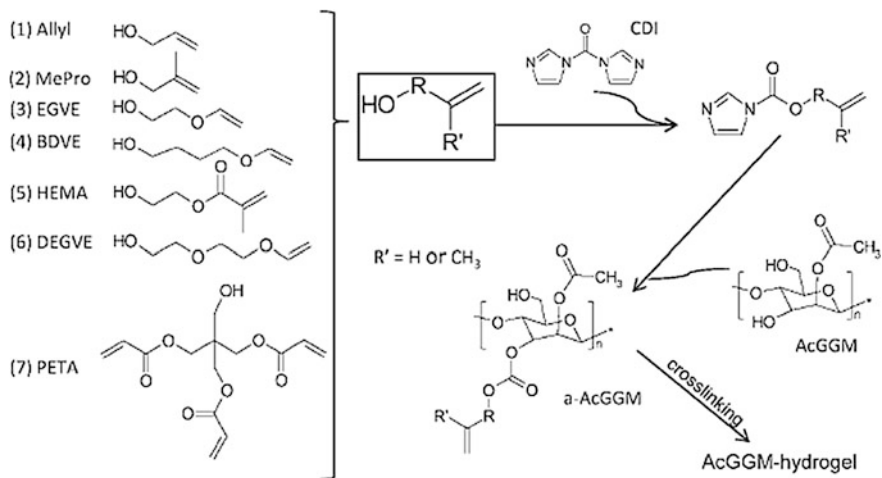


Fig. 6 The synthesis route of hydrogels (Voepel et al. 2010)

3.1.3 Semi-full Interpenetrating Hydrogels

Over the past few decades, interpenetrating polymer networks (IPNs) showed high potential in the biomedical fields applications, such as drug delivery. IPNs have promoted the development of bioengineering tissues, such as cartilage scaffolds, tissues, and bone substitutes greatly (Rokhade et al. 2007). IPNs comprise two or more networks which cannot be separated unless chemical bonds are broken because they are interlaced on a molecular scale but not covalently bonded to each other. Semi-IPNs are different from IPNs due to the compositions linear or branched polymers can be separated from the compositions polymer networks without the breakages of chemical bonds (Chikh et al. 2011). Semi-IPNs are considered as popular sensitive polymers with great mechanical strength, various sensitivity, and easy fabrication of devices (Zhao et al. 2006). Natural polysaccharide and its derivatives, such as hemicellulose, chitosan, sodium alginate and cellulose, which are biocompatible and biodegradable, could be used as linear macromolecule forming half interpenetrating networks. Moreover, their functional groups could respond to the environmental stimuli, and have been widely used in preparing biomedical materials. The formation of semi- and full interpenetrating hydrogels is shown Fig. 7.

Karaaslan et al. (2010, 2012) designed novel pH-responsive semi-IPN hydrogels to utilize hemicellulose and chitosan, which were synthesized with glutaraldehyde as the cross-linker. Swelling abilities have improved with the increase of hemicellulose content and mainly consisted of H-bonded bound water. Covalent cross-linkings rather than crystallites introduced through hemicellulose were the main factor that would influence the mechanical stability of hydrogels. In addition, konjac glucomannan-based (KGM) semi-IPNs hydrogels were synthesized by using

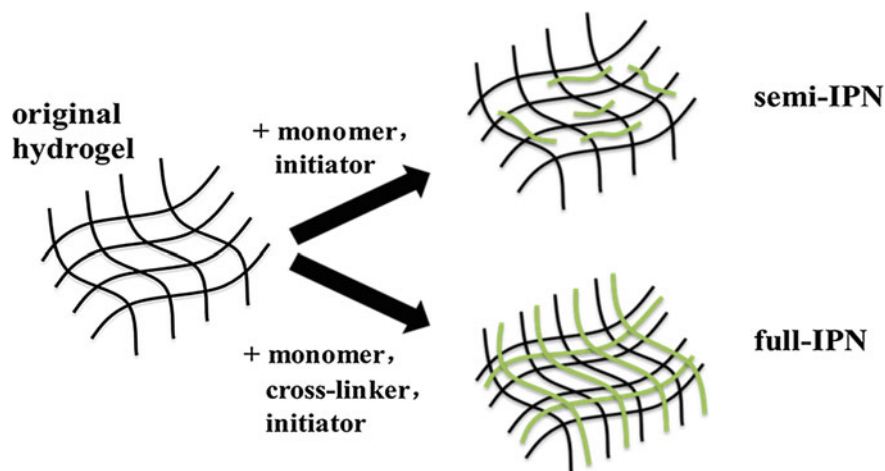


Fig. 7 Formation of semi- and full interpenetrating hydrogels

poly (aspartic acid) and KGM using trisodium trimetaphosphate as the cross-linker (Liu et al. 2010). These results indicated that these two semi-IPN hydrogels are suitable to be used as the polymeric carrier for designated site-specific drug delivery in the intestine. Zhang et al. (2012) prepared a pH-responsive semi-interpenetrating polymer network (semi-IPN) hydrogels based on methylacrylic acid (MAA) and Konjac glucomannan (KGM) reacted with different concentrations of initiator potassium persulfate (KPS) in the presence of *N,N*-methylene-bis-acrylamide (MBA) as the cross-linker through free radical polymerization. Moreover, a novel semi-IPNs were prepared by copolymerizing konjac glucomannan (KGM) and poly (ethylene glycol diacrylate) (PEGDA) with poly (*N*-vinyl pyrrolidinone) (PNVP) using 2-hydroxy-2-methyl-propiophenone (HMPP) as an initiator under UV curing (Fig. 8). And the study indicated that the KGM hydrogel could benefit wound healing (Shahbuddin et al. 2014).

3.2 Physically Cross-linking Hydrogel

Physically cross-linking hydrogels are three-dimensional networks due to the entanglement between molecules, and the interaction among ions, hydrogen bonds and hydrophobic effect (Guan et al. 2014a). For example, with the increase/decrease of temperature, polymers with random-string state distributed in the solution, the molecule motion increase led to the destruction of the random-string structure, and a spring-like structure formed due to the entanglement among molecules which could form a gel (Osato et al. 2003; Deszczynski et al. 2003). The gelation mechanism of temperature-responsive hydrogel is shown in Fig. 9. Ion embedding

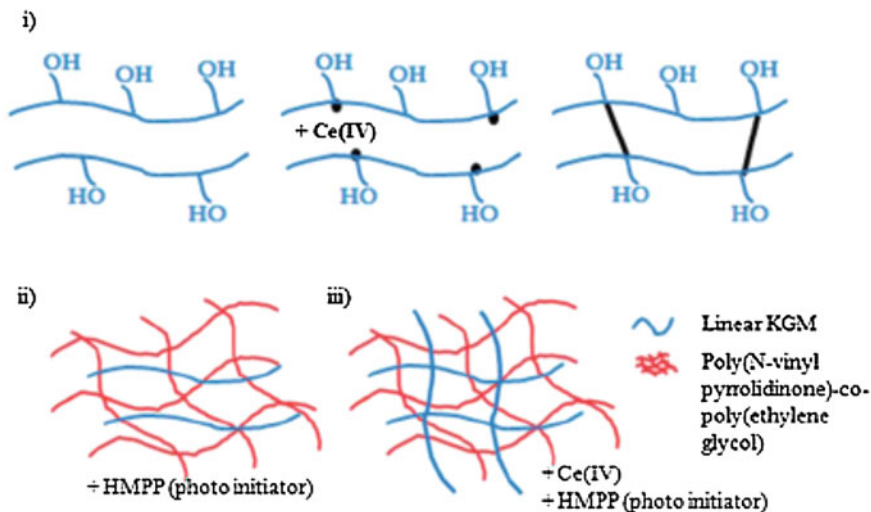


Fig. 8 Schematic representation of the formation of (i) cross-linking with liner KGM initiated by Ce (iv), (ii) semi-IPN of P(NVP-*co*-PEGDA) initiated by HMPP with uncrosslinked KGM and (iii) grafted conetwork of KGM and P (NVP-*co*-PEGDA) by Ce (iv) and HMPP (Shahbuddin et al. 2014)

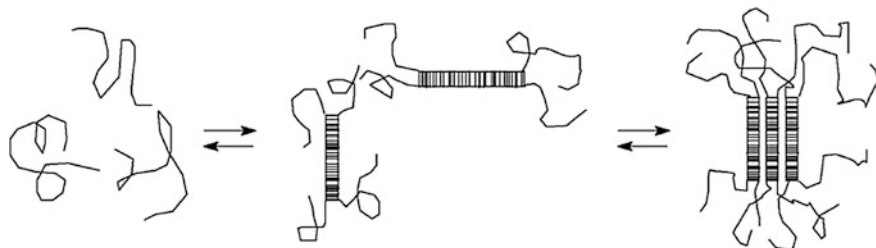


Fig. 9 Gelation mechanism of temperature response model of physical cross-linking hydrogels sol-gel transition diagram

type hydrogel is synthesized due to the polyelectrolyte polyvalent ionic bonds with opposite charges and timeliness (Fig. 10). But with opposite charges of two kinds of polyelectrolyte interaction to form the physical cross-linking system are called electrolysis compounds (Fig. 10).

For cross-linking hydrogels, entanglement among molecules, hydrophobic interaction between molecules and ionic bond areas could facilitate the formation of cluster structure, thus causing an irregular structure in hydrogels (Kweon and Noh 2001). Meanwhile, free chain end and link can also lead to instantaneous network defects. The ionic cross-linking with polyvalent counter ion is a simple way to form physical cross-linking hydrogels. However, such ions could exchange with soluble ions in body fluids, inevitably, resulting in loss of performance compared with the

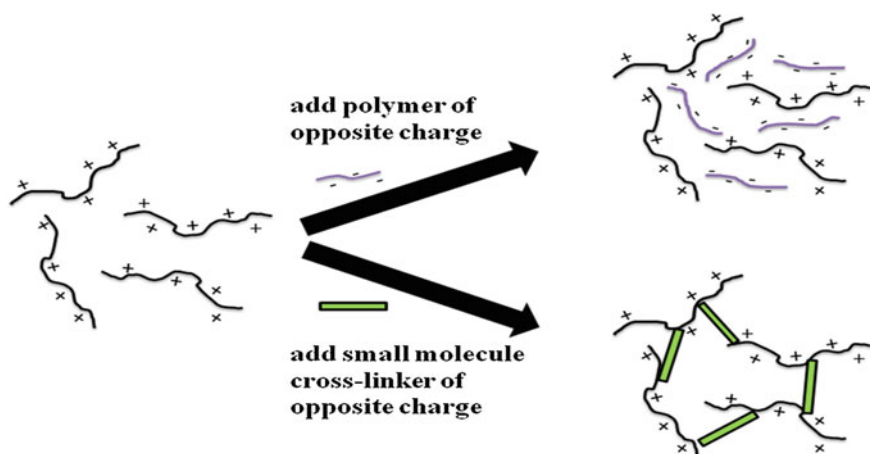


Fig. 10 Mechanisms of in situ physical gelation based on charge interactions

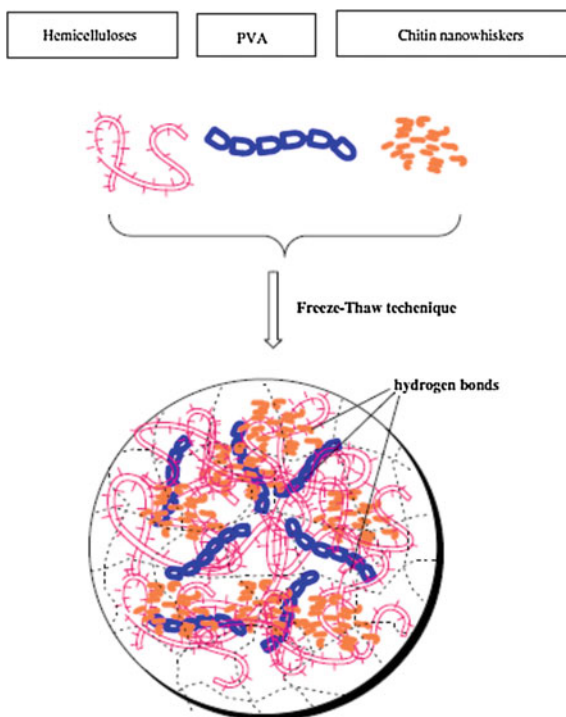
original performance. Therefore, cationic groups/anion groups on the backbone of hemicellulose could be incorporated to ensure the formation of hemicellulose-based hydrogels.

In addition, the polymer phase transition can also form hydrogels. For example, when the temperature reaches the lower critical solution temperature (LCST), small changes in temperature can make polymer sol phase transition into a gel.

Freeze–thaw processing is one method of preparing hydrogels without using chemical cross-linking agents (Nugent and Higginbotham 2007). This method is simple, convenient, and causes low pollution. The polymer is rejected from the growing ice crystallite when the solution freezes, resulting in the gelation of polymers, which is driven by phase separation. This process is refined with repeated cycling (Guan et al. 2014a) (Fig. 11). The more the cycles, a larger dimension of the crystallites could be obtained, and the final hydrogels consisted of water-filled pores, in which the ice has disappeared, surrounded by a polymer skeleton. Physical cross-linking in the form of crystalline polymeric regions and hydrogen bonds strengthens the gel structure.

PVA hydrogels designed by freeze/thaw cycling are excellent candidates for biomaterials as they possess a high swelling ratio in water, a rubbery elastic nature, are innocuous, noncarcinogenic, and good biocompatibility. The versatility of PVA hydrogels endows them with many biomedical applications, such as matrices for cell immobilization and for drug release. Guan et al. (2014b) reported a hybrid hydrogel which can be easily synthesized through physical cross-linking of hemicellulose, chitin nanowhiskers, and poly (vinyl alcohol phosphate) (P-PVA). This work emphasized the influence of the hydrogen bonds on polymers with a freeze–thaw method by comparing the structural and morphological properties, as well as the swelling and mechanical properties. The hydrogen-bonded network was easily formed among the polymers in the frozen state. However, when the water was

Fig. 11 Proposed synthesis route for the preparation of hemicellulose, chitin nanowhiskers, and PVA under a freeze–thaw technique (Guan et al. 2014b)



removed, the pores were retained with the increasing of temperature. This indicated that these hydrogels had a large number of hydroxyl bonds and that hydrogen-bonded network structures still kept a highly stable state at low temperatures.

3.3 Classification of Smart Hydrogels

3.3.1 Temperature-Responsive Hydrogels

Temperature-sensitive hydrogel is a type of hydrogels whose properties could change with temperature changes (Yang et al. 2011). When small changes occur in temperature, several or dozens of times in the volume would happen on hydrogels, when the changes reach or exceed the critical region, even discontinuous abrupt changes will happen, which is called volume phase transition (Cao et al. 2014). This kind of hydrogel has a certain proportion of hydrophobic and hydrophilic groups, and the change in temperature can affect the hydrophobic interaction and hydrogen bonding interaction between the macromolecular chains, so that the hydrogel structure changed, resulting in a volume phase transition, this temperature is called the volume phase transition temperature (VPTT) (Zhao et al. 2006) (Fig. 12; Tables 4 and 5).

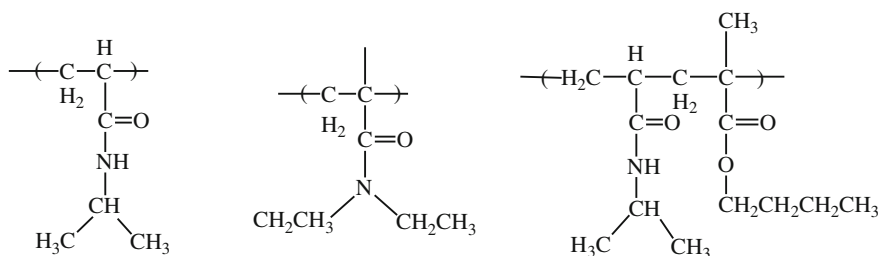


Fig. 12 Structures of typical temperature-sensitive polymers (Qiu et al. 2012)

Table 4 Groups which can cause temperature responding behavior

Alcohol functional groups	Hydroxypropyl acrylate
	Hydroxypropyl methacrylate
	Hydroxyethyl acrylate
	Hydroxypropyl methyl cellulose (HPMC)
	Hydroxyethyl cellulose
	Hydroxy propyl cellulose (HPC)
	Methylated cellulose (MC)
	Polyvinyl Alcohol and its derivatives
N-substituted amide functional group	Poly (N— <i>isopropyl</i> acrylamide)
	Polypropylene morpholine and Acrylic ester containing morpholine
Ether functional groups	PEO (polyethylene oxide)
	Copolymer and block copolymer of ethylene oxide/propylene oxide
	Polyvinyl methyl ether (PVME)
	PEO-PPO
	Alkyl—PEO block surfactant

Table 5 Groups used for prepare pH-sensitive hydrogels (Peng et al. 2011)

Anionic groups	$-\text{COO}^-$
	$-\text{OPO}_3^-$
Cationic groups	$-\text{NH}_3^+$
	$-\text{NRH}_2^+$
	$-\text{NR}_2\text{H}^+$
	$-\text{NR}_3^+$

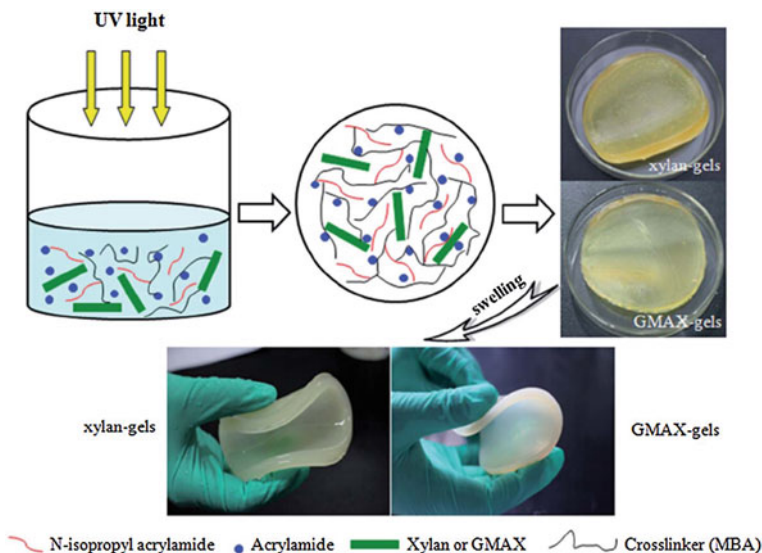


Fig. 13 Proposed synthesis route for the preparation of temperature-sensitive xylan-based hydrogels (Gao et al. 2015a)

Gao et al. (2015a) prepared a temperature/pH dual-responsive hydrogel by the grafting copolymerization of xylan derivative with *N*-isopropylacrylamide and acrylamide using *N,N'*-methylenebis-acrylamide as the cross-linking agent. The hydrogels exhibited a rapid phase transition temperature around 35 °C (Fig. 13).

3.3.2 pH-Sensitive Hydrogels

The swelling and shrinkage of pH-sensitive hydrogels are closely associated with the value of pH (Falamarzian and Varshosaz 1998; Gao et al. 2015a). Generally speaking, the networks of pH-responsive hydrogels containing a lot of acidic and alkaline groups such as carboxyl, sulfonic groups, and amino tend to decomposed or protonated (Zhao et al. 2006). Dissociation of these groups is easily affected by the pH value of the environment, which could damage the inner related hydrogen bonds of hydrogels, with the decrease of cross-linkings, resulting in a swelling of hydrogels. This kind of polymer with large amounts of ionization group is called the polyelectrolyte. Ionic strength, pH value, and the type of the counter ion could affect the swelling behavior of polyelectrolyte hydrogels due to the electrostatic repulsion like charges (Zhao et al. 2014a). The stimulus–response behaviors indicated that the hydrogel could be easily controlled by changing solvent pH and solvent type. The responsiveness of polyelectrolyte gel can be adjusted by copolymerization with neutralization monomer. Moreover, the introduction of 2-hydroxyethyl methyl methacrylate, methyl methacrylate (MMA) and maleic

anhydride can change the hydrophilicity of polymer (Sun et al. 2013), which can be used to adjust the responsiveness of hydrogels.

Sun et al. (2013) designed a novel pH-sensitive and biodegradable hemicellulose-based hydrogel which was prepared by grafting AAc into hemicellulose. The swelling ratio data showed apparent transitions at physiological pH.

3.3.3 Photosensitive Sensitive Hydrogels

Photosensitive molecules introduced into hydrogels could endow the hydrogel response to an environmental stimulus when the photosensitive absorbed light and then resulted in a change of temperature or electric field. Photosensitive compounds are chlorophyllin, dichromate, aromatic azides and diazo compound, aromatic nitro compounds and organic halogen compounds, etc. (Chiang and Chu 2015; Sumaru et al. 2006).

The mechanism of photo-responsiveness could fall into three categories: One is introducing special photosensitive molecules to temperature-sensitive materials, which could convert light into heat with the increase of temperature (Zhu et al. 2012). Hydrogels could response when the inner temperature achieves the phase inversion temperature. Another is that the photosensitive molecules ionized by light resulting in a light responsiveness. This kind of hydrogels could generate a large number of ions by light, resulting in a mutation in osmotic pressure, which could accelerate the swelling of hydrogels. The third responsive mechanism is the chromophoric group that in hydrogels, which can absorb light and come into being color (Szilagyi et al. 2007).

Polysaccharide-based multi-responsive hydrogels with light responsive abilities are of great interest for controlled drug and protein delivery systems. Cao et al. (2014) designed a novel photo-responsive hydrogel prepared by free radical copolymerization (Fig. 14). The synthesized hydrogel presented a light response behavior under the UV irradiation. The thermodynamically stable trans-conformation of azobenzene structure would convert into the cis-conformation under UV irradiation. However, as the cis-conformation of azobenzene was exposed to visible light or deposited in the dark, it would transfer into the trans-conformation again, resulting in a variation of the hydrophilic/hydrophobic balance causing by the trans-cis isomerization.

3.3.4 Electric-Responsive Hydrogels

Electric-responsive hydrogels, which can undergo significant physicochemical changes in response to electric stimuli, have drawn wide attention in many fields. Ionogens in the networks are the essential requirement for the polymer materials to response to the electrical stimulation. Electric sensitive hydrogels are consisted of polyelectrolyte (Osada et al. 1987). When placed into the electrolyte solution, the

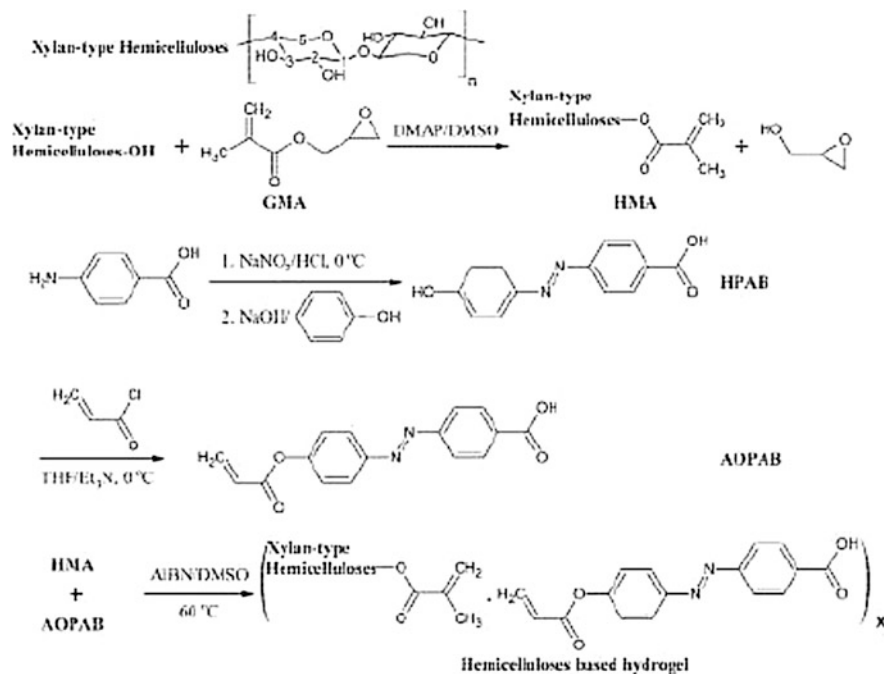


Fig. 14 Proposed synthesis route for the preparation of light-responsive xylan-type hemicellulose-based hydrogel (Cao et al. 2014)

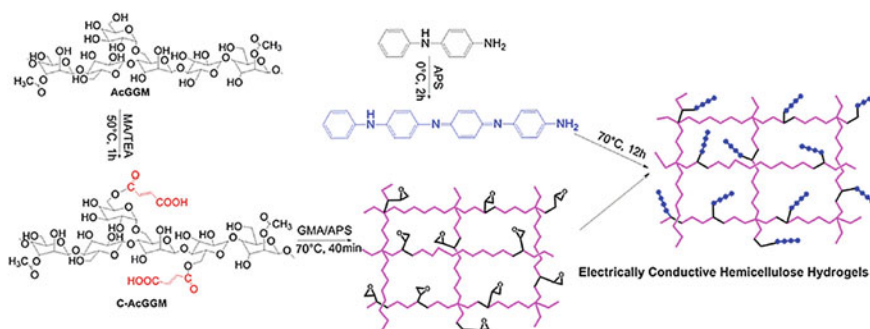


Fig. 15 Proposed synthesis route of electrically conductive hemicellulose hydrogels (ECHHs) (Zhao et al. 2014c)

size or shape of hydrogels would change under the stimulation of electricity to transform the electricity into mechanical energy.

Zhao et al. (2014c) designed a straightforward and robust approach by synthesizing electrically conductive hemicellulose hydrogels (ECHHs) based on AcGGM and conductive aniline tetramer (AT) (Fig. 15). The degree of substitution (DS) of the carboxylated AcGGM has a great influence on hydrogel swelling ratios (Fig. 16).

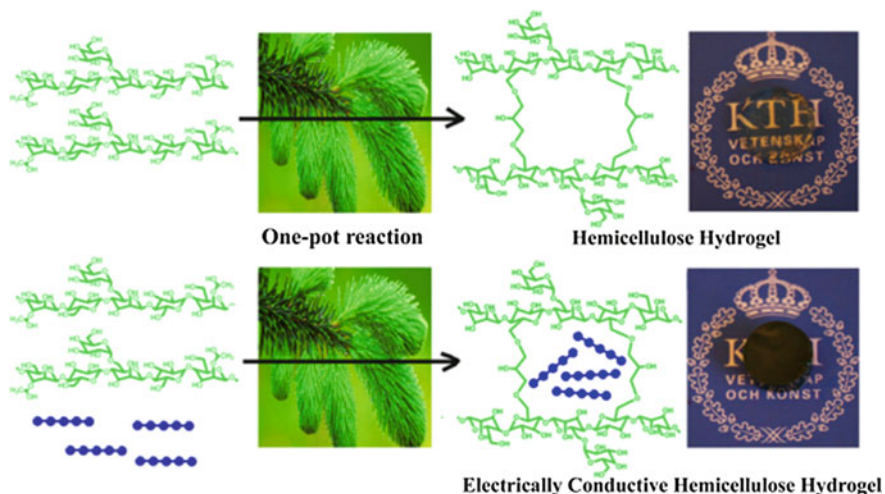


Fig. 16 The proposed mechanism of a one-pot reaction to synthesize electrically conductive hemicellulose hydrogels (Zhao et al. 2014b)

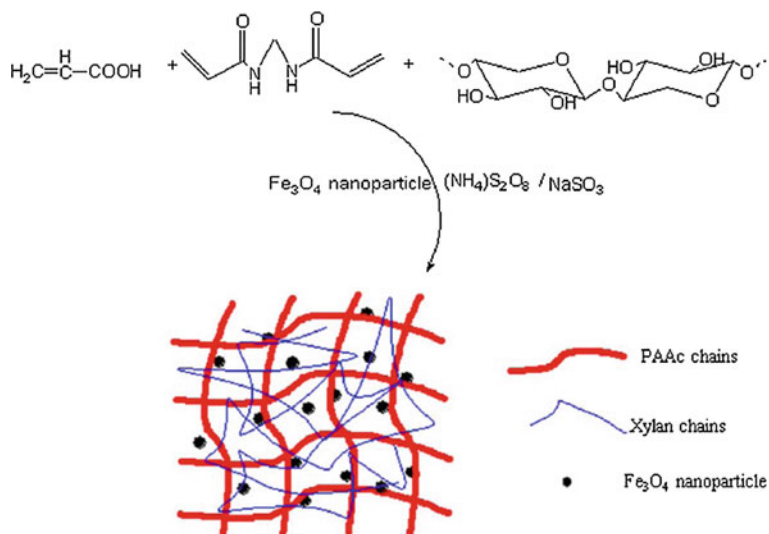


Fig. 17 The synthesis mechanism for xylan/PAAC semi-IPN magnetic hydrogel (Sun et al. 2015b)

Zhao et al. (2014b) designed a type of electrically conductive hemicellulose hydrogels (ECHHs) with macro-porous structures by cross-linking AcGGM with epichlorohydrin in the presence of conductive aniline pentamer (AP) through a facile method in water and at ambient temperature (Fig. 17). And the addition of

AP could improve the thermal stability of ECHHs. In addition, equilibrium swelling ratios were regulated by cross-linker concentration and AP content level. Therefore, EEHHs possess controllable conductivity, tunable swelling behavior, and acceptable mechanical properties.

3.3.5 Magnetic-Responsive Hydrogels

Magnetic-responsive hydrogel is a kind of intelligent hydrogel, whose swelling behavior can be responsive to environmental magnetic field. This kind of hydrogel could be separated rapidly by applied magnetic field. Recent years, there is a great interest in studying magnetic-responsive hydrogel used in the field of cellular segregation, enzyme immobilization, and targeted drugs (Lima-Tenorio et al. 2015; Sun et al. 2015a, b). For example, introducing Fe_3O_4 as a magnetic material into hydrogel systems could endow the hydrogel with magnetism, and they could be applied for separation, image enhancement, drug delivery, and remote-controlled actuators.

Li et al. (2014) synthesized a novel hemicellulose-based magnetic hydrogel through the graft copolymerization method, using H_2O_2 -Vc as a redox initiator system to initiate the hemicellulosic derivative and surface-modified Fe_3O_4 particles as the magnetic component. Results showed that the Fe_3O_4 particles were evenly distributed in the hydrogel matrix with the paramagnetic properties. Swelling behaviors of the hydrogels were simulated using Fickian and Schott kinetic models in a buffer solution (pH = 8). The size of the pore and swelling ratio of the prepared hydrogels increased with increasing the pH value due to the $-\text{COOH}$ groups in the hydrogels that were dissociated into $-\text{COO}^-$ at higher pH values. In this case, electrostatic interaction expanded the network of hydrogels. In addition, the adsorption ability of the magnetic hydrogel was much higher than that of a non-magnetic hydrogel when used to adsorb lysozyme, and the equilibrium adsorption data fitted the Freundlich and Temkin isotherm models well. Sun et al. (2015b) prepared a Fe_3O_4 nanocomposite hydrogels base on xylan and poly (acrylic acid) (Fig. 17), which exhibited magnetic- and pH-responsive properties and excellent thermal stability. Besides that, Sun et al. (2015c) designed the xylan/poly (acrylic acid) magnetic nanocomposite hydrogels adsorbent base on Fe_3O_4 nanoparticles and wheat straw xylan. The data showed that the removal percentage of methylene blue could reach above 90%, indicating that the prepared hydrogel adsorbent has a great potential for the water treatment.

3.4 Characterization Methods of Hydrogels

The structure of hydrogels is usually characterized by Fourier transform infrared spectroscopy (FTIR)/ultraviolet spectrophotometry (UV), scanning electron microscopy (SEM), transmission electron microscopy (TEM), and differential

scanning calorimetry (DSC). In addition, mechanical properties and swelling behavior are the important properties of hydrogels (Guan et al. 2015).

In addition to qualitative characterized for hydrogels using FTIR/UV, UV could also be used for the determination of LCST (Uraki et al. 2006). SEM is a main method that could observe the microstructure of hydrogels directly and it could magnify hydrogels' microstructure and surface morphology tens of thousands of times (Lima-Tenorio et al. 2015). TEM possesses high resolution and magnification and is used to evaluate the morphology, composition, and structure of fine particles or nanoparticles in hydrogels (Gao et al. 2014).

The interaction between absorbed water and hydrogel and the distribution of water in hydrogel have great influence on the application of hydrogel due to its excellent properties of absorbing water. The hydrogen bonds between water and hydrogel are helpful to the formation of bridge connection in polymer networks, which could plastify or anti-plastify the network of hydrogels. At present, many researchers think that water mainly exists in three states, which are free water, frozen bound water, and unfrozen bound water. Free water is also called unbound water, whose enthalpimetric, heat flow peak, and phase transition temperature are similar to pure water in shape using differential scanning calorimetry (DSC) (Gao et al. 2015a). The melting temperature of the frozen bond water is lower than pure water's phase transition temperature because of the weak strength adhesion forces. However, the strong interaction between unfrozen bond water and hydrogels inhibits the observation through DSC.

The mechanical properties of hydrogels could be explored through the mechanical tensile experiments, such as tensile strength, elongation at break, and elastic modulus. In general, the storage modulus (E') and loss modulus (E'') are very low when the hydrogel is at the swelling state and it will be higher when in contraction condition. The interaction (such as hydrogen bonds, electrostatic interaction, crystallization, and hydrophilic/hydrophobic interaction) among hydrogel molecules is in connection with hydrogel's storage modulus (E') and loss modulus (E'') (Kong et al. 2016). The equilibrium swelling experiments are usually performed by the gravimetric method (Sun et al. 2015a).

4 The Applications of Hemicellulose-Based Hydrogels

Natural polymers based intelligent hydrogels which have environmental multi-responsive sensitivity to temperature, pH, salt, light, etc., have aroused increasing interests due to the biodegradability, abundance, and biocompatibility of biopolymers (Gao et al. 2015a; Bhattarai et al. 2010). Additionally, natural macromolecules could be candidate for recyclable hydrogel design because they have plenty of hydrophilic groups and adsorb aqueous solutes (Ferrari et al. 2014). Nowadays, wastewater pollution especially heavy metals have brought serious damage to living environment, biomaterials like hemicellulose-based hydrogels

have been alternative absorbent materials for water pretreatment as well as other chemical adsorbents (Ayoub et al. 2013; Peng et al. 2012b; Sun et al. 2015a; Zhang et al. 2014a). Recent years, hemicellulose possessing the unique physiological properties have been widely reported and extensively studied among the fields of medical science (Barbat et al. 2008; Noaman et al. 2008; Oliveira et al. 2010), including histological scaffolds for tissue engineering, biosensors, immunization barriers for the cells encapsulation, and controlled drug delivery systems owing to their special properties (Dai et al. 2015; Gao et al. 2015a; Lee and Mooney 2001; Lin and Metters 2006; Qiu and Park, 2012; Sefton et al. 2000). Moreover, hemicellulose with a number of charged groups has attracted great attention to be conductive materials for application in biosensors, electronic devices, and tissue engineering fields (Guimard et al. 2007; Guo et al. 2013; Zhao et al. 2014c).

4.1 Adsorbent Materials

Nowadays, the increasing environmental issues have aroused global concern. One of most serious problems is water pollution by heavy metal ions derived from industrial wastes, mainly textile factories and metal workshops (Peng et al. 2012b). The heavy metal ions, such as cadmium, plumbum, zinc, nickel, and chromium, have brought serious threat to the human beings, living life organisms, and ecological resources worldwide, causing various heavy diseases and damage of natural environment (Ayoub et al. 2013; O'Connell et al. 2008; Wan Ngah and Hanafiah 2008). Different from organic wastes, heavy metals ions were difficult to remove and could be accumulated in the environment and living body. Furthermore, heavy metal ions exhibit toxic impact even at very low dosages. Recently, biodegradable hydrogels as adsorbent materials for removing heavy ions have been paid extensive attention instead of conventional methods from aqueous solutions including chemical precipitation, ion exchanges, chemical oxidation/reduction, electro dialysis, reverse osmosis, and ultrafiltration because hydrogels with a three-dimensional polymer network as adsorbents which have big porous structure, multifunctional groups, and high internal specific surface area (Zheng and Wang 2009). Biodegradable polysaccharides based hydrogels have apparent advantages, such as higher efficiency, high hydrophilicity, lower costs, minimization of chemical or biological sludge, flexibility, simplicity of design, good reusability, and good biodegradability (Ahluwalia and Goyal 2005; Crini and Badot 2008; Li and Bai 2006). The swelling abilities of polysaccharides-based hydrogels in water and their solutes adsorption could be controlled by their cross-linking density and chemical compositions (Ferrari et al. 2014).

Hemicellulose is a suitable resource to prepare bioadsorbents for removing metal ions and has been attracted important attention (Ayoub et al. 2013; Dax et al. 2014; Peng et al. 2012b; Sun et al. 2015a; Zhong et al. 2013). Peng et al. (2012b) prepared xylan-rich hemicellulose-based hydrogels as bioadsorbent by grafting copolymerization of AA and hemicellulose for the application of heavy metal ions (Pd^{2+} ,

Cd^{2+} , and Zn^{2+}) adsorption from aqueous solutions. AA was the most common hydrophilic monomer in adsorbent hydrogels because it is the simplest unsaturated carboxylic acid and has pH sensitivity. The adsorption kinetics study demonstrated that the optimum adsorption values of Pd^{2+} , Zn^{2+} , and Cd^{2+} were 859, 274, and 495 mg/g, respectively. More importantly, xylan-rich hemicellulose-grafting-AA hydrogels also showed highly efficient reusability and metal ion recovery efficiency. After plenty of repeated adsorption/desorption cycles, there were no noticeable loss of adsorption capacity emerging. Similarly, but to a less extent, a hydrogel for adsorbing Cu^{2+} and Ni^{2+} was prepared by cross-linking of arabinoxylan and AA (Zhong et al. 2013). Table 6 shows the comparison of adsorption values of metal ions (Pb^{2+} , Cd^{2+} , Zn^{2+} , Cu^{2+}) of different adsorbents. Hemicellulose-based hydrogels had the excellent adsorption capacities.

Superabsorbent hydrogels based on xylan and inorganic clay montmorillonite (MMT) were prepared by Zhang et al. (2014a). The hydrogels had very high swelling ratio due to the addition of hydrophilic AA and 2-acrylamido-2-methylpropanesulfonic acid (AMPS) as well as MMT with good absorption property. Furthermore, the increment of MMT content could increase the compression strength of hydrogels. The swelling ratio of the porous xylan-based hydrogels in the cationic salt solutions (LiCl , CaCl_2 , and FeCl_3) followed the order: $\text{Li}^+ > \text{Ca}^{2+} > \text{Fe}^{3+}$. Poly(amidoamine)/hemicellulose-based hydrogels were prepared from *O*-acetylated galactoglucomannan-rich plant and displayed a remarkable adsorption capacities for Cu^{2+} , Cd^{2+} , Pb^{2+} , Zn^{2+} , Ni^{2+} , Co^{2+} , and CrO_4^{2-} (Ferrari et al. 2014). In their study, two different polyacrylamide-based oligomers were synthesized and polysaccharide networks were formed by chemically radical grafting copolymerization. Generally, the order of adsorption affinity toward Me^{2+}

Table 6 Comparison of adsorption values (mg/g) of metal ions by different adsorbents

Adsorbents	Pb^{2+}	Cd^{2+}	Zn^{2+}	Cu^{2+}	References
Cellulose derivatives	≤ 105	≤ 169	≤ 27		O'Connell et al. (2008)
Sugarcane bagasse	500	256.4			Gurgel et al. (2008)
Chitosan-based derivatives	559.4				Tang et al. (2007)
Starch-based derivatives	416.9				Guo et al. (2006)
Carrageenan/AA hydrogels	202	239	216		Shawky et al. (2006)
Hemicellulose/AA hydrogels	859	495	274		Peng et al. (2012b)
Arabinoxylan/AA hydrogels				330.1	Zhong et al. (2013)
Modified plant wastes	≤ 313	≤ 313	≤ 83.3		Wan Ngah and Hanafiah (2008)
Magnetic nanoparticles	166.1	29.6	43.4	129.6	Ge et al. (2012)

was $\text{Cu}^{2+} > \text{Co}^{2+} > \text{Zn}^{2+} \approx \text{Ni}^{2+} > \text{Pb}^{2+} > \text{Cd}^{2+}$. All obtained hydrogels were had great potential as adsorbent materials. Dax et al. (2014) investigated GMA-modified *O*-acetyl galactoglucomannan-based hydrogels and their application for removing arsenic and chromium ions. The results revealed that hydrogels had a high surface area and were evaluated to have a great capacity to remove arsenic and chromate ions at different pH aqueous solutions. To separate the adsorbent simply and quickly from the solution system, additives such as Fe_3O_4 nanoparticles were introduced and separated by an external magnetic field (Sun et al. 2015c). The xylan/poly(acrylic acid) magnetic (Fe_3O_4 nanoparticles) nanocomposite hydrogel adsorbent for methylene blue removal from aqueous medium was prepared from wheat straw xylan by Sun et al. (2015c). Results showed that the optimal condition for methylene blue adsorption was at pH 8, adsorbent dosage was 3 g/L and a beginning concentration was 400 mg/L, and the final removal rate reached more than 90%. The addition of Fe_3O_4 nanoparticles could enhance the cyclic utilization of the xylan-based adsorbent. The adsorption isotherm of methylene blue was consistent with the Langmuir model. The hemicellulose-based adsorbent hydrogel materials will provide potential choice for water pretreatment and heavy metal removal.

4.2 Medical Materials

The major challenges in developing medical materials (e.g., drug delivery carriers, human tissues scaffold) were found to require suitable biomaterials and convenient preparation methods that would ensure excellent durability, nontoxicity, and biocompatibility (Reis et al. 2006). There is increasing interest in cooperating multi-sensitive monomers with natural polysaccharides as hydrogel materials for medical application. So many relevant researches on biopolymers (e.g., chitosan, cellulose, dextran, starch, and pullulan) based hydrogels have been reported in the past decades (Bhattacharai et al. 2010; Bostan et al. 2013; Fundueanu et al. 2008; Gao et al. 2015b; Hebeish et al. 2014; Li et al. 2012; Wang and Chen 2016; Zhang et al. 2004). However, hemicellulose-based intelligent hydrogels including temperature, pH, salt, light-sensitive hydrogel materials showed excellent application prospects in biomedical fields because xylan had unique physiological characteristics such as biocompatibility, anticancer effect and inhibiting growth rate of tumors, etc. (Barbat et al. 2008; Oliveira et al. 2010; Whistler et al. 1976). These unique and competitive advantages aroused broad interest among researchers in studying hemicellulose-based hydrogels which could be applied in the fields of drug-controlled delivery, immunity of the human body, and tissue engineering.

Xylan isolated from corn cobs was proved to be an appropriate additive in the pharmaceutical and immune fields (Hromadkova et al. 1999; Oliveira et al. 2010). Moreover, hemicellulose is proved to be stable in the human stomach and intestine (Oliveira et al. 2010). Therefore, hemicellulose and hemicellulose derivatives based hydrogels had promising application as sustained controlled release carriers in the

human digestive system (Ebringerová et al. 2002). Moreover, compared with other polysaccharides such as cellulose, starch, and chitosan, hemicellulose has relatively high solubility due to their low molecular weight and high substitution degree of side chain (Chimphango et al. 2012). Hence, hemicellulose could be easily dissolved in common solvents such as alkaline solution, DMF/LiCl, dimethyl sulfoxide (DMSO), and ionic liquid, which provide more chance for modification of hemicellulose with active hydroxyl groups (Peng et al. 2012b). Hemicellulose derivatives were also investigated to increase the reactivity of preparing hydrogels and overcome the shortcomings of hemicellulose, such as brittleness and relatively poor forming ability (Gabrielii et al. 2000; Gao et al. 2015a). Peng et al. (2012a) introduced methacryloyl groups (from GMA) onto hemicellulose by the transesterification reaction in the DMSO medium. Cao et al. (2014) prepared photosensitive hydrogels by the radical copolymerization of GMA-modified hemicellulose using 4-[(4-acryloyloxyphenyl)azo] benzoic acid (AOPAB), the resulting hydrogels showed multi-sensitive behaviors to pH, water/ethanol solutions and light. Vitamin B₁₂ (VB₁₂) was chosen as drug model to determine its in vitro release performance under UV irradiation at 37 °C. The maximum cumulative release rates of the hydrogel in pH 2.2 and 7.4 solutions were 78.2 and 89.3%, respectively. Besides, the cumulative VB₁₂ release of hemicellulose-based hydrogels under UV irradiation was higher than that without UV irradiation, which had a potential application in the light on-off drug delivery field. Temperature-sensitive hemicellulose-based hydrogels were prepared by grafting maleic anhydride (MA) to hemicellulose and then photocrosslinking with NIPAm in LiCl/DMF solvent to prepare the hydrogels (Yang et al. 2011). Maleic anhydride modified hemicellulose (Hce-MA) based hydrogels had well-defined honeycomb-like structure and temperature sensitivity. The LCST of hydrogels ranged approximately between 28 and 32 °C and increased with the increasing Hce-MA content due to the hydrophilicity of Hce-MA. The induced temperature-sensitive properties were induced by the balance of hydrophilic/hydrophobic in the hydrogels system induced sensitive hydrogels (Pan and Sano 2005). The Hce-MA-based hydrogels could be as drug controlled carriers in the further studies. The attributes of the raw materials and preparation methods are the main influence factors of the functionalities of hydrogels for using as encapsulation matrix. Hydrogels applied for controlled release delivery systems had the demanding of protecting the functionalities of the encapsulated agents (Coviello et al. 2007). Xylans are considered to possess excellent gelation for preparing hydrogels which could be used as coating materials for controlled release of bioactive agents (Chimphango et al. 2012). The oat spelt xylan hydrogels were prepared by recombinant-L-arabinofuranosidase (AbfB). The horseradish peroxidase (HRP) as bioactive agent was encapsulated in situ and was released actively for a period of 180 min. It was noticeable that the drug delivery behaviors of HRP were based on the sequence of addition during the preparation of hydrogels. The results revealed modification of xylan-based hydrogels as biodegradable encapsulation matrices were suitable for encapsulating bioactive agents to reach slow or targeted release. AcGGM-based hydrogels were prepared using APS and Na₂S₂O₅ by radical polymerization (Voepel et al. 2009). The drug release behaviors of

AcGGM-based hydrogels were determined by caffeine and vitasyn blue as drug models. The results showed molecular weight of drug and the amount of AcGGM had an important effect on the release behaviors. The caffeine released more over 80% after 120 min, while vitasyn blue released 250 min. The vitasyn blue had lower release rate than caffeine duo to higher molecular weight. Arabinoxylan-based hydrogels as drug vectors were prepared by peroxidase/peroxide oxidative cross-linking (Irvani et al. 2011), the caffeine as the drug model was chosen and released in the HCl and water solution, respectively. The results indicated that the caffeine release amount in the 0.1 M HCl solution was higher than in water. Moreover, it was indicative of that xylan-based hydrogels could not only be applied in the delivery of macromolecules like protein, but also have broad applications in small molecular drug controlled release in the gastrointestinal tract.

Afterwards, Sun et al. (2013) prepared pH-sensitive hydrogels for drug controlled delivery using hemicellulose isolated from wheat straw. Acrylic acid was added as pH-sensitive monomer and cross-linked with hemicellulose chain in the presence of MBA. The results showed that the resulted hydrogels had good biodegradability. Moreover, the swelling ratios, water uptake, and degradation of hydrogels could be adjusted by the amount of acrylic acid, cross-linkers, and initiator. The cumulative release of acetylsalicylic acid as drug model was approximately 85 and 25% in simulated intestinal and gastric fluid. Comparing the drug release of acetylsalicylic acid with theophylline (shown in Fig. 18), the difference between the cumulative release amounts of acetylsalicylic acid in the stimulated gastrointestinal solutions was more obvious than that of theophylline. The maximum drug release of acetylsalicylic acid in gastric solution was about 24%, far less than 50% of theophylline. This was indicative of that molecular structure of drug had significant influence on drug release performance. The comparison study of these two types of drugs revealed that drug release behavior was dominated by the hydrogels structure and drugs species.

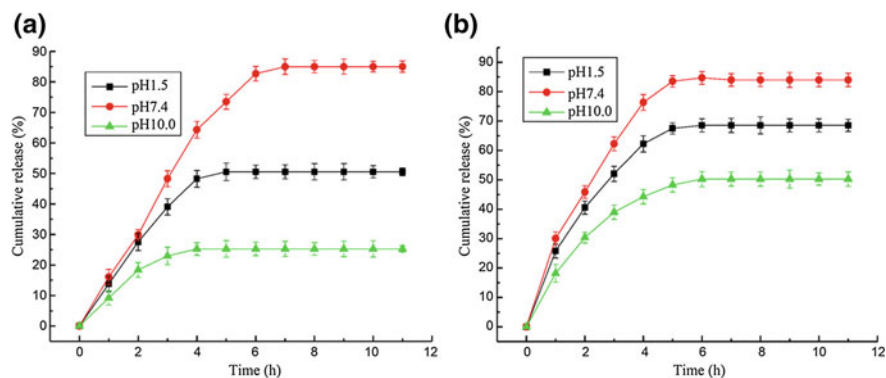
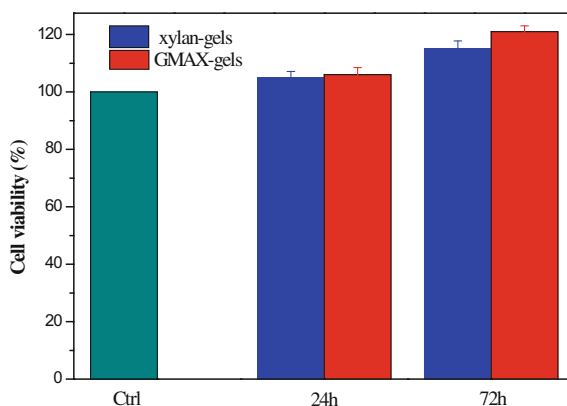


Fig. 18 Drug release performance of acetylsalicylic acid and theophylline loaded hydrogels as functions of pH at 37 °C (Sun et al. 2013)

Contrast researches on temperature and pH dual-sensitive xylan-based and GMA-modified xylan (GMAX) based hydrogels were investigated by Gao et al. (2015a). Both the two types of hydrogels had an LCST about 35 °C. Results indicated that introduce of methacryloyl groups (from GMA) onto xylan backbone had the great influence on the structure of xylan and preparation of hydrogels. In comparison, the cumulative release rate of acetylsalicylic acid for GMAX-based hydrogels (GMAX-gels) was higher (84.2%) than that of xylan-based gels (77.5%) in the pH 7.4 solution. Moreover, GMAX-gels had higher drug coating efficiency (95.21%) and lower drug release rate in gastric fluid due to denser and honeycomb-like network structure. This would reduce greatly the side effect of long-term use of acetylsalicylic acid, such as gastric ulcer, gastrorrhagia, and salicylism (Kent et al. 2008; Khalil 2015). NIH3T3 cells in GMAX-gels were proved to be biocompatible with NIH3T3 cells in Fig. 19. The results showed that the NIH3T3 cellviabilities of both xylan-gels and GMAX-gels were higher than the control group. Furthermore, the NIH3T3 cells had apparent proliferation after incubation for 3 days. Therefore, GMAX-based hydrogels with good mechanical properties and biocompatibility will have a promising potential in biomedical applications, especially in intestinal-targeted drug release system.

Hemicellulose-based hydrogels not only had broad researches on drug controlled release, but also had other medical applications. Guan et al. (2015) investigated hemicellulose-based hydrogels coated with Ag nanoparticles. *Staphylococcus aureus* (*S. aureus*) and *Escherichia coli* (*E. coli*) had small bacterial inhibition ring, in which the diameters were determined for 5 and 6 mm, respectively. This exhibited excellent antibacterial ability against the model microbes *E. coli* and *S. aureus*. Recently, in situ forming and injectable hydrogels have dominated in biomedical applications instead of traditional hydrogels because they could be inserted into the object region by straight injection accurately. Moreover, they provided homogeneous distribution of active molecules in the circumambient tissue (Kretlow et al. 2007; Van Tomme et al. 2008). In situ forming injectable hydrogels from xylan-tyramine (TA) conjugate were fabricated by enzymatic cross-linking

Fig. 19 Cell viability of NIH3T3 after incubating for 1 day and 3 days at 37 °C (Gao et al. 2015a)



(Kuzmenko et al. 2014). Tyramine (TA) side groups were cross-linked with xylan chains. Xylan-TA conjugate was formed using horseradish peroxidase (HRP) and H_2O_2 . The results showed that a 3D hydrogel network was formed in about 20 s at room temperature, which is the best result achieved for any hemicellulose-based hydrogel so far. The hydrogels had excellent swelling properties and maintained mechanical integrity for more than 2 months. Mesenchymal stem cells were able to differentiate into adipocytes inside the hydrogels. It was concluded that xylan had a promising precursor for in situ forming hydrogels and could be assessed further for tissue engineering.

4.3 Conduction Material

Biomaterials based hydrogels with electrical conductivity have the potential application in nerve regeneration because conductive properties could support the attachment and differentiation of neural-like cells with improved interactions (Green et al. 2012; Guarino et al. 2013). The conducting polymers (CPs) were firstly produced in the mid-1970s which are considered as the fourth generation of polymeric materials. The CPs show similar properties with metals and inorganic semiconductors. CPs can be prepared either chemically or electrochemically with each having advantages and disadvantages as summarized in Table 7 (Diaz and Bargon 1986). Chemical synthesis includes either condensation polymerization or addition polymerization, while electrochemical synthesis is conducted using a three-electrode configuration which is including working, counter, and reference electrodes in a mixture solution of the monomer, solvent, and electrolyte (Diaz and Kanazawa 1979; Guimard et al. 2007). There is increasing interest in studying on CPs owing to their special physicochemical properties, such as electroluminescence, electric conductivity, and electrochromism, which impart CPs promising prospects in various applications, such as photovoltaic devices, light-emitting

Table 7 Comparison of chemical and electrochemical CP polymerization

Polymerization approach	Advantages	Disadvantages
Chemical polymerization	• Larger scale production possible	• Cannot make thin film
	• Post-covalent modification of bulk CP possible	• Synthesis more complicated
	• More options to modify CP backbone covalently	
Electrochemical polymerization	• Thin film synthesis possible	• Difficult to remove film from electrode surface
	• Ease of synthesis	
	• Entrapment of molecules in CP	• Post-covalent modification of bulk CP is difficult
	• Doping is simultaneous	

diodes, and biomedical devices (Guarino et al. 2013; Heeger 2001). Furthermore, the CPs-based materials can improve the biodegradability and biocompatibility of products, especially in biomedical fields like scaffold. The CPs can also facilitate to increase the solubility in most solvents (Wang et al. 1996).

Electrically conductive *O*-acetylgalactoglucomannan based hydrogels and conductive aniline tetramer were prepared using a robust pathway by Zhao et al. (2014a). Combining electrically conductive aniline tetramer with degradable, hydrophilic, and nontoxic hemicellulose is a potential choice to surmount the deficiencies of conventional high molecular weight conductive polymers, such as poor polymerization and solubility, the absence of reaction sites, and low hydrophilicity (Guimard et al. 2007; Guo et al. 2013). When the aniline tetramer content increased from 10 to 40% (w/w), the swelling ratio (SR) decreased from 548 to 228% while simultaneously conductivities of hydrogels changed from 2.93×10^{-8} to 1.12×10^{-6} S/cm. The conductivities of the hydrogels increased with increasing aniline tetramer content. Thus, adjusting the amount of aniline tetramer could change the conductivities of hydrogels, which could be applied in biosensor field. Subsequently, Zhao et al. (2014b) synthesized conductive hemicellulose-based hydrogels by one-step reaction. These hydrogels were prepared by reacting *O*-acetyl-galactoglucomannan with epichlorohydrin in the existence of aniline pentamer via a facile and green approach in water. The results showed the thermostability of hydrogels was increased due to aniline pentamer. Besides, equilibrium swelling ratios (SR_{eq}) of hydrogels varied from 13.7 to 11.4 and could be controlled by cross-linker concentration. The SR_{eq} decreased from 9.6 to 6.0 by changing the aniline tetramer content from 10 to 40% (w/w). While conductivity of hemicellulose-based hydrogels changed from 9.05×10^{-9} to 1.58×10^{-6} S/cm which increased by three orders of magnitude. The excellent swelling and conductive properties impart hydrogels with broaden application prospects. Hemicellulose-based hydrogels with controllable swelling behavior and conductivity show promising application in biomedical aspects, especially in biosensors, electronic equipments, and histological engineering fields.

5 Conclusion

In this chapter, the structure of hemicellulose in plant and its physical-chemical prosperities were described and the type of hemicellulose-based hydrogels and their promising application were summarized. The preparation of hemicellulose and hemicellulose derivatives based hydrogels not only expands the application range of the hydrogel but also provides an effective way to realize the high-value utilization of hemicellulose. Moreover, the hemicellulose and hemicellulose derivatives based hydrogels can be widely used in industrial and medical fields because of their excellent features. In the future, more types of hemicellulose derivatives should be developed to synthesize hemicellulose-based intelligent hydrogels and the influencing mechanism of structure and the performance of hemicellulose-based

intelligent hydrogels should be established. In addition, hemicellulose-based nanocomposite hydrogels should be developed to improve the mechanical properties of hydrogels and expand the application of hemicellulose-based hydrogels while keeping their native structure, biodegradability, and biocompatibility.

Acknowledgements This work was supported by grants from National Natural Science Foundation of China (No. 21406080).

References

- Ahluwalia SS, Goyal D (2005) Removal of heavy metals from waste tea leaves from aqueous solution. *Eng Life Sci* 5:158–162
- Albertsson AC, Voepel J, Edlund U, Dahlgren O, Söderqvist-Lindblad M (2010) Design of renewable hydrogel release systems from fiberboard mill waste water. *Biomacromol* 11:1406–1411
- Ayoub A, Venditti RA, Pawlak JJ, Sadeghifar H, Salam A (2013) Development of an acetylation reaction of switch grass hemicellulose in ionic liquid without catalyst. *Ind Crop Prod* 44:306–314
- Bai L, Hu H, Xu J (2012) Influences of configuration and molecular weight of hemicelluloses on their paper-strengthening effects. *Carbohydr Polym* 88:1258–1263
- Barbat A, Gloaguen V, Moine C, Sainte-Catherine O, Kraemer M, Rogniaux H, Ropartz D, Krausz P (2008) Structural characterization and cytotoxic properties of a 4-O-methylglucuronoxylan from *Castanea sativa*. 2. Evidence of a structure-activity relationship. *J Nat Prod* 71:1404–1409
- Bhattarai N, Gunn J, Zhang MQ (2010) Chitosan-based hydrogels for controlled, localized drug delivery. *Adv Drug Deliver Rev* 62:83–99
- Bostan MS, Senol M, Cig T, Peker I, Goren AC, Ozturk T, Eroglu MS (2013) Controlled release of 5-aminosalicylic acid from chitosan based pH and temperature sensitive hydrogels. *Int J Biol Macromol* 52:177–183
- Buranov AU, Mazza G (2010) Extraction and characterization of hemicelluloses from flax shives by different methods. *Carbohydr Polym* 79:17–25
- Cao XF, Peng XW, Zhong LX, Sun RC (2014) Multiresponsive hydrogels based on Xylan-type hemicelluloses and photoisomerized azobenzene copolymer as drug delivery carrier. *J Agr Food Chem* 62:10000–10007
- Capek P, Alföldi J, Lišková D (2002) An acetylated galactoglucomannan from *Picea abies* L. *Karst. Carbohydr Res* 337:1033–1037
- Cheng Y, Luo X, Payne GF, Rubloff GW (2012) Biofabrication: programmable assembly of polysaccharide hydrogels in microfluidics as biocompatible scaffolds. *J Mater Chem* 22:7659–7666
- Chiang CY, Chu CC (2015) Synthesis of photoresponsive hybrid alginate hydrogel with photo-controlled release behavior. *Carbohydr Polym* 119:18–25
- Chikh L, Delhorbe V, Fichet O (2011) (Semi-)Interpenetrating polymer networks as fuel cell membranes. *J Membrane* 368:1–17
- Chimphango AFA, Zyl WHV, Görgens JF (2012) In situ enzymatic aided formation of xylan hydrogels and encapsulation of horse radish peroxidase for slow release. *Carbohydr Polym* 88:1109–1117
- Corobea MC, Muhlet O, Miculescu F, Antoniac IV, Vuluga Z, Florea D et al (2016) Novel nanocomposite membranes from cellulose acetate and clay-silica nanowires. *Polym Adv Technol* 27(12):1586–1595

- Coviello T, Matricardi P, Marianecchi C, Alhaique F (2007) Polysaccharides hydrogels for modified release formulations. *J Control Release* 119:5–24
- Crini G, Badot PM (2008) Application of chitosan, a natural aminopolysaccharide, for dye removal from aqueous solutions by adsorption processes using batch studies: A review of recent literature. *Prog Polym Sci* 33:399–447
- Dai QQ, Ren JL, Kong WQ, Peng F, Meng L (2015) Adsorption kinetics and thermodynamics of cellulose dinitrobenzoate prepared in ionic liquid for the removal of creatinine. *Bioresources* 10:3666–3681
- Dax D, Chávez MS, Xu C, Willför S, Mendonça RT, Sánchez J (2014) Cationic hemicellulose-based hydrogels for arsenic and chromium removal from aqueous solutions. *Carbohydr Polym* 111:797–805
- Deszczynski M, Kasapis S, Macnaughton W, Mitchell JR (2003) Effect of sugars on the mechanical and thermal properties of agarose gels. *Food Hydrocolloids* 17:793–799
- Diaz AF, Bargon J (1986) Electrochemical synthesis of conducting polymers. In: Skotheim TA (ed) *Handbook of conducting polymers*. New York, pp 81–115
- Diaz AF, Kanazawa KK (1979) Electrochemical polymerization of pyrrole. *J Chem Soc Chem Commun*, 635
- Ebringerová A (2005) Structural diversity and application potential of hemicelluloses. *Macromol Symp* 232:1–12
- Ebringerová A, Heinze T (2000) Xylan and xylan derivatives—biopolymers with valuable properties, 1. Naturally occurring xylans structures, isolation procedures and properties. *Macromol Rapid Comm* 21:542–556
- Ebringerová A, Kardošová A, Hromádková Z, Malovíková A, Hřibálová V (2002) Immunomodulatory activity of acidic xylans in relation to their structural and molecular properties. *Int J Biol Macromol* 30:1–6
- Ebringerová A, Hromádková Z, Heinze T (2005) *Hemicellulose*. Springer, Berlin, Heidelberg
- Edlund U, Albertsson AC (2008) A microspheric system: hemicellulose-based hydrogels. *J Bioact Compat Pol* 23:171–186
- Falamazian M, Varshosaz J (1998) The effect of structural changes on swelling kinetics of polybasic/hydrophobic pH-sensitive hydrogels. *Drug Dev Ind Pharm* 24:667–669
- Fang JM, Sun RC, Tomkinson J, Fowler P (2000) Acetylation of wheat straw hemicellulose B in a new non-aqueous swelling system. *Carbohydr Polym* 41:379–387
- Ferrari E, Ranucci E, Edlund U, Albertsson AC (2014) Design of renewable poly(amidoamine)/hemicellulose hydrogels for heavy metal adsorption. *J Appl Polym Sci* 132, <https://doi.org/10.1002/app.41695>
- Fréchet JM, Henmi M, Gitsov I, Aoshima S, Leduc MR, Grubbs RB (1995) Self-condensing vinyl polymerization—an approach to dendritic. *Mater Sci* 269:1080–1083
- Fundueanu G, Constantin M, Ascenzi P (2008) Preparation and characterization of pH- and temperature-sensitive pullulan microspheres for controlled release of drugs. *Biomaterials* 29:2767–2775
- Gabrielli I, Gatenholm P (1998) Preparation and properties of hydrogels based on hemicellulose. *J Appl Polym Sci* 69:1661–1667
- Gabrielli I, Gatenholm P, Glasser WG, Jain RK, Kenne L (2000) Separation, characterization and hydrogel-formation of hemicellulose from aspen wood. *Carbohydr Polym* 43:367–374
- Gao Y, Wei Z, Li F, Yang ZM, Chen YM, Zrinyi M, Osada Y (2014) Synthesis of a morphology controllable Fe₃O₄ nanoparticle/hydrogel magnetic nanocomposite inspired by magnetotactic bacteria and its application in H₂O₂ detection. *Green Chem* 16:1255–1261
- Gao CD, Ren JL, Kong WQ, Sun RC, Chen QF (2015a) Comparative study on temperature/pH sensitive xylan-based hydrogels: their properties and drug controlled release. *Rsc Adv* 5:90671–90681
- Gao LX, Chen JL, Han XW, Yan SX, Zhang Y (2015b) Electro-response characteristic of starch hydrogel crosslinked with glutaraldehyde. *J Biomat Sci-Polym E* 26:1–21

- Ge F, Li MM, Ye H, Zhao BX (2012) Effective removal of heavy metal ions Cd^{2+} , Zn^{2+} , Pb^{2+} , Cu^{2+} , from aqueous solution by polymer-modified magnetic nanoparticles. *J Hazard Mater* 211–212:366–372
- Green RA, Hassarati RT, Goding JA, Baek S, Lovell NH, Martens PJ (2012) Conductive hydrogels: mechanically robust hybrids for use as biomaterials. *Macromol Biosci* 12:494–501
- Guan Y, Bian J, Peng F, Zhang XM, Sun RC (2014a) High strength of hemicelluloses based hydrogels by freeze/thaw technique. *Carbohyd Polym* 101:272–280
- Guan Y, Zhang B, Bian J, Peng F, Sun RC (2014b) Nanoreinforced hemicellulose-based hydrogels prepared by freeze-thaw treatment. *Cellulose* 21:1709–1721
- Guan Y, Chen JH, Qi XM, Chen GG, Peng F, Sun RC (2015) Fabrication of biopolymer hydrogel containing Ag nanoparticles for antibacterial property. *Ind Eng Chem Res* 54:7393–7400
- Guarino V, Alvarez-Perez MA, Borriello A, Napolitano T, Ambrosio L (2013) Conductive PANi/PEGDA macroporous hydrogels for nerve regeneration. *Adv Healthc Mater* 2:218–227
- Guilherme MR, Reis AV, Takahashi SH, Rubira AF, Feitosa JPA, Muniz EC (2005) Synthesis of a novel superabsorbent hydrogel by copolymerization of acrylamide and cashew gum modified with glycidyl methacrylate. *Carbohyd Polym* 61:464–471
- Guimard NK, Gomez N, Schmidt CE (2007) Conducting polymers in biomedical engineering. *Prog Polym Sci* 32:876–921
- Gulati I, Park J, Maken S, Lee MG (2014) Production of carboxymethylcellulose fibers from waste lignocellulosic sawdust using $\text{NaOH}/\text{NaClO}_2$ pretreatment. *Fiber Polym* 15:680–686
- Guo L, Zhang SF, Ju BZ, Yang JZ, Quan X (2006) Removal of Pb (II) from aqueous solution by cross-linked starch phosphate carbamate. *J Polym Res* 13:213–217
- Guo BL, Glavas L, Albertsson AC (2013) Biodegradable and electrically conducting polymers for biomedical applications. *Prog Polym Sci* 38:1263–1286
- Gurgel LVA, Karnitz Júnior O, Gil RPF, Gil LF (2008) Adsorption of Cu(II), Cd(II), and Pb(II) from aqueous single metal solutions by cellulose and mercerized cellulose chemically modified with succinic anhydride. *Bioresour Technol* 99:3077–3083
- Habibi Y, Mahrouz M, Marais MF, Vignon MR (2004) An arabinogalactan from the skin of *Opuntia ficus-indica* prickly pear fruits. *Carbohyd Res* 339:1201–1205
- Hansen NM, Plackett D (2008) Sustainable films and coatings from hemicelluloses: a review. *Biomacromol* 9:1493–1505
- Hartman J, Albertsson AC, Lindblad MS, Sjöberg J (2006) Oxygen barrier materials from renewable sources: material properties of softwood hemicellulose-based films. *J Appl Polym Sci* 100:2985–2991
- Hawker CJ, Bosman AW, Harth E (2001) New polymer synthesis by nitroxide mediated living radical polymerizations. *Chem Rev* 101:3661–3688
- Hebeish A, Waly A, AbdelMohdy FA, Aly AS (1997) Synthesis and characterization of cellulose ion exchangers. I. Polymerization of glycidyl methacrylate, dimethylaminoethyl methacrylate, and acrylic acid with cotton cellulose using thiocarbonate- H_2O_2 redox system. *J Appl Polym Sci* 66:1029–1037
- Hebeish A, Farag S, Sharaf S, Shaheen TI (2014) Thermal responsive hydrogels based on semi interpenetrating network of poly (NIPAm) and cellulose nanowhiskers. *Carbohyd Polym* 102:159–166
- Heeger AJ (2001) Semiconducting and metallic polymers: the fourth generation of polymeric materials (Nobel lecture). *Angew Chem Int Ed* 40:2591–2611
- Hromadkova Z, Kovacicova J, Ebringerova A (1999) Study of the classical and ultrasound-assisted extraction of the corn cob xylan. *Ind Crop Prod* 9:101–109
- Iravani S, Fitchett CS, Georget DMR (2011) Physical characterization of arabinoxylan powder and its hydrogel containing a methyl xanthine. *Carbohyd Polym* 85:201–207
- Ishizu K, Mori A (2000) Synthesis of hyper branched polymers by self-addition free radical vinyl polymerization of photo functional styrene. *Macromol Rapid Comm* 21:665–668
- Ishizu K, Shen XX, Tsubaki KI (2000) Radical copolymerization reactivity of methacryloyl-terminated poly(ethylene glycol methylether) with vinylbenzyl-terminated polystyrene macromonomers. *Polym* 41:2053–2057

- Karaaslan AM, Tshabalala MA, Buschle-Diller G (2010) Wood hemicellulose/chitosan-based semi-interpenetrating network hydrogels: mechanical, swelling and controlled drug release properties. *BioResources* 5:1036–1054
- Karaaslan MA, Tshabalala MA, Yelle DJ, Buschle-Diller G (2011) Nanoreinforced biocompatible hydrogels from wood hemicelluloses and cellulose whiskers. *Carbohyd Polym* 86:192–201
- Karaaslan MA, Tshabalala MA, Buschle-Diller G (2012) Semi-interpenetrating polymer network hydrogels based on aspen hemicellulose and chitosan: Effect of crosslinking sequence on hydrogel properties. *J Appl Polym Sci* 124:1168–1177
- Kent K, Ganetsky M, Cohen J, Bird S (2008) Non-fatal ventricular dysrhythmias associated with severe salicylate toxicity. *Clin Toxicol* 46:297–299
- Khalil MS (2015) The postulated mechanism of the protective effect of ginger on the aspirin induced gastric ulcer: histological and immunohistochemical studies. *Histol Histopathol* 30:855–864
- Kiefer LL, York WS, Albersheim P, Darvill AG (1990) Structural characterization of an arabinose-containing heptadecasaccharide enzymically isolated from sycamore extracellular xyloglucan. *Carbohyd Res* 197:139–158
- Kim BS, Chen L, Gong JP, Osada Y (1999) Titration behavior and spectral transition of water-soluble polythiophenic carboxylic acids. *Macromolecules* 32:3964–3969
- Kong WQ, Ren JL, Wang SY, Chen Q (2014) Removal of heavy metals from aqueous solutions using acrylic-modified sugarcane bagasse-based adsorbents: equilibrium and kinetic studies. *BioResources* 9:3184–3196
- Kong WQ, Huang DY, Xu GB, Ren JL, Liu CF, Zhao LH, Sun RC (2016) A new design strategy for graphene oxide/polyacrylamide/aluminium ion-crosslinked carboxymethyl hemicelluloses nanocomposite hydrogels with highly tough and elastic properties. *Chem Asian J*. <https://doi.org/10.1002/asia.201600138>
- Kopecek J, Yang JY (2007) Review—Hydrogels as smart biomaterials. *Polym Inter* 56:1078–1098
- Kretlow JD, Klouda L, Mikos AG (2007) Injectable matrices and scaffolds for drug delivery in tissue engineering. *Adv Drug Deliver Rev* 59:263–273
- Kuzmenko V, Hägg D, Toriz G, Gatenholm P (2014) In situ forming spruce xylan-based hydrogel for cell immobilization. *Carbohyd Polym* 102:862–868
- Kweon JO, Noh IT (2001) Thermal, thermomechanical, and electrochemical characterization of the organic-inorganic hybrids poly (ethylene oxide) (PEO)-silica and PEO-silica-LiClO₄. *J Appl Polym Science* 81:2471–2479
- Lai JY, Wang TP, Li YT, Tu IH (2012) Synthesis, characterization and ocular biocompatibility of potential keratoprosthesis hydrogels based on photopolymerized poly(2-hydroxyethyl methacrylate)-co-poly(acrylic acid). *J Mater Chem* 22:1812–1823
- Lee KY, Mooney DJ (2001) Hydrogels for tissue engineering. *Chem Rev* 101:1869–1880
- Li YT, Armes SP (2005) Synthesis and chemical degradation of branched vinyl polymers prepared via ATRP: use of a cleavable disulfide-based branching agent. *Macromolecules* 38:8155–8162
- Li N, Bai RB (2006) Highly enhanced adsorption of lead ions on chitosan granules functionalized with poly(acrylic acid). *Ind Eng Chem Res* 45:7897–7904
- Li GY, Guo L, Chang XJ, Yang MY (2012) Thermo-sensitive chitosan based semi-IPN hydrogels for high loading and sustained release of anionic drug. *Int J Biol Macromol* 50:899–904
- Li YJ, Sun XF, Ye Q, Liu BC, Wu YG (2014) Preparation and properties of a novel hemicellulose-based magnetic hydrogel. *Acta Phys-Chim Sin* 30:111–120
- Lima-Tenorio MK, Tenorio-Neto ET, Garcia FP, Nakamura CV, Guilherme MR, Muniz EC (2015) Hydrogel nanocomposite based on starch and Co-doped zinc ferrite nanoparticles that shows magnetic field-responsive drug release changes. *J Mol Liq* 210:100–105
- Lin C, Gitsov I (2010) Preparation and characterization of novel amphiphilic hydrogels with covalently attached drugs and fluorescent markers. *Macromolecules* 43:10017–10030
- Lin CC, Metters AT (2006) Hydrogels in controlled release formulations: network design and mathematical modeling. *Adv Drug Deliver Rev* 58:1379–1408
- Lindblad MS, Ranucci E, Albertsson AC (2001) Biodegradable polymers from renewable sources. New hemicellulose-based hydrogels. *Macromol Rapid Comm* 22:962–967

- Liu Y, Ranucci E, Lindblad MS, Albertsson AC (2001) New biodegradable polymers from renewable sources: polyester-carbonates based on 1,3-propylene-co-1,4-cyclohexanedimethylene succinate. *J Polym Sci, Part A: Polym Chem* 39:2508–2519
- Liu ZL, Hu H, Zhuo RX (2004) Konjac glucomannan-graft-acrylic acid hydrogels containing azo crosslinker for colon-specific delivery. *J Polym Sci, Part A: Polym Chem* 42:4370–4378
- Liu C, Chen Y, Chen J (2010) Synthesis and characteristics of pH-sensitive semi-interpenetrating polymer network hydrogels based on konjac glucomannan and poly(aspartic acid) for in vitro drug delivery. *Carbohydr Polym* 79:500–506
- Miculescu M, Thakur VK, Miculescu F, Voicu SI (2016) Graphene-based polymer nanocomposite membranes: a review. *Polym Adv Technol* 27(7):844–859
- Morimoto N, Endo T, Iwasaki Y, Akiyoshi K (2005) Design of hybrid hydrogels with self-assembled nanogels as cross-linkers: interaction with proteins and chaperone-like activity. *Biomacromol* 6:1829–1834
- Mv S, Lahooti S, Mh BJM (2000) Making microencapsulation work: conformational coating, immobilization gels and in vivo performance. *J Control Release* 65:173–186
- Nagasaki Y, Ogawa R, Yamamoto S, Kato M, Kataoka K (1997) Synthesis of heterotelechelic poly(ethylene glycol) macromonomers. Preparation of poly(ethylene glycol) possessing a methacryloyl group at one end and a formyl group at the other end. *Macromolecules* 30:6489–6493
- Nghiem NP, Montanti J, Johnston DB, Drapcho C (2011) Fractionation of corn fiber treated by soaking in aqueous ammonia (SAA) for isolation of hemicellulose B and production of C5 sugars by enzyme hydrolysis. *Appl Biochem Biotechnol* 164:1390–1404
- Noaman E, El-Din NKB, Bibars MA, Abou Mossallam AA, Ghoneum M (2008) Antioxidant potential by arabinoxylan rice bran, MGN-3/biobran, represents a mechanism for its oncostatic effect against murine solid Ehrlich carcinoma. *Cancer Lett* 268:348–359
- Nugent MJD, Higginbotham CL (2007) Preparation of a novel freeze thawed poly(vinyl alcohol) composite hydrogel for drug delivery applications. *Eur J Pharm Biopharm* 67:377–386
- O’Connell DW, Birkinshaw C, O’Dwyer TF (2008) Heavy metal adsorbents prepared from the modification of cellulose: a review. *Bioresource Technol* 99:6709–6724
- Ohseido Y, Takashina R, Gong JP, Osada Y (2004) Surface friction of hydrogels with well-defined polyelectrolyte brushes. *Langmuir* 20:6549–6555
- Okazaki M, Hamada T, Fujii H, Kusudo O, Mizobe A, Matsuzawa S (1995) Development of poly(vinyl alcohol) hydrogel for waste water cleaning. II. Treatment of N, N -dimethylformamide in waste water with poly(vinyl alcohol) gel with immobilized microorganisms. *J Appl Polym Sci* 58:2243–2249
- Oliveira EE, Silva AE, Júnior TN, Gomes MCS, Aguiar LM, Marcelino HR (2010) Xylan from corn cobs, a promising polymer for drug delivery: production and characterization. *Bioresource Technol* 101:5402–5406
- Osada Y, Kish R, Hasebe M (1987) Anomalous chemomechanical characteristics of electro-activated polyelectrolyte gel. *Polymer Sci* 25:41–485
- Osato M, Yuko N, Hitoshi K, Yoshinobu I, Hitomi K, Hidetoshi S (2003) Effect of water potential on sol-gel transition and intermolecular interaction of gelatin near the transition temperature. *Biopolymers* 70:482–491
- Pan XJ, Sano Y (2005) Fractionation of wheat straw by atmospheric acetic acid process. *Bioresource Technol* 96:1256–1263
- Peng XW, Ren JL, Zhong LX, Cao XF, Sun RC (2010a) Microwave-induced synthesis of carboxymethyl hemicelluloses and their rheological properties. *J Agr Food Chem* 59:570–576
- Peng XW, Ren JL, Sun RC (2010b) Homogeneous esterification of xylan-rich hemicelluloses with maleic anhydride in ionic liquid. *Biomacromol* 11:3519–3524
- Peng XW, Ren JL, Zhong LX, Peng F, Sun RC (2011) Xylan-rich hemicelluloses-graft-acrylic acid ionic hydrogels with rapid responses to pH, salt, and organic solvents. *J Agri Food Chem* 59:8208–8215
- Peng XW, Ren JL, Zhong LX, Sun RC, Shi WB, Hu BJ (2012a) Glycidyl methacrylate derivatized xylan-rich hemicelluloses: synthesis and characterizations. *Cellulose* 19:1361–1372

- Peng XW, Zhong LX, Ren JL, Sun RC (2012b) Highly effective adsorption of heavy metal ions from aqueous solutions by macroporous xylan-rich hemicelluloses-based hydrogel. *J Agr Food Chem* 60:3909–3916
- Petzold K, Schwikal K, Günther W, Heinze T (2005) Carboxymethyl xylan-control of properties by synthesis. *Macromol Symp* 232:27–36
- Petzold K, Schwikal K, Heinze T (2006) Carboxymethyl xylan—synthesis and detailed structure characterization. *Carbohydr Polym* 64:292–298
- Pourjavadi A, Barzegar S, Mahdavinia GR (2004) Modified chitosan, 7-Graft copolymerization of methacrylonitrile onto chitosan using ammonium persulfate initiator. *E-Polym*
- Qiu Y, Park K (2012) Environment-sensitive hydrogels for drug delivery. *Adv Drug Deliver Rev* 53:321–339
- Reis CP, Neufeld RJ, Ribeiro AJ, Veiga F (2006) Nanoencapsulation I. Methods for preparation of drug-loaded polymeric nanoparticles. *Nanomed-Nanotechnol* 2:8–21
- Ren JL, Sun RC, Liu CF, Chao ZY, Luo W (2006) Two-step preparation and thermal characterization of cationic 2-hydroxypropyltrimethylammonium chloride hemicellulose polymers from sugarcane bagasse. *Polym Degrad Stabil* 91:2579–2587
- Ren JL, Sun RC, Liu CF, Cao ZN, Luo W (2007a) Acetylation of wheat straw hemicelluloses in ionic liquid using iodine as a catalyst. *Carbohydr Polym* 70:406–414
- Ren JL, Sun RC, Liu CF, Lin L, He BH (2007b) Synthesis and characterization of novel cationic scb hemicelluloses with a low degree of substitution. *Carbohydr Polym* 67:347–357
- Ren JL, Peng F, Sun RC, Liu CF, Cao ZN, Luo W (2008a) Synthesis of cationic hemicellulosic derivatives with a low degree of substitution in dimethyl sulfoxide media. *J Appl Polym Sci* 109:2711–2717
- Ren JL, Xu F, Sun RC, Peng B, Sun JX (2008b) Studies of the lauroylation of wheat straw hemicelluloses under heating. *J Agri Food Chem* 56:1251–1258
- Ren JL, Peng XW, Peng F, Sun RC (2011) The preparation and application of the cationic biopolymer based on xylan-rich hemicelluloses from agricultural biomass. *Adv Mater Res* 239–242:463–467
- Ren JL, Kong WQ, Sun RC (2014) Preparation of sugarcane bagasse/Poly(Acrylic Acid-co-Acrylamide) hydrogels and their application. *BioResources* 9:3290–3303
- Rokhade AP, Patil SA, Aminabhavi TM (2007) Synthesis and characterization of semi-interpenetrating polymer network microspheres of acrylamide grafted dextran and chitosan for controlled release of acyclovir. *Carbohydr Polym* 67:605–613
- Roos AA, Edlund U, Sjöberg J, Albertsson AC, Stålbrand H (2008) Protein release from galactoglucomannan hydrogels: influence of substitutions and enzymatic hydrolysis by beta-mannanase. *Biomacromol* 9:2104–2110
- Samuelsen AB (2000) Structural features of biologically active polysaccharide fractions from the leaves and seeds of *Plantago major* L. Springer, Netherlands
- Sandhu JS, Hudson GJ, Kennedy JF (1981) The gel nature and structure of the carbohydrate of ispaghula husk ex *Plantago ovata* Forsk. *Carbohydr Res* 93:247–259
- Schwikal K, Heinze T (2007) Dialkylaminoethyl xylans: Polysaccharide ethers with pH-sensitive solubility. *Polym Bull* 59:161–167
- Schwikal K, Heinze T, Ebringerová A, Petzold K (2005) Cationic xylan derivatives with high degree of functionalization. *Macromol Symp* 232:49–56
- Sefton MV, May MH, Lahooti S, Babensee JE (2000) Making microencapsulation work: conformal coating, immobilization gels and in vivo performance. *J Control Release* 65:173–186
- Shahbuddin M, Bullock AJ, MacNeil S, Rimmer S (2014) Glucomannan-poly(N-vinyl pyrrolidone) bicomponent hydrogels for wound healing. *J mater chem B* 2(6):727–738
- Shawky HA, El-Hag Ali A, El Sheikh RA (2006) Characterization and adsorption properties of the chelating hydrogels derived from natural materials for possible use in the improvement of groundwater quality. *J Appl Polym Sci* 99:2904–2912

- Singha AS, Shama A, Thakur VK (2008) X-ray diffraction, morphological, and thermal studies on methylmethacrylate graft copolymerized Saccharum ciliare fiber. *Int J Polym Anal Charact* 13 (6):447–462
- Sinha VR, Kumria R (2001) Polysaccharides in colon-specific drug delivery. *Int J Pharm* 224:19–38
- Sinha VR, Mittal BR, Bhutani KK, Kumria R (2004) Colonic drug delivery of 5-fluorouracil: an in vitro evaluation. *Int J Pharm* 269:101–108
- Stephen AM (1983) 3—Other plant polysaccharides. *Polysaccharides*, 97–193
- Stevens BJH, Selvendran RR (1980) Structural investigation of an arabinan from cabbage (*Brassica oleracea* var. *capitata*). *Phytochemistry* 19:559–561
- Sumaru K, Ohi K, Takagi T, Kanamori T, Shinbo T (2006) Photoresponsive properties of poly (N-isopropylacrylamide) hydrogel partly modified with spirobenzopyran. *Langmuir* 22:4353–4356
- Sun JX, Sun XF, Sun RC, Su YQ (2004a) Fractional extraction and structural characterization of sugarcane bagasse hemicelluloses. *Carbohydr Polym* 56:195–204
- Sun XF, Sun RC, Sun JX (2004b) Oleoylation of sugarcane bagasse hemicelluloses using N-bromosuccinimide as a catalyst. *J Sci Food Agr* 84:800–810
- Sun XF, Xu F, Zhao H, Sun RC, Fowler P, Baird MS (2005) Physicochemical characterisation of residual hemicelluloses isolated with cyanamide-activated hydrogen peroxide from organosolv pre-treated wheat straw. *Bioresource Technol* 96:1342–1349
- Sun XF, Wang HH, Jing ZX, Mohanathas R (2013) Hemicellulose-based pH-sensitive and biodegradable hydrogel for controlled drug delivery. *Carbohydr Polym* 92:1357–1366
- Sun XF, Gan Z, Jing Z, Wang H, Wang D, Jin Y (2015a) Adsorption of methylene blue on hemicellulose-based stimuli-responsive porous hydrogel. *J Appl Polym Sci* 132(10)
- Sun XF, Jing ZX, Wang HH, Liu YY (2015b) Physical-chemical properties of xylan/PAAC magnetic semi-interpenetrating network hydrogel. *Polym Comp* 36:2317–2325
- Sun XF, Liu BC, Jing ZX, Wang HH (2015c) Preparation and adsorption property of xylan/poly (acrylic acid) magnetic nanocomposite hydrogel adsorbent. *Carbohydr Polym* 118:16–23
- Szilagyí A, Sumaru K, Sugiura S, Takagi T, Shinbo T, Zrinyi M (2007) Rewritable microrelief formation on photoresponsive hydrogel layers. *Chem Mater* 19:2730–2732
- Tang XH, Zhang XM, Guo CC, Zhou AL (2007) Adsorption of Pb²⁺ on chitosan cross-linked with triethylene—tetramine. *Chem Eng Technol* 30:955–961
- Thakur VK, Thakur MK (2014) Recent trends in hydrogels based on psyllium polysaccharide: a review. *J Clean Prod* 82:1–15
- Thakur VK, Thakur MK (2015) Recent advances in green hydrogels from lignin: a review. *Int J Biol Macromol* 72:834–847
- Thakur MK, Thakur VK, Gupta RK, Pappu A (2016) Synthesis and applications of biodegradable soy based graft copolymers: a review. *ACS Sustain Chem Eng* 4(1):1–17
- Trache D, Hazwan Hussin M, Mohamad Haafiz MK, Kumar Thakur V (2017) Recent progress in cellulose nanocrystals: sources and production. *Nanoscale* 9(5):1763–1786
- Uraki Y, Imura T, Kishimoto T (2006) Body temperature-responsive gels derived from hydroxypropylcellulose bearing lignin II: adsorption and release behavior. *Cellulose* 13:225–234
- Van Tomme SR, Storm G, Hennink WE (2008) In situ gelling hydrogels for pharmaceutical and biomedical applications. *Int J Pharmaceut* 355:1–18
- Vermonden T, Censi R, Hennink WE (2012) Hydrogels for protein delivery. *Chem Rev* 112:2853–2888
- Voepel J, John Sjöberg MR, Albertsson AC, Hultin UK, Gasslander U (2009) Drug diffusion in neutral and ionic hydrogels assembled from acetylated galactoglucomannan. *J Appl Polym Sci* 112:2401–2412
- Voepel J, Edlund U, Albertsson AC (2010) Alkenyl-functionalized precursors for renewable hydrogels design. *J Polym Sci, Part A: Polym Chem* 47:3595–3606

- Voicu SI, Condruz RM, Mitran V, Cimpean A, Miculescu F, Andronesu C, Thakur VK (2016) Sericin covalent immobilization onto cellulose acetate membrane for biomedical applications. *ACS Sustain Chem Eng* 4(3):1765–1774
- Wan Ngah WS, Hanafiah MAKM (2008) Removal of heavy metal ions from wastewater by chemically modified plant wastes as adsorbents: a review. *Biores Technol* 99:3935–3948
- Wang QQ, Chen DJ (2016) Synthesis and characterization of a chitosan based nanocomposite injectable hydrogel. *Carbohydr Polym* 136:1228–1237
- Wang LX, SoczkaGuth T, Havinga E, Mullen K (1996) Poly(phenylenesulfidephenylenamine) (PPSA) e the ('compound') of polyphenylenesulfide with polyaniline. *Angew Chem Int Ed* 35:1495–1497
- Whistler RL, Bushway AA, Singh PP, Nakahara W, Tokuzen R (1976) Noncytotoxic, antitumor polysaccharides. *Adv Carbohydr Chem Bi* 32:235–275
- Xu F, Sun JX, Geng ZC, Liu CF, Ren JL, Sun RC (2007) Comparative study of water-soluble and alkali-soluble hemicelluloses from perennial ryegrass leaves (*Lolium persee*). *Carbohydr Polym* 67:56–65
- Yang L, Chu JS, Fix JA (2002) Colon-specific drug delivery: new approaches and in vitro/in vivo evaluation. *Int J Pharm* 235:1–15
- Yang JY, Fang J, Zhou XS (2011) Synthesis and characterization of temperature sensitive hemicellulose-based hydrogels. *Carbohydr Polym* 86:1113–1117
- Zhang XZ, Wu DQ, Chu CC (2004) Synthesis and characterization of partially biodegradable, temperature and pH sensitive Dex-MA/PNIPAAm hydrogels. *Biomaterials* 25:4719–4730
- Zhang C, Han HM, Qu P, Xu J, Zhou Y, Wang J, Zhao N, Xu J (2012) Initiator concentration effect on rheological properties of a pH-sensitive semi-IPN hydrogel based on konjac glucomannan and methacrylic acid. *Adv Mater Res* 627:730–733
- Zhang S, Guan Y, Fu GQ, Chen BY, Peng F, Yao CL, Sun RC (2014a) Organic/inorganic superabsorbent hydrogels based on xylan and montmorillonite. *J Nanomater* 1:3669–3676
- Zhang XQ, Chen MJ, Liu CF, Sun RC (2014b) Dual-component system dimethyl sulfoxide/LiCl as a solvent and catalyst for homogeneous ring-opening grafted polymerization of ϵ -caprolactone onto xylan. *J Agr Food Chem* 62:682–690
- Zhao Y, Kang J, Tan TW (2006) Salt-, pH- and temperature-responsive semi-interpenetrating polymer network hydrogel based on poly(aspartic acid) and poly(acrylic acid). *Polymer* 47:7702–7710
- Zhao L, Li W, Plog A, Xu YP, Buntkowsky G, Gutmann T, Zhang K (2014a) Multi-responsive cellulose nanocrystal-rhodamine conjugates: an advanced structure study by solid-state dynamic nuclear polarization (DNP) NMR. *Phys Chem Chem Phys* 16:26322–26329
- Zhao W, Glavas L, Odelius K, Edlund U, Albertsson AC (2014b) Facile and green approach towards electrically conductive hemicellulose hydrogels with tunable conductivity and swelling behavior. *Chem Mater* 26:4265–4273
- Zhao WF, Glavas L, Odelius K, Edlund U, Albertsson AC (2014c) A robust pathway to electrically conductive hemicellulose hydrogels with high and controllable swelling behavior. *Polymer* 55:2967–2976
- Zheng Y, Wang A (2009) Evaluation of ammonium removal using a chitosan-g-poly(acrylic acid)/rectorite hydrogel composite. *J Hazard Mater* 171:671–677
- Zhong LX, Peng XW, Song LX, Yang D, Cao XF, Sun RC (2013) Adsorption of Cu^{2+} and Ni^{2+} from aqueous solution by arabinoxylan hydrogel: equilibrium, kinetic, competitive adsorption. *Sep Sci Technol* 48:2659–2669
- Zhou C, Wu Q, Lei T, Negulescu II (2014) Adsorption kinetic and equilibrium studies for methylene blue dye by partially hydrolyzed polyacrylamide/cellulose nanocrystal nanocomposite hydrogels. *Chem Eng J* 1251:17–24
- Zhu CH, Hai ZB, Cui CH, Li HH, Chen JF, Yu SH (2012) In situ controlled synthesis of thermosensitive Poly(N-isopropylacrylamide)/Au nanocomposite hydrogels by gamma radiation for catalytic application. *Small* 8:930–936

Chapter 4

Updates on Stimuli-Responsive Polymers: Synthesis Approaches and Features



Ibrahim M. El-Sherbiny, Islam A. Khalil and Isra H. Ali

Abstract Stimuli-responsive polymers (SRPs) are a type of smart materials which can demonstrate noticeable changes in their characteristics as a response to their exposure to some environmental stimuli variations. The environmental stimuli could be physical (e.g., electric field, ionic strength, magnetic field, mechanical stress, pressure, radiation, and temperature), chemical (e.g., specific ions and chemical agents), or biochemical (e.g., enzyme substrates and ligands). Recently, SRPs were used in numerous applications including diagnostics, drug delivery systems, biosensors, regenerative medicine, and stem cells. This chapter illustrates the different categories of SRPs and highlights some of their synthesis approaches, unique features, major development, their different structures, and classifications.

Keywords Stimuli-responsive polymers · SRPs · Synthesis · Classifications

1 Polymers as Smart Materials

Responsive materials can demonstrate chemical and physical changes in their properties when triggered by surrounding environmental stimuli such as change in chemical composition, exposure to an electrical or magnetic field, irradiation with light, mechanical force, temperature, etc. In the last decade, advanced stimuli-responsive materials were playing a significant role in different applications, such as coatings, diagnostics, drug delivery, biosensors, regenerative medicine,

I. M. El-Sherbiny (✉) · I. A. Khalil · I. H. Ali
Center for Materials Science, University of Science and Technology (UST),
Zewail City of Science and Technology, 6th October City, Cairo 12588, Egypt
e-mail: ielsherbiny@zewailcity.edu.eg

I. A. Khalil
Department of Pharmaceutics and Industrial Pharmacy, College of Pharmacy,
Misr University of Science and Technology (MUST), 6th October City, Cairo 12566, Egypt

© Springer Nature Singapore Pte Ltd. 2018
V. K. Thakur and M. K. Thakur (eds.), *Polymer Gels*, Gels Horizons: From Science to Smart Materials, https://doi.org/10.1007/978-981-10-6086-1_4

smart optical systems, stem cells, microelectromechanical systems, and textiles. This chapter will review recent advances and challenges in the development of stimuli-responsive polymer materials and systems in thin films and nanostructures.

2 Polymers from Simple Networks to Smart Materials

Recently, an important evolution has been made in the field of hydrogels and their applications as biomaterials (Thakur and Thakur 2014a, b, 2015). The use of hydrogels in biomedical applications was limited due to both the toxicity and the physiological impacts of crosslinkers used during hydrogel formation. Biomaterials designing and synthesis require merging of the well knowledge of both polymer chemistry and biological processes (Trache et al. 2017; Corobea et al. 2016; Voicu et al. 2016; Miculescu et al. 2016). Hydrogel materials can be synthesized using various polymers either naturally derived or synthetic ones, where polymer chains are held together using different physical or chemical crosslinking agents. The developed hydrogel matrices have high capacity to carry pharmaceutical agents in their architecture and thus they are considered to be good candidates for the synthesis of biomaterials for controlled drug release and tissue regeneration applications. Although hydrogel matrices have many advantages, they still possess several limitations to be converted into clinical products. In this section, a historical overview of development of more sophisticated smart hydrogels using simple polymeric networks will be highlighted.

Hydrogels are three-dimensional polymer networks capable of retaining a significant amount of water in their swollen state due to the presence of many hydrophilic functional moieties within their structures such as $-\text{OH}$, $-\text{CONH}^-$, $-\text{CONH}_2$, $-\text{COOH}$, and $-\text{SO}_3\text{H}$. Hydrogels could be classified into three categories according to the nature of the building polymers: (a) natural, (b) synthetic, or (c) hybrid of both (Peppas and Khare 1993). Hydrogels can be crosslinked through (a) chemical covalent bonds, (b) physical non-covalent interactions, or (c) a combination of both interactions. The balance between forces within the hydrogel structure arises from water sorption including capillary property, osmotic forces or hydration, and the forces exerted by the crosslinked polymer chains retaining polymer matrix and resisting its expansion (Roorda et al. 1986).

In 1960s, Wichterle and Lim successfully applied hydrogels as contact lenses (Wichterle and Lim 1960). Later on, hydrogels have been commonly used as controlled drug delivery systems to enable both localized and sustained releases of drugs. In 1984, the Journal of Controlled Release has been launched to play a fundamental role in publishing the state-of-the-art of research work and review articles focusing on drug delivery using hydrogel matrices.

In this section, a presentation of the major progress in hydrogel research over the last 50 years, starting from relatively simple and chemically crosslinked networks in the 1960s to today's smart hydrogel matrices, would be described in details as illustrated in Fig. 1.

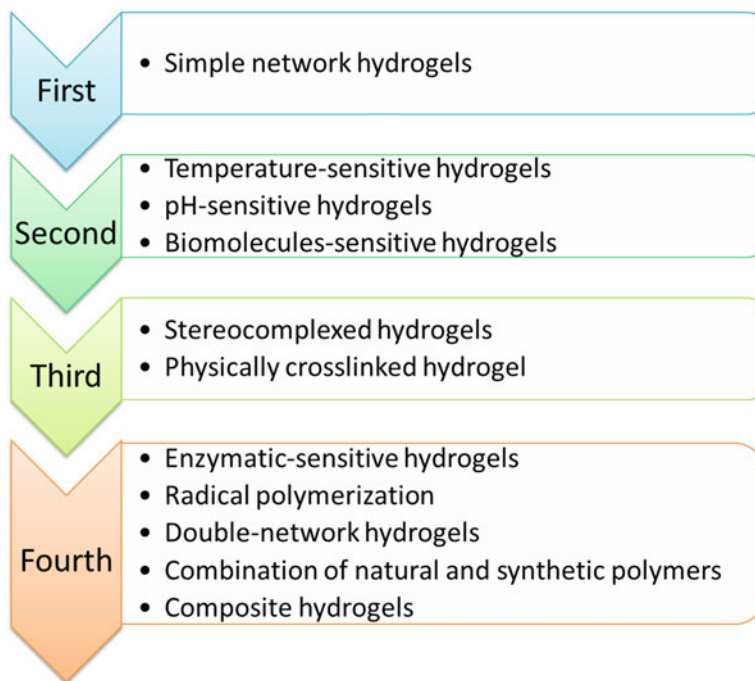


Fig. 1 Different generations of hydrogels

2.1 *First-Generation Hydrogels*

In 1894, hydrogel as term was first used in literature to describe crosslinked networks made of swellable polymeric chains (VanBemmelen 1894). Afterward, in 1960, a landmark paper about the fabrication of soft contact lenses using poly (2-hydroxyethyl methacrylate) pHEMA hydrogels was the first to report hydrogels as water-swollen crosslinked macromolecular networks (Wichterle and Lim 1960). Following that discovery, many scientific literature articles were reported focusing on the preparation of relatively simple and chemically crosslinked synthetic polymers networks to be used as hydrogels in ophthalmic and drug delivery applications. The two main strategies used for hydrogels preparation are either polymerization of monomers in the presence of a crosslinking agent or direct crosslinking of already abundant hydrophilic polymers. The famous first-generation hydrogels were pHEMA, poly(vinyl alcohol) (PVA), and poly(ethylene glycol) (PEG).

2.2 *Second-Generation Hydrogels*

Katchalsky research in the period between 1950s and 1960s opened a new era of the concept of transforming chemical energy into mechanical response (Kuhn et al.

1950; Steinberg et al. 1966). Starting the 1970s, the simple networks of hydrogels shifted to new materials with the capability to respond to external environmental conditions such as pH, temperature, etc. (Kopecek 2009). The external environmental stimuli can be used to induce specific response like gel formation or controlled drug release.

Temperature-sensitive hydrogels are the most famous environmentally responsive hydrogels. The significant features that create the crosslinkages are hydrogen bonding, physical entanglements, and hydrophobic interactions. In situ formation of hydrogels (Sol–Gels) is an important example of formation of the temperature-sensitive hydrogels. Simply, the sol–gels are polymer solutions converting from solutions to gels after injection in specific tissues or organs (Ruel-Gariépy and Leroux 2004; Ward and Georgiou 2011). The main advantage of the in situ formation of hydrogels is that it does not need any surgical procedures to be applied. Biological components can be simply incorporated within the polymeric network and then flow easily in the body leading to proper shape fitting to the surrounding tissue. The most extensively investigated hydrogels in this generation are poly(ethylene glycol)-polyester block copolymers, poly(N-isopropylacrylamide) (pNIPAAm), and polyN-(2-hydroxypropylacrylamide) (PHPMAm).

The second most used type of the in situ formed hydrogels is the pH-sensitive one. It has the advantages of responding to various pH values in the different parts of the human body. It contains either acidic or basic functional groups that can be ionized at low or high pH, respectively (Gupta et al. 2002; Qiu and Park 2012). Last member of second-generation hydrogels is biomolecule-sensitive hydrogel that could respond to different concentrations of biomolecules like hormones, glucose, etc. (Miyata et al. 2002). All of the second-generation sensitive hydrogels are mainly utilized for the synthesis of controlled delivery systems for drugs and therapeutics.

2.3 *Third-Generation Hydrogels*

In the 1990s, other physical interactions were used as crosslinkers that led to the improvement of degradation, thermal, and mechanical properties of hydrogels. These interactions used for the in situ hydrogel formation. The third-generation hydrogels include stereocomplexation, inclusion complex formation, metal–ligand coordination, and peptide interactions as crosslinking methods for the preparation of hydrogels.

Stereocomplexed hydrogel is a stereoselective interaction between two complementary stereoregular polymer chains, which interlock and form a new composite demonstrating altered physical property in comparison with the constituting polymers (Slager and Domb 2003). In 1953, Pauling and Corey reported the first example of stereocomplexation between polypeptide chains (Pauling and Corey 1953). In 1987, Ikada et al. studied stereocomplexation between enantiomeric polylactide chains (Ikada et al. 1987). Since 2000, stereocomplexation between enantiomeric PLLA and PDLA blocks in amphiphilic copolymers has been applied

for injectable hydrogels (De Jong et al. 1998; Fukushima and Kimura 2006; Tsuji 2005). Several examples of stereocomplexed hydrogels were prepared from pluronics (Chung et al. 2008), oligolactide-functionalized pHEMA (Lim et al. 2000), and 2-methacryloyloxyethyl phosphorylcholine (Takami et al. 2011) polymers. In 2012, Bertin summarized recent publications that focused on stereocomplex polymers in biomedical applications (Bertin 2012).

Cyclodextrins (CDs), cyclic oligosaccharides containing a hydrophobic cavity that can host a variety of molecules, are good examples for physically crosslinked hydrogels. In 1994, Li et al. reported the first hierarchical self-assembly process to create a physically crosslinked CDs hydrogel (Li et al. 1994). The low stability and long gelation times were the main disadvantages of these formed systems, where PEG was used as the guest (loaded) molecule. An improved version of physically crosslinked CDs hydrogels was obtained when their aqueous solutions were mixed with amphiphilic block copolymers like pluronics (Li et al. 2003), reverse pluronics (PPO-PEO-PPO) (Kuo and Lai 2011), and polycaprolactone (PCL)-based block copolymer, PCL-PEG-PCL (Zhao et al. 2006). Also, CDs hydrogels were prepared with PEG-dextran (Huh et al. 2001), PEG-chitosan (Huh et al. 2004), and PEG-heparin (Ma et al. 2010).

2.4 Fourth-Generation Hydrogels

In the last decade, various chemically crosslinked hydrogels have been synthesized through different organic synthesis techniques. The fourth-generation hydrogels were also called smart hydrogels due to their capability to enhance loaded drugs bioactivity through tailoring hydrogels properties like mechanical stability or control the release of the loaded drugs. These customized characteristics were accomplished via covalent or ionic crosslinking between polymer chains possessing complementary functional groups in order to form double-network hydrogels.

2.4.1 Enzymatic-Sensitive Hydrogels

Enzymatic-sensitive hydrogel can be crosslinked by enzymes such as horseradish peroxidase (Fig. 2) (Kurisawa et al. 2005), transglutaminase (Chen et al. 2003; Hu and Messersmith 2005), and tyrosinase (Chen et al. 2003). Tissue engineering is the main application for this class of hydrogels (Teixeira et al. 2012). However, the main drawback of enzymatic-sensitive hydrogels is the instability of many enzymes.

2.4.2 Radical Polymerization-Based Hydrogels

In radical polymerization technique, N,N,N',N'-tetramethylethylenediamine (TEMED) and potassium persulfate (KPS) are used as a catalyst and an initiator

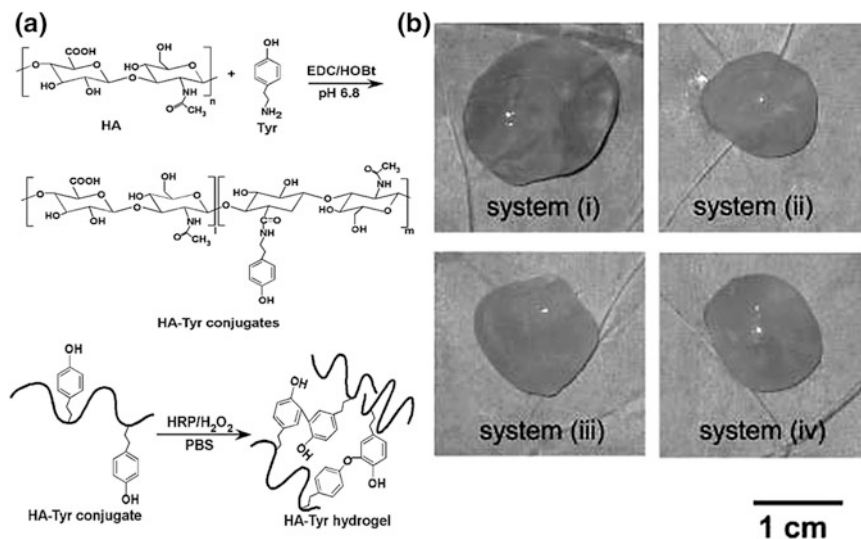


Fig. 2 Biodegradable hydrogels consisting of hyaluronic acid–tyramine conjugates; **a** synthesis of the conjugates and formation of the polymeric hydrogel via an enzyme-catalyzed oxidation reaction; **b** different hydrogel systems formed in vivo (Kurisawa et al. 2005)

receptively to synthesize crosslinked hydrogels using the corresponding monomer or macromeres containing methacrylate or acrylate moieties. In 1990, Saito et al. were the first to report hydrogels formed by redox reactions using the TEMED/KPS combination (Inomata et al. 1990; Otake et al. 1990). Hennink research group prepared dextran-hydroxy-ethyl-methacrylate (dex-HEMA) hydrogels using this redox reaction (Chung et al. 2005) that led to controlling the release of albumin, lysozyme, and IgG from these hydrogels (Hennink et al. 1997). Also, they succeeded in synthesizing hydrogels formed of methacrylated hyaluronic acid (Oudshoorn et al. 2007). However, in this technique, the presence of the unreacted persulfate and TEMED could damage, oxidize, and denature the encapsulated bioactive agent such as protein. So, a complete removal of these compounds is essential to apply this class of hydrogels in biomedical applications. The *in vitro* biocompatibility of biodegradable dextran-based hydrogels was examined using human fibroblasts. The results revealed that the cells have spider-like structures and contain intracellular granula (Fig. 3) (De Groot et al. 2001).

2.4.3 Double-Network Hydrogels

Physically crosslinked hydrogels possess very weak mechanical properties which limit their applications in tissue engineering, where mechanical stability is mandatory (Drury and Mooney 2003). On the other hand, *in situ* chemically crosslinked hydrogels show very poor gelation kinetics with rapid dissolution of the

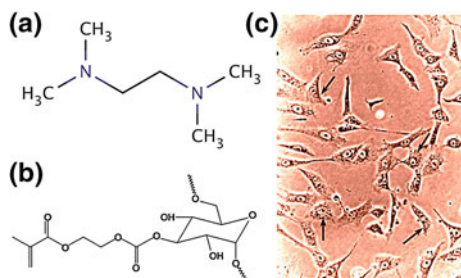


Fig. 3 In vitro biocompatibility of biodegradable dextran-based hydrogels examined using human fibroblast; **a** chemical structure of TEMED; **b** chemical structure of methacrylated dextran (Dex-MA); and **c** Human fibroblasts, cultured for 24 h in the presence of dex-MA (De Groot et al. 2001)

hydrogels. Therefore, a combination of both chemical and physical crosslinking approaches is an essential criterion to form more stable and smart double-network hydrogels with enhanced properties.

Furthermore, designing hydrogels by combining both physical and chemical crosslinking moieties allows the formation of smart sol-to-gel structure that could be triggered by certain stimuli such as temperature. In addition, building up hydrogels through combining ionically and covalently crosslinking networks can form the so-called interpenetrating networks (IPN) which incredibly synergistically affect the hydrogels properties (Fig. 4) (Matricardi et al. 2013; Sun et al. 2012).

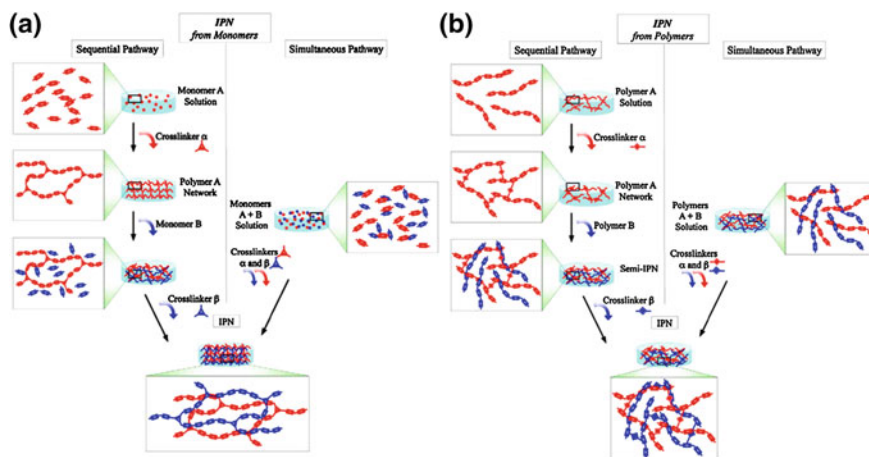


Fig. 4 Schematic illustration of the interpenetrating polymeric network (IPN) and semi-IPN formation; **a** IPN preparation pathway from monomers; **b** IPN preparation pathway from polymers (Matricardi et al. 2013)

2.4.4 Hydrogels Made of a Combination of Natural and Synthetic Polymers

Synthetic polymers are combined with natural polymers to obtain hydrogels with enhanced mechanical properties (Langer and Tirrell 2004; Sionkowska 2011). Many natural polymers are used in the synthesis of hydrogels such as agarose, alginate, cellulose, gelatin, chitosan, collagen, fibrin, hyaluronic acid, lignin, soya bean, and matrigel (Fig. 5) (Hoffman 2012; Lee and Mooney 2001). The non-chemically crosslinked hydrogels of these polymers showed enhanced cell adhesion and improved mechanical properties (Cascone et al. 1995; Coombes et al. 2002; Santin et al. 1996). Recently, hybrid hydrogels formed of natural and synthetic polymers have been designed through covalent crosslinking of the functional groups abundant in both polymers (Censi et al. 2010). In situ crosslinked hydrogels were synthesized using PNIPAAm-based polymers and natural carbohydrate polymers such as methylcellulose, carboxymethyl cellulose (CMC), hyaluronic acid, and dextran (Patenaude and Hoare 2012). Furthermore, many examples of hybrid hydrogels were successfully prepared through a combination of gelatin-methacrylamide, gelatin-PEG (Daniele et al. 2014), fibrin-polyurethane (Huang et al. 2013), and chitosan-PEG (Tan et al. 2013).

2.4.5 Composite Hydrogels

The mechanical properties and bioactivity of the formed hydrogels could be improved by incorporation of fillers within the polymeric matrices of the hydrogels to be used for certain applications. For instance, small inorganic molecules such as

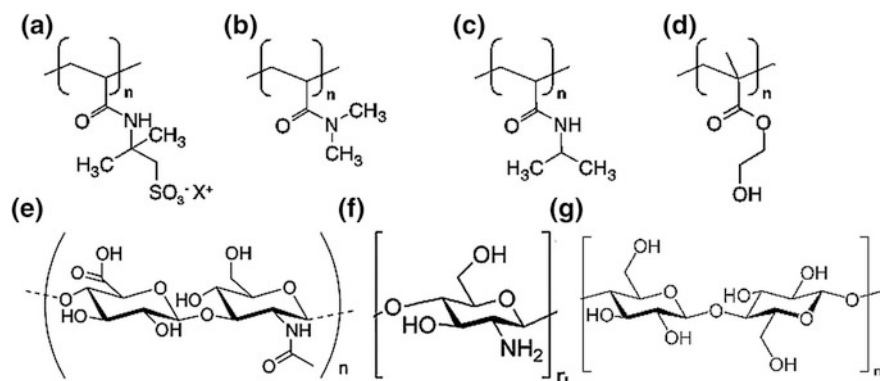


Fig. 5 Structures of some natural and synthetic polymers; **a** poly(2-acrylamido-2-methylpropanesulfonic acid) (PAMPS); **b** polyacrylamide (PAAm); **c** poly(N-isopropylacrylamide) (pNIPAAm); **d** poly(hydroxyethylmethacrylate) (pHEMA); **e** hyaluronan; **f** chitosan; **g** cellulose

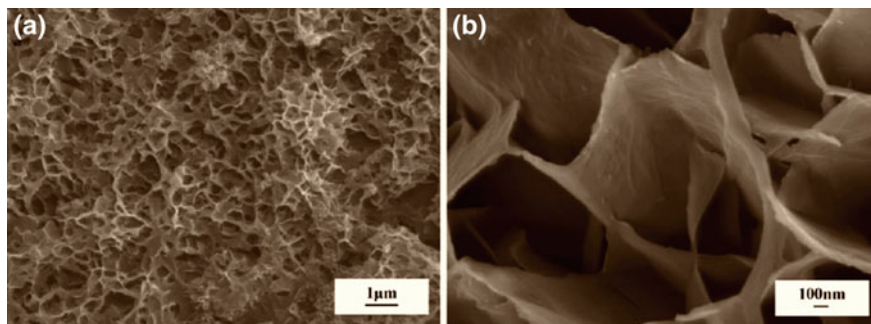


Fig. 6 SEM images of intensively mineralized supramolecular hydrogels; **a** intact macroporous calcium phosphate hydrogel architecture after disassembly of the self-assembled matrix; and **b** highly magnified image of an interconnected mineralized wall structure (Schnepp et al. 2006)

hydroxyapatite and calcium phosphate were used as fillers in the fabrication of composite hydrogels for bone tissue mineralization (Fig. 6) (Leeuwenburgh et al. 2007; Na et al. 2007; Schnepp et al. 2006). Also, Habraken et al. studied ceramics–hydrogel composites for tissue regeneration and drug delivery (Habraken et al. 2007).

3 Forms of Nanostructured Stimuli-Responsive Polymer Materials

Stimuli-responsive nanostructured polymeric materials and systems could be constructed in two forms according to their application. The architecture of materials and systems are either two-dimensional (2D) (films) or three-dimensional (3D) (particulates and their assemblies) as summarized in Fig. 7.

3.1 Two-Dimensional Architecture (2D-Films)

The construction of thin film surfaces could be summarized in different categories such as (a) spontaneously traditional shaped polymer surfaces in bulk materials, (b) polymer brushes formed through grafting polymer thin films, and (c) multilayered self-assembled thin films. Examples of the abovementioned categories are demonstrated in Fig. 2a.

The stimuli-responsive properties of modified thin polymer films can be used in biotechnological and biomedical applications (Alexander and Shakesheff 2006; Bajpai et al. 2008; Mendes 2008). First, the possibility of regulating adhesion property between stimuli-responsive films at one side and proteins and cells at the

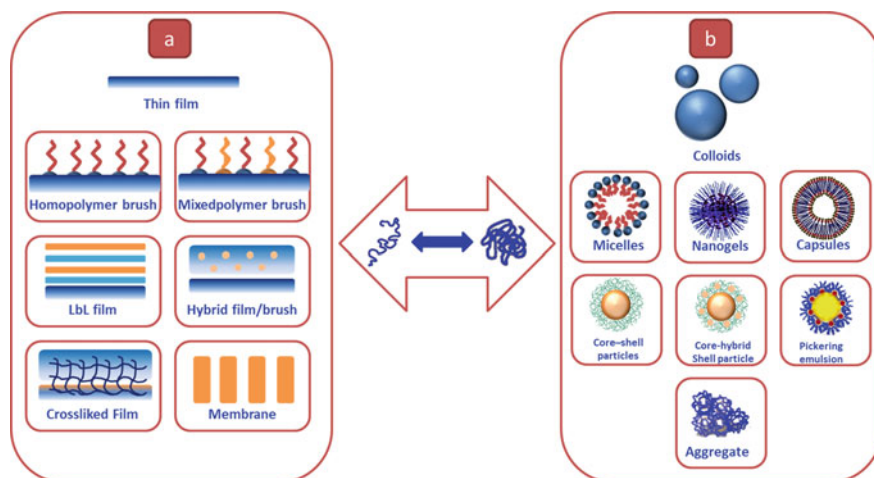


Fig. 7 Different architectures of nanostructured stimuli-responsive polymer materials. **a** Thin film design and **b** nanoparticles

other side has been explored and used for bioseparation and tissue regeneration (de las Heras Alarcón et al. 2005; Ionov et al. 2009; Lutolf et al. 2003). Second, the possibility of controlling functional moieties at the film surfaces has been explored for regulating signals and associated biomolecule activity modulation in bioengineering (Ebara et al. 2004; Hayashi et al. 2007). Third, surface-grafted stimuli-responsive polymers provide an opportunity for controlling molecules permeation through cellular membranes (Lue et al. 2008), interaction of biomolecules with film responsive surfaces (Motornov et al. 2009) in bioseparation (Wong et al. 2009), or controlling drug permeation by nano/microporous membranes (Lue et al. 2008).

3.2 *Three-Dimensional Architecture (3D-Particles)*

The rearrangement of polymer molecules could form different types of nanoparticles such as aggregates, capsules, core-shell particles, hybrid particle-in-particle structures, micelles, nanogels, pickering emulsion, and vesicles. Stimuli-responsive particles represent a vast growing and a fundamental category of the materials that could be applied for protection, stabilization, and delivery of different cargos.

The design of responsive nanoparticles can be typically found in a core-shell nanoparticle prepared by the self-assembly of some amphiphilic copolymers. Also, modifications of the polymeric particles using specific functional moieties could develop smart stimuli-responsive hydrogels. Finally, core-forming polymers developed stimuli-responsive polymeric hydrogels that could respond to the

externally applied specific stimuli in order to stimulate the self-assembled formation, reversible or irreversible disintegration, aggregation, swelling, and adsorption (Stuart et al. 2010).

4 Classification of Stimuli-Responsive Polymers

This section discusses the state-of-the-art in stimuli-responsive polymeric delivery systems. These systems are capable of controlling a cargo release in response to a physiological need or external stimuli. Special attention is paid to proteins as therapeutic drugs, presenting the advantages and disadvantages of different categories. Schematic representation of these categories is demonstrated in Fig. 8.

4.1 Physiological Stimuli-Responsive Polymers

4.1.1 pH-Sensitive Polymers

Some of the stimuli-responsive polymeric nanosystems have been synthesized to possess specific pH-sensitive moieties in order to be able to target specific locations inside the human body depending on the physiological pH gradients. For example, those smart polymeric systems have been extensively designed to target specific organs, intracellular organelles, or even pathological sites such as cancerous and inflammatory tissues (Mura et al. 2013). Upon exposure to the external pH stimulus, these smart hydrogel nanosystems are capable of being physically and/or chemically altered in terms of swelling, fusing membranes, converting charges, and disrupting or cleaving bonds (Mo et al. 2012). To design such smart pH-responsive nanosystems, two major strategies could be followed. The first strategy is to utilize

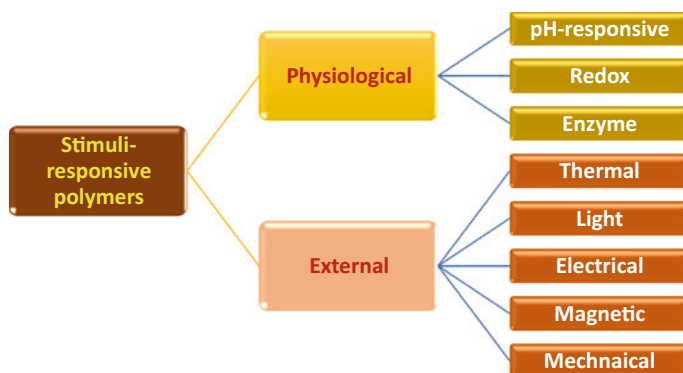


Fig. 8 Different types of stimuli-triggered polymers and hydrogels

the protonation of polymer ionizable groups (Gu et al. 2013; Lee et al. 2005), while the second strategy is to integrate acid-cleavable bonds in polymer chains (Bae and Kataoka 2009; Bae et al. 2003).

4.1.2 Redox-Responsive Polymers

Tripeptide-reducing agent, glutathione, is found at a higher level than cytosol in the extracellular fluids which renders intracellular redox potential. Therefore, redox-responsive carriers are designed to degrade and release drugs into the cytosol. Various reducing agents could be used to reversibly convert disulfides to thiol groups through redox reactions (Kamada et al. 2010). This redox-responsive behavior of thiol–disulfide exchange offers a chance to control drug release using redox as a potential trigger (Zhang et al. 2003). To achieve this reversible redox-responsive approach, disulfide bonds can be incorporated into either polymer backbone or the crosslinkers structures.

4.1.3 Enzyme-Responsive Polymers

One of the important targets for certain applications such as drug delivery is the abundance of certain enzymes with certain concretions as they play a vital role in biochemical processes within the human body cells (la Rica et al. 2012). Polymers can be designed in such a way to release certain cargoes in response to specific enzymatic levels in target tissue. Enzyme-based carriers are able to program delivery of sensitive bioactive materials such as proteins with both high sensitivity and selectivity to target sites (Guo et al. 2012). In the past few years, significant numbers of articles have been published in the field of enzyme-responsive protein delivery systems (Guo et al. 2012).

4.2 External Stimuli-Responsive Polymers

4.2.1 Thermal-Responsive Polymers

The main characteristic of thermal-responsive materials is the nonlinear relationship between their temperature and solubility. At a sharp temperature transition, the solubility of thermal-responsive materials either increases or decreases extensively (Schmaljohann 2006). Temperature-responsive polymers possess a phase transition at a specific temperature which depends on the hydrophilic and hydrophobic moieties balance within their structure (Heskins and Guillet 1968). A class of covalently crosslinked hydrogels is a major class of temperature-responsive systems that are beneficial in biomedical applications such as targeted drug delivery, controlled release, and tissue engineering.

4.2.2 Light-Responsive Polymers

Light-responsive polymeric delivery systems can remotely trigger cargo release with very high accuracy. It can be regulated through the adjustment of any parameters like wavelength, light intensity, duration of exposure, and beam diameter (Fomina et al. 2012). For instance, titanium oxide containing nanomaterials has photocatalytic activity along with their excellent biocompatibility; therefore, many publications are considered it as a good light-triggered delivery system (Zhou et al. 2006).

4.2.3 Electric-Responsive Polymers

Electric-responsive systems are either an indirect or direct trigger system. The indirect trigger system is a pH-sensitive polymer where the local pH could be regulated by the presence or absence of an electric current. Consequently, electric stimuli have been utilized to trigger drug release. So, this system could be considered as a derivative of pH-responsive delivery systems (Lee et al. 2004). Kwon et al. developed an indirect electric-responsive system consisting of a complex of poly(methacrylic acid) and poly(ethylloxazoline) formed via hydrogen bonding between the carboxylic group and the oxazoline group, respectively. A complex formation is precipitated at pH below 5; however, this precipitate would dissolve instantly at pH above 5.4 (Kwon et al. 1991).

The indirect trigger system is the passage of counterions and water molecules in the non-degradable polymer matrix. Florence et al. described the behavior of crosslinked hyaluronic acid-based hydrogel when exposed to electric stimuli (Tomer et al. 1995). The developed crosslinked hyaluronic acid system showed a pulsatile release of protein cargo. Upon switching on the applied electric field, cargo release behavior stopped. On contrary, upon switching off the applied electric field, hydrogel swelled up leading to cargo release.

4.2.4 Magnetic-Responsive Polymers

Magnetic-responsive nanosystems are capable of targeting tumors under the influence of applied magnetic field (Chorny et al. 2011). Huang et al. developed different amino-functionalized mesoporous magnetic hollow nanoparticles (MMHs) and investigated their intracellular trafficking using BSA as a model cargo (Huang et al. 2008). Modified MMHs were prepared using a reported procedure, where a template of negatively charged polystyrene (PS) nanospheres was used and then removed to form the mesoporous hollow structure (Huang and Tang 2005). The modified MMHs with amino groups showed high drug-loading efficiency with intracellular drug delivery and release capability into specific subcellular compartments.

4.2.5 Mechanical-Responsive Polymers

Mechanical-responsive nanosystems were used recently to control drug release by applying mechanical force to external stimuli. Lee et al. developed vascular endothelial growth factor (VEGF)-loaded alginate hydrogels with pulsatile release as a response to different strain amplitudes of compressive forces (Lee et al. 2004). VEGF was released upon compression while release stopped once the strain was removed as the hydrogel resumed its initial volume.

5 Future Prospective of Stimuli-Responsive Polymers

Stimuli-responsive polymeric nanosystems could be used for a variety of applications, such as adhesives, protecting coatings, sensors, and drug delivery. In reality, it is a challenge to develop complex systems that are responsive to physiological signals or external stimuli on the nanoscale. Such systems need a complex, hierarchical organization of the responsive particles abovementioned in this chapter to accommodate various possible mechanisms. Another challenge is to develop systems that could respond to several stimuli in an intelligent way. These systems could target specific physiological condition with controlled release profile. Although several trials have been reported recently, much more effort is still required before practical applications are viable. Responsive materials can also be introduced into many systems with a very thin coating layer to which certain functional moieties could be linked in order to enhance the targeting capability of such smart systems.

References

- Alexander C, Shakesheff KM (2006) Responsive polymers at the biology/materials science interface. *Adv Mater* 18:3321–3328
- Bae Y, Fukushima S, Harada A, Kataoka K (2003) Design of environment-sensitive supramolecular assemblies for intracellular drug delivery: polymeric micelles that are responsive to intracellular pH change. *Angew Chem Int Ed* 42:4640–4643
- Bae Y, Kataoka K (2009) Intelligent polymeric micelles from functional poly (ethylene glycol)-poly (amino acid) block copolymers. *Adv Drug Deliv Rev* 61:768–784
- Bajpai A, Shukla SK, Bhanu S, Kankane S (2008) Responsive polymers in controlled drug delivery. *Prog Polym Sci* 33:1088–1118
- Bertin A (2012) Emergence of polymer stereocomplexes for biomedical applications. *Macromol Chem Phys* 213:2329–2352
- Cascone MG, Sim B, Sandra D (1995) Blends of synthetic and natural polymers as drug delivery systems for growth hormone. *Biomaterials* 16:569–574
- Censi R, Fietsen PJ, di Martino P, Hennink WE, Vermonden T (2010) In situ forming hydrogels by tandem thermal gelling and Michael addition reaction between thermosensitive triblock copolymers and thiolated hyaluronan. *Macromolecules* 43:5771–5778

- Chen T, Embree HD, Brown EM, Taylor MM, Payne GF (2003) Enzyme-catalyzed gel formation of gelatin and chitosan: potential for in situ applications. *Biomaterials* 24:2831–2841
- Chorny M, Fishbein I, Forbes S, Alferiev I (2011) Magnetic nanoparticles for targeted vascular delivery. *IUBMB Life* 63:613–620
- Chung HJ, Lee Y, Park TG (2008) Thermo-sensitive and biodegradable hydrogels based on stereocomplexed Pluronic multi-block copolymers for controlled protein delivery. *J Control Release* 127:22–30
- Chung J, Vlught-Wensink K, Hennink W, Zhang Z (2005) Effect of polymerization conditions on the network properties of dex-HEMA microspheres and macro-hydrogels. *Int J Pharm* 288:51–61
- Corobea MC, Muhulet O, Miculescu F, Antoniac IV, Vuluga Z, Florea D et al (2016) Novel nanocomposite membranes from cellulose acetate and clay-silica nanowires. *Polym Adv Technol* 27(12):1586–1595
- Coombes A, Verderio E, Shaw B, Li X, Griffin M, Downes S (2002) Biocomposites of non-crosslinked natural and synthetic polymers. *Biomaterials* 23:2113–2118
- Daniele MA, Adams AA, Naciri J, North SH, Ligler FS (2014) Interpenetrating networks based on gelatin methacrylamide and PEG formed using concurrent thiol click chemistries for hydrogel tissue engineering scaffolds. *Biomaterials* 35:1845–1856
- De Groot CJ, Van Luyn MJ, Van Dijk-Wolthuis WN, Cadée JA, Plantinga JA, Den Otter W, Hennink WE (2001) In vitro biocompatibility of biodegradable dextran-based hydrogels tested with human fibroblasts. *Biomaterials* 22:1197–1203
- De Jong S, van Dijk-Wolthuis W, Kettenes-Van den Bosch J, Schuyl P, Hennink W (1998) Monodisperse enantiomeric lactic acid oligomers: preparation, characterization, and stereo-complex formation. *Macromolecules* 31:6397–6402
- De las Heras Alarcón C, Farhan T, Osborne VL, Huck WT, Alexander C (2005) Bioadhesion at micro-patterned stimuli-responsive polymer brushes. *J Mater Chem* 15:2089–2094
- Drury JL, Mooney DJ (2003) Hydrogels for tissue engineering: scaffold design variables and applications. *Biomaterials* 24:4337–4351
- Ebara M, Yamato M, Aoyagi T, Kikuchi A, Sakai K, Okano T (2004) Temperature-responsive cell culture surfaces enable “on-off” affinity control between cell integrins and RGDS ligands. *Biomacromol* 5:505–510
- Fomina N, Sankaranarayanan J, Almutairi A (2012) Photochemical mechanisms of light-triggered release from nanocarriers. *Adv Drug Delivery Rev* 64:1005–1020
- Fukushima K, Kimura Y (2006) Stereocomplexed polylactides (Neo-PLA) as high-performance bio-based polymers: their formation, properties, and application. *Polym Int* 55:626–642
- Gu X, Wang J, Wang Y, Wang Y, Gao H, Wu G (2013) Layer-by-layer assembled polyaspartamide nanocapsules for pH-responsive protein delivery. *Colloids Surf, B* 108:205–211
- Guo D-S, Wang K, Wang Y-X, Liu Y (2012) Cholinesterase-responsive supramolecular vesicle. *J Am Chem Soc* 134:10244–10250
- Gupta P, Vermani K, Garg S (2002) Hydrogels: from controlled release to pH-responsive drug delivery. *Drug Discov Today* 7:569–579
- Habraken W, Wolke J, Jansen J (2007) Ceramic composites as matrices and scaffolds for drug delivery in tissue engineering. *Adv Drug Deliv Rev* 59:234–248
- Hayashi G, Hagihara M, Dohno C, Nakatani K (2007) Photoregulation of a peptide-RNA interaction on a gold surface. *J Am Chem Soc* 129:8678–8679
- Hennink W, Franssen O, van Dijk-Wolthuis W, Talsma H (1997) Dextran hydrogels for the controlled release of proteins. *J Control Release* 48:107–114
- Heskins M, Guillet JE (1968) Solution properties of poly (N-isopropylacrylamide). *J Macromol Sci Chem* 2:1441–1455
- Hoffman AS (2012) Hydrogels for biomedical applications. *Adv Drug Deliv Rev* 64:18–23
- Hu BH, Messersmith P (2005) Enzymatically cross-linked hydrogels and their adhesive strength to biosurfaces. *Orthod Craniofac Res* 8:145–149

- Huang X, Meng X, Tang F, Li L, Chen D, Liu H, Zhang Y, Ren J (2008) Mesoporous magnetic hollow nanoparticles—protein carriers for lysosome escaping and cytosolic delivery. *Nanotechnology* 19:445101
- Huang Y, Zhang B, Xu G, Hao W (2013) Swelling behaviours and mechanical properties of silk fibroin-polyurethane composite hydrogels. *Composites Science and Technology* 84:15–22
- Huang Z, Tang F (2005) Preparation, structure, and magnetic properties of mesoporous magnetite hollow spheres. *J Colloid Interface Sci* 281:432–436
- Huh KM, Cho YW, Chung H, Kwon IC, Jeong SY, Ooya T, Lee WK, Sasaki S, Yui N (2004) Supramolecular Hydrogel Formation Based on Inclusion Complexation Between Poly (ethylene glycol)-Modified Chitosan and alpha-Cyclodextrin. *Macromol Biosci* 4:92–99
- Huh KM, Ooya T, Lee WK, Sasaki S, Kwon IC, Jeong SY, Yui N (2001) Supramolecular-structured hydrogels showing a reversible phase transition by inclusion complexation between poly (ethylene glycol) grafted dextran and alpha-cyclodextrin. *Macromolecules* 34:8657–8662
- Ikada Y, Jamshidi K, Tsuji H, Hyon SH (1987) Stereocomplex formation between enantiomeric poly (lactides). *Macromolecules* 20:904–906
- Inomata H, Goto S, Saito S (1990) Phase transition of N-substituted acrylamide gels. *Macromolecules* 23:4887–4888
- Ionov L, Houbenov N, Sidorenko A, Stamm M, Minko S (2009) Stimuli-responsive command polymer surface for generation of protein gradients. *Biointerphases* 4:FA45–FA49
- Kamada J, Koynov K, Corten C, Juhari A, Yoon JA, Urban MW, Balazs AC, Matyjaszewski K (2010) Redox responsive behavior of thiol/disulfide-functionalized star polymers synthesized via atom transfer radical polymerization. *Macromolecules* 43:4133–4139
- Kopecek J (2009) Hydrogels: From soft contact lenses and implants to self-assembled nanomaterials. *J Polym Sci, Part A: Polym Chem* 47:5929–5946
- Kuhn W, Hargitay B, Katchalsky A, Eisenberg H (1950) Reversible dilation and contraction by changing the state of ionization of high-polymer acid networks. *Nature* 165:514–516
- Kuo W-Y, Lai H-M (2011) Morphological, structural and rheological properties of beta-cyclodextrin based polypseudorotaxane gels. *Polymer* 52:3389–3395
- Kurisawa M, Chung JE, Yang YY, Gao SJ, Uyama H (2005) Injectable biodegradable hydrogels composed of hyaluronic acid-tyramine conjugates for drug delivery and tissue engineering. *Chem Commun* 4312–4314
- Kwon IC, Bae YH, Kim SW (1991) Electrically erodible polymer gel for controlled release of drugs. *Nature* 354:291–293
- La Rica R, Aili D, Stevens MM (2012) Enzyme-responsive nanoparticles for drug release and diagnostics. *Adv Drug Delivery Rev* 64:967–978
- Langer R, Tirrell DA (2004) Designing materials for biology and medicine. *Nature* 428:487–492
- Lee ES, Na K, Bae YH (2005) Doxorubicin loaded pH-sensitive polymeric micelles for reversal of resistant MCF-7 tumor. *J Control Release* 103:405–418
- Lee K, Yoon J, Lee J, Kim S, Jung H, Kim S, Joh J, Lee H, Lee D, Lee S (2004) Sustained release of vascular endothelial growth factor from calcium-induced alginate hydrogels reinforced by heparin and chitosan. In: *Transplantation proceedings*, pp 2464–2465
- Lee KY, Mooney DJ (2001) Hydrogels for tissue engineering. *Chem Rev* 101:1869–1880
- Leeuwenburgh SC, Jansen JA, Mikos AG (2007) Functionalization of oligo (poly (ethylene glycol) fumarate) hydrogels with finely dispersed calcium phosphate nanocrystals for bone-substituting purposes. *J Biomater Sci Polym Ed* 18:1547–1564
- Li J, Harada A, Kamachi M (1994) Sol-gel transition during inclusion complex formation between alpha-cyclodextrin and high molecular weight poly (ethylene glycol) s in aqueous solution. *Polym J* 26:1019–1026
- Li J, Ni X, Zhou Z, Leong KW (2003) Preparation and characterization of polypseudorotaxanes based on block-selected inclusion complexation between poly (propylene oxide)-poly (ethylene oxide)-poly (propylene oxide) triblock copolymers and alpha-cyclodextrin. *J Am Chem Soc* 125:1788–1795

- Lim DW, Choi SH, Park TG (2000) A new class of biodegradable hydrogels stereocomplexed by enantiomeric oligo (lactide) side chains of poly (HEMA-g-OLA) s. *Macromol Rapid Commun* 21:464–471
- Lue SJ, Hsu J-J, Wei T-C (2008) Drug permeation modeling through the thermo-sensitive membranes of poly (N-isopropylacrylamide) brushes grafted onto micro-porous films. *J Membr Sci* 321:146–154
- Lutolf M, Lauer-Fields J, Schmoekel H, Metters A, Weber F, Fields G, Hubbell J (2003) Synthetic matrix metalloproteinase-sensitive hydrogels for the conduction of tissue regeneration: engineering cell-invasion characteristics. *Proc Natl Acad Sci* 100:5413–5418
- Ma D, Tu K, Zhang L-M (2010) Bioactive supramolecular hydrogel with controlled dual drug release characteristics. *Biomacromol* 11:2204–2212
- Matricardi P, Di Meo C, Coviello T, Hennink WE, Alhaique F (2013) Interpenetrating polymer networks polysaccharide hydrogels for drug delivery and tissue engineering. *Adv Drug Deliv Rev* 65:1172–1187
- Mendes PM (2008) Stimuli-responsive surfaces for bio-applications. *Chem Soc Rev* 37:2512–2529
- Miyata T, Uragami T, Nakamae K (2002) Biomolecule-sensitive hydrogels. *Adv Drug Deliv Rev* 54:79–98
- Miculescu M, Thakur VK, Miculescu F, Voicu SI (2016) Graphene-based polymer nanocomposite membranes: a review. *Polym Adv Technol* 27(7):844–859
- Mo R, Sun Q, Xue J, Li N, Li W, Zhang C, Ping Q (2012) Multistage pH-responsive liposomes for mitochondrial-targeted anticancer drug delivery. *Adv Mater* 24:3659–3665
- Motornov M, Tam TK, Pita M, Tokarev I, Katz E, Minko S (2009) Switchable selectivity for gating ion transport with mixed polyelectrolyte brushes: approaching ‘smart’ drug delivery systems. *Nanotechnology* 20:434006
- Mura S, Nicolas J, Couvreur P (2013) Stimuli-responsive nanocarriers for drug delivery. *Nat Mater* 12:991–1003
- Na K, won Kim S, Sun BK, Woo DG, Yang HN, Chung HM, Park KH (2007) Osteogenic differentiation of rabbit mesenchymal stem cells in thermo-reversible hydrogel constructs containing hydroxyapatite and bone morphogenic protein-2 (BMP-2). *Biomaterials* 28:2631–2637
- Otake K, Inomata H, Konno M, Saito S (1990) Thermal analysis of the volume phase transition with N-isopropylacrylamide gels. *Macromolecules* 23:283–289
- Oudshoorn MH, Rissmann R, Bouwstra JA, Hennink WE (2007) Synthesis of methacrylated hyaluronic acid with tailored degree of substitution. *Polymer* 48:1915–1920
- Patenaude M, Hoare T (2012) Injectable, mixed natural-synthetic polymer hydrogels with modular properties. *Biomacromol* 13:369–378
- Pauling L, Corey RB (1953) Two rippled-sheet configurations of polypeptide chains, and a note about the pleated sheets. *Proc Natl Acad Sci USA* 39:253
- Peppas NA, Khare AR (1993) Preparation, structure and diffusional behavior of hydrogels in controlled release. *Adv Drug Deliv Rev* 11:1–35
- Qiu Y, Park K (2012) Environment-sensitive hydrogels for drug delivery. *Adv Drug Delivery Rev*
- Roorda W, Bodde H, De Boer A, Junginger H (1986) Synthetic hydrogels as drug delivery systems. *Pharmaceutisch Weekblad* 8:165–189
- Ruel-Gariépy E, Leroux JC (2004) In situ-forming hydrogels—review of temperature-sensitive systems. *Eur J Pharm Biopharm* 58:409–426
- Santin M, Huang S, Iannace S, Ambrosio L, Nicolais L, Peluso G (1996) Synthesis and characterization of a new interpenetrated poly (2-hydroxyethylmethacrylate)—gelatin composite polymer. *Biomaterials* 17:1459–1467
- Schmaljohann D (2006) Thermo-and pH-responsive polymers in drug delivery. *Adv Drug Deliv Rev* 58:1655–1670
- Schnepf ZA, Gonzalez-McQuire R, Mann S (2006) Hybrid biocomposites based on calcium phosphate mineralization of self-assembled supramolecular hydrogels. *Adv Mater* 18:1869–1872

- Sionkowska A (2011) Current research on the blends of natural and synthetic polymers as new biomaterials: Review. *Prog Polym Sci* 36:1254–1276
- Slager J, Domb AJ (2003) Biopolymer stereocomplexes. *Adv Drug Deliv Rev* 55:549–583
- Steinberg I, Oplatka A, Katchalsky A (1966) Mechanochemical engines. *Nature* 210:568–571
- Stuart MAC, Huck WTS, Genzer J, Müller M, Ober C, Stamm M, Sukhorukov GB, Szleifer I, Tsukruk VV, Urban M, Winnik F, Zauscher S, Luzinov I, Minko S (2010) Emerging applications of stimuli-responsive polymer materials. *Nat Mater* 9:101–113. <https://doi.org/10.1038/nmat2614>
- Sun J-Y, Zhao X, Illeperuma WR, Chaudhuri O, Oh KH, Mooney DJ, Vlassak JJ, Suo Z (2012) Highly stretchable and tough hydrogels. *Nature* 489:133–136
- Takami K, Watanabe J, Takai M, Ishihara K (2011) Spontaneous formation of a hydrogel composed of water-soluble phospholipid polymers grafted with enantiomeric oligo (lactic acid) chains. *J Biomater Sci Polym Ed* 22:77–89
- Tan H, Luan H, Hu Y, Hu X (2013) Covalently crosslinked chitosan-poly (ethylene glycol) hybrid hydrogels to deliver insulin for adipose-derived stem cells encapsulation. *Macromol Res* 21:392–399
- Thakur VK, Thakur MK (2014a) Recent trends in hydrogels based on psyllium polysaccharide: a review. *J Clean Prod* 82:1–15
- Thakur VK, Thakur MK (2014b) Recent advances in graft copolymerization and applications of Chitosan: a review. *ACS Sustain Chem Eng* 2(12):2637–2652
- Thakur VK, Thakur MK (2015) Recent advances in green hydrogels from lignin: a review. *Int J Biol Macromol* 72:834–847
- Teixeira LSM, Feijen J, van Blitterswijk CA, Dijkstra PJ, Karperien M (2012) Enzyme-catalyzed crosslinkable hydrogels: emerging strategies for tissue engineering. *Biomaterials* 33:1281–1290
- Tomer R, Dimitrijevic D, Florence AT (1995) Electrically controlled release of macromolecules from cross-linked hyaluronic acid hydrogels. *J Control Release* 33:405–413
- Trache D, Hazwan Hussin M, Mohamad Haafiz MK, Kumar Thakur V (2017) Recent progress in cellulose nanocrystals: sources and production. *Nanoscale* 9(5):1763–1786
- Tsujii H (2005) Poly (lactide) stereocomplexes: formation, structure, properties, degradation, and applications. *Macromol Biosci* 5:569–597
- VanBemmelen JM (1894) Der Hydrogel und das kristallinische Hydrat des Kupferoxydes. *Z Anorg Chem* 5:466
- Voicu SI, Condruz RM, Mitran V, Cimpean A, Miculescu F, Andronesu C, Thakur VK (2016) Sericin covalent immobilization onto cellulose acetate membrane for biomedical applications. *ACS Sustain Chem Eng* 4(3):1765–1774
- Ward MA, Georgiou TK (2011) Thermoresponsive polymers for biomedical applications. *Polymers* 3:1215–1242
- Wichterle O, Lim D (1960) Hydrophilic gels for biological use. *Nature* 185:117–118
- Wong VN, Fernando G, Wagner AR, Zhang J, Kinsel GR, Zauscher S, Dyer DJ (2009) Separation of peptides with polyionic nanosponges for MALDI-MS analysis. *Langmuir* 25:1459–1465
- Zhang W, Tichy SE, Pérez LM, Maria GC, Lindahl PA, Simanek EE (2003) Evaluation of multivalent dendrimers based on melamine: kinetics of thiol-disulfide exchange depends on the structure of the dendrimer. *J Am Chem Soc* 125:5086–5094
- Zhao S-P, Zhang L-M, Ma D (2006) Supramolecular hydrogels induced rapidly by inclusion complexation of poly (varepsilon-caprolactone)-poly (ethylene glycol)-poly (varepsilon-caprolactone) block copolymers with alpha-cyclodextrin in aqueous solutions. *J Phys Chem B* 110:12225–12229
- Zhou H, Gan X, Liu T, Yang Q, Li G (2006) Electrochemical study of photovoltaic effect of nano titanium dioxide on hemoglobin. *Bioelectrochemistry* 69:34–40

Chapter 5

Polysaccharide-Based Polymer Gels



Tamás Fekete and Judit Borsa

Abstract Hydrogels are special polymer systems with unique properties due to their high water content. They hold a relative large importance in several application fields, especially in the medicine and sanitary products. Moreover, their potential utility is intensively studied in several other fields. While most commercially available hydrogels are synthetic polymer-based, there is an increasing interest in the use of various renewable resources. Such materials have several advantageous properties, like biodegradability and good biocompatibility. Polysaccharides are the most important group of the renewable materials due to their abundance and low cost. In the present chapter, we give an account of the potential use of polysaccharide systems for the formation of hydrogels. After a short introduction to the chemical structure of polysaccharides, their dissolution, possible crosslinking methods, and the studies related to the most important representatives are discussed. The modification of gel properties by grafting, copolymerization, and blending is also a very common route. The non-polysaccharide component can range from other renewable resources like polypeptides to synthetic polymers to inorganic additives. Finally, we give a summary of the potential applications of the polysaccharide-based hydrogels.

Keywords Polysaccharide · Hydrogel · Superabsorbent · Crosslinking

T. Fekete
Centre for Energy Research, Hungarian Academy of Sciences,
Institute for Energy Security and Environmental Safety, Budapest
114, P.O. Box 49, 1525, Hungary
e-mail: feketet@energia.mta.hu

J. Borsa (✉)
Faculty of Light Industry and Environmental Engineering, Óbuda-University,
Doberdó str. 6, Budapest 1034, Hungary
e-mail: borsa.judit@rkk.uni-obuda.hu

1 Introduction

Gels are special three-dimensional polymer networks where the polymer matrix is filled with liquid or gas. The polymer network can be physically or chemically crosslinked. In case of physical gels, the network formation occurs due to various weak interactions, like the entanglement of the polymer chains, hydrogen bonds, or van der Waals interactions. Such structures are usually not permanent and they dissolve over the time when immersed in their solvents. However, the polymer chains can also be crosslinked through chemical reactions, leading to strong covalent bonds. The chemically crosslinked network is much more stable and cannot be dissolved without the degradation of the polymer. Therefore, chemical gels are usually preferable in the majority of the application fields.

Hydrogels are special gels filled with water or are capable of absorbing large amounts of it. The swelling behavior heavily depends on the chemical structure of the polymer: for high water uptake, the presence of hydrophilic groups in the polymer backbone is favored. Moreover, other effects like the electrostatic repulsion between charged groups also contribute to the network expansion, leading to improved swelling. Hydrogels with an exceedingly high water absorbing capacity (usually hundreds or even thousands times of their own weight) are called super-absorbents. The high water content has a major impact on the gel behavior: such gels are very soft and special properties like biocompatibility are also easier to develop. Moreover, depending on the chemical structure, hydrogels can also exhibit responsive behavior to the environmental conditions, such as the pH or the temperature. This sensitivity can be very advantageous and allows new possible applications.

Nowadays hydrogels already have a wide array of commercial applications due to the intensive research thanks to their unique properties. They are especially widespread in the medicine and pharmacy, where they are used mainly in drug delivery, tissue engineering, and wound dressing. Their use is widespread in hygienic products like diapers, as well. Moreover, there are a large number of studies focusing on the application in new fields such as the agriculture and wastewater treatment. Most commercially available hydrogels are synthetic polymer-based. The use of acrylates (various salts and esters of acrylic acid) holds an especially important place in the hydrogel production and application. Such gels exhibit excellent swelling properties, non-toxicity, and responsive behavior. However, in certain fields their potential use is limited. For example, their agricultural application is hindered by their poor biodegradability.

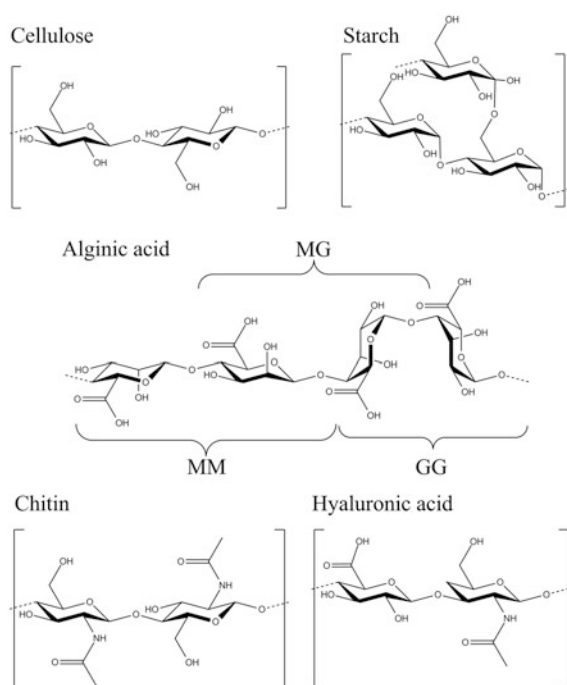
There is also a growing interest in the replacement of synthetic polymers with different renewable resources. Such materials are not only cheap and available in abundance but also more environmentally friendly. A very important aspect is the lack of toxicity: unlike their polymers, the acrylate monomers are toxic; thus, their residues need to be carefully removed after the synthesis. Hydrogels based on natural polymers show excellent biodegradability, which is a possible requirement depending on the application. The most important renewable materials are the

polysaccharides. The major focus is on the most abundant polysaccharides, such as the cellulose, chitin, starch, and alginate. These polymers are not only used in their native form, but the utilization of their derivatives is also significant. The modification is relatively easy and cheap due to the reactive hydroxyl or other pendant groups. A very important aspect that led to the investigation of their derivatives is the dissolution: depending on the chemical structure and molecular properties, water solubility can be easily achieved for the derivatives of polymers normally insoluble in water; thus, no special solvents are required. Moreover, the substituents introduced with the functionalization also lead to new gel properties.

2 Chemical Structure of Polysaccharides

The chemical structure of the various polysaccharides holds a lot of similarities (Trache et al. 2017; Corobea et al. 2016; Voicu et al. 2016; Miculescu et al. 2016). The most common structural unit is the glucose and its derivatives, but other saccharides also common components in certain polymers (Fig. 1). Due to the differences in the structural units and in the supramolecular structures, their properties are very different; thus, the crosslinking strategies differ significantly. Therefore, a short overview is given for the most common polysaccharides used for hydrogels.

Fig. 1 Chemical structure of the most common polysaccharides



2.1 Cellulose and Its Derivatization

Cellulose is the most abundant material in the world. It is present mostly in plant cells, but it is synthesized by some bacteria, as well. It consists of β -D-glucose units which form a linear chain with $\beta(1 \rightarrow 4)$ linkages. The presence of hydroxyl groups leads to the formation of intermolecular and intramolecular hydrogen bonds, while apolar parts of the macromolecules are linked with van der Waals interactions (Gross and Chu 2010). The cellulose chains form a semicrystalline structure consisting of crystalline and amorphous regions. Moreover, in the latter region, semi-ordered structures are also present to a certain degree. The polysaccharide has multiple crystalline polymorphs: Cellulose I, II, III, and IV. In the nature, Cellulose I is the dominant structure, which consists of parallel polymer chains and is formed by two different phases: the monoclinic I_{α} and the triclinic I_{β} . While both phases are present simultaneously, in higher plants the I_{β} , in bacteria and algae the I_{α} phase are the dominant (Sugiyama et al. 1991). The other cellulose polymorphs are usually synthesized by the conversion of Cellulose I, but the natural formation of the thermodynamically more stable Cellulose II was also observed (Hirai et al. 2002).

Due to the strong intermolecular interactions, the cellulose is insoluble in water. However, the partial substitution of hydroxyl groups results in the weakening of these bonds, leading to improved solubility. The water solubility increases with the degree of substitution which leads to weaker polymer–polymer interactions. For the hydrogel synthesis, mostly the cellulose ethers are utilized; the importance of its esters is minimal in this field. Cellulose ethers are important industrial materials with a wide array of applications such as surfactants, coatings, and thickeners. During the derivatization, the cellulose is disintegrated first in concentrated alkali followed by the substitution reaction (the alkaline environment also functions as a catalyst) (Woodings 2001). Carboxymethylcellulose is prepared with the addition of chloroacetic acid, leading to the formation of the sodium salt of the derivative. For the synthesis of alkylcelluloses alkyl chloride, in case of hydroxyalkylcelluloses alkene oxide is used as a reagent. Alkylhydroxyalkylcelluloses are also common derivatives, where both types of pendant groups are present in the structure.

2.2 Starch

Starch is another major polysaccharide which consists of α -D-glucose units. It is mostly present in plant cells as granules for energy storage. The glucose units form two different macromolecular structures: amylose and amylopectin. The amylose is a linear macromolecule where the glucose units are linked with $\alpha(1 \rightarrow 4)$ bonds. Amylopectin has a similar structure but it also has branches due to the $\alpha(1 \rightarrow 6)$ linkages. There is also a major difference in the molecular weight as the linear amylose is a significantly smaller macromolecule. The chains organized in double

helices which form the crystalline structure. Starch has two allomorphs: type A and type B starch (Buléon et al. 1998). Both structures consist of ordered double helices, but their position differs significantly. In A-type starch, the helices are closely packed, and the water molecules are positioned between the helices. For B-type starch, the helices form a hexagonal lattice, where the water is inside the hexagonal structure. C-type starch consisting of the mixture of the A and B-type structures also exists, though related studies are limited (Bogacheva et al. 1998). The oriented helices form the crystal lamellae, while the branch points are part of the amorphous phase, leading to a semicrystalline structure. Starch is present in the plant cells in granule form, which consists of alternating amorphous and crystalline regions; lipids and proteins are also present on its surface. Moreover, other components like phosphates and phospholipids are also found in the granule depending on the source. As the granular structure is not destroyed before the starch is used for the hydrogel synthesis, it has a major effect on the mechanism of the gelation.

While there is a large interest in the derivatization of the starch (Gotlieb and Capelle 2005), currently only the carboxymethylation (prepared with chloroacetic acid in sodium hydroxide solution similarly to the other polysaccharides) is relevant for the gel synthesis.

2.3 Chitin and Its Derivatization

Chitin is the most abundant material after the cellulose. It is a very important structural unit in the nature, especially for the fungi in the cell walls and as the exoskeleton for a wide array of animals. The chemical structure of chitin is similar to the structure of cellulose. It consists of β -D-glucose groups linked by $\beta(1 \rightarrow 4)$ linkages, but the hydroxyl groups in the C(2) position are substituted by an acetamido group; thus, *N*-acetyl- β -D-glucosamine is the structural unit. There are strong intermolecular interactions between the chitin chains due to the hydrogen bonds between the NH and CO groups, leading to a strong crystalline structure and insolubility in water. Chitin forms three different crystalline polymorphs: α -chitin consists of antiparallel chains, and β -chitin is formed by parallel macromolecules, while the γ polymorph has a more unique structure as two parallel chains are followed by an antiparallel one (Hudson and Smith 1998). Unlike the cellulose, all three polymorphs are present in the nature.

Chitin derivatization is usually achieved through modification of the acetamido groups. The most important derivative is the chitosan which is prepared by the deacetylation of chitin, leading to amino groups in the C(2) position. While full deacetylation is possible (Domard and Rinaudo 1983), the process is usually incomplete; thus, *N*-acetyl- β -D-glucosamine units are still present in the polymer structure. Unlike the chitin, chitosan is soluble in aqueous solutions at acidic pH due to the protonation of the amine groups (Rinaudo et al. 1999).

The hydroxyl groups in the polymer chain can also be utilized for the functionalization. For example, by introducing carboxymethyl groups, a fully

water-soluble chitin and chitosan derivative can be prepared (Muzzarelli 1988). However, these derivatives hold much smaller importance than the chitosan.

2.4 Alginate

Alginates are the salts of the alginic acid, from which the sodium salt is present in abundance in the nature. Alginate is synthesized by various algae and bacteria; for the industrial use, usually brown algae is used as alginate source. Unlike alginic acid, the alginate is water soluble. It is a linear copolymer of two monomers: β -D-mannuronic acid (M) and α -L-guluronic acid (G), with (1 \rightarrow 4) linkages between the units. These bonds can also form between the same units, leading to the formation of homopolymer (GG and MM) and copolymer blocks (MG) with different properties in an alternating structure (Donati and Paoletti 2009). The properties of the alginate heavily depend on the ratio of the two monomers and the distribution of the blocks (Johnson et al. 1997).

2.5 Hyaluronic Acid

Hyaluronan or hyaluronic acid is a unique polysaccharide due to its versatility. It is naturally present throughout the body of mammals in its salt form. The repeating unit consists of D-glucuronic acid and N-acetyl-D-glucosamine units with β (1 \rightarrow 3) linkage. These disaccharide units are linked with β (1 \rightarrow 4) bonds, forming a linear macromolecule of very large molecular weight (Fraser et al. 1997). While it is not as easily available as other abundant polysaccharides, there is a major interest in it due to its favorable properties for medical applications.

3 Dissolution of Polysaccharides

While gels can be synthesized from both solution and in dry state, the latter method is very rarely used for polysaccharide-based systems; thus, the dissolution of the polysaccharide is a key factor in the gel preparation. Unlike low molecular weight molecules, the dissolution of macromolecules is much more difficult. The solubility depends on the polymer–solvent and polymer–polymer interaction: if the latter one is dominant, the solvent cannot disrupt the intermolecular bonds between the macromolecules. Thus, the solvent properties are decisive. The most important solvent is the water due to its advantages. A wide array of polysaccharides like alginate and hyaluronic acid are water soluble. Therefore, water is the standard solvent for these polymers unless other water-insoluble components are also added. However, the most abundant polysaccharides (cellulose, starch, and chitin) are not

soluble in water; thus, special solvents are required. While a wide array of solvents are available for the dissolution of these polymers, in the following section, only solvents utilized for the hydrogel synthesis are reviewed.

3.1 *Dissolution of Cellulose and Its Derivatives*

The dissolution of cellulose was extensively studied in the past decades. There were major efforts to find cost-effective, environmentally friendly solvents. For the hydrogel synthesis, usually its industrial solvents are used, but there is strong interest toward novel systems like ionic liquids, as well. However, not all common solvents were investigated for this application so far. For example, dimethyl sulfoxide (DMSO)-based solvent systems are mostly used only for the synthesis of aerogels (Innerlohinger et al. 2006). Similarly, *N*-methylmorpholine-*N*-oxide, the solvent used for manufacturing regenerated cellulose fibers (e.g., Lyocel, Tencel), currently holds little importance in the gel preparation, but it might gain more attention in the future. Several solvents, such as cupriethylenediamine (CUEN) hydroxide, depend on the formation of metal–ion complexes with cellulose. CUEN and its relatives with different metals and ammonium hydroxide find substantial industrial use (Johnson 1985). Cuprammonium hydroxide (a mixture of copper hydroxide and ammonium hydroxide) and phosphorous acid had been used for regenerated cellulose fiber production for a long time (Kotek 2007); they might attract the interest of the cellulosic gel producers in the future.

For the hydrogel synthesis, multiple solvents of cellulose are widely used. The dimethylacetamide/lithium chloride (DMAc/LiCl) system is one of the most common such solvents. The mechanism of the process was in-depth investigated: the hydrogen bonds between the cellulose chains break up due to the chloride ions forming hydrogen bonds with the hydroxyl groups (Striegel 1997). Solvent exchange further improves the dissolution: the cellulose is immersed in water, which is gradually exchanged to methanol, and finally to DMAc/LiCl (McCormick et al. 1985). Such systems are not only stable, but the dissolution occurs without degradation even for high molecular weight cellulose at low temperatures (Dupont 2003). However, Potthast et al. (2002b) observed that elevated temperatures (over 85 °C) lead to the rapid degradation of the polymer.

Another method to dissolve cellulose is the addition of urea or thiourea to alkali hydroxide aqueous solutions. Sodium hydroxide is a cheap solvent of cellulose, but it is suitable only for the dissolution of low molecular weight polymer (Isogai and Atalla 1998). However, the introduction of urea or thiourea leads to the significantly improved solubility of the polysaccharide. The process is explained by the stabilizing effect of the components: Na⁺ cations interact with the hydrophilic groups of the cellulose (Cai and Zhang 2005), while the urea stabilizes the hydrophobic parts, preventing the intermolecular interactions between the polymer chains (Xiong et al. 2014). Due to this dual effect, the ratio of the two components is important: both too high hydroxide and too high urea content lead to decline in the solubility (Zhang et al. 2010).

Recently, the use of ionic liquids as novel solvents is also showing a growing tendency. Ionic liquids are organic salts with melting point below 100 °C, commonly even below the room temperature. Unlike the aforementioned solvents, they offer a more environmentally friendly option due to the low toxicity and biodegradability. However, this is not universally true for all salts: depending on the chemical structure, some ionic liquids not only show poor biodegradability but also are more hazardous than conventional solvents (Gatherhood et al. 2004; Romero et al. 2008). The chemical structure of the salt also plays a major role in the process: it not only affects the dissolution but some salts can also react with the cellulose (Clough et al. 2015). The latter process may lead to undesirable changes in the polymer properties; thus, it should be avoided. Swatlowksi et al. (2002) investigated the dissolution of cellulose in different alkyl-methylimidazolium systems and noted that the alkyl chain and the anion have a major effect on the solubility. While a wide array of methylimidazolium-based ionic liquids proved to be an efficient solvent (Feng and Chen 2008), most commonly 1-allyl-3-methylimidazolium chloride (AMIMCl) is used for the hydrogel synthesis (Zhang et al. 2005b). These salts are not only capable of dissolving large amounts of cellulose, but the polymer degradation is observed only at high temperatures. While they also have some disadvantages like the high viscosity or the slow dissolution, its widespread use is mainly hindered by the high production costs compared to the classic solvents.

Another method to achieve water solubility is the partial substitution of the hydroxyl groups, which weakens the strong intermolecular interactions, thus improving water–polymer interactions. Water solubility heavily depends on the molecular mass, degree of substitution (D_S), and substituent, as well. For example, a minimum D_S of 0.4 is required for carboxymethylcellulose to be fully water soluble (Wertz et al. 2010). In case of nonpolar substituents like methyl groups, an even higher degree of substitution is needed for optimal solubility. Moreover, heterogeneous distribution also leads to a decrease in the solubility, as the intermolecular bonds are not disrupted in certain segments of the chains. The derivatization is especially important for the cellulose, for which a wide array of substituents groups are used. The most common derivatives are the carboxyalkyl, alkyl, hydroxyalkyl, and alkylhydroxyalkylcelluloses.

3.2 *Dissolution of Starch and Its Derivatives*

Similarly to the cellulose, native starch does not dissolve in water due to the strong polymer–polymer interactions. Amylose and amylopectin, the two components of starch form a semicrystalline granule structure. These granules are resistant to external effects and while they show some swelling in water, they are insoluble. However, increasing the temperature of the aqueous dispersion leads to gelatinization: the interactions between the polymer chains are weakened, the ordered structure is disrupted, and the swelling of the granules increases significantly (Miles et al. 1985; Hoover 2001). The high viscosity of the gelatinized starch allows the

homogeneous dispersion of the crosslinking agents and other monomers in the system. This method is widely used for the preparation of copolymer gels as water is sufficient instead of more expensive and less “green” solvents.

Derivatization is also a possible way to achieve water solubility. However, opposed to the cellulose, for starch the derivatization is much less significant as the more convenient gelatinization is preferred. Moreover, only the gelation of its carboxymethyl derivative was investigated so far in this field (Nagasawa et al. 2004).

3.3 *Dissolution of Chitin and Chitosan*

Chitin is highly crystalline as the acetamide groups also participate in the formation of the intermolecular bonds. Solvents similar to the ones utilized for the cellulose dissolution are used to disrupt the intermolecular interactions. For example, sodium hydroxide/urea system proved to be excellent solvents for the chitin (Hu et al. 2007). Low temperature promotes the destruction of the intermolecular bonds as the polymer–solvent interactions become more stable (Chang et al. 2011a). Another popular solvent is the so-called Ca solvent, which is CaCl_2 dihydrate dissolved in methanol. The water present in the CaCl_2 also plays a major role in the mechanism as Ca solvent prepared from anhydrous chloride salt does not dissolve the chitin (Tamura et al. 2006). Tetrabutylammonium fluoride/dimethyl sulfoxide and lithium chloride systems were also applied successfully; for the latter system, *N*-methyl-2-pyrrolidone was used for the dissolution of the salt (Yoshimura et al. 2005). Recently, the application of ionic liquids was also studied and the imidazolium salts proved to be very efficient.

Chitosan, the deacetylated derivative of chitin is an even more popular choice for the hydrogel preparation. While pure water is an inadequate solvent, aqueous solution of chitosan can be prepared in presence of acidic medium like acetic acid; thus, the gel synthesis is easier compared to chitin. However, chitosan is also often derivatized further to modify the gel properties: the swelling properties of the hydrogels significantly improve at nonacidic pH if carboxymethyl groups are introduced to the polymer (Vaghani et al. 2012). Thus, the carboxymethylchitosan is also a major subject of such experiments. Moreover, carboxymethylation is also a viable route to increase the water solubility of the chitin polymer; thus, deacetylation is not required to allow the use of aqueous solutions for the gelation (Zhao et al. 2001).

4 Crosslinking Methods

The dissolution of the polysaccharide is followed by the crosslinking the polymer chains to form the three-dimensional network. In solutions, the polymer chains are highly mobile; thus, the crosslink formation is easier. A wide variety of methods are

employed for the synthesis of hydrogels. The properties of the polysaccharide are the determining factor which crosslinking steps are applicable; thus, the preferred method is polymer-dependent. For the physical crosslinking, three major strategies are available: gelation induced by high temperature, solvent exchange, or complexation through ionic interactions. On the other hand, chemical crosslinks are reached by adding crosslinking agents or initiating the formation of reactive free radicals. The latter method can be initiated either by chemical initiators or by high-energy irradiation. In the following, a short general summary is given for these methods.

4.1 Physical Gelation

4.1.1 Thermal Gelation

Temperature-induced gelling is a classic method for the preparation of physical hydrogels. In aqueous solution, the polymer chains are surrounded by the water molecules which weaken the polymer–polymer interaction. However, increasing the temperature leads to the gradual dehydration of the chains; thus, the macromolecules can interact again with each other, leading to the aggregation of the polymer chains. This method is very commonly used for polymers containing various hydrophobic groups like alkyl chains due to the increasing hydrophobic interactions at elevated temperatures (Sarkar 1979). The thermal gelation is usually thermoreversible: the physical network gradually falls apart at low temperatures due to the hydration. However, for some polymers like native cellulose the process are irreversible; thus, the cooling has no effect on the gel structure (Cai and Zhang 2006).

The low temperatures also help the strong interaction between the polymer chains. In the freeze-thawing method, the solution is stored in frozen state and then thawed in multiple freezing cycles (Yang et al. 2008). In the frozen solution, multiple phases are present: the frozen solvent, the polymer-rich phase, and the transition between them. The high polymer concentration leads to strong interaction between the chains, aiding the interactions. Moreover, the polymer-rich region is not frozen due to the significantly lower freezing point. The chain mobility in moderately frozen state not only allows the formation of physical networks, but it can even be utilized for chemical crosslinking at low temperatures (Yang et al. 2008).

4.1.2 Coagulation by Solvent Exchange

An interesting method to prepare physical gels is the solvent exchange. After the dissolution a non-solvent is added to the solution—as the ratio of the good solvent decreases, the interaction between the macromolecules increases, ultimately leading

to aggregation and formation of the physical gel. To utilize this method for the hydrogel formation, the polymer must be insoluble in water so they do not dissolve in the aqueous environment. This strategy is mostly used for the cellulose-based gels, where the cellulose is dissolved in various solvents and then water is added to promote the gel formation (Potthast et al. 2002a; Kadokawa et al. 2008; Östlund et al. 2009). However, gelation of the whole system occurs only over a critical polymer concentration: in very dilute solutions only the aggregation and precipitation of the polymer was observed (Ishii et al. 2006). In LiCl/DMAc solutions the ionic strength is also a determining factor in the dissolution of cellulose. Therefore, the deionization of the system also leads to reduced solubility and gelation. The precipitation method is also used in the manufacturing of some regenerated cellulose fibers: after dissolution of cellulose in NMMO/water system, the precipitation is carried out by stepwise addition of water (Loubinox and Chaunis 1987). As this technology shows, the change of the solvent system properties to promote the aggregation does not necessarily need the introduction of another solvent.

4.1.3 Complexation (Ionic Crosslinking)

The ionic interactions can also be exploited for the formation of physical crosslinks. Several polysaccharides have charged pendant groups on the polymer chains, most commonly carboxylic groups. These groups can interact with their counterions and weak ionic bonds are formed between them. However, if multivalent counterions or polymers with oppositely charged groups are present, they can interact with multiple charged pendant groups and form intramolecular and intermolecular bonds (George and Abraham 2006). This method allows a relatively easy gel formation, though the physical network is relatively weak. The ion complexation is the most important gelation method for the alginates, including the industrial production. Alginate gels are formed with the addition of calcium ions through the interaction with the carboxyl groups, leading to a special egg-box structure (Grant et al. 1973). However, not only other divalent cations proved to be efficient crosslinkers (Yang et al. 2013) but also the ion complexes formed with trivalent cations like Al^{3+} led to an even stronger network structure (Rochefort et al. 1986). Moreover, valence is not the singular determining factor as ions with the same valence show different efficiency in the gel formation (Menakbi et al. 2016).

4.2 Chemical Gelation

4.2.1 Chemical Crosslinking with Crosslinking Agents

The most common method for chemical crosslinking is the use of crosslinking agents. These reagents contain groups which can easily react with the pendant functional groups on the polymer backbone. To form crosslinks, the crosslinking

agents need to be at least bifunctional so they can react with at least two pendant groups on different chains. For polysaccharides, usually a large number of reactive hydroxyl groups are present on the polymer backbone; therefore, crosslinkers which easily react with these groups have the largest importance. Reactions involving other common pendant groups like carboxyl groups are also common, but their utility is more limited.

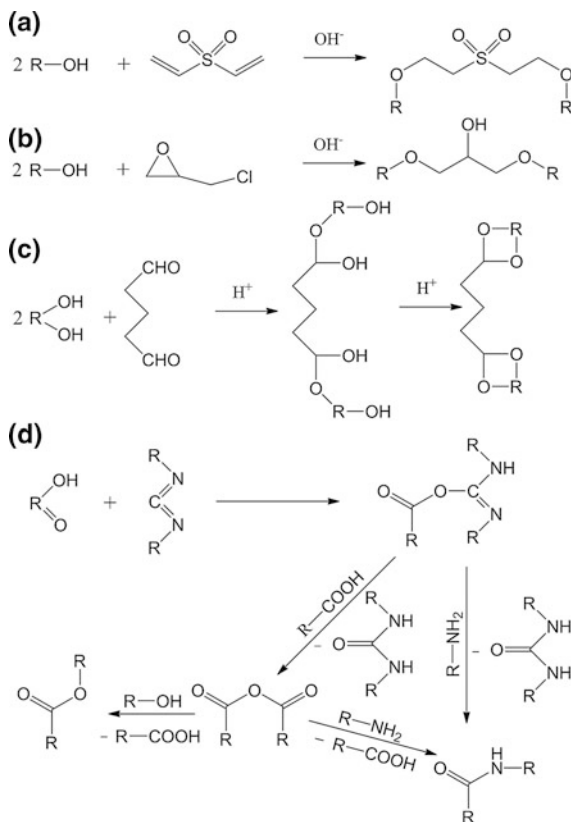
One of the major crosslinking agents is the divinyl sulfone (DVS). The crosslink formation occurs through the reaction of the vinyl and hydroxyl groups (Fig. 2a). However, this requires alkaline pH because the hydroxyl groups are needed to be deprotonated. Therefore, dilute aqueous solutions of potassium hydroxide are used as solvents instead of water to promote the crosslinking (Esposito et al. 1996). The major drawback of the DVS is the high toxicity: while it does not have a harmful effect on the environment after the reaction, the unreacted molecule itself is hazardous. As it has a negative impact on the biocompatibility (Yeom et al. 2010), the unreacted DVS needs to be removed by washing from the gel structure. Recently, new methods for the treatment of the DVS-polluted water were established. UV irradiation in presence of TiO_2 photocatalyst is capable of fully degrading the remains of the crosslinker (Marci et al. 2006). This method allows a more environmentally friendly application of the divinyl sulfone as the wastewater is reusable.

Epichlorohydrin (ECH) is another very significant crosslinking molecule. The reaction is similar to the divinyl sulfone as it needs alkaline environment to catalyze the reaction with the hydroxyl groups (McKelvey et al. 1963) (Fig. 2b). This makes it an excellent reagent for a wide array of polysaccharides. However, similarly to the DVS, its toxicity is a major disadvantage.

Crosslinking with glutaraldehyde and other dialdehydes is also a relatively common method due to their low toxicity. As the aldehyde groups can easily react with amine groups, it is usually used for the crosslinking of various proteins (Hopwood et al. 1970); thus, for the polysaccharides it is relatively rarely used with the exception of the chitosan, as the presence of amine groups makes it a perfect candidate for the reaction. However, the aldehyde groups can also react with the hydroxyl groups, leading to the formation of hemiacetal or even acetal if there is another nearby hydroxyl group (Tomihata and Ikada 1997b) (Fig. 2c). This requires acid component to catalyze the reaction, which is generally achieved with the addition of hydrochloric acid.

Carbodiimides are also primarily used to crosslink various polypeptides. The monomer, depending on the conditions, can easily react with a carboxyl groups and form an unstable intermediate which can then react with an amine (Nakajima and Ikada 1995). Unlike most crosslinking agents, the carbodiimide is a zero-length crosslinker: it only helps the crosslink formation between the two pendant groups, the crosslinking molecule itself is not part of the formed crosslink (Fig. 2d). As various carbodiimides are somewhat toxic, this is a big advantage as the removal of all crosslinkers after the gelation is possible. This makes it more favorable compared to other toxic molecules. They are usually used to crosslink carboxyl and amine groups, which is rarely exploitable for polysaccharides. However, the

Fig. 2 Crosslinking mechanism of divinyl sulfone (a), epichlorohydrin (b), glutaraldehyde (c), and carbodiimide (d)



carbodiimide can also be utilized to crosslink the chains with carboxyl and hydroxyl groups. After the reaction with a carboxyl group, the anhydride formation with another nearby carboxyl substituent is promoted, which is followed by a reaction with a hydroxyl group. This method was successfully applied for multiple polysaccharides, like hyaluronic acid (Tomihata and Ikada 1997a) and carboxymethylcellulose (Sannino et al. 2010).

The largest problem of the major crosslinking agents is their toxicity. Therefore, there is a considerable interest in the use of more environmentally friendly crosslinking agents like various polycarboxylic acids. Under normal conditions, the ester bond formation does not occur between the carboxyl and hydroxyl groups. However, if the polycarboxylic acid is dehydrated, the anhydride formed from two carboxyl groups can easily react with a hydroxyl pendant group (Fig. 3). The formation of anhydride is easily reached by heat treatment as even moderate temperatures (70–80 °C) promote the water loss. After esterification, one carboxyl group is freed up and it can participate in the anhydride formation with another nearby carboxyl group. Therefore, at least three carboxyl groups are required for the crosslinking effect. Due to the relatively low cost, the most important polycarboxylic acid is the citric acid which contains three carboxyl groups (Demetri et al.

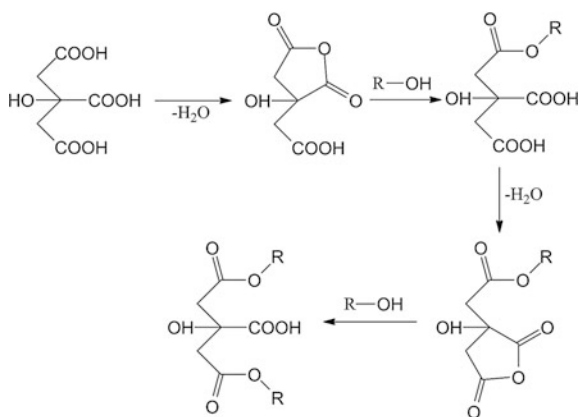
2008; Shi et al. 2008). However, the application of various tetracarboxylic acids was also investigated (Nazari et al. 2009). Usually, low temperatures and long treatment times are used. The latter is due to the water content of the solutions: the presence of the water molecules hinders the anhydride formation. The application of these green crosslinking agents was mostly investigated for the preparation of cellulose derivative gels, and in other areas like for fixation of cellulosic fiber structure in order to get crease resistant textiles.

The number of less common crosslinking agents is large. The crosslinking of *N*, *N'*-methylene-bis-acrylamide occurs through free-radical crosslinking; thus, it will be discussed in the next section. Other crosslinkers are rather specific and are used only for the crosslinking of certain polysaccharides; thus, they are reviewed in Sect. 5 under the subsection of the corresponding polymer.

4.2.2 Free-Radical Crosslinking

The crosslinking reactions can also occur through the highly reactive free radicals. The process requires initiation, which leads to the formation of the radicals. The radicals initiating the process are usually formed either during the degradation of the initiators or directly on the polymer chain by high energy irradiation. The radicals easily react with another macromolecule and the resulting product can also participate in further reactions. The reaction is terminated by the disproportionation or the combination of radicals. However, it is important to note that the radicals can not only initiate the crosslinking, but their reactions may also lead to chain scission, hindering the network formation. The relationship of the two processes heavily depends on various environmental parameters such as the presence of the solvent and the atmosphere, thus conditions favoring the crosslinking should be used. Crosslinking agents are also often introduced even for high energy irradiation to improve the crosslink formation, most common being the *N*, *N'*-methylene-bis-acrylamide.

Fig. 3 Crosslinking mechanism of citric acid



However, other monomers capable of gelation (network formation) such as acrylates are also often used.

The established method for the initiation is the addition of various chemical initiator systems (Ahmed 2015). The most common chemical initiators are the redox systems, most notable being persulfates (especially potassium (KPS) and ammonium (APS) persulfate). These agents are sensitive to the thermal degradation, thus elevated temperatures lead to the formation of radicals (Misra et al. 1984; Bao et al. 2011). The ionic interactions also affect the reaction mechanism as anionic radicals are the products of the degradation process. The macroradicals are formed through proton transfer to the sulfate radicals; the initiation requires acidic environment. Cerium ammonium nitrate is also a common chemical initiator: the Ce^{4+} cation forms a complex with the polysaccharide and the radicals are formed during its reduction to Ce^{3+} (Rahman et al. 2000). Similarly to the persulfate acidic medium is required, which is usually provided by the addition of nitric acid, although high acid concentration has a negative impact on the radical formation (Dhiman et al. 2008). While there are other common redox initiator systems, their importance in the synthesis of polysaccharide hydrogels is very small so far. The method is mainly used to prepare polysaccharide/acrylate copolymer hydrogels as the macroradicals easily react with molecules containing vinyl groups.

The formation of free-radicals can also be initiated by high energy irradiation. In these experiments usually gamma-irradiation or electron beam is used. In the first experiments regarding the irradiation of polysaccharide solutions only the degradation of the polymer was observed. However, Fei et al. (2000) discovered that the crosslink formation process becomes dominant when solutions with very high polymer concentration are irradiated. The macroradicals are formed by the cleavage of various chemical bonds in the structure. While a wide array of macroradicals can form, for the polysaccharides usually the C–H bonds are the most sensitive in the polymer backbone, leading to the highest radical yield. However, the presence of various pendant groups due to the derivatization also affects the process (Wach et al. 2003a, b). The gelation is heavily dependent on the molar properties such as the degree of substitution and the molecular weight. Moreover, besides the absorbed dose the dose rate is also an important factor as higher dose rates lead to better gelation. While the crosslink formation also occurs in air atmosphere, the presence of the oxygen hinders the process (Liu et al. 2002). Thus using vacuum or inert gas atmosphere helps the gelation as the free radicals do not react with oxygen. As solutions are used for the gelation, the solvent–irradiation interaction also affects the process. In aqueous solutions the radiolysis of water occurs, leading to the formation of reactive intermediates. These radicals can also attack the covalent bonds in the polymer (most important being the hydroxyl radicals), leading to the formation of macroradicals (Rosiak and Ulański 1999). The reactivity of these intermediates also shows large differences, the hydroxyl radicals showing significantly higher reactivity; moreover, the solution pH is also an important factor (Ulański and von Sonntag 2000; Wach et al. 2004).

UV irradiation is another possible route for the initiation. However, this method requires the addition of photoinitiators to the solution for the radical formation

(Fouassier and Lalevée 2012). Another common strategy is the functionalization of the polymer with chemical groups sensitive to the irradiation; for this methacrylation is the most popular choice (Smeds and Grinstaff 2001). Due to the smaller energy, UV irradiation allows in situ gelation without harmful effects, thus it is widely used in certain medical applications. However, for gels aimed at other fields the high energy irradiation shows higher potential.

4.3 Formation of Interpenetrating and Semi-interpenetrating Networks

If two or more polymers are present in the solution, different polymer networks can be formed depending on their chemical structure and the crosslinking method. Usually, the two components contain same reactive groups; thus, one crosslinking agent can react with both polymers. This method is the most common as it makes the crosslinking process much simpler. The polymers can also contain different groups which can react with each other, thus making the formation of the copolymer possible.

The two polymers do not need to be necessarily connected with covalent bonds, they can also form an interpenetrating network (IPN) structure (Dragan 2014). In this case, the polymer networks are not chemically crosslinked but their entanglement sterically prevents their separation. Such gels are usually synthesized in two steps where only one polymer is crosslinked in each step. This is most commonly achieved by the addition of two different crosslinking agents. However, as multiple polymers are present, gel can form even if a single component is crosslinked: the three-dimensional network forms the gel matrix, while the intermolecular interactions prevent the not crosslinked polymer component from leaving the gel structure during the swelling. Such structures are called semi-interpenetrating networks (semi-IPN). Similarly to the synthesis of IPN gels, crosslinking agents which react with a single component are needed for their preparation.

5 Polysaccharide-Based Hydrogels

While the aforementioned crosslinking strategies are widely used for polysaccharide systems, the importance of the individual methods shows a large difference depending on the type of the carbohydrate. Moreover, there is a wide array of other crosslinking routes which were only utilized for specific polymers so far, thus were not discussed previously. Therefore, in the following section, studies related to the gelation of different polysaccharide-based systems are reviewed separately, highlighting the specific considerations and unique methods for the various systems.

5.1 *Hydrogels Based on Cellulose and Its Derivatives*

5.1.1 Native Cellulose

Unmodified cellulose as a hydrogel material is widely studied due to its very low cost, but insolubility in water renders it less important than its derivatives. While chemically crosslinked gels were also prepared, the physical gelation has a much bigger role. The physical network is usually achieved by solvent exchange or temperature change. In the former method, water is used to disrupt the solvent–polymer interactions. Potthast et al. (2002a) investigated the behavior of cellulose dissolved in LiCl/DMAc and observed the slow aggregation of cellulose chains due to the hydrogen bonds. However, the presence of water even in very low concentrations led to the formation of larger aggregates. Ishii et al. (2006) prepared physical gels by two methods: coagulation with water and deionization with ion exchange resins. The addition of water led to instantaneous gel formation, while the slower deionization resulted in a more homogenous structure. Similar behavior was observed for tetrabutylammonium fluoride (TBAF)/DMSO solutions: the water disrupted the interaction between the hydroxyl groups of the cellulose and the fluoride; thus, intermolecular hydrogen bonds between the cellulose chains became dominant (Östlund et al. 2009). As very low water concentrations are required for the process, even the storage in humid environment is enough for the gelation of the solution (Patchan et al. 2013). The method is applicable for cellulose dissolved in ionic liquids, as well (Kadokawa et al. 2008).

The gelation can be induced by the change in the temperature, as well. Frey et al. (1996) studied the gelation of cellulose/ammonia/ammonium thiocyanate systems and observed that lower temperatures led to shorter gelling time. There is a much richer literature available about NaOH systems. Opposed to the ammonia/ammonium thiocyanate system, increasing the temperature was beneficial for the self-association of the cellulose in this solvent (Roy et al. 2003). Interestingly, lowering the temperature has a similar effect: Cai and Zhang (2006) studied the behavior of cellulose/NaOH/urea systems at different temperatures and noted that hydrophobic interactions between the cellulose chain become stronger at low temperatures (under 0 °C). LiOH-based systems were also used for the gelation of cellulose with higher molecular weight (Wang et al. 2013d). It is also important to note that unlike the physical gels of methylcellulose, the thermal gelation of the cellulose is an irreversible process under such conditions.

Epichlorohydrin (ECH) is the most common monomer for the chemical crosslinking of cellulose hydrogels. Westman and Lindström (1981) used cellulose xanthan as a precursor: the solution of the derivative was crosslinked with ECH, followed by regeneration with acid hydrolysis. However, recent studies focus on the direct crosslinking of cellulose. The method is similar to the physical gelation: cellulose is dissolved in NaOH/urea, stored in frozen state and after thawing the crosslinking agent is added. The chemical reaction occurs at room or slightly elevated temperature (Zhou et al. 2007). Chang et al. (2010b) also investigated the

effect of the post-treatment of the hydrogels: the samples were frozen or heated for 20 h. The former method resulted in better mechanical properties, while gels treated with the latter one had higher water uptake and better optical properties. There were also considerable efforts toward the copolymerization of cellulose with synthetic polymers. Chang et al. (2008) compared cellulose/PVA hydrogels both chemical gels with epichlorohydrin and physically crosslinked samples: the properties of the latter were inferior compared to the chemical gels. Wu et al. (2012a) used free-radical crosslinking to synthesize cellulose/acrylic acid/acrylamide hydrogels in the presence of MBA crosslinker. In a later work, Chang et al. (2011b) combined the two methods: after the gelation of cellulose with ECH, they prepared poly(*N*-isopropylacrylamide) (PNIPAAm)/cellulose gels by free-radical crosslinking the cellulose gel and the NIPAAm monomers.

5.1.2 Cellulose Derivatives

Unlike for most polysaccharides, the gelation of a wide array of derivatives is investigated for the cellulose. These polymers are cheap and have been used for a long time in the industry; thus, their properties are well known (Pappu et al. 2015, 2016). The literature focuses especially on the carboxymethylcellulose due to its advantageous properties, but other derivatives like the hydroxyalkyl, alkyl, and alkylhydroxyalkyl celluloses are also common subjects of the studies.

Carboxymethylcellulose hydrogels

The carboxymethyl derivatives of cellulose and other polysaccharides are a popular choice for the gel formation due to their excellent swelling properties. This is related to the carboxyl groups which are deprotonated at nonacidic pH: the electrostatic repulsion helps the expansion of the gel network which leads to better swelling (Barbucci et al. 2000). The process is affected by the Donnan effect, as well: the charged carboxyl groups and their counterions result in a high ion concentration in the hydrogel compared to the solvent environment. This leads to an osmotic effect promoting the diffusion of the water into the gel structure. These effects also mean that the carboxymethylcellulose hydrogels are highly sensitive to the environmental conditions, such as the pH and the ionic strength, while having higher water uptake than hydrogels based on alkyl and hydroxyalkyl derivatives of cellulose (Fekete et al. 2014).

Studies related to the physical gelation of carboxymethylcellulose are relatively limited. The easiest route is the complexation with multivalent cations. While the ionic crosslinking was also used for pure carboxymethylcellulose solutions (Saglam et al. 2002), it is much more prevalent in the synthesis of copolymer gels with other natural polymers containing anionic groups, most notably being alginate. For these blends CaCl_2 , the classic crosslinker for alginate-based gels is widely used (Mai et al. 2013; Ren et al. 2016), but exchanging it to the salts of various trivalent ions such as Fe^{3+} and Al^{3+} leads to a stronger structure (Nie et al. 2004; Kim et al. 2012; Swamy and Yun 2015). However, the importance of the complexation is small compared to the chemical crosslinking of the cellulose derivative.

Chemical gelation of carboxymethylcellulose with crosslinking agents is the most established strategy. The classic crosslinkers for the derivative are the epichlorohydrin and the divinyl sulfone. While both reagents are capable of crosslinking pure carboxymethylcellulose solution, the electrostatic repulsion between the chains hinders the crosslinking, leading to the formation of intramolecular crosslinks. However, by introducing a nonionic polymer such as the hydroxyethylcellulose, the intermolecular reactions are easier and the gelation improves significantly (Anbergen and Oppermann 1990; Esposito et al. 1996). In such systems, not only the interaction between the carboxyl groups is weaker, but also the nonionic polymer is not affected by the charged groups; thus, it easily participates in the crosslinking process.

In recent studies, the interest is shifted toward the more environmentally friendly crosslinking agents. The polycarboxylic acids are major contenders in this field. Besides the low toxicity, mild synthesis conditions are sufficient and some of these reagents are relatively cheap. The first experiments involved the application of citric acid as crosslinking agent (Demitri et al. 2008), but recently other polycarboxylic acids like succinic acid, maleic acid (Hashem et al. 2013), and 1,2,3,4-butanetetracarboxylic acid (Nazari et al. 2009) were also used for the crosslinking. Fumaric acid is also viable reagent; however, unlike other polycarboxylic acids, it requires highly acidic environment (Akar et al. 2012). The crosslinking is initiated by a mild heat treatment at 70–80 °C. Similarly to the toxic crosslinkers, the presence of nonionic cellulose derivatives improves the crosslink formation. The gel properties can be changed by implementing post-treatment after the crosslinking: Hashem et al. (2013) improved the gelation by a second short, high-temperature curing step after mild heating. Besides carboxylic acids, carbodiimide was also successfully utilized as a green crosslinker due to the zero-length linkages (Sannino et al. 2010). The reaction requires acidic initiation, which was provided by dilute citric acid solution.

Free-radical chemical crosslinking is also a common way for the preparation of carboxymethylcellulose gels. Generally, ammonium persulfate is used as a chemical initiator in the presence of *N,N'*-methylene-bis-acrylamide (MBA) crosslinking agent. However, chemical initiation is mostly used for the synthesis of copolymer gels with synthetic polymers. For pure carboxymethylcellulose solutions, the initiation by high-energy irradiation is the preferred method.

High-energy irradiation is an excellent way to prepare chemically crosslinked carboxymethylcellulose gels without any additives. While pure carboxymethyl hydrogels are synthesized from aqueous solutions, for the synthesis of copolymer gels other solvents are also used if the other polymer is insoluble in water (Tang et al. 2014). The crosslink formation requires relatively high solute concentrations as in dilute solutions the degradation processes dominate due to the hindering effect of the electrostatic repulsion (Fei et al. 2000). The critical concentration also depends on several factors such as the degree of substitution. Moreover, recently Wach et al. (2014) also successfully prepared hydrogels with dilute solutions. The native pH of the CMC-Na solution is slightly alkaline; thus, the carboxyl groups are deprotonated and the electrostatic repulsion between them hinders the crosslink

formation. Shifting the pH toward acidic character led to the protonation of the carboxyl groups and the lack of interaction between them promoted the gelation. Several other factors such as the storage time before the irradiation (Wach et al. 2000) also affected the gel fraction. Liu et al. (2002) observed that not only the lack of oxygen leads to better gelation, but the type of the inert atmosphere also has an impact on the process. The radiation-initiated crosslinking can be further improved by adding crosslinking agents in low concentrations. While they are used mostly for the synthesis of copolymer gels, they can also improve the gelation of pure cellulose derivative solutions (Fekete et al. 2016a). In their presence, the crosslinking requires significantly milder conditions and better gel properties can be achieved than for the crosslinker-free hydrogels.

Methylcellulose hydrogels

The most important representative of the alkylcelluloses is the methylcellulose. It is a major additive in the food industry, where its thermogelling behavior is also utilized to affect the baking of pastes (Sanz et al. 2004). The gelation mechanism of the methylcellulose is explained with the interaction of the hydrophobic methyl substituents (Sarkar 1979). At low temperatures, the hydrophobic interactions are hindered by the hydration of the polymer chains; however, increasing the temperature leads to lower hydration, thus the interactions between the methyl groups are less obstructed. Haque and Morris (1993) attributed the gelation also to the changes in the solution structure. During the derivatization of the cellulose, the crystalline structure is not completely destroyed; thus, small aggregates are present in the methylcellulose solution. However, at high temperatures, the aggregates are partly broken up and the free ends of the polymer chains forming the aggregates also become more mobile. The degree of substitution and the distribution of the substituents also affect the gelling behavior. Higher degree of substitution leads to lower gel temperature due to the higher number of hydrophobic groups. This also explains the importance of the distribution of the substituents: the regions with higher degree of substitution play a larger role in the gelation than other regions (Desbrières et al. 1998). High molecular weight is also beneficial for the process, leading to a shift toward lower gelation temperatures (Takahashi et al. 2001). The required temperature can also be altered by chemical modification: Liu et al. (2004) prepared *N*-isopropylacrylamide/methylcellulose copolymers, where the ratio of the two components determined the gelation temperature.

The chemical gelation of methylcellulose holds a relatively small significance due to the importance of the thermal gelation. Chemically crosslinked hydrogels of methylcellulose were prepared through free-radical crosslinking: Wach et al. (2003a) crosslinked concentrated methylcellulose solutions by high-energy irradiation. They found electron beam significantly more efficient than gamma irradiation, leading to higher gelation. Methylcellulose gels showed good swelling properties but were inferior to hydroxyethylcellulose-based hydrogels due to the hydrophobic pendant groups. Photoinitiated crosslinking also proved to be a viable route, but in this case, acrylate was also present in the system besides the photoinitiator. Aouada et al. (2009) synthesized methylcellulose/polyacrylamide copolymer gels in presence of

MBA crosslinking agent. The application of previously modified methylcellulose was also investigated: Stalling et al. (2009) used methacrylated methylcellulose for photoinitiated gelation. The modified cellulose derivative was prepared by reaction of the polymer with methacrylic acid anhydride. Rimdusit et al. (2012) also compared high-energy irradiation and crosslinking with glutaraldehyde: while the presence of the crosslinking agent also led to gelation, the properties proved to be inferior compared to the irradiation-crosslinked gels.

Hydroxyalkylcellulose-based hydrogels

Hydroxyethylcellulose and hydroxypropylcellulose are the hydroxyalkylcellulose with the largest industrial application; thus, unsurprisingly studies of gelation are also limited to these two derivatives. While there are more studies related to the synthesis of chemical gels, their thermal behavior was also examined (Klug 1971). Heating the aqueous solutions of hydroxyalkylcelluloses promotes the aggregation through the hydrophobic interactions. However, unlike the methylcellulose, this process leads to precipitation due to the phase separation instead of gel formation.

The chemical crosslinking of hydroxyalkylcelluloses is usually achieved by divinyl sulfone crosslinker. Chemical gels of hydroxyethylcellulose were mostly prepared in the presence of another polymer component. In copolymer hydrogels with carboxymethylcellulose, the role of the HEC was to promote the intermolecular crosslinking (Anbergen and Oppermann 1990). A similar method was used for the synthesis of copolymers with hyaluronic acid (Kwon et al. 2015) and gelatin (Kajjari et al. 2011); in the latter case, glutaraldehyde was utilized instead of divinyl sulfone. On the other hand, hydroxypropylcellulose gels were also prepared without the addition of a second polymer. Besides DVS, other crosslinkers like epichlorohydrin were also used (Yan et al. 2009). Another strategy for the synthesis of hydrogel nanoparticles is the temperature-induced aggregation: increasing the temperature led to the formation of small aggregates, where the polymer chains can be crosslinked chemically in a second step (Gao et al. 2001). However, the phase transition does not necessarily need the change of the temperature: by introducing surfactant (Lu et al. 2000) or electrolyte (Xia et al. 2003) into the cellulose derivative system the water-polymer interactions become weaker and aggregation occurs at lower temperature.

Free-radical crosslinking is usually initiated by UV irradiation. First studies involved the synthesis of hydroxypropylcellulose hydrogels either after chemical modification (Marsano et al. 2000) or in the presence of a synthetic polymer (Marsano and Bianchi 2002). Later the focus is shifted toward the pure cellulose derivative systems. Petrov et al. (2006) investigated the cryotropic gelation of hydroxypropylcellulose. Aqueous solutions of the polymer and the photoinitiator were frozen which led to phase separation. The formation of the frozen solvent fraction leads to high polymer concentration in the other phase; thus, the crosslinking processes of the free radicals become dominant opposed to the degradation. This made possible the gelation even in semi-dilute solutions. In a later study, the method was successfully utilized for the gelation of hydroxyethylcellulose, as well (Petrov et al. 2007). Moreover, they observed that the radical formation also occurs in the presence of hydrogen peroxide (a common chemical

redox initiator with Fe^{2+}). This allowed the substitution of the (4-benzoylbenzyl) trimethylammonium chloride photoinitiator with a more environmentally friendly additive.

High-energy irradiation was used for initiation to a lesser extent. Both hydroxyalkylcelluloses formed gels when their concentrated solutions were irradiated (Wach et al. a, b). The dependence of the properties on the synthesis parameters was similar to the carboxymethylcellulose systems. Moreover, the introduction of low concentrations of MBA crosslinker had a positive impact on the gel formation (Fekete et al. 2016a).

Alkylhydroxyalkylcellulose-based hydrogels

The gelation of alkylhydroxyalkylcelluloses was investigated only for two representatives: the hydroxypropylmethylcellulose and the ethylhydroxyethylcellulose. Similarly to the methylcellulose, the physical crosslinking by heat treatment shows a large importance due to the industrial applications. However, the hydrogel synthesis of the two derivatives was investigated at somewhat different conditions. For the hydroxypropylmethylcellulose, the thermal gelation is very similar to the behavior of the methylcellulose due to the methyl substituents in both derivatives (Sarkar 1979). On the other hand, the presence of the hydroxypropyl groups hinders the gelation process, leading to higher gelation temperature. This is attributed to two effects: the hydroxypropyl groups are less hydrophobic than the methyl groups and the larger substituents also sterically interfere with the formation of the hydrophobic ordered structures (Haque et al. 1993).

The thermal behavior of the ethylhydroxyethylcellulose is quite different. Its aqueous solution shows a decrease in the viscosity with the temperature. Above the cloud point phase, separation occurs, leading to even lower viscosity. However, the presence of ionic surfactants significantly alters this process: the hydrophobic polymer–surfactant interactions promote the formation of the polymer–polymer interactions, leading to the formation of physical gels (Carlsson et al. 1990). The effect also heavily depends on the type of the surfactant as depending on the chemical structure it interacts differently with the polymer chains (Nyström and Lindman 1995; Wang and Olofsson 1995).

Pure cellulose derivative chemical gels were only prepared from hydroxypropylmethylcellulose. Pekel et al. (2004) used gamma irradiation to crosslink HPMC solution. The swelling of the gels was sensitive to the pH and the temperature. The sensitivity was further improved by introducing phthalate groups into the polymer structure (Xu et al. 2002b). However, the phthalate derivative has low solubility in water; thus, it requires the addition of Na_2CO_3 for full dissolution.

5.2 Hydrogels Based on Starch and Its Derivatives

The application of starch as a hydrogel material is less widely studied than the other major polysaccharides. Moreover, studies focus on the use of starch as a copolymer

instead of the preparation of pure starch hydrogels. Usually, various reactive monomers like acrylic acid or acrylamide are added to starch (Kiatkamjornwong et al. 2000), but polyvinyl alcohol and other synthetic polymers with relatively low molecular weight are also used (Pal et al. 2006). The dispersion of the other components is achieved through the pregelatinization of the aqueous dispersion of starch, which results in a highly viscous solution due to the improved swelling of the granules. The gelation occurs through free-radical crosslinking; both chemical initiator systems like potassium persulfate/KOH (Xiao and Yang 2006) and high-energy irradiation (Zhai et al. 2002) are widely used for the initiation. The process can be further improved by introducing other crosslinking agents, *N,N'*-methylene-bis-acrylamide being the most common choice. While the crosslinking through free radicals is by far the most important method, there were efforts to crosslink starch systems through chemical reactions, as well. The gel properties are not only determined by the synthesis parameters, but the properties of the starch also play a major role. The starch source not only affects the amylose/amylopectin ratio but also the concentration of other minor components, like the lipids; the amylose/amylopectin ratio is an especially important factor during the crosslinking process. Zhai et al. (2002) prepared PVA copolymer gels with pure amylose and amylopectin besides cornstarch. Amylose-based systems showed significantly better properties as the polyvinyl-alcohol reacted more easily with the amylose than the amylopectin. Pal et al. (2006) synthesized starch/poly(vinyl alcohol) crosslinking copolymer hydrogel membranes with glutaraldehyde as a crosslinker.

Carboxymethylation of starch offers a different route to the gelation due to the water solubility. Nagasawa et al. (2004) synthesized superabsorbent gels from aqueous solutions of carboxymethylstarch. Similarly to the water-soluble derivatives of cellulose, the gelation improved significantly with the increasing solute concentration, but led to worse swelling properties. Separate study of carboxymethylated amylose and amylopectin proved that the amylopectin ratio was a determining factor in gel formation of the derivatives, but the tendency is reversed compared to the non-modified starch described earlier: in the presence of PVA, the branched amylopectin gelled even at relatively low solute concentrations, while the amylose showed gelling behavior only at 50 wt% concentration.

5.3 Hydrogels Based on Chitin and Its Derivatives

5.3.1 Chitin

Precipitation is a common method for the preparation of chitin hydrogels due to the water insolubility of the polymer: chitin is dissolved by one of its solvents and the solution is slowly added to a water bath. The dissolution is usually achieved by CaCl_2 /methanol solvent system (Tamura et al. 2006; Nagahama et al. 2008), but in some experiments hydrogels were prepared from chitin dissolved in NaOH/urea by freeze-drying (Chang et al. 2011a) and in DMA/LiCl systems (Tsiptsias and

Panayiotou 2008), as well. There is also a large interest regarding the composites from physically crosslinked chitin gels, where the nanoparticles are incorporated into the gel structure after the precipitation. As the application of chitin-based physical gels is centered on the medical field, achieving antibacterial activity by silver (Madhumathi et al. 2010) or metal oxide (Kumar et al. 2013) particles is widely studied.

Multiple crosslinking strategies were examined for the preparation of chemically crosslinked networks. Tang et al. (2012) crosslinked dissolved chitosan with epichlorohydrin through the hydroxyl groups. NaOH/urea was used as solvent which also provided the alkaline environment required for the reaction. Epichlorohydrin was also utilized for the preparation of chitin-based copolymer gel with carboxymethylcellulose (Tang et al. 2014) and composite with hydroxyapatite (Chang et al. 2013).

Crosslinking with the more environmentally friendly polycarboxylic acids was also studied. Yoshimura et al. (2005) used succinic anhydride to crosslink chitosan solution: the acid anhydride reacted with the hydroxyl groups of the chitin. Moreover, the free carboxyl group formed after the reaction could also react with another hydroxyl group. The solvent present during the crosslinking had a major effect on the gelation: in DMSO/TBAF solutions, the chemical crosslinks easily formed, while in LiCl/*N*-methyl-2-pyrrolidone (NMP) solutions, the second reaction was inhibited; thus, minimal gelation was observed. Opposed to the polycarboxylic acids, the use of anhydride and the lack of water allowed bypassing the heat treatment. Kono and Zakimi (2013) synthesized gels with the dianhydride of butanetetracarboxylic acid from blends of chitin and cellulose in LiCl/NMP. The two anhydride groups allowed the formation of crosslinks despite the free carboxyl groups not participating in the crosslinking. However, the presence of non-reacted carboxyl groups led to responsive behavior: unlike the native polymers, the copolymer exhibited sensitivity to the pH of the environment.

5.3.2 Chitosan

Chitosan-based physical gels are prepared either by various additives which interact with the chitosan chains or by chemical modification. In the latter case, new functional groups are introduced into the polymer structure by grafting; thus, the gel formation can occur through new mechanisms. Qu et al. (1999) prepared lactic acid modified chitosan through heat treatment. The lactic acid reacted with the amine group, which was followed by polyesterification. The formation of the physical gel was attributed to the hydrophobic interactions between the substituents and the hydrogen bonds. By introducing hydrophobic groups thermoreversible gelling can be also achieved: grafting chitosan with poly(ethylene glycol) led to a water-soluble chitosan derivative, but at higher temperature, the stronger hydrophobic interactions resulted in physical gelation (Bhattarai et al. 2005). Freeze-thawing is also a possible method for gelation: Yang et al. (2008) prepared PVA/chitosan solution by multiple freeze-thaw cycles at $-20\text{ }^{\circ}\text{C}$.

The second strategy for the physical gelation is the introduction of various additives to the chitosan solution. These can also induce the thermal gelation of the solution through hydrophobic interactions. Such behavior was observed in the presence of polyols. Chenite et al. (2001) used β -glycerophosphate disodium salt to neutralize the chitosan solution, leading to thermogelating systems at body temperature. Other polyols exhibited similar effect on the chitosan systems (Schuetz et al. 2008). Chitosan gels grafted with monomers of thermosensitive polymers like *N*-isopropylacrylamide exhibited similar behavior (Chen and Cheng 2006). The gelation is often achieved through ionic interactions, as well. This requires the presence of polymers with negative charges which can interact with amine groups in the chitosan backbone. As anionic polymers are relatively common in the nature, most studies focus on the application of various natural polymers for the synthesis as a cheap, green alternative to synthetic polymers (Berger et al. 2004). While polymers with carboxyl groups are the most common choice, the addition of polysaccharides containing sulfate or phosphate groups is also a viable route.

Glutaraldehyde is a common chemical crosslinker for chitosan as the aldehyde groups easily react with the amines (Mirzaei et al. 2013). However, the crosslink formation can be initiated by a single aldehyde group, as well. Singh et al. (2006a) utilized formaldehyde to gelate chitosan solution at acidic pH. The reaction of the formaldehyde and the amine pedant group resulted in the formation of imine which in acidic environment can react with a second amine, thus forming a crosslink. A more environmental friendly alternative is the genipin due to its low toxicity, which is isolated from gardenia fruits. The molecule with a carboxyl and two hydroxyl groups does not only react with the amine groups to form crosslinks, but its homopolymerization is also observed (Mi et al. 2000). The pH has a major effect on the reaction. Alkaline environment promotes the formation of homopolymer chains; thus, long crosslinks are formed between the chitosan macromolecules. On the other hand, in acidic environment, the crosslinks are short (dimers, trimers, and tetramers of genipin), and the more compact gel structure leads to worse swelling properties (Mi et al. 2005).

Free-radical crosslinking is usually initiated by UV irradiation. Ono et al. (1999) prepared water-soluble photocrosslinkable chitosan by reacting chitosan with azide (p-azidobenzoic acid) and lactose (lactobionic acid). The introduction of lactose groups improved the solubility in water; thus, aqueous solutions formed even at neutral pH. On the other hand, the azide group is sensitive to the UV irradiation, leading to the formation of reactive nitrene group which reacts with another nitrene or a free amine group to form azo crosslinks.

Vinyl groups are also commonly introduced for easier crosslink formation. Hong et al. (2006) achieved this by grafting methacrylic acid on chitosan, while grafted lactic acid provided the water solubility. The crosslinking reaction was initiated via ammonium persulfate and *N,N,N',N'*-tetramethylethylenediamine redox system. Due to the fast gelation at body temperature, these gels show large potential as injectable hydrogels.

High-energy irradiation also proved to be suitable for the gelation of chitosan. Yang et al. (2008) synthesized chitosan/poly(vinyl alcohol) gels by gamma

irradiation. While the gels showed high water uptake, the mechanical properties were poor. However, irradiated samples treated with freeze-thawing had higher mechanical strength.

5.3.3 Derivatives of Chitin and Chitosan

Hydrogels based on water-soluble derivatives of chitin have a relatively small literature. Zhao et al. (2001) modified chitin by carboxylation: the carboxymethylated derivative was water soluble and was crosslinked with chitosan in aqueous solution with glutaraldehyde. The formed copolymer had better properties than the gels synthesized from either derivative. Zhao et al. (2003a, b) also prepared hydrogels from carboxymethylated derivatives of chitin and chitosan by high-energy irradiation. Similarly to the cellulose derivatives, by irradiating high concentrated solutions no additives were required for the gelation. Gels of both derivatives had good swelling properties and carboxymethylchitosan gels also exhibited antibacterial activity.

Similarly to the chitin, carboxymethylated of chitosan is the only chitosan derivative for which the hydrogel formation was studied. Pure carboxymethylchitosan hydrogels were prepared from aqueous solutions with glutaraldehyde by Zamani et al. (2010). The drying method after the crosslinking was also a determining factor for the swelling behavior: freeze-drying and foaming with pentane resulted in porous gels with very high water uptake compared to oven-drying. Bidgoli et al. (2010) also investigated the effect of the carboxymethylation: the water uptake improved with the concentration of the carboxyl groups; thus, higher degree of substitution was favorable for the synthesis of superabsorbents. Carboxymethylchitosan-based copolymer gels were also investigated: besides the copolymers formed with chitin discussed previously (Zhao et al. 2003a), gelatin was also used to prepare green hydrogels. The solution of the two polymers was crosslinked by gamma irradiation; thus, no additives were needed (Yang et al. 2010).

5.4 Hydrogels Based on Alginate

The crosslinking of alginate systems has a wide literature, the most important gelation method being the complex formation with multivalent ions. The application of divalent cations was extensively studied, from which the calcium cation has the largest significance. The interaction between the Ca^{2+} and the alginate chains leads to the formation of an egg-box structure, where the cations are surrounded by the polymer layers (Grant et al. 1973). The calcium complexes are still held a large importance due to the easily achieved gelation and are widely used especially in medical fields. The calcium source has a major effect on the gelation. Usually, CaCl_2 is used due to its good water solubility and fast crosslink formation. While

short gelation times are preferred in the practice, too fast gelation can lead to an inhomogeneous structure. Calcium salts with low solubility like CaCO_3 allow an even distribution of the cations at the expense of slower gelation, leading to homogeneous gel (Kuo and Ma 2001). A major disadvantage of the Ca-alginate gels is the low stability which leads to cation release during application (Ng and Cheng 2007); thus, the applicability of other divalent ions like Fe^{2+} (Kroll et al. 1996), Sr^{2+} , Ba^{2+} , and Zn^{2+} (Yang et al. 2013; Harper et al. 2014) was also investigated: the cation type had a significant effect on the gel properties. Interestingly, while Mg^{2+} is often considered as a non-gelling cation, in very high ion concentrations (5–10 times higher than for Ca^{2+}) in fact it is capable of crosslinking the alginate; however, the gelation is very slow compared to other multivalent cations (Topuz et al. 2012). Trivalent ions also show a large potential as they can interact stronger with the alginate, leading to faster gelation and a more stable structure. Rochefort et al. (1986) investigated the effect of the treatment of weakly crosslinked Ca-alginate with $\text{Al}(\text{NO}_3)_3$ solution. The presence of the Al^{3+} ions led to a significant improvement in the gelation. Al-alginate complexes can also form without a pre-crosslinking step with calcium ions. Banerjee et al. (2013) prepared alginate/methylcellulose hydrogels where the Al-complex provided the gel structure. Depending on the other components in copolymer systems, the cations can also interact with the other polymer: in alginate/carboxymethylxanthan systems, the cations interacted with both polymers due to the carboxyl groups (Ray et al. 2011). Menakbi et al. (2016) also investigated the complexation of several trivalent cations like Sc^{3+} , Cr^{3+} , and La^{3+} . The binding strength depended on the cation, but in all cases, it was stronger than for the divalent cations.

While the ionic crosslinking with multivalent cations is a simple method, it also has disadvantages like the sensitivity to the presence of non-crosslinking ions. Therefore, other possible crosslinking paths were also investigated. Physical crosslinking can be achieved alternatively by modifying the chemical structure of the alginate so new interactions appear between the chains. Boisseson et al. (2004) introduced long alkyl chains through substitution: the hydrophobic interaction between the alkyl chains resulted in a gel stable in the presence of ions, although complexing multivalent cations further improved the stability of the network structure.

Alginate gels crosslinked with covalent bonds were also prepared both by chemical crosslinking agents and free-radical crosslinking. In the former case, both the hydroxyl and carboxyl groups can participate in the crosslink formation depending on the crosslinking agent. Crosslinkers containing amine groups can easily react with the carboxyl groups. Moreover, derivatives of hydrophilic polymers like poly(ethylene glycol) used as crosslinking agents also improve the swelling of the gels (Lee et al. 2000a). On the other hand, glutaraldehyde crosslinks alginate by reacting with the hydroxyl groups in acidic environment (Kulkarni et al. 2000). Kim et al. (2000b) also used this agent to synthesize alginate-based gel fibers. Water-soluble carbodiimides as zero-length crosslinking agents were used to form crosslinks between the hydroxyl and carboxyl groups of the alginate (Xu et al. 2002a).

Free-radical crosslinking is also a viable strategy for the gel formation. It is mostly used for the preparation of alginate-based composite or copolymer gels. Chemical initiation is generally used for the radical formation: ammonium persulfate is added as initiator, while MBA monomer participates in the crosslinking. Copolymer gels with other polymers like carboxymethylcellulose (Pourjavadi et al. 2006) were also prepared, but most studies focus on the synthesis of alginate/clay composites (Yadav and Rhee 2012). For photoinitiated crosslinking only the gelation of methacrylated alginate was studied (Jeon et al. 2009; Smeds and Grinstaff 2001). While radiation-initiated crosslinking was also used for the synthesis of alginate/methacrylate copolymer gels (Bardajee et al. 2012), currently its significance is still very small.

5.5 Hydrogels Based on Hyaluronic Acid

Studies focus solely on the chemical gelation of the hyaluronic acid. The crosslinking routes are somewhat different than for the other polysaccharides: hyaluronic acid is usually chemically modified by the introduction of new pendant groups before the gelation. However, the gelation of unmodified hyaluronic acid was also studied to a smaller extent. First experiments involved crosslinking with glutaraldehyde (Tomihata and Ikada 1997b); the removal of solvent by freeze-drying led to a porous chemical gel structure (Collins and Birkinshaw 2011). Divinyl sulfone is another classic crosslinker which was first utilized for the preparation of cellulose derivative/hyaluronic acid hydrogels (Sannino et al. 2004). However, later the focus is shifted to the crosslinking of pure hyaluronic acid systems. Collins and Birkinshaw (2008) compared the gelation by DVS, glutaraldehyde, and freeze-thawing. Covalently crosslinked systems showed better mechanical properties than the physical gels; moreover, the crosslinking efficiency of the two molecules also differed as the addition of glutaraldehyde led to higher crosslink density. It is also important to note that high DVS concentration has a negative impact on the cytocompatibility, which is a crucial factor for medical applications (Lai 2014). Ibrahim et al. (2010) also observed that the modification of gel properties is possible through addition of hyaluronic acid oligomers. Carbodiimides also play an important role in the synthesis of hyaluronic acid gels: during the chemical modification of the carboxyl groups, the introduction of the new functional groups is often carried out with its utilization due to the zero-length crosslinking. However, the direct crosslinking of the polysaccharide is also feasible with crosslinking agents containing multiple amine groups: Jeon et al. (2007) used this method to prepare hyaluronic acid/polyethylene-glycol copolymer gels by crosslinking hyaluronan with the diamine derivative of PEG. Carbodiimide crosslinker was also utilized for the crosslinking of pure hyaluronan through esterification (Tomihata and Ikada 1997a).

As discussed above, there is an even larger interest toward the use of chemically modified hyaluronic acids. These newly introduced functional groups are not only

the participants of the crosslinking process but also affect the gel properties. Even the formation of autocrosslinkable hyaluronic acid gels is possible, where the presence of air is adequate to initiate the gelation: through the oxidation of thiol groups by the oxygen disulfide crosslinks form between the macromolecules (Shu et al. 2002). The rate of the crosslink formation can be increased by the addition of crosslinkers which easily react with thiols such as the α,β -unsaturated esters and amides of poly(ethylene glycol) (Shu et al. 2004). A large variety of substituents were investigated, typically molecules containing hydrazide, thiol, or aldehyde groups (Burdick and Prestwich 2011). Acryloyl groups are especially popular as they are not only capable to react with certain groups like thiols (Hahn et al. 2006) but also allow the free-radical crosslinking of the polymer. Most commonly methacrylate groups are introduced through the functionalization with glycidyl methacrylate (Leach et al. 2003) or methacrylic anhydride (Burdick et al. 2005), but other acrylates are also often utilized (Sahoo et al. 2008). The formation of free radicals is usually initiated by UV irradiation in the presence of photoinitiators; the application of redox initiators is rarely used. The degree of substitution has a major impact on the gel properties: Bencherif et al. (2008) noted that the crosslink density increased with the degree of methacrylation, leading to better mechanical properties at the expense of lower water uptake. To promote the crosslink formation, co-monomers such as *N*-vinyl-2-pyrrolidone (NVP) are also sometimes added to the functionalized hyaluronic acid (Patterson et al. 2010).

5.6 Hydrogels Based on Other Polysaccharides

While gelation of the aforementioned polysaccharides is in the center of interest, studies do not focus solely on them. However, while other polysaccharides are widely used in industrial applications as additives, their importance in the gel preparation is so far much smaller than for the above-mentioned, more common polysaccharides. Therefore, only a short overview is given on them.

5.6.1 Dextran

Dextran is a group of water-soluble polysaccharides consisting of a backbone of D-glucose groups with $\alpha(1 \rightarrow 6)$ and/or $\alpha(1 \rightarrow 3)$ linkages, with branches in different positions; they are produced from glucose by bacterial fermentation. Chemical gels from unmodified dextran were prepared with various crosslinkers such as diisocyanates (Hovgaard and Brønsted 1995) or sodium trimetaphosphate (Wintgens et al. 2015); moreover, even enzymatic crosslinking with divinyl adipate crosslinker was achieved (Ferreira et al. 2005). However, the polysaccharide is also very often functionalized. After carboxymethylation, the chemical gelation of the derivative can be carried out with carbodiimides, thus forming zero-length crosslinks (Zhang et al. 2005c). Its dialdehyde derivative is applicable for

copolymerization with polymers containing amine groups like gelatin (Draye et al. 1998) or chitosan (Gómez-Mascaraque et al. 2014); the synthesis of pure dextran hydrogels is also possible with adipic acid dihydrazide modification (Maia et al. 2005). Methacrylated dextran is easily crosslinked in presence of chemical initiator through free-radical crosslinking (van Dijk-Wolthuis et al. 1997). Moreover, the acrylated (Kim et al. 1999) and methacrylated (Kim and Chu 2000) derivatives are used for the formation of photocrosslinkable hydrogels.

5.6.2 Agarose

Agarose is a linear polysaccharide extracted from seaweeds consisting of alternating D-galactose and 3,6-anhydro-L-galactose units with $\alpha(1 \rightarrow 3)$ and $\beta(1 \rightarrow 4)$ linkages. While it is not water soluble at room temperature, it readily dissolves in hot water. Cooling its solution leads to thermoreversible gel formation. Most studies involving such systems focused on its application for the controlled release of various bioactive molecules (Wang and Wu 1997; Meilander et al. 2003; Liu and Li 2005; Liang et al. 2006), incorporation of nanoparticles (Luo et al. 2016; Wang et al. 2016) and gel electrophoresis (Serwer 1983). Chemical gels with citric acid (Awadhiya et al. 2016) and epichlorohydrin (Zhang et al. 2012) were also prepared, but their importance is much smaller compared to the more convenient thermal gelation.

5.6.3 Xanthan

Xanthan is a water-soluble heteropolysaccharide with a $\beta(1 \rightarrow 4)$ linked D-glucose backbone and side chains consisting of D-glucuronic acid and D-mannose containing acetyl and pyruvate groups; it is produced from carbohydrates by bacterial fermentation. Despite its good water solubility, physical gels can be prepared by annealing (change in the ordered structure) at high temperature and subsequent cooling its aqueous solution (Quinn et al. 1994). The presence of charged groups allows the ionic crosslinking of the polymers with multivalent cations (Izawa et al. 2009) or cationic polymers like chitosan (Dumitriu et al. 1994; Chellat et al. 2000). Chemical crosslinking is also viable with molecules containing amine groups in the presence of carbodiimide (Bejenariu et al. 2008). For the chemical crosslinking of xanthan solution, a number of crosslinking agents are applicable, such as epichlorohydrin (Alupej et al. 2002), citric acid (Bueno et al. 2013), and trisodium trimetaphosphate (Bejenariu et al. 2009). There is also a large interest toward free-radical copolymerization with various acrylates and methacrylates (Gils et al. 2009; Kulkarni and Sa 2009a; Mittal et al. 2014).

5.6.4 Chondroitin Sulfate

Chondroitin sulfate is a linear polymer with alternating D-glucuronic acid and N-acetyl-D-galactosamine units with sulfate residues; it is extracted from cartilage

of various animals. Due to its water solubility, mainly the chemical gelation was investigated. While pure chondroitin sulfate gels can be prepared with crosslinkers like ethylene glycol diglycidyl ether (Jensen et al. 2002), most studies focus on the synthesis of copolymer hydrogels with various natural and synthetic polymers. The chondroitin sulfate functionalization with *N*-hydroxysuccinimide (Strehin et al. 2010), adipic acid dihydrazide (Gilbert et al. 2004; Zhang et al. 2011b), methacrylates (Bryant et al. 2004; Li et al. 2004), or through oxidation (Dawlee et al. 2005) is carried out for the covalent crosslinking with the other polymer component even for systems capable of forming ionic complexes like chondroitin sulfate/gelatin solutions (Kuijpers et al. 2000). The copolymerization can also occur without functionalization with appropriate crosslinkers like epichlorohydrin (Oprea et al. (2012).

5.6.5 Other Polysaccharides

A wide array of other polysaccharides like the guar gum (Das et al. 2006), tara gum (Huang et al. 2007, Abd Alla et al. 2012), tragacanth gum (Singh and Sharma 2014), carrageenan (Xu et al. 2003), lignin (Thakur and Thakur 2015), pectin (Sutar et al. 2008), hemicellulose (Gabrieli and Gatenholm 1998), and psyllium polysaccharide (Thakur and Thakur 2014) were also investigated to a lesser extent for the hydrogel formation. Sometimes their pure solution is also used for gel formation (especially for thermogelling polymers), but usually, they are added as a natural component for the copolymerization with synthetic polymers, although rarely they are also mixed with natural polymers to modify their properties.

6 Copolymer and Composite Hydrogels

The modification of hydrogels by introducing another component is very common; mixing polysaccharides and synthetic polymers has a large literature due to their importance in the practical use. However, there is also a major interest in the blends and copolymers with other natural polymers to keep them more environmentally friendly. Another interesting strategy is the incorporation of inorganic components in the gel network, either to reduce the costs or achieve novel properties. In the following, these three types of modifications are in-depth reviewed.

6.1 Blends and Copolymers with Other Natural Polymers

A green route to modify the properties of the polysaccharide hydrogels is the introduction of other natural polymers instead of synthetic ones. This allows achieving novel properties without the application of nonrenewable materials.

A large part of such studies focuses on the blends and copolymers of different polysaccharides due to the similarities in the chemical structure. However, the modification with other major natural polymers used for hydrogel synthesis such as collagen also plays an important role.

6.1.1 Hydrogels Based on Multiple Polysaccharides

The introduction of another polysaccharide can serve multiple purposes. The preparation of blends allows the modification of the hydrogel properties without the introduction of additives or synthetic components; thus, the hydrogels keep the advantageous properties of polysaccharides, such as the good biocompatibility, biodegradability, and the sole use of renewable materials. While similarities such as the presence of hydroxyl groups offer a convenient route for the crosslinking of different polymers, the different functional groups also allow the preparation of semi-IPN and IPN hydrogels through separate polymer networks (Chen et al. 2004).

Despite the larger importance of chemical crosslinking, physical hydrogels were also in-depth investigated. Thermal crosslinking of these blends is rare, as thermogelling systems are usually modified with various additives or by grafting monomers of thermosensitive synthetic polymers. On the other hand, precipitation and ionic crosslinking are commonly utilized for these systems. The former method is usually used if both polymers are insoluble in water, like the blends of cellulose, chitin, and chitosan (Sun et al. 2009; Liu et al. 2012). In such cases, solvents capable of dissolving all components like ionic liquids are required. If one of the polymers is water soluble, usually a post-crosslinking step is used to make the hydrogel more stable (Chiaoprakobkij et al. 2011).

Ionic interactions are also very important for the crosslinking of multiple polysaccharides. Not only several native polysaccharides contain charged (mainly carboxyl) groups, but the carboxymethylation is a common derivatization method for the nonionic polymers, as well. In such systems, the use of multivalent cations is very popular as they interact with all polymers containing anionic pendant groups. The most common component for these hydrogels is the alginate, which is mixed with other anionic polymers (Lin et al. 2005; Kim et al. 2012; Tran et al. 2013). Chitosan is also an important polymer due to its cationic character. As the protonated amino groups can interact with the carboxyl groups of an anionic polymer, the formation of polyionic hydrogel system occurs without the need of complexing ions (George and Abraham 2006).

The chemical crosslinking of different polysaccharides is carried out relatively easily due to the similarities in the functional groups. Certain crosslinking agents like divinyl sulfone (Sannino et al. 2004), epichlorohydrin (Chang et al. 2009, 2010a) or polycarboxylic acids (Kono and Zakimi 2013) react with the hydroxyl groups; thus, they are widely used for crosslinking different polysaccharides. Crosslinkers containing aldehyde groups also need a special mention: besides the application of common crosslinkers like glutaraldehyde (Işiklan 2006), the aldehyde groups are also often introduced into the polymer component through

oxidation; thus, they fulfill the function of the crosslinker (Li et al. 2012b). Nonionic polymers are often used to improve the gelation: while the electrostatic repulsion between polymer chains containing charged groups hinders the crosslinking process, the nonionic component is not affected by it; thus, the crosslinks form more easily between the macromolecules. Hydroxyethylcellulose is a good example as it is often utilized to help the crosslink formation of carboxymethylcellulose systems (Demitri et al. 2008).

6.1.2 Carbohydrate/Amino Acid-Based Hydrogels

Collagen-based blend and copolymer hydrogels

Polypeptides form the other major group of natural polymers. For the modification of polysaccharide hydrogels, collagen is their most important representative. It is insoluble in water, but slightly acidic pH is sufficient for its dissolution. While several different types of collagen are present in animals, studies related to the hydrogel synthesis investigate mainly the application of collagen I, the most common one, an important component of skin, tendon, and bone. Studies focus mainly on its utilization with hyaluronic acid and chitosan; the interest toward blends and copolymers with other polysaccharides is much smaller. The largest attention toward such copolymer structures is shown in the field of tissue engineering for the preparation of hydrogel scaffolds.

Methods used for the synthesis of hyaluronic acid/collagen hydrogels show a large variety. Besides covalently crosslinking the two polymers, the formation of semi-IPN and IPN structures is also common. Semi-interpenetrating network is often achieved by the methacrylation of hyaluronic acid, leading to photocrosslinkable semi-IPN hydrogels (Brigham et al. 2009). Such systems are advantageous for the preparation of injectable hydrogels crosslinkable in situ with UV irradiation (Omlor et al. 2012). If this property is not required, the addition of chemical crosslinkers like poly(ethylene glycol) diglycidyl ether (PEGDGE) is also a viable strategy if the collagen is added after the crosslinking in a separate step (Kim et al. 2007). However, the collagen component can also form the three-dimensional network through self-assembly (fibrillogenesis) (Harris et al. 2013). Both processes can be simultaneously utilized, leading to IPN hydrogels with superior mechanical properties compared to the semi-IPN structures (Suri and Schmidt 2009). Composite hydrogels were also utilized by adding collagen fibers prepared by electrospinning into hyaluronic acid/gelatin solution during the gelation process (Ekaputra et al. 2011). For chemical crosslinking of the two polymers, carbodiimide is an excellent crosslinker due to the presence of carboxyl and amine groups (Park et al. 2003; Kim et al. 2008c). PEGDGE can be also utilized if the agent is added when both polymers are present in the solution (Segura et al. 2005b).

Chitosan is another popular choice for the copolymer synthesis. For chemical gelation, crosslinking agents capable of reacting with the amino groups present in

both polymers are generally used. While mostly glutaraldehyde is utilized (Wu et al. 2007), other less common crosslinkers containing aldehyde groups such as glyoxal (Wang and Stegemann 2011) or formaldehyde (Zhang et al. 1997) are also used to a lesser extent. Other agents like genipin (Yan et al. 2010) and carbodiimide/*N*-hydroxysuccinimide system (Rafat et al. 2008; Deng et al. 2010) were likewise utilized in some studies; the latter one was also used to crosslink hydrogels based on collagen and the carboxymethyl derivative of chitosan (Chen et al. 2006). The physical gelation is usually achieved by incubation at 37 °C to promote the formation of the fibrous structure of collagen, while the chitosan is aggregated with the increase of the pH (Tan et al. 2001; Chiu and Radisic 2011; Reis et al. 2012). There is a major interest in the preparation of systems capable of thermal gelation, as well. Most studies investigated chitosan/ β -glycerophosphate systems where the addition of collagen has a beneficial effect on several properties: such systems not only gel faster, but they show lower cytotoxicity and slower degradation (Song et al. 2010; Wang and Stegemann 2010; Li et al. 2012a). As even body temperature is sufficient for the thermal gelation, these properties make such systems an excellent material for injectable hydrogels in the medical field.

In case of cellulose-based copolymers, most commonly the native (especially bacterial) cellulose is used as a second polymer with collagen. Due to the poor water solubility of the components, the preparation of physical gels is very common. Two different strategies were utilized: either the two polymers were dissolved simultaneously and then precipitated (Wang et al. 2013b), or the prepared cellulose gel is immersed in the collagen solution to allow its absorption and interaction with the cellulose chains (Zhijiang and Guang 2011). Chemical crosslinking of the two components is also possible through chemical modification: Saska et al. (2012) used amino acid or its derivative to modify the polysaccharide, which then covalently reacted with the collagen in presence of carbodiimide crosslinker. This zero-length crosslinker was also utilized for the solution of carboxymethyl derivative of cellulose and collagen in presence of adipic acid dihydrazide (Liu et al. 2013). On the other hand, Cheng et al. (2014) directly introduced aldehyde groups into the cellulose structure through oxidation, which then reacted with the amine groups of the collagen.

The literature regarding alginate/collagen hydrogels is even more limited, despite the complexation of alginate with multivalent cations allowing easy formation of physical composite gels (de Cunha et al. 2014). Moreover, similarly to the carboxymethylcellulose, the chemical crosslinking of the two polymers with carbodiimide is also possible due to the presence of carboxyl pendant groups on the alginate chain (Liu et al. 2008b).

Gelatin-based blend and copolymer hydrogels

While non-modified collagen is widely used, there is an even larger interest in the utilization of gelatin, the product of the degradation or denaturation of collagen. Unlike the original polymer, gelatin is soluble in water over 30 °C and cooling its solution leads to the formation of physical gels (Eldridge and Ferry 1954; Hayashi and Oh 1983). While chemical crosslinking strategies used for the collagen gelation

are also applicable for the gelation, due to its larger importance the utilized methods are much more diverse. Similarly to the collagen, the most commonly used copolymer polysaccharides are the hyaluronic acid and the chitosan, but there is a major interest in alginate/gelatin systems and mixing with starch, cellulose, and its derivatives, as well.

For the synthesis of hyaluronic acid/gelatin hydrogels, the chemical gelation is utilized in most studies. Similarly to hyaluronic acid/collagen copolymers, carbodiimides are the usual chemical crosslinking agents (Zhang et al. 2011a; Zhou et al. 2013a, b). Derivatization is another common approach for the chemical gelation. Unlike the collagen-based gels, gelatin is also modified along with the hyaluronic acid component; thus, both polymers participate in the chemical gelation. Methacrylation is very common to prepare autocrosslinkable hydrogels (Skardal et al. 2010; Camci-Unal et al. 2013), but reagents containing thiol groups are also often used to modify both polymers, which then react with each other to form disulfide crosslinks when exposed to air (Shu et al. 2003). Moreover, the introduction of crosslinkers like derivatives of poly(ethylene glycol) does not only increase the gelation rate of the thiolated derivatives, but it also offers a convenient way to modify the gel properties (Mironov et al. 2005; Vanderhoogz et al. 2009). Enzymatic crosslinking was also used to a lesser extent: Crescenzi et al. (2002) utilized transglutaminase-catalyzed copolymerization after the modification of hyaluronan with dipeptide.

Physical gels of chitosan and gelatin are prepared in multiple steps: the two components are dissolved separately by adding acid or heating, the two solutions are mixed, followed by cooling and neutralization (Chang et al. 2002; Nagahama et al. 2009). For crosslinking through the amine groups, several crosslinking agents were utilized, such as glutaraldehyde (Yao et al. 1995; Zhao et al. 2002; Franco et al. 2011), genipin (Cui et al. 2014), and proanthocyanidins (Kim et al. 2005). They are usually added to the polymer solution, but the immersion of physical gels in the crosslinker solution is also possible (Shen et al. 2000). Carbodiimides are also applicable, although in this case only gelatin has the carboxyl groups required for the crosslink formation; thus, the chitosan chains are not directly crosslinked (Gorgieva and Kokol 2012). The molecule was utilized for the synthesis of hyaluronic acid/chitosan/gelatin hydrogels, as well (Tan et al. 2009). Enzymatic crosslinking catalyzed by transglutaminase is also more advantageous for copolymerization with chitosan than for hyaluronic acid/gelatin systems, as the former polysaccharide does not require functionalization due to the amine groups (Chen et al. 2003). Besides the chitosan its carboxymethyl derivative was also used for the copolymerization: Yang et al. (2010) utilized gamma irradiation to initiate the free-radical crosslinking. Moreover, gelatin-based composite hydrogels containing chitin nanofibers showed excellent mechanical properties (Hassanzadeh et al. 2016).

While combining alginate with collagen was barely studied, the use of its denatured form was in-depth investigated. Like for other polysaccharide/gelatin systems, glutaraldehyde is commonly utilized as a chemical crosslinker for semi-IPN hydrogels (Dong et al. 2006; Liu and Zhao 2006). The addition of Ca^{2+}

cations is also often used to achieve IPN structures from semi-IPN through the ionic crosslinking of alginate (Fadnavis et al. 2003). Another interesting approach is the enzymatic crosslinking of gelatin instead of the addition of classic crosslinker molecules (Wen et al. 2014). Moreover, IPN structure was also observed under the sol-gel temperature of gelatin: in this case, both polymers form physical networks (Awad et al. 2004; Duan et al. 2013). The major strategy for the covalent crosslinking of the polymers is the derivatization of alginate through oxidation, which then reacts with the amine groups in presence of catalyst (usually borax) (Balakrishnan et al. 2005); the application of such hydrogels is widely investigated as scaffolds in tissue engineering. Another possible route is the addition of carbodiimide for the formation of amide groups (Yang et al. 2009). Aroguz et al. (2014) used a two-step crosslinking process: first crosslinked oxidized alginate with adipic dihydrazide and in the following step, the gelatin was added with the carbodiimide. The modified alginate can also function as a crosslinker: Sakai et al. (2008) prepared Ca-alginate/gelatin hydrogel fibers, which were then immersed into a solution containing oxidized alginate to crosslink the gelatin component, as well.

The application of native cellulose with gelatin is more limited compared to the collagen. Nakayama et al. (2004) prepared IPN structures by chemically crosslinking gelatin with carbodiimide, while the cellulose formed a separate physical network. On the other hand, Dash et al. (2013) used oxidized cellulose nanowhiskers to covalently crosslink the gelatin solution. However, there is also an interest toward the use of cellulose derivatives; in these experiments, the formation of IPN hydrogels was carried out by the addition of glutaraldehyde crosslinker. This method was used for the gelation of solutions formed with the carboxymethyl (Rathna et al. 1996; Rokhade et al. 2006) and hydroxyethyl (Kajjari et al. 2011) derivatives of cellulose, as well.

For starch-based systems, physical gelation is the standard route for the gel formation. Elevated temperatures, sufficient not only for the gelatin dissolution but also for the gelatinization of the starch, are used in this process (Abdulmola et al. 1996). Besides the ratio of two polymers, the starch type also has a major impact on the gel properties (Mallick et al. 2014). Porous gels were also prepared from such systems: Jaya et al. (2009) used microwave vacuum drying as a more efficient method compared to freeze-drying for starch/gelatin/hydroxyapatite composites.

Copolymers based on other amino acid-based polymers

Other polypeptides like albumin were also utilized to a very small extent. Tada et al. (2007) chemically crosslinked alginate with albumin in presence of carbodiimide crosslinker; thus, the polypeptide formed the crosslinks between the polysaccharide chains. On the other hand, Boppana et al. (2010) prepared IPN hydrogel from carboxymethylcellulose and albumin: multivalent cations were used for the physical crosslinking of the cellulose derivative, while albumin was crosslinked with glutaraldehyde. Interestingly, oligopeptides were also capable to crosslink functionalized dextran to form hydrogels (Lévesque and Shoichet 2007).

6.2 Grafting and Copolymerization with Synthetic Polymers

The literature related to synthetic polymer-based hydrogels is vast compared to the polysaccharide gels. Therefore, unsurprisingly there are numerous studies related to the preparation of their blends and copolymers. The ratio of the polysaccharide and synthetic polymer content used in the studies show a large variety, but the amount of the synthetic component is usually considerable, often higher than polysaccharide content. Thus, investigations focus on the blends and copolymers with the most important commercial polymers.

6.2.1 Acrylates and Methacrylates

Most commercial products are based on acrylates due to their low cost and advantageous properties like responsivity to various environmental conditions. Therefore, it is not surprising that the copolymers formed with acrylates are the most widely studied. The first studies involved the application of acrylic acid for the copolymer gel formation with chitosan: a large advantage over the other polysaccharides is the presence of amine groups, as in charged form they can interact with the carboxyl groups of the acrylic acid depending on the pH. Such copolymers were prepared by Wang et al. (1997) first: the chitosan was chemically crosslinked with glutaraldehyde, while the poly(acrylic acid) was bound by the electrostatic interaction. Moreover, the chemical crosslinking of chitosan is not required for the formation of such physical gels (de la Torre et al. 2003). While in this case the acrylic acid was added as a polymer, in most studies its monomer is used instead. Chemical initiators (Yazdani-Pedram et al. 2000), UV (Lee et al. 1999) and high-energy irradiation (Shim and Nho 2003) are all common methods to initiate the reactions of the acrylic acid. Hydrogels by grafting acrylic acid on chitin (Tanodekaew et al. 2004) and alginate (Yin et al. 2008) were also prepared, but currently their importance is very small. As for the cellulose, only its carboxymethyl derivative was gelled in presence of the acrylic acid (Bajpai and Mishra 2004; Zhang et al. 2014a). In most studies very high acrylic acid content is used compared to the polysaccharide; however, very low amount of acrylic acid can be also utilized to improve the gelation of the polysaccharide solution. This leads to not only better gel properties but also milder synthesis conditions are required (Fekete et al. 2016b).

Acrylamide is another common acrylic monomer; its polymerization is likewise achieved through free radicals. Similarly to the acrylic acid, copolymerization with chitosan was in-depth studied (Risbud and Bhone 2000; Kumbhar et al. 2003; Xia et al. 2005). While usually chemical initiator/MBA crosslinker systems are used, Sokker et al. (2011) also achieved gel formation by high-energy irradiation in the absence of the crosslinking agent. The irradiation method is also common for the carboxymethylcellulose/acrylamide systems; while MBA monomer is often used to improve the gelation (El-Din et al. 2010; Hemvichian et al. 2014), crosslinker-free

gels were also synthesized (Abd El-Mohdy 2007). Alternatively, the carboxyl groups of the cellulose derivative allow the preparation of semi-IPN gels by multivalent cations with polyacrylamide (Aalaie et al. 2013). Alginate/acrylamide gels also have considerable literature; such gels are synthesized in two-step crosslinking: acrylamide is crosslinked by free-radical crosslinking, while multivalent cations are added for the complexation of the alginate (Omidian et al. 2006). Ca^{2+} cations are usually used as a crosslinker, but better mechanical properties can be reached through their replacement with trivalent ions (Yang et al. 2013). Moreover, free-radical crosslinking alone is also capable of crosslinking alginate/acrylamide solutions (Kulkarni and Sa 2009b). An interesting method to accelerate the process is microwave irradiation: Singh et al. (2006b) observed that the gelation was significantly faster and low initiator content and air atmosphere proved to be adequate.

While both acrylic acid and acrylamide are widely used separately for copolymerization as discussed above, the copolymer of the two is also common due to the excellent swelling properties related to the presence of both amine and carboxyl groups. Their first polysaccharide-based copolymers were prepared with starch via free-radical grafting (Athawale and Lele 2000; Kiatkamjornwong et al. 2000). The ratio of the two monomers had a major impact on the water uptake: the use of their mixtures led to better swelling properties than when only one of them was added. Acrylic acid-co-acrylamide gels were prepared with several polysaccharides such as cellulose (Wu et al. 2012a), chitosan (Mahdavinia et al. 2004), and their derivatives (Suo et al. 2007; Yin et al. 2007). Alginate-based copolymers were also synthesized: in this case, crosslinking with multivalent cations was also utilized next to the chemical crosslinking (Yahşi et al. 2005). Other components like methacrylates (Li 2010) or clay minerals (Rashidzadeh et al. 2014) are also commonly introduced to improve the properties. While the acrylamide and acrylic acid is mostly added in monomer form, other synthesis routes are also available: Sadeghi and Hosseinzadeh (2007) copolymerized CMC and polyacrylonitrile (PAN); the amino and carboxyl groups were formed by the alkaline hydrolysis of PAN in presence of ammonia.

An even more intensively studied monomer is the *N*-isopropylacrylamide (NIPAAm) as its thermosensitivity even at low temperatures makes it an excellent candidate for medical hydrogels. Copolymer and IPN hydrogels formed with alginate and chitosan have the largest literature. The former polysaccharide is used mostly for the preparation of IPN structures achieved by free-radical crosslinking of the alginate/NIPAAm solution, followed by complexation of the alginate with Ca^{2+} cations (Guilherme et al. 2005; Petrusic et al. 2012). Semi-IPN structures are also attainable: Ju et al. (2002) and Shi et al. (2006) used the polymer of the acrylamide derivative to prepare ionically crosslinked alginate/PNIPAAm solution: the physically crosslinked alginate matrix bound the acrylate chains through weak interactions. However, the alginate does not necessarily form the crosslinked network: if only the free-radical crosslinking of the mixture solution is carried out, then the covalently crosslinked network is formed by the PNIPAAm (Zhang et al. 2005a; Dumitriu et al. 2010). Semi-IPN gels show better swelling properties than their full-IPN counterparts, but the deswelling is slower (Lee et al. 2006). Functionalization also offers another route to chemically crosslink the two

polymers: Ju et al. (2001) introduced amine groups to the PNIPAAm polymer which the Ca-alginate in the presence of carbodiimide.

For chitosan-based hydrogels, the synthesis of semi-IPN structure by crosslinking the NIPAAm monomer is the most common route (Wang et al. 2000; Verestiuc et al. 2004). If full interpenetrating network is the goal, then glutaraldehyde crosslinking agent is added after the first polymerization step (Lee and Chen 2001; Alvarez-Lorenzo et al. 2005). Grafting offers an alternative for gels with different properties: the monomer is grafted on the chitosan and the modified polysaccharide forms the three-dimensional network (Kim et al. 2000a; Lee et al. 2004a; Cai et al. 2005). Such gels also exhibit thermal sensitivity due to the acrylate side chains. The crosslinking method affects the gel properties, as well: grafted copolymer gels show better responsivity to the environmental parameters at the expense of lower water uptake compared to IPN hydrogels (Kim et al. 2000a). Grafting glycidyl methacrylate in a second step to the polymer backbone leads to photocrosslinkable systems—this property is utilized for the formation of injectable hydrogels in medicine (Zhang et al. 2014b). Similarly to the alginate, the chemical reaction of the two components is also a viable route for grafting, but in this case, the PNIPAAm is functionalized with reagents containing carboxyl groups (Lee et al. 2004b; Chen and Cheng 2006). NIPAAm is also often used with carboxymethylchitosan as such gels have better pH-sensitivity compared to copolymers containing unmodified chitosan (Guo and Gao 2007; Ma et al. 2007a, b).

While first studies of cellulose/NIPAAm systems involved the modification of cotton fibers by radiation-initiated grafting (Jun et al. 2001), in later experiments, hydrogels were also synthesized by free-radical crosslinking (Gupta and Khandekar 2003; Wang et al. 2013c). Cellulose derivatives were also utilized for the modification of the PNIPAAm gels: the copolymerization with carboxymethylcellulose leads to pH and thermosensitive systems (Ma et al. 2007b; Ekici 2011), while the thermal sensitivity can be changed with hydroxypropyl (Chauhan et al. 2004; Xu et al. 2010) and methyl (Liu et al. 2010) derivatives. Grafting with *N*-isopropylacrylamide is also an interesting route to prepare thermosensitive hyaluronic acid gels as the polysaccharide component has minimal effect on the thermal behavior of NIPAAm (Ohya et al. 2001). Polymerization of the synthetic monomer in presence of the hyaluronan is also a common strategy for formation of semi-IPN structure (Santos et al. 2010; Coronado et al. 2011).

Copolymerization is not limited to the aforementioned monomers. Methacrylate monomers such as the hydroxyethylmethacrylate (Mandal and Ray 2013), 2-dimethylaminoethylmethacrylate (Salama et al. 2016), and alkylmethacrylates (Li 2010) were also used among other acrylate and methacrylate components. However, their crosslinking mechanism is very similar to the one discussed for the above-mentioned monomers and their importance is very small; thus, they will not be further discussed.

6.2.2 Polyvinylpyrrolidone

Synthetic polymers other than acrylates are also widely used for the copolymerization with polysaccharides. Other common synthetic polymers, especially ones widely applied in the medical field, are also investigated to achieve better properties than the homopolymer gels. Polyvinylpyrrolidone is a popular material for hydrogel synthesis as its thermosensitivity is very advantageous in the medicine similarly to the PNIPAAm. However, the relatively low swelling and poor mechanical properties (especially fragility) led to the investigation of its copolymers to counter these disadvantages, for which polysaccharides also proved to be effective besides the usual acrylate copolymers (Wang et al. 2007). While in some studies the monomer of the PVP was added to the solution (Işıklan et al. 2008), usually its polymer with varying molecular weight is utilized. There is an especially large focus on chitosan/PVP hydrogels; in earlier studies, semi-IPN gels were synthesized by chemically crosslinking the chitosan with glutaraldehyde (Risbud et al. 2001; Risbud and Bhat 2001) or genipin (Khurma et al. 2005). However, recently the interest shifted toward the radiation-induced crosslinking (Nho and Park 2002; Dergunov et al. 2005; Archana et al. 2013). The latter method was also used for the copolymers formed with carboxymethylchitosan (Zhao et al. 2006), starch (Zhai et al. 2002), and alginate (Singh and Singh 2012), as well. For the latter polysaccharide, complexation was also utilized for the preparation of physical gels (Doria-Serrano et al. 2002). Out of the cellulose-based copolymer gels, the major focus is on the carboxymethylcellulose (Wang et al. 2007; Lü et al. 2010); besides the chemical crosslinking, heat treatment under pressure similarly proved to be a viable method for physical gel formation (Roy et al. 2010). The addition of hydroxypropyl (Marsano and Bianchi 2002) and methylhydroxyethyl (Plungpongpan et al. 2013) derivatives of cellulose also had a positive impact on the properties of PVP gels. PVP is also a frequent copolymer for less studied polysaccharides like pectin (Mishra et al. 2008) and κ -carrageenan (Relleve et al. 1999; Abad et al. 2003) in the hydrogel formation.

6.2.3 Poly(Vinyl Alcohol)

Poly(vinyl alcohol) (PVA) is a popular hydrogel material for biomedical applications due to its excellent biocompatibility. For polysaccharide/PVA systems, the physical gelation holds larger importance than the chemical crosslinking as it can be easily achieved via freeze-thawing the PVA solution (Yokoyama et al. 1986); this is often utilized for the polysaccharide/PVA blends, as well. The gelation method also heavily depends on the polysaccharide type; the most common copolymer for PVA being the chitosan. Physical gels are prepared by both freeze-thawing and elevated temperatures. The former route is widely used (Sung et al. 2010), despite the presence of chitosan hindering the association of the PVA molecules in frozen state, leading to a weaker structure (Cascone et al. 1999). On the other hand, at high temperatures, the stronger hydrophobic interactions between the polymer chains

lead to the gel formation (Minoura et al. 1998). Moreover, while heat treatment at higher temperatures is common (Koyano et al. 1998; Jin and Bai 2002; Zhu et al. 2012), the gelation may occur under body temperature or even room temperature depending on the ratio of the components, making it ideal for medical applications (Tang et al. 2007). Chemical gels were also prepared by various methods, such as the addition of glutaraldehyde (Wang et al. 2004b; Costa-Júnior et al. 2009; Kumar et al. 2009), ethylene glycol diglycidyl ether (Liu et al. 2010), UV (Kim et al. 2003), or gamma irradiation (Nho and Park 2002). Yang et al. (2008) combined freeze-thawing and irradiation: they observed that even the order of the two crosslinking steps affected significantly the gel properties. Besides chitosan, its carboxymethylated derivative was also used for the formation of physical (Lee et al. 2009) and chemical (Zhao et al. 2003b) gels with PVA. For starch/PVA systems, the pregelatinization of the starch is generally utilized. While films were also prepared through pure physical crosslinking by heat treatment (Spiridon et al. 2008; Tang et al. 2008), for the hydrogel synthesis, the pregelatinized systems are also chemically crosslinked in the following step. This is achieved with crosslinkers capable of reacting with hydroxyl groups like citric acid (Shi et al. 2008) or formaldehyde (Han et al. 2009); free-radical crosslinking initiated with gamma irradiation is another possible way to avoid the use of such additives (Zhai et al. 2002). Interestingly, physical gels were also prepared by freeze-thawing after grafting PVA onto the starch backbone (Xiao and Yang 2006). Studies involving unmodified cellulose hydrogels focused on its physical gelation by the freezing method (Millon and Wan 2006; Chang et al. 2008). On the other hand, for the carboxymethyl derivative physical (Barkhordari et al. 2014), chemical crosslinking (Taleb et al. 2009; Rao et al. 2012) and a mixture of the two steps (El-Salmawi 2007) were also examined. So far there was only minor interest in other cellulose derivatives, although Park et al. (2001) studied the gelation of methylcellulose/PVA solutions in presence of glutaraldehyde. For hyaluronic acid-based copolymers, both physical crosslinking with freeze-thawing (Guerra et al. 1994) and chemical gelation with glutaraldehyde (Kim et al. 2004) were investigated.

6.2.4 Poly(Ethylene Glycol)

Poly(ethylene glycol) (PEG) (also known as polyethylene oxide (PEO), although it is usually used for its high molecular weight variant) is another common material for hydrogel formation. Unlike the above-mentioned polymers, it is mainly utilized as a spacer macromolecule; this allows the formation of longer and more mobile crosslinks, leading to better swelling properties. Most studies involve the application of low molecular weight PEG, but gelation with large spacer molecules (over 10^5 Da) was also reported (El-Din et al. 2013). As PEG does not react directly with the polysaccharides, the addition of various crosslinking agents or chemical modification is required. The most common crosslinker for this purpose is the divinyl sulfone. The chemical crosslinking can occur in the simultaneous presence of all three components (Esposito et al. 2005), but the polyethylene-glycol can be

previously functionalized through reaction with DVS, as well (Jin et al. 2010). Likewise, PEG is also often chemically modified with various reagents to make the direct reaction with the polysaccharide possible. The diglycidyl ether of PEG is an excellent crosslinker due to the reactive epoxy groups (Kono 2014). Another good example is the introduction of amine groups which in the presence of carbodiimide crosslinker easily react with polymer containing carboxyl groups, such as the alginate (Eiselt et al. 1999) or hyaluronic acid (Jeon et al. 2007). UV-initiated crosslinking is a viable strategy if vinyl groups are present in the polymer—this is usually achieved by various acrylates (Leach and Schmidt 2005; Zhong et al. 2010). In such systems, both PEG and the polysaccharide are modified to contain double bonds. The two components can also be functionalized using different groups which easily react with each other: Shu et al. (2004) used thiolated hyaluronic acid and PEG modified with various acrylates for chemical crosslinking. If only PEG is functionalized, hydrogels with interpenetrating network can be prepared; this is especially characteristic for chitosan/PEG systems, where the chitosan is cross-linked with glutaraldehyde, while the reaction of the acrylated PEG is initiated by UV irradiation (Lee et al. 2000b; Kaewpirom and Boonsang 2006). The gelation is often carried out by high-energy irradiation, as well; this allows the crosslinking without the functionalization of the polymers due to the free radical formation. This strategy was utilized for carboxymethylcellulose/PEG copolymer hydrogels (Lee et al. 2005; El-Din et al. 2013).

6.3 Composite Hydrogels with Inorganic Components

Recently, there are major efforts for the use of various inorganic materials for the preparation of composite gels. Studies focus on two major groups of inorganic components: clays and metal nanoparticles. The application of the two groups is fueled by very different goals. Clays are very cheap resources available in abundance. While their presence also modifies the gel properties, the main reason for their use is to reduce the costs of the gel preparation. On the other hand, the aim of the metal nanoparticle incorporation is the introduction of novel properties, such as the antibacterial behavior. The mineral content of the composites shows a large variety: in some experiments, only very low amounts of it are added, while in others the inorganic content is over 50%.

6.3.1 Minerals

Studies investigating the incorporation of minerals in polysaccharide hydrogels show a huge variety in the type of the added inorganic component. While the goal is the reduction of the production costs by lowering the polysaccharide content, it is a major requirement that the inorganic component should not negatively affect the swelling properties. Therefore, the polymer is generally mixed with materials

containing hydrophilic pendant groups like silicates or double layered hydroxides. The mineral component is added in powder form to the solution before the crosslinking process; the particle size is usually under 100 μm , but several experiments use particles even in the nanometer range as this allows the formation of homogeneous dispersions.

The most important minerals with hydrophilic properties are the silicates, where the hydrophilic surface is provided by the silanol groups. Studies focus on the application of various aluminosilicate clay minerals such as the kaolinite (Pourjavadi et al. 2007), montmorillonite (Liu et al. 2008a), palygorskite (also known as attapulgite) (Wang et al. 2009), illite (Wang et al. 2013f), and vermiculite (Xie and Wang 2009). Kaolinite is mostly added in the form of kaolin (kaolinite-rich clay), but other minerals are mainly used as pure minerals, although the use of bentonite (rich in montmorillonite) instead of pure montmorillonite is also common (Oh et al. 2011). Other silicates like mica minerals, sericite being their most important representative, are utilized to a lesser extent, as well (Wu et al. 2000). Earlier studies involved the modification of polysaccharide/acrylate copolymers to further reduce the production costs. Due to the acrylate component, the gelation is carried out by free-radical crosslinking; this also allows the formation of covalent bonds between the mineral and the polymer besides the weak interaction of the components. While most studies use chemical initiators, gamma irradiation also proved to be a viable route (El Salmawi and Ibrahim 2011). Wu et al. (2000, 2003) investigated the effect of the addition of three types of clays (kaolin, bentonite, and sericite) on the gel properties in starch/acrylamide systems. The mineral not only made the synthesis more cost-effective, but it also led to improved swelling at low mineral concentration. However, very high silicate content had a negative impact on the water uptake. The mineral type also proved to be an important parameter as the differences in the hydration affected the crosslinking process. The synthesis of superabsorbent polysaccharide/acrylate/mineral composites was accomplished with other natural polymers such as the cellulose (Anidhuran et al. 2011), chitosan (Xie and Wang 2009), alginate (Pourjavadi et al. 2007), and guar gum (Wang and Wang 2009), as well. Moreover, there are also recent studies involving the gelation of the carboxymethyl (Wang and Wang 2010; Bao et al. 2011) and methyl (Bortolin et al. 2013) derivatives of cellulose in composite systems.

Despite the large interest in the copolymer composite gels, pure polysaccharide/mineral composites offer an alternative way to prepare cheaper and more environmentally friendly gels. Alginate is a popular choice due to the easy physical crosslinking via complexation. The first such system was prepared by Céspedes et al. (2007) with the addition of CaCl_2 to alginate/clay solutions, while Singh et al. (2009b) further introduced starch into the alginate/clay system. Their method was similar but hot water was required in the latter case to form a homogeneous solution due to the presence of starch. Besides the alginate, chitosan was also utilized to form physical gels with montmorillonite (Celis et al. 2012). Chemical crosslinking is also a viable strategy for such composites: Yang et al. (2012) synthesized alginate/modified rectorite composites by free-radical crosslinking initiated by potassium persulfate in presence of *N,N'*-methylene-bis-acrylamide crosslinker.

While minerals are usually added in their natural form to lower the production costs, the chemical modification of clays is also an interesting approach to adjust their properties depending on the application field. So far, only the organic modification (achieved through the replacement of cations with molecules containing hydrophobic groups like cationic surfactants) is relevant for the hydrogels, especially in case of montmorillonite. The change in the structure leads to a more hydrophobic character which hinders the gelation process (Xu et al. 2006). However, this property can be utilized in the water treatment: the hydrophobic interactions participate in the adsorption of certain pollutants, leading to higher adsorption capacity (Wang and Wang 2013). Recently, organically modified illite was also employed for the preparation of composite gels with alginate for dye adsorption (Wang et al. 2013g).

Double layered hydroxides (DLH) have a very different structure compared to the silicates. The cations form a layer structure which is surrounded by the anions and other molecules like water. Hydrotalcite is the most often used native mineral, but synthetic double layered hydroxides are also significant. The multivalent ions present in their structure interact with negatively charged groups on the polymers, thus leading to complex formation. Barkhordari et al. (2014) prepared carboxymethylcellulose/DLH composite hydrogels by heating the alkaline solution of the two components; the high pH promoted the deprotonation of the carboxyl groups so it was possible for the multivalent metal ions to interact with them. The cationic layer can also bind other anions; thus, they also show potential as adsorbents (see Sect. 7.2). The cations present in the structure also affect the gel properties: Yadollahi et al. (2015c) compared different carboxymethylcellulose/DLH composites, and they found that DLH containing zinc or copper cations also provided antibacterial activity to the gels.

6.3.2 Metal Nanoparticles

The preparation of gels containing metal particles has two major requirements: the nanoparticles need to be homogeneously dispersed in the gel structure and interactions with the polymer should prevent their diffusion into the environment. They are usually added in salt form to the polymer gel: as they are present as ions due to the dissociation, charged groups on the polymer chain can bind them to the gel network. In earlier studies, copolymers with synthetic polymers were used, but recently the nanoparticles were also incorporated in a wide array of pure polysaccharide hydrogels: systems based on cellulose derivatives (Hebeish et al. 2013), starch (Villanueva et al. 2016), chitin and chitosan (Kumar et al. 2012, 2013), alginate (Obradovic et al. 2012), and even dextran (Ma et al. 2009). The synthesis heavily depends on the metal type. Silver is a very popular choice for antibacterial nanoparticles; it is added to the gel as aqueous solution of AgNO_3 . There are two available methods: either the crosslinked gel is immersed in the silver nitrate solution (Ma et al. 2009), or the salt is added to the dissolved polymer before the crosslinking (Yadollahi et al. 2015a); this ensures the homogeneous dispersion

of the nanoparticle. The next step is the reduction of the silver cations, leading to the formation of silver particles. Antibacterial hydrogels containing gold nanoparticles were also synthesized. Marsich et al. (2011) used HAuCl_4 precursor to prepare modified chitosan/alginate/gold hydrogels.

While the effect of the silver and gold nanoparticles is widely studied, their high cost is a relatively big disadvantage, leading to the investigation of the applicability of cheaper alternatives. Various metal oxides with antibacterial properties like the copper (Yadollahi et al. 2015b) and zinc (Kumar et al. 2012) oxides proved to be perfect candidates. Similarly to the silver, they are added in salt precursor form (CuCl_2 , $\text{Zn}(\text{NO}_3)_2$, or zinc acetate); the synthesis is analogous to the silver nanocomposite gels: the hydrogels are immersed in their solution and oxides are formed during an oxidation step. Metal oxide nanoparticles exhibit very good antibacterial properties despite their significantly lower cost; thus, their importance shows a constant growth. Titan dioxide is another interesting nanoparticle as it not only exhibits antibacterial activity but also improves the mechanical strength of the hydrogel (Archana et al. 2013). Unlike other oxides, it is mixed with the polysaccharide solution in its oxide form instead of using precursors.

Another interesting application is the preparation of hydrogels with magnetic properties. This is especially advantageous in the utilization as adsorbents, where the hydrogel is used in form of small beads or particles. Incorporating the magnetic particles allows the removal of these beads from the water by a magnetic field, making their recovery a lot easier. The polysaccharide also plays a major role in the synthesis: the polymer forms a coating around the nanoparticles, preventing their aggregation. Magnetic properties were first achieved by Fe_2O_3 (Kroll et al. 1996); however, in more recent experiments Fe_3O_4 nanoparticles are used as magnetic nanoparticles (Shen et al. 2011).

7 Application of Polysaccharide-Based Hydrogels

While there is a vast literature available about the potential application of hydrogels, studies related to polysaccharide-based gels are much more limited and focused on certain fields. The largest interest toward their use is in the medical field due to the biocompatibility and the common responsive behavior. The absorption and desorption of various chemicals are also utilized in the water treatment and agricultural applications—the good biodegradability is another important advantage in the latter field. Studies related to applications in other fields are so far pretty limited; thus, only a short summary is given for them.

7.1 Medical Applications

Studies focus mainly on three major applications: controlled drug delivery systems, wound dressings, and scaffolds for tissue engineering. However, to a lesser extent,

the utility of carbohydrate-based systems was investigated for the use as bulking agents and components for contact lenses, as well. Moreover, it is important to note that these applications are not strictly separate: for example, wound dressings and scaffolds often contain bioactive agents; thus, such systems function as drug delivery systems, as well.

7.1.1 Drug Delivery

The most significant medical application of hydrogels is in the field of drug delivery. Hydrogels allow the controlled release of the bioactive molecules over an extended period of time, leading to constant drug concentration in the environment and a long-term effect. The properties of the loaded molecule also play a crucial part as it determines the possible routes for their incorporation and release (Hoare and Kohane 2008). While the diffusion of small molecules occurs easily, the process is hindered by the gel network at larger molecular size. However, the swelling of the hydrogel leads to an expanded polymer network, allowing the release of larger molecules, as well. Covalent binding to the polymer backbone or the use of polymers which interact with the molecules (e.g., through ionic interactions) are also common to control the process: in this case, the interactions between the polymer and the loaded molecule need to be disrupted.

Stimuli-responsive polymers are especially favored in this field, as the dependence of the swelling behavior on the environmental properties offers another way to control the release (Qiu and Park 2001). The abundance of polyelectrolytes and polymers with thermogelling properties among polysaccharides is also a major reason for the large interest in their application (George and Abraham 2006). While gels may show sensitivity to various properties of the environment, for carbohydrate-based hydrogels, only the pH and thermal sensitivity are generally studied. The presence of charged groups leads to sensitivity to the pH due to the protonation or deprotonation. This not only affects the gel expansion, but it can also disrupt the ionic interaction with the loaded molecules. This property is crucial as it allows a convenient route for the delivery of orally administered drugs due to the varying pH in the digestive system; however, it also plays an important role in other internal applications. While a lot of polysaccharides show pH-responsive behavior, chitosan is the only common cationic representative among them, thus exhibiting significantly different responsiveness. On the other hand, polysaccharides with anionic (especially carboxyl) groups are relatively common, especially due to the widely used carboxymethylation of nonionic polymers. This led a large interest toward the chitosan as it can be utilized in a different environment than the anionic polysaccharides (Bhattacharai et al. 2010). However, other considerations also need to be taken during the hydrogel formation. While the destruction of the gel network often also plays a part in the controlled delivery, usually this process should be avoided as it may lead to the rapid release of the drug. For example, carboxymethylcellulose hydrogels crosslinked with Fe^{3+} are unstable in acidic environment, but the introduction of alginate copolymer improves the gel stability (Kim et al. 2012).

Thermal sensitivity is another important factor. Several polysaccharides also exhibit thermogelling behavior. If the sol-gel transition occurs under the body temperature, it allows the preparation of solutions gelling only after being injected into the body; thus, implantation is achieved without surgery. Multiple polysaccharide-based systems show thermogelling behavior at low temperatures, such as the chitosan/ β -glycerol phosphate solutions (Chenite et al. 2001). The phosphate additive not only makes the chitosan solution thermogellable, but its concentration offers an easy way to control the gel temperature. The temperature also affects the drug release in such systems, a property which needs to be taken into account, as well (Amin et al. 2012).

The preparation of injectable hydrogels does not necessarily need thermogelling behavior: photocrosslinkable systems (usually prepared through methacrylation) allow *in vivo* gelation through UV irradiation (Jameela et al. 2002). However, such systems are usually utilized for tissue engineering rather than as pure drug delivery systems.

7.1.2 Wound Dressing

Another major application of the hydrogels is the wound dressing. The function of the dressings is not only to prevent the infection but also promote the healing process. Moreover, several factors can hinder the healing—for such healing-impaired wounds, further considerations are required in the dressing preparation. Hydrogels are only one of the numerous types of dressings, but their properties such as the high water content or the ability to absorb wound fluids make them preferable compared to other products (Stashak et al. 2004). This not only provides a cooling effect for the damaged skin, but the moist environment is also beneficial during the healing process. Physically crosslinked alginate dressings are especially important polysaccharide-based systems; such products are widely available even in commercial use (Boateng et al. 2008). However, they are mostly used in non-gel form like fibers. Moreover, recently adverse effects were also reported during their application due to the high Ca^{2+} concentration in the product (Ng and Cheng 2007).

Chitosan and other chitin derivatives are subjects of intense research as materials for hydrogel dressings. The degradation during their use leads to the release of various glucosamine monomer and oligomer molecules which accelerate the healing processes (Muzzarelli 1993). The healing is even faster if tissue culture medium is incorporated in the hydrogel (Kiyozumi et al. 2006). Due to these degradation products, they are also often added to other dressing systems such as alginate fibers (Knill et al. 2004) or grafted polypropylene fabrics (Yang and Lin 2004) to enhance their beneficial effect. Pure chitosan systems are mostly utilized for the preparation of photocrosslinkable hydrogels; this method offers a noninvasive way to protect the wound: the chitosan is chemically modified and after the injection onto the surface it is gelled by UV irradiation (Ishihara et al. 2001; Lu et al. 2010).

While the utilization of hyaluronic acid was in-depth investigated (Price et al. 2005), it is rarely used in hydrogel form. Cellulose-based gels also hold little importance in this application, although there are recent investigations concerning the use of hydrogels of poly(vinyl alcohol) combined with cellulose (Gonzalez et al. 2014) or its acetate derivative (Abd El-Mohdy 2013).

Hydrogels in this field often contain other components which further enhance their positive effects. Additives exhibiting antibacterial activity are especially common as the disinfection of the wound also accelerates the healing. Such effect is easily achieved by the incorporation of various antibiotics, where controlled release ensures its long-term effect. Usually, chitosan-based hydrogels are used for such systems (partly due to the antibacterial activity of native chitosan), although hydrogels based on other carbohydrates like alginate were also investigated to a lesser extent. A wide array of drugs like ciprofloxacin lactate (Yu et al. 2006) sulfadiazine (Mi et al. 2002), nitrofurazone (Kim et al. 2008b), and minocycline (Sung et al. 2010) were used as model molecules. However, there are major efforts to avoid the use of such drugs. Honey is a natural material very effective to help the healing process; it was used as a bioactive component in chitosan/gelatin hydrogels (Wang et al. 2012). Chitosan/fucoidan (sulfated polysaccharide extracted from algae) hydrogels similarly showed superior properties compared to pure chitosan (Sezer et al. 2008).

Various metal nanoparticles also exhibit antimicrobial behavior; thus, such dressings are capable to disinfect the wound. In hydrogels, the nanoparticles are dispersed in the polymer matrix (see 5.6.3.2). Silver nanoparticles are widely known for their antibacterial activity. While there is a large interest in chitosan-based composites (Lu et al. 2008), this property is also useful for polysaccharides which do not exhibit antibacterial activity like cellulose (Maneerung et al. 2008). Madhumathi et al. (2010) also observed faster blood clotting when chitin/silver nanoparticle hydrogel was applied to the wound. However, due to the relatively high cost, cheaper alternatives like metal oxides were also investigated. Archana et al. (2013) utilized TiO₂ nanoparticles to enhance the properties of chitosan–PVP gels as they show minimal cytotoxicity compared to other nanoparticles. Similar results were observed when ZnO was dispersed in chitosan hydrogel (Kumar et al. 2012).

7.1.3 Tissue Engineering

Tissue engineering is a rapidly developing medical field due to growing demand toward organs and tissues, while there is a lack of donors for transplantation. The use of polymer scaffolds for the growth of new tissues offers an alternative route to meet the demand. Hydrogels can fulfill multiple functions as scaffolds, like bulking agents providing structural integrity, but their use for the cell delivery and local controlled release of various drugs is also very important (Drury and Mooney 2003). There are several crucial requirements toward hydrogels in this field, such as good mechanical properties or porosity to allow the three-dimensional growth of the tissue. Biodegradability is another advantageous property of the

polysaccharide-based systems: the enzymatic degradation of the polymer allows the development of the tissue from the encapsulated cells (Nicodemus and Bryant 2008). There is also a large interest toward injectable hydrogels (Kretlow et al. 2007) as they allow a minimally invasive way to deliver the polymer system into the body where the gelation occurs. However, it is also important to take into consideration that *in vivo* and *in vitro* effects of hydrogel scaffolds are different (Yang et al. 2009). There are several routes available for *in vivo* gelation: the use of systems containing reactive components with a well-defined gelation time, photoinitiated crosslinking by UV irradiation (e.g., methacrylated hyaluronic acid), thermal gelation (systems capable of gel formation at body temperature such as chitosan/ β -glycerophosphate-based hydrogels), or ionic crosslinking (most notably alginate-based scaffolds). Another advantage of this method is that the polymer fills the available space; thus, no shaping is required. The delivery of various molecules such as DNA or growth factors can be used to promote the growth of the cells (Chung and Park 2007); these systems proved to be much more effective than agent-free polymer scaffolds (Kolambkai et al. 2011) or individual injection of the bioactive agents (Simmons et al. 2004) due to the slow release. *In vitro* preparation also has its advantages: such 3D scaffolds are suitable for evaluating the effect of new bioactive molecules on the target cells as they provide more precise information than 2D models (Gurski et al. 2009).

The application requirements vary heavily as specific considerations are required depending on the cell type (Kim et al. 2011). Therefore, the literature regarding the application of polysaccharide-based hydrogels in this field is very diverse. There is also a huge variety of the hydrogel systems utilized: such studies rarely involve pure polysaccharide hydrogels with the exception of bacterial cellulose, instead they are used as a component for various copolymers, blends, and composites formed with other polysaccharides, polypeptides, synthetic polymers, or even minerals (Van Vlierberghe et al. 2011). The most important representatives are chitosan (Kim et al. 2008a) and hyaluronic acid (Collins and Birkinshaw 2013), but cellulose (Svensson et al. 2005) and alginate (Venkatesan et al. 2015) show a large potential, as well. As it was mentioned previously, the literature shows large diversity based on the targeted tissue; however, the cartilage (Svensson et al. 2005; Muzzarelli et al. 2012), bone (Venkatesan et al. 2015; LogithKumar et al. 2016), and skin (Fu et al. 2013) tissue engineering is an outstanding field for the application of polysaccharide hydrogels. The number of polysaccharides investigated for the sole delivery of various bioactive molecules is much smaller compared to the preparation of scaffolds for cell delivery: studies focus mostly on hydrogel systems based on hyaluronic acid (Segura et al. 2005a; Ekaputra et al. 2011; Lei et al. 2011) and alginate (Simmons et al. 2004; Krebs et al. 2010; Jeon et al. 2011).

7.1.4 Bulking Agents

An interesting application of hydrogels is their utilization as space-filling materials. Their role in the tissue engineering as bulking agents was previously discussed;

however, their medical utility is not solely limited to this field as they show a large potential in the urology, as well. Urinary incontinence is a common disorder for women and injectable hydrogels allow a minimally invasive way for its treatment. Currently, only hyaluronic acid-based bulking agents are available in the commercial use as polysaccharide-based products (Vaizey and Kamm 2005; Mohr et al. 2013). However, Thornton et al. (2004) also investigated the application of various alginate hydrogels. They noted that covalently crosslinked alginate shows good potential for such use, although very high crosslink density increases the inflammatory response.

There are some advances toward their use in the dietary applications, as well. Such products are utilized to promote the weight loss as an alternative for more drastic strategies like surgery. Hydrogels offer a novel way to achieve such effect compared to the currently available products due to their very high water absorbing capacity. Sannino et al. (2006, 2010) investigated the use of carboxymethylcellulose/hydroxyethylcellulose hydrogels as stomach bulking agents: the copolymer not only showed high water uptake at acidic pH, but the results of tests regarding biocompatibility were also favorable. Another interesting approach for the hydrogel utilization is the preparation of oil bulking agents: by incorporating oil droplets in the gel structure, such systems can serve as replacement for animal fat (Ruiz-Capillas et al. 2013; Herrero et al. 2014).

7.1.5 Contact Lenses

The preparation of contact lenses is another field where the properties of the hydrogels excel. However, studies related to the preparation of polysaccharide-based contact lenses are much more limited. While contact lenses based on chitosan/gelatin composites were successfully synthesized and the products showed good properties (Shi and Tan 2004), no further advancement toward their commercial use was made. On the other hand, the incorporation of non-crosslinked hydrophilic polysaccharides such as hyaluronic acid (Ali and Byrne 2009) and hydroxypropylmethylcellulose (White et al. 2011) in contact lens offers a way to reduce ocular dryness caused by the lenses and reduced protein sorption through their slow release, effectively functioning as a wetting agent on the lens surface. A more long-term effect can be achieved by photocrosslinked hyaluronic acid, where the properties are also affected by the crosslink density (Weeks et al. 2012). Moreover, polysaccharide coatings even allow the incorporation of bioactive molecules to prepare lenses capable of controlled drug delivery (Hu et al. 2014).

7.2 Water Treatment

Wastewater usually contains a large amount of contaminants which are often harmful to the health; thus, they need to be removed from the water. There are

several different methods available, for example, the precipitation of pollutants or the application of adsorbents. In the latter method, hydrogels with superabsorbent properties show a large potential due to their excellent swelling properties, which helps the removal of the contaminants. This requires interaction between the pendant groups on the polymer and the pollutant so that the molecules do not leave with the water from the gel matrix during the immersion. The adsorption can be achieved even by weak interactions, like hydrogen bonds or hydrophobic interactions. However, in presence of charged (usually carboxyl) groups on the polymer backbone, strong ionic interactions can form with pollutant if the latter is also present in dissociated form, leading to significantly better adsorption. In this case, the sorption occurs either by ion exchange with the counterions of the charged groups or by complex formation (Veglio and Beolchini 1997). Charged groups can also be introduced to the gel by various copolymers; thus, the application of a wide variety of the polysaccharide-based gels was investigated. Studies focus mostly on the adsorption of the positively charged pollutants; chitosan-based gels were used for the removal of anionic contaminants, as well.

Heavy metals form one of the most important pollutant groups as industrial wastewater is often contaminated by them. A lot of them are highly toxic even in very low concentration; thus, their removal during the water treatment is crucial (Sud et al. 2008). As the metal ions are positively charged, the polymer must have negatively charged pendant groups to bind the metal ions. The use of Ca-alginate complexes was intensively studied. On the one hand, the pollutants disrupt the ionically crosslinked network; thus, the cations used for the gelation are released to the environment. However, if the alginate complexes are protonated via acid treatment, the metal ions are bound through the ion exchange with the protons, while the egg-box structure formed by the crosslinker ions is not affected by the change in the environment (Ibáñez and Umetsu 2002). The mechanical stability of the gels is also crucial: Wang et al. (2013a) significantly improved the mechanical properties of alginate beads by SiO₂ doping with minimal change in the adsorption capacity. The alginate complexes showed good efficiency for adsorbing several heavy metals like Cr³⁺ or Cd²⁺ from polluted water (Ibáñez and Umetsu 2002, 2004; Papageorgiou et al. 2006). Moreover, studies of the interaction with multi-valent ions (Menakbi et al. 2016) indicate that they are capable of binding other common metal ion contaminants, as well.

Another interesting method is the synthesis of magnetic hydrogels. In this case, various magnetic particles like Fe₃O₄ are coated with the polysaccharide hydrogel, leading to the formation of very small gel particles (Liu et al. 2012) which are easily removed from the treated water by a strong magnetic field.

Dyes are also common pollutants of the wastewater, especially in the textile industry. While not as toxic as heavy metal, several dyes are regarded as hazardous materials due to their health risk. The chemical structure of the dye is a key factor which determines the possible binding mechanism. The application of hydrogel adsorbents for dye adsorption was investigated only for dyes with charged groups. While the interaction of hydroxyl and other groups with the dye molecule also leads

to the adsorption of the pollutant, excellent adsorption can be only achieved when charged groups capable of ionic interactions are present.

For pure polysaccharide hydrogels, the adsorption of anionic dyes was mainly investigated. For this application, chitosan-based hydrogels show a large potential. The amine groups at low pH become protonated; thus, they form ionic bonds with the anionic dye. Opposed to the adsorbents used for cationic dyes, chitosan-based gels show the highest adsorption at acidic pH. Increasing pH leads to the deprotonation of amine groups and the dye is bound only with weak interactions, resulting in a significantly lower adsorption capacity. The adsorption capacity can be further enhanced by additives like surfactants (Chatterjee et al. 2009). Shen et al. (2000) also compared chitosan with chitosan-Fe(III) hydrogels prepared from FeCl_3 solution. The Fe(III) groups can also interact with the dye molecules, improving their sorption. By introducing Fe_3O_4 nanoparticles, the chitosan-Fe(III) complex also exhibited magnetic properties. Cationic hydrogels can be prepared from other polysaccharides, as well. Yan et al. (2009) synthesized hydroxypropylcellulose gels by crosslinking the polymer with epichlorohydrin and ammonia at alkaline pH. The amino groups in the crosslinks led to a high adsorption capacity toward anionic dyes.

Studies related to the removal of cationic dyes are more limited. While alginate hydrogels showed good potential in this field (Aravindhan et al. 2007), most studies investigated the use copolymer systems formed with acrylates (Cai et al. 2013; Zhang et al. 2014a). Composite gels with a mineral component are also commonly used for this application. The cationic dyes interact with the anionic clay through the exchange of cations surrounding the surface (Wang et al. 2004a).

Polymers with charged groups were also utilized for other pollutants. Methylcellulose/acrylamide hydrogels proved to be successful in adsorbing paraquat pesticide from water (Aouada et al. 2009). Chatterjee and Woo (2009) used chitosan hydrogels for the removal of nitrate as an alternative method for denitrification. However, the efficiency of the adsorption heavily depends on the pollutant, as well. Sowyma and Meenakshi (2013) investigated the effect of various ionic molecules on the adsorption: different ions showed different affinity toward the hydrogels; thus, the hydrogels show a degree of selectivity toward certain pollutants. This is advantageous as lower adsorption capacity is required for the removal of target pollutants during water treatment.

7.3 Agricultural Applications

Agricultural applications of superabsorbents also show a large potential. In the present, most commercially available products are acrylate-based superabsorbents; thus, agricultural studies mostly focus on their utilization, as well. However, recently there is a growing interest toward the application of renewable resources as a greener alternative. A major advantage of the carbohydrate-based superabsorbents is the excellent biodegradability in soil. Studies related to the agricultural use can be

separated into two categories: delivery of chemicals and soil conditioning. As the cost efficiency is a major factor due to the volume of the hydrogels required for the modification of the soil, only the most abundant polysaccharides are of large interest.

7.3.1 Fertilizer Release

The delivery of various compounds into the soil in a controlled manner is an application analogous with the drug delivery in pharmacy: the gel allows the slow release of the chemicals; thus, they exhibit their beneficial effect over a long period of time. As the bioactive agent is enclosed in the polymer matrix, the gel network needs to expand to allow the release of the incorporated molecule. While in the drug delivery can be controlled by a wide array of environmental parameters such as the pH or temperature, in the agriculture the gel expansion is controlled by the presence of moisture, leading to the swelling of the hydrogel, as other properties show a large variance between the soil types. The incorporated molecule can have multiple functions: the addition of fertilizers improves the plant growth, while other agents like pesticides and fungicides offer pest control. Such applications were widely studied with acrylate-based gels (Rudzinski et al. 2002); investigations related to the polysaccharide-based ones are more limited and even then, such systems are mainly copolymers formed with synthetic polymers. Characteristically acrylates are added as copolymers, most notable being the acrylic acid and acrylamide. However, other hydrophilic polymers such as the PVA (Han et al. 2009; Jamnongkan and Kaewpirom 2010; Li et al. 2015) are also relatively frequent components.

Urea, a common nitrogen fertilizer is the most common model molecule for the investigation of desorption kinetics, although the release of other components like phosphates was also studied (Rashidzadeh and Olad 2014). There are two major methods for the incorporation of the fertilizer: either the bioactive agent is added as a powder during the gel synthesis, or the crosslinked sample is immersed in its solution to allow the sorption. In the latter case, composites containing clay minerals are common, as the inorganic component improves the sorption of the organic molecule (Bortolin et al. 2013). Moreover, the interaction also leads to slower release compared to pure hydrogels (Rashidzadeh et al. 2014). For the production of fertilizers, copolymers of alginate (Abd El-Rehim 2006; Wang et al. 2013e) and chitosan (Jamnongkan and Kaewpirom 2010) are of major interest due to their advantageous properties. These polymers not only offer good biodegradability, but degradation products like oligo-alginates also promote the plant growth (González et al. 2012). A novel method for the preparation of chitosan-based nanoparticle fertilizers was also created, where the particles were formed with an inner chitosan and an outer acrylate coating (Wu and Liu 2008; Corradini et al. 2010). The application of starch (Guo et al. 2005; Han et al. 2009) and cellulose-based copolymers (Bortolin et al. 2012, 2013; Li et al. 2015) was also investigated due to their lower cost. Sulfonated starch/PAA hydrogels were used to prepare a phosphate fertilizer from phosphate rock, a normally difficult-to-utilize phosphorus source

(Zhong et al. 2013). Recently, pure polysaccharide-based gels were also investigated for slow fertilizer delivery. Both ionically (Davidson et al. 2013) and chemically (Ni et al. 2011) crosslinked cellulose derivative superabsorbents proved to be a viable alternative for the copolymer-based fertilizers. Interestingly, chemical cellulose acetate hydrogels crosslinked with polycarboxylic acid were also studied besides the usual cellulose ethers (Senna et al. 2015).

7.3.2 Pest Control

While the focus of the studies is on the application as fertilizers, hydrogels also allow the controlled release of other chemicals, which offer protection against pests (pesticide), weeds (herbicide), and fungi (fungicide). The largest interest is shown toward the controlled release of pesticides. The incorporation of the molecules is similar to the method detailed for fertilizers. A wide array of pesticides were examined in such experiments, and the release kinetics was also determined. This is important because the chemical structure of the bioactive agents also affects the release kinetics (Abd El-Mohdy et al. 2011). First, such experiments were carried out with starch matrices crosslinked with formaldehyde (Kulkarni et al. 1999; Kumbar et al. 2001), but later the interest shifted toward alginate-based systems. Both ionically and chemically crosslinked alginate system showed good potential for the incorporation. While Ca^{2+} cations are the standard crosslinkers of the physical gels (Roy et al. 2009). Işıklan (2007) observed that by using different multivalent cations, the release kinetics is controllable. Chemical crosslinking with glutaraldehyde was utilized for blends with other polysaccharides and polypeptides (Kulkarni et al. 2001; Işıklan 2006). Chitosan-based controlled release systems were also prepared: while Rao et al. (2006) used AAm-g-PVA IPN structured gels, Yi et al. (2011) avoided the use of crosslinkers and copolymers by using azide functionalized photocrosslinkable chitosan.

Herbicides were investigated to a smaller extent, despite their encapsulation in starch already being studied decades ago (Trimmell et al. 1985). Cellulose derivative-based gels show a large potential in this field. In earlier experiments, the copolymers of hydroxyethylcellulose were used (Rehab et al. 1991), but recently the carboxymethylcellulose/clay gels became more important: the easy ionic crosslinking through the carboxyl groups renders the copolymers redundant (Li et al. 2008, 2009). The presence of clay not only slows the release of the agent, but its rate can be adjusted by the clay type and ratio. The encapsulation also leads to lower environmental impact: Grillo et al. (2014) observed that herbicide in chitosan gels showed lower toxicity despite its activity being not affected.

Studies related to the controlled release of fungicides are few. Singh et al. (2007, 2009a, b) investigated the application of various starch gels in this field. While copolymers with acrylates were also prepared, the addition of ionically crosslinked alginate proved to be a good alternative for the synthetic polymer component. Experiments were carried out with thiram as a model fungicide; the release rate was controlled by the crosslink density.

7.3.3 Soil Conditioning

Another application field with a growing significance is the soil conditioning: the goal is to improve the water retention of the soil, thus increasing the yield of the agricultural plants and lowering the need of the irrigation. Moreover, such modification may allow cultivation even in lands with very poor retention such as sandy soil. Superabsorbents are capable of trapping large amounts of water, thus decreasing the gravitational drain of free water after the irrigation. However, the water is not strongly bound in the gel structure; thus, it is available for the plants. As gels with superabsorbent properties are used usually for the controlled release of bioactive agents, a large part of the related studies also investigated the effect of the gels on the water retention and plant growth. Similarly, the majority of such experiments used polysaccharide/acrylate systems as model superabsorbents. Acrylamide is an especially popular co-monomer which was used for copolymerization with carboxymethylcellulose (Ibrahim et al. 2007), starch (Qiao et al. 2016) and alginate (Abd El-Rehim 2006). The application of pure polysaccharide superabsorbents was also studied. Nnadi and Brave (2011) prepared carboxymethylcellulose/starch gels by pregelatinization and ionic crosslinking. The superabsorbent mixed into the soil in 0.3–0.6% concentration significantly promoted the plant growth. Biodegradability is also a crucial factor in this field. Superabsorbent gels from succinic acid-crosslinked starch (Yoshimura et al. 2006) showed similar or only slightly slower biodegradability than pure starch depending on the synthesis conditions. Alginate and chitosan hydrogels are also very good candidates for this application: as mentioned previously, the products of the hydrogel degradation promote the plant growth, leading to more desirable properties (Abd El-Rehim 2006). In the future, chitosan-based gels might also have a larger role, as they show fungicidal activity (Badawy et al. 2004).

7.4 Other Applications

The potential application of hydrogels is much wider than the fields covered so far in this section. However, there are only a few studies related to these uses concerning polysaccharide-based hydrogels. For example, while the application of polysaccharides in catalysis was investigated, especially in case of chitosan (Guibal 2005), they are not utilized in hydrogel form. In the few available studies, the polysaccharide hydrogels are used as a matrix for the immobilization of the nanoparticle catalyst (Saha et al. 2010; Wu et al. 2012b). In some cases, the hydrogel itself catalyzes the reaction: Reddy et al. (2006) used chitosan gel as a catalyst for aldol and Knoevenagel reactions. In sensors, the hydrogel functions as the structural component; glucose (Brown et al. 2005), phenol (Zhang and Ji 2010), and enzyme-sensing (Ebrahimi and Schonherr 2014) systems were prepared from chitosan-based hydrogels. Another interesting utility is the synthesis of self-healing gels. In such systems, defects and cracks can heal over time; thus, the structural

integrity is maintained—this is very advantageous in numerous applications to improve the performance of the material (Thakur and Kessler 2015). Although there is little literature available for polysaccharide-based self-healing hydrogels, recently there is a rapidly growing interest in their utilization as multiple polysaccharides like alginate (Miao et al. 2015; Pettignano et al. 2017), cellulose (Zheng et al. 2015; Liu et al. 2016) and chitosan derivatives (Wei et al. 2015) proved to be capable to form such systems.

8 Conclusions

The application of polysaccharides for hydrogel formation has a bright future. They are not only cheap and abundant materials, but a wide array of methods are available for the gel formation. The large variety in the functional groups results in properties advantageous in several applications, such as the responsive behavior. Moreover, the easy chemical modification and mixing with other natural polymers allow a convenient way to achieve the desired properties. Such systems offer a more environmentally friendly and sustainable alternative for the acrylate-based products. Currently, the main interest lies in copolymers and blends with synthetic polymers; thus, the advantages of both components can be utilized simultaneously. However, the trend is shifting toward pure polysaccharide and other natural polymer-based systems as they proved to be a good substitute for acrylates in an increasing number of fields.

References

- Aalaie J, Vasheghani-Farahani E, Rahmatpour A, Semzarszadeh MA (2013) Gelation rheology and water absorption behavior of semi-interpenetrating polymer networks of polyacrylamide and carboxymethyl cellulose. *J Macromol Sci B* 52:604–613
- Abad LV, Relleve LS, Aranilla CT, Dela Rose AM (2003) Properties of radiation synthesized PVP-kappa carrageenan hydrogel blends. *Radiat Phys Chem* 68:901–908
- Abd Alla SG, Sen M, El-Naggar AWM (2012) Swelling and mechanical properties of superabsorbent hydrogels based on Tara gum/acrylic acid synthesized by gamma irradiation. *Carbohydr Polym* 89:478–485
- Abd El-Mohdy HL (2007) Water sorption behavior of CMC/PAM hydrogels prepared by γ -irradiation and release of potassium nitrate as agrochemical. *React Funct Polym* 67:1094–1102
- Abd El-Mohdy HL (2013) Radiation synthesis of nanosilver/poly vinyl alcohol/cellulose acetate/gelatin hydrogels for wound dressing. *J Polym Res* 20:177–188
- Abd El-Mohdy HL, Hegazy EA, El-Nesr EM, El-Wahab MA (2011) Control release of some pesticides from starch/(ethylene glycol-co-methacrylic acid) copolymers prepared by γ -irradiation. *J Appl Polym Sci* 122:1500–1509
- Abd El-Rehim HA (2006) Characterization and possible agricultural application of acrylamide/sodium alginate crosslinked hydrogels prepared by ionizing radiation. *J Appl Polym Sci* 101:3572–3580

- Abdulmola NA, Hember MWN, Richardson RK, Morris ER (1996) Application of polymer blending laws to starch-gelatin composites. *Carbohydr Polym* 31:53–63
- Ahmed EM (2015) Hydrogel: preparation, characterization, and applications: a review. *J Adv Res* 6:105–121
- Akar E, Altunışık A, Seki Y (2012) Preparation of pH- and ionic-strength responsive biodegradable fumaric acid crosslinked carboxymethyl cellulose. *Carbohydr Polym* 90:1634–1641
- Ali M, Byrne ME (2009) Controlled release of high molecular weight hyaluronic acid from molecularly imprinted hydrogel contact lenses. *Pharm Res* 26:714–726
- Alupeı IC, Popa M, Hamcerencu M, Abadie MJM (2002) Superabsorbant hydrogels based on xanthan and poly(vinyl alcohol): 1. The study of the swelling properties. *Eur Polym J* 38:2313–2320
- Alvarez-Lorenzo C, Concheiro A, Dubovik AS, Grinberg NV, Burova TV, Grinberg VY (2005) Temperature-sensitive chitosan-poly(*N*-isopropylacrylamide) interpenetrated networks with enhanced loading capacity and controlled release properties. *J Control Release* 102:629–641
- Amin MCIM, Ahmad N, Halib N, Ahmad I (2012) Synthesis and characterization of thermos- and pH-responsive bacterial cellulose/acrylic acid hydrogels for drug delivery. *Carbohydr Polym* 88:465–473
- Anbergen U, Oppermann W (1990) Elasticity and swelling behaviour of chemically crosslinked cellulose ethers in aqueous systems. *Polymer* 31:1854–1858
- Anidhuran TS, Tharun AR, Rejeena SR (2011) Investigation on poly(methacrylic acid)-grafted cellulose/bentonite superabsorbent composite: synthesis, characterization, and adsorption characteristics of bovine serum albumin. *Ind Eng Chem Res* 50:1866–1874
- Aouada FA, Pan Z, Orts WJ, Mattoso LHC (2009) Removal of paraquat pesticide from aqueous solutions using a novel adsorbent material based on acrylamide and methylcellulose hydrogels. *J Appl Polym Sci* 114:2139–2148
- Aravindhnan R, Fathima NN, Rao JR, Nair BU (2007) Equilibrium and thermodynamic studies on the removal of basic black dye using calcium alginate beads. *Colloid Surf* 299:232–238
- Archana D, Singh BK, Dutta J, Dutta PK (2013) In vivo evaluation of chitosan-PVP-titanium dioxide nanocomposite as wound dressing material. *Carbohydr Polym* 95:530–539
- Aroguz AZ, Baysal K, Adiguzel Z, Baysal BM (2014) Alginate/polyoxyethylene and alginate/gelatin hydrogels: preparation, characterization, and application in tissue engineering. *Appl Biochem Biotechnol* 173:433–448
- Athawale VD, Lele V (2000) Factors influencing absorbent properties of saponified starch-g-(acrylic acid-co-acrylamide). *J Appl Polym Sci* 77:2480–2485
- Awad HA, Wickham MQ, Leddy HA, Gimble JM, Guilak F (2004) Chondrogenic differentiation of adipose-derived adult stem cells in agarose, alginate, and gelatin scaffolds. *Biomaterials* 25:3211–3222
- Awadhiya A, Kumar D, Verma V (2016) Crosslinking of agarose bioplastic using citric acid. *Carbohydr Polym* 151:60–67
- Badawy MEI, Rabea EI, Rogge TM, Stevens CV, Smagge G, Steurbaut W, Höfte M (2004) Synthesis and fungicidal activity of new *O*, *N*-acyl chitosan derivatives. *Biomacromol* 5:589–595
- Bajpai AK, Mishra A (2004) Ionizable interpenetrating polymer networks of carboxymethyl cellulose and polyacrylic acid: evaluation of water uptake. *J Appl Polym Sci* 93:2054–2065
- Balakrishnan B, Mohanty M, Umashankar PR, Jayakrishnan A (2005) Evaluation of an in situ forming hydrogel wound dressing based on oxidized alginate and gelatin. *Biomaterials* 26:6335–6342
- Banerjee S, Singh S, Bhattacharya SS, Chattopadhyay P (2013) Trivalent ion cross-linked pH-sensitive alginate-methyl cellulose hydrogel beads from aqueous template. *Int J Biol Macromol* 57:297–307
- Bao Y, Ma J, Li N (2011) Synthesis and swelling behaviors of sodium carboxymethyl cellulose-g-poly(AA-co-AM-co-AMPS)/MMT superabsorbent hydrogel. *Carbohydr Polym* 84:76–82

- Barbucci R, Magnani A, Consumi M (2000) Swelling behavior of carboxymethylcellulose hydrogels in relation to cross-linking, pH, and charge density. *Macromolecules* 33:7475–7480
- Bardajee GR, Hooshyar Z, Zehtabi F, Pourjavadi A (2012) A superabsorbent hydrogel network based on poly ((2-dimethylaminoethyl) methacrylate) and sodium alginate obtained by γ -radiation: synthesis and characterization. *Iran Polym J* 21:829–836
- Barkhordari S, Yadollahi M, Namazi H (2014) pH-sensitive nanocomposite hydrogel beads based on carboxymethyl cellulose/layered double hydroxide as drug delivery systems. *J Polym Res* 21:454–462
- Bejenariu A, Popa M, Le Cerf D, Picton L (2008) Stiffness xanthan hydrogels: synthesis, swelling characteristics and controlled release properties. *Polym Bull* 61:631–641
- Bejenariu A, Popa M, Dulong V, Picton L, Le Cerf D (2009) Trisodium trimetaphosphate crosslinked xanthan networks: synthesis, swelling, loading and releasing behavior. *Polym Bull* 62:525–538
- Bencherif SA, Srinivasan A, Horkay F, Hollinger JO, Matyjaszewski K, Washburn NR (2008) Influence of the degree of methacrylation on hyaluronic acid hydrogel properties. *Biomaterials* 29:1739–1749
- Berger J, Reist M, Mayer JM, Felt O, Gurny R (2004) Structure and interactions in chitosan hydrogels formed by complexation or aggregation for biomedical applications. *Eur J Pharm Biopharm* 57:35–52
- Bhattarai N, Ramay HR, Gunn J, Matsen FA, Zhang M (2005) PEG-grafted chitosan as an injectable thermosensitive hydrogel for sustained protein release. *J Control Release* 103: 609–624
- Bhattarai N, Gunn J, Zhang M (2010) Chitosan-based hydrogels for controlled, localized drug delivery. *Adv Drug Deliver Rev* 62:83–99
- Bidgoli H, Zamani A, Taherzadeh MJ (2010) Effect of carboxymethylation conditions on the water-binding capacity of chitosan-based superabsorbents. *Carbohydr Res* 345:2683–2689
- Boateng JS, Matthews KH, Stevens HNE, Eccleston GM (2008) Wound healing dressings and drug delivery systems: a review. *J Pharm Sci* 97:2892–2923
- Bogacheva TY, Morris VJ, Ring SG, Hedley CL (1998) The granular structure of C-type pea starch and its role in gelatinization. *Biopolymers* 45:323–332
- Boissesson MRD, Leonard M, Hubert P, Marchal P, Steuert A, Castel C, Favre E, Dellacherie E (2004) Physical alginate hydrogels based on hydrophobic or dual hydrophobic/ionic interactions: bead formation, structure, and stability. *J Colloid Interf Sci* 273:131–139
- Boppana R, Kulkarni RV, Mutalik SS, Setty CM, Sa B (2010) Interpenetrating network hydrogel beads of carboxymethylcellulose and egg albumin for controlled release of lipid lowering drug. *J Microcapsul* 27:337–344
- Bortolin A, Aouada FA, de Moura MR, Ribeiro C, Longo E, Mattoso LHC (2012) Application of polysaccharide hydrogels in adsorption and controlled-extended release of fertilizers processes. *J Appl Polym Sci* 123:2291–2298
- Bortolin A, Aouada FA, Mattoso LHC, Ribeiro C (2013) Nanocomposite PAAm/methyl cellulose/montmorillonite hydrogel: evidence of synergistic effects for the slow release of fertilizers. *J Agric Food Chem* 61:7431–7439
- Brigham MD, Bick A, Lo E, Bendali A, Burdick JA, Khademhosseini A (2009) Mechanically robust and bioadhesive collagen and photocrosslinkable hyaluronic acid semi-interpenetrating networks. *Tissue Eng A* 15:1645–1653
- Brown JQ, Srivastava R, McShane MJ (2005) Encapsulation of glucose oxidase and an oxygen-quenched fluorophore in polyelectrolyte-coated calcium alginate microspheres as optical glucose sensor systems. *Biosens Bioelectron* 21:212–216
- Bryant SJ, Davis-Arehard KA, Luo N, Shoemaker RK, Arthur JA, Anseth KS (2004) Synthesis and characterization of photopolymerized multifunctional hydrogels: water-soluble poly(vinyl alcohol) and chondroitin sulfate macromers for chondrocyte encapsulation. *Macromolecules* 37:6726–6733
- Bueno VB, Bentini R, Catalini LH, Petri DFS (2013) Synthesis and swelling behavior of xanthan-based hydrogels. *Carbohydr Polym* 92:1091–1099

- Buléon A, Colonna P, Planchot V, Ball S (1998) Starch granules: structure and biosynthesis. *Int J Biol Macromol* 23:85–112
- Burdick JA, Prestwich GD (2011) Hyaluronic acid hydrogels for biomedical applications. *Adv Mater* 23:41–56
- Burdick JA, Chung C, Jia X, Randolph MA, Langer R (2005) Controlled degradation and mechanical behavior of photopolymerized hyaluronic acid networks. *Biomacromol* 6:386–391
- Cai L, Zhang L (2005) Rapid dissolution of cellulose in LiOH/urea and NaOH/urea aqueous solutions. *Macromol Biosci* 5:539–548
- Cai J, Zhang L (2006) Unique gelation behavior of cellulose in NaOH/urea aqueous solution. *Biomacromol* 7:183–189
- Cai H, Zhang ZP, Sun PC, He BL, Zhu XX (2005) Synthesis and characterization of thermo- and pH-sensitive hydrogels based on chitosan-grafted *N*-isopropylacrylamide via γ -radiation. *Radiat Phys Chem* 74:26–30
- Cai T, Yang Z, Li H, Yang H, Li A, Cheng R (2013) Effect of hydrolysis degree of hydrolyzed polyacrylamide grafted carboxymethyl cellulose on dye removal efficiency. *Cellulose* 20:2605–2614
- Camci-Unal G, Cuttica D, Annabi N, Demarchi D, Khademhosseini A (2013) Synthesis and characterization of hybrid hyaluronic acid-gelatin hydrogels. *Biomacromol* 14:1085–1092
- Carlsson A, Karlström G, Lindman B (1990) Thermal gelation of nonionic cellulose ethers and ionic surfactants in water. *Colloid Surf* 47:147–165
- Cascone MG, Maltinti S, barbani N, Laus M (1999) Effect of chitosan and dextran on the properties of poly(vinyl alcohol) hydrogels. *J Mater Sci Mater M* 10:431–435
- Celis R, Adelino MA, Hermosin MC, Cornejo J (2012) Montmorillonite-chitosan bionanocomposites as adsorbents of the herbicide clopyralid in aqueous solution and soil/water suspensions. *J Hazard Mater* 209–210:67–76
- Céspedes FF, Sánchez MV, Garcia SP, Pérez MF (2007) Modifying sorbents in controlled release formulations to prevent herbicides pollution. *Chemosphere* 69:785–794
- Chang Y, Xiao L, Tang Q (2002) Preparation and characterization of a novel thermosensitive hydrogel based on chitosan and gelatin blends. *J Appl Polym Sci* 113:400–407
- Chang C, Lue A, Zhang L (2008) Effects of crosslinking methods on structure and properties of cellulose/PVA hydrogels. *Macromol Chem Phys*
- Chang C, Duan B, Zhang L (2009) Fabrication and characterization of novel macroporous cellulose–alginate hydrogels. *Polymer* 50:5467–5473
- Chang C, Duan B, Cai J, Zhang L (2010a) Superabsorbent hydrogels based on cellulose for smart swelling and controllable delivery. *Eur Polym J* 46:92–100
- Chang C, Zhang L, Zhou J, Zhang L, Kennedy JF (2010b) Structure and properties of hydrogels prepared from cellulose in NaOH/urea aqueous solutions. *Carbohydr Polym* 82:122–127
- Chang C, Chen S, Zhang L (2011a) Novel hydrogels prepared via direct dissolution of chitin at low temperature: structure and biocompatibility. *J Mater Chem* 21:3865–3871
- Chang C, Han K, Zhang L (2011b) Structure and properties of cellulose/poly(*N*-isopropylacrylamide) hydrogels prepared by IPN strategy. *Polym Adv Technol* 22:1329–1334
- Chang C, Peng N, He M, Teramoto Y, Nishio Y, Zhang L (2013) Fabrication and properties of chitin/hydroxyapatite hybrid hydrogels as scaffold nano-materials. *Carbohydr Polym* 91:7–13
- Chatterjee S, Woo SH (2009) The removal of nitrate from aqueous solutions by chitosan hydrogel beads. *J Hazard Mater* 164:1012–1018
- Chatterjee S, Lee DS, Lee MW, Woo SH (2009) Congo red adsorption from aqueous solutions by using chitosan hydrogel beads impregnated with nonionic or anionic surfactant. *Bioresour Technol* 100:3862–3868
- Chauhan GS, Lal H, Mahajan S (2004) Synthesis, characterization, and swelling responses of poly(*N*-isopropylacrylamide)- and hydroxypropyl cellulose-based environmentally sensitive biphasic hydrogels. *J Appl Polym Sci* 91:479–488
- Chellat F, Tabrizian M, Dumitriu S, Chornet E, Magny P, Rivard CH, Yahia L (2000) In vitro and in vivo biocompatibility of chitosan-xanthan polyionic complex. *J Biomed Mater Res* 51:107–116

- Chen JP, Cheng TH (2006) Thermo-responsive chitosan-graft-poly(*N*-isopropylacrylamide) injectable hydrogel for cultivation of chondrocytes and meniscus cells. *Macromol Biosci* 6:1026–1039
- Chen T, Embree HD, Brown EM, Taylor MM, Payne GF (2003) Enzyme-catalyzed gel formation of gelatin and chitosan: potential for in situ applications. *Biomaterials* 24:2831–2841
- Chen SC, Wu YC, Mi FL, Lin YH, Yu LC, Sung HW (2004) A novel pH-sensitive hydrogel composed of *N*, *O*-carboxymethyl chitosan and alginate cross-linked by genipin for protein drug delivery. *J Control Release* 96:285–300
- Chen RN, Wang GM, Chen CH, Ho HO, Sheu MT (2006) Development of *N*, *O*-(carboxymethyl) chitosan/collagen matrixes as a wound dressing. *Biomaterials* 7:1058–1064
- Cheng Y, Lu J, Liu S, Zhao P, Lu G, Chen J (2014) The preparation, characterization and evaluation of regenerated cellulose/collagen composite hydrogel films. *Carbohydr Polym* 107:57–64
- Chenite A, Buschmann M, Wang D, Chaput C, Kandani N (2001) Rheological characterisation of thermogelling chitosan/glycerol-phosphate solutions. *Carbohydr Polym* 46:39–47
- Chiaoprakobkij N, Sanchavanakit N, Subbalekha K, Pavasant P, Phisalaphong M (2011) Characterization and biocompatibility of bacterial cellulose/alginate composite sponges with human keratinocytes and gingival fibroblasts. *Carbohydr Polym* 85:548–553
- Chiu LLY, Radisic M (2011) Controlled release of thymosin β 4 using collagen–chitosan composite hydrogels promotes epicardial cell migration and angiogenesis. *J Control Release* 155:376–385
- Chung HJ, Park TG (2007) Surface engineered and drug releasing pre-fabricated scaffolds for tissue engineering. *Adv Drug Deliver Rev* 59:249–262
- Clough MT, Geyer K, Hunt PA, Son S, Vagt U, Welton T (2015) Ionic liquids: not always innocent solvents for cellulose. *Green Chem* 17:231–243
- Collins MN, Birkinshaw C (2008) Physical properties of crosslinked hyaluronic acid hydrogels. *J Mater Sci Mater Med* 19:3335–3343
- Collins MN, Birkinshaw C (2011) Morphology of crosslinked hyaluronic acid porous hydrogels. *J Appl Polym Sci* 120:1040–1049
- Collins MN, Birkinshaw C (2013) Hyaluronic acid based scaffolds for tissue engineering—a review. *Carbohydr Polym* 92:1262–1279
- Corobea MC, Muhulet O, Miculescu F, Antoniac IV, Vuluga Z, Florea D et al (2016) Novel nanocomposite membranes from cellulose acetate and clay-silica nanowires. *Polym Adv Technol* 27(12):1586–1595
- Coronado R, Pekerar S, Lorenzo AT, Sabino MA (2011) Characterization of thermo-sensitive hydrogels based on poly(*N*-isopropylacrylamide)/hyaluronic acid. *Polym Bull* 67:101–124
- Corradini E, de Moura MR, Mattoso KHC (2010) A preliminary study of the incorporation of NPK fertilizer into chitosan nanoparticles. *Express Polym Lett* 4:509–515
- Costa-Júnior ES, Barbose-Stancioli EF, Mansur AAP, Vasconcelos WL, Mansur HS (2009) Preparation and characterization of chitosan/poly(vinyl alcohol) chemically crosslinked blends for biomedical applications. *Carbohydr Polym* 76:472–481
- Crescenzi V, Francescangeli A, Talenti A (2002) New gelatin-based hydrogels via enzymatic networking. *Biomacromol* 3:1384–1391
- Cui L, Jia J, Guo Y, Liz Y, Zhu P (2014) Preparation and characterization of IPN hydrogels composed of chitosan and gelatin cross-linked by genipin. *Carbohydr Polym* 99:31–38
- Das A, Wadhwa S, Srivastava AK (2006) Cross-linked guar gum hydrogel discs for colon-specific delivery of ibuprofen: Formulation and in vitro evaluation. *Drug Deliver* 12:139–142
- Dash R, Foston M, Ragauskas AJ (2013) Improving the mechanical and thermal properties of gelatin hydrogels cross-linked by cellulose nanowhiskers. *Carbohydr Polym* 91:638–645
- Davidson DW, Verma MS, Gu FX (2013) Controlled root targeted delivery of fertilizer using an ionically crosslinked carboxymethyl cellulose hydrogel matrix. *SpringerPlus* 2:318–326
- Dawlee S, Sugandhi A, Balakrishnan B, Labarre D, Jayakrishnan A (2005) Oxidized chondroitin sulfate-cross-linked gelatin matrixes: a new class of hydrogels. *Biomacromol* 6:2040–2048

- de Cunha CB, Klumpers DD, Li WA, Koshy ST, Weaver JC, Chaudhuri O, Granja PL, Mooney DJ (2014) Influence of the stiffness of three-dimensional alginate/collagen-I interpenetrating networks on fibroblast biology. *Biomaterials* 35:8927–8936
- de la Torre PM, Torrado S, Torrado S (2003) Interpolymer complexes of poly(acrylic acid) and chitosan: influence of the ionic hydrogel-forming medium. *Biomaterials* 24:1459–1468
- Demitri C, Sole RD, Scaler F, Sannino A, Vasapollo G, Maffezzoli A, Ambrosio L, Nicolais L (2008) Novel superabsorbent cellulose-based hydrogels crosslinked with citric acid. *J Appl Polym Sci* 110:2453–2460
- Deng C, Zhang P, Vulesevic B, Kuraitis D, Li F, Yang AF, Griffith M, Ruel M, Suuronen EJ (2010) A collagen–chitosan hydrogel for endothelial differentiation and angiogenesis. *Tissue Eng A* 16:3099–3109
- Dergunov SA, Nam IK, Mun GA, Nurkeeva ZS, Shaikhutdinov EM (2005) Radiation synthesis and characterization of stimuli-sensitive chitosan-polyvinyl pyrrolidone hydrogels. *Radiat Phys Chem* 72:619–623
- Desbrières J, Hirrien M, Rinaudo M (1998) A calorimetric study of methylcellulose gelation. *Carbohydr Polym* 37:145–152
- Dhiman PK, Kaur I, Mahajan RK (2008) Synthesis of a cellulose-grafted polymeric support and its application in the reductions of some carbonyl compounds. *J Appl Polym Sci* 108:99–111
- Domard A, Rinaudo M (1983) Preparation and characterization of fully deacetylated chitosan. *Int J Biol Macromol* 5:49–52
- Donati I, Paoletti S (2009) Material properties of alginates. In: Rehm BHA (ed) *Alginates: biology and applications*. Springer, Berlin, pp 1–54
- Dong Z, Wang Q, Du Y (2006) Alginate/gelatin blend films and their properties for drug controlled release. *J Membrane Sci* 280:37–44
- Doria-Serrano MC, Riva-Palacio G, Ruiz-Trevino FA, Hernández-Esparza M (2002) Poly(*N*-vinyl pyrrolidone)–calcium alginate (PVP-Ca-alg) composite hydrogels. Physical properties and activated sludge immobilization for wastewater treatment. *Ind Eng Chem Res* 41:3163–3168
- Dragan ES (2014) Design and applications of interpenetrating polymer network hydrogels: a review. *Chem Eng J* 243:572–590
- Draye JP, Delaey B, van de Voorde A, van den Bulcke A, de Reu B, Schacht E (1998) In vitro and in vivo biocompatibility of dextran dialdehyde cross-linked gelatin hydrogel films. *Biomaterials* 19:1677–1687
- Drury JL, Mooney DJ (2003) Hydrogels for tissue engineering: scaffold design variables and applications. *Biomaterials* 24:4337–4351
- Duan B, Hockaday LA, Kang KH, Butcher JT (2013) 3D bioprinting of heterogeneous aortic valve conduits with alginate/gelatin hydrogels. *J Biomed Mater Res A* 101:1255–1264
- Dumitriu S, Magny P, Montané D, Vidal PF, Chornet E (1994) Polyionic hydrogels obtained by complexation between xanthan and chitosan: their properties as supports for enzyme immobilization. *J Bioact Compat Pol* 9:184–209
- Dumitriu RP, Mitchell GR, Vasile C (2010) Multi-responsive hydrogels based on *N*-isopropylacrylamide and sodium alginate. *Polym Int* 60:222–233
- Dupont AL (2003) Cellulose in lithium chloride/*N*, *N*-dimethylacetamide, optimisation of a dissolution method using paper substrates and stability of the solutions. *Polymer* 44:4117–4126
- Ebrahimi MMS, Schonherr H (2014) Enzyme-sensing chitosan hydrogels. *Langmuir* 30:7842–7850
- Eiselt P, Lee KY, Mooney DJ (1999) Rigidity of two-component hydrogels prepared from alginate and poly(ethylene glycol)–diamines. *Macromolecules* 32:5561–5566
- Ekaputra AK, Prestwich GD, Cool SM, Huttmacher DW (2011) The three-dimensional vascularization of growth factor-releasing hybrid scaffold of poly(ϵ -caprolactone)/collagen fibers and hyaluronic acid hydrogel. *Biomaterials* 32:8108–8117
- Ekici S (2011) Intelligent poly(*N*-isopropylacrylamide)-carboxymethyl cellulose full interpenetrating polymeric networks for protein adsorption studies. *J Mater Sci* 46:2843–2850

- El Salmawi KM, Ibrahim SAM (2011) Characterization of superabsorbent carboxymethylcellulose/clay hydrogel prepared by electron beam irradiation. *Macromol Res* 19:1029–1034
- El-Din HMN, Abd Alla SG, El-Naggar AWM (2010) Swelling and drug release properties of acrylamide/carboxymethyl cellulose networks formed by gamma irradiation. *Radiat Phys Chem* 79:725–730
- El-Din HMN, El-Naggar AWM, Abu-El Fadle FI (2013) Radiation synthesis of pH-sensitive hydrogels from carboxymethylcellulose/poly(ethylene oxide) blends as drug delivery systems. *Int J Polym Mater Polym Biomater* 62:711–718
- Eldridge JE, Ferry JD (1954) Studies of the cross-linking process in gelatin gels. III. Dependence of melting point on concentration and molecular weight. *J Phys Chem* 58:992–995
- El-Salmawi KM (2007) Application of polyvinyl alcohol (PVA)/carboxymethyl cellulose (CMC) hydrogel produced by conventional crosslinking or by freezing and thawing. *J Macromol Sci A* 44:619–624
- Esposito F, Del Nobile MA, Mensitieri G, Nicolais L (1996) Water sorption in cellulose-based hydrogels. *J Appl Polym Sci* 60:2403–2407
- Esposito A, Sannino A, Cozzolino A, Quinriliano SN, Lamberti M, Ambrosio L, Nicolais L (2005) Response of intestinal cells and macrophages to an orally administered-PEG based polymer as a potential treatment for intractable edemas. *Biomaterials* 26:4101–4110
- Fadnavis NW, Sheelu G, Kumar BM, Bhalariao MU, Desphande AA (2003) Gelatin blends with alginate: gels for lipase immobilization and purification. *Biotechnol Prog* 19:557–564
- Fei B, Wach RA, Mitomo H, Yoshii F, Kume T (2000) Hydrogel of biodegradable cellulose derivatives. I. Radiation-induced crosslinking of CMC. *J Appl Polym Sci* 78:278–283
- Fekete T, Borsa J, Takács E, Wojnárovits L (2014) Synthesis of cellulose derivative based superabsorbent hydrogels by radiation induced crosslinking. *Cellulose* 21:4157–4165
- Fekete T, Borsa J, Takács E, Wojnárovits L (2016a) Synthesis of cellulose-based superabsorbent hydrogels by high-energy irradiation in the presence of crosslinking agent. *Radiat Phys Chem* 118:114–119
- Fekete T, Borsa J, Takács E, Wojnárovits L (2016b) Synthesis of carboxymethylcellulose/acrylic acid hydrogels with superabsorbent properties by radiation-initiated crosslinking. *Radiat Phys Chem* 124:135–139
- Feng L, Chen Z (2008) Research progress on dissolution and functional modification of cellulose in ionic liquids. *J Mol Liq* 142:1–5
- Ferreira L, Gil MH, Cabrita AM, Dordick JS (2005) Biocatalytic synthesis of highly ordered degradable dextran-based hydrogels. *Biomaterials* 26:4707–4016
- Fouassier JP, Lalevée J (2012) Photoinitiators for polymer synthesis: scope, reactivity, and efficiency. Wiley-VCH Verlag & Co., KGaA, Germany
- Franco RA, Nguyen TH, Lee BT (2011) Preparation and characterization of electrospun PCL/PLGA membranes and chitosan/gelatin hydrogels for skin bioengineering applications. *J Mater Sci Mater Med* 22:2207–2218
- Fraser JRE, Laurent TC, Laurent UBG (1997) Hyaluronan: its nature, distribution, functions and turnover. *J Intern Med* 242:27–33
- Frey MW, Cuculo JA, Khan SA (1996) Rheology and gelation of cellulose/ammonia/ammonium thiocyanate solutions. *J Appl Polym Sci* 34:2375–2381
- Fu L, Zhang Yang G (2013) Present status and applications of bacterial cellulose-based materials for skin tissue repair. *Carbohydr Polym* 92:1432–1442
- Gabrieli I, Gatenholm P (1998) Preparation and properties of hydrogels based on hemicellulose. *J Appl Polym Sci* 69:1661–1667
- Gao J, Haidar G, Lu X, Hu Z (2001) Self-association of hydroxypropylcellulose in water. *Macromolecules* 34:2242–2247
- Gatherhood N, Garcia MT, Scammels PJ (2004) Biodegradable ionic liquids: Part I. Concept, preliminary targets and evaluation. *Green Chem* 6:166–175
- George M, Abraham TE (2006) Polyionic hydrocolloids for the intestinal delivery of protein drugs: alginate and chitosan—a review. *J Control Release* 114:1–14

- Gilbert E, Kirker KR, Gray SD, Ward PD, Szakacs JG, Prestwich GD, Orlandi RR (2004) Chondroitin sulfate hydrogel and wound healing in rabbit maxillary sinus mucosa. *Laryngoscope* 114:1406–1409
- Gils PS, Ray D, Sahoo PK (2009) Characteristics of xanthan gum-based biodegradable superporous hydrogel. *Int J Biol Macromol* 45:364–371
- Gómez-Mascaraque LG, Méndez JA, Fernández-Gutiérrez M, Vázquez B (2014) Oxidized dextrans as alternative crosslinking agents for polysaccharides: application to hydrogels of agarose–chitosan. *Acta Biomater* 10:798–811
- Gonzalez JS, Ludueña LN, Ponce A, Alvarez VA (2014) Poly(vinyl alcohol)/cellulose nanowhiskers nanocomposite hydrogels for potential wound dressings. *Mater Sci Eng C* 34:54–61
- González A, Castro J, Vera J, Moenne A (2012) Seaweed oligosaccharides stimulate plant growth by enhancing carbon and nitrogen assimilation, basal metabolism, and cell division. *J Plant Growth Regul* 32:443–448
- Gorgieva S, Kokol V (2012) Preparation, characterization, and in vitro enzymatic degradation of chitosan-gelatine hydrogel scaffolds as potential biomaterials. *J Biomed Mater Res A* 100:1655–1667
- Gotlieb KF, Capelle A (2005) Starch derivatization: fascinating and unique industrial opportunities. Wageningen Academic Publishers, The Netherlands
- Grant GT, Morris ER, Rees DA, Smith PJC, Thom D (1973) Biological interactions between polysaccharides and divalent cations: the egg-box model. *FEBS Lett* 32:195–198
- Grillo R, Pereira AES, Nishisaka CS, de Lima R, Oehlke K, Greiner R, Fraceto LF (2014) Chitosan/tripolyphosphate nanoparticles loaded with paraquat herbicide: an environmentally safer alternative for weed control. *J Hazard Mater* 278:163–171
- Gross AS, Chu JW (2010) On the molecular origins of biomass recalcitrance: the interaction network and solvation structures of cellulose microfibrils. *J Phys Chem B* 114:13333–13341
- Guerra RSD, Cascone MG, Barbani N, Lazzeri L (1994) Biological characterization of hydrogels of poly(vinyl alcohol) and hyaluronic acid. *J Mater Sci-Mater M* 5:613–616
- Guibal (2005) Heterogeneous catalysis on chitosan-based materials: a review. *Prog Polym Sci*, 71–109
- Guilherme MR, de Moura M, Radovanovic E, Geuskens G, Rubira AF, Muniz EC (2005) Novel thermo-responsive membranes composed of interpenetrated polymer networks of alginate-Ca²⁺ and poly(*N*-isopropylacrylamide). *Polymer* 46:2668–2674
- Guo BL, Gao QY (2007) Preparation and properties of a pH/temperature-responsive carboxymethyl chitosan/poly(*N*-isopropylacrylamide)semi-IPN hydrogel for oral delivery of drugs. *Carbohydr Res* 342:2416–2422
- Guo M, Liu M, Zhan F, Wu L (2005) Preparation and properties of a slow-release membrane-encapsulated urea fertilizer with superabsorbent moisture preservation. *Ind Eng Chem Res* 44:4206–4211
- Gupta KC, Khandekar K (2003) Temperature-responsive cellulose by ceric(IV) ion-initiated graft copolymerization of *N*-isopropylacrylamide. *Biomacromol* 4:758–765
- Gurski LA, Jha AK, Zhang C, Jia X, Farach-Carson MC (2009) Hyaluronic acid-based hydrogels as 3D matrices for in vitro evaluation of chemotherapeutic drugs using poorly adherent prostate cancer cells. *Biomaterials* 30:6076–6085
- Hahn SK, Oh EJ, Miyamoto H, Shimobouji T (2006) Sustained release formulation of erythropoietin using hyaluronic acid hydrogels crosslinked by Michael addition. *Int J Pharm* 322:44–51
- Han X, Chen S, Hu X (2009) Controlled-release fertilizer encapsulated by starch/polyvinyl alcohol coating. *Desalination* 240:21–26
- Haque A, Morris ER (1993) Thermogelation of methylcellulose. Part I: molecular structures and processes. *Carbohydr Polym* 22:161–173
- Haque A, Richardson RK, Morris ER (1993) Thermogelation of methylcellulose. Part II: effect of hydroxypropyl substituents. *Carbohydr Polym* 22:175–186

- Harper BA, Barbut S, Lim LT, Marcone MF (2014) Effect of various gelling cations on the physical properties of “wet” alginate films. *J Food Sci* 79:562–567
- Harris JR, Soliakov A, Lewis RJ (2013) In vitro fibrillogenesis of collagen type I in varying ionic and pH conditions. *Micron* 49:60–68
- Hashem M, Sharaf S, Abd El-Hady MM, Hebeish A (2013) Synthesis and characterization of novel carboxymethylcellulose hydrogels and carboxymethylcellulose-hydrogel-ZnO-nanocomposites. *Carbohydr Polym* 95:421–427
- Hassanzadeh P, Kazemzadeh-Narbat M, Rosenweig R, Zhang X, Khademhosseini A, Annabi N, Rolandi M (2016) Ultrastrong and flexible hybrid hydrogels based on solution self-assembly of chitin nanofibers in gelatin methacryloyl (GelMA). *J Mater Chem* 4:2539–2543
- Hayashi A, Oh SC (1983) Gelation of gelatin solution. *Agric Biol Chem* 47:1711–1716
- Hebeish A, Abd El-Hady MM, Sharaf S (2013) Development of CMC hydrogels loaded with silver nano-particles for medical applications. *Carbohydr Polym* 92:407–413
- Hemvichian K, Chanthawong A, Suwanmala P (2014) Synthesis and characterization of superabsorbent polymer prepared by radiation-induced graft copolymerization of acrylamide onto carboxymethyl cellulose for controlled release of agrochemicals. *Radiat Phys Chem* 103:167–171
- Herrero AM, Carmona P, Jiménez-Colmenero F, Ruiz-Capillas C (2014) Polysaccharide gels as oil bulking agents: technological and structural properties. *Food Hydrocolloid* 36:374–381
- Hirai A, Tsuji M, Horii F (2002) TEM study of band-like cellulose assemblies produced by acetobacter xylinum at 4 °C. *Cellulose* 9:105–113
- Hoare TR, Kohane DS (2008) Hydrogels in drug delivery: progress and challenges. *Polymer* 49:1993–2007
- Hong Y, Mao Z, Wang H, Gao C, Shen J (2006) Covalently crosslinked chitosan hydrogel formed at neutral pH and body temperature. *J Biomed Mater Res A* 79:913–922
- Hoover R (2001) Composition, molecular structure, and physicochemical properties of tuber and root starches: a review. *Carbohydr Polym* 45:253–267
- Hopwood D, Allen CR, McCabe M (1970) The reactions between glutaraldehyde and various proteins. An investigation of their kinetics. *Histochem J* 2:137–150
- Hovgaard L, Brønsted H (1995) Dextran hydrogels for colon-specific drug delivery. *J Control Release* 36:15–166
- Hu X, Du Y, Tang Y, Wang Q, Feng T, Yang J, Kennedy JF (2007) Solubility and property of chitin in NaOH/urea aqueous solution. *Carbohydr Polym* 70:451–458
- Hu XH, Tan HP, Li D, Gu MY (2014) Surface functionalization of contact lenses by CS/HA multilayer film to improve its properties and deliver drugs. *Mater Technol* 29:8–13
- Huang Y, Yu H, Xiao C (2007) pH-sensitive cationic guar gum/poly (acrylic acid) polyelectrolyte hydrogels: swelling and in vitro drug release. *Carbohydr Polym* 69:774–783
- Hudson SM, Smith C (1998) Polysaccharides: chitin and chitosan: chemistry and technology of their use as structural materials. In: Kaplan DL (ed) *Biopolymers from renewable resources*. Springer, Berlin, pp 96–118
- Ibáñez JP, Umetsu Y (2002) Potential of protonated alginate beads for heavy metals uptake. *Hydrometallurgy* 64:89–99
- Ibáñez JP, Umetsu Y (2004) Uptake of trivalent chromium from aqueous solutions using protonated dry alginate beads. *Hydrometallurgy* 72:327–334
- Ibrahim SM, El Salmawi KM, Zahran AH (2007) Synthesis of crosslinked superabsorbent carboxymethyl cellulose/acrylamide hydrogels through electron-beam irradiation. *J Appl Polym Sci* 104:2003–2008
- Ibrahim S, Kang QK, Ramamurthi A (2010) The impact of hyaluronic acid oligomer content on physical, chemical, and biologic properties of divinyl sulfone-crosslinked hyaluronic acid hydrogels. *J Biomed Mater Res A* 94:355–370
- Innerlohinger J, Weber HK, Kraft G (2006) Aerocellulose: aerogels and aerogel-like materials made from cellulose. *Macromol Symp* 244:126–135

- Ishihara M, Ono K, Sato M, Nakanishi K, Saito Y, Yura H, Matsui T, Hattori H, Fujita M, Kikuchi M, Kurita A (2001) Acceleration of wound contraction and healing with a photocrosslinkable chitosan hydrogel. *Wound Repair Regen* 9:513–521
- Ishii D, Tatsumi D, Matsumoto T, Murata K, Hayashi H, Yoshitani H (2006) Investigation of the structure of cellulose in LiCl/DMAc solution and its gelation behavior by small-angle X-ray scattering measurements. *Macromol Biosci* 6:293–300
- Işiklan N (2006) Controlled release of insecticide carbaryl form sodium alginate, sodium alginate/gelation, and sodium alginate/sodium carboxymethyl cellulose blend beads crosslinked with glutaraldehyde. *J Appl Polym Sci* 99:1310–1319
- Işiklan N (2007) Controlled release study of carbaryl insecticide from calcium alginate and nickel alginate hydrogel beads. *J Appl Polym Sci* 105:718–725
- Işiklan N, İnal M, Yiğitoğlu M (2008) Synthesis and characterization of poly(*N*-vinyl-2-pyrrolidone) grafted sodium alginate hydrogel beads for the controlled release of indomethacin. *J Appl Polym Sci* 110:481–493
- Isogai A, Atalla RH (1998) Dissolution of cellulose in aqueous NaOH solutions. *Cellulose* 5:309–319
- Izawa H, Kaneko Y, Kadokawa J (2009) Unique gel of xanthan gum with ionic liquid and its conversion into high performance hydrogel. *J Mater Chem* 19:6969–6972
- Jameela SR, Lakshmi S, James NR, Jayakrishnan A (2002) Preparation and evaluation of photocrosslinkable chitosan as a drug delivery matrix. *J Appl Polym Sci* 86:1873–1877
- Jamnongkan T, Kaewpirom S (2010) Potassium release kinetics and water retention of controlled-release fertilizers based on chitosan hydrogels. *J Polym Environ* 18:413–421
- Jaya S, Durance TD, Wang R (2009) Porous composite scaffold fabricated using novel microwave energy under vacuum technique. *J Compos Mater* 43:1451–1460
- Jensen M, Hansen PB, Murdan S, Frokjaer S, Florence AT (2002) Loading into and electro-stimulated release of peptides and proteins from chondroitin4-sulphate hydrogels. *Eur J Pharm Sci* 15:139–148
- Jeon O, Song SJ, Lee KJ, Park MH, Lee SH, Hahn SK, Kim S, Kim BS (2007) Mechanical properties and degradation behaviors of hyaluronic acid hydrogels cross-linked at various cross-linking densities. *Carbohydr Polym* 70:251–257
- Jeon O, Bouhadir KH, Mansour JM, Alsberg E (2009) Photocrosslinked alginate hydrogels with tunable biodegradation rates and mechanical properties. *Biomaterials* 30:2724–2734
- Jeon O, Powell C, Solorio LD, Krebs MD, Alsberg E (2011) Affinity-based growth factor delivery using biodegradable, photocrosslinked heparin-alginate hydrogels. *J Control Release* 154:258–266
- Jin L, Bai R (2002) Mechanisms of lead adsorption on chitosan/PVA hydrogel beads. *Langmuir* 18:9765–9770
- Jin R, Teixeira LSM, Krouwels A, Dijkstra PJ, van Blitterswijk CA, Karperien M, Feijen J (2010) Synthesis and characterization of hyaluronic acid-poly(ethylene glycol) hydrogels via Michael addition: an injectable biomaterial for cartilage repair. *Acta Biomater* 6:1968–1977
- Johnson DC (1985) Solvents for cellulose. In: Nevell TP, Zeronian SH (eds) *Cellulose chemistry and its applications*. Ellis Horwood Ltd., Chichester, pp 181–201
- Johnson FA, Craig CQ, Mercer AD (1997) Characterization of the block structure and molecules weight of sodium alginates. *J Pharm Pharmacol* 49:639–643
- Ju HK, Kim SY, Lee YM (2001) pH/temperature-responsive behaviors of semi-IPN and comb-type graft hydrogels composed of alginate and poly(*N*-isopropylacrylamide). *Polymer* 42:6851–6857
- Ju HK, Kim SY, Kim SJ, Lee YM (2002) pH/temperature-responsive semi-IPN hydrogels composed of alginate and poly(*N*-isopropylacrylamide). *J Appl Polym Sci* 83:1128–1139
- Jun L, Jun L, Min Y, Hongfei H (2001) Solvent effect on grafting polymerization of NIPAAm onto cotton cellulose via γ -preirradiation method. *Radiat Phys Chem* 60:625–628
- Kadokawa J, Murakami M, Kaneko Y (2008) A facile preparation of gel materials from a solution of cellulose in ionic liquid. *Carbohydr Polym* 343:769–772
- Kaewpirom S, Boonsang S (2006) Electrical response characterisation of poly(ethylene glycol) macromer (PEGM)/chitosan hydrogels in NaCl solution. *Eur Polym J* 42:1609–1616

- Kajjari PB, Manjeshwar LS, Aminabhavi TM (2011) Semi-interpenetrating polymer network hydrogel blend microspheres of gelatin and hydroxyethyl cellulose for controlled release of theophylline. *Ind Eng Chem Res* 50:7833–7840
- Khurma JR, Rohindra DR, Nand AV (2005) Swelling and thermal characteristics of genipin crosslinked chitosan and poly(vinyl pyrrolidone) hydrogels. *Polym Bull* 54:195–204
- Kiatkamjornwong S, Chomsaksakul W, Sonsuk M (2000) Radiation modification of water absorption of cassava starch by acrylic acid/acrylamide. *Radiat Phys Chem* 59:413–427
- Kim SH, Chu CC (2000) Synthesis and characterization of dextran–methacrylate hydrogels and structural study by SEM. *J Biomed Mater Res* 49:517–527
- Kim SH, Won CY, Chu CC (1999) Synthesis and characterization of dextran-based hydrogel prepared by photocrosslinking. *Carbohydr Polym* 40:183–190
- Kim SY, Cho SM, Lee YM, Kim SJ (2000a) Thermo- and pH-responsive behaviors of graft copolymer and blend based on chitosan and *N*-isopropylacrylamide. *J Appl Polym Sci* 78:1381–1391
- Kim YJ, Yoon KJ, Ko SW (2000b) Preparation and properties of alginate superabsorbent filament fibers crosslinked with glutaraldehyde. *J Appl Polym Sci* 78:1797–1804
- Kim SJ, Park SJ, Kim SI (2003) Swelling behavior of interpenetrating polymer network hydrogels composed of poly(vinyl alcohol) and chitosan. *React Funct Polym* 55:53–59
- Kim SJ, Yoon SG, Lee YM, Kim HC, Kim SI (2004) Electrical behavior of polymer hydrogel composed of poly(vinyl alcohol)-hyaluronic acid in solution. *Biosens Bioelectron* 19:531–536
- Kim S, Nimni ME, Yang Z, Han B (2005) Chitosan/gelatin-based films crosslinked by proanthocyanidin. *J Biomed Mater Res B* 75:442–450
- Kim JK, Lee JS, Jung HJ, Cho JH, Heo JI, Chang YH (2007) Preparation and properties of collagen/modified hyaluronic acid hydrogel for biomedical application. *J Nanosci Nanotechnol* 7:3852–3856
- Kim IY, Seo SJ, Moon HS, Yoo IY, Kim BC, Cho CS (2008a) Chitosan and its derivatives for tissue engineering applications. *Biotechnol Adv* 26:1–21
- Kim JO, Park JK, Kim JH, Jin SG, Yong CS, Li DX, Choi JY, Woo JS, Yoo BK, Lyoo WS, Kim JA, Choi HG (2008b) Development of polyvinyl alcohol-sodium alginate gel-matrix-based dressing system containing nitrofurazone. *Int J Pharm* 359:76–86
- Kim TG, Chung HJ, Park TG (2008c) Macroporous and nanofibrous hyaluronic acid/collagen hybrid scaffold fabricated by concurrent electrospinning and deposition/leaching of salt particles. *Acta Biomater* 4:1611–1619
- Kim IL, Mauck RL, Burdick JA (2011) Hydrogel design for cartilage tissue engineering: a case study with hyaluronic acid. *Biomaterials* 32:8771–8782
- Kim MS, Park SJ, Gu BK, Kim CH (2012) Ionically crosslinked alginate-carboxymethyl cellulose beads for the delivery of protein therapeutics. *Appl Surf Sci* 262:28–33
- Kiyozumi T, Kanatani Y, Ishihara M, Saitoh D, Shimizu J, Yura J, Suzuki S, Okada Y, Kikuchi M (2006) Medium (DMEM/F12)-containing chitosan hydrogel as adhesive and dressing in autologous skin grafts and accelerator in the healing process. *J Biomed Mater Res B* 79:129–136
- Klug ED (1971) Some properties of water-soluble hydroxylalkyl celluloses and their derivatives. *J Polym Sci C* 36:491–508
- Knill CJ, Kennedy JF, Mistry J, Mirafat M, Smart G, Grocock MR, Williams H (2004) Alginate fibres modified with unhydrolysed and hydrolysed chitosans for wound dressing. *Carbohydr Polym* 55:65–76
- Kolambkai YM, Dupont KM, Boerckel JD, Huebsch N, Mooney DJ, Huttmacher DW, Goldberg RE (2011) An alginate-based hybrid system for growth factor delivery in the functional repair of large bone defects. *Biomaterials* 32:65–74
- Kono H (2014) Characterization and properties of carboxymethyl cellulose hydrogels crosslinked by polyethylene glycol. *Carbohydr Polym* 106:84–93
- Kono H, Zakimi M (2013) Preparation, water absorbency, and enzyme degradability of novel chitin- and cellulose/chitin-based superabsorbent hydrogels. *J Appl Polym Sci* 128:572–581

- Kotek R (2007) Regenerated cellulose fibers. In: Lewin M, Perce EM (eds) Handbook of fiber chemistry, 3rd edn. Marcel Dekker, New York, pp 667–772
- Koyano T, Minoura N, Nagura M, Kobayashi K (1998) Attachment and growth of cultured fibroblast cells on PVA/chitosan-blended hydrogels. *J Biomed Mater Res* 39:486–490
- Krebs MD, Salter E, Chen E, Sutter KA, Alsberg E (2010) Calcium phosphate-DNA nanoparticle gene delivery from alginate hydrogels induces in vivo osteogenesis. *J Biomed Mater Res A* 92:1131–1138
- Kretlow JD, Klouda L, Mikos AG (2007) Injectable matrices and scaffolds for drug delivery in tissue engineering. *Adv Drug Deliver Rev* 59:263–273
- Kroll E, Winnik FM, Ziolo RF (1996) In situ preparation of nanocrystalline γ -Fe₂O₃ in iron(II) cross-linked alginate gels. *Chem Mater* 8:1594–1596
- Kuijpers AJ, Engbers GHM, Meyvis TKL, de Smedt SSC, Demeester J, Krijgsveld J, Zaat SAJ, Danker J, Feijen J (2000) Combined gelatin–chondroitin sulfate hydrogels for controlled release of cationic antibacterial proteins. *Macromolecules* 33:3705–3713
- Kulkarni RV, Sa B (2009a) Electroresponsive polyacrylamide-grafted-xanthan hydrogels for drug delivery. *J Bioact Compat Pol* 24:368–384
- Kulkarni RV, Sa B (2009b) Polyacrylamide-grafted-alginate-based pH-sensitive hydrogel beads for delivery of ketoprofen to the intestine. *J Biomater Sci* 20:235–251
- Kulkarni AR, Soppimath KS, Aminabhavi TM, Dave AM, Mehta MH (1999) Urea-formaldehyde crosslinked starch and guar gum matrices for encapsulation of natural liquid pesticide [Azadirachta Indica A. Juss. (neem) seed oil]: swelling and release kinetics. *J Appl Polym Sci* 73:2437–2446
- Kulkarni AR, Soppimath, KS, Aminabhavi TM, Dave AM, Mehta, MH (2000) Glutaraldehyde crosslinked sodium alginate beads containing liquid pesticide for soil application. *J Control Release* 63:97–105
- Kulkarni AR, Soppimath KS, Aminabhavi TM, Rudzinski WE (2001) In-vitro release kinetics of cefadroxil-loaded sodium alginate interpenetrating network beads. *Eur J Pharm Biopharm* 51:127–133
- Kumar M, Tripathi BP, Shahi VK (2009) Crosslinked chitosan/polyvinyl alcohol blend beads for removal and recovery of Cd(II) from wastewater. *J Hazard Mater* 172:1041–1048
- Kumar PTS, Lakshmanan VK, Anilkumar TV, Ramya C, Reshmi P, Unnikrishnan AG, Nair SV, Jayakumar R (2012) Flexible and microporous chitosan hydrogel/nano ZnO composite bandages for wound dressing: in vitro and in vivo evaluation. *ACS Appl Mater Interfaces* 4:2618–2629
- Kumar PTS, Lakshmanan VK, Mincy R, Raja B, Tamura H, Nair SV, Jayakumar R (2013) Evaluation of wound healing potential of β -chitin hydrogel/zinc oxide composite bandage. *Pharm Res* 30:523–537
- Kumbar SG, Kulkarni AR, Dave AM, Aminabhavi TM (2001) Encapsulation efficiency and release kinetics of solid and liquid pesticides through urea formaldehyde crosslinked starch, guar gum, and starch + guar gum matrices. *J Appl Polym Sci* 82:2863–2866
- Kumbar SG, Soppimath KS, Aminabhavi TM (2003) Synthesis and characterization of polyacrylamide-grafted chitosan hydrogel microspheres for the controlled release of indomethacin. *J Appl Polym Sci* 87:1525–1536
- Kuo CK, Ma PX (2001) Ionically crosslinked alginate hydrogels as scaffolds for tissue engineering: Part 1. Structure, gelation rate and mechanical properties. *Biomaterials* 22:511–521
- Kwon SS, Kong BJ, Park SN (2015) Physicochemical properties of pH-sensitive hydrogels based on hydroxyethyl cellulose-hyaluronic acid and for applications as transdermal delivery systems for skin lesions. *Eur J Pharm Biopharm* 92:146–154
- Lai JY (2014) Relationship between structure and cytocompatibility of divinyl sulfone cross-linked hyaluronic acid. *Carbohydr Polym* 101:203–212
- Leach JB, Schmidt CE (2005) Characterization of protein release from photocrosslinkable hyaluronic acid-polyethylene glycol hydrogel tissue engineering scaffolds. *Biomaterials* 26:125–135

- Leach JB, Bivens KA, Partick CW, Schmidt CE (2003) Photocrosslinked hyaluronic acid hydrogels: natural, biodegradable tissue engineering scaffolds. *Biotechnol Bioeng* 82:578–589
- Lee WF, Chen YJ (2001) Studies on preparation and swelling properties of the *N*-isopropylacrylamide/chitosan semi-IPN and IPN hydrogels. *J Appl Polym Sci* 82:2487–2496
- Lee JW, Kim SY, Kim SS, Lee YM, Lee KH, Kim SJ (1999) Synthesis and characteristics of interpenetrating polymer network hydrogel composed of chitosan and poly(acrylic acid). *J Appl Polym Sci* 73:113–120
- Lee KY, Rowley JA, Eiselt P, Moy EM, Bouhadir KH, Mooney DJ (2000a) Controlling mechanical and swelling properties of alginate hydrogels independently by cross-linker type and cross-linking density. *Macromolecules* 33:4291–4294
- Lee SJ, Kim SS, Lee YM (2000b) Interpenetrating polymer network hydrogels based on poly(ethylene glycol) macromer and chitosan. *Carbohydr Polym* 41:197–205
- Lee JW, Jung MC, Park HD, Park KD, Ryu GH (2004a) Synthesis and characterization of thermosensitive chitosan copolymer as a novel biomaterial. *J Biomater Sci Polymer Edn* 15:1065–1079
- Lee SB, Ha DI, Cho SK, Kim SJ, Lee YM (2004b) Temperature/pH-sensitive comb-type graft hydrogels composed of chitosan and poly(*N*-isopropylacrylamide). *J Appl Polym Sci*, 2612–2620
- Lee JH, Nho YC, Lim YM, Son TI (2005) Prevention of surgical adhesions with barriers of carboxymethylcellulose and poly(ethylene glycol) hydrogels synthesized by irradiation. *J Appl Polym Sci* 96:1138–1145
- Lee SB, Park EK, Lim YM, Cho SK, Kim SY, Lee YM, Nho YC (2006) Preparation of alginate/poly(*N*-isopropylacrylamide) semi-interpenetrating and fully interpenetrating polymer network hydrogels with γ -ray irradiation and their swelling behaviors. *J Appl Polym Sci* 100:4439–4446
- Lee SJ, Pereira BP, Yusof N, Selvaratnam L, Yu Z, Abbas AA, Kamrul T (2009) Unconfined compression properties of a porous poly(vinyl alcohol)–chitosan-based hydrogel after hydration. *Acta Biomater* 5:1919–1925
- Lei Y, Rahim M, Ng Q, Sagura T (2011) Hyaluronic acid and fibrin hydrogels with concentrated DNA/PEI polyplexes for local gene delivery. *J Control Release* 153:255–261
- Lévesque SG, Shoichet MS (2007) Synthesis of enzyme-degradable, peptide-cross-linked dextran hydrogels. *Bioconjug Chem* 18:874–885
- Li S (2010) Removal of crystal violet from aqueous solution by sorption into semi-interpenetrated networks hydrogels constituted of poly(acrylic acid-acrylamide-methacrylate) and amylose. *Bioresour Technol* 101:2197–2202
- Li Q, Williams CG, Sun DDN, Wang J, Leong K, Elisseeff H (2004) Photocrosslinkable polysaccharides based on chondroitin sulfate. *J Biomed Mater Res A* 68:28–33
- Li J, Li Y, Dong H (2008) Controlled release of herbicide acetochlor from clay/carboxymethylcellulose gel formulations. *J Agric Food Chem* 56:1336–1346
- Li J, Lu J, Li Y (2009) Carboxymethylcellulose/bentonite composite gels: water sorption behavior and controlled release of herbicide. *J Appl Polym Sci* 112:261–268
- Li X, Ma X, Fan D, Zhu C (2012a) New suitable for tissue reconstruction injectable chitosan/collagen-based hydrogels. *Soft Matter* 8:3781–3790
- Li X, Weng Y, Kong X, Zhang B, Li M, Diao K, Zhang Z, Wang X, Chen H (2012b) A covalently crosslinked polysaccharide hydrogel for potential applications in drug delivery and tissue engineering. *J Mater Sci Mater Med* 23:2857–2865
- Li X, Li Q, Su Y, Yue Q, Gao B, Su Y (2015) A novel wheat straw cellulose-based semi-IPN superabsorbent with integration of water-retaining and controlled release. *J Taiwan Inst Chem E* 55:170–179
- Liang S, Xu J, Weng L, Dai H, Zhang X, Zhang L (2006) Protein diffusion in agarose hydrogel in situ measured by improved refractive index method. *J Control Release* 115:189–196
- Lin YH, Liang HF, Chung CK, Chen MC, Sung HW (2005) Physically crosslinked alginate/*N*, *O*-carboxymethyl chitosan hydrogels with calcium for oral delivery of protein drugs. *Biomaterials* 26:2105–2113

- Liu J, Li L (2005) SDS-aided immobilization and controlled release of camptothecin from agarose hydrogel. *Eur J Pharm Sci* 25:237–344
- Liu G, Zhao X (2006) Electroresponsive behavior of gelatin/alginate semi-interpenetrating polymer network membranes under direct-current electric field. *J Macromol Sci A* 43:345–354
- Liu P, Zhai M, Li J, Peng J, Wu J (2002) Radiation preparation and swelling behavior of sodium carboxymethyl cellulose hydrogels. *Radiat Phys Chem* 63:525–528
- Liu W, Zhang B, Lu WW, Li X, Zhu D, Yao KD, Wang Q, Zhao C, Wang C (2004) A rapid temperature-responsive sol-gel reversible poly(*N*-isopropylacrylamide)-*g*-methylcellulose copolymer hydrogel. *Biomaterials* 25:3005–3012
- Liu KH, Liu TY, Chen SY, Liu DM (2008a) Drug release behavior of chitosan–montmorillonite nanocomposite hydrogels following electrostimulation. *Acta Biomater* 4:1038–1045
- Liu W, Griffith M, Li F (2008b) Alginate microsphere-collagen composite hydrogel for ocular drug delivery and implantation. *J Mater Sci Mater Med* 19:3365–3371
- Liu Y, Cao X, Hua R, Wang Y, Liu Y, Pang C, Wang Y (2010) Selective adsorption of uranyl ion on ion-imprinted chitosan/PVA cross-linked hydrogel. *Hydrometallurgy* 104:150–155
- Liu Z, Wang H, Liu C, Jiang Y, Yu G, Mu X, Wang X (2012) Magnetic cellulose-chitosan hydrogels prepared from ionic liquids as reusable adsorbent for removal of heavy metal ions. *Chem Commun* 48:7350–7352
- Liu B, Ma X, Zhu C, Mi Y, Fan D, Li X, Chen L (2013) Study of a novel injectable hydrogel of human-like collagen and carboxymethylcellulose for soft tissue augmentation. *e-Polymers* 13:380–390
- Liu H, Sui X, Xu H, Zhang L, Zhong Y, Mao Z (2016) Self-healing polysaccharide hydrogels based on dynamic covalent enamine bonds. *Macromol Mater Eng* 301:725–732
- LogithKumar R, KeshavNarayan A, Dhivya S, Chawla A, Saravanan S, Selvamurugan N (2016) A review of chitosan and its derivatives in bone tissue engineering. *Carbohydr Polym* 151:172–188
- Loubinoux D, Chaunis S (1987) An experimental approach to spinning new cellulose fibers with *N*-methylmorpholine-oxide as a solvent. *Text Res J* 57:61–65
- Lu X, Hu Z, Gao J (2000) Synthesis and light scattering study of hydroxypropyl cellulose microgels. *Macromolecules* 33:8698–8702
- Lu S, Gao W, Gu HY (2008) Construction, application and biosafety of silver nanocrystalline chitosan wound dressing. *Burns* 34:623–628
- Lu G, Ling K, Zhao P, Xu Z, Deng C, Zheng H, Huang J, Chen J (2010) A novel in situ-formed hydrogel wound dressing by the photocross-linking of a chitosan derivative. *Wound Repair Regen* 18:70–79
- Lü S, Liu M, Ni B, Gao C (2010) A novel pH- and thermo-sensitive PVP/CMC semi-IPN hydrogel: swelling, phase behavior, and drug release study. *J Polym Sci B* 48:1749–1756
- Luo F, Chen Z, Megharaj M, Naidu R (2016) Simultaneous removal of trichloroethylene and hexavalent chromium by green synthesized agarose-Fe nanoparticles hydrogel. *Chem Eng J* 294:290–297
- Ma J, Xu Y, Fan B, Liang B (2007a) Preparation and characterization of sodium carboxymethylcellulose/poly(*N*-isopropylacrylamide)/clay semi-IPN nanocomposite hydrogels. *Eur Polym J* 43:2221–2228
- Ma J, Xu Y, Zhan Q, Zha L, Liang B (2007b) Preparation and characterization of pH- and temperature-responsive semi-IPN hydrogels of carboxymethyl chitosan with poly (*N*-isopropyl acrylamide) crosslinked by clay. *Colloid Polym Sci* 285:479–484
- Ma YQ, Yi JZ, Zhang LM (2009) A facile approach to incorporate silver nanoparticles into dextran-based hydrogels for antibacterial and catalytic application. *J Macromol Sci A* 46:643–648
- Madhumathi K, Kumar PTS, Abhilash S, Sreeja V, Tamura H, Manzoor K, Nair SV, Jayakumar R (2010) Development of novel chitin/nanosilver composite scaffolds for wound dressing applications. *J Mater Sci* 21:807–813

- Mahdavinia GR, Pourjavadi A, Hosseinzadeh H, Zohuriaan MJ (2004) Modified chitosan 4. Superabsorbent hydrogels from poly(acrylic acid-co-acrylamide) grafted chitosan with salt- and pH-responsiveness properties. *Eur Polym J* 40:139–1407
- Mai THA, Tran VN, Le VVM (2013) Biochemical studies on the immobilized lactase in the combined alginate-carboxymethyl cellulose gel. *Biochem Eng J* 74:81–87
- Maia J, Ferreira L, Carvalho R, Ramos MA, Gil MH (2005) Synthesis and characterization of new injectable and degradable dextran-based hydrogels. *Polymer* 46:9604–9614
- Mallick SP, Sagiri SS, Singh VK, Pal DK, Pradhan DK, Bhattacharya MK (2014) Effect of processed starches on the properties of gelatin-based physical hydrogels: characterization, in vitro drug release and antimicrobial studies. *Polym-Plast Technol* 53:700–715
- Mandal B, Ray SK (2013) Synthesis of interpenetrating network hydrogel from poly(acrylic acid-co-hydroxyethyl methacrylate) and sodium alginate: modeling and kinetics study for removal of synthetic dyes from water. *Carbohydr Polym* 98:257–269
- Maneering T, Tokura S, Rujiravanit R (2008) Impregnation of silver nanoparticles into bacterial cellulose for antimicrobial wound dressing. *Carbohydr Polym* 72:43–51
- Marci G, Mele G, Palmisano L, Pulito P, Sannino A (2006) Environmentally sustainable production of cellulose-based superabsorbent hydrogels. *Green Chem* 8:439–444
- Marsano E, Bianchi E (2002) A new class of hydrogels based on hydroxypropylcellulose and polyvinylpyrrolidone. *Polymer* 43:3371–3374
- Marsano E, Gagliardi S, Ghioni F, Bianchi E (2000) Behavior of gels based on (hydroxypropyl) cellulose methacrylate. *Polymer* 41:7691–7698
- Marsich E, Travan A, Donati I, Luca AD, Benincasa M, Crosera M, Paoletti S (2011) Biological response of hydrogels embedding gold nanoparticles. *Colloid Surf B* 83:331–339
- McCormick CL, Callais PA, Hutchinson BH (1985) Solution studies of cellulose in lithium chloride and *N*, *N*-dimethylacetamide. *Macromolecules* 18:2394–2401
- McKelvey JB, Benerito RR, Berni RJ, Burgis BG (1963) The action of epichlorohydrin in the presence of alkalis and various salts on the crease recovery of cotton. *J Appl Polym Sci* 7:1371–1389
- Meilander NJ, Pasumathy MK, Kowalczyk TH, Cooper MJ, Bellamkonda RV (2003) Sustained release of plasmid DNA using lipid microtubules and agarose hydrogel. *J Control Release* 88:321–331
- Menakki C, Quignard F, Mineva T (2016) Complexation of trivalent metal cations to mannuronate type alginate models from a density functional study. *J Phys Chem B* 120:3615–3623
- Mi FL, Sung HW, Shyu SS (2000) Synthesis and characterization of a novel chitosan-based network prepared using naturally occurring crosslinker. *J Polym Sci A* 38:2804–2814
- Mi FL, Wu YB, Shyu SS, Schoung JY, Huang YB, Tsai YH, Hao JY (2002) Control of wound infections using a bilayer chitosan wound dressing with sustainable antibiotic delivery. *J Biomed Mater Res* 59:438–449
- Mi FL, Shyu SS, Peng CK (2005) Characterization of ring-opening polymerization of genipin and pH-dependent cross-linking reactions between chitosan and genipin. *J Polym Sci A* 43:1985–2000
- Miao T, Fenn SL, Charron PN, Oldinski RA (2015) Self-healing and theroresponsive dual-cross-linked alginate hydrogels based on supramolecular inclusion complexes. *Biomacromol* 16:3740–3750
- Miculescu M, Thakur VK, Miculescu F, Voicu SI (2016) Graphene-based polymer nanocomposite membranes: a review. *Polym Adv Technol* 27(7):844–859
- Miles MJ, Morris VJ, Orford PD, Ring SG (1985) The roles of amylose and amylopectin in the gelation and retrogradation of starch. *Carbohydr Res* 135:271–281
- Millon LE, Wan WK (2006) The polyvinyl alcohol–bacterial cellulose system as a new nanocomposite for biomedical applications. *J Biomed Mater Res B* 79:245–253
- Minoura N, Koyano T, Koshizaki N, Umehara H, Nagura M, Kobayashi K (1998) Preparation, properties, and cell attachment/growth behavior of PVA/chitosan-blended hydrogels. *Mater Sci Eng C* 6:275–280

- Mironov V, Kasyanov V, Shu XZ, Eisenberg C, Eisenberg L, Gonda S, Trusk T, Markwald RR, Prestwich GD (2005) Fabrication of tubular tissue constructs by centrifugal casting of cells suspended in an in situ crosslinkable hyaluronan-gelatin hydrogel. *Biomaterials* 26:7628–7635
- Mirzaei BE, Ramazani SAA, Shafiee M, Danaei M (2013) Studies on glutaraldehyde crosslinked chitosan hydrogel properties for drug delivery systems. *Int J Polym Mater Polym Biomater* 62:605–611
- Mishra RK, Datt M, Banthia AK (2008) Synthesis and characterization of pectin/PVP hydrogel membranes for drug delivery system. *AAPS PharmSciTech* 9:395–403
- Misra BN, Mehta IK, Khetarpal RC (1984) Grafting onto cellulose. VIII. Graft copolymerization of poly(ethylacrylate) onto cellulose by use of redox initiators. Comparison of initiator reactivities. *J Polym Sci A* 22:2767–2775
- Mittal H, Parashar V, Mishra SB, Mishra AK (2014) Fe₃O₄ MNPs and gum xanthan based hydrogels nanocomposites for the efficient capture of malachite green from aqueous solution. *Chem Eng J* 255:471–482
- Mohr S, Siegenthaler M, Mueller MD, Kuhn A (2013) Bulking agents: an analysis of 500 cases and review of the literature. *Int Urogynecol J* 24:241–247
- Muzzarelli RAA (1988) Carboxymethylate chitins and chitosans. *Carbohydr Polym* 8:1–21
- Muzzarelli RAA (1993) Biochemical significance of exogenous chitins and chitosans in animals and patients. *Carbohydr Polym* 20:7–16
- Muzzarelli RAA, Greco F, Busilacchi A, Sollazzo V, Gigante A (2012) Chitosan, hyaluronan and chondroitin sulfate in tissue engineering for cartilage regeneration: a review. *Carbohydr Polym* 89:732–739
- Nagahama H, Nwe N, Jayakumar R, Koiwa S, Furuike T, Tamura H (2008) Novel biodegradable chitin membranes for tissue engineering applications. *Carbohydr Polym* 73:295–302
- Nagahama H, Meada H, Kashiki T, Jayakumar R, Furuike T, Tamura H (2009) Preparation and characterization of novel chitosan/gelatin membranes using chitosan hydrogel. *Carbohydr Polym* 76:255–260
- Nagasawa N, Yagi T, Kume T, Yoshii F (2004) Radiation crosslinking of carboxymethyl starch. *Carbohydr Polym* 58:109–113
- Nakajima N, Ikada Y (1995) Mechanism of amide formation by carbodiimide for bioconjugation in aqueous media. *Bioconjug Chem* 6:123–130
- Nakayama A, Kakugo A, Gong JP, Osada Y, Takai M, Erata T, Kawano S (2004) High mechanical strength double-network hydrogel with bacterial cellulose. *Adv Funct Mater* 14:1124–1128
- Nazari A, Montazer M, Rashidi A, Yazdanshenas M, Anary-Abbasinejad M (2009) Nano TiO₂ photo-catalyst and sodium hypophosphite for crosslinking cotton with poly carboxylic acids under UV and high temperature. *Appl Catal A-Gen* 371:10–16
- Ng RW, Cheng YL (2007) Calcium alginate dressing-related hypercalcemia. *J Burn Care Res* 28:203–204
- Nho YC, Park KR (2002) Preparation and properties of PVA/PVP hydrogels containing chitosan by radiation. *J Appl Polym Sci* 85:1787–1794
- Ni B, Liu S, Lü S, Xie L, Wang Y (2011) Environmentally friendly slow-release nitrogen fertilizer. *J Agric Food Chem* 59:10169–10175
- Nicodemus GD, Bryant SJ (2008) Cell encapsulation in biodegradable hydrogels for tissue engineering applications. *Tissue Eng B* 14:149–165
- Nie H, Liu M, Zhan F, Guo M (2004) Factors on the preparation of carboxymethylcellulose hydrogel and its degradation behavior in soil. *Carbohydr Polym* 58:185–189
- Nnadi F, Brave C (2011) Environmentally friendly superabsorbent polymers for water conservation in agricultural lands. *J Soil Sci Environ Manage* 2:206–211
- Nyström B, Lindman B (1995) Dynamic and viscoelastic properties during the thermal gelation process of a nonionic cellulose ether dissolved in water in the presence of ionic surfactants. *Macromolecules* 28:967–974

- Obradovic B, Stojkovsak J, Jovanovic Z, Miskovic-Stankovic V (2012) Novel alginate based nanocomposite hydrogels with incorporated silver nanoparticles. *J Mater Sci Mater Med* 23:99–107
- Oh ST, Kim WR, Kim SH, Chung YC, Park JS (2011) The preparation of polyurethane foam combined with pH-sensitive alginate/bentonite hydrogel for wound dressings. *Fiber Polym* 12:159–165
- Ohya S, Nakayama Y, Matsuda T (2001) Thermoresponsive artificial extracellular matrix for tissue engineering: hyaluronic acid bioconjugated with poly(*N*-isopropylacrylamide) grafts. *Biomacromol* 2:856–863
- Omidian H, Rocca JG, Park K (2006) Elastic, superporous hydrogel hybrids of polyacrylamide and sodium alginate. *Macromol Biosci* 6:703–710
- Omlor GW, Nerlich AG, Lorenz H, Burkner T, Richter W, Pfeiffer M, Gühring T (2012) Injection of a polymerized hyaluronic acid/collagen hydrogel matrix in an in vivo porcine disc degeneration model. *Eur Spine J* 21:1700–1708
- Ono K, Saito Y, Yura H, Ishikawa K, Kurita A, Akaike T, Ishihara M (1999) Photocrosslinkable chitosan as a biological adhesive. *J Biomed Mater Res* 49:289–295
- Oprea AM, Profire L, Lupusoru CE, Ghiciuc CM, Ciolacu D, Vasile C (2012) Synthesis and characterization of some cellulose/chondroitin sulphate hydrogels and their evaluation as carriers for drug delivery. *Carbohydr Polym* 87:721–729
- Östlund , Lundberg D, Nordstierna L, Holmberg K, Nydén M (2009) Dissolution and gelation of cellulose in TBAF/DMSO solutions: the roles of fluoride ions and water. *Biomacromol* 10:2401–2407
- Pal K, Banthia AK, Majumdar DK (2006) Preparation of transparent starch based hydrogel membrane with potential application as wound dressing. *Trends Biomater Artif Organs* 20: 59–67
- Papageorgiou SK, Katsaros FK, Kouvelos EP, Nolan JW, Deit HL, Kanellopoulos NK (2006) Heavy metal sorption by calcium alginate beads from *Laminaria digitata*. *J Hazard Mater* 137:1765–1772
- Pappu A, Patil V, Jain S, Mahindrakar A, Haque R, Thakur VK (2015) Advances in industrial prospective of cellulosic macromolecules enriched banana biofibre resources: a review. *Int J Biol Macromol* 79:449–458
- Pappu A, Saxena M, Thakur VK, Sharma A, Haque R (2016) Facile extraction, processing and characterization of biorenewable sisal fibers for multifunctional applications. *J Macromol Sci Part A* 53(7):424–432
- Park JS, Park JW, Ruckenstein E (2001) Thermal and dynamic mechanical analysis of PVA/MC blend hydrogels. *Polymer* 42:4271–4280
- Park SN, Lee HJ, Lee KH, Suh H (2003) Biological characterization of EDC-crosslinked collagen–hyaluronic acid matrix in dermal tissue restoration. *Biomaterials* 24:1631–1641
- Patchan M, Graham JL, Xia Z, Maranchi JP, McCally R, Schein O, Elisseeff JH, Trexler MM (2013) Synthesis and properties of regenerated cellulose-based hydrogels with high strength and transparency for potential use as an ocular bandage. *Mater Sci Eng C* 33:3069–3076
- Patterson J, Siew R, Herring SW, Lin ASP, Guldberg R, Stayton PS (2010) Hyaluronic acid hydrogels with controlled degradation properties for oriented bone regeneration. *Biomaterials* 31:6772–6781
- Pekel N, Yoshii F, Kume T, Güven O (2004) Radiation crosslinking of biodegradable hydroxypropylmethylcellulose. *Carbohydr Polym* 55:139–147
- Petrov P, Petrova E, Stamenova R, Tsvetanov CB, Riess G (2006) Cryogels of cellulose derivatives prepared via UV irradiation of moderately frozen systems. *Polymer* 47:6481–6484
- Petrov P, Petrova E, Tchorbanov B, Tsvetanov CB (2007) Synthesis of biodegradable hydroxyethylcellulose cryogels by UV irradiation. *Polymer* 48:4943–4949
- Petrusic S, Lewandowski M, Giraud S, Jovanic P, Bugarski B, Ostojic S, Koncar V (2012) Development and characterization of thermosensitive hydrogels based on poly(*N*-isopropylacrylamide) and calcium alginate. *J Appl Polym Sci* 124:890–903

- Pettignano A, Häring M, Bernardi L, Tanchoux N, Quignard F, Díaz Díaz D (2017) Self-healing alginate–gelatin biohydrogels based on dynamic covalent chemistry: elucidation of key parameters. *Mater Chem Front* 1:73–79
- Plungpongpan K, Koyanukkul K, Kaewvilai A, Nootsuwan N, Kewsuwan P, Laobuthee A (2013) Preparation of PVP/MHEC blended hydrogels via gamma irradiation and their calcium ion uptaking and releasing ability. *Energia Procedia* 34:775–781
- Potthast A, Rosenau T, Buchner R, Röder T, Ebner G, Bruglachner H, Sixta H, Kosma P (2002a) The cellulose solvent system *N, N*-dimethylacetamide/lithium chloride revisited: the effect of water on physicochemical properties and chemical stability. *Cellulose* 9:41–53
- Potthast A, Rosenau T, Sixta H, Kosma P (2002b) Degradation of cellulosic materials by heating in DMAc/LiCl. *Tetrahedron Lett* 43:7757–7759
- Pourjavadi A, Barzengar S, Mahdavinia GR (2006) MBA-crosslinked Na-Alg/CMC as a smart full-polysaccharide superabsorbent hydrogels. *Carbohydr Polym* 66:386–395
- Pourjavadi A, Ghasemzadeh H, Soleyman R (2007) Synthesis, characterization, and swelling behavior of alginate-g-poly(sodium acrylate)/kaolin superabsorbent hydrogel composites. *J Appl Polym Sci* 105:2631–2639
- Price RD, Myers S, Leigh IM, Navsaria HA (2005) The role of hyaluronic acid in wound healing. *Am J Clin Dermatol* 6:393–402
- Qiao D, Liu H, Yu L, Bao X, Simon GP, Petinakis E, Chen L (2016) Preparation and characterization of slow-release fertilizer encapsulated by starch-based superabsorbent polymer. *Carbohydr Polym* 147:146–154
- Qiu Y, Park K (2001) Environment-sensitive hydrogels for drug delivery. *Adv Drug Deliver Rev* 53:321–329
- Qu X, Wirsén A, Albertsson AC (1999) Synthesis and characterization of pH-sensitive hydrogels based on chitosan and D, L-lactic acid. *J Appl Polym Sci* 74:3193–3202
- Quinn FX, Hatakeyama T, Takahashi M, Hatakeyama H (1994) The effect of annealing on the conformational properties of xanthan hydrogels. *Polymer* 35:1248–1252
- Rafat M, Li F, Fagerholm P, Lagali NS, Watsky MA, Munger R, Matsuura T, Griffith M (2008) PEG-stabilized carbodiimide crosslinked collagen–chitosan hydrogels for corneal tissue engineering. *Biomaterials* 29:3960–3972
- Rahman L, Silong S, Zin WM, Rahman MZA, Ahmad M, Haron J (2000) Graft copolymerization of methyl acrylate onto sago starch using ceric ammonium nitrate as an initiator. *J Appl Polym Sci* 76:516–523
- Rao KSVM, Naidu BVK, Subha MCS, Sairam M, Aminabhavi TM (2006) Novel chitosan-based pH-sensitive interpenetrating network microgels for the controlled release of cefadroxil. *Carbohydr Polym* 66:333–344
- Rao KM, Mallikarjuna B, Krishna Rao KSV, Prabhakar MN, Chowdoji Rao K, Subha MCS (2012) Preparation and characterization of pH sensitive poly(vinyl alcohol)/sodium carboxymethyl cellulose IPN microspheres for in vitro release studies of an anti-cancer drug. *Polym Bull* 68:1905–1919
- Rashidzadeh A, Olad A (2014) Slow-released NPK fertilizer encapsulated by NaAlg-g-poly (AA-co-AAm)/MMT superabsorbent nanocomposite. *Carbohydr Polym* 114:269–278
- Rashidzadeh A, Olad A, Salari D, Reyhanitabar (2014) On the preparation and swelling properties of hydrogel nanocomposite based on sodium alginate-g-poly(acrylic acid-co-acrylamide)/clinoptilolite and its application as slow release fertilizer. *J Polym Res* 21:344–358
- Rathna GVN, Rao DVM, Chatterji PR (1996) Hydrogels of gelatin-sodium carboxymethylcellulose: synthesis and swelling kinetics. *J Macromol Sci A* 33:1199–1207
- Ray R, Maity S, Mandal S, Chatterjee TK, Sa B (2011) Cross-linked homopolymeric and interpenetrating network hydrogel beads of carboxymethyl xanthan and sodium alginate. *Adv Polym Tech* 30:1–11
- Reddy KR, Rajgopal K, Maheswari CU, Kantam ML (2006) Chitosan hydrogel: a green and recyclable biopolymer catalyst for aldol and Knoevenagel reactions. *New J Chem* 30:1549–1552

- Rehab A, Akelah A, Issa R, D'Antone S, Solaro R, Chiellini E (1991) Controlled release of herbicides supported on polysaccharide based hydrogels. *J Bioact Comp Polym* 6:52–63
- Reis LA, Chiu LLY, Liang Y, Hyunh K, Momen A, Radisic M (2012) A peptide-modified chitosan-collagen hydrogel for cardiac cell culture and delivery. *Acta Biomater* 8:1022–1036
- Relleve L, Yoshii F, dela Rosa A, Kume T (1999) Radiation-modified hydrogel based on poly(*N*-vinyl-2-pyrrolidone) and carrageenan. *Angew Makromol Chem* 273:63–68
- Ren H, Gao Z, Wu D, Jiang J, Sun Y, Luo C (2016) Efficient Pb(II) removal using sodium alginate-carboxymethyl cellulose gel beads: preparation, characterization, and adsorption mechanism. *Carbohydr Polym* 137:402–409
- Rimdisut S, Somsaeng K, Kewsuwan P, Jubsilp C, Tiptipakorn S (2012) Comparison of gamma radiation crosslinking and chemical crosslinking on properties of methylcellulose hydrogel. *Eng J* 16:15–28
- Rinaudo M, Pavlov G, Desbrières J (1999) Influence of acetic acid concentration on the solubilization of chitosan. *Polymer* 40:7029–7032
- Risbud MV, Bhat SV (2001) Properties of polyvinyl pyrrolidone/ β -chitosan hydrogel membranes and their biocompatibility evaluation by haemorheological method. *J Mater Sci Mater M* 12:75–79
- Risbud MV, Bhonde RR (2000) Polyacrylamide-chitosan hydrogels: in vitro biocompatibility and sustained antibiotic release studies. *Drug Deliv* 7:69–75
- Risbud M, Hardikar A, Bhonde R (2001) Growth modulation of fibroblasts by chitosan-polyvinyl pyrrolidone hydrogel: implications for wound management. *J Biosci* 25:25–31
- Rocheffort WE, Rehg T, Chau PC (1986) Trivalent cation stabilization of alginate gel for cell immobilization. *Biotechnol Lett* 8:115–120
- Rokhade AP, Agnihotri SA, Patil SA, Mallikarjuna NN, Kulkarni PV, Aminabhavi TM (2006) Semi-interpenetrating polymer network microspheres of gelatin and sodium carboxymethyl cellulose for controlled release of ketorolac tromethamine. *Carbohydr Polym* 65:242–252
- Romero A, Santos A, Tojo J, Rodríguez A (2008) Toxicity and biodegradability of imidazolium ionic liquids. *J Hazard Mater* 151:268–273
- Rosiak JM, Ulański P (1999) Synthesis of hydrogels by irradiation of polymers in aqueous solution. *Radiat Phys Chem* 55:139–151
- Roy C, Budtova T, Navard P (2003) Rheological properties and gelation of aqueous cellulose-NaOH solutions. *Biomacromol* 4:259–264
- Roy A, Bajpai J, Bajpai AK (2009) Dynamics of controlled release of chlorpyrifos from swelling and eroding biopolymeric microspheres of calcium alginate and starch. *Carbohydr Polym* 76:221–231
- Roy N, Saha N, Kitano T, Saha P (2010) Novel hydrogels of PVP-CMC and their swelling effect on viscoelastic properties. *J Appl Polym Sci* 117:1703–1710
- Rudzinski WE, Dave AM, Vaishnav UH, Kumbar SG, Kulkarni AR, Aminabhavi TM (2002) Hydrogels as controlled release devices in agriculture. *Design Monomers Polym* 5:39–65
- Ruiz-Capillas C, Carmona P, Jiménez-Colmenero F, Herrero AM (2013) Oil bulking agents based on polysaccharide gels in meat batters: a Raman spectroscopy study. *Food Chem* 141:3688–3694
- Sadeghi M, Hosseinzadeh H (2007) Synthesis and superswelling behavior of carboxymethylcellulose-poly(sodium-acrylate-co-acrylamide) hydrogel. *J Appl Polym Sci* 108:1142–1151
- Saglam A, Yalcinkaya Y, Denizli A, Arica MY, Genc Ö, Bektas S (2002) Biosorption of mercury by carboxymethylcellulose and immobilized *Phanerochaete chrysosporium*. *Microchem J* 71:73–81
- Saha S, Pal A, Kundu S, Basu S, Pal T (2010) Photochemical green synthesis of calcium-alginate-stabilized Ag and Au nanoparticles and their catalytic application to 4-nitrophenol reduction. *Langmuir* 26:2885–2893
- Sahoo S, Cung C, Khetan S, Burdick JA (2008) Hydrolytically degradable hyaluronic acid hydrogels with controlled temporal structures. *Biomacromol* 9:1088–1092

- Sakai S, Yamaguchi S, Takei T, Kawakami K (2008) Oxidized alginate-cross-linked alginate/gelatin hydrogel fibers for fabricating tubular constructs with layered smooth muscle cells and endothelial cells in collagen gels. *Biomacromol* 9:2036–2041
- Salama A, El-Sakhawy M, Kamel S (2016) Carboxymethyl cellulose based hybrid material for sustained release of protein drugs. *Int J Biol Macromol* 93:1647–1652
- Sannino A, Madaghiele M, Conversano F, Mele G, Maffezzoli A, Netti PA, Ambrosio L, Nicolais L (2004) Cellulose derivative–hyaluronic acid-based microporous hydrogels cross-linked through divinyl sulfone (DVS) to modulate equilibrium sorption capacity and network stability. *Biomacromol* 5:92–96
- Sannino A, Madaghiele M, Lionetto MG, Schettino T, Maffezzoli A (2006) A cellulose-based hydrogel as a potential bulking agent for hypocaloric diets: an in vitro biocompatibility study on rat intestine. *J Appl Polym Sci* 102:1524–1530
- Sannino A, Madaghiele M, Demitri C, Scalera F, Esposito A, Esposito V, Maffezzoli A (2010) Development and characterization of cellulose-based hydrogels for use as dietary bulking agent. *J Appl Polym Sci* 115:1438–1444
- Santos JR, Alves NM, Mano JF (2010) New thermo-responsive hydrogels based on poly(*N*-isopropylacrylamide)/hyaluronic acid semi-interpenetrated polymer networks: swelling properties and drug release studies. *J Bioact Compat Polym* 25:169–184
- Sanz T, Slavador A, Fiszman SM (2004) Effect of concentration and temperature of methylcellulose-added batters application to battered, fried seafood. *Food Hydrocolloid* 18:127–131
- Sarkar N (1979) Thermal gelation properties of methyl and hydroxypropyl methylcellulose. *J App Polym Sci* 24:1073–1087
- Saska S, Teixeira LN, de Oliveira PT, Gaspar AMM, Ribeiro SJL, Messaddeq Y, Marchetto R (2012) Bacterial cellulose-collagen nanocomposite for bone tissue engineering. *J Mater Chem* 22:22102–22112
- Schuetz YB, Gurny R, Jordan O (2008) A novel thermoresponsive hydrogel based on chitosan. *Eur J Pharm Biopharm* 68:19–25
- Segura T, Anderson BC, Chung PH, Webber R, Shull KR, Shea LD (2005a) Crosslinked hyaluronic acid hydrogels: a strategy to functionalize and pattern. *Biomaterials* 26:359–371
- Segura T, Chung PH, Shea LD (2005b) DNA delivery from hyaluronic acid-collagen hydrogels via a substrate-mediated approach. *Biomaterials* 26:1575–1584
- Senna AM, do Carmo JB, da Silva JMS, Botaro VR (2015) Synthesis, characterization and application of hydrogel derived from cellulose acetate as a substrate for slow-release NPK fertilizer and water retention in soil. *J Environ Chem Eng* 3:996–1002
- Serwer P (1983) Agarose gels: properties and use for electrophoresis. *Electrophoresis* 4:375–382
- Sezer AD, Cevher E, Hatipoğlu Z, Baş AL, Akbuğa J (2008) Preparation of fucoidan-chitosan hydrogel and its application as burn healing accelerator on rabbits. *Biol Pharm Bull* 31:2326–2333
- Shen F, Cui YL, Yang LF, Yao KD, Dong XH, Jia WY, Shi HD (2000) A study on the fabrication of porous chitosan/gelatin network scaffold for tissue engineering. *Polym Int* 49:1596–1599
- Shen C, Shen Y, Wen Y, Wang H, Liu W (2011) Fast and highly efficient removal of dyes under alkaline conditions using magnetic chitosan-Fe(III) hydrogel. *Water Res* 45:5200–5210
- Shi XY, Tan TW (2004) New contact lens based on chitosan/gelatin composites. *J Bioact Compat Polym* 19:467–479
- Shi J, Alves NM, Mano JF (2006) Drug release of pH/temperature-responsive calcium alginate/poly(*N*-isopropylacrylamide) semi-IPN beads. *Macromol Biosci* 6:358–363
- Shi R, Bi J, Zhang Z, Zhu A, Chen D, Zhou X, Zhang L, Tain W (2008) The effect of citric acid on the structural properties and cytotoxicity of the polyvinyl alcohol/starch films when molding at high temperature. *Carbohydr Polym* 74:763–770
- Shim JW, Nho YC (2003) Preparation of poly(acrylic acid)–chitosan hydrogel by gamma irradiation and in vitro drug release. *J Appl Polym Sci* 90:3660–3667
- Shu XZ, Liu Y, Luo Y, Roberts MC, Prestwich GD (2002) Disulfide cross-linked hyaluronan hydrogels. *Biomacromolecules* 3:1304–1311

- Shu XZ, Liu Y, Palumbo F, Prestwich GD (2003) Disulfide-crosslinked hyaluronan-gelatin hydrogel films: a covalent mimic of the extracellular matrix for in vitro cell growth. *Biomaterials* 24:3825–3834
- Shu XZ, Liu Y, Palumbo FS, Luo Y, Prestwich GD (2004) In situ crosslinkable hyaluronan hydrogels for tissue engineering. *Biomaterials* 25:1339–1348
- Simmons CA, Alsberg E, Hsiong S, Kim WJ, Mooney DJ (2004) Dual growth factory delivery and controlled scaffold degradation enhance in vivo bone formation by transplanted bone marrow stromal cells. *Bone* 35:562–569
- Singh B, Sharma V (2014) Influence of polymer network parameters of tragacanth gum-based pH responsive hydrogels on drug delivery. *Carbohydr Polym* 101:928–940
- Singh R, Singh D (2012) Radiation synthesis of PVP/alginate hydrogel containing nanosilver as wound dressing. *J Mater Sci Mater Med* 23:2649–2658
- Singh A, Narvi SS, Dutta PK, Pandey ND (2006a) External stimuli response on a novel chitosan hydrogel crosslinked with formaldehyde. *Bull Mater Sci* 29:233–238
- Singh V, Tiwari A, Pandey S, Singh SK (2006b) Microwave-accelerated synthesis and characterization of potato starch-g-poly(acrylamide). *Starch* 58:536–543
- Singh B, Sharma DK, Gupta A (2007) Controlled release of thiram fungicide from starch-based hydrogels. *J Environ Sci Heal B* 42:677–695
- Singh B, Sharma DK, Gupta A (2009a) A study towards release dynamics of thiram fungicide from starch-alginate beads to control environmental and health hazards. *J Hazard Mater* 161:208–216
- Singh B, Sharma DK, Kumar R, Gupta A (2009b) Controlled release of the fungicide thiram from starch-alginate-clay based formulation. *Appl Clay Sci* 45:76–82
- Skardal A, Zhang J, McCoard L, XU X, Oottamasathien S, Prestwich GD (2010) Photocrosslinkable hyaluronan-gelatin hydrogels for two-step bioprinting. *Tissue Eng A* 16:2675–2685
- Smeds KA, Grinstaff MW (2001) Photocrosslinkable polysaccharides for in situ hydrogel formation. *J Biomed Mater Res* 54:115–121
- Sokker HH, El-Savvy NM, Hassan MA, El-Anadouli BE (2011) Adsorption of crude oil from aqueous solution by hydrogel of chitosan based polyacrylamide prepared by radiation induced grafting polymerization. *J Hazard Mater* 190:359–365
- Song K, Yiao M, Liu T, Jiang B, Macedo HM, Ma X, Cui Z (2010) Preparation, fabrication and biocompatibility of novel injectable temperature-sensitive chitosan/glycerophosphate/collagen hydrogels. *J Mater Sci Mater Med* 21:2835–2842
- Sowmya A, Meenakshi S (2013) An efficient and regenerable quaternary amine modified chitosan beads for the removal of nitrate and phosphate anions. *J Environ Chem Eng* 1:906–915
- Spiridon I, Popescu MC, Bodârlău R, Vasile C (2008) Enzymatic degradation of some nanocomposites of poly(vinyl alcohol) with starch. *Polym Degrad Stabil* 93:1884–1890
- Stalling SS, Akintoye SO, Nicoll SB (2009) Development of photocrosslinked methylcellulose hydrogels for soft tissue reconstruction. *Acta Biomater* 5:1911–1918
- Stashak TS, Farsvedt E, Othic A (2004) Update on wound dressing: indications and best use. *Clin Tech Equine Pract* 3:148–163
- Strehin I, Nahas Z, Arora K, Nguyen T, Elisseff (2010) A versatile pH sensitive chondroitin sulfate-PEG tissue adhesive and hydrogel. *Biomaterials* 31:2788–2797
- Striegel AM (1997) Theory and applications of DMAC/LICL in the analysis of polysaccharides. *Carbohydr Polym* 34:267–274
- Sud D, Mahajan G, Kaur MP (2008) Agricultural waste material as potential adsorbent for sequestering heavy metal ions from aqueous solutions—a review. *Bioresour Technol* 99:6017–6027
- Sugiyama J, Vuong R, Chanzy H (1991) Electron diffraction study on the two crystalline phases occurring in native cellulose from an algal cell wall. *Macromolecules* 24:4168–4175
- Sun X, Peng B, Ji Y, Chen J, Li D (2009) Chitosan(chitin)/cellulose composite biosorbents prepared using ionic liquid for heavy metal ions adsorption. *AIChE J* 55:2062–2069

- Sung JH, Hwang MR, Kim JO, Lee JH, Kim YI, Kim JH, Chang SW, Jin SG, Kim JA, Lyoo WS, Han SS, Ku SK, Yong CS, Choi HG (2010) Gel characterisation and in vivo evaluation of minocycline-loaded wound dressing with enhanced wound healing using polyvinyl alcohol and chitosan. *Int J Pharm* 392:232–240
- Suo A, Qian J, Yao Y, Zhang W (2007) Synthesis and properties of carboxymethyl cellulose-graft-poly(acrylic acid-co-acrylamide) as a novel cellulose-based superabsorbent. *J Appl Polym Sci* 103:1382–1388
- Suri S, Schmidt CE (2009) Photopatterned collagen-hyaluronic acid interpenetrating polymer network hydrogels. *Acta Biomater* 5:2385–2397
- Sutar PB, Mishra RK, Pal K, Banthia AK (2008) Development of pH sensitive polyacrylamide grafted pectin hydrogel for controlled drug delivery system. *J Mater Sci Mater Med* 19:2247–2253
- Svensson A, Nicklasson E, Harrah T, Panilaitis B, Kaplan DL, Brittberg M, Gatenholm P (2005) Bacterial cellulose as a potential scaffold for tissue engineering of cartilage. *Biomaterials* 26:419–431
- Swamy BY, Yun YS (2015) In vitro release of metformin from iron (III) cross-linked alginate-carboxymethyl cellulose hydrogel beads. *Int J Biol Macromol* 77:114–119
- Swatowski RP, Spear SK, Holbrey JD, Rogers RD (2002) Dissolution of cellulose with ionic liquids. *J Am Chem Soc* 124:4974–4975
- Tada D, Tanabe T, Tachibana A, Yamauchi K (2007) Albumin-crosslinked alginate hydrogels as sustained drug release carrier. *Mater Sci Eng* 27:870–874
- Takahashi M, Shimazaki M, Yamamoto J (2001) Thermoreversible gelation and phase separation in aqueous methyl cellulose solutions. *J Polym Sci B Polym Phys* 39:91–100
- Taleb MFA, El-Mohdy HLA, Abd El-Rehim HA (2009) Radiation preparation of PVA/CMC copolymers and their application in removal of dyes. *J Hazard Mater* 168:68–75
- Tamura H, Nagahama H, Tokura S (2006) Preparation of chitin hydrogel under mild conditions. *Cellulose* 13:357–364
- Tan W, Krishnaraj R, Desai TA (2001) Evaluation of nanostructured composite collagen–chitosan matrices for tissue engineering. *Tissue Eng* 7:203–210
- Tan H, Wu J, Lao L, Gao C (2009) Gelatin/chitosan/hyaluronan scaffold integrated with PLGA microspheres for cartilage tissue engineering. *Acta Biomater* 5:328–337
- Tang YF, Du YM, Hu XW, Shi XW, Kennedy JF (2007) Rheological characterisation of a novel thermosensitive chitosan/poly(vinyl alcohol) blend hydrogel. *Carbohydr Polym* 67:491–499
- Tang S, Zou P, Xiong H, Tang H (2008) Effect of nano-SiO₂ on the performance of starch/polyvinyl alcohol blend films. *Carbohydr Polym* 72:521–526
- Tang H, Zhou W, Zhang L (2012) Adsorption isotherms and kinetics studies of malachite green on chitin hydrogels. *J Hazard Mater* 209–210:218–225
- Tang H, Chen H, Duan B, Lu A, Zhang L (2014) Swelling behaviors of superabsorbent chitin/carboxymethylcellulose hydrogels. *J Mater Sci* 49:2235–2242
- Tanodekaew S, Prasitsilp M, Somporn S, Boonlom T, Pothsree Pateepasen R (2004) Preparation of acrylic acid grafted chitin for wound dressing application. *Biomaterials* 25:1453–1460
- Thakur VK, Kessler MR (2015) Self-healing polymer nanocomposite materials: a review. *Polymer* 69:369–383
- Thakur VK, Thakur MK (2014) Recent trends in hydrogels based on psyllium polysaccharide: a review. *J Clean Prod* 82:1–15
- Thakur VK, Thakur MK (2015) Recent advances in green hydrogels from lignin: a review. *Int J Biol Macromol* 72:834–847
- Thornton AJ, Alsberg E, Hill EE, Mooney DJ (2004) Shape retaining injectable hydrogels for minimally invasive bulking. *J Urol* 172:763–768
- Tomihata K, Ikada Y (1997a) Crosslinking of hyaluronic acid with water-soluble carbodiimide. *J Biomed Mater Res* 37:243–251
- Tomihata K, Ikada Y (1997b) Crosslinking of hyaluronic acid with glutaraldehyde. *Polym Chem* 35:3553–3559

- Topuz F, Henke A, Richtering W, Groll J (2012) Magnesium ions and alginate do form hydrogels: a rheological study. *Soft Matter* 8:4877–4881
- Trache D, Hazwan Hussin M, Mohamad Haafiz MK, Kumar Thakur V (2017) Recent progress in cellulose nanocrystals: sources and production. *Nanoscale* 9(5):1763–1786
- Tran THA, Tran VN, Le VVM (2013) Biochemical studies on the immobilized lactase in the combined alginate-carboxymethyl cellulose gel. *Biochem Eng J* 74:81–87
- Trimmell D, Shasha BS, Otey FH (1985) The effect of α -amylases upon the release of trifluralin encapsulated in starch. *J Control Release* 1:183–190
- Tsiptsias C, Panayiotou C (2008) Foaming of chitin hydrogels processed by supercritical carbon dioxide. *J Supercrit Fluid* 47:302–308
- Ulanski P, von Sonntag C (2000) OH-radical-induced chain scission of chitosan in the absence and presence of dioxygen. *J Chem Soc Perkin Trans 2*(2000):2022–2028
- Vaghani SS, Patel MM, Satish CS (2012) Synthesis and characterization of pH-sensitive hydrogel composed of carboxymethyl chitosan for colon targeted delivery of ornidazole. *Carbohydr Res* 347:76–82
- Vaizey CJ, Kamm MA (2005) Infectable bulking agents for treating faecal incontinence. *Brit J Surg* 92:521–527
- van Dijk-Wolthuis WNE, Hoozeboom JAM, van Steenberghe MJ, Tsang SKY, Hennink WE (1997) Degradation and release behavior of dextran-based hydrogels. *Macromolecules* 30:4639–4645
- Van Vlierberghe S, Dubruel P, Schacht E (2011) Biopolymer-based hydrogels as scaffolds for tissue engineering applications: a review. *Biomacromol* 12:1387–1408
- Vanderhoogz JL, Alcoutlabi M, Magda JJ, Prestwich GD (2009) Rheological properties of cross-linked hyaluronan–gelatin hydrogels for tissue engineering. *Macromol Biosci* 9:20–28
- Veglio F, Beolchini F (1997) Removal of metals by biosorption: a review. *Hydrometallurgy* 44:301–316
- Venkatesan J, Bhatnagar I, Manivasagan P, Kang KH, Kim SK (2015) Alginate composites for bone tissue engineering: a review. *Int J Biol Macromol* 72:269–281
- Verestiu L, Ivanov C, Barbu E, Tsiouklis J (2004) Dual-stimuli-responsive hydrogels based on poly(*N*-isopropylacrylamide)/chitosan semi-interpenetrating networks. *Int J Pharm* 269:185–194
- Villanueva ME, del Rosario Diez AM, González JA, Pérez CJ, Orrego M, Piehl L, Teves S, Copello GJ (2016) Antimicrobial activity of starch hydrogel incorporated with copper nanoparticles. *ACS Appl Mater Interfaces*. <https://doi.org/10.1021/acsami.6b02955> (in press)
- Voicu SI, Condruz RM, Mitran V, Cimpean A, Miculescu F, Andronesu C, Thakur VK (2016) Sericin covalent immobilization onto cellulose acetate membrane for biomedical applications. *ACS Sustain Chem Eng* 4(3):1765–1774
- Wach RA, Mitomo H, Yoshii F, Kume T (2000) Hydrogel of biodegradable cellulose derivatives. II. Effect of some factors on radiation-induced crosslinking of CMC. *J Appl Polym Sci* 81:3030–3037
- Wach RA, Mitomo H, Nagasawa N, Yoshii F (2003a) Radiation crosslinking of methylcellulose and hydroxyethylcellulose in concentrated aqueous solutions. *Nucl Instrum Meth B* 211:533–544
- Wach RA, Mitomo H, Nagasawa N, Yoshii F (2003b) Hydrogel of radiation-induced cross-linked hydroxypropylcellulose. *Macromol Mater Eng* 287:285–295
- Wach RA, Kudoh H, Zhai M, Nagasawa N, Muroya Y, Yoshii F, Katsumura Y (2004) Rate constants of reactions of carboxymethylcellulose with hydrated electron, hydroxyl radical and the decay of CMC macroradicals. A pulse radiolysis study. *Polymer* 45:8165–8171
- Wach RA, Rokita B, Bartoszek N, Katsumura Y, Ulanski P, Rosiak JM (2014) Hydroxyl radical-induced crosslinking and radiation-initiated hydrogel formation in dilute aqueous solutions of carboxymethylcellulose. *Carbohydr Polym* 112:412–415
- Wang G, Olofsson G (1995) Ethyl(hydroxyethyl)cellulose and ionic surfactants in dilute solution. Calorimetric viscosity study of the interaction with SDS and some cationic surfactants. *J Phys Chem* 99:5588–5596

- Wang L, Stegemann JP (2010) Thermogelling chitosan and collagen composite hydrogels initiated with β -glycerophosphate for bone tissue engineering. *Biomaterials* 31:3976–3985
- Wang L, Stegemann JP (2011) Glyoxal crosslinking of cell-seeded chitosan/collagen hydrogels for bone regeneration. *Acta Biomater* 7:2410–2417
- Wang W, Wang A (2009) Preparation, characterization and properties of superabsorbent nanocomposites based on natural guar gum and modified rectorite. *Carbohydr Polym* 77:891–897
- Wang W, Wang A (2010) Nanocomposite of carboxymethylcellulose and attapulgite as a novel pH-sensitive superabsorbent: synthesis, characterization and properties. *Carbohydr Polym* 82:83–91
- Wang M, Wang L (2013) Synthesis and characterization of carboxymethyl cellulose/organic montmorillonite nanocomposites and its adsorption behavior for Congo Red dye. *Water Sci Eng* 6:272–282
- Wang N, Wu XS (1997) Preparation and characterization of agarose hydrogel nanoparticles for protein and peptide drug delivery. *Pharm Dev Technol* 2:135–142
- Wang H, Li W, Lu Y, Wang Z (1997) Studies on chitosan and poly(acrylic acid) interpolymer complex. I. Preparation, structure, pH-sensitivity, and salt sensitivity of complex-forming poly(acrylic acid): chitosan semi-interpenetrating polymer network. *J Appl Polym Sci* 65:1445–1450
- Wang M, Qiang J, Fang Y, Hu D, Cui Y, Fu X (2000) Preparation and properties of chitosan-poly(*N*-isopropylacrylamide) semi-IPN hydrogels. *J Polym Sci A* 38:474–481
- Wang CC, Juanf LC, Hsu TC, Lee CK, Lee JF, Huang FC (2004a) Adsorption of basic dyes onto montmorillonite. *J Colloid Interf Sci* 273:80–86
- Wang T, Turhan M, Gunasekaran S (2004b) Selected properties of pH-sensitive biodegradable chitosan-poly(vinyl alcohol) hydrogel. *Polym Int*, 911–918
- Wang M, Xu L, Hu H, Zhai M, Peng J, Nho Y, Li J, Wei G (2007) Radiation synthesis of PVP/CMC hydrogels as wound dressing. *Nucl Instrum Meth B* 265:385–389
- Wang Q, Zhang J, Wang A (2009) Preparation and characterization of a novel pH-sensitive chitosan-g-poly(acrylic acid)/attapulgite/sodium alginate composite hydrogel bead for controlled release of diclofenac sodium. *Carbohydr Polym* 78:731–737
- Wang T, Zhu XK, Xue XT, Wu DY (2012) Hydrogel sheets of chitosan, honey and gelatin as burn wound dressings. *Carbohydr Polym* 88:75–83
- Wang F, Zhao J, Pan F, Zhou H, Yang X, Li W, Liu H (2013a) Adsorption properties toward trivalent rare earths by alginate beads doping with silica. *Ind Eng Chem Res* 52:3453–3461
- Wang J, Wei L, Ma Y, Li K, Li M, Yu Y, Wang L, Qiu H (2013b) Collagen/cellulose hydrogel beads reconstituted from ionic liquid solution for Cu(II) adsorption. *Carbohydr Polym* 98:736–743
- Wang J, Zhou X, Xiao H (2013c) Structure and properties of cellulose/poly(*N*-isopropylacrylamide) hydrogels prepared by SIPN strategy. *Carbohydr Polym* 94:749–754
- Wang Q, Cai J, Zhang L, Xu M, Cheng H, Han CC, Kuga S, Xiao J, Xiao R (2013d) A bioplastic with high strength constructed from a cellulose hydrogel by changing the aggregated structure. *J Mater Chem A* 1:6678–6686
- Wang Y, Liu M, Ni B, Xie L (2013e) κ -carrageenan–sodium alginate beads and superabsorbent coated nitrogen fertilizer with slow-release, water-retention, and anticompaction properties. *Ind Eng Chem Res* 51:1413–1422
- Wang Y, Wang W, Shi X, Wang A (2013f) A superabsorbent nanocomposite based on sodium alginate and illite/smectite mixed layer clay. *J Appl Polym Sci* 130:161–167
- Wang Y, Wang W, Wang A (2013g) Efficient adsorption of methylene blue on an alginate-based nanocomposite hydrogel enhanced by organo-illite/smectite clay. *Chem Eng J* 228:132–139
- Wang J, Hu H, Yang Z, Wei J, Li J (2016) IPN hydrogel nanocomposites based on agarose and ZnO with antifouling and bactericidal properties. *Mater Sci Eng C* 61:376–386
- Weeks A, Morrison D, Alauzun JG, Brook MA, Jones L, Sheardown H (2012) Photocrosslinkable hyaluronic acid as an internal wetting agent in model conventional and silicone hydrogel contact lenses. *J Biomed Mater Res A* 100:1972–1982

- Wei Z, Yang JH, Liu ZQ, Xu F, Zhou JX, Zrinyi M, Osada Y, Chen YM (2015) Novel biocompatible polysaccharide-based self-healing hydrogel. *Adv Funct Mater* 25:1352–1359
- Wen C, Lu L, Li X (2014) Mechanically robust gelatin–alginate IPN hydrogels by a combination of enzymatic and ionic crosslinking approaches. *Macromol Mater Eng* 299:504–513
- Wertz JL, Bédoué O, Mercier JP (2010) Cellulose science and technology. EPFL Press, Switzerland
- Westman L, Lindström T (1981) Swelling and mechanical properties of cellulose hydrogels. I. Preparation, characterization and swelling behavior. *J Appl Polym Sci* 26:2519–2532
- White CJ, McBride MK, Pate KM, Tieppo A, Byrne ME (2011) Extended release of high molecular weight hydroxypropyl methylcellulose from molecularly imprinted, extended wear silicone hydrogel contacts. *Biomaterials* 32:5698–5705
- Wintgens V, Lorthioir C, Dubot P, Sébille B, Amiel C (2015) Cyclodextrin/dextran based hydrogels prepared by cross-linking with sodium trimetaphosphate. *Carbohydr Polym* 132:80–88
- Woodings C (ed) (2001) Regenerated cellulose fibres. Woodhead Publishing Ltd., England
- Wu L, Liu M (2008) Preparation and properties of chitosan-coated NPK compound fertilizer with controlled-release and water-retention. *Carbohydr Polym* 72:240–247
- Wu J, Lin J, Zhou M, Wei C (2000) Synthesis and properties of starch-graft-polyacrylamide/clay superabsorbent composite. *Macromol Rapid Commun* 21:1032–1034
- Wu J, Wei Y, Lin J, Lin S (2003) Study on starch-graft-acrylamide/mineral powder superabsorbent composite. *Polymer* 44:6513–6520
- Wu X, Black L, Santacana-Laffitte G, Partick CW (2007) Preparation and assessment of glutaraldehyde-crosslinked collagen-chitosan hydrogels for adipose tissue engineering. *J Biomed Mater Res A* 81:59–65
- Wu F, Zhang Y, Liu L, Yao J (2012a) Synthesis and characterization of a novel cellulose-g-poly (acrylic acid-co-acrylamide) superabsorbent composite based on flax yarn waste. *Carbohydr Polym* 87:2519–2525
- Wu J, Zhao N, Zhang X (2012b) Cellulose/silver nanoparticles composite microspheres: eco-friendly synthesis and catalytic application. *Cellulose* 19:1239–1249
- Xia X, Tang S, Lu X, Hu Z (2003) Formation and volume phase transition of hydroxypropyl cellulose microgels in salt solution. *Macromolecules* 36:3695–3698
- Xia Y, Guo T, Song M, Zhang B, Zhang B (2005) Hemoglobin recognition by imprinting in semi-interpenetrating polymer network hydrogel based on polyacrylamide and chitosan. *Biomacromol* 6:2601–2606
- Xiao C, Yang M (2006) Controlled preparation of physically cross-linked starch-g-PVA hydrogel. *Carbohydr Polym* 64:37–40
- Xie Y, Wang A (2009) Study on superabsorbent composites XIX. Synthesis, characterization and performance of chitosan-g-poly(acrylic acid)/vermiculite superabsorbent composites. *J Polym Res* 16:143–150
- Xiong B, Zhao P, Hu K, Zhang L, Cheng G (2014) Dissolution of cellulose in aqueous NaOH/urea solution: role of urea. *Cellulose* 21:1183–1192
- Xu JB, Bartley JP, Johnson RA (2002a) Preparation and characterization of alginate hydrogel membranes crosslinked using a water-soluble carbodiimide. *J Appl Polym Sci* 90:747–753
- Xu L, Nagasawa N, Fumio Y, Kume T (2002b) Syntheses of hydroxypropyl methylcellulose phthalate hydrogels in Na₂CO₃ aqueous solution with electron-beam irradiation. *J Appl Polym Sci* 89:2123–2130
- Xu JB, Bartley JP, Johnson RA (2003) Preparation and characterization of alginate–carrageenan hydrogel films crosslinked using a water-soluble carbodiimide (WSC). *J Membr Sci* 218:131–146
- Xu Y, Ren X, Hanna MA (2006) Chitosan/clay nanocomposite film preparation and characterization. *J Appl Polym Sci* 99:1684–1691
- Xu FJ, Zhu Y, Liu FS, Nie J, Ma NJ, Yang WT (2010) Comb-shaped conjugates comprising hydroxypropyl cellulose backbones and low-molecular-weight poly(*N*-isopropylacrylamide) side chains for smart hydrogels: synthesis, characterization, and biomedical applications. *Bioconjug Chem* 21:456–464

- Yadav M, Rhee KY (2012) Superabsorbent nanocomposite (alginate-g-PAMPS/MMT): Synthesis, characterization and swelling behavior. *Carbohydr Polym* 90:165–173
- Yadollahi M, Farhoudian S, Namazi H (2015a) One-pot synthesis of antibacterial chitosan/silver bio-nanocomposite hydrogel beads as drug delivery systems. *Int J Biol Macromol* 79:37–43
- Yadollahi M, Gholamali I, Namazi H, Aghazadeh M (2015b) Synthesis and characterization of antibacterial carboxymethylcellulose/CuO bio-nanocomposite hydrogels. *Int J Biol Macromol* 73:109–114
- Yadollahi M, Namazi H, Aghazadeh M (2015c) Antibacterial carboxymethyl cellulose/Ag nanocomposite hydrogels cross-linked with layered double hydroxides. *Int J Biol Macromol* 79:269–277
- Yağış A, Şahin F, Demirel G, Tümtürk H (2005) Binary immobilization of tyrosinase by using alginate gel beads and poly(acrylamide-co-acrylic acid) hydrogels. *Int J Biol Macromol* 36:253–258
- Yan L, Shuai Q, Gong X, Gu Q, Yu H (2009) Synthesis of microporous cationic hydrogel of hydroxypropyl cellulose (HPC) and its application on anionic dye removal. *Clean* 37:392–398
- Yan LP, Wang YJ, Ren L, Wu G, Caridade SG, Fan JB, Wang LY, Ji PH, Oliveira JM, Oliveira JT, Mano JF, Reis RL (2010) Genipin-cross-linked collagen/chitosan biomimetic scaffolds for articular cartilage tissue engineering applications. *J Biomed Mater Res A* 95:465–475
- Yang JM, Lin HT (2004) Properties of chitosan containing PP-g-AA-g-NIPAAm bigraft nonwoven fabric for wound dressing. *J Membr Sci* 243:1–7
- Yang X, Liu Q, Chen X, Yu F, Zhu Z (2008) Investigation of PVA/ws-chitosan hydrogels prepared by combined γ -irradiation and freeze-thawing. *Carbohydr Polym* 73:401–408
- Yang C, Frei H, Rossi F, Burt HM (2009) The differential in vitro and in vivo responses of bone marrow stromal cells on novel porous gelatin–alginate scaffolds. *J Tissue Eng Regen M* 3:601–614
- Yang C, Xu L, Zhou Y, Zhang X, Huang X, Wang M, Han Y, Zhai M, Wei S, Li J (2010) A green fabrication approach of gelatin/CMC-chitosan hybrid hydrogel for wound healing. *Carbohydr Polym* 82:1297–1305
- Yang L, Ma X, Guo N (2012) Sodium alginate/Na⁺-rectorite composite microspheres: preparation, characterization, and dye adsorption. *Carbohydr Polym* 90:853–858
- Yang CH, Wang MX, Haider H, Yang JH, Sun JY, Chen YM, Zhou J, Suo Z (2013) Strengthening alginate/polyacrylamide hydrogels using various multivalent cations. *ACS Appl Mater Interfaces* 5:10418–10422
- Yao KD, Yin YJ, Xu MX, Wang YF (1995) Investigation of pH-sensitive drug delivery system of chitosan/gelatin hybrid polymer network. *Polym Int* 38:77–82
- Yazdani-Pedram M, Retuert J, Quijada R (2000) Hydrogels based on modified chitosan, 1. Synthesis and swelling behavior of poly(acrylic acid) grafted chitosan. *Macromol Chem Phys* 201:923–930
- Yeom J, Bhang SH, Kim BS, Seo MS, Hwang EJ, Cho IH, Park JK, Hahn SK (2010) Effect of cross-linking reagents for hyaluronic acid hydrogel dermal fillers on tissue augmentation and regeneration. *Bioconj Chem* 21:240–247
- Yi Y, Xu S, Sun H, Chang D, Yin Y, Zheng H, Xu H, Lou Y (2011) Gelation of photocrosslinkable carboxymethyl chitosan and its application in controlled release of pesticide. *Carbohydr Polym* 86:1007–1013
- Yin L, Fei L, Cui F, Tang C, Yin C (2007) Superporous hydrogels containing poly(acrylic acid-co-acrylamide)/O-carboxymethyl chitosan interpenetrating polymer networks. *Biomaterials* 28:1258–1266
- Yin Y, Ji X, Dong H, Ying Y, Zheng H (2008) Study of the swelling dynamics with overshooting effect of hydrogels based on sodium alginate-g-acrylic acid. *Carbohydr Polym* 71:682–689
- Yokoyama F, Masada I, Shimamura K, Ikawa T, Monobe K (1986) Morphology and structure of highly elastic poly(vinyl alcohol) hydrogel prepared by repeated freezing-and-melting. *Colloid Polym Sci* 264:595–601

- Yoshimura T, Uchikoshi I, Yoshiura Y, Fujioka R (2005) Synthesis and characterization of novel biodegradable hydrogels based on chitin and succinic anhydride. *Carbohydr Polym* 61:322–326
- Yoshimura T, Yoshimura R, Seki C, Fujioka R (2006) Synthesis and characterization of biodegradable hydrogels based on starch and succinic anhydride. *Carbohydr Polym* 64:345–349
- Yu H, Xu X, Chen X, Hao J, Jing X (2006) Medicated wound dressings based on poly(vinyl alcohol)/poly(*N*-vinyl pyrrolidone)/chitosan hydrogels. *J Appl Polym Sci* 101:2453–2463
- Zamani A, Henriksson D, Taherzadeh MJ (2010) A new foaming technique for production of superabsorbents from carboxymethyl chitosan. *Carbohydr Polym* 80:1091–1101
- Zhai M, Yoshii F, Kume T, Hashim K (2002) Syntheses of PVA/starch grafted hydrogels by irradiation. *Carbohydr Polym* 50:295–303
- Zhang Y, Ji C (2010) Electro-induced covalent cross-linking of chitosan and formation of chitosan hydrogel films: its application as an enzyme immobilization matrix for use in a phenol sensor. *Anal Chem* 82:5275–5281
- Zhang Q, Liu L, Ren L, Wang F (1997) Preparation and characterization of collagen–chitosan composites. *J Appl Polym Sci* 64:2127–2130
- Zhang GQ, Zha LS, Zhou MH, Ma JH, Liang BR (2005a) Preparation and characterization of pH- and temperature responsive semi-interpenetrating polymer network hydrogels based on linear sodium alginate and crosslinked poly(*N*-isopropylacrylamide). *J Appl Polym Sci* 97:1931–1940
- Zhang H, Wu J, Zhang J, He J (2005b) 1-allyl-3-methylimidazolium chloride room temperature ionic liquid: a new and powerful nonderivatizing solvent for cellulose. *Macromolecules* 38:8272–8277
- Zhang R, Tang M, Bowyer A, Eisenthal R, Hubble J (2005c) A novel pH- and ionic-strength-sensitive carboxy methyl dextran hydrogel. *Biomaterials* 26:4677–4683
- Zhang S, Li FX, Yu JY, Hsieh YL (2010) Dissolution behavior and solubility of cellulose in NaOH complex solution. *Carbohydr Polym* 81:668–674
- Zhang F, He C, Cao L, Feng W, Wang H, Mo X, Wang J (2011a) Fabrication of gelatin–hyaluronic acid hybrid scaffolds with tunable porous structures for soft tissue engineering. *Int J Biol Macromol* 48:474–481
- Zhang L, Li K, Xiao W, Zheng L, Xiao Y, Fan H, Zhang X (2011b) Preparation of collagen–chondroitin sulfate–hyaluronic acid hybrid hydrogel scaffolds and cell compatibility in vitro. *Carbohydr Polym* 84:118–125
- Zhang LM, Wu CX, Huang JY, Peng XH, Chen P, Tanf SQ (2012) Synthesis and characterization of a degradable composite agarose/HA hydrogel. *Carbohydr Polym* 88:1445–1452
- Zhang G, Yi L, Deng H, Sun P (2014a) Dyes adsorption using a synthetic carboxymethyl cellulose-acrylic acid adsorbent. *J Environ Sci* 26:1203–1211
- Zhang L, Wang L, Guo B, Ma PX (2014b) Cytocompatible injectable carboxymethyl chitosan/*N*-isopropylacrylamide hydrogels for localized drug delivery. *Carbohydr Polym* 103:110–118
- Zhao X, Kato K, Fukumoto Y, Nakamae K (2001) Synthesis of bioadhesive hydrogels from chitin derivatives. *Int J Adhes Adhes* 21:227–232
- Zhao F, Yin Y, Lu WW, Leong JC, Zhang W, Zhang J, Zhang M, Yao K (2002) Preparation and histological evaluation of biomimetic three-dimensional hydroxyapatite/chitosan-gelatin network composite scaffolds. *Biomaterials* 23:3227–3234
- Zhao L, Mitomo H, Nagasawa N, Yoshii F, Kume T (2003a) Radiation synthesis and characteristic of the hydrogels based on carboxymethylated chitin derivatives. *Carbohydr Polym* 51:169–175
- Zhao L, Mitomo H, Zhai M, Yoshii F, Nagasawa N, Kume T (2003b) Synthesis of antibacterial PVA/CM-chitosan blend hydrogels with electron beam irradiation. *Carbohydr Polym* 53:439–446
- Zhao L, Xu L, Mitomo H, Yoshii F (2006) Synthesis of pH-sensitive PVP/CM-chitosan hydrogels with improved surface property by irradiation. *Carbohydr Polym* 64:473–480
- Zheng WJ, Gao J, Wei Z, Zhou J, Chen YM (2015) Facile fabrication of self-healing carboxymethyl cellulose hydrogels. *Eur Polym J* 72:514–522

- Zhijiang C, Guang Y (2011) Bacterial cellulose/collagen composite: characterization and first evaluation of cytocompatibility. *J Appl Polym Sci* 120:2938–2944
- Zhong C, Wu J, Reinhart-King CA, Chu CC (2010) Synthesis, characterization and cytotoxicity of photo-crosslinked maleic chitosan-polyethylene glycol diacrylate hybrid hydrogels. *Acta Biomater* 6:3908–3918
- Zhong K, Lin ZT, Zhen XL, Jiang GB, Fang YS, Mao XY, Liao ZW (2013) Starch derivative-based superabsorbent with integration of water-retaining and controlled-release fertilizers. *Carbohydr Polym* 92:1367–1376
- Zhou J, Chang C, Zhang R, Zhang L (2007) Hydrogels prepared from unsubstituted cellulose in NaOH/urea aqueous solution. *Macromol Biosci* 7:804–809
- Zhou ZH, He SL, Huang TL, Liu LH, Liu QQ, Zhao YM, Ou BL, Zeng WN, Yang ZM, Cao D (2013a) Degradation behavior and biological properties of gelatin/hyaluronic acid composite scaffolds. *Mater Res Innov* 17:420–424
- Zhou Z, Yang Z, Huang T, Liu L, Liu Q, Zhao Y, Zeng W, Yi Q, Cao D (2013b) Effect of chemical cross-linking on properties of gelatin/hyaluronic acid composite hydrogels. *Polym Plast Technol* 52:45–50
- Zhu HY, Fu YQ, Jiang R, Yao J, Xiao L, Zeng GM (2012) Novel magnetic chitosan/poly(vinyl alcohol) hydrogel beads: preparation, characterization and application for adsorption of dye from aqueous solution. *Bioresour Technol* 105:24–30

Chapter 6

Polysaccharide Containing Gels for Pharmaceutical Applications



Catalina Natalia Cheaburu-Yilmaz, Sakine Tuncay Tanriverdi,
Ozgen Ozer and Cornelia Vasile

Abstract Bio-derived polymers are falling into the needs of pharmaceutical formulations for topical applications due to their gelling ability. Generally, in topical delivery, as an alternative way for local and systemic application of active substances, formulations in gelling form are preferred as they have multiple advantages, e.g., minimize systemic side effects, avoid gastrointestinal irritation, prevent the metabolism of the active substance in liver, etc. The present chapter reviews bio-based polymers with special reference to polysaccharides-based hydrogels with respect to their pharmaceutical applications.

Keywords Polymeric gels · Hydrogels · Biopolymers · Polysaccharides
Pharmaceutical formulations · Topical delivery · Gel systems

1 Introduction

The topical delivery treatment is a preferred route for various skin diseases. Most of the medicated products are applied directly on the skin or at the level of the mucous membrane which either enhances or restores a fundamental functions of the skin. Such products are referred as dermal or transdermal products. Within Fig. 1 is shown a representative image of the skin describing its physiology and functions described by Venus et al. (2011).

The dermal preparations are applied to local act. The drug remains on the skin surface or in some cases, it penetrates through the epidermal layers and may reach the dermis. For local applications, the drugs are not absorbed into the blood

C. N. Cheaburu-Yilmaz (✉) · C. Vasile
Department of Physical Chemistry of Polymers, “Petru Poni”
Institute of Macromolecular Chemistry, 700487 Iasi, Romania
e-mail: duncaty@gmail.com

C. N. Cheaburu-Yilmaz · S. T. Tanriverdi · O. Ozer
Department of Pharmaceutical Technology, Faculty of Pharmacy,
Ege University, 35100 Izmir, Turkey

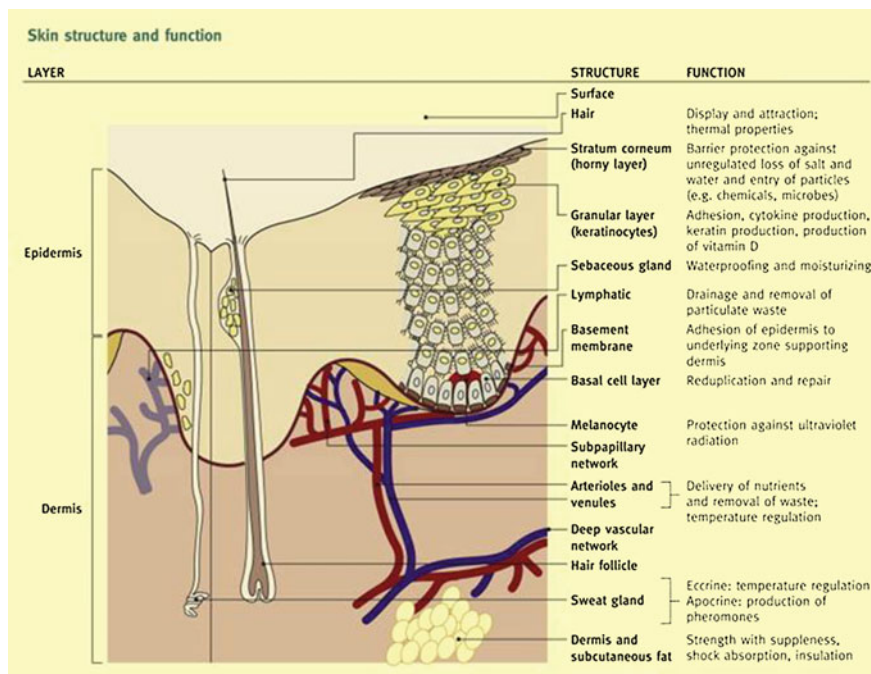


Fig. 1 Structure of the skin. With permission from Elsevier from (Venus et al. 2011)

circulation. The transdermal formulations are applied to obtain a systemic effect of drugs. In this case, drugs are delivered into the general blood circulation to achieve a specific therapeutic response. Corticosteroids, antifungals, antivirals, antibiotics, antiseptics, local anesthetics, and antineoplastics are applied topically in different vehicles.

Conventionally topical vehicles are classified as liquid, semisolid, and solid systems. Powders, patches, gauzes, tapes, and sticks are examples of solid topical dosage forms. Liquid topical forms are lotions, suspensions, and solutions while semisolid topical dosage forms are collodions, foams, ointments, pastes, creams, and gels (Ueda et al. 2009; Murthy and Shivakumar 2010).

Gel systems represent an important group of semisolid preparations and transdermal gels both commonly used in cosmetics and in pharmaceutical preparations. In pharmaceutical fields, they could be used for a localized drug delivery system anywhere in the body through ophthalmic, rectal, vaginal, nasal, and skin as topical routes. The gelling agents, mostly the polymeric matrix, and water are the primary ingredients used to form gel systems.

The optimal composition for polymers to be used was chosen to be between 1 and 5% in topical gel formulation. They offer advantage by their non-greasy properties because they can easily provide a washable film on the skin.

Many of biodegradable polymers are coming from natural sources (Trache et al. 2017; Corobea et al. 2016; Voicu et al. 2016; Miculescu et al. 2016). They become even more attractive by the time passing as combination of their properties e.g. biocompatibility, lack of toxicity, biodegradability some of them exhibiting specific characteristics like responsiveness to external stimuli, gelling abilities, susceptibility to be chemically modified to obtain new materials; moreover, the natural polymers have more than one functional group on the structural unit as compared with synthetic polymers, therefore an increased reactivity and possibility to form inter-polymeric associations (Kontogiorgos et al. 2015; Cheaburu and Bumbu 2009; Pappu et al. 2015, 2016).

In the last decades a huge number of scientific reports were dedicated to gels/hydrogels and many having as common subject of biopolymers within pharmaceutical, food and medical applications, fields which all require non-toxicity for human health (Sagiri et al. 2014; Pamfil and Vasile 2017). The class of bio-derived polymers which are found naturally, includes proteins (peptides, proteins, collagen, silk, keratin, elastin, etc.), nucleic acids (e.g., self-assembling DNA *hydrogel* (Nishida et al. 2016); Y-shaped DNA units functionalized with Ag-nanoclusters as fluorescent *hydrogels* (Guo et al. 2013), *lignin* (Thakur and Thakur 2015) and polysaccharides (chitosan, alginate, carragenan, hyaluronic acid, psyllium, etc.) (Babu et al. 2013; Thakur and Thakur 2014). These bio-based polymers have shown enormous interest in recent years as regarding the developments in their structure modification and their applications.

The present chapter deals with the reviewing of state-of-art of gel/hydrogels used for pharmaceutical applications, emphasizing on the role of polysaccharides-based systems within the prepared formulations for different topical applications.

Conventionally, polymers were used just as tablet binders; in modern and advanced dosage forms, the role of polymers became more important as they need to protect the loaded drug for a determined time period, mask the taste, to release drugs in a controlled manner and to target them to a specific site, therefore the drug bioavailability will increase as well. The rheology modification represents another property that is considered important in liquid dosage forms (Sagiri et al. 2014).

2 General Aspects

2.1 Definition Classification

The concept of gel was mentioned for the first time by (Papkov 1974) and later by (Tanaka 1985).

The terms, gels and hydrogels are interchangeably used by scientists to describe polymeric crosslinked network structures able to absorb a high amount of liquids, respectively water (Gulrez et al. 2011). Rogovina et al. (2008) described a gel as being a solid which comprises at least two constituents, the polymeric one, which may form the three-dimensional network via covalent or noncovalent bonding

(giving chemical and physical gels, respectively) in the medium of the second constituent (a liquid one). The minimum amount of the liquid is theoretically enough to ensure elastic properties to the gel. The network structure is formed as result of physical bonding (namely, physical gels) or chemical bonding (i.e., chemical gels), crystallites or other junctions persisting in the same state within the extending fluid (Huang et al. 2002). Peppas and Buri (1985) reported a theory for polymer gels based on so-called Single-Chain Mean-Field (SCMF) theory. This theory uses the mesh chain or the star polymer as the characteristic units for the polymer gels, and it grants the study of chain conformation in its different gel stages.

A general accepted classification of the gels/hydrogels was done by various researchers and two main categories were evidenced: permanent or chemical gel; the terms “permanent” or “chemical” gels reflect the covalently crosslinked networks and reversible or physical gels (Hennink and Nostrum 2002). The permanent type of gel reaches a steadiness of swelling state (equilibrium) which depends on the polymer–water interaction parameter and the crosslink density (Rosiak and Yoshii 1999).

In the second one the crosslinks are clamped together by molecular entanglements, and/or secondary forces including ionic, hydrogen bonding, or hydrophobic interactions. In the case of these gels, dissolution is limited by physical interactions, which exist between the different polymer chains (Hennink and Nostrum 2002). All of these interactions are reversible, and can be destroyed by the changes which occur in physical conditions or in the case of a stress or shear load application (Rosiak and Yoshii 1999).

Gels are also categorized as weak or strong depending on their flow behavior in steady state (Russo 1987; Ferry 1961) Singhal and Gupta in their comprehensive review (Singhal and Gupta 2016) took into account the presence or absence of electrical charge located in the crosslinked chains and classified the gels accordingly.

2.2 Biopolymer Gel Network Formation

In past decades an increased interest on the gel preparation was observed as the applicative aspect started to become more important. Correlations between the characteristics of the polymeric material and the practical needs in various fields became a “must.” Various reports and reviews were published emphasizing the importance of the preparation method of the gel/hydrogels to obtain the desired properties for specific applications (Singhal and Gupta 2016; Ahmad and Asifm Mahmood 2016; Secchi et al. 2013).

As a general accepted concept, gelation process is assigned to the phenomena of linking the macromolecular chains together, up to the structure of polymers and their conformation producing a highly branched polydisperse, yet soluble polymers defined as “sol.”

Propagation of the linking process leads to the increasing the extent of the crosslinked polymer with decreasing solubility. This “limitless polymer” is named as “gel” or “network” (Gulrez et al. 2011).

This evolution from a system with soluble finite branched polymer to infinite molecules is claimed as being a “sol-gel transition” (or “gelation”) and the crucial point at what gel is firstly formed is so-called the “gel point” (Rubinstein and Colby 2003).

Most of the biopolymers form gels more readily in water than in organic solvents, e.g., renaturation to the triple helical conformation in gelatin and double helical conformation in polysaccharides controls the nucleation and growth of crystallites during gel formation. At high temperatures, they have a random coiled conformation (Jeong et al. 2012). As temperature decreased, they form double helices and aggregates and further behave like crosslinking joints. One example on how a polysaccharide-based matrix is forming the gel in water is shown in Fig. 2. The random coils are changing the conformations into helices-like, which further aggregate and form the gel with its junction’s sites.

An example was reported by Jeong et al. (2012). They attached hydrophilic segments on the water insoluble cellulose and obtained water-soluble cellulose derivatives. At a specific hydrophilic and hydrophobic balance, macromolecular chains suffer a sol-to-gel transition in water, depending on the type and degree of substitution of cellulose at the hydroxyl group (Jeong et al. 2012). As water evolves

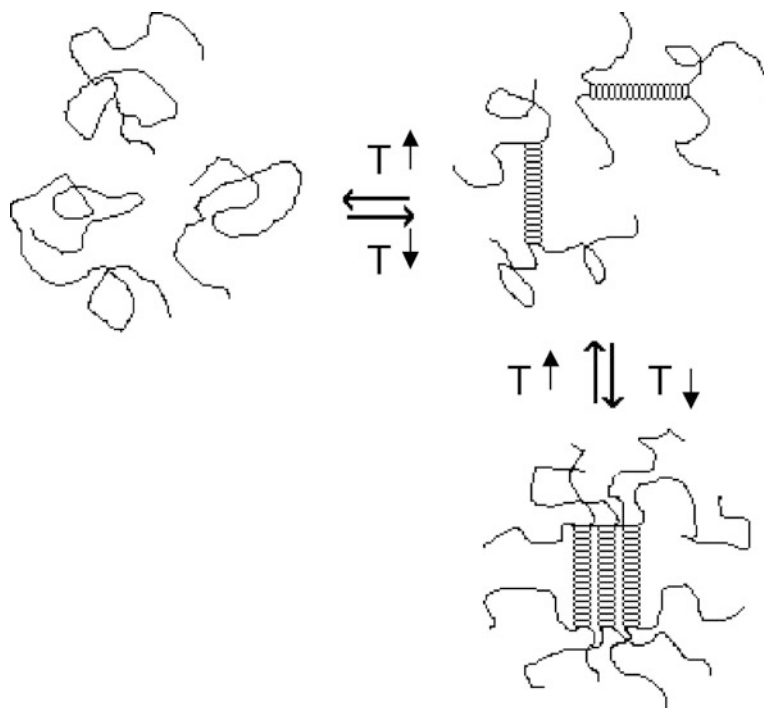


Fig. 2 Gelation of polysaccharides in water. With permission from Elsevier from (Jeong et al. 2012)

towards to a poor solvent once temperature is increased and polymer–polymer interactions become dominant at higher temperatures, the gel is formed (Bekturov and Bimendina 1981; Cheaburu and Bumbu 2009).

An interesting inverse thermo-gelation of a mixture of chitosan and glycerol phosphate disodium salt was reported by Chenite et al. (2000). They reported that by mixing a solution of chitosan and glycerophosphate disodium salt solution, at neutral pH and at room temperature, the mixture was homogeneous and a clear liquid which becomes a gel close to 37 °C. The gelation temperature increased as the degree of deacetylation of the polymer decreased and was not strongly influenced by the molecular weight of the chitosan. The dominant gelation drawing force was supposed to be based on the hydrophobic interactions between neutral chitosan molecules; additionally the gelation strength is complemented by the action of glycerol.

Nie et al. (2015) studied the oriented structure of a multilayered chitosan (CS) hydrogel prepared free of an auxiliary crosslinking agent. They studied as well the gelation process of solubilized CS in acidic aqueous medium. CS behaves like a polyelectrolyte due to the protonation of $-\text{NH}_2$ groups in acidic medium. The solution of CS can be turned into a hydrogel in alkaline medium. The sol-gel transition of CS occurs around pH 6–6.5, the hydrogel being formed at higher pH values (Cheaburu-Yilmaz et al. 2015a). The development of the layers could be clarified by the Liesegang Ring Phenomenon. This lead to periodical precipitation in the medium at the interphase between the internal and the external electrolyte layer (Nie et al. 2015).

According to Nie et al. (2015), gelation debuted with the closeness of the surface layer of CS solution reached coagulation bath. As primary hydrogel layer was formed and it further acted as the interface for the second layer, between the system and OH^- source. The process is progressive as the crosslinks are not formed simultaneously in the whole system. This gelation mechanism was found as a layer-wise characteristic. Therefore it could be form of multilayers hydrogels (Nie et al. 2015).

Physical gels/hydrogels differ from chemical ones in respect with the type of crosslinks, the random character of the network formation, and the effects of these parameters on the rigidity and elastic moduli of the crosslinked structures (Singhal and Gupta 2016).

3 Preparation Methods

3.1 General Aspects

Various gel/hydrogel preparation procedures were reported in the past years (Ullah et al. 2015; Ahmed 2015; Gulrez et al. 2011; Aroguz et al. 2010; Hoare and Kohane 2008; Buwalda et al. 2014). Natural biopolymers, e.g., alginate, chitosan, carrageenan, hyaluronan, carboxymethyl cellulose (CMC), pectin, etc., were preferred within the pharmaceutical formulations and various preparation techniques were adopted up to the aimed properties of the final gel/hydrogel.

Generally, the methods are classified into physical crosslinking, chemical crosslinking, grafting polymerization techniques, and radiation induced crosslinking (Hennink and Nostrum 2002; Guilherme et al. 2015; Thakur et al. 2016). Different ways to form physical and chemical gels were summarized within Table 1 comprising the specificity of the method and selected examples as there are so numerous reviews and books reporting this aspect (Hennink and Nostrum 2002; Guilherme et al. 2015).

Present sub-chapter comprises the discussion over the mostly used methods to prepare gel/hydrogels used in pharmaceutical application, highlighting the last trends, and developments. Ionic gelation of alginate represents the most used method in pharmacy to encapsulate drugs and other active substances and it was given a special attention in the following.

3.2 *Ionic Gelation of Alginate*

Alginate gels are consistently developed via physical based crosslinking procedures (ionic bonds with divalent cations such as Ca^{2+} and Mg^{2+}). Ionic gelation with Ca^{2+} represents the most applied method to obtain hydrogels and its mechanism was explained based on the distinct and effective interactions between calcium ions and blocks of galacturonic and guluronic acid residues (Braccini and Perez 2001).

Calcium ions induce chain–chain associations and form joint regions which are responsible for the gel formation. Grant and Morris developed before a model for the joint zone, well-known as the “egg box” (Grant et al. 1973; Morris et al. 1978). According to the model proposed, couples of helical chains are packed by the calcium ions placed between the helices forming the “boxes.” A representative illustration is presented within the Fig. 3.

It was assumed that polyguluronates segments are responsible for the egg boxes formation. Plazinski (2011) improved the theory of (Braccini and Perez 2001) and (Morris et al. 1978) proving by using a theoretical approach that Guluronic acid residues (G blocks) onward the alginate chains took a helical conformation; two of such chains are packed together with the calcium ions located between them.

3.3 *Radiation-Induced Gelation*

Another crosslinking method has been proposed as physical gelation can lead to structural inhomogeneity and by chemical crosslinking, structural biocompatibility can be reduced due to the presence of the crosslinking agents. Radiation-induced crosslinking is considered more efficient and milder than the other two methods (Fan et al. 2016). In the gelation induced by irradiation, there is no need of adding additional crosslinking agents. Fan et al. used γ -irradiation to prepare a hydrogel composed of chitosan/gelatin/PVA. They found as an optimal parameter for the

Table 1 Summary of the preparation methods for gels/hydrogel preparation with selected examples for each type

Preparation method	Structural characteristics	Selected examples	Composition	Application	References
Physical methods	Hydrogen bonding	<ul style="list-style-type: none"> - Hydrogen bonds between the functional groups - pH dependent swelling of the gels 	Alginate acid—poly (N-isopropyl acryl amide) (AgA/PNIPAAm)	In situ gelling systems	Cheaburu and Vasile (2008)
	UV-induced polymerization	Obtaining the polymer through a chain reaction initiated by light	PVA/betacyclodextrin	Sustained release of ocular therapeutics	Xu et al. (2010)
	Freeze-thawing	Exposure to freeze and thaw cycles resulting a low strength gel; crystalline junctions are formed and the strength of the gel is increased	PVA/chitosan hydrogels Poly (vinyl alcohol)/-cyclodextrin blends (CD)	Ciprofloxacin carriers Drug delivery	Pamfil et al. (2016), Păduraru et al. (2010)
Freeze-drying	A porous like structure is obtained Matrix become more suitable for transport	Hydroxyethylcellulose (HEC) and polyacrylic acid (PAA)	10 wt%	Drug delivery and improve of the solubility of the anti-HIV drug, efavirenz	Ahmad and Asifm Mahmood (2016)
Ionic gelation	Interaction of an ionic polymer with oppositely charge ion to initiate Cross linking	Ionic gelation of alginate with Ca ²⁺ with the formation of "egg-box" like structures	1–3wt%	Drug delivery, encapsulation of protein or other active constituents	Leong et al. (2016)

(continued)

Table 1 (continued)

Preparation method	Structural characteristics	Selected examples	Composition	Application	References
		Chitosan (CS)-based nanoparticles (NPs) loaded with ketorolac tromethamine (KT)	CS solutions 1, 1.25, 1.75 and 2 mg/mL in acetic acid 1% 2.5:1 v/v of CS:TPP	Ocular delivery of KT	Fathalla et al. (2016)
		Chitosan nanoparticles	CTS:TPP 2:1 until 6:1 ^a	Pharmaceutical applications	De Pinho Neves et al. (2014)
		Dermatan sulfate/chitosan (CS/DS)	1:1, 2:1, 3:1 and 9:1 v/v ^b	Endothelial uptake and vascular disease, drug delivery	Rasente et al. (2016)
	Double physically crosslinked magnetic hydrogel beads ^c	Sodium alginate and poly(vinyl alcohol) (PVA) containing magnetic laponite RD	1:1 w/w%	Magnetic response of hydrogels for adsorption of bovine serum albumin (BSA) on the hydrogels	Mahdavinia et al. (2016)
Polymer-polymer complexes	Complex structure directly depends on the degree of ionization of cationic and anionic polymers that, in turn, is determined by the pH and ionic strength of the reaction environment	Chitosan (CH) and carboxymethylcellulose (CMC)	CH/CMC 1:3 ^d	Colon delivery of vancomycin (VM) ^e	Cerchiara et al. (2016)
	Solid and liquid active constituents are encapsulated by a polymer solution through the	Chitosan/hyaluronic acid (CS/HA)	SCS/HA and CS/HA PECs 1:1 mass ratio	Sulfadiazine release	Dumitriu et al. (2015)
Spray drying		Cross-linked alginate microcapsules (CLAMs)	Emulsion: alginate suspension 1:1 (w/w) ^e	Drug delivery	Strobel et al. (2016)

(continued)

Table 1 (continued)

Preparation method	Structural characteristics	Selected examples	Composition	Application	References
	use of a crosslinking agent and hot air to bring about desired physiochemical changes within the encapsulated moiety	Spray freeze-drying of chitosan (SFDC) or alginate (SFDA)	1% (w/v) chitosan-acetic acid solution: sodium TPP at 0.3% (w/v) Sodium alginate 1% (w/v)	Colon delivery	Gamboia et al. (2015)
Combination of physical crosslinking procedure with microfluidic technology	Self-assembling behavior of chitosan into 3D nanofiber network without crosslinking agent	Chitosan microspheres with an ECM-mimicking nanofibrous structure	Chitosan 1–2% (w/v) Oil phase 3% (v/v) span-8	Scaffolds for tissue engineering	Zhou et al. (2016)
	Physical crosslinking and lyophilization	Hydroxyethylcellulose (HEC) and polyacrylic acid (PAA)	10 wt%	Drug delivery and improved solubility of the anti-HIV drug, efavirenz	Mabrouk et al. (2015)
Chemical	Water/oil/water emulsion Core-shell particles	Alginate-poly (lactide-co-glycolide) (PLGA)	4.5% (w/v) sodium alginate (NaAlg): 10% (w/v) PLGA solution	Drug delivery	Lim et al. (2013)
Chemical crosslinking	Addition of a chemical crosslinking agent e.g. glutaraldehyde, tripolymphosphate, etc	Nanocomposite hydrogels based on chitosan (CS) and montmorillonite (MMT) β -cyclodextrins (β CD) crosslinked with epichlorohydrin (EP)	1:1–1:3 v/v/% ^g	Topical application, drug delivery systems	Cojocariu et al. (2012), Cheaburu-Yilmaz et al. (2015b)
			EP: CD ratio was 11:1, T 25–60 °C	Drug delivery	Machin et al. (2012)

(continued)

Table 1 (continued)

Preparation method	Structural characteristics	Selected examples	Composition	Application	References
Grafting reactions	Coupling reaction in the presence of a water-soluble carbodiimide as a crosslinker and <i>N</i> -hydroxysuccinimide	β -cyclodextrin-grafted carboxymethyl chitosan hydrogels	17 mmol CMC: 3 mmol CMC 17 mmol CMC: 6 mmol CMC 17 mmol CMC: 9 mmol CMC ^h	Controlled drug delivery	Kono and Teshirogi (2015)
	Carbodiimide coupling reaction ⁱ	Chitosan/pluronic composite hydrogels	0.5 and 1 wt%: and Plu-SH 4 and 16 wt%	Tissue adhesives and hemostatic materials	Ryu et al. (2011)
Controlled radical polymerization reactions	Click chemistry technique	Layer by layer hydrogels based on alkynyl functional hyaluronic acid/ chitosan-N3	1:1 (w/w %) per functional unit	Drug delivery	Hu and Gong (2016)
Michael addition reaction	Involves formation of thiol-acrylate networks for hydrogel microparticles that is due to chemical modification of functional groups of polymer	Dex-I-DTT hydrogel ^l	Dextran 62 mmol glucopyranosyl ring/ 4-dimethylaminopyridine (DMAP) (15.5 mmol)/ glycidyl methacrylate (GMA, 31 mmol)	3D cell encapsulation	Liu et al. (2015)
Interpenetrated polymeric networks	Covalently cross-linked with <i>N</i> , <i>N'</i> -methylenebisacrylamide	Mixed-interpenetrated polymeric networks based on sodium alginate (ALG) and poly (<i>N</i> -isopropylacryl amide) (PNIPAAm)	NIPAAm-to-alginate percentage weight ratios (99/1, 80/20, and 75/25 NIPAAm/ALG)	Drug delivery	Dumitriu et al. (2014)

(continued)

Table 1 (continued)

Preparation method	Structural characteristics	Selected examples	Composition	Application	References
Radiation induced gelation	Gelation of alginate undergoing ionic crosslinking upon ultraviolet (UV) irradiation	Alginate with calcium carbonate (CaCO ₃) particles and a photoacid generator (PAG)	4 wt/vol% alginate, 60 mM PAG, and 30 mM CaCO ₃	Topical applications	Higham et al. (2014)

^aCrosslinking was done with tripolyphosphate (TPP) at an adjusted pH 4.5, average diameter of 76.2 nm and zeta potential of 32.6 mV were obtained
^bpH 3.5, the ratio 3:1 was the optimal determined

^cSodium alginate and PVA were physically crosslinked by Ca²⁺ and freezing–thawing cycles

^dWas selected based on the encapsulation efficiency, water-uptake and drug release rate

^eEmulsion (corn oil, Tween 80, 2% (w/w) succinic Acid): 4% alginate, 0.2% CaHPO₄, and 0.06% sodium citrate dehydrate, pH adjusted at 5.6

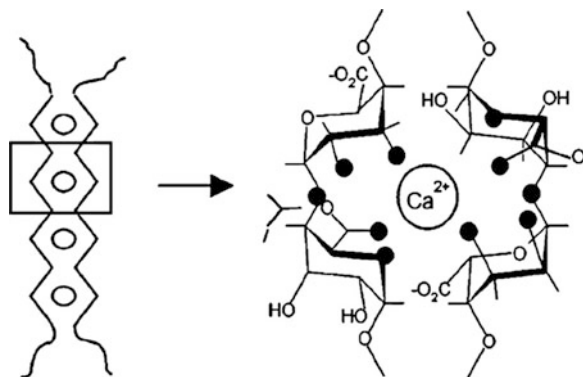
^fPolyvinyl alcohol (PVA) was used as a plasticizer [Crosslinked Hydrogel Composite (CHC)]

^gCrosslinking degree of CS with GA at the ratio of 1:0.3 v/v%. PVA-poly (vinyl alcohol)

^hYield of the dried hydrogel obtained from the reaction of CMC and CMCD was found the highest

ⁱChitosan conjugated with multiple catechol groups in the backbone was crosslinked with terminally thiolated Pluronic F-127 triblock copolymer to obtain temperature-sensitiveness and adhesive sol-gel transition
^j“l” means “linked-by”

Fig. 3 Illustration of the “egg-box” model for calcium alginate gel and the interaction between calcium cations and oxygen atoms (filled circles) on the guluronic acid monomers. With permission from Springer from (Fu et al. 2011)



hydrogel preparation, the gamma radiation dose as being of 40 kGy. For this value, properties of the gels were very good and it was noticed that with the addition of chitosan the crosslinking density of the polymer molecules was increased leading to enhanced mechanical properties of the hydrogel.

Javvaji et al. (2011) studied photogelation of alginate or any other biopolymer by using a simple method of physically (noncovalently) crosslinking, namely the UV irradiation. They combined a non-soluble salt of a cation (e.g., calcium carbonate, CaCO_3) with an aqueous solution of the biopolymer (e.g., alginate) and a third constituent, a photoacid generator (PAG). During the UV irradiation, the PAG dissociated and released H^+ ions, which further reacted with the CaCO_3 generating free Ca^{2+} which bind the alginate chains creating the crosslinked network (“egg-box” junctions) (Dumitriu 2004). Javvaji et al. (2011) claimed that the same method can be applied for other biopolymers and the formed gels seem to be reversible as calcium chelators were added, e.g., sodium citrate.

Similar results were obtained also by Higham et al. (2014). They detailed the gelation of alginate by ionic crosslinking under the ultraviolet (UV) irradiation treatment and characterized the gels by in situ dynamic rheology. They found out that the gel point is inversely proportional to UV intensity (I), gelling point being expressed as $\text{GP} \sim I^{-0.65}$. Lowering the UV intensity, the emitted energy is less causing a delay of the release of the acidic species from the PAG and thus, the crosslinking in the presence of Ca^{2+} . As result they observed also that the network structure developed slower and forming a compact structure.

Recently, ionic gelation of alginate in the presence of Ca^{2+} was induced by X-ray scattering and reported by Yoshiaki et al. (2016). They found out that the short oligoguluronates, oligoG’s affected the gelation mechanism.

An interesting study was reported by Molina et al. (2014). They analyzed the effect of atmospheric dielectric barrier discharge (DBD) plasma on the gelation/crosslinking process of chitosan. The DBD plasma chitosan gelation process did not damage the chemical structure of the biopolymer. During the plasma treatment, solvent evaporation and local heating of the chitosan solutions were observed after 15 min of treatment. It is assumed that partial de-protonation of amide group

occurred (Fig. 4) and additional hydrogen bonding with hydroxyl groups of other chitosan molecules were formed.

The bombardment of charged ions on the surface of the chitosan aqueous solution advanced to the formation of reactive radicals of H, OH and the solvated electrons. After the reaction with new molecules of chitosan, carbonyl (i.e., aldehyde) groups were mostly formed (Prasertsung et al. 2012). The higher plasma treatment duration is the stronger gel is formed due to formation of covalent bonds by Shift-base reactions between chitosan polymeric chains (Fig. 4) A higher concentration of chitosan (up to 2%) seemed to be optimal as Molina et al. (2014) observed from rheological results.

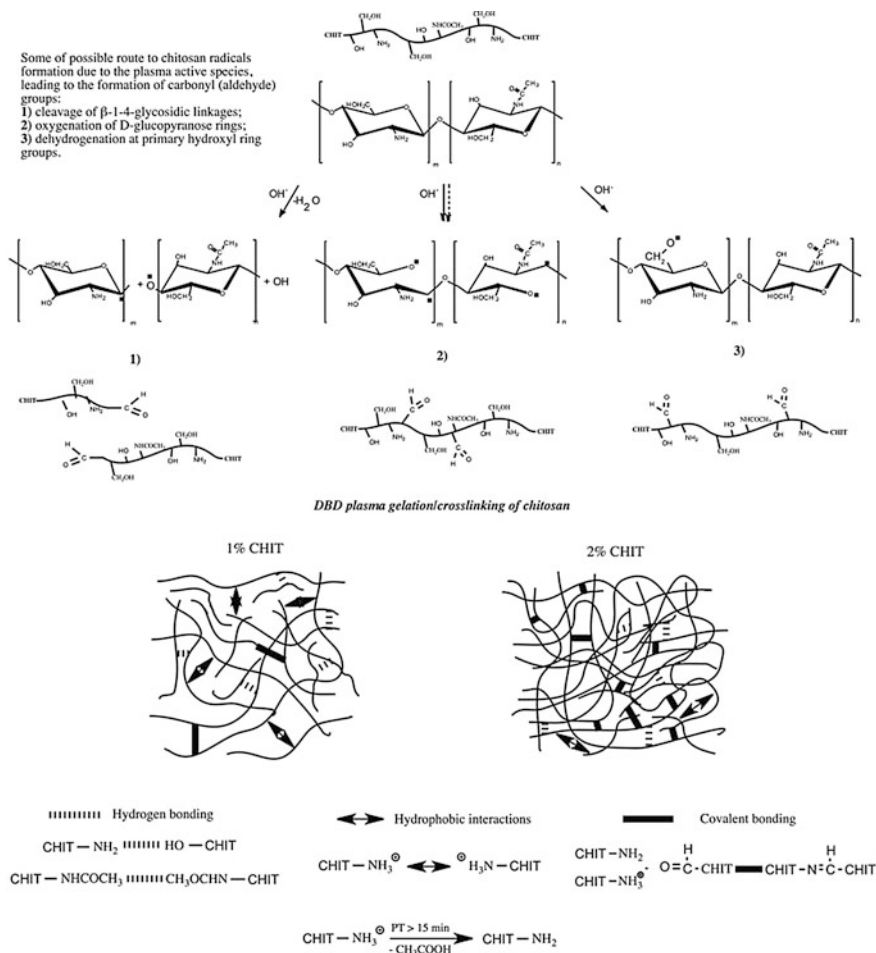


Fig. 4 Scheme of chitosan gelation under plasma treatment. With permission from Elsevier from (Molina et al. 2014)

3.4 Chemical Crosslinking

Chemically crosslinked gels present covalent bonds between different polymer chains. Despite of their stability and difficulty to be dissolved in solvents, the chemically crosslinked hydrogels are avoided to be used within pharmaceutical applications due to the possible toxicity of the used crosslinking agents. By comparison, dissolution of physically crosslinked gels is prevented only by physical interactions, between the different polymer chains, which make them less stable in organic solvents or physiological medium but strong enough to fulfill the requirements of a pharmaceutical formulation (Ebara et al. 2014). It is mentioned that crosslinking process can take place at room temperature and physiological pH.

Generally, crosslinking agents are molecules having two reacted functional groups able to interconnect by covalent bonds two other macromolecular chains (e.g., polymers, proteins, etc.). The type and position of the functional groups group are criteria to classify the crosslinking agents into two classes: homobifunctional and heterobifunctional. In the case of homobifunctional ones the reactive groups are located at the side chain of the molecule and the reactive groups are the same type. Table 2 summarizes the main classes of crosslinking agents and their characteristics. The heterobifunctional crosslinking agents comprise different reactive groups of the two sides of the molecule. The second class of crosslinkers is more likely as it is more selective and controlled as the first class is causing also unwanted crosslinks like intramolecular crosslinks. The reactive groups on the molecule of crosslinking agent classify them into another category: carboxyls, amines, sulfhydryls, and hydroxyls based. They are generally selected taking into account their reactivity with the protein or polymers chains, length, and solubility. They can be also activated by light or presents of specific functional groups.

3.5 Hydrogels with Special Structural Configurations

Formation of gels leads to improvement of the mechanical properties, viscoelasticity, better entrapment of the drug within the matrix, better interactions with the drug and therefore controlled delivery at the desired site, etc.

Poor mechanical strength of hydrogels in swollen state represents a nowadays limitation for pharmaceutical topical applications. New structures of hydrogels were developed with the motivation to overcome this problem, e.g., slide ring gels, double-network hydrogels, nanocomposite gels, interpenetrated networks, etc. (Tomsic et al. 2008; Johnson et al. 2010).

Interpenetrated networks (IPN) are frequently prepared by polymerization and crosslinking of one complete polymer network, followed by polymerization and crosslinking of a second polymer in the presence of the first polymeric network. If the two polymerizations processes separately occur, the network formation may be performed simultaneously.

Table 2 Type of crosslinking agents and their characteristics

Crosslinking agent	Specific characteristics
<i>N</i> -Hydroxysuccinimide esters (NHS esters)	NHS esters react with amines to give stable amide groups. Optimal reaction conditions are slightly alkaline conditions (pH 7.2–8) The rate of hydrolysis increases with increasing pH, so the pH of the buffer solution must be closer controlled
Imidoesters	Form amidines with primary amines optimal reaction pH is 8 and 10
Carbodiimides, e.g., EDC [1-ethyl-3-(3-dimethylaminopropyl) carbodiimide]	Form amide bond between a carboxylic acid group and an amine group of another molecule as specificity, they do not become as part of final macromolecule
Maleimides	Is used in the reaction of sulfhydryls based chains at physiological pH to produce a stable thioether linkage
Haloacetyls	Are used within reactions of chains with sulfhydryl groups at physiological pH to give a thioether linkage
Pyridyl disulfides	React with sulfhydryls to form disulfide bonds; optimal pH is 4–5
Diazirines	They are photoreactive; they are inert until activated by exposure to ultraviolet light Specific for protein–protein interactions

Double-network gels are formed from two independently crosslinked networks, one consists of a flexible uncharged polymer, and the other, of a rigid polyelectrolyte. As the crosslinking degree is getting higher, gels would have very good mechanical properties (Peak et al. 2013). The improved mechanical strength of these double-network hydrogels is mainly due to the high concentration of second constituent, which may be much higher than the concentration of the first polymer. This is a way to prevent the crack propagation leading to failure (Johnson et al. 2010; Na 2013; Chen et al. 2015).

The double-network hydrogels seems to be a new alternative of getting materials with enhanced viscoelastic and mechanical properties which are also likely for pharmaceutical formulations. Recently, Xu et al. (2016) synthesized the double-network hydrogels of a responsive double-network poly (N_{ϵ} -acryloyl L-lysine)/hyaluronic acid (pLysAAm/HA) via a two-steps photo-polymerization process. For the first network HA-Cys-GMA chains were used and pLysAAm chains for the second network. The synthesis method was described within Fig. 5.

The area of **nanocomposite hydrogels** is one of fashion topic as a large number of publications are published (Cheaburu-Yilmaz 2015a; Butnaru et al. 2015; Lim et al. 2011; Singh and Singh 2012). The nanofiller, which can be organic or anorganic, e.g., nanosized silicates layers or other inorganic clay minerals, is incorporated within the hydrogel matrix in order to obtain increased thermal

stability, mechanical properties, viscoelastic behavior, etc.; up to the desired applications (Gaharwar et al. 2014; Zhou and Wu 2011).

Combination of physical and chemical crosslinking can bring multiple advantages to obtain hydrogels comprising both characteristics of a physical gel and a chemical crosslinked one—Table 1. Regarding the mechanical properties, physical hydrogels showed lower moduli due to the reversible physical interactions. By increasing the crosslinking degree, thus the molecular motion is hindered, mechanical properties are superior. Biocompatibility can be also achieved by combining both physical and chemical crosslinking in a single hydrogel system (Malda et al. 2013).

Techniques like thermo-gelation, photo-polymerization, click chemistry, and stereo-complexation started to be applied with the aim of obtaining both physical and chemical crosslinking. The main advantage of combination of the two crosslinking methods is the outcome of a faster gelification, improved mechanical and physical properties by comparison with neat polymers. Different crosslinked networks which can be obtained by different methods are illustrated within Fig. 6.

Vulpe et al. (2016) prepared hydrogels based on collagen, sericin, and hyaluronic acid by crosslinking the natural polymers via carbodiimide chemistry, in the presence of 1-ethyl-3-(3-dimethylaminopropyl) carbodiimide (EDAC) and *N*-hydroxysuccinimide (NHS). The procedure is schematically represented within Fig. 7.

The method was chosen on the base on the stability and mechanical properties of the final hydrogel. This concern came out from the susceptibility of the collagen of being easily degraded.

β -cyclodextrins (β CD) are cyclic oligosaccharides which have been widely handled for pharmaceutical applications. The insoluble polymers with a disc-like shape, were synthesized by crosslinking β -cyclodextrins in the presence of epichlorohydrin as crosslinker (Machín et al. 2012) while cyclodextrin/PEG hydrogels for drug delivery were obtained by reaction of hexamethylene isocyanate (Salmaso et al. 2007) The lysozyme loading degree increased and the release was faster as the CD/PEG ratio decreased while the incorporation of β -estradiol and quinine and their release rate showed inverse correlation with respect to the CD/PEG ratio.

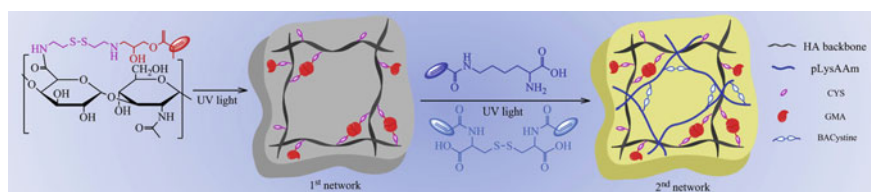


Fig. 5 Schematic diagram for the preparation of pLysAAm/HA hydrogels with dually crosslinked networks. With permission from Elsevier from (Xu et al. 2016)

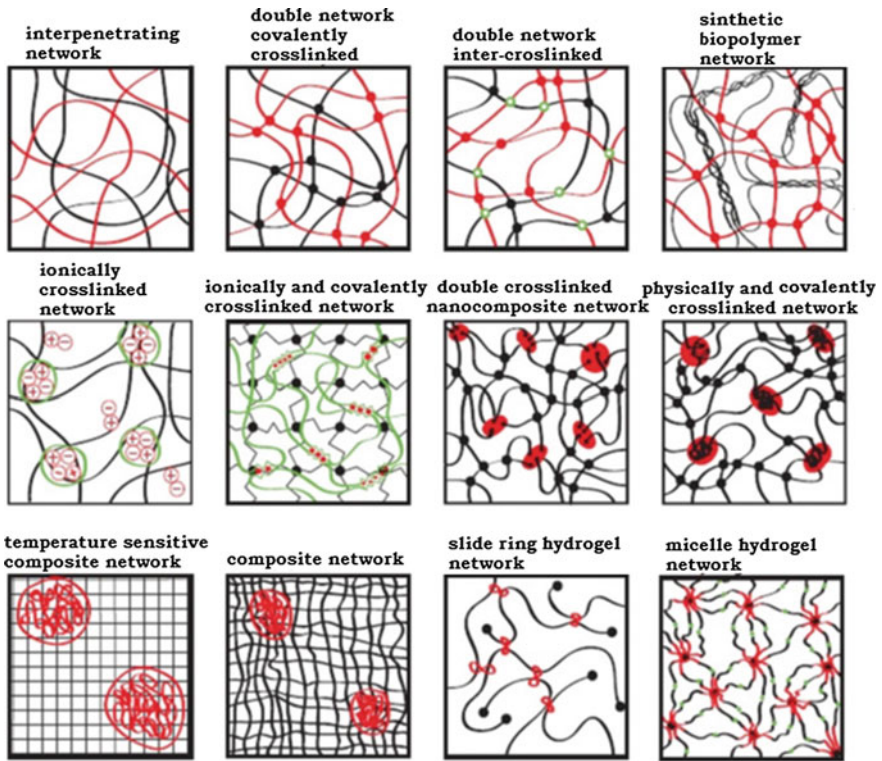


Fig. 6 Crosslinked networks formed by different gelation techniques. With permission from Springer modified from (Peak et al. 2013)

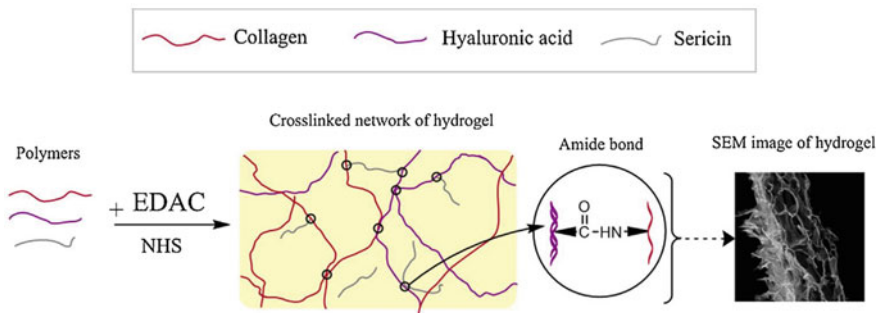


Fig. 7 Schematic representation of hydrogel preparation by carbodiimide crosslinking. With permission from Elsevier from (Vulpe et al. 2016)

The supramolecular self-assembly of cyclodextrins and polymers led to the development of new supramolecular hydrogels for drug delivery applications (Gidwani and Vyas 2015). Cyclodextrins (CDs) and polymers based on polypseudorotaxane supramolecular hydrogels showed potential applications as injectable hydrogel drug delivery systems due to their thixotropic nature and biocompatibility. Furthermore novel CD–polypseudorotaxane hydrogels with new stimuli-responsive properties are still under development (Liu et al. 2011).

Supramolecular hydrogels crosslinked via host–guest interactions with high elasticity and toughness were prepared without chemical crosslinker by polymerization of the inclusion complexes between β -cyclodextrin acrylamide and adamantane acrylamide monomers (Kakuta et al. 2013).

4 Properties of Pharmaceutical Gels

4.1 Thermosensitivity

Temperature is one of the most common stimuli to control the responsive hydrogels. At higher (i.e., LCST) or lower (i.e., UCST) temperatures, the aqueous solutions of temperature responsive polymers show a sol-gel transition together with a self-assembly process taking place due to hydrophobic interactions (Singh and Lee 2014). The thermosensitive hydrogels, as a type of smart hydrogels, have attracted considerable attention, because their aqueous polymeric solution have low viscosity at ambient temperature, which favors the drug encapsulation and further the drug delivery. Thermogels exhibit a reversible sol-gel transition as temperature changes. This phase change behavior at the temperature variation is reversible as the gel is formed by physical crosslinks between the polymer chains. These thermo-responsive polymers or copolymers consist of hydrophilic and hydrophobic segments, which can self-assemble into polymeric micelles in water. The hydrophobic segments form the core of the micelles while the hydrophilic chains interact with water molecules at the corona (Liow et al. 2016; Klouda 2015).

The most common thermosensitive polymers, especially among the polysaccharide are: methylcellulose (LCST 60–80 °C), xyloglucan, carrageenan, agars, gelatin, guar gum, etc. Also, they can be obtained by chemical derivatization, grafting/blending of polysaccharides such as chitosan, alginate, cellulose, dextran and their derivatives with thermosensitive polymers (Klouda and Mikos 2008; Prabakaran and Mano 2006).

Wang et al. (2013) reported a chitosan derivative, *N*-[(2-hydroxy-3-trimethylammonium) propyl] chitosan chloride, which interacted with glycerophosphate to produce a thermosensitive hydrogel. Gels with high mechanical strength are obtained by crosslinking in the presence of glutaraldehyde (GA) and polyvinyl alcohol (PVA), aiming intratumoral delivery of paclitaxel (PTX).

Thermosensitivity was also achieved by combining the properties of alginate (AgA) with the thermo-responsive poly (Nisopropylacrylamide) (PNIPAAm), in various architectures like interpolymeric complexes (IPC), block and graft copolymers or hydrogels (Vasile et al. 2009; Dumitriu et al. 2011, 2014).

The associative behavior of the copolymer in aqueous solutions seemed to be composition and temperature dependent. Copolymers exhibited a reversible thermo-thickening behavior in aqueous solutions when the degree of grafting, the concentration, and the temperature values were higher than some critical ones.

This type of temperature-responsivity is a key characteristic especially in the case of in situ gelling formulations and liquid dosage forms. Recent developments of thermosensitive systems based on polysaccharides are summarized within Table 3.

4.2 pH Sensitivity

pH variations occur at several body sites, e.g., the gastrointestinal tract, vagina, and blood vessels and there can provide an adequate medium for pH-responsive hydrogels aimed as drug carriers. Additionally the pH changes in response to specific substrates can be used for controlling the drug release. Generally, the pH-responsive drug delivery systems are aimed to be used for per oral controlled drug delivery, taste-masking of bitter drugs or intravascular drug release (Gupta et al. 2002).

Many polysaccharide components such as chitosan, alginate, hyaluronic acid, heparin, carboxy methyl cellulose, cyclodextrin, confer to hydrogels pH-responsiveness. Among the various hydrogels, the pH-sensitive type, which are based on biocompatible polymers or copolymers have been used extensively in drug delivery systems (Shi et al. 2004; Jabeen et al. 2016; Guo and Kaletunc 2016; Mercado and Slater 2016; Cheaburu-Yilmaz et al. 2017).

Their special particular pH sensitivity combined with the fact that pH varies throughout the digestive system make them suitable for oral administration when targeting the intestinal tract, especially the colon. More specific, most of the in vitro and in vivo experiments supported that when drugs are to be delivered to the gastrointestinal tract, they are usually sustained and protected within the hydrogel in the acidic gastric environment (pH 1.2), while in the less acidic intestinal regions (pH 6.8–7.4), swelling of the hydrogel basically releases the drugs.

A pH-sensitive system was reported by Eldin et al. (2015) from grafted alginate hydrogel-based matrix for protein controlled release applications. L-arginine was grafted onto the alginate backbone via amine groups and the system was designed to enhance the sustained protein release especially in acidic medium, by comparison with neat alginate hydrogels. They found out that the increase of L-arginine concentration, pH, time, and temperature of grafting reaction increased the grafting efficiency and swelling ability of the crosslinked Arg-g-Alg hydrogels.

Table 3 Examples of thermo-responsive polysaccharide-based hydrogels for pharmaceutical applications

System	Thermo-responsive behavior	Parameters influencing T-responsive	Application	References
Chitosan, β -glycerophosphate, and glycerol	Tunable sol-to-gel temperature from 35 to 56 °C	Composition ^a	Wound healing in endorectal ultrasonography	(Huang et al. 2016)
Carboxymethylcellulose (CMC) and poly (<i>N</i> -isopropylacrylamide)	Water retention values decreased significantly above ~ 32 °C	Faster swelling rates (SR) and slower swelling; presence of loaded enzyme	Proteins delivery	(Dutta et al. 2016; Bokias et al. 2001)
Sodium alginate, polyethylene oxide and acrylic acid with cyclodextrine	pH-dependent structure and properties ^b	pH of the synthesis medium	Drug delivery of ibuprofen	(Jabeen et al. 2016)
Poly (<i>N</i> -isopropylacrylamide) [poly(NIPAAm)] in the presence of carboxymethylchitosan (CMC) and magnetite nanoparticles (MNPs) and crosslinked with glutaraldehyde	Water swelling responses to the change in solution pH and temperature	Ratios of CMC, NIPAAm, glutaraldehyde and surfactant (Tween-20) ^c	Controlled drug release	(Rodkate and Rutnakornpituk 2016)

^aOptimized formulation 0.5% CS, 5% β -GP, and 25% glycerol

^bHydrogel prepared at neutral pH had the desirable viscoelasticity, higher encapsulation capacity and comparatively faster release rate

^cEffects on morphology of the particles and the spherical shape-like

Guo and Kaletunc (2016) designed a system based on alginate and pectin. The mixture of the two polymers resulted in a hydrogel when the pH was below 3.0, showing pH responsivity. This pH responsivity was due to the presence of a high amount of carboxylate groups on the polymer chains and inducing a strong hydrophilic character. Guo et al. claimed that they can control the particles size and it can be formed disc-shaped particles which can potentially enhance the particle adhesion in intestines. Their study reported a model to predict the dissolution of alginate-pectin hydrogels under various pH and temperature conditions in order to release the biologically active compounds.

A self-healing pH-responsive polysaccharide-based hydrogel was prepared by Liu et al. (2016). They mixed cellulose acetoacetate (CAA) aqueous solution with chitosan aqueous solution at room temperature. Prior to this, they synthesized CAA by means of reaction of cellulose with tert-butyl acetoacetate (t-BAA) in ionic liquid 1-allyl-3-methylimidazo-lium chloride (AMIMCl). The pH response of the polysaccharide hydrogel was assessed and described as shown within Fig. 8.

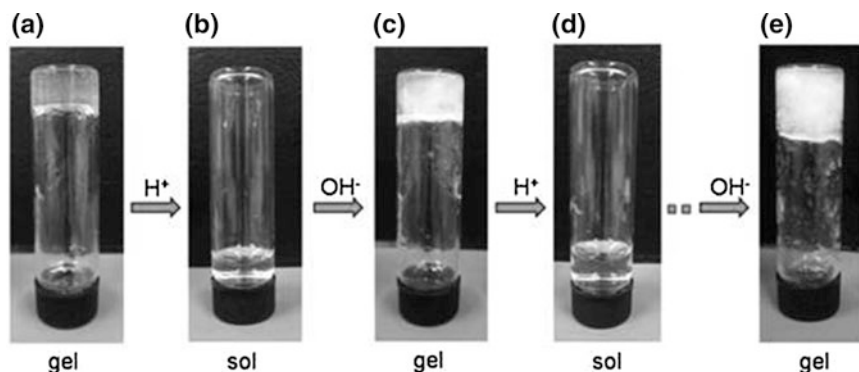


Fig. 8 pH responsiveness of the hydrogel. **a** neat hydrogel, **b** sol phase after addition of aqueous HCl, **c** regeneration of the hydrogel after addition of aqueous solution of NaOH, **d** regenerated hydrogel converted into hydrosol after addition of aqueous solution of HCl, **e** regenerated hydrogel after five cycles. With permission from John Wiley and Sons, from (Liu et al. 2016)

The pH-responsive behavior can be also evidenced by means of rheological studies as Jabeen et al. reported (2016). They prepared pH and temperature responsive hydrogels based on sodium alginate, polyethylene oxide, and acrylic acid with cyclodextrin as hydrocolloid. Interestingly, the viscoelastic properties response at pH variation showed like three different formulations with the same constituents. The elastic properties were illustrated within Fig. 9.

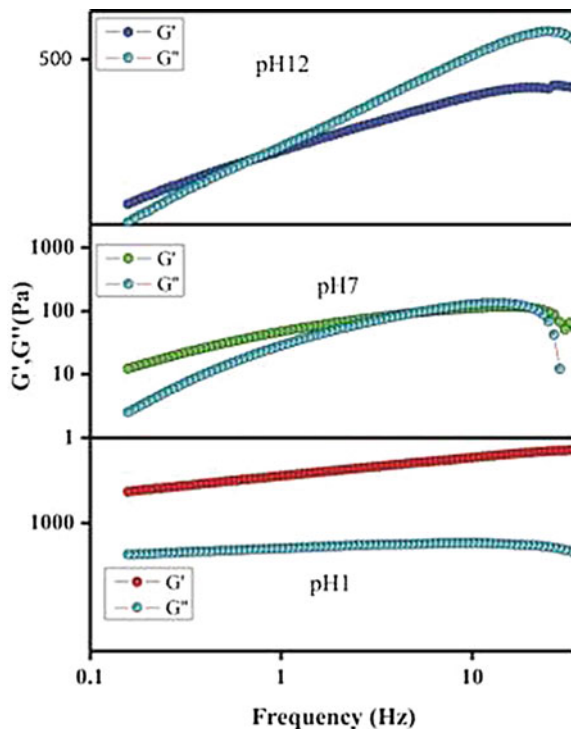
As shown within Fig. 9, when hydrogels were prepared at low pH (around 1), elastic gels were obtained as the storage modulus (G') took higher values than loss modulus (G''). Jabeen et al. claimed that the viscoelastic properties were not influenced by temperature or frequency change. Neutral pH induced to the obtained hydrogels viscoelastic and thermo-reversible characteristics; furthermore hydrogel exhibited the sol-gel transition by appearing the crossover point. At higher pH (pH 12) the viscous character is more dominant, hydrogel having the lowest tensile strength, thus is unstable to temperature variation and had fast drug release rate. The optimal formulation regarding the pharmaceutical needs was considered the one prepared at neutral pH as it showed the higher drug loading and the slowest release of the drug.

4.3 Swelling

One of the main characteristic of a gel/hydrogel is considered to be its ability to retain water within the network (Gulrez et al. 2011) The presence of the polar hydrophilic groups favors the hydration leading to the formation of primary bound water.

Upon the contact with water, the hydrogel is swollen, phenomena caused by the interaction of hydrophylic groups with water molecules The hydrophobic groups

Fig. 9 Viscoelastic properties as function of pH of the preparation medium. With permission from Science direct from (Jabeen et al. 2016)



are also capable of interacting with water molecules. In this case it is named as “secondary bound water” or hydrophobically bound water. Primary and secondary bound water form “total bound water.”

Thanks to the osmotic driving force of the network chains, hydrogel’s network continues to absorb additional water up to infinite dilution. The supplementary swelling is prevented by the covalent or physical crosslinks, leading to an elastic network retraction force. Thus, the hydrogel will reach an equilibrium swelling level.

The additional absorbed water, called as “free water” or “bulk water,” is expected to fill the space between the network chains, and/or the center of larger pores, macropores, or voids. Further swelling, depends on the nature and composition of the hydrogel and, may lead to the disintegration and/or dissolution of the matrix if the network chain or crosslinks are degradable.

Generally the swelling ability is determined by swelling degree defined by applying the kinetic model and the mechanism of swelling/drug release can be established (Korsmeyer et al. 1968)

$$\frac{W_t}{W_{eq}} = k_{sw} t^{n_{sw}}, \quad (1)$$

where: W_t and W_{eq} represent the amount of solution absorbed by the matrices at time t and at equilibrium, respectively; k_{sw} is the swelling rate constant or specific

rate characteristic of the system and n_{sw} is the power diffusion law exponent which takes into account the type of solvent transport. Equation (1) applies to initial stages of swelling (swelling degree less than 60%).

Recently, Tulain et al. (2016) explained that pH and ionic concentration are the principal parameters which influence the swelling ability of pH-sensitive hydrogels as result of electrostatic repulsion between the ionic charges. At high pH, an ionic polymeric network (due to acidic or basic functionalities) exhibited higher swelling. They developed a pH-responsive hydrogel prepared via free radical polymerization in aqueous media aimed to protect the rabeprazole sodium from acidic environment from stomach. They reported that the swelling behavior of prepared hydrogels in buffer solutions of various pH indicated highly pH-dependent swelling of hydrogels. The swelling ratio of the hydrogel was low in acidic medium and high with the increasing pH. This was due to the presence of ionized COOH groups of acrylic acid groups at pH 7.4. At low pH values, the anionic group is protonated, swelling rate and ratio being low.

4.4 Rheological and Thixotropic Characteristics

Rheological and thixotropic characteristics are very important when manufacturing of topical products. It is likely to obtain for the new formulation a predictable and smooth filling process and therefore a material that contributes effectively when subjected to a high stress (e.g., physical load). For the topical or transdermal application the product should likely have a low viscosity at high shear rates but in the same way to be capable to quickly recover and return to a higher viscosity upon standing. More specifically, a topical cream should easily flow out from the tube when a patient press and apply a physical load and spreading the medication over the skin, yet it should return to a sufficient viscosity as to remain on the skin and not flow off after application.

Patient compliance and therapeutic efficiency of the semisolid product would vary according to the flow property (i.e., spreadability) changes and the speed of spreading on the skin (Mastropietro et al. 2013). The viscosity change with the variation of shear rate can be indicative for the assessment of the properties of the gel/hydrogel. More specifically it can be obtained information on the structure and composition of the formulation.

Generally, the rheological response of the hydrogels is connected with the contributions of crosslinks such as covalent bonds and physical crosslinks, e.g., electrostatic interactions and hydrogen bonds and also some topological interactions among the polymeric entanglements. The crosslinks cause a decrease of the intrinsic mobility of the polymer chains that are not able to release stress; consequently the material shows a predominant elastic behavior ($G' > G''$) and behaves as a three-dimensional network where deformation is the consequence of the applied stress.

Borzacchiello et al. (2015) studied hydrogels of hyaluronic acid (HA), obtained by crosslinking with divinyl sulfone (DVS) using a solvent-free method. They found out that HA/DVS weight ratio and HA concentration influenced their rheological properties even though the gels still behaved as strong gels.

The influence of hyaluronic acid (HA) within a methylcellulose matrix on the thermo-gelation was studied by Mayol et al. (2014). Thermo-gelation was evidenced by means of rheological experiments showing for the blends with hyaluronic acid a typical behavior of a viscous fluid or entangled solutions at 20 °C and at 37 °C, of a weak gel since $G' > G''$ in all the frequency range. The contribution of hyaluronic acid on the final rheological properties was found to be revealed by the values of storage modulus at a frequency of 1 Hz, particularly at 37 °C; G' of methyl cellulose (MC) was 7.2 Pa while G' of the blend (MC/LMWHA) was 40 and 30 Pa from blends containing, respectively, 1 and 2% w/v of low molecular weight HA (LMWHA). The further increase of concentration would increase excessively and would not fulfill the injectability requirements of the matrix.

Thixotropy of the pharmaceutical gels is a characteristic which refers to the ability of the gel to reform slowly its structure after a shear load without altering the other structural characteristics (Davis 1971; Mezger 2006). One of the first definitions of thixotropy was given by Freundlich and Barnes (Freundlich and Rawitzer 1927; Barnes 1997) who stated that “*By thixotropy is meant the phenomena of concentrated gels ... which solidify to gels which may again be liquefied to sols. The re-solidification occurs repeatedly, at constant temperature with a constant speed.*” Thixotropic property is directly associated with the therapeutic efficiency of the pharmaceutical formulations and contributes to the extension of the retention time at the targeted site and enhancing systemic bioavailability (Leea et al. 2009). The non-Newtonian behavior of the thixotropic sol-gel system is revealed by the yield stress values. Yield stress value and plastic viscosity are material characteristics, whereas the thixotropy mainly is reflected by the shear history of the material and the degree of dispersion. Mezger and Leea showed that the increase of the yield stress indicates the gradual strengthening of the three-dimensional network structure for the thixotropic formulations (Mezger 2006; Leea 2009).

Al-Kassas et al. (2016) found recently for their propranolol-HCl loaded chitosan nanoparticles (Al-a thixotropic behavior. Formulations obtained by ionic gelation method, were aimed as transdermal delivery system, due to their potential to improve the systemic bioavailability and the therapeutic efficacy of propranolol-HCl.

Gel formulations subjected to shear stress showed a viscosity decrease due to the time-dependent reformation of the secondary structure. They showed a hysteresis loop which was bigger for the gel containing propranolol nanoparticles than that for the free drug gel indicating a significant structural breakdown and thixotropy of this formulation, shown in Fig. 10. This is a more preferable property for a topical formulation because as the greater the thixotropy is, the lower the settling and sedimentation rate of the nanoparticles in the system.

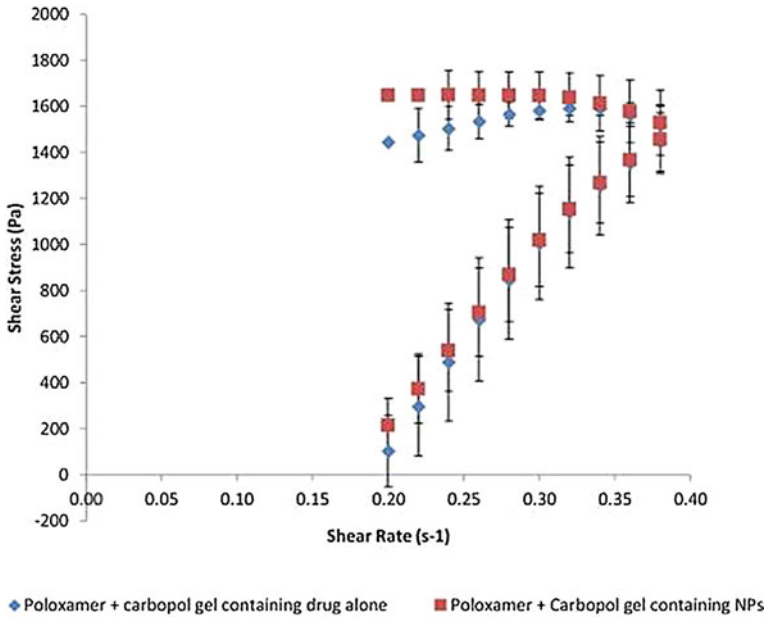


Fig. 10 Hysteresis loop of chitosan nanoparticles when subjected to a shear load. With permission from Elsevier from (Al-Kassas et al. 2016)

4.5 Thermo-Mechanical Properties

Thermal and mechanical stability of the gel formulation is considered when it is applied at the level of skin. Tomsic et al. (2008) reported sol-gel and gel-sol thermal transition of mixtures based of methylcellulose (MC) and κ -carrageenan (KC) investigated by means of small-angle X-ray scattering (SAXS), differential scanning calorimetry (DSC) and oscillatory rheological experiments in a 20–80 °C temperature range. The main motivation of the study was to prove a sort of “tricky” gel from a mixture of KC/MC/water which should behave as a gel in a narrow temperature range and as liquid solution facilitates homogeneous incorporation of functional particles.

Sionkowska et al. (2016) reported thermogravimetry (TG) to characterize the thermal destruction of several 3D porous composites based on blends of chitosan, collagen, and hyaluronic acid synthesized by means of freeze dry process. They used differential thermogravimetric analysis (DTG) to measure the thermal event which took place during the heating of the hydrogel at higher temperature. They found out that the peak between 40 and 110 °C could be assigned to the removal of bonded water of hydrogen bonds existing between collagen and polysaccharides. A second peak on the DTG curve which was assigned to the decomposition of biopolymers and they reported that by hyaluronic acid addition up to 5%, the

maximum decomposition temperature increases, thus the thermal stability of the composites is much higher.

Texture Profile Analysis (TPA tests) is a very popular double compression test for determining the textural properties of gels and widely used for characterizing the pharmaceutical formulations and cosmetics. TPA tests supposes a twice compression using a texture analyzer to provide information on the textural features of the gel formulations. Texture profile analysis (TPA) was firstly introduced as a method to characterize semisolid drug dosage forms by Jones et al. (1997). They described the beneficial aspects that contribute to the patient compliance and therapeutic efficiency of the formulations. Ease of removal of product from the container, good spreadability on the substrate (e.g., skin, mucous membranes), good bioadhesion (to ensure retention at the site of application), acceptable viscosity, and drug release and absorption are considered as optimal, mechanical properties by Jones et al. (1997).

Hurler et al. (2012) developed a fast and efficient method to characterize texture properties of hydrogels, e.g., cohesiveness, adhesiveness, and hardness.

As they emphasized topical applications for wound treatment contain additional ingredients to favor the gelling characteristics of polymer, e.g., drugs, solvent, humectants, i.e., glycerol or drug carrier systems such as liposomes, providing sustained release of the drug. Evaluating the effect of various additives within the gel formulation they found out that after compression test high molecular weight chitosan gel lost almost all of its original hardness, as it retained only 8% of its original hardness and addition of liposome within the chitosan gel containing 10% glycerol, was found to be the most stable. Incorporation of liposomes within the chitosan hydrogel network increased the stability of the final gel formulation even at increased temperatures of 40 °C.

Baloglu's group (Ay Senyigit et al. 2014; Rencher et al. 2016) correlated the textural characteristics of chitosan-based hydrogels with the mucoadhesivity of the material on the substrate.

Spreadability of the gel formulations indicates the extent of area to which a gel is readily spreads over at the level of the skin or another injured part of body. The therapeutic efficiency of a formulation depends on its spreading-ability value. Spreadability can be evaluated also from texture analysis. The method is based on the "slip" and "drag" characteristics of the gels. It is expressed as time in seconds taken by two slides to slip off from gel which is placed in between the slides under the direction of certain load. A good spreadability can be interpreted by lower time values needed for the separation of two slides.

4.6 Erosion/Degradability

Most enzyme-degradable hydrogels are prepared from natural polymers, such as polypeptides and polysaccharides. Biodegradable conductive hydrogels, films, and scaffolds found applications for cardiovascular, tissue engineering, and controlled drug delivery. Borzacchiello et al. (2015) performed in vitro degradation for the

hyaluronic acid based hydrogels they prepared. As degrading enzyme, a solution of hyaluronase was used in a concentration of 43.9 Units/mL. Gel formulations with the prepared enzyme solution were mixed by vortex in a volume ratio of 10:1 v/v% to obtain a final enzyme concentration of 4 Units/mL. The degradation of the hydrogel was evidenced by measuring the rheological parameters after degradation by comparison with those ones obtained from un-degraded sample at a frequency of 0.1 Hz as function of time.

Hydrogels containing higher amount of crosslinking agent showed a good stability against enzyme action.

4.7 Morphology

The concentration of the polymer within the gel played an important role as for different concentrations, different morphologies could be observed. Particularly, in the case of a chitosan-based hydrogel or a concentration lower than 0.5 wt%, an ordinary random 3D network could be considered as isotropic (Nie et al. 2015). With the increasing concentration, higher than 1.0 wt%, a different type, a more complex one, in three dimensions, may be attributed. This complex 3D morphology can be as: multilayered structure, an oriented structure which had been observed in the hydrogel of Nie et al. (2015) they found out that the arrangement appeared to be onward the direction of OH^- diffusion and joined every layer at about 90° . It is seems that between that spatial arrangement and direction of diffusion process is an interrelationship. The last 3D orientation of the complex hydrogel structure is based on a structural conversion with the increasing distance between the primary and the afterward hydrogel layer. The region located right close to the initial hydrogel layer has a smooth and compact structure. At higher distance, oriented region appeared and transformed into porous structure. Analyzing the characteristics of the obtained gel, Nie et al. (2015) referred to a typical structure as a layered-wise-oriented structure, described within Fig. 11.

4.8 Drug Release Ability

In last decade, controlled drug delivery systems and the polymers used in these systems have become much more complex, with more broaden functions. Diffusion is the main mechanism for the drug delivery and its rate depends on the physical structure of the polymer network and its chemical nature. If the gel is highly hydrated the drug could diffuse through the pores. In gels with lower hydration the release of the drug could be completed either by dissolution in the polymer or could be transported through the network. The crosslinking degree also modifies diffusion rate.

Recent studies aimed developing of these types of biopolymeric-based systems meant to improve the drug release efficiency. Li et al. (2016) prepared thiolated

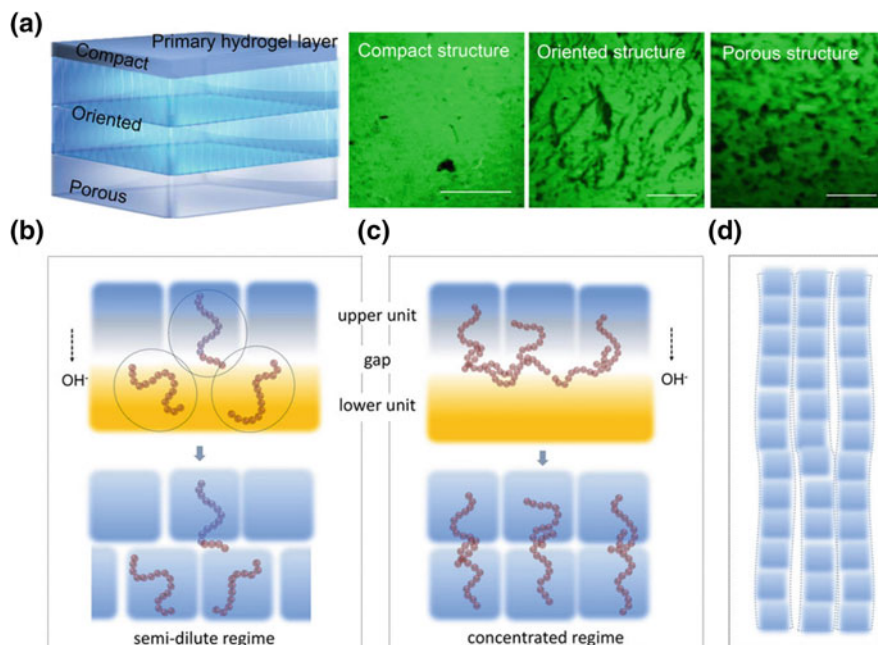


Fig. 11 Schematic representation of the layered CS hydrogel and the possible mechanism. **a** CLSM images assigned to the compact region, oriented region and porous region **b–d** Macromolecular interactions in “gel-sol consecutive reaction units” during the gelation process, **b** semi-dilute regime, **c** concentrated regime, and **d** formation of oriented structure by stacking of reaction units. With permission from Nature from (Nie et al. 2015)

chitosan by covalent binding between *N*-acetyl-L-cysteine and chitosan in order to modify the surface of the nanostructured lipid carrier loaded curcumin. They proposed these systems for topical ocular administration of curcumin. As reported, released amount of curcumin from unmodified chitosan matrix was 98.38% within 12 h, while the amount of drug released from the nanostructured lipid carrier loaded curcumin was 63.07% after 72 h.

A much prolonged release process was evidenced for the coated nanostructured lipid carrier, this being correlated with the adhesiveness and gel-like properties of the CS derivatives. By coating the nanoparticles with a chitosan derivative layer proved that the curcumin release can be modulated in an effective way, increasing more than 10 times the apparent permeability coefficients compared with the nanostructured lipid carrier loaded curcumin and the self-made eye drops.

Another recent example of thiolated chitosan for topical delivery was reported by Lucero et al. (2016). They studied a system comprising crosslinked chitosan-*N*-acetyl-D, L-homocysteine conjugate polymer (crosslinked thiolated chitosan, CTS), as controlled drug delivery system for topical use. They performed the chemical modification of chitosan by reaction with *N*-acetyl-L, D-homocysteine thiolactone aiming the attachment of thiol groups into the polymer backbone. They applied this

method not only as additionally crosslinking path but also to enhance and to control the cohesive properties of the final formulation based on thiolated chitosan. The obtained a high cohesiveness of the formulation and dependency on the polymer concentration. The optimal composition was found to be the one containing 3% CTS regarding mechanical and viscoelastic properties which are likely to be obtained for topical applications. Additionally their texture studies confirmed the same outcome.

The same composition was found to release the most efficient and a more controlled drug release profile was achieved.

Chitosan nanoparticles loaded with dexamethasone sodium phosphate (DEX) for topical ocular delivery were prepared by (Kalam 2016) aiming to improve the precorneal retention and corneal permeability. The chitosan nanoparticles based formulation was optimized in the way of improving the mucoadhesiveness of the formulation and to delay the release of dexamethasone. For this purpose the chitosan nanoparticles were coated with hyaluronic acid (HA), and the burst release profile of the drug obtained for the uncoated formulation was overcome and, additionally, the release of dexamethasone was slowed down.

Similar results regarding the delayed release of dexamethasone was obtained by Calles et al. (2016a) in their approach to use crosslinked crosslinked hyaluronic acid and itaconic acid films loaded with dexamethasone sodium phosphate salt (DEX) for topical treatment of surface inflammatory ocular diseases. The crosslinking of the mixture was done with polyethylene glycol diglycidyl ether.

Wick's group (Carmona-Moran et al. 2016) reported a transdermal drug delivery formulation. They prepared a semisolid gel and a solid hydrogel film formulations with gellan gum as a rheology modifier agent. The effect of penetration intensifier (e.g., dimethylsulphoxide, etc.) and gellan gum on the transport of sodium diclofenac from the semisolid gel and solid hydrogel film formulations were studied by using a synthetic membrane and a Transwell diffusion system. The main parameters affecting the transport of sodium diclofenac were the concentration of gellan within the formulation and the temperature. Low gellan content induced low permeability and concentration of transported sodium diclofenac in the semisolid formulation and higher concentration in the solid hydrogel film. This behavior was assigned to a specific 3D swollen configuration of the polymer in the solid hydrogel film, in this case the delivery being diffusion controlled. The Transwell diffusion system provided a way to quantify the drug diffusion for many types of formulations. This system together with the thermo-responsive properties of the nanogels provided a better control over the drug release mechanism.

4.9 Bioadhesive Properties

Bioadhesion describes the interfacial forces that hold together two bodies that one or both of them, are of biological nature, for extended periods of time (Solomonidou et al. 2001).

Bioadhesion is an essential feature for a successful application of a bioadhesive drug delivery system having a gelled polymeric matrix. The strength of the joint between the dosage form and the biological tissue is important for an effective treatment. The polymers with strong anionic charges and a number of carboxyl or hydroxyl groups have good binding potential and exhibit bioadhesive properties. Several parameters which influence the strength of the adhesion and the mechanism itself should be mentioned as molecular weight, chain flexibility, conformation of the polymer, crosslinking ratio, particle size, functionality, surface area and energy as well as the environmental factors like pH, temperature, hydration of the substrates, applied forces (e.g., duration of the contact, other forces applied), etc. To allow interpenetration into the biological substrate, a bioadhesive polymer should have sufficient chain flexibility or to possess flexible side chains which can be easily involved in the adhesion. Moreover, a high surface area would favor the adhesion between the two substrates as well as contact time may have a contribution to the strength of the formed joints. It also should have favorable surface energy properties to facilitate spreading over the biological surface of the polymeric layer and a sufficient macromolecular size to produce an interpenetrating layer and entanglements. It was reported that generally, natural and polyacrylic acid based polymers possess good bioadhesive properties (Smart et al. 1984; Park and Robinson 1984; Peppas and Buri 1985).

For in vitro determination of bioadhesion, several techniques have been reported, e.g., tensile testing (Park and Robinson 1985) shear stress testing and adhesion weight method (Smart et al. 1984), fluorescent probe method (Park et al. 1985), flow channel techniques (Mikos and Peppas 1986) and texture analysis (Wong et al. 1999; Tanriverdi and Ozer 2013).

4.10 Skin Irritation

The skin irritation studies of gel formulations could be tested by in vivo study. As a general accepted procedure, the gel formulation is applied directly on human or animal skin and irritation potential of formulation is measured. The shaved skin from back area is marked on both sides. One side serves as control while the other side is for the test. Gel/hydrogel is applied for certain time and the site is monitored for any sensitivity such as erythema and melanin by using a Mexameter device (Langasco et al. 2016). Gavini's group (Langasco et al. 2016) measured the skin parameters, e.g., skin hydration, elasticity, and sebum content before application and after different application time periods of gel formulations and obtained favorable results due to their slow and linear drug permeation profile.

5 Applications

Topical delivery is an interesting route for local and systemic application of drug. Topical application has many advantages by comparison with the conventional routes. The gastrointestinal (GI)-irritation could be avoided, the drug metabolism in the liver would be prevented and drug bioavailability increased via this route. Topical formulations include creams, ointments, pastes, gels, etc. Gel systems have better application properties and stability than cream and ointment. The gel formulations should be prepared with a gelling agent that is inert, safe and compatible with other components. The topical gel should not be tacky and it should be sterile if it is ophthalmic gel. Gel formulations can have prolonged drug contact at the site of application due to their rheological and mucoadhesive properties.

The smart polymer gels are in focus of pharmaceutical research. Polymers could change the physicochemical properties in response to an altered environment and they are easy to administer into desired body cavities. From pharmaceutical point of view, smart polymeric gels are defined as liquid formulations which are transformed to solid or semisolid after application by external stimuli as temperature, pH and ionic strength (He et al. 2008; Gupta et al. 2002; Chaterji et al. 2007).

5.1 Vaginal Applications

Vagina as a route for drug delivery (Hussain and Ahsan 2005) provides various advantages such as easy and accessible path, delayed retention of the formulations, high surface and permeation area, high vascularization, relative low enzymatic activity and it avoids first-pass metabolism (Das Neves and Bahia 2006; Bernkop-Schnurch and Hornof 2003). Vaginal formulations could be prepared under various pharmaceutical forms, e.g., semisolids, tablets, capsules, liquid preparations, vaginal films, vaginal rings, foams, and tampons. Among all these, the most used are semisolid preparations, i.e., cream, ointments, and gels (Das Neves and Bahia 2006) due to their patient acceptability, easy preparation methods, and feasibility. The only limitations reported for these types of formulations were leakage and rapid removal from the treated site.

Vaginal administration was used to treat various diseases like osteoporosis, hormone replacement therapy, contraception, infections, infertility, and other female-related conditions as is a feasible alternative way compared to oral or parenteral administration. By comparison, conventional gel formulations have difficulties to be applied onto the infected site of the vagina. The use of mucoadhesive polymers such as thiomers could offer not only an easy application but also enhancement of the intravaginal retention time of the drug delivery systems. Furthermore, the therapeutic efficiency of locally acting drugs could be improved by their prolonged availability at the target membrane (Bernkop-Schnurch and Hornof 2003).

Smart polymer gels and in situ gelling systems, offer multiple advantages as they are combining the advantages of both gels and solutions (Patel and Patel 2015). These formulations are liquid formulations before the administration but turn into gel after administration into the vaginal cavity due to the action of the environmental stimuli like temperature and pH. Mucoadhesive, thermosensitive vaginal gels with prolonged release were formulated for a better therapeutic efficacy and improved patient compliance. The formulation should stay long enough inside the vagina for the best therapeutic effect. The conventional formulations are removed faster from vagina and therefore a constant cure could not obtain, varying the efficiency of the cure and decreasing the bioavailability of the drug. Patel et al. (2015) reported in situ gel formulations of clindamycin HCl comprising hydroxyl-propyl-methyl cellulose (HPMC) as bioadhesive polymer (0.1%) and gellan gum (as gelling agent) in order to modulate the sol-gel transition temperature so that to obtain gelation at physiological conditions. Addition of mucoadhesive polymer decreased the gelation temperature but it is still close body temperature. Gel of hydroxyethylcellulose (HEC) alone or mixed with chitosan (CS) or its derivative 5-methylpyrrolidinone-chitosan (MPCS) and loaded with the antibacterial metronidazole (MET) (0.75%) were prepared by Perioli et al. (2008). They tried to optimize the local vaginal therapy by increasing the formulation retention and increasing drug–mucosa contact time. They found out that CS amount plays an important role on drug release. A higher concentration of CS would decrease the drug diffusion through the gel network. A correlation between gel consistency (i.e., viscosity) and drug release was observed; higher content of CS higher the gel consistency is; polymeric network would be very dense and responsible for tortuous channel formation would decrease the MET diffusion.

Another reports state that the liquid applied on the topical areas is transformed into gel by varying several parameters, e.g., pH of cellulose acetate phthalate, the concentration of calcium ions for gellan gum, temperature for poloxamers, etc. (Gupta and Sharma 2009; Patel and Koyani 2014). Bioadhesion and retention at the site of application could be obtained by incorporating bioadhesive polymers like hydroxypropyl methylcellulose (HPMC) within the formulations.

A study on mucoadhesive chitosan was done by Ay Senyigit et al. (2014) on chitosan with different molecular masses and viscosity properties. They claimed that chitosan was very successful as a vaginal mucoadhesive gel base for econazole nitrate and miconazole nitrate, drugs used to topical fungal and yeast infections. Drug release was directed by the gel viscosity; increased gel viscosity of the gel led to slower release of the drug. Choosing the adequate gel consistency which is done based on the rheological characteristics of the prepared gels, makes the gel formulation to remain over 24 h over the vaginal mucosa ensuring a complete treatment. This was observed by infrared imaging techniques (Ay Senyigit et al. 2014).

The combination of a natural polymer of marine origin, e.g., like chitosan or kappa-carrageenan, with a semisynthetic polymer such as hydroxyl-propyl-methylcellulose (HPMC) in solid compacted formulations for sustained release of acyclovir (ACV) was studied by Veiga's group (Sanchez et al. 2015).

They observed a full and sustained release of acyclovir during a 220–260 h period. The prepared formulation could adhere onto the vaginal mucosa and remain adhered for 72 h. They found out that the swelling of the formulations played a fundamental role. HPMC had a higher degree of swelling than chitosan and kappa-carrageenan and less erodible. They controlled the swelling ability and degradability with the addition of anhydrous calcium hydrogen phosphate within the system. Chitosan-based formulations were the best as it is concerns of mucoadhesive properties and sustained delivery of ACV, showing a defensive effect of chitosan against the cell damage.

5.2 *Buccal Applications*

Mucosa of the buccal cavity is considered a very convenient and easily accessible site for the drugs administration aimed for both local and systemic delivery (Russo et al. 2016).

Recently Russo et al. reviewed the polymers used for preparation of buccal dosage forms and the general requirements of a polymeric system to fall into relevant field. They listed general requirements for an ideal muco-buccal delivery system to be considered when this type of system is planned to be designed

- Particle size up to 1–3 cm² and a daily dose of 25 mg or less (Alur et al. 2001)
- Duration of the buccal delivery up to 4–6 h
- To mask the taste-masking strategies, on the basis of target population;
- To reduce the possible mucosal irritation at the site of application;
- To have adequate mechanical and rheological properties, e.g., thixotropic, pseudoplastic, or plastic flow so that the buccal formulations to be easy to apply;
- To possess hardness and resistance to handling.

The conventional dosage forms have difficulties to maintain their effects in buccal cavity. They are easily eliminated by salivation, temperature controlled, tongue movement, and swallowing. The mucoadhesive polymers are suitable to improve duration of formulation in cavity (Gandhi and Robinson 1994; Fini et al. 2011). The most proper dosage forms are the semisolid one like gels because of their large and soft surface area by comparison with the solid and liquid forms. Moreover, the delivery in the buccal area can take place for an extended period of time, due to their viscosity (Ishida et al. 1983; Khairnar and Sayyad 2010).

A characteristic “must have” of polymeric-based gel formulation is mucoadhesivity. Mucoadhesion is similarly defined as the bioadhesion having one of the substrate a mucosal surface (Shaikh et al. 2011).

Adhesive gels used in local delivery of drugs for buccal application were reported. Among them chlorhexidine was used for the treatment of periodontitis, for infectious diseases fluconazole, for inflammatory benzydamine hydrochloride, with high efficacy and patient acceptability (Senel et al. 2000; Vinholis et al. 2001).

Spray dried microparticles of chitosan and metformin were synthesized by (Sander et al. 2013) They prepared the microparticles taking into account the interdependency between the molecular weight and polymer chain length. With the aim of improving the bioadhesive properties of metformin microparticles they used chitosan grades with various polymer chain lengths obtaining as main outcome higher degree of interpenetration of mucosal residues also higher viscosities of the swelled particles. The encapsulation efficiency of metformin microparticles was influenced by the content of chitosan within the particle; particularly, encapsulation increased from 82 to 96% with decreasing chitosan: metformin ratio; the optimum ratio found was chitosan: metformin 1:3. The mucoadhesion between the polymeric drug delivery platform and mucosal substrate has a complex mechanism which comprises several steps such as wetting, adsorption, and interpenetration of polymer chains with mucosal substrate. Crosslinking degree, chain length and the presence of other functional groups. The side chains may have a major contribution to the mucoadhesion (Salamat-Miller et al. 2005; Andrews et al. 2009).

Smart (2005) reviewed the mechanism of mucoadhesion and found out that a favorable molecular weight for mucoadhesion can be between 104 and 4×10^6 Da. In the case of a lower molecular weight polymers, at the interphase with the substrate weak gels would be formed and the possibility to dissolve is high. The flexibility of polymer chains is another key parameter for the mucoadhesion process as it influences the penetration and entanglement, facilitating the interaction between the binding groups. Furthermore the crosslinking degree affects the mobility as a strong polymeric gel would hinder the mucoadhesion. In the case of anionic polymeric based matrices the pH of the medium may have a fundamental contribution, as groups would be ionized at pHs below the pKa of the polymer.

5.3 Transdermal and Dermal Application

Transdermal systems are desirable for drug delivery due to their advantages by comparison with other routes of delivery (Paudel et al. 2010; Vintiloiu and Leroux 2008). Transdermal delivery was described as a beneficial and pain-free self-administration route for patients. By this method, frequent and overdoses are avoided and plasma level peaks of the drug showed a constant concentration, the main motivation of these being the compliance of the patient, especially when a long period cure is needed, e.g., chronic pain treatment or smoking cessation therapy. Another advantage of the transdermal route reported is that the hepatic first-pass metabolism is prevented (Paudel et al. 2010; Vintiloiu and Leroux 2008). Thus the amount of delivered drug is lower and safer in the case of hepato-compromised patients and avoiding the side effects. Transdermal systems are generally cheap when compared with other therapies and, as patches, are designed to deliver drugs for a period from 1 to 7 days. Another advantage of transdermal delivery is the possibility to use successive doses, on-demand or various delivery rates of drugs by using the latest technology regarding programmable

devices. Micro-needle arrays (MN) is an alternative method for transdermal delivery as the drug is included inside the hydrogel-forming MN patch, thus decreasing the amount of drug to be delivered (Larraneta et al. 2016).

Transdermal absorption supposes the deterioration of the skin barrier function in order to direct specific molecules down to dermis. This process comprises of three different steps: the penetration of molecules in the outer stratum of the skin, the transport of the molecules through the layers (i.e., permeation) and the resorption at the level of dermis and vascular system. The quantification of the drug penetration efficiency in the skin is generally described by Fick's diffusion law. Liuzzi et al. (2016) recently explained the transport of microemulsions through the skin giving details on the transport efficiency in transdermal drug delivery emphasizing the role of the microstructure of microemulsions on the skin permeation.

A transdermal delivery gel commonly is formed of a vehicle, most commonly pluronic lecithin organogel (PLO gel), which delivers drug via the transdermal route to the bloodstream (Prabha 2013; Ibrahim et al. 2013). The micellar composition of PLO gel contributes to the enhancement of skin penetration of the pharmaceutical agent. PLO gel is generally well tolerated and is nontoxic if ingested. However, not all drugs are suitable for transdermal application, and there are relatively few studies of the bioavailability of drugs from compounded transdermal gels.

Trovatti et al. (2012) reported a bacterial cellulose (BC) hydrogel used for transdermal delivery of lidocaine hydrochloride and ibuprofen. They analyzed the permeation through the skin of the formulation with drugs and the conventional ones. They claimed that they obtained lower rates of the permeation for lidocaine hydrochloride in BC membranes by comparison with the conventional formulations. Their results are relevant for using the system for pathologies which require hydrophilic drugs with a more prolonged release of the drug formulations.

Similar results obtained also Silva et al. (2014) for BC membranes. These systems based on cellulose proved to be worthwhile in the design of transdermal drug delivery systems due to their property to absorb exudates and to easily adhere to irregular skin surfaces, along with their conformability.

Aktar et al. (2014) reported a transdermal system based on alginate loaded with metoclopramide hydrochloride (MTC). They optimized the system by adding different permeation enhancers, e.g., terpinolene, nerolidol, eucalyptol or dl-limonene. They found out that the released amount of MTC from transdermal films was higher for the systems where terpinolene was used as permeation enhancer. The *in vitro* adhesion results confirmed that transdermal films formulation of MTC with terpinolene and nerolidol showed the highest adhesion force values, results very likely for the transdermal delivery of the drugs.

Recently, transdermal delivery of isoliquiritigenin, an inhibitor of prostate cancer growth, was reported to be used as a hydrogel formulation based on hyaluronic acid (HA)-hydroxyethylcellulose (HEC) (Kong et al. 2016). This hydrogel formulation had a porous structure able to swell and to act as a reservoir which retains a large amount of water. This ability was useful in the skin absorption of drug which was very much increased. Comparable results were obtained by Tariverdi et al. (2016)

for an emulgel system based on hyaluronic acid/PVA for controlled delivery of melatonin.

A thermo-responsive graft copolymer of chitosan and poly (*N*-vinyl caprolactam) (PNVCL) was prepared by Indulekha et al. (2016) and named as “heat triggered transdermal drug delivery system (TDDS).” This type of system was designed to act like a pulsatile drug system which is responsive to the variation of the temperature. By combining the properties of PNVCL with the ones of chitosan they claimed that obtained a pH and temperature responsive transdermal system. Drug release profiles obtained showed higher amount released both for hydrophilic and hydrophobic at 39 °C (above LCST) and pH 5.5 when compared to other release conditions. In vitro skin permeation showed enhanced drug release when the skin was heated up to 39 °C. Also the skin permeation was influenced by the hydrophobicity or hydrophilicity of the drug, the hydrophilic one showing better results.

5.4 Ocular Applications

Hyaluronic acid based hydrogels are used for ophthalmic preparations and wound healing due to non-irritating properties of polymer. Sodium hyaluronate gels are used to separate tissues during ophthalmic surgery and prevent postoperative adhesion formation. Hyaluronic based gels also improve duration of drug on site of application due to mucoadhesive properties (Saettone et al. 1989). Recently, Calles et al. (2016b) proposed a system based on hyaluronic acid itaconic acid to be used within ocular delivery. They studied the effect of the homogeneous crosslinking of hyaluronic acid and itaconic acid in the presence of glutaraldehyde and triacetin as plasticizers on the properties of the materials. They found out that crosslinking with glutaraldehyde showed favorable results regarding the bioadhesive properties of the hyaluronan based hydrogels. Addition of itaconic acid increased even more the adhesiveness and lowered the wettability and swelling capacities. Thus the materials become more fragile and less elastic. To overcome exceeded stiffness required used plasticizers (Calles et al. 2016b).

Collagen is connective fundamental combinatorial tissue protein in animals. Collagen gels with a transparent appearance have been considered adequate for ophthalmic drug delivery applications. The patented ocular inserts of collagen are soluble devices for drug delivery (Miyata et al. 1979).

Pilocarpine hydrochloride loaded crosslinked collagen inserts are maintaining constant and controlled release of drug for 5–15 days (Vasanthra et al. 1988; Agban et al. 2016) Agban et al. (2016) found out that crosslinked collagen shields which they developed are suitable for topical ocular drug delivery devices. They observed that the nanoparticles (NPs) based on ZnO/polyvinyl pyrrolidone (PVP) seemed to be the best as crosslinker as concerning the cytotoxicity, shield transparency, and tensile strength. The optimum ratio was found as 1:1 collagen to ZnO/PVP NPs.

Rose et al. (2014) reviewed the possibility of using gelatin within the pharmaceutical formulations due to its good biocompatibility, it is inexpensive, ease of processing and availability. Gelatin and its derivatives were mostly handled as potential scaffolds for corneal epithelium (De la Mata et al. 2013), corneal endothelium (Lai et al. 2013a) and retinal pigment epithelium (Lai 2013b) and as a potential bioadhesive in treatment of retinal detachment (Yamamoto et al. 2013). They also highlighted methods of crosslinking which are exhibiting a low risk of toxicity.

5.5 Nasal Applications

Nasal application is an unconventional route of drug administration for gels. There are two reported nasal gels were developed up to now and these are already marketed. One is vitamin B-12 gel, Nascobal, used commonly as a dietary supplement. A hydrophilic cellulose derivative was used as gelling agent and the gel was apparently odorless, non-irritating and adheres to nasal mucous. Other gel is Neo-Synephrine Viscous that was formulated with methylcellulose as hydrophilic gelling agent.

Karavasili and Fatouros (2016) reviewed recent developments on the in situ gelling systems based on polysaccharides as a novel way in intranasal release of therapeutics. They focused on the tunable gelation properties up to the used polysaccharides (e.g., pectin, chitosan, etc.) with backbone of galacturonic acids units linked by α -1,4 bonds (Illum 2012). Chitosan was mentioned as being an efficient nasal absorption enhancer for small molecular weight drugs but also for proteins and peptides. A mechanism of enhanced absorption caused by the presence of chitosan within the in situ gels was proven by different studies on cell cultures and it was shown as being non-irritating with low local and systemic toxicity and accordingly to the regulations in Europe and USA. A marketed product for nasal delivery is based on chitosan which was found to be a successful absorption enhancing agent for nasal delivery of morphine, e.g., RylomineTM.

6 Conclusions and Future Perspectives

Present chapter reviews hydrogel/gels based polysaccharides; the concept of what is a hydrogel or gel was highlighted and the main preparation methods were summarized. Herein the concept of hydrogel/gel is at the borderline between two domains, i.e., polymer chemistry and pharmaceutical sciences. The present chapter aims the fusion between the chemistry sciences and pharmaceutical and medical sciences in order to bring contribution to scientists on the selection of the adequate material for a specific application by taking into account the properties.

As the conventional pharmaceutical formulations were incorporating before the polymeric moieties just for a better binding of the constituents, nowadays the role of polymers became more important as they need to protect the loaded drug for a determined period of time, mask the taste, to release drugs in a controlled manner (up to the desired conditions) and to target them to the specific site, therefore the drug bioavailability will increase as well. Sensibility to the external medium seems to have increased importance as a temperature, pH or other external response will allow to scientists to tailor the properties of the delivery systems accordingly. When a polymer matrix is intended to be used as a pharmaceutical formulation, a series of tests are priorly made, e.g., toxicity studies, thermo-mechanical properties, swelling, rheological and thixotropical, ability to release under controlled conditions (specific pH and temperature), gelling ability, erosion/degradability. The present chapter brought recent examples summarizing the needed properties and relevant values to get an idea about the pharmaceutical formulation needs.

Polysaccharides became attractive by the time passing as combination of their properties, e.g., biocompatibility, lack of toxicity, biodegradability, some of them exhibiting specific characteristics like responsivity to external stimuli, gelling abilities, susceptibility to be chemical modification to obtain new materials and with new architectures. The tremendous number of publications within this field proves that the developments already done are still limited and the potential of these materials is enormous.

Acknowledgements This work was partially supported by “The Scientific and Technological Research Council of Turkey (TUBITAK), cofunded by Marie Curie Actions under FP7,” project number 115C078; Romanian National Authority for Scientific Research, ANCS-UEFISCDI, project number PN-II-ID-PCE-2011-3-0906/274/2011 and grant BIONANOMED no 164/2012.

References

- Agban Y, Lian J, Prabakar S, Seyfoddin A, Rupenthal ID (2016) Nanoparticle cross-linked collagen shields for sustained delivery of pilocarpine hydrochloride. *Intern J Pharm* 501:96–101
- Ahmad M, Asifmehmood SMR (2016) Hydrogel microparticles as an emerging tool in pharmaceutical field: a review. *Adv Polym Technol* 21:535
- Ahmed EM (2015) Hydrogel: preparation, characterization, and applications: a review. *J Adv Res* 6:105–121
- Aktar B, Erdal MS, Sagirli O, Gungor Ozsoy Y (2014) Optimization of biopolymer based transdermal films of metoclopramide as an alternative delivery approach. *Polymers* 6:1350–1365
- Al-Kassas R, Wen J, En-Miao A, Amy C, Kim MJ, Sze S, Liu M, Yu J (2016) Transdermal delivery of propranolol hydrochloride through chitosan nanoparticles dispersed in mucoadhesive gel. *Carbohydr Polym*. <https://doi.org/10.1016/j.carbpol.2016.06.096>
- Alur HH, Johnston TP, Mitra AK (2001) Encyclopedia of pharmaceutical technology. In: Superbrick J, Boylan JC (eds) *Peptides and proteins: buccal absorption*. Marcel Dekker Inc., New York pp, pp 193–218

- Andrews GP, Lavery TP, Jones DS (2009) Mucoadhesive polymeric platforms for controlled drug delivery. *Eur J Pharm Biopharm* 71:505–518
- Aroguz AZ, Baysal K, Baysal BM (2010) Preparation and characterization of hydrogels of several polysaccharides for biomaterials applications hydrogels. Chap. 7 in biomaterials applications contemporary science of polymeric materials. ACS Symp Ser 1061:93–110
- Ay Senyigit Z, Karavana SY, Erac B, Gursel O, Hosgor Limoncu M, Baloglu E (2014) Evaluation of chitosan based vaginal bioadhesive gel formulations for antifungal drugs. *Acta Pharm* 64:139–156
- Babu RP, O'Connor K, Seeram R (2013) Current progress on bio-based polymers and their future trends. *Progr in Biomater* 2:8–16
- Barnes HA (1997) Thixotropy a review. *J Non-Newtonian Fluid Mech* 70:1–33
- Bekturov EV, Bimendina LA (1981) Interpolymer complexes. *Adv Polym Sci* 41:99–147
- Bernkop-Schnurch A, Hornof M (2003) Intravaginal drug delivery: design, challenges and solutions. *Am J Drug Deliv* 1:241–254
- Bokias G, Mylonas Y, Staikos G, Bumbu GG, Vasile C (2001) Synthesis and aqueous solution properties of novel thermoresponsive graft copolymers based on a carboxymethylcellulose backbone. *Macromolecules* 34:4958–4964
- Borzacchiello A, Russo L, Malle BM, Schwach-Abdellaoui K, Ambrosio L (2015) Hyaluronic acid based hydrogels for regenerative medicine applications. *BioMed Res Int* 2015 871218:12
- Braccini I, Perez S (2001) Molecular basis of Ca^{2+} -induced gelation in alginates and Pectins: the egg-box model revisited. *Biomacromol* 2:1089–1096
- Butnaru E, Cheaburu CN, Yilmaz O, Pricope GM, Vasile C (2015) Poly(vinyl alcohol)/chitosan/montmorillonite nanocomposites for food packaging applications: influence of montmorillonite content. *High Perform Polym* (0954008315617231)
- Buwalda SJ, Boere KWM, Dijkstra PJ, Feijen J, Vermonden T, Hennink WE (2014) Hydrogels in a historical perspective: from simple networks to smart materials. *J Controlled Release* 190:254–273
- Calles JA, Lopez-García A, Valles EM, Palma SD, Diebol Y (2016a) Preliminary characterization of dexamethasone-loaded cross-linked hyaluronic acid films for topical ocular therapy. *Intern J Pharm* 509:237–243
- Calles JA, Ressia JA, Llabot JM, Valles EM, Palma SD (2016b) Hyaluronan-itaconic acid-glutaraldehyde films for biomedical applications: preliminary studies. *Sci Pharm* 84:61–72
- Carmona-Moran CA, Zavgorodny O, Penman AD, Kharlampiev E, Bridges SL Jr, Hergenrother RW, Singh JA, Wick TM (2016) Development of gellan gum containing formulations for transdermal drug delivery: component evaluation and controlled drug release using temperature responsive nanogels. *Intern J Pharm* 509:465–476
- Cerchiara T, Abruzzo A, Parolina C, Vitali B, Bigucci F, Gallucci MC, Nicolettac FP, Luppi B (2016) Microparticles based on chitosan/carboxymethylcellulose polyelectrolyte complexes for colon delivery of vancomycin. *Carbohydr Polym* 143:124–130
- Corobea MC, Muhulet O, Miculescu F, Antoniac IV, Vuluga Z, Florea D et al (2016) Novel nanocomposite membranes from cellulose acetate and clay-silica nanowires. *Polym Adv Technol* 27(12):1586–1595
- Chaterji S, Kwon IK, Park K (2007) Smart polymeric gels: redefining the limits of biomedical devices. *Progr Polym Sci.* 32:1083–1122
- Cheaburu CN, Bumbu GG (2009) Degradable interpolymeric complexes, Chap. 10. In: Vasile C, Zaikov G, Brill (eds) Environmentally degradable materials based on multicomponent polymeric systems, 654 pages
- Cheaburu CN, Vasile C (2008) Responsive freeze-drying interpolymeric associations of alginic acid and poly (N-Isopropyl Acrylamide). II. Transition and temperature dependence on pH and composition. *Cell Chem Technol* 42:207–212
- Cheaburu-Yilmaz CN, Yilmaz O, Vasile C (2015a) Eco-friendly chitosan-based nanocomposites: chap. In eco-friendly Polymer Nanocomposites. In: Thakur VK, Thakur, MK (eds) Chem Appl Adv Struct Mater 74:341–386

- Cheaburu-Yilmaz CN, Dumitriu RP, Nistor MT, Lupusoru C, Popa MI, Profire L, Silvestre C, Vasile C (2015b) Biocompatible and biodegradable chitosan/clay nanocomposites as new carriers for theophylline controlled release. *Br J Pharm Res* 6:228–254
- Cheaburu-Yilmaz CN, Bibire N, Yilmaz O, Pamfil D, Lupusoru C, Lupusoru RV, Vasile C (2017) Freeze-thaw PVA/hyaluronic acid hydrogels for controlled delivery of methotrexate for psoriasis therapy (in press)
- Chen Q, Chen H, Zhu L, Zheng J (2015) Fundamentals of double network hydrogels. *J Mater Chem B* 3:3654–3676
- Chenite A, Chaput C, Wang D, Combes C, Buschmann MD, Hoemann CD, Leroux JC, Atkinson BL, Binette F, Selmani A (2000) Novel injectable neutral solutions of Chitosan form biodegradable gels in situ. *Biomaterials* 21:2155–2161
- Cojocariu A, Profire L, Cheaburu C, Vasile C (2012) Chitosan/montmorillonite composites as matrices for prolonged delivery of some novel nitric oxide donor compounds based on theophylline and paracetamol. *Cell Chem Technol* 46:35–43
- Das Neves J, Bahia MF (2006) Gels as vaginal drug delivery systems. *Intern J Pharm* 318:1–14
- Davis SS (1971) Viscoelastic properties of pharmaceutical semisolids IV: destructive oscillatory testing. *J Pharm Sci* 60:1356–1360
- De la Mata A, Nieto-Miguel T, Lopez-Paniagua M, Galindo S, Aguilar MR, García-Fernandez L, Gonzalo S, Vazquez B, Roman JS, Corrales RM (2013) Chitosan-gelatin biopolymers as carrier substrata for limbal epithelial stem cells. *J Mater Sci Mater Med* 24:2819–2829
- De Pinho Neves AL, Cardoso Milioli C, Muller L, Gracher Riella H, Kuhnena NC, Stulzer HK (2014) Factorial design as tool in chitosan nanoparticles development by ionic gelation technique. *Colloids and surfaces a: physicochem. Eng Aspects* 445:34–39
- Dumitriu RP, Mitchell GR, Vasile C (2011) Rheological and thermal behaviour of poly (N-isopropylacrylamide)/alginate smart polymeric networks. *Polym Intern* 60:1398–1407
- Dumitriu RP, Oprea AM, Cheaburu CN, Nistor MT, Novac O, Ghiciuc CM, Profire L, Vasile C (2014) Biocompatible and biodegradable alginate/poly (N-isopropylacrylamide) hydrogels for sustained theophylline release. *J Appl Polym Sci* 131:40733
- Dumitriu RP, Profire L, Nita LE, Dragostin OM, Ghetu N, Peptu D, Vasile C (2015) Sulfadiazine-chitosan conjugates and their polyelectrolyte complexes with hyaluronate destined in the management of burn wounds. *Materials* 8:317–338
- Dumitriu S (2004) Polysaccharides: structural diversity and functional versatility, 2nd Edn. CRC Press, Science, p 1224
- Dutta S, Samanta P, Dhara D (2016) Temperature, pH and redox responsive cellulose based hydrogels for protein delivery. *Intern J Biol Macromol* 87:92–100
- Ebara M, Kotsuchibashi Y, Narain R, Idota N, Kim YJ, Hoffman JM, U to K, Aoyagi T (2014) Smart hydrogels Chap. 2 in smart biomaterials. Springer, p 118
- Eldin MSM, Kamoun EA, Sofan MA, Elbayomi SM (2015) L-Arginine grafted alginate hydrogel beads: a novel pH-sensitive system for specific protein delivery. *Arab J Chem* 8:355–365
- Fan L, Yang H, Yang J, Peng M, Hu J (2016) Preparation and characterization of chitosan/gelatin/PVA hydrogel for wound dressings. *Carbohydr Polym* 146:427–434
- Fathalla ZMA, Khaled KA, Hussein AK Alany RG, Vangala A (2016) Formulation and corneal permeation of ketorolac tromethamine-loaded chitosan nanoparticles. *Drug Dev Ind Pharm* 42:514–524
- Ferry JD (1961) Viscoelastic properties of polymers. Wiley, New York, p 391
- Fini A, Bergamante V, Ceschel GC (2011) Mucoadhesive gels designed for the controlled release of chlorhexidine in the oral cavity. *Pharmaceutics* 3:665–679
- Freundlich H, Rawitz W (1927) Influence of metals on thixotropic sols and gels. *Kolloid-Z* 41:102–104
- Fu S, Thacker A, Sperger DM, Boni RL, Buckner IS, Velankar S, Munson EJ, Block LH (2011) Relevance of rheological properties of sodium alginate in solution to calcium alginate gel properties. *AAPS Pharmscitech* 12:453–460
- Gaharwar AK, Peppas NA, Khademhosseini A (2014) Nanocomposite hydrogels for biomedical applications. *Biotechnol Bioeng* 111:441–453

- Gamboa A, Araujo V, Caro N, Gotteland M, Abugoch L, Tapia C (2015) Spray freeze-drying as an alternative to the ionic gelation method to produce chitosan and alginate nano-particles targeted to the colon. *J Pharm Sci* 104:4373–4385
- Gandhi RB, Robinson JR (1994) Oral cavity as a site for bioadhesive drug delivery. *Adv Drug Deliv Rev* 13:43–74
- Gidwani B, Vyas A (2015) A comprehensive review on cyclodextrin-based carriers for delivery of chemotherapeutic cytotoxic anticancer drugs. *BioMed Res Intern* 198268:15. <http://dx.doi.org/10.1155/2015/198268>
- Grant GT, Morris ER, Rees DA, Smith PJC, Thom D (1973) Biological interactions between polysaccharides and divalent cations: the egg-box model. *FEBS Lett* 32:195–198
- Guilherme MR, Aouada FA, Fajardo AR, Martins AF, Paulino AT, Davi MT, Rubira AF, Muniz EC (2015) Superabsorbent hydrogels based on polysaccharides for application in agriculture as soil conditioner and nutrient carrier: a review. *Eur Polym J* 72:365–385
- Gulrez KHS, Phillips GO, Al-Assaf S (2011) Hydrogels: methods of preparation, characterisation and applications. In: *Progress in molecular and environmental bioengineering—from analysis and modeling to technology applications*. InTech Ed Carpi A (ISBN: 978-953-307-268-5)
- Guo J, Kaletunc G (2016) Dissolution kinetics of pH responsive alginate-pectin hydrogel particles. *Food Res Intern*. <https://doi.org/10.1016/j.foodres.2016.05.020>
- Guo W, Orbach R, Mironi-Harpaz I, Seliktar D, Willner I (2013) Fluorescent DNA hydrogels composed of nucleic acid-stabilized silver nanoclusters. *Small* 9:3748–3752
- Gupta H, Sharma A (2009) Ion activated bioadhesive in situ gel of clindamycin for vaginal application. *Int J Drug Deliv* 10:32–40
- Gupta P, Vermani K, Garg S (2002) Hydrogels: from controlled release to pH-responsive drug delivery. *Drug Discov Today* 7:569–579
- He CL, Kim SW, Lee DS (2008) In situ gelling stimuli-sensitive block copolymer hydrogels for drug delivery. *J Control Release* 127:189–207
- Hennink WE, Nostrum CFV (2002) Novel crosslinking methods to design hydrogels. *Adv Drug Delivery Rev* 54:13–36
- Higham AK, Bonino CA, Raghavan SR, Khan SA (2014) Photo-activated ionic gelation of alginate hydrogel: real-time rheological monitoring of the two-step crosslinking mechanism. *Soft Matter* 10:4990–5002
- Hoare TR, Kohane DS (2008) Hydrogels in drug delivery: progress and challenges. *Polymer* 49:1993–2007
- Hu X, Gong X (2016) A new route to fabricate biocompatible hydrogels with controlled drug delivery behavior. *J Colloid Interf Sci* 470:62–70
- Huang CL, Chen YB, Lo YL, Lin YH (2016) Development of chitosan/ β glycerophosphate/glycerol hydrogel as a thermosensitive coupling agent. *Carbohydr Polym* 147:409–414
- Huang Y, Szleifer I, Peppas NA (2002) A molecular theory of polymer gels. *Macromolecules* 35:1373–1380
- Hurler J, Engesland A, Kermany BP, Skalko-Basnet N (2012) Improved texture analysis for hydrogel characterization: gel cohesiveness, adhesiveness, and hardness. *J Appl Polym Sci* 125:180–188
- Hussain A, Ahsan F (2005) The vagina as a route for systemic drug delivery. *J Control Release* 103:301–313
- Ibrahim MM, Hafez SA, Mahdy MM (2013) Organogels, hydrogels and bigels as transdermal delivery systems for diltiazem hydrochloride. *Asian J Pharm Sci* 8:48–57
- Illum L (2012) Nasal drug delivery—recent developments and future prospects. *J Control Release* 161:254–263
- Indulekha S, Arunkumar P, Bahadur D, Srivastava R (2016) Thermoresponsive polymeric gel as an on-demand transdermal drug delivery system for pain management. *Mat Sci Eng C* 62:113–122
- Ishida M, Nambu N, Nagai T (1983) Highly viscous gel ointment containing Carbopol for application to the oral mucosa. *Chem Pharm Bull* 31:4561–4564

- Jabeen S, Maswal M, Chat OA, Rather GM, Dar AA (2016) Rheological behavior and Ibuprofen delivery applications of pH responsive composite alginate hydrogels. *Colloids Surf B: Biointerfaces* 139:211–218
- Javvaji V, Baradwaj AG, Payne GF, Raghavan SR (2011) Light-activated ionic gelation of common biopolymers. *Langmuir* 27:12591–12596
- Jeong B, Kim SW, Bae YH (2012) Thermosensitive sol–gel reversible hydrogels. *Adv Drug Delivery Rev* 64:154–162
- Johnson JA Turro N, Koberstein JT, Mark JE (2010) Some hydrogels having novel molecular structures. *Prog Polym Sci* 35:332–337
- Jones DS, Woolfson AD, Brown AF (1997) Textural, viscoelastic and mucoadhesive properties of pharmaceutical gels composed of cellulose polymers. *Intern J Pharm* 151:223–233
- Kakuta T, Takashima Y, Harada A (2013) Highly elastic supramolecular hydrogels using host-guest inclusion complexes with cyclodextrins. *Macromolecules* 46:4575–4579
- Kalam MA (2016) Development of chitosan nanoparticles coated with hyaluronic acid for topical ocular delivery of dexamethasone. *Intern J Biol Macromol* 89:127–136
- Karavasili C, Fatouros DG (2016) Smart materials: in situ gel-forming systems for nasal delivery. *Drug Discovery Today* 21:157–166
- Khairnar GA, Sayyad FJ (2010) Development of buccal drug delivery system based on mucoadhesive polymers. *Int J PharmTech Res* 2:719–735
- Klouda L (2015) Thermoresponsive hydrogels in biomedical applications a seven-year update. *Eur J Pharm Biopharm* 97:338–349
- Klouda L, Mikos AG (2008) Thermoresponsive hydrogels in biomedical applications—a review. *Eur J Pharm Biopharm* 68:34–45
- Kong BJ, Kim A, Park SN (2016) Properties and in vitro drug release of hyaluronic acid-hydroxyethylcellulose hydrogels for transdermal delivery of isoliquiritigenin. *Carbohydr Polym* 147:473–481
- Kono H, Teshirogi T (2015) Cyclodextrin-grafted chitosan hydrogels for controlled drug delivery. *Intern J Biol Macromol* 72:299–308
- Kontogiorgos V, Smith AM, Morris GA (2015) The parallel lives of polysaccharides in food and pharmaceutical formulations. *Curr Opin Food Sci* 4:13–18
- Korsmeyer RW, Lustig SR, Peppas NA (1968) Solute and penetrant diffusion in swellable polymers. I. Mathematical modeling. *J Polym Sci Part B: Polym Phys* 24:395–408
- Lai JY (2013) Influence of solvent composition on the performance of carbodiimide cross-linked gelatin carriers for retinal sheet delivery. *J Mater Sci Mater Med* 24:2201–2210
- Lai JY, Ma DHK, Lai MH, Li YT, Chang RJ, Chen LM (2013) Characterization of cross-linked porous gelatin carriers and their interaction with corneal endothelium: biopolymer concentration effect. *PLoS ONE* 8:540–558
- Langasco R, Spada G, Tuncay Tanriverdi S, Rassa G, Giunchedi P, Ozer O, Gavini E (2016) Bio-based topical system for enhanced salicylic acid delivery: preparation and performance of gels. *J Pharm Pharmacol* 68:999–1009
- Larraneta E, Lutton REM, Woolfson AD, Donnelly RF (2016) Microneedle arrays as transdermal and intradermal drug delivery systems: materials science, manufacture and commercial development. *Mater Sci Eng R* 104:1–32
- Leea CH, Moturia V, Lee Y (2009) Thixotropic property in pharmaceutical formulation. *J Control Release* 136:88–98
- Leong JY, Lam WH, Ho KW, Voo WP, Lee MFX, Lim HP, Lim SL, Tey BT, Poncelet D, Chan ES (2016) Advances in fabricating spherical alginate hydrogels with controlled particle designs by ionotropic gelation as encapsulation systems. *Particuology* 24:44–60
- Li J, Liu D, Tana G, Zhao Z, Yang X, Pan W (2016) A comparative study on the efficiency of chitosan-N-acetylcysteine, chitosan oligosaccharides or carboxymethyl chitosan surface modified nanostructured lipid carrier for ophthalmic delivery of curcumin. *Carbohydr Polym* 146:435–444

- Lim MPA, Lee WL, Widjaja E, Loo SCJ (2013) One-step fabrication of core-shell structured alginate-PLGA/PLLA microparticles as a novel drug delivery system for water soluble drugs. *Biomater Sci* 1:486–493
- Lim YM, Gwon HJ, Park JS, Nho YC Shim JW, Kwon IK, Kim SE, Baik SH (2011) Synthesis and properties of hyaluronic acid containing copolymers crosslinked by γ -ray irradiation. *Macromol Res* 19:436–441
- Liow SS, Dou Q, Kai D, Karim AA, Zhang K, Xu F, Loh XJ (2016) Thermogels. In *Situ gelling biomaterial*. *ACS Biomater Sci Eng* 2:295–316
- Liu H, Sui X, Xu H, Zhang L, Zhong Y, Mao Z (2016) Self-healing polysaccharide hydrogel based on dynamic covalent enamine bonds. *Macromol Mater Eng* 301:725–732
- Liu KL, Zhang Z, Li J (2011) Supramolecular hydrogels based on cyclodextrin-polymer polypseudorotaxanes: materials design and hydrogel properties. *Soft Matter* 7:11290–11297
- Liu ZQ, Wei Z, Zhu XL, Huang GY, Xu F, Yang JH, Osada Y, Zrinyig M, Yong JHL, Chena M (2015) Dextran-based hydrogel formed by thiol-michael addition reaction for 3D cell encapsulation. *Colloids Surf, B* 128:140–148
- Liuzzi R, Carciati A, Guido S, Caserta S (2016) Transport efficiency in transdermal drug delivery: What is the role of fluid microstructure? *Colloids Surf, B* 139:294–305
- Lucero MJ, Ferris C, Sánchez-Gutiérrez CA, Jiménez-Castellanos MR, de-Paz MV (2016) Novel aqueous chitosan-based dispersions as efficient drug delivery systems for topical use. Rheological, textural and release studies. *Carbohydr Polym* 151:692–699
- Mabrouk M, Chejara DR, Mulla JAS, Badhe RV, Choonara YE, Kumar P, du Toit LC, Pillay V (2015) Design of a novel crosslinked HEC-PAA porous hydrogel composite for dissolution rate and solubility enhancement of efavirenz. *Intern J Pharm* 490:429–437
- Machín R, Isasi JR, Velaz I (2012) β -cyclodextrin hydrogels as potential drug delivery systems. *Carbohydr Polym* 87:2024–2030
- Mahdavinia GR, Mousanezhad S, Hosseinzadeh H, Darvishi F, Sabzi M (2016) Magnetic hydrogel beads based on PVA/sodium alginate/laponite RD and studying their BSA adsorption. *Carbohydr Polym* 147:379–391
- Malda J, Visser J, Melchels FP, Jüngst T, Hennink WE, Dhert WJA, Groll J, Huttmacher DW (2013) 25th anniversary article: engineering hydrogels for biofabrication. *Adv Mater* 25:5011–5028
- Mastropietro DJ, Nimrooz R, Omidian H (2013) Rheology in pharmaceutical formulations—a perspective. *J Dev Drugs* 2:108–116
- Mayol L, De Stefano D, De Falco F, Carnuccio R, Maiuri MC, De Rosa G (2014) Effect of hyaluronic acid on the thermogelation and biocompatibility of its blends with methyl cellulose. *Carbohydr Polym* 112:480–485
- Mercado SA, Slater NKH (2016) The functional and structural effects of an amphipathic pH responsive biopolymer: a comprehensive study in osteosarcoma cells. *Eur Polymer J* 74:158–167
- Mezger TG (2006) *The rheology handbook: for users of rotational and oscillatory rheometers*, 2nd revised edn. Vincentz Network, Hannover
- Mikos AG, Peppas NA (1986) Comparison of experimental technique for measurement of the bioadhesive forces of polymeric materials with soft tissues. *Proc Int Symp Control Release Bioact Mater* 13:97–100
- Miculescu M, Thakur VK, Miculescu F, Voicu SI (2016) Graphene-based polymer nanocomposite membranes: a review. *Polym Adv Technol* 27(7):844–859
- Miyata T, Rubin AL, Stenzel KH, Dunn MW (1979) US Patent 4, 164, 559
- Molina R, Jovancic P, Vilchez S, Tzanov T, Solans C (2014) In situ chitosan gelation initiated by atmospheric plasma treatment. *Carbohydr Polym* 103:472–479
- Morris ER, Rees DA, Thom D, Boyd J (1978) Chiroptical and stoichiometric evidence of a specific, primary dimerisation process in alginate gelation. *Carbohydr Res* 66:145–154
- Murthy S, Shivakumar H (2010) Topical and transdermal drug delivery. *Handbook of Non-Invasive Drug Delivery Systems*, pp 1–36

- Na YH (2013) Double network hydrogels with extremely high toughness and their applications. *Korea-Aust Rheol J* 25:185–196
- Nie J, Lu W, Ma J, Yang L, Wang Z, Qin A, Hu Q (2015) Orientation in multi-layer chitosan hydrogel: morphology. *Mech Des Principle Sci Rep* 5:7635
- Nishida Y, Ohtsuki S, Araie Y, Umeki Y, Endo M, Emura T, Hidaka K, Sugiyama H, Takahashi Y, Takakura Y, Nishikawa M (2016) Self-assembling DNA hydrogel-based delivery of immunoinhibitory nucleic acids to immune cells. *Nanomedicine: nanotechnology. Biol Med* 12:123–130
- Păduraru OM, Vasile C, Pațachia S, Grigoras C, Oprea AM (2010) Membranes based on poly (vinyl alcohol)/beta-cyclodextrin blends. *Polimery* 55:473–478
- Pamfil D, Butnaru E, Vasile C (2016, Aug) Poly (vinyl alcohol)/chitosan cryogels as pH responsive ciprofloxacin carriers. *J Polym Res* 23(8). <https://doi.org/10.1007/s10965-016-1042-1>
- Pamfil D, Vasile C (2017) Nanogels of natural polymers Chap. 4 in handbook on “Polymer Gels”. Section “polymer gels: science and fundamentals” (in press)
- Papkov SP (1974) Gel-like state of polymers. *Khimiya, Moscow*
- Park H, Robinson JR (1985) Physicochemical properties of water insoluble polymers important to mucin/epithelial adhesion. *J Control Rel* 2:257–275
- Park K, Robinson JR (1984) Bioadhesive polymers as platforms for oral-controlled drug delivery: method to study bioadhesion. *Int J Pharm* 198:107–127
- Patel P, Patel P (2015) Formulation and evaluation of clindamycin HCl in situ gel for vaginal application. *Intern J Pharm Investig* 5:50–56
- Pappu A, Patil V, Jain S, Mahindrakar A, Haque R, Thakur VK (2015) Advances in industrial prospective of cellulosic macromolecules enriched banana biofibre resources: a review. *Int J Biol Macromol* 79:449–458
- Pappu A, Saxena M, Thakur VK, Sharma A, Haque R (2016) Facile extraction, processing and characterization of biorenewable sisal fibers for multifunctional applications. *J Macromol Sci Part A* 53(7):424–432
- Patel PV, Koyani V (2014) Smart polymers: innovative drug delivery system. *World J Pharm Pharm Sci* 3:508–527
- Paudel KS, Milewski M, Swadley CL, Brogden NK, Ghosh P, Stinchcomb AL (2010) *Ther Deliv* 1:109–131
- Peak CW, Wilker JJ, Schmidt G (2013) A review on tough and sticky hydrogels. *Colloid Polym Sci* 291:2031–2047
- Peppas NA, Buri PA (1985) Surface, interfacial and molecular aspects of polymer bioadhesion on soft tissues. *J Control Release* 2:257–275
- Perioli L, Ambrogi V, Venezia L, Pagano C, Ricci M, Rossi C (2008) Chitosan and a modified chitosan as agents to improve performances of mucoadhesive vaginal gels. *Colloids Surf, B* 66:141–145
- Plazinski W (2011) Molecular basis of calcium binding by polyguluronate chains. Revising the egg-box model. *J Comput Chem* 32:2988–2995
- Prabaharan M, Mano JF (2006) Stimuli-responsive hydrogels based on polysaccharides incorporated with thermo-responsive polymers as novel biomaterials. *Macromol Biosci* 8:991–1008
- Prasertung I, Damrongsakkul S, Terashima C, Saito N, Takai O (2012) Preparation of low molecular weight chitosan using solution plasma system. *Carbohydr Polym* 87:2745–2749
- Rasente RY, Imperiale JC, Lázaro-Martínez JM, Gualco L, Oberkersch R, Sosnik A, Calabrese GC (2016) Dermatan sulfate/chitosan polyelectrolyte complex with potential application in the treatment and diagnosis of vascular disease. *Carbohydr Polym* 144:362–370
- Rencher S, Karavana SY, Ay Şenyigit Z, Erac B, Hosgor Limoncu M, Baloglu E (2016) Mucoadhesive in situ gel formulation for vaginal delivery of clotrimazole: formulation, preparation, and in vitro/in vivo evaluation. *Pharm Develop Tech*. <https://doi.org/10.3109/10837450.2016.1163385>

- Rodkate N, Rutnakornpituk M (2016) Multi-responsive magnetic microsphere of poly (N-isopropylacrylamide)/carboxymethylchitosan hydrogel for drug controlled release. *Carbohydr Polym* 151:251–259
- Rogovina LZ, Vasilev VG, Braudo EE (2008) Definition of the Concept of Polymer Gel. *Polymer Sci Ser C* 50:85–92
- Rose JB, Pacelli S, El Haj AJ, Dua HS, Hopkinson A, White LJ, Rose FRAJ (2014) Gelatin-based materials in ocular tissue engineering. *Materials* 7:3106–3135
- Rosiak JM, Yoshii F (1999) Hydrogels and their medical applications. *Nucl Instr Meth Phys Res B* 151:56–64
- Rubinstein M, Colby RH (2003) *Polymer physics*. Oxford University Press, Oxford
- Russo E, Selmin F, Baldassari S, Gennari CGM, Caviglioli G, Cilurzo F, Minghetti P, Parodi B (2016) A focus on mucoadhesive polymers and their application in buccal dosage forms. *J Drug Delivery Sci Techn* 32:113–125
- Russo PS (1987) A perspective on reversible gels and related systems. In: Russo PS (eds) Chapter 1 in reversible polymeric gels and related systems 350:1–21
- Ryu JH, Lee Y, Kong WH, Kim TG, Park TG, Lee H (2011) Catechol-functionalized chitosan/pluronic hydrogels for tissue adhesives and hemostatic materials. *Biomacromol* 12:2653–2659
- Saettone MF, Cheton P, Torracca MT, Burgalassi S, Giannaccini B (1989) Evaluation of muco-adhesive properties and in vivo activity of ophthalmic vehicles based on hyaluronic acid. *Int J Pharm* 51:203–212
- Sagiri SS, Behera B, Rafanan RR, Bhattacharya C, Pal K, Banerjee I, Rousseau D (2014) Organogels as matrices for controlled drug delivery: a review on the current state. *Soft Mater* 12:47–72
- Salamat-Miller N, Chittchang M, Johnston TP (2005) The use of mucoadhesive polymers in buccal drug delivery. *Adv Drug Delivery Rev* 57:1666–1691
- Salmaso S, Semenzato A, Bersani S, Matricardi P, Rossi F, Caliceti P (2007) Cyclodextrin/PEG based hydrogels for multi-drug delivery. *Int J Pharm* 345:42–50
- Sanchez MP, Martín-Illana A, Ruiz-Caro R, Bermejo P, Abad MJ, Carro R, Bedoya LM, Tamayo A, Rubio J, Fernández-Ferreiro A, Otero-Espinar F, Veiga MD (2015) Chitosan and kappa-carrageenan vaginal acyclovir formulations for prevention of genital herpes. In vitro and ex vivo evaluation. *Mar Drugs* 13:5976–5992
- Sander C, Madsen DK, Hyrup B, Nielsen HM, Rantanen J, Jacobsen J (2013) Characterization of spray dried bioadhesive metformin microparticles for oromucosal administration. *Eur J Pharm Biopharm* 85:682–688
- Secchi E, Roversi T, Buzzaccaro S, Piazza L, Piazza R (2013) Biopolymer gels with “physical” cross-links: gelation kinetics, aging, heterogeneous dynamics, and macroscopic mechanical properties. *Soft Matter* 9:3931–3944
- Senel S, İkinci G, Kas S, Yousefi-Rad A, Sargon MF, Hınca AA (2000) Chitosan films and hydrogels of chlorhexidine gluconate for oral mucosal delivery. *Int J Pharm* 193:197–203
- Shaikh R, Singh TRR, Garland MJ, Woolfson AD, Donnelly RF (2011) Mucoadhesive drug delivery systems. *J Pharm Bioallied Sci* 3:89–100
- Shi L, Yang L, Chen J, Pei Y, Chen M, Hui B, Li J (2004) Preparation and characterization of pH-sensitive hydrogel of chitosan/poly (acrylic acid) co-polymer. *J Biomater Sci Polym Ed* 15:465–474
- Silva NHCS, Rodrigues AF, Almeida IF, Costa PC, Rosado C, Neta CP, Silvestre AJD, Freire CSR (2014) Bacterial cellulose membranes as transdermal delivery systems for diclofenac: in vitro dissolution and permeation studies. *Carbohydr Polym* 106:264–269
- Prabha SB (2013) Preparation and evaluation of pluronic lecithin organogel containing ricinoleic acid for transdermal drug delivery. Theses and dissertations. Paper 32
- Singh NK, Lee DS (2014) In situ gelling pH- and temperature-sensitive biodegradable block copolymer hydrogels for drug delivery. *J Control Release* 193:214–227
- Singh R, Singh D (2012) Radiation synthesis of PVP/alginate hydrogel containing nanosilver as wound dressing. *J Mater Sci: Mater Med* 23:2649–2658

- Singhal R, Gupta K (2016) A review: tailor-made hydrogel structures (classifications and synthesis parameters). *Polymer-Plastics Technol Eng* 55:54–70
- Sionkowska A, Kaczmarek B, Lewandowska K, Grabska S, Pokrywczynska M, Kloskowski T, Drewa T (2016) 3D composites based on the blends of chitosan and collagen with the addition of hyaluronic acid. *Intern J Biol Macromols* 89:442–448
- Smart JD (2005) The basics and underlying mechanisms of mucoadhesion. *Adv Drug Delivery Rev* 57:1556–1568
- Smart JD, Kellaway IW, Worthington HEC (1984) An in vitro investigation of mucosa adhesive materials for use in controlled drug delivery. *J Pharm Pharmacol* 36:295–299
- Solomonidou D, Cremer K, Krumme M, Kreuter J (2001) Effect of carbomer concentration and degree of neutralization on the mucoadhesive properties of polymer films. *J Biomat Sci* 12:1191–1205
- Strobel SA, Scher HB, Nitin N, Jeoh T (2016) In situ cross-linking of alginate during spray-drying to microencapsulate lipids in powder. *Food Hydrocolloids* 58:141–149
- Tanaka T (1985) in encyclopedia of polymer science and engineering. In: Klingsberg A, Piccinini P (eds), vol 7. Wiley, New York, p 514
- Tanriverdi ST, Ozer O (2013) Novel topical formulations of terbinafine-HCl for treatment of onychomycosis. *Eur J Pharm Sci* 48:628–636
- Tanriverdi ST, Cheaburu-Yilmaz CN, Carbone S, Özer Ö (2016) Preparation and in vitro evaluation of melatonin loaded HA/PVA gel formulations. *Pharm Develop Technol*. <https://doi.org/10.1080/10837450.2016.1268158>
- Thakur VK, Thakur MK (2014) Recent trends in hydrogels based on psyllium polysaccharide: a review. *J Cleaner Prod* 82:1–15
- Thakur VK, Thakur MK (2015) Recent advances in green hydrogels from lignin: a review. *Int J Biol Macromol* 72:834–847
- Thakur MK, Thakur VK, Gupta RK, Pappu A (2016) Synthesis and applications of biodegradable soy based graft copolymers: a review. *ACS Sustain Chem Eng* 4:1–17
- Tomsic M, Prossnigg F, Glatter O (2008) A thermoreversible double gel: characterization of a methylcellulose and κ -carrageenan mixed system in water by SAXS, DSC and rheology. *J Colloid Interface Sci* 322:41–50
- Trovatti E, Freire CSR, Pinto PC, Almeida IF, Costa P, Silvestre AJD, Neto CP, Rosado C (2012) Bacterial cellulose membranes applied in topical and transdermal delivery of lidocaine hydrochloride and ibuprofen: in vitro diffusion studies. *Intern J Pharm* 435:83–87
- Trache D, Hazwan Hussin M, Mohamad Haafiz MK, Kumar Thakur V (2017) Recent progress in cellulose nanocrystals: sources and production. *Nanoscale* 9(5):1763–1786
- Tulain UR, Ahmad M, Rashid A, Malik MZ, Iqbal FM (2016, Mar) Fabrication of pH-responsive hydrogel and its in vitro and in vivo evaluation. *Adv Polym Technol*. <https://doi.org/10.1002/adv.21668>
- Ueda CT, Shah VP, Derdzinski K, Ewing G, Flynn G, Maibach H, Marques M, Rytting H, Shaw S, Thakker K, Yacobi (2009) A topical and transdermal drug products. *Pharmacoepial Forum* 35(3):750–764
- Ullah F, Othman MBH, Javed F, Ahmad Z, Md Akil H (2015) Classification, processing and application of hydrogels: a review. *Mater Sci Eng, C* 57:414–433
- Vasantra R, Sehgl PK, Rao KP (1988) Collagen ophthalmic inserts for pilocarpine drug delivery system. *Int J Pharm* 47:95–102
- Vasile C, Dumitriu RP, Cheaburu C, Oprea AM (2009) Architecture and composition influence on the properties of some smart polymeric materials designed as matrices in drug delivery systems. *A Comp Study. Appl Sur Sci* 256:65–71
- Venus M, Waterman J, McNab I (2011) Basic physiology of the skin. *Surgery (Oxford)* 29:471–474
- Vinholis AHC, de Figueiredo LC, Marcantonio E Jr, Marcantonio RAC, Salvador SLS, Goissis G (2001) Subgingival utilization of a 1% chlorhexidine collagen gel for the treatment of periodontal pockets. A clinical and microbiological study. *Braz Dent J* 12:209–213

- Vintiloiu A, Leroux JC (2008) Organogels and their use in drug delivery—a review. *J Control Release* 125:179–192
- Voicu, SI, Condruz RM, Mitran V, Cimpean A, Miculescu F, Andronescu C, Miculescu M, Thakur VK (2016) Sericin covalent immobilization onto cellulose acetate membrane for biomedical applications. *ACS Sustain Chem Eng* 4(3):1765–1774
- Vulpe R, Popa M, Picton L, Balan V, Dulong V, Butnaru M, Verestiuc L (2016) Crosslinked hydrogels based on biological macromolecules with potential use in skin tissue engineering. *Int J Biol Macromol* 84:174–181
- Wang W, Zhang P, Shan W, Gao J, Liang W (2013) A novel chitosan-based thermosensitive hydrogel containing doxorubicin liposomes for topical cancer therapy. *J Biomater Sci Polym Ed* 24:1649–1659
- Wong CF, Yuen KH, Kok KP (1999) An in vitro method for buccal adhesion studies: importance of instrument variables. *Int J Pharm* 180:47–57
- Xu J, Li X, Sun F, Cao P (2010) PVA hydrogels containing beta-cyclodextrin for enhanced loading and sustained release of ocular therapeutics. *J Biomater Sci Polym Ed* 21:1023–1038
- Xu W, Qian J, Zhang Y, Suo A, Cui N, Wang J, Yao Y, Wang H (2016) A double-network poly (Ne-acryloyl L-lysine)/hyaluronic acid hydrogel as a mimic of the breast tumor microenvironment. *Acta Biomater* 33:131–141
- Yamamoto S, Hirata A, Ishikawa S, Ohta K, Nakamura K, Okinami S (2013) Feasibility of using gelatin-microbial transglutaminase complex to repair experimental retinal detachment in rabbit eyes. *Graefe's Arch Clin Exp Ophthalmol* 251:1109–1114
- Yoshiaki Y, Padol HA, Draget AM, Ingar K, Torger SB (2016) Local structure of Ca²⁺ induced hydrogels of alginate–oligoguluronate blends determined by small-angle-X-ray scattering. *Carbohydr Polym*. <https://doi.org/10.1016/j.carbpol.2016.07.020>
- Zhou C, Wu Q (2011) A novel polyacrylamide nanocomposite hydrogel reinforced with natural chitosan nanofibers. *Coll Surf B Biointer* 84:155–162
- Zhou Y, Gao HL, Shen LL, Pan Z, Mao LB, Wu T, He JC, Zou DH, Zhang ZY, Yu SH (2016) Chitosan microspheres with an extracellular matrix-mimicking nanofibrous structure as cell carrier building blocks for bottom-up cartilage tissue engineering. *Nanoscale* 8:309–317

Chapter 7

Design of Multifunctional Nanogels with Intelligent Behavior



G. Rimondino, C. Biglione, M. Martinelli, C. Alvarez Igarzábal and M. Strumia

Abstract The design of polymeric nanogels with novel properties (dimensional structure, mechanics, high water content, and biocompatibility) continues to attract the attention of both scientific researchers and biomedical industries seeking new materials for application in areas such as tissue engineering, cell immobilization, separation of biomolecules or cells, biomedical implants, for use as diagnostic agents and in theranostics. The impressive progress in material and pharmaceutical sciences has given rise to the design of a broad range of nanogels of diverse size, architecture, and surface properties. The nanoscopic scale of these nanocarriers permits systemic (intravenous) or local (mucosal) administration and facilitates their diffusion within the cell. Moreover, surface functionalization methodologies can impart to the nanocarriers the ability to control pharmacokinetic and bio-distribution. Interest in intelligent nanogels has grown in recent years owing to their capacity to regulate behavior in response to external physical, chemical and biological stimuli. The different methods of nanogel synthesis and the adequate structure/property ratio for intelligent behavior and novel applications will be described and discussed in this chapter, presenting the most significant progress achieved in recent years in the field of nanocarriers in biomedical applications.

Keywords Multifunctional nanogels · Intelligent nanogels · Polymeric nanogels Structure/property ratio

G. Rimondino · C. Biglione · M. Martinelli · C. Alvarez Igarzábal · M. Strumia (✉)
Departamento de Química Orgánica, Facultad de Ciencias Químicas, Instituto de Investigación y Desarrollo En Ingeniería de Procesos y Química Aplicada (IPQA), CONICET, Universidad Nacional de Córdoba. Ciudad Universitaria, X5000HUA Córdoba, Argentina

© Springer Nature Singapore Pte Ltd. 2018
V. K. Thakur and M. K. Thakur (eds.), *Polymer Gels*, Gels Horizons: From Science to Smart Materials, https://doi.org/10.1007/978-981-10-6086-1_7

1 Introduction

A gel is a soft three-dimensional network of flexible polymer chains. The gel is formed by elements connected in the form of a tangled network in a determined manner, and swollen by a liquid. The organogel contains an organic solvent and the hydrogel contains water, both types forming swollen spatial polymeric networks. When the solvent is a water–organic mixture, different intermediate variants are possible. Gels combine the properties of solids and fluids and their properties depend on the interaction between these two components. The presence of liquid in the structure prevents the network from collapsing into an insoluble compact mass and the solid prevents the liquid from flowing freely. Gels vary in consistency from viscous fluids to almost rigid solids. They can be classified into two main types, depending on the connections of the three-dimensional network of which they are composed. In both types, the macromolecular chains connect to form a 3D network. Gels commonly classified as covalent are those with chemical crosslinking and non-covalent gels are those with physical crosslinking. It is important to note that the bulk morphology (homophase or heterophase) of the gel depends both on the chemical structure of the constituent polymers and the method of preparation.

In general, gels have a high number of hydrophilic groups or domains and thus high affinity for water. This feature confers on them the same property of being able to transport liquids, especially in the case of molecules significantly smaller than the gel pore size.

Particular interest has been focused on nanogels (NGs), which are nanosized polymeric networks (50–200 nm) formed by physical or chemical crosslinking. These products represent unique structures with a well-defined 3D architecture and tunable properties, positioning them as platforms with huge application potential in several fields, particularly in nanomedicine. Nanogels have similar characteristics to macroscopic gels, but all contained within a smaller size, facilitating particle penetration at the cellular level. In general, the most attractive features of NGs can be described in terms of their high biocompatibility, biodegradability, soft nature, design versatility, particle size suitable for permeation, swelling capacity in aqueous medium in a short time, good dispersibility, and colloidal stability in aqueous medium, rapid response to external stimuli, non-immune response, possibility of prolonged circulation times in the bloodstream, and high drug loading capacity and subsequent release. The drug-load capacity is strongly dependent on the presence of functional groups to chemically attach a drug or a targeting agent by bio-conjugation or in other cases to form a hydrogen bridge or van der Waals interactions (Sivaram et al. 2015). These properties are significantly influenced by temperature, the presence of hydrophilic/hydrophobic groups in the network, crosslinking density, and the type of crosslinking bonds present in the polymer networks.

As will be seen in the methodology section, one useful technique for preparing NGs involves surfactants; however, this calls for a subsequent purification step and furthermore can lead to non-reacted and/or undesired side-products being formed in

the process. As the presence of surfactants or monomers can obviously impart toxicity, and due to the high cost of the purification step, this feature can be considered as the main disadvantage of NGs.

There are various types of NGs but new trends in polymer science have led to the development of nanomaterials with specific features: sensitive or responsive nanogels, which respond to physical, chemical, or biological stimuli of the environment, and hybrid nanogels, which synergistically combine the characteristics of a hydrogel system with a nano-structured inorganic particle.

1.1 *Intelligent Materials*

Intelligent materials are those that can respond predictably to certain external stimuli by modifying some of their properties. These materials differ from intelligent “devices” in that they do not require complex sensor systems, sampling and calculations to provide feedback and respond to the stimulus (Hu et al. 2012): the response of smart materials is inherent to their nature.

The preparation of synthetic intelligent materials able to respond to stimuli in a controllable and predictable manner is an important objective at both the scientific and technological levels. Nature provides several examples of biological systems that can assist researchers in designing new materials, among which are: the rotation of sunflowers towards the sun for a phototropic effect; the change in skin color of chameleons by rearrangement of the crystals within the specialized skin cells; and the case of the *Mimosa pudica* plant collapsing rapidly when touched or the *Dionaea muscipula*, which traps insects upon closing (Teyssier et al. 2015). There are a variety of polymers comparable to the materials involved in these systems which respond to stimuli such as temperature, pH, ionic strength, light, electric field, magnetic field, among others by undergoing physical or chemical change. The materials can also be designed to respond to more than one stimulus at a time, making multiple responses possible (Ayano et al. 2012; Thomas et al. 2012; Nash et al. 2012; Li et al. 2014). These stimuli can cause changes in dimension and/or in form, as well as in some mechanical properties such as stiffness, flexibility, opacity, porosity, among others. Depending on the final form in which these materials are obtained—as gels, nanoparticles, films, etc.—intelligent materials have potential applications in modern technologies for controlled drug delivery, tissue engineering, cell immobilization, separation of biomolecules, theranostics, diagnostic agents, packaging, biosensors, optoelectronics, and others.

To yield an intelligent polymeric material, it is very important to achieve high efficiency in the reversible response of the used polymers and thus be able to transfer the material to a particular application. The criteria for choosing the monomers in terms of the degree of crosslinking, the functional groups present in the structure and the final physical shape required of the polymeric material, are crucial. The desired properties can also be achieved through a combination of more than one polymer or other material, inorganic or organic, conforming hybrid

materials. New or improved materials with particularly versatile or handy properties have an even more promising future as platforms for multiple applications. More recently developed synthetic methodologies using simple procedures are capable of achieving well-defined polymers with predictable structural organization.

A special class of smart material is the hydrogel, in which the presence of specific functional groups and hydrophobic/hydrophilic domain-handling can confer substantial changes on the properties of these materials, giving them the ability to react to specific stimuli (pH, temperature, light, ionic strength and electric or magnetic pulses, among others). Immediate changes in their swelling or in their mechanical properties can lead to some interesting applications such as modulating the ability to contain or release a specific drug and subsequently biodegrade, converting them into ideal materials to be used as controlled release matrices. Interest in the design and development of macroscopic intelligent materials at the nanoscale has intensified over the last few years.

In the field of biomedicine in particular, nanomaterials that are biocompatible and responsive to external stimuli have become the new generation of smart materials. In general, as in the case of macroscopic materials, the principle behind stimulus-responsive nanomaterials resides in the fact that different external environmental factors trigger a cascade of changes in the structure of the material with consequent changes in their properties (Wu et al. 2010a). In the case of NGs, they can be designed to swell or dissolve, and release a therapeutic agent in response to changes in the surrounding medium. The possibility of tailored structure/surface adjustment and the ability to incorporate drugs in their cavities opens up opportunities for use as nano-transporters of drugs at the cellular level (Kabanov and Vinogradov 2009; Chacko et al. 2012). The advantage of using NGs with an encapsulated drug means that the drug can then be released at a specified site, thus protecting those drugs with low stability in the bloodstream. Furthermore, NGs may contain functional groups (acids, amines, alcohol) to chemically bond a drug whose junction can then be hydrolyzed (enzymatically, labile bonds at pH), releasing it at the desired site of action. Some drugs can be attached to NGs, remaining stable at a given pH chemical bond, and then be hydrolyzed with a change. NGs can also be prepared in a specific manner such that once they reach the site and respond to a stimulus the drug can diffuse out and be released by changes in stimuli mentioned above (Morimoto et al. 2013; Chen et al. 2013).

The development of NGs meeting these requirements is an interesting challenge (Yallapu et al. 2011; Oh et al. 2008; Wu et al. 2010b; Fleige et al. 2012; Chacko et al. 2012). In sensitive NGs, the transitions occur even when changes in external variations are small. Their size can be reduced and collapsed into a compact form, expanded in the order of seconds, or they can expel water absorbed in response to external stimuli (Zhan et al. 2011; Mura et al. 2013; Yallapu et al. 2011; Fleige et al. 2012; Kabanov and Vinogradov 2009; Sivaram et al. 2015). In general the swelling can be controlled both by NG structure (monomer or polymer chemical structure, degree of crosslinking, charge density, among others) and by environmental parameters.

As NGs are reticular crosslinked particles, their links drastically reduce the mobility of the chains and their conformational entropy. However, crosslinking allows the preparation of NGs with a more complex architecture, leading to the introduction of functional groups at different positions within, which may affect the overall degree of swelling. It is known that a balance between the osmotic pressure and elasticity of the polymer determines the physical dimensions of an NG particle. Osmotic pressure results from the net difference between the concentration of mobile ions inside the nanogel particle and the solution outside. In the case of ionic NGs, the charged groups attract hydrated counterions that tend to expand the nanogel, while conformational entropy elasticity of the crosslinked polymer chains counteracts this expansion. The neutralization of the nanogel reduces the difference in the net concentration of the ions, resulting in the dehydration of the nanogel and a diminution of its volume (Rayo and Guerrero 2014).

As stimuli-responsive nanostructures based on polymeric compositions, smart NGs are one of the most interesting nanomaterials. Thermo-sensitive NGs, in particular, have shown great potential in biomedical areas. Two types of swelling transitions are observed; the transition from upper solution critical temperature (UCST) (generally for acrylic acid derivatives) and lower critical solution temperature (LCST) (for *N*-acrylamide derivatives). LCST-type nanogels swell abruptly at temperatures below a critical point whereas UCST-type nanogels swell sharply at temperatures above a critical point. Since NGs do not dissolve, the temperature at which the nanogel passes from a swollen to a collapsed state is called volume phase transition temperature (VPTT) (Rayo and Guerrero 2014; Cuggino et al. 2011; Witting et al. 2015; Quesada-Perez et al. 2014).

The structure–property relationship of polymeric systems provides the basis for the development of intelligent stimuli-responsive NGs. Success in obtaining a smart NG requires synthetic design criteria that combine the right choice of functional groups present in the nanostructure, flexibility and the final shape of the chains in the structure to be used.

This Chapter covers various topics: in the first part, the different methodologies for synthesizing nanogels are detailed. Following this, the second part comments on prominent work relating to the structure/properties ratio required for intelligent behavior and novel application properties. In the third part, desirable characteristics for smart and hybrid NGs are described. Finally, the last part describes the importance of size for different applications and reports on the most significant progress achieved in recent years in the field of nanocarriers for biomedical applications.

2 Synthesis Methodologies

There are two major approaches for creating nanometer-scale particles: the top-down approach (lithography) and the bottom-up approach, in which the nanometer scale is controlled by designing molecular structures and assemblies.

This latter methodology is the most widespread in nanotechnology and the formation of polymeric NGs is an example. The synthesis of NGs, like classical polymers, can be carried out through polymerization of functionalized monomers or from preformed polymers. Natural (Wang et al. 2014) or synthetic (Chem et al. 2012) polymers may be employed, depending on the application. Precursor polymers, such as amphiphilic copolymers, can form nanogels by self-assembly in solution, physical crosslinking or by chemical crosslinking, depending on the reactive sites. Synthesis via monomer polymerization is more efficient and the yielded crosslinked NGs show great promise as drug delivery vehicles (Zhang et al. 2015). Generally, NGs in the size range of 20–200 nm are useful for the treatment of a variety of diseases.

Depending on the structure and functionality of monomers, radical, cationic and anionic polymerizations are synthetic alternatives. Due to the difficulty in controlling the molecular architecture through these mechanisms, new synthetic routes were opened up by the use of controlled radical polymerization (CRP). In recent years, CRP techniques such as radical polymerization atom transfer (ATRP) (Huang et al. 2007; Zampano et al. 2009; Wang et al. 2011), nitroxide mediated polymerization (NMP) (Gromadzki et al. 2010) and transfer polymerization reversible addition-fragmentation chain (RAFT) (Roy et al. 2005) have been used. Both ATRP and RAFT are based on the dynamic equilibrium between active and disabled species. CRP techniques are a good way of yielding NGs with controlled molecular weight and low polydispersity (Jafari and Kaffashi 2016). RAFT in water has emerged as a simple method of preparing well-defined NGs with core-shell structures (Liu et al. 2012). Other methodologies including ring opening, coupling reactions, and click chemistry are also used to synthesize NGs from functional monomers. A series of pH-responsive disulfide crosslinked NGs based on poly(L-histidine) has been synthesized by a one-step ring-opening polymerization process (Bilalis et al. 2016). The progress in copper-free click chemistry such as that involved in strain-promoted azide-alkyne cycloaddition, radical mediated thiolene chemistry, Diels-Alder reaction, tetrazole-alkene photo-click chemistry, and oxime reaction has enabled the formation of NGs without the use of potentially toxic catalysts (for example copper catalyst) or immunogenic enzymes that are commonly used in both chemical and physical crosslinking, as in the crosslinking of casein with microbial transglutaminase (Jiang et al. 2014). The combination of controlled polymerization techniques with efficient chemical reactions is fundamental in the synthesis of NGs. By combining the ATRP method and click chemistry it was possible to synthesize well-defined crosslinked poly(styrene) nanoparticles with diameter in the range of 50–150 nm (Xu et al. 2009).

Crosslinks are essential for the structural stability of the NGs since they prevent dissolution of the polymer chains in the aqueous environment. The physical crosslinkings can be promoted by hydrophobic and electrostatic interactions, chain entanglements, Van der Waals forces or hydrogen bond between the polymer chains of the nanogel. NGs formed by physical crosslinking in aqueous media and mild conditions can easily collapse as a result of changes in their environment. Environmental parameters such as pH value, ionic strength, temperature, and

others, that affect particle size, must be controlled. Atiyoshi et al. reported the first physically crosslinked NGs using self-assembly of polysaccharides. The system was colloidally stable with monodisperse nanoparticles above the critical concentration (Akiyoshi et al. 1993). Chemical crosslinking involves the formation of covalent bonds rendering stable, rigid structures; the bonds are formed during polymerization, employing a bifunctional crosslinking agent, or after polymerization with reactive groups present in the monomers. The reactions generally require purification steps to remove residual monomers and/or crosslinking agents. It is therefore convenient to design efficient reactions between functional groups to avoid the use of crosslinking agents. Michael additions of amines and thiols or condensation reactions between acids and amines or alcohols are examples of such reactions (Rahimian et al. 2015). Many precursors used for addition or coupling reactions are biologically inert and this is important when NGs are to be used in biomedicine. In particular, the formation of a disulfide bond between polymer chains using suitably functionalized monomers avoids the use of additional crosslinking agents (Gyarmati et al. 2013). Moreover, a disulfide bond is biodegradable to biochemical reductants and the nanogel is stimuli-responsive to specific analytes (Heffernan and Murthy 2009). The first chemically crosslinked NGs were prepared by crosslinking polyethyleneimine with carbonyldiimidazole-activated poly(ethylene glycol) (PEG) for the delivery of oligonucleotides. The synthesis was reported by Kabanov and col. (Vinogradov et al. 1999). The developed NGs showed effective diameters ranging from 20 to 220 nm and were stable in solution, revealing no aggregation. The NGs showed enhanced drug loading capacity and improved drug release behavior compared to common nanoparticles.

In order to avoid the use of crosslinkers in chemical crosslinking, an alternative approach is to use ionizing radiation (gamma rays, X-rays, accelerated electrons, ion beams, or ultraviolet rays), which is useful for the synthesis of NGs from linear polymers in aqueous medium. This method avoids the use of monomers, crosslinking agents, initiators and surfactants. The water molecules absorb most of the radiation, generating reactive species (hydroxyl protons, solvated electrons, hydrogen peroxide) which react with the polymer chains, producing radicals. The effect of irradiation on the polymer depends on its chemical structure, concentration, molecular weight and the irradiation conditions (Jafari and Kaffashi 2016; Dailing et al. 2015). The crosslinking may be intra- or intermolecular, depending on the average number of radicals per chain. By increasing irradiation, the average number of radicals per chain also increases and the probability of intramolecular recombination is greater.

The degree of crosslinking determines the swelling degree of NGs, which is one of their most important properties.

3 Synthesis Techniques

Various polymerization techniques have been used to prepare NGs by direct polymerization of monomers (emulsion or inverse emulsion) or polymerization-induced phase separation. Regardless of the method of preparation of the NGs, colloidal stability is of great importance in the synthetic process and rigorous control over the size of nanocolloids is essential for different biomedical applications. Figure 1 shows different preparation methods of NGs.

The radical polymerization of hydrophilic monomers in inverse emulsion and polymerization-induced phase separation represent the most widely used methods to convert monomers directly into NGs. The progress in controlled polymerization techniques has significantly propelled the development of phase separation methods, the most well-known example of the latter being precipitation polymerization.

Precipitation polymerization is performed in cases where the monomers and polymers are soluble and insoluble, respectively, in a specific solvent. It is a useful methodology for the preparation of thermo-responsive NGs such as poly(*N*-isopropylacrylamide) (pNIPAm) NGs.

At the temperature of the reaction the polymer chains reach a critical length and collapse upon themselves, producing precursors of particles. The chains collapse because the polymerization temperature is higher than the VPPT or phase transition temperature of the nanogel. All components, (monomers, initiator and crosslinking

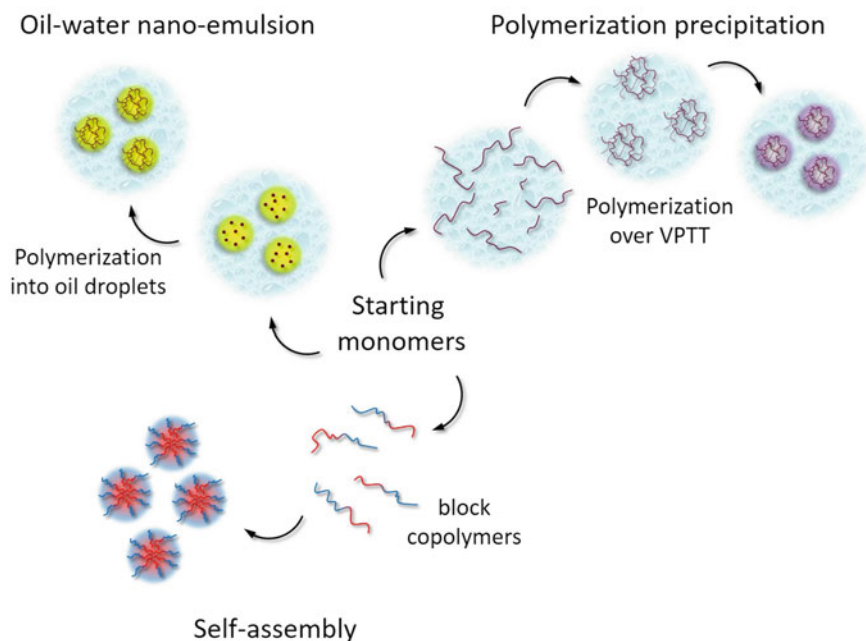


Fig. 1 Synthetic routes for the preparation of NGs

agent) are dissolved in water, including a surfactant in some cases (Chem et al. 2012).

As the reaction proceeds, a precursor of particles can be added to form a colloidally stable system. In addition, when the chains reach a critical size, the charge incorporated from a radical initiator gives rise to an electrostatic stabilization mechanism. The temperature is subsequently lowered to below the transition temperature and the swollen nanogel particles are stabilized by a steric mechanism as a consequence of the formation of a hydrogen bond between the polymer chains and water molecules. An ionic surfactant can be added to impart colloidal stability during the polymerization reaction. The diameter of the particles depends on the concentration of surfactant, so small particles can be obtained by increasing the surfactant concentration (McPhee et al. 1993).

Miniemulsion and inverse miniemulsion polymerization require the surfactants to be oil dispersed in water and water in oil emulsions, respectively. Miniemulsion polymerization is conducted using surfactants such as sodium dodecyl sulfate (SDS) or sodium dodecylbenzene sulfonate (SDBS), which is dissolved in water. The hydrophobic monomers and crosslinkers are added to the aqueous solution and polymerized in oil dispersed in excess water. After polymerization, the surfactant is removed by dialysis. Controlled polymerization methods have been used in miniemulsions to prepare NGs.

The inverse nanoemulsion (water/oil) system has been used to prepare NGs by direct polymerization of hydrophilic monomers such as electrolyte monomers and PEG-containing monomers. In this methodology, the hydrophilic monomers and the crosslinker agent are dissolved in water droplets emulsified into a continuous hydrophobic phase. The aqueous droplets in the presence of oil-soluble surfactants [sorbitan monooleate, Span—80 or sodium bis(2-ethylhexyl)sulfosuccinate, AOT] are generated by sonication in an organic solvent as the continuous phase. The thermodynamically stable emulsion is reached at a surfactant concentration below or near its critical micelle concentration. Cationic [(3-acrylamidopropyl) trimethylammonium chloride], (Sahiner et al. 2006) anionic (2-acrylamido-2-methylpropane sulfonic acid) (Bhardwaj et al. 2009) and neutral monomers (*N*-vinylformamide) were polymerized via inverse miniemulsion (Shi et al. 2008).

Hydrophilic drugs including anticancer drugs (e.g., doxorubicin, DOX) and biomacromolecules (e.g., DNA and proteins) can be incorporated into NGs using inverse emulsion. Several NGs coated in PEG chains have been synthesized by emulsion (Iijima and Nagasaki 2006).

An alternative is an oil-in-water emulsion achieved by stirring (suspension polymerization), useful for hydrophobic monomers which do not require the surfactant to be removed after polymerization.

Nanoemulsion synthesis can be applied to different mechanisms of controlled radical polymerization such as RAFT and atomic transfer radical polymerization (ATRP) (Raemdonck et al. 2009; Kuo et al. 2015).

Several examples have been reported for the synthesis of NGs from gelatin using this methodology. Crosslinked NGs from gum arabic aldehyde and gelatin nanoparticles were prepared by the inverse miniemulsion process. The nanosize and

spherical particles were nontoxic and showed high potential for application in drug and gene delivery (Sarika and James 2015).

For biomedical applications, the synthesis and purification of the delivery system should be easy and scalable. Several polymerization conditions in emulsion require the use of surfactants, which as mentioned, need to be removed after synthesis (Chacko et al. 2012). Surfactants always favor the stabilization of nanogel particles and minimize the aggregation process; they also lower interfacial tension and reduce the size of nanogels. Park et al. reported an emulsion-free surfactant of heparin NGs (Bae et al. 2008). This green alternative was used by An et al. in the synthesis of a dual-responsive NG. Hydroxypropylcellulose (HPC) NGs were synthesized using HPC as a template in surfactant-free aqueous media. The concentration of the crosslinker determined the size of the NGs, which show promise for use as nano-biomaterials (An et al. 2015).

Others technologies have emerged for the preparation of NGs with well-defined molecular architectures (Liu and An 2014), for instance liposomes (Hong et al. 2008) and inorganic nanoparticles (Singh et al. 2007) as nanosized reactors. Also, hollow NGs can be prepared using nanoparticles as template. For example, gold and monodisperse silica nanoparticles were used as a nanotemplate to grow a polymer shell, after which the template was removed to yield a hollow nanogel. These NGs possess the ability to function as nanocapsules (Liu et al. 2015).

4 Characterization Methods

NG properties can be conveniently studied by methods developed for macromolecules in solution. The most important characterization techniques are: light scattering, gel permeation chromatography, viscosimetry, calorimetry, microscopy, and spectroscopy.

Light scattering measures provide information on the structure and molecular dynamics of the particles. Static light scattering determines the average molecular weight. The measurement range of the particle size is 10 nm–3.5 μ m and the radius of gyration can be obtained. Dynamic Light Scattering (DLS) indicates the distribution of the hydrodynamic diameters in a range of particle size from 1 nm to 6 μ m and can also be used to study the real-time kinetic of NG formation. Similarly, viscosity measurements are often used to follow relative changes in the hydrodynamic dimensions of the NGs in terms of their average molecular weight, structure and size. The relationship between the average radius of gyration and the hydrodynamic diameter is a particularly valuable indicator of the nanogel structure. Surface loading effects, such as electrophoretic mobility, can be investigated by measuring the zeta potential.

The structural differences in NGs of the same chemical composition but synthesized by different methods can be determined by small-angle neutron scattering measurements, which are complementary to light scattering.

Melting temperatures and crystallization, particularly phase transition temperatures (VPTT) of NGs, changes in enthalpy and entropy, and the glass transition temperature can be determined by Differential Scanning Calorimetry (DSC). Furthermore, the presence of associated and non-associated water in the NGs is useful for determining the swelling degree. Different techniques such as Scanning Electron Microscopy (SEM), Transmission Electron Microscopy (TEM) and Atomic Force Microscopy (AFM) can be used to study the topology of the NG surface at different scales, measuring the forces between the particles and determining the elastic properties of micro- and nanoparticles. SEM produces high-resolution images (3–4 nm) of the nanogel surface; TEM provides images with a resolution of 0.2 nm, so individual particles of NGs and/or monolayers can be observed; AFM shows higher resolution images (lower than 1 nm) and provides information about nanogel structure at the atomic and molecular level.

Finally, the chemical composition of NGs can be determined by UV-Visible and Infrared (IR) Spectroscopy. Electron spin resonance (ESR) and nuclear magnetic resonance (NMR) spectroscopies provide information on the structure and dynamics of the NG environment. Integrating different techniques enables one not only to characterize the final material, but also to manage the variables of the reaction with a view to designing a tailor-made material. The results obtained from each methodology permit an evaluation of the effect of each variable on the size and morphology of the synthesized product. The NGs of HPC synthesized in a solvent-free medium were characterized using the DLS, IR, AFM, and TEM techniques. The results led to determination of the interdependence between size temperature and concentration of the crosslinker, and the effect of the HPC concentration on the reaction mixture (An et al. 2015).

5 Intelligent Nanogels

As explained in the introductory section of this Chapter, smart NGs can undergo a reversible phase transition in response to external or internal stimuli. Several recently published and reviewed papers have reported nanosystems responding to

Table 1 Environmental stimuli

Physical	Chemical	Biomedical
Temperature	pH	Enzymes
Light	Specific ions	Ligands
Electric field	Chemical agents	Biochemical agents
Magnetic field		
Ionic Strength		
Solvents		
Sonic radiation		
Mechanical stress		

changes in different environmental conditions (Maya et al. 2013; Giubudagian et al. 2014; Sierra-Martin and Fernandez-Barbero 2015), classifying the stimulus into the three main groups as presented in Table 1 (Hoffman et al. 2000).

As with macrogels, major changes or transitions are observed in the phase volume, optical density, surface charge or hydrophilic/hydrophobic balance of NGs. Due to their unique properties, smart NGs have been widely tested mainly in the biomedical field. As mentioned, they are used as drug carriers and/or delivery systems, for diagnosis and gene therapy, among other applications (Molina et al. 2015).

The key to the successful design of a smart nanogel with implications for further applications is the use of different chemical building blocks or monomer compositions to confer the appropriate functionality and triggered response capability.

Among the fascinating, multiple materials that have been developed recently, thermo- and/or pH-sensitive NGs are the most widely used and have spread into nanoscale polymer science. Their reproducibility, facility of synthetic process and use of classic and commercially available monomers, are the major advantages compared with other systems. The following section focuses on NGs based on a single stimulus response, with temperature and pH taken as representative examples; basic and high-precision concepts are explained and a brief presentation is provided of redox-sensitive materials with a view to exploring promising new materials for application in biomedicine.

5.1 *Thermo-Responsive Nanogels*

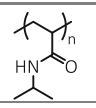
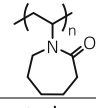
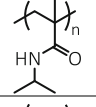
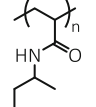
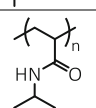
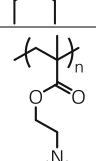
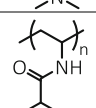
Of special interest are nanoparticles prepared from polymers having a lower critical temperature or VPTT in water, giving rise to a reversible collapsing process triggered by a shape-temperature change in the surrounding medium.

For this particular class of polymer networks, the enthalpy term, mostly caused by the hydrogen-type bonding between polar groups of polymer and solvent, water in this case, dominates at temperatures below VPTT, leading to the swelling of the system. Above VPTT, the entropic term arises due to the hydrophobic polymer-polymer interactions, resulting in a shrinking nanogel, and the consequent solvent expulsion of the network (Jeong et al. 2002; Schild 1992; Nayak and Andrew Lyon 2005).

N-Substituted acrylamides are very attractive monomers owing to their ability to generate polymer networks with lower critical temperatures. Table 2 summarizes some homopolymer structures and experimentally determined VPTT (Müllen and Ober 2013).

One of the first reports of thermo-responsive NGs was the pioneer work published by Pelton and Chibante in 1986, which described the principles of the thermo precipitation-polymerization technique, using NIPAm and *N,N'*-methylene bisacrylamide (BIS) as model monomer and crosslinker, respectively, for the preparation of aqueous lattices with different VPTT (Pelton and Chibante 1986).

Table 2 VPTT of N-substituted acrylamide based polymers

Polymer	Structure	VPTT (°C)
Poly(<i>N</i> -isopropylacrylamide) (pNiPAm)		32–34
Poly(vinylcaprolactam) (pVCL)		32–40
Poly(<i>N</i> -isopropylmethacrylamide)		38–42
Poly(<i>N</i> -ethyl- <i>N</i> -methylacrylamide)		56
Poly(<i>N,N</i> -diethylacrylamide)		32
Poly(<i>N,N</i> -dimethyl aminoethyl methacrylate)		50
Poly(vinylisobutyroamide)		35

Since then, numerous articles have focused on the synthesis and characterization of smart nanoparticles based on thermo-sensitive polymers.

NiPAm and vinyl caprolactame (VCL) monomers and their base polymers are probably the most widely used since their VPTT is close to the physiological one. As seen before, both monomers are excellent candidates for nanogel formation via the polymerization-precipitation method. Surfactant-free polymerization or the use of ionic surfactant was previously reported, showing a high degree of ruggedness of both monomers to form thermo-responsive nanogels under different conditions. Figure 2 shows a schematic representation of pNiPAm and pVCL nanogels and the reversible phase transition equilibrium.

As regards synthetic procedures, NiPAm is a very robust monomer, while VCL can undergo a hydrolysis process as a competitive reaction during polymerization in acid media. Ramos and coworkers reported the hydrolysis of the polymerizable vinyl group of VCL, leading to caprolactam and acetaldehyde as products.

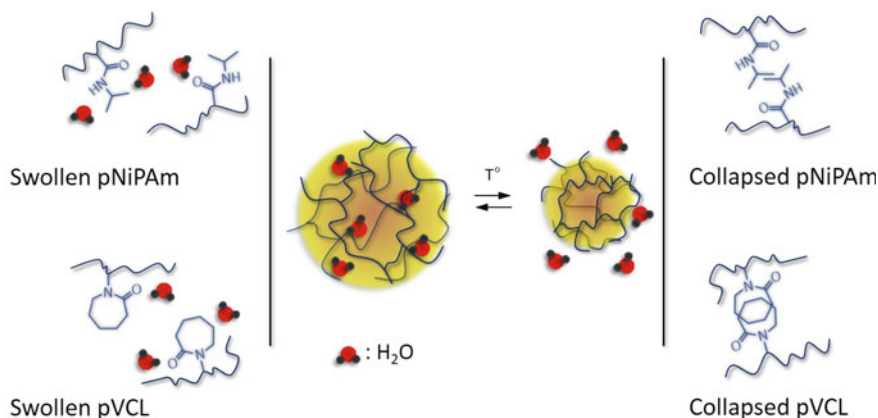


Fig. 2 Schematic representation of polymer–solvent and polymer–polymer interaction of pNiPAm and pVCL

Nevertheless, the problem can be solved by carrying out the polymerization in buffered medium to avoid the pH decrease (Ramos et al. 2012).

Although both pVCL and pNiPAm are widely used in the biomedical field, the latter's biocompatibility gives it an advantage over pVCL (Vihola et al. 2005; Lau and Wu 1999).

As with macrogels, VPTT of NiPAm or VCL-based NGs can be tuned by copolymerization with other monomers or different crosslinkers. Examples of this include utilization of hydrophilic monomers such as acrylic acid (AAc) and 2-hydroxy ethylmethacrylate (HEMA), to shift the transition point to higher values (Rzaev et al. 2007; Lee et al. 2008; Wang et al. 2013; Cortez-Lemus and Licea-Claverie 2015). There are several examples of this kind of NGs as drug delivery agents (Madhusudana Rao et al. 2013; Wang et al. 2013).

Owing to the thermo-sensitivity of this particular class of nanomaterials, different stimuli can generate the phase transition in the site of interest. Light hyperthermia in diseased cells is the most important internal stimulus. Localized warm sites can be irradiated by laser, near infrared probes, or by a combination of alternating magnetic fields and magnetic nanoparticles (Zhang et al. 2014; Chiang et al. 2013).

Over the last few years, polymers based on oligo (ethylene glycol) acrylates or methacrylates (OEGa and OEGm, respectively) have been employed as starting materials for the synthesis of thermo-responsive systems. Although these polymers do not show the N-substituted acrylamide presented in Table 2, the presence of repetitive hydrophobic units of ethylene and hydrophilic oxygen-based functions leads to a hydrophilic/hydrophobic equilibrium in the monomer backbone. As a result of the high variety of OEG-based monomers and their combination in copolymeric formulations, a huge range of VPTT, from 5 to 95 °C, were reported (Vancoillie et al. 2014).

Oligo(ethylene oxide) monomethyl ether methacrylate is extensively used in nanogel preparations via inverse miniemulsion. The principal advantage of this system is the nontoxicity and biodegradability of the easily tunable NGs (Hu et al. 2010).

5.2 pH-Responsive Nanogels

The other important group of smart NGs besides thermo-responsive NGs are pH-sensitive polymer-based nanomaterials. This class of materials is formed by synthetic or natural polymer networks containing ionizable pendant groups, capable of donating or accepting protons from the surrounding medium. The equilibrium between the protonated and deprotonated state is achieved at pKa value. When the pH of the environment reaches the pKa value, the degree of ionization of the polymer backbone changes dramatically, triggering the presence of an absolute charge at the nanogel structure. A non-charged nanogel shows a collapsed conformation owing to the polymer–polymer predominant interactions, whereas when the polymer is charged, it adopts an expanded or swelling state as a result of electrostatic repulsion between chains and the consequent entry of solvent.

Two different types of pH-dependent monomers can be used to generate this kind of smart NGs. Monomers containing acid functionalities, mainly carboxylic acids or sulfonates, can transfer their acid proton when the pH of the surrounding medium rises up to pKa, leaving a negative charge value. In this case, AAc and methacrylic acid (pKa: 4.2 and 4.6, respectively) are the most frequently used monomers for preparing pH-responsive NGs (Cuggino et al. 2016; Abu Samah and Heard 2013; Peng et al. 2013; Oh et al. 2009). Alternatively, amine-based monomers or polymers are employed to give polymeric structures that arrest protons from the medium, giving a net positive charge on the nanogel when the pH is lower than pKa (Salehi et al. 2015; Fleige et al. 2012).

In this kind of NGs, different physiological pH values can trigger the reversible phase transition. In the human body, two different behaviors give rise to a similar result: changes in normal tissues or changes in sick tissues. Inside healthy cells, the physiological pH gradient ranges from a neutral value close to 7.4 at the cytosol to a relatively acidic condition inside lysosomal compartments with pH values of 4.5–5.0, or a basic condition at the mitochondria, in which pH values rises to 8.0 (Asokan and Cho 2002). The pH values presented by pathologic tissues such as in cases of cancer, infection or inflammation, are significantly different. The cytosolic pH of a cell undergoing an inflammatory reaction drops to 6.5 compared to the cytosolic pH of normal tissues. Thus, the high glycolytic activity in tumor cells produces a slight diminution in the pH of damaged tissue (Gerweck and Seetharaman 1996; Ganta et al. 2008).

The rational design of smart NGs leads to materials that can undergo a phase transition during the endocytosis process or a response at a particular intracellular

site, providing a promising platform for drug-carrier and stimuli-mediated delivery systems.

Although they are still not widely used, the design of redox-sensitive NGs presents one of the most appealing challenges. As mentioned before, diseased tissues as in cancer cells present slight alterations in redox potential, pH values or temperature (Cheng et al. 2013; Asokan and Cho 2002). The focus on redox-sensitive materials, monomers or crosslinkers containing disulfide functions would thus appear to be the simplest and most effective way of achieving the desired objective since they can be rapidly reduced to thiols under the mild reductive environment inside cells (Meng et al. 2009; Saito et al. 2003).

Several examples of the synthesis of NGs containing a disulfide bond have been reported over the last few years. 3,3'-dithiodipropionic acid or similar diacids, and cystamine bis acrylamide, among other divinyllic crosslinkers, are most widely used for the synthesis of redox-sensitive NGs; the synthesis of block copolymers containing a disulfide linkage is also common. Reduction of disulfides leads to the cleavage of polymer crosslinkings with the subsequent degradation of NG matrices, thus under specific conditions triggering for example a drug delivery system.

As already stated, different strategies have been developed opening up greater opportunities for the design and use of smart polymeric nano-devices. In this section we have mentioned only single stimulus-responsive NGs, but scientific efforts are being focused on a wide span of multi stimuli-responsive materials. As will be seen in the next section, building different polymeric compositions is not the only way of achieving the sought-after goal: the use of inorganic materials constitutes a new stage in the design of NGs.

6 Hybrid Nanogels

Hybrid NGs are those where inorganic particles are incorporated into the polymer matrix. Montoro et al. classified hybrid NGs into three categories according to their morphology: (1) core-shell hydrogels with the inorganic nanoparticles placed in the core; (2) inorganic nanoparticles distributed in the hydrogel matrix; and (3) hydrogels covered with inorganic nanoparticles (Montoro et al. 2014). Different nanoparticles (NPs) such as magnetic nanoparticles (MNPs), gold nanoparticles (AuNPs), silicate nanoparticles, quantum dots (QDs), silver nanoparticles (AgNPs), etc., have been used in hybrid NG synthesis. Depending on the nature of the inorganic NP, different functionalities can be achieved. Figure 3 shows an example of a multifunctional hybrid nanogel (Online 2015).

There are two main ways of incorporating inorganic NPs into the polymer network, one physical the other covalent: they can be introduced physically into the NG matrix before or after gelation, so that they become trapped in the NG; or they can be covalently incorporated using NPs as crosslinkers or moieties having a covalent interaction between the matrix and NPs (Thoniyot et al. 2015).

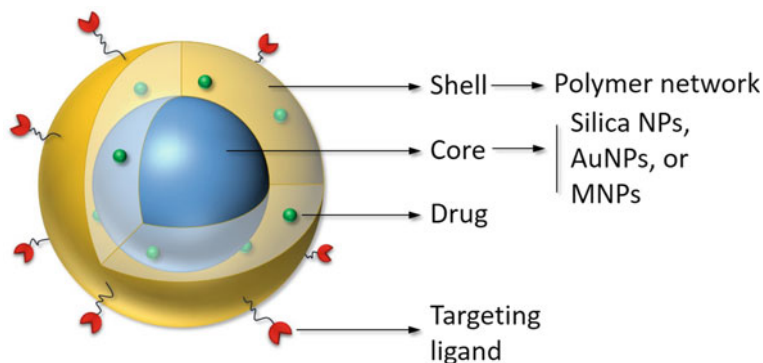


Fig. 3 Schematic representations of multifunctional hybrid nanogel

Owing to their unique potential in combining the characteristics of a hydrogel system with an inorganic nanoparticle, hybrid NGs have gained considerable attention in recent years as one of the most promising nano-sized drug delivery systems. The synergistic sum of different functions, all of interest in their own right, becomes even more appealing when integrated within a nano-sized object (Ryu et al. 2012; Liu et al. 2015). The incorporation of NPs into a matrix introduces an additional advantage: the type of nanoparticle incorporated regulates the kind of stimuli that can be used to release the drug under the desired conditions, enhancing the delivery in different parts of the body, allowing the transport of hydrophobic drugs or creating multi stimuli-responsive systems (Merino et al. 2015). The stimulus can be a magnetic field, near infrared irradiation, or others. Moreover, in some cases the incorporation of NPs such as mesoporous silica can enhance the loading of a drug.

Among all hybrid NGs, those having inorganic nanoparticles such as magnetic NPs (MNPs), gold nanoparticles (AuNPs) or silica NPs have gained all the attention of general researchers because of their potential use in optical sensing, diagnostic imaging and drug delivery. The following describes the most appealing characteristics of each hybrid.

6.1 *Magnetic Nanogels (MNGs)*

The most common magnetic nanoparticles (MNPs) used are iron oxide NPs (IONPs), magnetite (Fe_3O_4) and maghemite (Fe_2O_3), alone or with another metal such as manganese or zinc as dopant. Various MNPs have been synthesized using ZnS or CoPt, among others (Peng et al. 2015; Dürr et al. 2013). MNPs are an important class of biomaterials used for a variety of purposes such as imaging, cell labeling, drug delivery, gene delivery and hyperthermia (Choi et al. 2012). Treatment with MNPs produces intracellular heat stress in the temperature range of

41–46 °C, which leads to activation and/or initiation of intracellular and extracellular degradation (Verma et al. 2014). The ability of MNPs to generate heat under the influence of external high-frequency field (Alternating Magnetic Field, AMF) makes them a promising device for hyperthermia treatment (Karimi et al. 2016).

In addition, imaging is one of the most important tools in cancer diagnostics. MNPs can be used for Magnetic Resonance Imaging (MRI), the standard clinical test for determining the presence, location and size of a tumor. MNPs are ideal for localized therapy, such as chemotherapy, radiation, immunotherapy or hyperthermia, or a combination of these (Brazel 2009). For example, the combination of MNPs and a thermo-responsive network facilitates the optimal release of drugs, since the heat generated by MNPs under AMF increases the temperature of the nanogels above their VPTT, enhancing drug diffusion across the nanogel into the blood (Merino et al. 2015). Some of the polymers used for obtaining MNG are pNIPAm, thermo-responsive polyglycerol, oligoethylenglycol-based polymers, etc. (Chen et al. 2011; Asadian-birjand et al. 2016; Boularas et al. 2015).

6.2 AuNPs-Hybrid Nanogels

The potential use of AuNPs as a simultaneous imaging and therapeutic agent has been demonstrated by many researchers, mainly because they are bio-inert and can be easily modified with various biomolecules or chemical moieties (Choi et al. 2012). The shape of Au Nanorods generates several interesting characteristics such as unique optical absorption and photo-thermal properties (Ryu et al. 2012). Gold nanoparticles are able to absorb from visible to near infrared (NIR) which can be used to generate local heat for use in photo-thermal therapy (PTT). In the presence of an incident light at a specific wavelength, free electrons in the gold surface undergo collective coherent oscillations known as surface plasmon resonance (SPR) that can decay by heat emission (Online 2015).

The local heating produced by the nanoparticles after light stimulation causes tissue necrosis, together with controlled delivery of the entangled chemotherapeutic molecules (Merino et al. 2015). In addition to the direct effect of these particles on heat delivery to the site when illuminated using an NIR laser, the transduction of heat to thermo-responsive drug reservoirs, such as nanogels, allows a more efficient delivery (Yeh 2014). Furthermore, AuNPs can also generate secondary electrons under X-ray or gamma radiation, becoming ideal radiosensitizers that lead to DNA and protein breakdown.

Several AuNPs-hybrid NGs have been synthesized using different AuNPs, such as spherical NPs, nanorods, nanoshells, nanocages, and nanostars. Combining them with different polymer matrices, a number of smart NGs have been designed with responsiveness to one or more stimuli such as pH, temperature, and NIR among others (Vigderman and Zubarev 2013). The most common polymers used in this kind of NGs are polyacrylamide, poly(oligoethylenglycol), polyglycerol, poly(vinyl

alcohol), and pVCL, known for their stimuli-responsive behavior (Lu et al. 2013; Fuchs et al. 2015; Lutz 2011; Motornov et al. 2010).

6.3 *Silica NP-Hybrid Nanogels*

Silica NPs are robust, bio-inert and easy to control in terms of size and morphology. There are two main types of silica NPs—mesoporous silica NPs (MSNPs) and amorphous NPs. MSNPs have been at the center of attention of researchers for several reasons: they have finely controllable pores and considerable pore volume; they can incorporate or bind high concentrations of a wide variety of molecules; their diverse honeycomb-like architecture provides a large surface area and pore diameter (Choi et al. 2012); the nanoplatform can be fine-tuned during synthesis; their inner part can be modified in order to improve the interaction with the cargo loaded inside and also the surface with a polymer matrix (Baek et al. 2015).

Combining MSNPs with a stimuli-responsive polymer matrix can improve drug delivery by encapsulation of the active molecule not only in the polymer network but also in the NPs. Furthermore, delivery can be triggered by an external stimulus such as temperature or pH. The polymer used for the synthesis of silica NP-hybrid nanogels are polyglycerol, oligoethylenglycol-based polymers, poly(*N*-vinylcarprolactam) and others (Wu et al. 2015).

6.4 *Importance of NGs in Medicine*

The impact of polymers on medicine has been widely recognized for more than 40 years, during which time they have received acclaim not only for their use as biomedical materials but also for their application in pharmaceutical and biotechnology products. Their biodegradability, yielding optimal materials for resorbable sutures, orthopaedic implants and macro or microscale drug delivery systems; their versatility and adaptability to different forms; and their targeting capacity and tailored mechanical properties all make them valuable materials for applications in different areas of medicine, particularly in controlled release therapy and as diagnostic agents. (Molina et al. 2015; Calderón et al. 2010).

The application of nanotechnology to the development of safer and more effective medicines, giving rise to nanomedicine, has signified an enormous challenge for the pharmaceutical and biotechnology industries. NGs play a very important role in new advances in this field: in addition to their nanometer size advantage, their chemical composition can be tailor-made to address specific requirements.

As mentioned, the design of polymeric NGs with new properties represents a field of constant interest owing to their 3D dimensional structure, good mechanical properties, high water content and biocompatibility. They are usually the material of

choice for introducing improvements into existing applications and for the development of new applications in tissue engineering, as diagnostic agents and for cell immobilization drug release and specific therapies (Chacko et al. 2012).

Undoubtedly, the nanometer size of NGs is the most important property in terms of promising use in delivery systems. The key aspects for the design of nanovehicle-based delivery systems will now be briefly dealt with.

- *Toxicity and biodegradability*: monomers or polymers used for synthesising NGs should ideally be biodegradable and nontoxic and the nontoxicity of their degradation products should also be assured. Another requirement is the controlled release of the loaded drug at the specific site and in the appropriate concentration, since its release above the therapeutic window would cause toxic or other undesirable side effects.
- *Stability*: the ability to maintain their integrity and size once the NGs are circulating in the bloodstream is key for the effectiveness of nanosystems. Furthermore, the encapsulation stability of the loaded agent is essential to avoid premature leakage of the drug during circulation: faced with the turbulent flow conditions of the vascular system, delivery vehicles encounter blood cells, serum, lipid membranes, and several potential hydrophobic components which can trigger undesired drug leakage. Previous works reporting a lack of correlation between in vitro and in vivo studies highlighted the need to measure stability in more quantifiable and universal terms (McNeil 2005; Jeong et al. 2002; Liggins and Burt 2002). The encapsulation factor, when the NGs are employed as a delivery system, is reported as the weight percent of the drug loaded per unit weight of the vehicle, which is the thermodynamic distribution coefficient of the drug molecule from the interior of the nanocarrier. Values considered reasonable fall in the range between 5 and 25% (Bickerton et al. 2012).

While the stability of the drug encapsulated in a carrier is desirable during circulation, the drug will only be effective if released once it reaches its intended target. As discussed in the previous section, this can be achieved by designing the chemical composition of the carrier to be effective against a particular stimulus or to recognize the site of action through target receptors.

- *Long circulation time*: it is important for NGs to be able to remain in circulation for sufficiently long to reach the site of the disorder, avoiding natural clearance routes. Unfortunately, most nanocarriers are eliminated by the reticuloendothelial system within minutes after injection. NGs are taken up by liver and spleen macrophages via phagocytosis. Opsonins serve as an adjunct immune system, combining with blood proteins at the surface and accelerating nanogel elimination. In general, nanoparticles of 30–200 nm in diameter show longer circulation times, shifting the equilibrium to extravasation and leading to improved accumulation in the tumor. The slightly negative zeta potential of nanoparticles also predicts reduced clearance (Khandare et al. 2012). In order to reduce interactions with serum proteins, achieve prolonged circulation time in

the blood and prevent accumulation of NGs in non-specific sites, it is essential to modify the surface of the NGs with inert hydrophilic polymers such as poly (ethylene glycol) (PEG). PEGylated nanocarriers have been developed to reduce particle opsonization and consequently enhance their circulation half-life (Hatakeyama et al. 2011).

Nevertheless, the majority of PEGylated carriers is still eliminated from circulation within hours after intravenous injection and can trigger an immunological response in the body. The development of better and safer materials is thus crucial in order to overcome this disadvantage (Romberg et al. 2008; Kamaly et al. 2012).

- *Passive targeting*: Passive targeting relies on the so-called enhanced permeability and retention effect (EPR), which is based on the abnormal physiology of the capillary endothelium present in the growing tumor, whose cells are poorly packed, often separated by spaces between 200 and 600 nm (Fig. 4). This fact, together with the increase in neovasculature formation, allows the passage of NGs through the circulatory system to the diseased region. Furthermore, their accumulation in tumor tissue is favored by the lack of lymphatic clearance in this environment and the endocytic capacity of tumor cells. Thus, the transport of NGs through intracellular spaces to the interstitial tumor zone and the subsequent accumulation in these tissues, determines the passive targeting of nanometric systems.

This design aspect is key to the targeting of several diseases, especially cancer and arthritis.

- *Active targeting*: This type of directing refers to the active orientation of NGs and site-specific accumulation in tumor tissues as a consequence of their marked specificity towards target cells. This specificity is achieved through the over-expression of cell-recognition processes, taking advantage of various types of receptors on the tumor cell surface. The accumulation of NGs on tumor

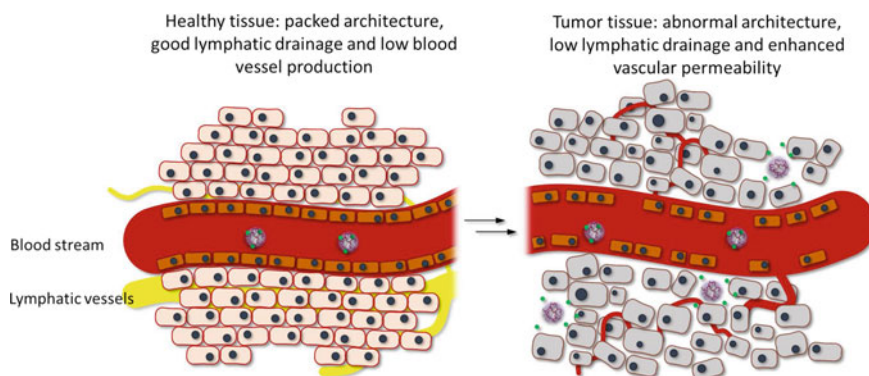


Fig. 4 Enhanced permeability and retention effect (EPR)

significantly increases the effectiveness of therapeutic drugs and reduces the appearance of collateral damage.

The mechanism of action in the body is in general terms as follows: after intravenous injection, the NGs float freely in the bloodstream in the smaller vessels and capillaries, reaching the site or specific tissue by exploiting the physiological mechanism of depuration. Drug release occurs after absorption of the NGs into the cells of the target tissue. This strategy is used to target specific disease phenotypes and the design of a delivery system should therefore take into account the ability to attach ligands to the carrier in order to achieve the action in one specific site.

The combination of the advantages of NGs with intelligent properties and the benefits of incorporating inorganic NPs offers the possibility of finding unique properties that facilitate the development of new nanometric platforms.

There is an urgent need for a new generation of formulations able to provide safer and more effective delivery by way of various pharmaceutical agents in a simple and scalable nanocarrier platform. This is particularly the case in certain types of therapies requiring high doses of extremely toxic drugs and in those where the therapy can be effective in the desired organ but negatively affects healthy tissues.

One of such therapies is that used in the treatment of cancer, the incidence of which continues to rise, making it one of the major causes of mortality and morbidity worldwide. The devastating course of this disease has created an urgent need to find successful NP-based drug delivery systems.

One of the great advances in the development of nanotechnology is theranostics (diagnosis + therapy), a system involving nanocarriers with combination ability of imaging and therapeutic agents and thus of great utility for real-time monitoring of

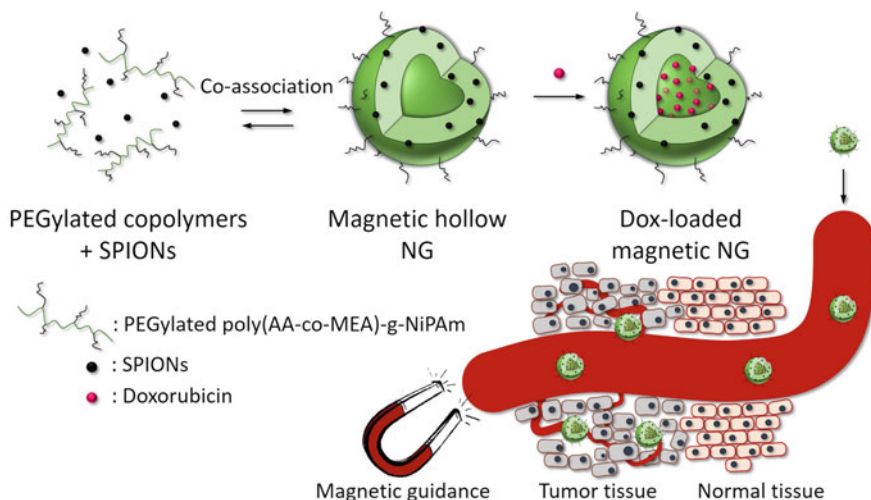


Fig. 5 Hollow hybrid nanogel

therapeutic efficacy. The report published by Hsin-Cheng Chiu et al. (Chiang et al. 2013) provides an interesting example of a well-designed nanosystem with the mentioned double function (see Fig. 5).

The reported hollow hybrid nanogel system with theranostics properties was prepared via the covalent stabilization of the co-assembly of magnetic nanoparticles with poly(AA-co-MEA)-g-mPEG/pNiPAm. As previously commented, the presence of co-monomers such as AA and NiPAm conferred pH- and thermo-sensitivity, respectively, on the nanogels. PEG segments were used as stabilizer to prevent particle aggregation and to enhance biocompatibility and long-time circulation. The incorporation of MNPs enables magnetic resonance imaging contrast, magnetic guidance and hyperthermia therapy, which trigger rapid drug release as a consequence of the thermo-responsiveness of the conjugated polymer. Doxorubicine (Dox), a well-studied anthracycline used in chemotherapy, was incorporated into the NGs, and both controlled drug elution and cellular uptake were observed. The nanocarriers enter into the blood circulation at 37 °C and are guided by a magnetic field to the targeted site of action. As a consequence of the hyperthermia produced by magnetic resonance or by changes in pH values, the drug is released at the tumor site. All these desirable characteristics lead to a prominent *in vitro* cytotoxic effect against tumor cells. Although an evaluation of the *in vivo* performance of this system is obviously required, this work demonstrates the great potential of the multimodal theranostics system for cancer treatment.

Another important example, but using gold NPs, is presented in the paper by Chunying Chen et al. (Zhang et al. 2014).

Figure 6 shows a photo-thermal and thermo-responsive nanocomposite with a core of Au@SiO₂. These NPs were coated with a polymer shell of thermo-responsive pNiPAm. The activation stimulus in this work was an NIR laser. NIR radiation range (from 650 to 900 nm) can penetrate deeply into the body and causes minimal damage. Gold NPs served as transducers for NIR transformation into confined local heat, which could be used to promote the size control of NGs and trigger drug release. This system showed low cytotoxicity and high biocompatibility in cell experiments. The improved accumulation in tumor with NIR laser

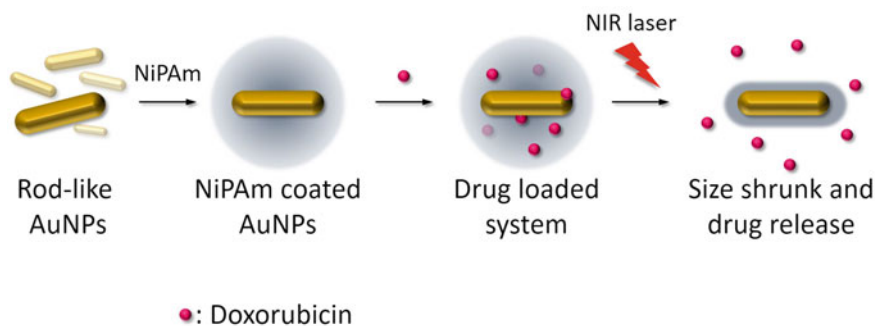


Fig. 6 Stimuli-responsive nanocomposite with a core of Au@SiO₂

irradiation induced sufficient increase in temperature to almost completely inhibit tumor growth, showing the very promising potential of the nanocomposite for tumor ablation.

7 Conclusions and Future Perspectives

In summary, the new generations of polymeric nanometric systems with targeted and controlled release are designed to navigate the complex live environment and incorporate features for achieving target specificity, control of the kinetics of drug concentration and exposure at the cell and subcellular levels of tissue.

Undoubtedly, such novel nanosystems will be a substantial improvement on those currently used in traditional medicine.

What is clear is the need for an intelligent design bringing together all the following features in one single system: improved pharmacological properties of drugs so that these remain unaltered during encapsulation and transport; the ability to target a drug to a specific site without damaging healthy tissue; the possibility of remaining in the bloodstream for longer without the risk of elimination; the ability to offer different therapeutic products regardless of their physical–chemical properties; the ability to fulfill more than one function at a time, such as delivering a therapeutic drug, providing images and at the same time allowing real-time monitoring of therapeutic efficacy. Materials with these beneficial properties will undoubtedly have a promising future in therapeutic techniques and accelerate the advancement of nanomedicine.

References

- Abu Samah NH, Heard CM (2013) Enhanced in vitro transdermal delivery of caffeine using a temperature- and pH-sensitive nanogel, poly(NIPAM-co-AAc). *Int J Pharm* 453(2):630–640
- Akiyoshi K, Deguchi S, Moriguchi N, Yamaguchi S, Sunamoto J (1993) Self-aggregates of hydrophobized polysaccharides in water. Formation and characteristics of nanoparticles. *Macromolecules* 26:3062–3068
- An D et al (2015) Synthesis of surfactant-free hydroxypropylcellulose nanogel and its dual-responsive properties. *Carbohydr Polym* 134:385–389
- Asadian-birjand M et al (2016) Transferrin decorated thermoresponsive nanogels as magnetic trap devices for circulating tumor cells. *Macromol Rapid Commun* 37:439–445
- Asokan A, Cho MJ (2002) Exploitation of intracellular pH gradients in the cellular delivery of macromolecules. *J Pharm Sci* 91(4):903–913
- Ayano E et al (2012) Poly(N-isopropylacrylamide)-PLA and PLA blend nanoparticles for temperature-controllable drug release and intracellular uptake. *Colloids Surf, B* 99:67–73
- Bae KH, Mok H, Park TG (2008) Biomaterials synthesis, characterization, and intracellular delivery of reducible heparin nanogels for apoptotic cell death. *Am J Hematol* 29:3376–3383
- Baek SM et al (2015) Smart multifunctional drug delivery towards anticancer therapy harmonized in mesoporous nanoparticles. *Nanoscale* 7:14191–14216

- Bhardwaj P et al (2009) Poly(acrylamide-co-2-acrylamido-2-methyl-1-propanesulfonic Acid) Nanogels made by inverse microemulsion polymerization. *J Macromol Sci Part A* 46 (11):1083–1094
- Bickerton S, Jiwpanich S, Thayumanavan S (2012) Interconnected roles of scaffold hydrophobicity, drug loading, and encapsulation stability in polymeric nanocarriers. *Mol Pharm* 9 (12):3569–3578
- Bilalis P et al (2016) Preparation of hybrid triple-stimuli responsive nanogels based on poly (L-histidine). *J Polym Sci, Part A: Polym Chem* 54(9):1278–1288
- Boullaras M et al (2015) Design of smart oligo(ethylene glycol)-based biocompatible hybrid microgels loaded with magnetic nanoparticles. *Macromol Rapid Commun* 36(1):79–83
- Brazel CS (2009) Magnetothermally-responsive nanomaterials: combining magnetic nanostructures and thermally-sensitive polymers for triggered drug release. *Pharm Res* 26(3):644–656
- Calderón M et al (2010) Functional dendritic polymer architectures as stimuli-responsive nanocarriers. *Biochimie* 92(9):1242–1251
- Chacko RT et al (2012) Polymer nanogels: a versatile nanoscopic drug delivery platform. *Adv Drug Deliv Rev* 64(9):836–851
- Chem P, Brian P, Currently V (2012) Temperature-sensitive nanogels: poly(*N*-vinylcaprolactam) versus poly(*N*-isopropylacrylamide). *Polym Chem* 3:852
- Chen T et al (2011) Preparation and characterization of thermosensitive organic–inorganic hybrid microgels with functional Fe₃O₄ nanoparticles as crosslinker. *Polymer* 52(1):172–179
- Chen W et al (2013) In situ forming reduction-sensitive degradable nanogels for facile loading and triggered intracellular release of proteins. *Biomacromol* 14(4):1214–1222
- Cheng R et al (2013) Dual and multi-stimuli responsive polymeric nanoparticles for programmed site-specific drug delivery. *Biomaterials* 34(14):3647–3657
- Chiang W et al (2013) Superparamagnetic hollow hybrid nanogels as a potential guidable vehicle system of stimuli-mediated MR imaging and multiple cancer therapeutics. *Langmuir* 29:6434–6443
- Choi KY et al (2012) Theranostic nanoplatfoms for simultaneous cancer imaging and therapy: current approaches and future perspectives. *Nanoscale* 4(2):330–342
- Cortez-Lemus NA, Licea-Claverie A (2015) Poly(*N*-vinylcaprolactam), a comprehensive review on a thermoresponsive polymer becoming popular. *Prog Polym Sci*
- Cuggino JC et al (2016) Responsive nanogels for application as smart carriers in endocytic pH-triggered drug delivery systems. *Eur Polym J* 78:14–24
- Cuggino JC et al (2011) Thermosensitive nanogels based on dendritic polyglycerol and *N*-isopropylacrylamide for biomedical applications. *Soft Matter* 7(23):11259
- Dailing EA et al (2015) Soft matter photopolymerizable nanogels as macromolecular precursors to covalently crosslinked water-based networks. *Soft Matter*
- Dürr S et al (2013) Magnetic nanoparticles for cancer therapy. *Nanotechnol Rev* 2(4):395–409
- Fleige E, Quadir MA, Haag R (2012) Stimuli-responsive polymeric nanocarriers for the controlled transport of active compounds: concepts and applications. *Adv Drug Deliv Rev* 64(9):866–884
- Fuchs AV, Gemmell AC, Thurecht KJ (2015) Utilising polymers to understand diseases: advanced molecular imaging agents. *Polym Chem* 6:868–880
- Ganta S et al (2008) A review of stimuli-responsive nanocarriers for drug and gene delivery. *J Controlled Release* 126(3):187–204
- Gerweck LE, Seetharaman K (1996) Cellular pH gradient in tumor versus normal tissue: potential exploitation for the treatment of cancer. *Can Res* 56:1194–1198
- Giulbudagian M et al (2014) Fabrication of thermoresponsive nanogels by thermo-nanoprecipitation and in situ encapsulation of bioactives. *Polym Chem* 5:6909–6913
- Gyarmati B, Nmety R, Szilgyi A (2013) Reversible disulphide formation in polymer networks: a versatile functional group from synthesis to applications. *Eur Polym J* 49(6):1268–1286
- Hatakeyama H, Akita H, Harashima H (2011) A multifunctional envelope type nano device (MEND) for gene delivery to tumours based on the EPR effect: a strategy for overcoming the PEG dilemma. *Adv Drug Deliv Rev* 63(3):152–160

- Heffernan MJ, Murthy N (2009) Disulfide-crosslinked polyion micelles for delivery of protein therapeutics. *Ann Biomed Eng* 37(10):1993–2002
- Hoffman AS et al (2000) Really smart bioconjugates of smart polymers and receptor proteins. *J Biomed Mater Res* 52(4):577–586
- Hong JS et al (2008) Liposome-templated supramolecular assembly of responsive alginate nanogels. *Langmuir* 24(8):4092–4096
- Hu J et al (2012) Recent advances in shape-memory polymers: structure, mechanism, functionality, modeling and applications. *Prog Polym Sci* 37(12):1720–1763
- Hu Z, Cai T, Chi C (2010) Thermoresponsive oligo(ethylene glycol)-methacrylate-based polymers and microgels. *Soft Matter* 6:2115–2123
- Iijima M, Nagasaki Y (2006) Synthesis of poly[*N*-isopropylacrylamide-*g*-poly(ethylene glycol)] with a reactive group at the poly(ethylene glycol) end and its thermosensitive self-assembling character. *J Polym Sci, Part A: Polym Chem* 44(4):1457–1469
- Jafari M, Kaffashi B (2016) Pure and applied chemistry synthesis and characterization of a novel solvent-free dextran-HEMA-PNIPAM thermosensitive nanogel. *Pure Appl Chem* 53(2):68–74
- Jeong B, Kim SW, Bae YH (2002) Thermosensitive sol-gel reversible hydrogels. *Adv Drug Deliv Rev* 54(1):37–51
- Jiang Y et al (2014) Click hydrogels, microgels and nanogels: emerging platforms for drug delivery and tissue engineering. *Biomaterials* 35(18):4969–4985
- Kabanov AV, Vinogradov SV (2009) Nanogels as pharmaceutical carriers: finite networks of infinite capabilities. *Angew Chem Int Ed* 48(30):5418–5429
- Kamaly N et al (2012) Targeted polymeric therapeutic nanoparticles: design, development and clinical translation. *Chem Soc Rev* 41(7):2971–3010
- Karimi M et al (2016) Smart micro/nanoparticles in stimulus-responsive drug/gene delivery systems. *R Soc Chem* 45:1457–1501
- Khandare J et al (2012) Multifunctional dendritic polymers in nanomedicine: opportunities and challenges. *Chem Soc Rev* 41(7):2824–2848
- Kuo C-Y et al (2015) Thermo- and pH-induced self-assembly of P(AA-*b*-NIPAAm-*b*-AA) triblock copolymers synthesized via RAFT polymerization. *J Polym Sci, Part A: Polym Chem* 54:1109–1118
- Lau ACW, Wu C (1999) Thermally sensitive and biocompatible poly(*N*-vinylcaprolactam): synthesis and characterization of high molar mass linear chains. *Macromolecules* 32:581–584
- Lee C-F, Lin C-C, Chiu W-Y (2008) Thermosensitive and control release behavior of poly(*N*-isopropylacrylamide-co-acrylic acid) latex particles. *J Polym Sci, Part A: Polym Chem* 6:5734–5741
- Li Z et al (2014) Sonochemical fabrication of dual-targeted redox-responsive smart microcarriers. *ACS Appl Mater Interfaces* 6(24):22166–22173
- Liggins RT, Burt HM (2002) Polyether-polyester diblock copolymers for the preparation of paclitaxel loaded polymeric micelle formulations. *Adv Drug Deliv Rev* 54(2):191–202
- Liu G, An Z (2014) Frontiers in the design and synthesis of advanced nanogels for nanomedicine. *Polym Chem* 5(5):1559
- Liu G, Qiu Q, An Z (2012) Development of thermosensitive copolymers of poly(2-methoxyethyl acrylate-co-poly(ethylene glycol) methyl ether acrylate) and their nanogels synthesized by RAFT dispersion polymerization in water. *Polym Chem* 3:504
- Liu J et al (2015) Design of hybrid nanovehicles for remotely triggered drug release: an overview. *J Mater Chem B* 3:6117–6147
- Lu S et al (2013) Polyacrylamide hybrid nanogels for targeted cancer chemotherapy via co-delivery of gold nanoparticles and MTX. *J Colloid Interface Sci* 412:46–55
- Lutz J-F (2011) Thermo-switchable materials prepared using the OEGMA-platform. *Adv Mater* 23(19):2237–2243
- Madhusudana Rao K et al (2013) Novel thermo/pH sensitive nanogels composed from poly(*N*-vinylcaprolactam) for controlled release of an anticancer drug. *Colloids Surf, B* 102:891–897

- Maya S et al (2013) Smart stimuli sensitive nanogels in cancer drug delivery and imaging: a review. *Curr Pharm Des* 19:7203–7218
- McNeil SE (2005) Nanotechnology for the biologist. *J Leukoc Biol* 78(3):585–594
- McPhee W, Tam KC, Pelton R (1993) Poly(*N*-isopropylacrylamide) latices prepared with sodium dodecyl sulfate. *J Colloid Interface Sci* 156:24–30
- Meng F, Hennink WE, Zhong Z (2009) Reduction-sensitive polymers and bioconjugates for biomedical applications. *Biomaterials* 30(12):2180–2198
- Merino S et al (2015) Nanocomposite hydrogels: 3D polymer-nanoparticle synergies for on-demand drug delivery. *ACS Nano* 9(5):4686–4697
- Molina M et al (2015) Stimuli-responsive nanogel composites and their application in nanomedicine. *Chem Soc Rev* 44(17):6161–6186
- Montoro SR, de Fátima Medeiros S, Alves GM (2014) Nanostructured hydrogels. Elsevier Inc.
- Morimoto N et al (2013) Self-assembled pH-sensitive cholesteryl pullulan nanogel as a protein delivery vehicle. *Biomacromolecules* 14(1):56–63
- Motornov M et al (2010) Stimuli-responsive nanoparticles, nanogels and capsules for integrated multifunctional intelligent systems. *Prog Polym Sci* 35(1–2):174–211
- Müllen K, Ober CK (2013) Polymers for advanced functional materials. In: Matyiazewski K, Möller M (eds) *Polymer science: a comprehensive reference*. Elsevier, Amsterdam, pp 1–502
- Mura S, Nicolas J, Couvreur P (2013) Stimuli-responsive nanocarriers for drug delivery. *Nat Mater* 12(11):991–1003
- Nash MA et al (2012) Multiplexed enrichment and detection of malarial biomarkers using a stimuli-responsive iron oxide and gold nanoparticle reagent system. *ACS Nano* 6(8):6776–6785
- Nayak S, Andrew Lyon L (2005) Soft nanotechnology with soft nanoparticles. *Angew Chem Int Ed* 44(47):7686–7708
- Oh JK et al (2008) The development of microgels/nanogels for drug delivery applications. *Prog Polym Sci (Oxford)* 33(4):448–477
- Oh JK, Lee DI, Park JM (2009) Biopolymer-based microgels/nanogels for drug delivery applications. *Prog Polym Sci (Oxford)* 34(12):1261–1282
- Online VA (2015) Multifunctional hybrid nanogels for theranostic applications. *Soft Matter* 11:8205–8216
- Pelton RH, Chibante P (1986) Preparation of aqueous latices with *N*-isopropylacrylamide. *Colloids Surf* 20(3):247–256
- Peng E, Wang F, Xue JM (2015) Nanostructured magnetic nanocomposites as MRI. *J Mater Chem B: Mater Biol Med* 00:1–36
- Peng J et al (2013) Controlled release of cisplatin from pH-thermal dual responsive nanogels. *Biomaterials* 34(34):8726–8740
- Quesada-Perez M, Ahualli S, Martin-Molina A (2014) Temperature-sensitive nanogels in the presence of salt: explicit coarse-grained simulations. *J Chem Phys* 141(12)
- Raemdonck K, Demeester J, De Smedt S (2009) Advanced nanogel engineering for drug delivery. *Soft Matter* 5:707–715
- Rahimian K, Wen Y, Oh JK (2015) Redox-responsive cellulose-based thermoresponsive grafted copolymers and in-situ disulfide crosslinked nanogels. *Polymer* 72:387–394
- Ramos J, Imaz A, Forcada J (2012) Temperature-sensitive nanogels: poly(*N*-vinylcaprolactam) versus poly(*N*-isopropylacrylamide). *Polym Chem* 3:852–856
- Rayo E, Guerrero Q (2014) *Administración De Fármacos*, pp 17–38
- Romberg B, Hennink WE, Storm G (2008) Sheddable coatings for long-circulating nanoparticles. *Pharm Res* 25(1):55–71
- Ryu JH et al (2012) Tumor-targeting multi-functional nanoparticles for theragnosis: new paradigm for cancer therapy. *Adv Drug Deliv Rev* 64(13):1447–1458
- Rzaev ZMO, Dinçer S, Pişkin E (2007) Functional copolymers of *N*-isopropylacrylamide for bioengineering applications. *Prog Polym Sci (Oxford)* 32(5):534–595
- Sahiner N et al (2006) Microgel, nanogel and hydrogel-hydrogel semi-IPN composites for biomedical applications: synthesis and characterization. *Colloid Polym Sci* 284(10):1121–1129

- Saito G, Swanson JA, Lee K-D (2003) Drug delivery strategy utilizing conjugation via reversible disulfide linkages: role and site of cellular reducing activities. *Adv Drug Deliv Rev* 55(2):199–215
- Salehi R, Rasouli S, Hamishehkar H (2015) Smart thermo/pH responsive magnetic nanogels for the simultaneous delivery of doxorubicin and methotrexate. *Int J Pharm* 487:274–284
- Sarika PR, James NR (2015) Preparation and characterisation of gelatin-gum arabic aldehyde nanogels via inverse miniemulsion technique. *Int J Biol Macromol* 76:181–187
- Schild HG (1992) Poly(*N*-isopropylacrylamide): experiment, theory and application. *Prog Polym Sci* 17(2):163–249
- Shi L et al (2008) Poly (*N*-vinylformamide) nanogels capable of pH-sensitive protein release. *Society* 41:6546–6554
- Sierra-Martin B, Fernandez-Barbero A (2015) Multifunctional hybrid nanogels for theranostic applications. *Soft Matter* 11(42):8205–8216
- Singh N et al (2007) Au nanoparticle templated synthesis of pNIPAm nanogels. *Chem Mater* 19(4):719–726
- Sivaram AJ et al (2015) Nanogels for delivery, imaging and therapy. *Wiley Interdisc Rev: Nanomed Nanobiotechnol*
- Teyssier J et al (2015) Photonic crystals cause active colour change in chameleons. *Nature* 1–7
- Thomas CS, Xu L, Olsen BD (2012) Kinetically controlled nanostructure formation in self-assembled globular protein-polymer diblock copolymers. *Biomacromol* 13(9):2781–2792
- Thoniyot P et al (2015) Nanoparticle-hydrogel composites: concept, design, and applications of these promising, multi-functional materials. *Adv Sci* 2(1–2)
- Vancoillie G, Frank D, Hoogenboom R (2014) Thermoresponsive poly(oligo ethylene glycol acrylates). *Prog Polym Sci* 39(6):1074–1095
- Verma J, Lal S, Van Noorden CJF (2014) Nanoparticles for hyperthermic therapy: synthesis strategies and applications in glioblastoma. *Int J Nanomed* 9:2863–2877
- Vigderman L, Zubarev ER (2013) Therapeutic platforms based on gold nanoparticles and their covalent conjugates with drug molecules. *Adv Drug Deliv Rev* 65(5):663–676
- Vihola H et al (2005) Cytotoxicity of thermosensitive polymers poly(*N*-isopropylacrylamide), poly(*N*-vinylcaprolactam) and amphiphilically modified poly(*N*-vinylcaprolactam). *Biomaterials* 26(16):3055–3064
- Vinogradov S, Batrakova E, Kabanov A (1999) Poly(ethylene glycol)-polyethyleneimine NanoGel (TM) particles: novel drug delivery systems for antisense oligonucleotides. *Colloids Surf, B* 16:291–304
- Wang Y et al (2014) Investigation of dual-sensitive nanogels based on chitosan and *N*-isopropylacrylamide and its intelligent drug delivery of 10-hydroxycamptothecin. *Drug Deliv* 7544:1–11
- Wang Y et al (2013) Poly(vinylcaprolactam)-based biodegradable multiresponsive microgels for drug delivery. *Biomacromolecules* 14(9):3034–3046
- Witting M et al (2015) Thermosensitive dendritic polyglycerol-based nanogels for cutaneous delivery of biomacromolecules. *Nanomed Nanotechnol Biol Med* 11(5):1179–1187
- Wu L, Glebe U, Böker A (2015) Surface-initiated controlled radical polymerizations from silica nanoparticles, gold nanocrystals, and bionanoparticles. *Polym Chem* 6(29):5143–5184
- Wu W et al (2010a) Chitosan-based responsive hybrid nanogels for integration of optical pH-sensing, tumor cell imaging and controlled drug delivery. *Biomaterials* 31(32):8371–8381
- Wu W et al (2010b) Core-shell hybrid nanogels for integration of optical temperature-sensing, targeted tumor cell imaging, and combined chemo-photothermal treatment. *Biomaterials* 31(29):7555–7566
- Xu LQ et al (2009) Simultaneous “click chemistry” and atom transfer radical emulsion polymerization and prepared well-defined cross-linked nanoparticles. *Macromolecules* 42(17):6385–6392
- Yallapu MM, Jaggi M, Chauhan SC (2011) Design and engineering of nanogels for cancer treatment. *Drug Discovery Today* 16(9–10):457–463

- Yeh C (2014) Near-infrared light-responsive nanomaterials in cancer therapeutics. *Chem Soc Rev* 43(17):6254–6287
- Zhan F et al (2011) Acid-activatable prodrug nanogels for efficient intracellular doxorubicin release. *Biomacromolecules* 12(10):3612–3620
- Zhang X et al (2015) Micro- and nanogels with labile crosslinks—from synthesis to biomedical applications. *Chem Soc Rev* 44(7):1948–1973
- Zhang Z et al (2014) Near infrared laser induced targeted cancer therapy using thermo-responsive polymer encapsulated gold nanorods. *J Am Chem Soc* 136:7317–7326

Chapter 8

Radiation Dosimetry—A Different Perspective of Polymer Gel



Deena Titus, E. James Jebaseelan Samuel
and Selvaraj Mohana Roopan

Abstract Medical physics has gained much interest in the past few decades with the introduction of polymer gels which act both as a phantom and a dosimeter. These polymer gels act as the substrate for the dose to act upon, after which the distribution can be read three-dimensionally. Mainly consisting of a gelling agent, monomer, crosslinker, and an antioxidant, these dosimeters on exposure to ionizing radiation polymerize as a function of the absorbed dose. This dose can be readout using modalities like MRI, X-ray CT, optical CT scanner, etc. Various combinations of polymer gels are presented including ones made with modifications to the present ingredients or addition of nanoparticles. The additions of nanoparticles enhance the dose for improved therapeutic efficiency. Being tissue equivalent and having good spatial resolution make it a new class of dosimeter which can replace the conventional dosimeters. The fundamental science behind the technique, gel preparation, and areas of future potential developments to improve the validation for lower dose than current fractional radiotherapy dose is also discussed.

Keywords Polymer gel · Dosimeter · Dose · Three-dimensional Ionizing radiation · Tissue equivalent · Radiotherapy

1 Introduction

The wide applications of polymer material are familiar to the modern era. Increasing usage of these in medicine and drug delivery has benefits due to their unique properties. Several biorenewable polymers have drawn interest for its

D. Titus · E. J. J. Samuel

Medical Gel Dosimetry Lab, Department of Physics, School of Advanced Sciences,
Vellore Institute of Technology, Vellore 632014, Tamil Nadu, India

S. M. Roopan (✉)

Department of Chemistry, School of Advanced Sciences, Chemistry of Heterocycles &
Natural Product Research Laboratory, Vellore Institute of Technology, Vellore 632014,
Tamil Nadu, India

e-mail: mohanaroopan.s@gmail.com; mohanaroopan.s@vit.ac.in

© Springer Nature Singapore Pte Ltd. 2018

V. K. Thakur and M. K. Thakur (eds.), *Polymer Gels*, Gels Horizons: From Science to Smart Materials, https://doi.org/10.1007/978-981-10-6086-1_8

309

diverse applications which include water purification, biomedical, etc. (Thakur and Thakur 2014, 2015). Some polymer nanocomposites possess self-healing property (Thakur and Kessler 2015). Moreover, polymer-loaded nanoparticles which are capable to target-specific cells are also in demand. Here, we bring to you another aspect of polymer gels which are of greater importance in the field of radiotherapy.

The current-day practice of sophisticated techniques in the field of cancer therapy includes Three-Dimensional Conformal Radiotherapy (3D CRT), Image-Guided Radiotherapy (IGRT), Intensity-Modulated Radiotherapy (IMRT), Brachytherapy, Stereotactic Radiosurgery/Radiotherapy (SRS/SRT), particle therapy, and so on. All these methods need a qualitative assessment prior to application on patient. Although the conventional methods like ionization chambers provide point dose measurement, films, being a two-dimensional dosimeter, provide better spatial resolution and relative dose measurement and so does the thermoluminescent dosimeters (TLDs) and other detectors. There was always a constant need for a radiation dosimetry technique which allows to capture the dose distribution three-dimensionally and that led to the development of radiation sensitive gels as we call it the gel dosimeter.

Gel dosimeter as the name suggests, a type of dosimeter, is tissue equivalent and enacts the role of both the phantom and a dosimeter. The history with the gels started off with the development of ferrous sulfate-doped gel (Fricke and Morse 1927). Later on, radiation-induced color change was observed in dyed gels especially methylene blue which paved way for the proposal of the use of gels for radiation therapy (Day and Stein 1950). Further investigation was done in-depth dose measurements using chloral hydrate agar gel with the aid of pH probe and spectrophotometry (Andrews et al. 1957). Then, the dose distribution via NMR imaging was introduced (Gore et al. 1984). Easy preparation, tissue equivalent nature of Fricke, which depended on the conversion of ferrous ions to ferric ions by radiation, gained much interest but had a limitation of ion diffusion, thereby not able to retain a spatially stable dose distribution. This put forth a time constraint between the time of irradiation and the time of scanning which is a maximum of two hours. So, soon after the irradiation, the dosimeters have to be scanned for results (Olsson et al. 1992). The problem of diffusion was reduced with the addition of glyoxal but the gel got partially bleached (Kalin and Mequanint 2013). Fricke Xylenol Orange is the common recipe studied and reported (Bero et al. 2000) which contain Xylenol orange which acts as the metal ion indicator and gelatin as the gel matrix. Fricke gels are composed of ferrous sulfate solution in gelatin matrix. The metal ion indicator used here is xylenol orange, to identify the conversion of ferrous ions to ferric ions. The indicator shows light orange color in ferrous environment and turns to dark brown in ferric. This property (color change) is used for scanning via optical CT scanner. The irreplaceable role of Fricke in the gel dosimetry field is evident from the progress of considerably more stable Fricke systems (Schreiner 2004) and improved optical technologies to view the dose pattern.

Through the polymer gel introduction, an alternative aspect based on the radiation-stimulated polymerization of monomers in solution, the problem of diffusion as in Fricke was solved. Figure 1 shows the basic idea of gel dosimetry.

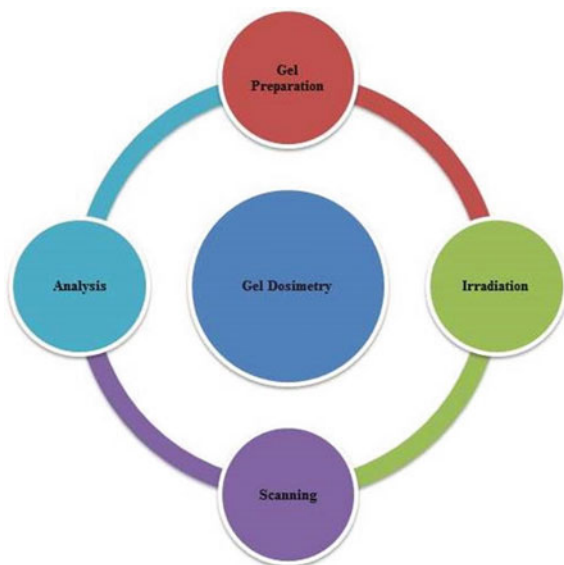
Various recipes of polymer gels have been described which increased the stability and sensitivity of the gel. This chapter gives an outline of the polymer gel dosimetry, its development, fundamental science sustaining the technique, different combinations, applications, and future scope.

2 Evolution of Polymer Gel Dosimetry

The effects of ionizing radiation on polymethyl methacrylate were proposed by (Alexander et al. 1954), and further led to a proposal on radiation polymerization in liquid-based dosimeter (Hoecker and Watkins 1958) and then later to a polyacrylamide gamma dosimeter (Boni 1961). A new recipe with the acronym BANANA was formulated which stands for its ingredients *N,N*-methylene-bis-acrylamide, Acrylamide, nitrous oxide, and agarose (Maryanski et al. 1992). The basic ingredient in a typical polymer gel dosimeter consisted of a monomer, a crosslinker, an oxygen-free environment, and a gelling agent. Nitrous oxide was used in this type of gel to remove the oxygen in the solution. The gel thus was termed as anoxic or hypoxic gel. Agarose in BANANA was replaced by gelatin and so termed as BANG (Maryanski et al. 1994a) as gelatin gave much clearer and transparent gel, thereby making the polymerized region much more visible to the naked eye and even to the imaging modalities.

Preparation became much simpler with the development of normoxic gels (Fong et al. 2001) as this is used an oxygen scavenger instead of nitrogen environment to

Fig. 1 Basic methodology for gel dosimetry



remove the oxygen in the gel solution. The first normoxic gel developed was named as MAGIC that stands for methacrylic acid, ascorbic acid, gelatin, and copper. Ascorbic acid along with copper takes away the oxygen (De Deene et al. 2002). Later on, the usage of tetrakis (hydroxymethyl) phosphonium chloride (THPC) was introduced as an oxygen scavenger (Baldock 2006). Some of the advancements in the field include the introduction of the gels namely MAGAT monomer–methacrylic acid (De Deene et al. 2002), PAGAT, monomer–acrylamide (Venning et al. 2005a), BANG (Maryanski et al. 1994a), and MICELLE are radiochromic gels which used dyes like leuco violet crystal and leucomalachite green (Jordan and Avvakumov 2009) and PRESAGE (Adamovics and Maryanski 2003). The potential hazards of the chemicals used in the manufacture are identified and suggested some less harmful gels like NIPAM, which uses *N*-isopropylacrylamide as the monomer (Senden et al. 2006), GENIPIN (Jordan 2009), HEMA, 2-hydroxyethyl methacrylate (Trapp et al. 2005), and other variations in the abovementioned formulae.

Reviews on polymer gel dosimeters have already been reported (Baldock et al. 2010; McJury et al. 2000) and additional works have been reported in the DOSGEL conference proceedings (DOSGEL 1999, 2001, 2004, 2006, 2008).

The basic methodology includes the fabrication of the gel dosimeter, irradiation using Co-60 or linear accelerators, and finally scanning (imaging).

2.1 Preparation

Polymer gels are majorly composed of 80% water, a monomer, crosslinker, gelling agent, and an oxygen scavenger. Monomer, such as acrylamide, is added, which is upon irradiation to ionizing radiation polymerizes. It also consists of a gelling agent, gelatin, which acts as the stabilizing agent as well as the gel matrix where the polymer is kept intact. Deionized distilled water is used in order to remove any oxygen present in it. The preparation was formerly done using glove box with nitrogen environment or in sealed reaction flasks. Oxygen scavengers are used for this purpose nowadays to get rid of any oxygen present in the mixture while preparing. On exposure to oxygen, the free radicals created and might interfere the process of polymerization. A crosslinker is also added to link the monomers. Gels are prepared and stored in PET containers which are then kept for refrigeration for further use. The prepared gel samples are irradiated using Co 60 or LINAC which are then scanned to extract the dose information (Baldock et al. 2010).

Similar preparation methods are reported and mentioned by the authors and sometimes slight variations in the combinations are adapted, which improve the stability and sensitivity of the gel.

2.2 *Principle of Mechanism*

The radiation sensitive chemicals when exposed to ionizing radiation will exhibit changes in the properties of the gel which are further analyzed by various techniques. 80% of the gel is composed of water; basically, polymer gels are hydrogels containing dissolved vinyl monomers present in it. The radiation induces free radical production by water radiolysis. These free radicals further lead to polymerization of the gel. For Fricke gel dosimeter, the radiation-induced free radicals help in ferrous to ferric ion conversion and so the color changes, whereas in polymer gels the monomers get converted into polymer which is instigated by the free radical produced by water radiolysis and there is significant change in the density, optical density, and binding of the water molecules. All these properties are made use of in choosing the appropriate modality for scanning the gel dosimeter for extracting the dose distribution. The polymers stay intact in place with the help of gelatin which acts as the stabilizing agent here. The exposed region in gel turns from colorless (transparent) to milky white (opaque) which can be seen visually. The amount of polymerization depends on the absorbed dose.

2.3 *Irradiation*

Gel dosimeters rely on the radiation-induced chemical changes. Though different types of radiation are being tested using gel dosimeters, commonly studied radiation types are gamma rays from Co-60 source and X-rays of higher energy from linear accelerator. Other radiation types include heavy ions and protons.

2.4 *Scanning Modalities*

As mentioned earlier, depending on the alteration in physical properties of the gel after radiation, the scanning techniques are selected. For polymer gels, widely used are the three modalities, namely Magnetic Resonance Imaging (MRI), X-ray Computed Tomography (X-ray CT), and Optical Computed Tomography (Optical CT).

2.4.1 *Magnetic Resonance Imaging*

The water molecules in the gel before and after irradiation play a significant role here. Polymerization of gel has an influence on the nearby water in the gel, which changes the binding of water molecules. It is this change which can be assessed by the two parameters of MRI, namely spin–lattice relaxation rate (R_1) and spin–spin

relaxation rate (R_2). Though R_1 has been found to vary only slightly, R_2 is the parameter often used as this varies with regard to the absorbed dose, as the extent of polymerization increases (Maryanski et al. 1993).

2.4.2 X-Ray CT

There is an increase in the physical density of the gel as the polymer chain is formed and the resultant variation in attenuation coefficient can be readout using X-ray CT. The density change which is apparently small is found to be proportional to the dose absorbed. When examined with CT, this eventually leads to variation in the CT number (Hilts et al. 2000). Image averaging and filtering techniques should be done for multiple acquisitions in order to get high signal-to-noise ratio (Hilts and Duzenli 2004).

2.4.3 Optical CT

Optical CT scanners obtain the sample's optical attenuation as a function of the spatial position by obtaining a set of projections. The irradiated regions of the gel become opaque and thus this helps in the scanning. A technique similar to the first-generation X-ray CT, instead of X-ray source a visible light (laser) source, is used. Several optical scanners have been developed using the principle of filter back projection for reconstructing the cross-sectional images. Due to factors like unavailability and high cost of MRI, this technique is used as an alternative to MRI and has got high spatial resolution and low noise as it uses photodiode for detection.

A typical optical CT scanner is analogous to the first-generation X-ray CT scanners as explained by Gore et al. (1996). The basic components are a laser beam, a photodetector. With the use of stepper motors, the laser and detector move with respect to the phantom and capture the sample gel images. Each full scan of the sample by the laser corresponds to a projection in one dimension. After each such projection, the sample is rotated by an angle and scanned again for a number of projections. An aquarium is used to keep the gel on a rotating table controlled by stepper motor so as to rotate the gel by small angles for scanning purpose. Artifacts due to refractive index can be cleared by adding a refractive matching liquid to the aquarium so that it matches with the refractive index of the gel. The images obtained are reconstructed using filter back projection algorithm to get the dose distribution three-dimensionally. A major drawback of the first-generation scanner is its slow scanning time.

Various optical scanners have been reported (Gore et al. 1996; Oldham et al. 2001; Doran et al. 2001; Wu et al. 2003; Van Doorn et al. 2005; Krstajic and Doran 2006; Sakhalkar and Oldham 2008).

In addition, the conversion of monomers to polymer can be demonstrated with the aid of FT-Raman vibration spectroscopy. Thus, it has been investigated to

understand the fundamental properties and structure of the dosimeter (Baldock et al. 1998b). Ultrasound computed tomography scanner was also developed to evaluate the dose distribution (Mather et al. 2003) as this makes use of the ultrasonic speed and attenuation which are dependent on the absorbed dose.

3 Gel Dosimeter—Characteristics

The process of polymerization is dependent on the various factors (Kumar and Samuel 2012) that are discussed below.

3.1 *Influence of Light and Oxygen*

The gel mixture, after adding the monomer and crosslinker, should be kept away from light and oxygen as it can degrade the sensitivity of the gel made. Photopolymerization can happen when exposed to light and free radical-induced polymerization can be stopped as the oxygen can react with the free radicals produced making it impossible to polymerize (Maryanski et al. 1993, 1994b; Baldock et al. 1998a).

3.2 *Gel Fogging*

Nitrogen bubbling into the gel can lead to fogging of the gel dosimeter. Use of high-grade chemicals is instructed as any free radical impurities present in the gel (chemical) can be responsible for this. Polymerization prior to irradiation does not serve the purpose of dosimetry (Maryanski et al. 1993, 1994b).

3.3 *Influence of Temperature*

Temperature is yet another important factor which has to be noted while the preparation, irradiation, and scanning. The corresponding temperature has to be maintained during preparation as some overheating can damage the gel. Though effect of temperature has not much effect on the irradiation part, it plays a major role in scanning. Decrease in temperature increases the relaxation rate of gelatin. Hence, the gels are to be maintained at uniform temperature before doing MRI. The temperature of the calibration gels and the experimental gel has to match (Maryanski et al. 1994b, 1997; Vachier and Rutledge 1996).

3.4 Gel Aging

It might take hours or even weeks for the complete polymerization of the gel once irradiated. Imaging the gel few hours of the irradiation can lead to errors. So it has to be kept overnight for stable complete polymerization for better results (McJury et al. 1999a).

3.5 Gel Matrix

Various gelling agents are used like agar-agar, agarose, gelatin, Sephadex, and polyvinyl alcohol (PV-A). Gelatin replaced the formerly used agarose as the gels made were much clearer than those made of agarose. 300 Bloom Gelatin is usually used (Vachier and Rutledge 1996), as the gel strength is more and so there is an increase in the melting point. Usually used in 5% by weight for the preparation, gelatin plays an important role by keeping the polymer intact in place forming a matrix. Increasing the concentration affects the sensitivity of the gel (Maryanski et al. 1994b).

3.6 Toxicity

The major component which is acrylamide (monomer) is a carcinogenic chemical, a neurotoxin, which can cause skin irritation and can even lead to nervous system on repeated exposure. Much care has to be taken while handling and disposal of the gel after use. Some gel combinations have replaced acrylamide with other monomers like acrylic acid for BANG-2 gel, methacrylic acid for MAGIC, *N*-isopropylacrylamide-NIPAM, and 2-hydroxyethyl methacrylate—HEMA which are considered as less toxic (Kumar and Samuel 2012).

3.7 High-Dose Edge Effects

Maryanski et al. (1994b) noticed edge enhancing effects at relatively high dose levels in the polymer gels near the regions of high-dose gradient. Outcome of the high dose in a particular region is the monomer depletion in that region, and thus the monomers start diffusing from low-dose to high-dose region and react with the polymer macro-radicals that are generated in the high-dose area. This can be a reason for the overshoot in the dose near the edge of the region exposed to high dose. The dependency of post-irradiation time with the overshoot amplitude was also discussed (De Deene et al. 2002). Based on the hypothesis that the

macro-radicals are accountable for the temporal and spatial instabilities detected in gel post-radiation, a mathematical model was proposed (Vergote et al. 2004). Increasing the gelatin concentration reduces the monomer diffusion constant; however, a decrease in sensitivity is also observed.

3.8 *pH Effect*

To investigate the nature of water macromolecule interactions, magnetization transfer was measured by varying the pH and monomer. The dependency of pH on the structure of macromolecule plays an important role in the magnetization transfer. There was a rise in the magnetization transfer at higher pH values greater than 8 and this was consistent with the chemical-exchange-mediated interaction between the polymer and water protons (Kennan et al. 1996). Later, it was found that the dependency of pH on the magnetization rate was inconsistent with acid or base-catalyzed chemical exchange (Gochberg et al. 1998).

3.9 *Influence of Concentration of Monomer and Crosslinker*

The dose sensitivity and the R_2 max were found to be dependent on the crosslinker fraction. The dose saturation point is extended which can be due to the monomer reactivity and the relaxation properties of gel (Baldock et al. 1996; Maryanski et al. 1997; Farajollahi et al. 1997). Kennan et al. (1996) and Maryanski et al. (1997) found that due to the low reactivity of BIS, crosslinker when compared to acrylamide, as the crosslinker fraction increases, the monomer-to-polymer conversion per unit dose decreases thereby decreasing the sensitivity of the gel.

4 Tissue Equivalency and Radiological Properties

The tissue equivalent nature of the gel is yet another important aspect which is one of the major criteria for a gel dosimeter. Before applying, one must always estimate the water equivalence of the polymer gel. The gel dosimeters should display water equivalent radiological properties. The water equivalence of a particular gel can be estimated using effective atomic number (Khan 2003) denoted as Z_{eff} ,

$$Z_{\text{eff}} = (a_1 Z_1^{2.94} + a_2 Z_2^{2.94} + a_3 Z_3^{2.94} + \dots + a_i Z_i^{2.94})^{1/2.94}$$

$$= \left(\sum a_i Z_i^{2.94} \right)^{1/2.94} \text{ where, } a_i \text{ is the fractional weight of the } i\text{th element.}$$

Also, the electron density is given by the formula

$$\rho_e = \rho_m N_A \left(\sum a_i Z_i^{2.94} \right)^{1/2.94}$$

$$a_i = (w_i Z_i / A_i) / \left(\sum w_i Z_i / A_i \right)$$

where A_i is the atomic weight

N_A —Avogadro's number

Z_i —atomic number

ρ_m —mass density

As the Compton and photoelectric interaction of photon beam with a particular compound is determined by the Z_{eff} and ρ_e , the required condition is that the electron density and effective atomic number should be that of the water. Radiation transport parameters are also calculated by knowing the photon mass energy absorption coefficient (μ_{en}/ρ), photomass attenuation coefficient (μ/ρ), and the total stopping power $(S/\rho)_{\text{tot}}$ which are the basic quantities used in the calculation. All these calculations can be done using ESTAR and XCOM database which are available online (<http://physics.nist.gov/>). These factors were found by combining the values of the elements that are present in the respective gel type according to their proportion.

These calculations have been reported by (Sellakumar et al. 2007) for investigating the radiation transport properties and water equivalence of 14 different polymer gels. The study revealed that the Z_{eff} of the gels were very close to that of water and also concluded that at energies less than 80 keV, the gel dosimeters cannot be considered water equivalent. The radiological properties have also been studied by Venning et al. (2005b) for MAGIC, MAGAS, and MAGAT gel dosimeters using Monte Carlo modeling. So before using the polymer gel dosimeter in the therapeutic energy range, we must consider the electron and mass densities to find out the water equivalent nature of the gel.

5 Calibration

Each gel prepared should be calibrated individually at the time of use for getting the proper response (Baldock et al. 1998a). The sensitivity and accuracy of the gel depend on the conditions of preparation and the chemicals used. Any impurity present or carelessness can lead to damage to the gel and its behavior. Different methods are adopted by which the gels are shifted to calibration phantoms and are irradiated with doses known. MRI scanning of the calibrated phantom produces T_2 relaxation. A plot of R_2 ($1/T_2$) against the doses is made, and this was used as a standard to calibrate the rest of the data (Maryanski et al. 1994b). Errors in fitting the data can determine the quality of the method and also on the quality of the gel.

The three methods used for the calibration are multibeam method, multiflask method, and depth dose method.

Multibeam method comprises the irradiation of a large volume of gel with several small beams. Depending on the sensitivity of the gel used, a number of doses can be given over a range (Oldham et al. 1998). Alternate to this, Maryanski et al. (1996) did a method where the phantom was irradiated with odd number of circular beams such that it converges at a central target point for which the dose was calibrated at D_{\max} . Major disadvantages include the use of a large amount of gel and only few numbers of data points could be obtained for the plot.

For multiflask method, small flasks are taken, packed with the respective gel and each flask is subjected to radiation to a known dose with parallel-opposed beam arrangement so as to get a uniform dose throughout the gel sample. Similar errors in multibeam method can happen here but only less gel is needed for this method. The flasks should be taken such that they are thin walled and completely filled with gel with no space for air cavity and should be surrounded by tissue equivalent phantom which is safe enough to ensure equilibrium. This removes the issue of the inter flask variation, thus ensuring that the conditions of full backscatter are met. The gels will therefore get a uniform irradiation which leads to error in calibration fit (Back et al. 1998; Baldock et al. 1998a; Ibbott et al. 1997).

In a water tank, a long test tube containing gel is vertically positioned and from the closed end it is irradiated with a single beam. This contributes to the characteristic depth dose distribution; the data should be plotted against ion chamber measurements or known depth dose distribution for the beam energy. To cover the entire range of 0–10 Gy, using multiple short test tubes may be ideal than using a single test tube taking into consideration the limitation of RF coil homogeneity. To increase the signal-to-noise ratio, adjacent points were averaged together at each depth (Ibbott et al. 1997; Maryanski et al. 1994b).

6 Recipes for Polymer Gel Preparation

The first ever made gel for dosimetric purpose was BANANA, a hypoxic polymer gel which was prepared by agarose infused with the co-monomers *N,N*-methylene-bis-acrylamide (BIS) and Acrylamide, nitrous oxide and agarose. Later, gelatin replaced the agarose in BANANA and the new formulation was referred to as BANG (Maryanski et al. 1992, 1994a). The two current models of BANG gel available are BANG-1TM, which uses powdered form of acrylamide and BANG-2TM, acrylic acid replaces the acrylamide together with NaOH. Improved gel response was seen in BANG-2TM. BANG-3TM replaced acrylic acid with methacrylic acid which delivered good MRI and optical response (McJury et al. 2000; Oldham et al. 2001).

Fong et al. (2001) introduced the normoxic polymer gels which can be prepared in normal atmospheric conditions. Here, the nitrogen environment used for oxygen

scavenging was replaced by the use of oxygen scavengers. First such developed gel is MAGIC which is the acronym for methacrylic acid, gelatin, ascorbic acid, and copper sulfate. Methacrylic acid here acts both as the monomer and crosslinker. The function of copper sulfate and ascorbic acid is that of an oxygen scavenger (De Deene et al. 2002). Later, different compositions and formulations of MAGIC dosimeter were developed. The use of tetrakis (hydroxymethyl) phosphonium chloride (THPC) was investigated which brought profound interest to the field (Baldock 2006). MAGAT was one among the findings which composed of methacrylic acid, gelatin, and THPC. For making a 500 g of gel sample, 430 g of distilled water is mixed with 40 g of gelatin under continuous stirring heated to a temperature of 48 °C for the complete dissolution of gelatin in the solution. The mixture was then allowed to cool and when it reached 35 °C, 30 g of methacrylic acid was added and mixed properly. 0.117 g of THPC was added at the end, mixed, and cooled (Govi et al. 2013).

A vital factor that can restrict the wider use of MAGIC gel is temperature; if the gel melts, it can take away the three-dimensional information. This was overcome by the addition of formaldehyde to the gel (Fernandes et al. 2008) during preparation, thus gaining an increase in the melting point making it viable to use in warmer conditions. 3% formaldehyde raised the melting point of the gel to 69 from 25 °C and a 12.5% increase in gel sensitivity was accomplished.

Sensitivity of MAGIC gel was studied with the addition of inorganic salts like LiCl, NaCl, KCl, and MgCl₂ which can act as the accelerator for polymerization. Among the salts examined, MgCl₂ acted as the most effective sensitizer (Hayashi et al. 2012). Urea and glucose added to MAGIC gel resulted in the increase of sensitivity and tissue equivalence (Zhu et al. 2010). Cho et al. (2014) examined the dose–response of MAGIC gel with several saccharide types to clarify its role in polymerization.

PAGAT was yet another invention. The commonly used PAGAT recipe followed is 5% gelatin mixed with 89% of double distilled water and the solution is heated to 40 °C. As the gelatin gets dissolved, it is continuously stirred using a magnetic stirrer. Once it is dissolved, the crosslinker namely *N,N*-methylene-bis-acrylamide is added to the solution and heated till 45 °C. After dissolving, the solution is allowed to cool and when it reached 40 °C, the monomer acrylamide is added to it and finally 10 mm THPC added at around room temperature (32 °C). The gel solutions are then poured into PET containers and kept for refrigeration (4 °C) overnight for complete gelation (Venning et al. 2005a; Subramanian et al. 2006).

Figure 2 shows the UV–Visible spectrum for PAGAT, and Fig. 3 shows the irradiated PAGAT gel. This shows the increase in the intensity as the dose progresses as depicted in the graph and visually. The gels were irradiated with 0–18 Gy (Samuel et al. 2015). PAGAT was also studied with the addition of formaldehyde (Yun et al. 2010) and succeeded in attaining an increase in the melting point and good linear response for the doses absorbed. Another modification of PAGAT gel by replacing the THPC with green tea due to its antioxidant nature was reported (Samuel et al. 2015). Green tea extract inhibits the

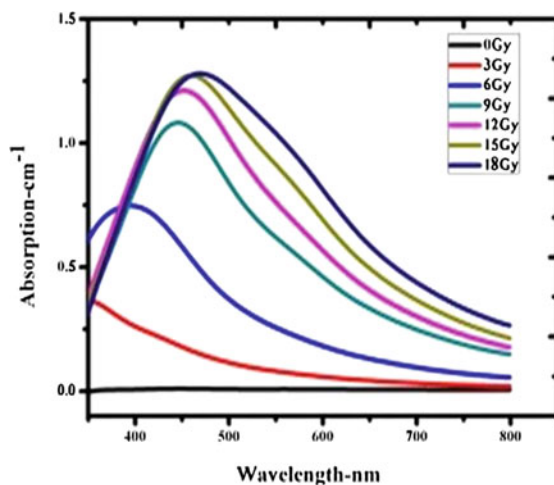


Fig. 2 UV-Vis spectrum of PAGAT



Fig. 3 Irradiated PAGAT with varying doses

polymerization in gel but when used in small quantity with sugar, it allows polymerization and increased the sensitivity.

PRESAGE is a new class of polymer gel, first proposed in 2003 (Adamovics and Maryanski 2003) which was based on leucomalachite green, a leuco dye, combined with clear polyurethane. The ingredients consist of an alkyl di-isocyanate pre-polymer and a hydroxyl reactive polyol together with a catalyst. This is

commercially available dosimeter which is insensitive to the atmosphere and so it is robust to use in a lab environment. The dosimeter does not require an external phantom or container. Higher accuracy readout is enabled as the radiochromic color change absorbs light. Imaging in optical CT is further enhanced due to the lack of containers and phantoms which minimizes the problem of refractive index matching thereby resulting in an accurate measurement of the dosimeter. By varying the amounts of leuco dye and other components, the dose sensitivity can be adjusted in this type of dosimeter. Variety of shapes can be achieved by proper machining and further can be used for various applications. Although not suitable for MRI, they exhibit maximum absorbance at around 633 nm making it apt for He-Ne laser source (Krstajic and Doran 2007).

Jordan and Avvakumov (2009) introduced the MICELLE gels, which contain leuco dyes, initially colorless, mixed with hydrogel matrix. It used 4% gelatin, 1 mM LCV, 25 mM trichloroacetic acid, and 4 mM Triton X-100 with triple distilled water. As discussed for other gels, the gelatin is added to the water and heated to 30 °C using a magnetic stirrer. At the same time, trichloroacetic acid, Triton X-100, and LCV were added to water and mixed for half an hour at 45 °C. Both the solutions were then mixed after the temperature of the second solution dropped from 45 to 30 °C. A bluish violet-colored gel was obtained and was kept for refrigeration. Upon reacting with the free radicals produced by the process of water radiolysis, the leuco dye molecules change to colored. Micelles have hydrophobic and hydrophilic parts. After a particular concentration, critical micelle concentration, the hydrophilic part comes in contact with the water, whereas the hydrophobic part repels from water toward the micelle center. Better spatial stability and low diffusion were the highlights of using this type of dosimeter. Furthermore, the easiness in preparation and less time involved make it suitable as a tool for dose information. Maximum absorption was found at 600 nm and so yellow LEDs are found suitable as the light source (Babic et al. 2009). It is suggested that within 6 h post-irradiation dose has to be read out.

Genipin was developed by Jordan (2009) with 2% gelatin, 2×10^{-5} % genipin, and 0.2 M H₂SO₄. Gelatin and genipin were made to dissolve in the distilled water, stirred for 18 h at 45 °C, and sulfuric acid was added, thereby forming the stock gel. Genipin crosslinks with gelatin and forms blue pigment as a result of crosslinking. A clear benefit of these gels is non-diffusion nature, thereby preventing diffusion in dose gradient regions. These deliver good stability and sensitivity, and have higher melting point.

Over the years, toxicity of gel was an important concern discussed among the researchers since the common monomer ingredient namely acrylamide (carcinogenic) can contribute to the overall gel toxicity, thus making the preparation and disposal difficult. Development of less toxic gels was a start to manage this issue and furthermore a breakthrough in the field. Senden et al. (2006) reported a dosimeter-less harmful than the available polymer gel dosimeters which can be made to suit the wide applications when compared with polyacrylamide gels. The toxic acrylamide is replaced by *N*-isopropylacrylamide (NIPAM). 5% of gelatin with 3% of BIS and 3% of NIPAM is mixed. At the end of the preparation, 10 mM

THPC is added which acts as the antioxidant. The dose, dose rate, temperature dependence, and post-irradiation time were observed and were in agreement with the previously reported PAGAT gel dosimeter. The dose–response was linear for a greater range than the PAGAT and better sensitivity. A co-solvent isopropanol was incorporated in NIPAM with the purpose of increasing the concentration of total monomer/crosslinker. Poor contrast and reduced dose resolution which arise due to the low-dose sensitivity of the PAGAT were improved with this ingredient. The gels made were stable and reproducible (Jirasek et al. 2010).

A new combination which makes use of 2-hydroxyethyl methacrylate (HEMA) as an alternative to the methacrylic acid in MAGIC gel was introduced. 82.48% of water was mixed with 8% gelatin, 0.5% ascorbic acid, 0.02% copper sulfate, and 9% HEMA, which was used as the formulation of the recipe (Trapp et al. 2005). Another combination reported with HEMA was with the use of polyethylene glycol 400 dimethacrylate (9G), triethylene glycol monoethyl ether monomethacrylate (TGMEMA), THPC, and gellan gum (gelling agent) (Hiroki et al. 2001). A linear dose–response which depended on the concentration of HEMA was seen in the case of gel with 9G and HEMA, while for the other gel having HEMA, TGMEMA, and 9G, the exposed region exhibited a thermos-responsive behavior and the absorbance increased after a certain dose. Yet, another using HEMA along with 9G and hydroxypropylcellulose (HPC) gel, a gelling agent used in place of gelatin, was studied for doses from 1 to 10 gray and the response was linear (Hiroki et al. 2013).

An additional class of polymer gel was developed with propylene acid based named DEMBIG. The preparation is as follows. Deionized water was filled with argon which was done in a glove box and then mixed with 7% gelatin under continuous stirring. The solution is heated to 45 °C for the gelatin to dissolve just like other preparation. Here, 5% DEMA and 4% BIS were added to the mixture and stirred again for some time. Then, the gel was filled with argon for half an hour, transferred to tubes and kept for cooling (Hsieh et al. 2011).

Turnbull dye-based dosimeter involves a gel matrix and an acidic medium with potassium ferricyanide and ferric compound. An insoluble dye $K [Fe^{II}Fe^{III}(CN)_6]$ is formed upon irradiation as the ferric ions get converted to ferrous ions and showed maximum absorption at 600 nm. When compared with the PAGAT gel, advantages of TB gel are its inhibited diffusion when compared to Fricke dosimeter and linearity for 0–400 gray (Solc and Spevacek 2009). Disadvantage includes gel aging due to interaction of ferric ions with other organic compounds. While preparing larger volumes, solidification can take several days and this was another problem which was encountered (Pilarova et al. 2014). PAGAT has a linear range up to 9 Gy, higher noise level in the response than TB gels, and also the toxicity issues due to monomer.

N-(Hydroxymethyl) acrylamide (NHMA)-based polymer gels (Basfar et al. 2015) were fabricated in a nitrogen glove box. 8% NHMA monomer was combined with 3% BIS, 4% gelatin, and 0.02 mM hydroquinone. For at least 5 hours, nitrogen was used in the chamber to remove the oxygen which can inhibit the polymerization of gels. The same procedure methods were used for the manufacture

and were characterized using MRI. The rate of polymerization was dose-dependent, that is irradiated to 20 Gy and studied the effect of dose rate and radiation energy but found no effect on the same.

Two dyed gelatin gels were formulated. The first gel makes use of Fuchsin acid cyanide dye (Gafar and El-Ahdal 2015) which diffuses in gelatin, thereby changing the colorless sample to a pink color after radiation. Using UV–Visible spectroscopy, the absorption was found at 550 nm. By varying the concentration of the dye, the formulations were studied and evaluated the radiation chemical yield, its stability, and sensitivity. Toluene Blue O (TBO) gelatin gel dosimeter (Gafar et al. 2014) was the second one which was studied with UV–Visible spectrophotometer having an absorbance at 635 nm. The G value increased with the dye concentration and the useful range being 1–150 Gy. The parameters like sensitivity, storage, and dose–response were also investigated.

A reusable radiochromic polymer gel named crystal ball was studied for its accuracy and for use in patient QA in proton therapy. It is tissue equivalent as well as commercially available (Avery et al. 2015). Mattea et al. (2015) studied a polymer gel using itaconic acid and BIS.

Yao et al. (2014) used the monomer tertiary-butyl acrylate, TBA which played the role of forming a transparent, quasi-rigid and 3D gel matrix and also the role of going through the process of polymerization with the fluorogenic material. The various combinations of gel are listed in (Table 1).

7 Nanoparticle-Embedded Gel Dosimetry

To improve the sensitivity and efficiency of the polymer gel, researchers are spending quality time on as to being used for lower dose range also that is below 1 gray. Aiming at giving minimum dose to the healthy tissues and maximum to the tumor cells, several approaches are implemented to serve the purpose. One of the novel methods is the incorporation of nanoparticle into the polymer gel dosimeter. Nanoparticle which finds its extensive application in almost all fields (Kalaiselvi et al. 2015; Elango and Roopan 2016; Kumar et al. 2015; Surendra et al. 2016; Helan et al. 2016) is a boon to the modern medical field. Interaction of the ionizing radiation with the healthy tissues may damage DNA, and therefore further care has to be taken to spare the healthy tissues.

Nanoparticles of the order of 1–100 nm have been in use in the past few years. It has been used for drug delivery, diagnostics, and treatment. The nanoscale particle has significant properties comparing the bulk material such as magnetic properties, fluorescence, and others. Prepared via various means, the nanoparticles exhibit properties which are applicable in medical field. Physical, chemical, and biological methods of preparation are the main methods of preparation. The physical method being a top-down approach includes ball milling, laser ablation, bead milling, etc., whereas the chemical method involves the use of chemicals as reducing agent to reduce the metal ions to nanoparticles. Electrochemical method, microwave

Table 1 Recipe summary

Normoxic dosimeters	Polymer gel dosimeter formulation
BANANA	Acrylamide, <i>N,N</i> -methylene-bis-acrylamide, nitrous oxide, and agarose
BANG	Acrylamide, <i>N,N</i> -methylene-bis-acrylamide, nitrous oxide, and gelatin
BANG-1 TM	Acrylamide (powdered form), <i>N</i> -methylene-bis-acrylamide, nitrous oxide, and gelatin
BANG-2 TM	Acrylic acid, NaOH, <i>N,N</i> -methylene- bis-acrylamide, and gelatin
BANG-3 TM	Methacrylic acid, gelatin
MAGIC	Methacrylic acid, ascorbic acid, CuSO ₄ ·5H ₂ O, and gelatin
MAGAS	Methacrylic acid, ascorbic acid, and gelatin (required a post-manufacture irradiation delay time of several days since no oxygen scavenger)
MAGAT	Methacrylic acid, tetrakis (hydroxymethyl) phosphonium chloride, and gelatin
nMAG	Methacrylic acid, <i>N,N</i> -methylene- bis-acrylamide, tetrakis (hydroxymethyl)phosphonium sulfate, and gelatin
PAGAS	Acrylamide, <i>N,N</i> -methylene- bis-acrylamide, ascorbic acid, and gelatin
PAGAT	Acrylamide, <i>N,N</i> -methylene-bis-acrylamide, tetrakis (hydroxymethyl) phosphonium chloride, (hydroquinone), and gelatin
nPAG	Acrylamide, <i>N,N</i> -methylene-bis-acrylamide, [tetrakis (hydroxymethyl) phosphonium] sulfate, and gelatin
PRESAGE	Alkyl di-isocyanate prepolymer and a hydroxyl reactive polyol along with a catalyst
NIPAM	<i>N</i> -isopropylacrylamide, tetrakis (hydroxymethyl) phosphonium chloride, and gelatin
MICELLE	Gelatin, sodium dodecyl sulfate, chloroform, trichloroacetic acid and leucomalachite green OR Gelatin, LCV, Trichloroacetic acid, and Triton X-100
GENIPIN	Gelatin, Genipin, H ₂ SO ₄
HEMA	2-hydroxyethyl methacrylate, gelatin, ascorbic acid, and copper sulfate
DEMBIG	Gelatin, 2-(Dimethylamino) ethyl acrylate, <i>N,N</i> -methylene-bis-acrylamide

irradiation, sonication, co-reduction method, micelle, and sol–gel are some of the methods opted for fabrication. An alternative to these methods is the biological method which is using plant extract and microorganisms which in turn reduces the metal ions. Plant-mediated synthesis or green synthesis is much more preferred as the microorganism-based synthesis is difficult to maintain. Prepared nanoparticles are then characterized using UV–Visible spectrophotometry for initial confirmation and further on to X-ray Diffraction (XRD) for finding the crystalline nature, Scanning Electron Microscope (SEM), Atomic Force Microscope (AFM), and Transmission Electron Microscope (TEM) for studying the morphology, topology, and size of the particle, Energy-Dispersive X-ray Spectroscopy (EDAX) for elemental composition, vibrating sample magnetometer for studying magnetic

properties, and various other methods depending on the need (Cheow et al. 2013; Roopan et al. 2012, 2014; Kumar et al. 2014; Pal et al. 2011; Elango et al. 2015; El-Alaily et al. 2015).

High atomic number nanoparticles have the ability to enhance the dose. Materials like gold, platinum, bismuth, etc. can be used for this purpose. The principle behind radiosensitization is discussed: When a target or metal is hit by an X-ray, part of the incident radiation energy will be imparted to eject an electron from its orbital and part of the energy goes as its kinetic energy. The corresponding kinetic energy can be calculated as the difference between the binding energy of the electron and the energy of the wave. The photoelectric effect is dependent on the atomic number of the material and also on the incident wave energy. Possibility of auger electron generations is also there if elements, with mid- to high atomic number, are ionized by X-ray or gamma ray; this can also enhance the dose. Here, the vacancy of the electron is filled by another electron and the energy is released (Khan 2003; Kobayashi et al. 2010). Depending on the size of the particle, its composition, uptake of these particles into the cells, and the energy of the applied radiation, the nanoparticles can provide radiation dose enhancements. Figure 4 depicts the dose enhancement mechanism.

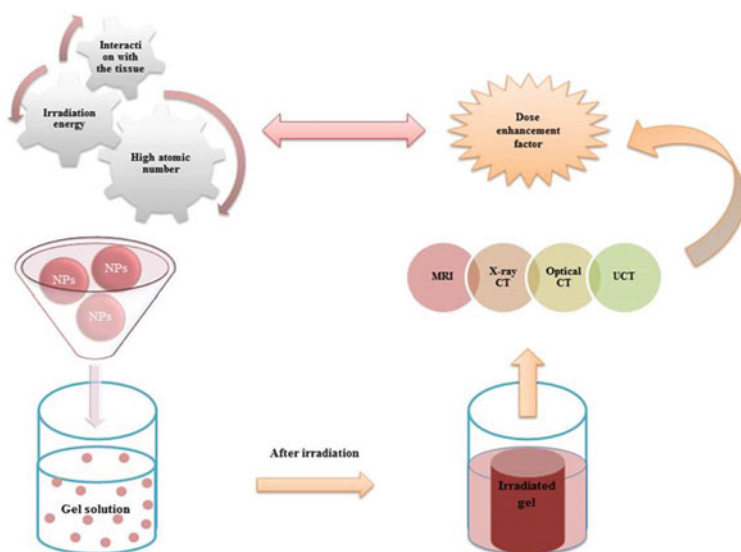


Fig. 4 Mechanism of dose enhancement

7.1 Gold Nanoparticle-Assisted Therapy

Gold, having atomic number $Z = 79$, nanoparticle (Au NP) considered as one of the less toxic and has been demonstrated to overcome the limitations of renal toxicity, short imaging timing, and poor contrast by other X-ray contrast agents. When compared to iodine, gold nanoparticles delivered 2.7% higher contrast (Hainfeld et al. 2006). No toxicity was observed with reduced bone interference and improvement in delineation of blood capillaries. The characteristics like being inert to interactions with the tissues and high atomic number element make it promising for photosensitization reaction. As radiosensitizer, these can perform well as it enhances the radiotherapy efficiency. When used combined with the kV X-rays, the nanoparticles enhance the dose deposited in the tumor and an increase in the absorption was seen as a result of the element's photoelectric cross section. The process which utilizes Au NPs as means for dose amplification is referred to as the gold nanoparticle-assisted radiation therapy abbreviated as GNRT (McMahon et al. 2008). Radiosensitization effect is governed by factors like the size, concentration of the particle, and the incident X-ray energy (Brun et al. 2009). The possibility of using GNRT via brachytherapy was done by Cho et al. (2009). Other GNRT works are reported by Rahman et al. (2009), Van den Heuvel et al. (2010), Leung et al. (2011), Zhang et al. (2012), Kakade and Sharma (2015), and review works have been reported (Jelveh and Chithrani 2011; Butterworth et al. 2012; Jain et al. 2012; Babaei and Ganjalikhani 2014; Su et al. 2014).

Au NPs of 2–3 μm average diameter were synthesized and mixed with MAGIC—f (methacrylic acid, ascorbic acid, gelatin, copper sulfate, and formaldehyde) in three different concentrations and subjected to irradiation using a 250 kV X-ray beam. Monte Carlo simulations were executed and the dose enhancement due to the Au NPs matched with the Monte Carlo simulations (Marques et al. 2010). Further, the dose variation due to Ag NPs was quantified in nPAG dosimeters using synchrotron and conventional beams used for radiotherapy (Rahman et al. 2010). Kamiar et al. (2013) prepared Au NPs of size 57 nm by reduction of gold precursor using trisodium citrate. These prepared NPs increased the effectiveness of radiation dose by about 21% and at 400 ppm; they exhibited major antibacterial property against *Escherichia coli*. The performance evaluation and the physicochemical characterization were thus done.

MAGICA gel was utilized to demonstrate the effect of dose enhancement due to Au NPs when used with megavoltage therapy. The R_2 increased with the addition of Au NPs and the optimum concentration was found out to be 0.1 mM which contributed to 10% dose enhancement (Khadem et al. 2013). Comparison studies with the Monte Carlo simulations were done too. Also, the effect of percentage depth dose was studied using energy in MV range in MAGICA gel. It was concluded that for concentrations greater than 0.1 mM, shielding effect was created and the simulation work suggests that the increase in gold concentration decreases the absorbed dose enhancement factor (Mahdavi et al. 2013).

Atae et al. (2015) compared the dose enhancement in 0.1 mM concentration of Au NPs using 6–8 MV photon beam. Gel used for this study was MAGICA and the outcome brought an increase in absorbed dose because of the addition of Au NPs. The extent of polymerization of the gels after irradiation with and without the presence of Au NPs was found to be more for 6 MV when compared to 18 MV energy. The predominance of pair production at higher energies and photoelectric effect at lower energies can be the reason for this. This was explained by Hainfield et al. (2004). Au NPs having 15 nm were prepared by chemical route and in 0.1 mM concentration was added to a new formulation of MAGIC-f polymer gel dosimeter. The setup was irradiated with Ir-192 source and 18 mV beam. The absolute doses from gel and Monte Carlo simulations were compared and an enhancement up to 15 and 8% was observed for internal external therapy (Khosravi et al. 2015).

Although the gold nanoparticles are considered to be less toxic for use in medical applications, higher concentrations can lead to the risk of toxicity. And also the dose enhancement factor may reduce when used in low concentration (Jeremic et al. 2013).

7.2 *Platinum-Promising Candidate*

Another promising material (high atomic number) proven for cancer therapy is platinum (Pt, $Z = 78$). Based on the addition of platinum nanoparticles with the fast ion irradiation like in hadron therapy, a new approach was formulated (Porcel et al. 2010). Fatal damage could happen to the DNA due to the presence of nanoparticles. The efficiency was calculated to be a factor of about 2. The enhancement is due to the auto-amplified electron cascades which are in the nanoparticles. Consequently, Pt NPs were combined with X-ray energies of different ranges to study the effect on DNA. The effect predominant in this study was the photoelectric effect and the platinum atoms were ionized by the photoelectrons. Any high atomic number nanoparticle can enhance the radiation dose irrespective of the nature of ionizing radiation and also is dependent on the source of the energy used for irradiation (Porcel et al. 2011).

The feasibility of using Pt NPs, produced by the technique of laser ablation having an average size of 10 nm, with PAGAT gel dosimeter was studied. Deyhimighighi et al. (2014) considered this possibility to investigate the usage of platinum nanoparticle as a dosimeter and as a tool for dose enhancer. Using Co-60, the nanoparticle-embedded PAGAT gel has been irradiated for different concentrations of NPs. The samples were analyzed with the presence and absence of the nanoparticle to study the enhancement effect. Here, the predominant effect is Compton effect since the mean energy of Co-60 is 1.25 meV and Z is 78. The results showed that 1×10^{-2} mg/l contributed to an increase of about 27.10% in dose, which is considered to be as the optimum concentration.

7.3 Silver

Anti-inflammatory and antimicrobial activities of silver nanoparticles (Ag NPs) are of great importance in this new era. Depending on the need, the preparatory standards can be chosen. Green synthesis is of great importance as of now due to its less toxic nature. Silver nanoparticles prepared by gamma radiation are already reported, so it is with gelatin and other gelling agents such as hydroxypropyl methylcellulose (Dong et al. 2014) but the introduction of the same as a dosimeter in therapy field was new. This method is free from any reducing agent and nanoparticles can be yielded in the pure form (Temgire and Joshi 2004; Kumar et al. 2005; Lai et al. 2007). Ag NP-based gel dosimeter was developed and investigated for its potential use in radiotherapy treatment. Here, the silver nitrate was mixed in gelatin (8%), since gelatin acts as the stabilizing agent and in higher percentage to minimize diffusion rate and agglomeration of Ag NPs (Vegeera and Zimon 2006), and the gel matrix was irradiated with gamma radiation which on subjection, produced silver nanoparticles as the radiation reduced the silver ions present in the solution to silver nanoparticles. Reduction reaction is displayed by a color change in the solution, and slightly yellow to dark brown could be made out visually. The resultant radio chromic gel with different concentrations of silver nitrate was reported (Soliman 2014) and was characterized using UV–Visible spectrophotometer which revealed the surface plasmon resonance at 450 nm. Tested for 3–100 gray, the gel responded to the dose linearly and exhibited good stability and the total uncertainty was 4.65% for 5–100 Gy. Similar works can be identified and tried for the introduction of new dosimeters. Other parameters are yet to be found on this dosimeter and further investigations have to be carried out to find out the radiological properties and other preparation methods.

7.4 Bismuth

Bismuth has high electron density, having atomic number 83, and makes it a better dose enhancer. Properties like less toxicity and less expensive nature of the Bismuth make it exceptional to use inefficient radiotherapy. All these were taken into consideration and investigation on the use of bismuth sulfide nanoparticles on the imaging technique namely computed tomography was explored. The polymer-coated nanoparticle was presented as an injectable CT imaging agent instead of the conventional iodine as they overcome the limitations (Rabin et al. 2006). Remarkable absorption than iodine, stability at 0.25 M Bi^{3+} , more than 2 h circulation time of the agent makes it more efficient and safer when compared to the conventional iodine agent. In vivo imaging can be enhanced utilizing these nanoparticles as agents.

Gold nanoparticle having high atomic number has already been reported to absorb the low-energy X-rays and was found to achieve dose enhancement within

the tumors. Introduction of a novel technique using a multi-compartment radiochromic radiation dosimeter was achieved so as to validate its application in nanoparticle-enhanced radiation therapy. It was designed to mimic 50 nm size Au NP-loaded tumor at a concentration of 0.5 mM which is surrounded by the normal tissue. Sensitivity-Modulated Advanced Radiation Therapy (SMART) dosimeter consists of an inner compartment coated with Au Nps and an outer compartment with tissue equivalent material. Irradiation of the dosimeter was done using 100 kV and 6 MV X-ray energies. Spectrophotometry and optical CT were used for the dose enhancement calculations. The changes in optical density were measured and compared between the two compartments. Stability of the dosimeter as well as the interbatch and intrabatch viability was also evaluated. DEF of 1.77 and 1.11 was obtained, respectively. The first ever three-dimensional visualization of the dose enhancement was depicted through the experiment. This invention is a boon as the current methods fail to do so and hence a novel-independent approach was proposed (Alqathami et al. 2012). In a similar way, the first ever evaluation of bismuth oxide nanoparticles for the effect of enhancement of dose was validated using SMART dosimeter. The inner compartment of the dosimeter coated with 0.1 mM of Bi_2O_3 -Nps and the outer compartment being tissue equivalent, irradiated to 100 kV, 10 Gy, a significant increase of about 80% in the radiation dose was observed which could solely be due to the presence of bismuth oxide nanoparticles which has the potential for dose enhancement (Alqathami et al. 2013).

7.5 Gadolinium and Iodine

Commonly used contrast agents for X-ray CT and MRI are iodine having atomic number 53 and gadolinium having atomic number 64 can be opted as a radioenhancer. Contrast agent iodine was incorporated in NIPAM gels and studied that led to measurable dose enhancement ratio post-irradiation with low energy (Meesat et al. 2009; Chang et al. 2013).

Gadolinium, in addition to being used as a contrast agent, has a high atomic number. Ultra-small gadolinium-based nanoparticles exhibit an interesting potential for image-guided radiotherapy. Equally, a radio-sensitizing effect and a contrast for MRI are favored by these nanoparticles (Le Duc et al. 2011, 2014). Polysiloxane shell where the Gd_2O_3 nanoparticles were encapsulated was delivered to be a potential IGRT tool in aglio sarcoma rat model. The nanoparticle accumulation was shown using MRI, and the rats were subjected to microbeam therapy. Miladi et al. 2013 used a brain tumor rat model with Gd nanoparticle. Effect of 0.1 mM of gadolinium oxide nanoparticles in dose enhancement with MAGIC-f gel was estimated. The gadolinium nanoparticles are much more effective than the contrast agents. Taupin et al. 2015 demonstrated the radiosensitization using both materials and found that enhancement is dependent on energy. The mechanism behind the increase in dose enhancement in Gd NPs may be due to the alterations in cell cycle, whereas in contrast agent, secondary electron emission plays the key role.

7.6 *Hafnium*

Hafnium oxide has not been introduced to a dose enhancer to the field of gel dosimetry as it causes stress damage to cell and is believed to be a good agent for enhancement. Theoretically, using Monte Carlo calculations, the effectiveness of Hafnium oxide was proved. NBTXR3 nanoparticles, when exposed to the ionizing radiation, act as a dose enhancer (Maggiorella et al. 2012). Another study revealed the dependence of dose enhancement on radiosensitivity of cancer cell line and the delivered dose showed in vitro that the radioenhancement depended on the dose delivered (Marill et al. 2014). This can further be investigated and used, it means that can improve the therapy. The different methods of preparation can be adapted and can be used with some polymer gels to validate the dose enhancing nature of the material.

7.7 *Iron Nanoparticles*

Superparamagnetic iron oxide nanoparticles (SPIONS) having good magnetic properties exhibit good dose enhancing properties and can also be used in imaging. Various studies have looked at the property of iron oxide nanoparticle. SPIONS catalyzes ROS formation which can lead to radiosensitization in tumor. Uncoated SPIONS triggered dark toxicity and the citrate coated stayed non-toxic in radiation absence, while the fluorescence intensity of dichlorofluorescein diacetate increased to 300% (Cooper et al. 2014). For 1 mg/mL concentration, an enhancement factor of 1.2 was seen on irradiating with 6 meV on prostate carcinoma cell line (Khoei et al. 2014).

In other nanoparticles like titanium oxide, non-metal-based nanoparticles like silica, quantum dots can also be studied used for the purpose and can be used along with gel dosimetry with proper techniques of preparation and analysis (Kwatra et al. 2013).

8 Extensive Applications

Polymer gel dosimetry has been utilized to confirm and validate several procedures. Validation of gel response was of focus exploring the three-dimensional imaging. The validated applications of gel dosimeters till date include depth dose, wedge profiles and penumbra, basic dosimetry in photon, neutron, electron and proton beams, conformal therapy SRS, IMRT, low dose rate and high dose rate brachytherapy, internal dosimetry, and estimation of heterogeneities in tissue. Some of the developments have been discussed below.

8.1 *Stereotactic Radiosurgery*

Targeting heavy doses to a small region of interest is the focus of stereotactic radiosurgery. It is a radiotherapy treatment not a procedure or surgery, used generally to target abnormal areas mainly tumors in brain. As the irradiated volumes of target are very small and can contain dose gradient regions, utmost care must be taken while the dosimeter is used. High spatial resolution is needed. Using Gamma knife system, from simple to complex that involve multiple targets too, dose distributions have been planned and were found to be in agreement with the dose calculated at the isocentre regions but the dose measured was less than that predicted by the planning system (Ibbott et al. 1996, 1997; Maryanski et al. 1996).

8.2 *Brachytherapy*

An advanced treatment of cancer which deals with placing radioactive sources is close toward the tumor area and provides high radiation dose to the tumor with reduced effect on the healthy tissues. Conventional dosimeters can give rise to errors as they quantify dose at a single point and so has limited resolution. The source is placed near to the tumor area with the help of a catheter which is positioned by using a remote afterloading equipment. The use of BANG gel in brachytherapy has been evaluated. The catheter containing the radiation source was placed inside the phantom containing gel. ^{192}Ir and ^{137}Cs sources were studied, and the catheter was placed at the center of the phantom. The absolute dose was observed to be within 7% of that of the dose (Maryanski et al. 1994b, 1996; Audet et al. 1996; McJury et al. 1999b)

8.3 *Intensity-Modulated Radiotherapy*

Gel dosimeters are good candidate for evaluating IMRT dose distribution. Simple phantoms are used generally but anthropomorphic phantoms are also used which can allow direct comparison of measurements done with film or TLD. Several methods have been adopted (Vergote et al. 2003; Low et al. 1999).

8.4 *Other Applications*

The modern techniques require a three-dimensional measurement of dose which makes gel dosimeters applicable in the field. Boron Neutron Capture Therapy (BNCT) is one among such procedures where gel dosimetry has drawn its attention.

Gambarini et al. (1994) worked with gel dosimeter and BNCT. Using BANG3 gel, the exactness of ArcCHECK-3DVH system was evaluated. Accurate estimation of dose distribution was done. But due to MRI noise, slight variations were found between iPAGAT and 3DVH planning (Ono et al. 2015; Watanabe and Nakaguchi 2013).

Nagahata et al. (2014) proposed a useful method with semi-solid polymer gel making use of agar to deal with metallic substances. In addition, Hassani et al. 2014 validated the help of polymer gels in getting three-dimensional distributions in small field sizes as the highly complex treatments like SRS or IMRT use small fields, thus becoming very useful for the treatment.

Also, polymer gels are being used for HDR and verification with treatment planning system (TPS) (Senkesen et al. 2014) as well as for validating circular irradiation fields of 10–30 mm diameter. The results are compared with the planned data (Kawamura et al. 2013).

9 Future Scope and Conclusion

Gel dosimetry fits in place for the idea of acquiring three-dimensional distribution of the absorbed dose when used with complex radiotherapy techniques. The necessary requisites for a typical gel dosimeter are in terms of tissue equivalence, stability, dose rate, spatial integrity, energy dependence, and temperature insensitivity. Since the ultimate goal is to verify the response three-dimensionally and this is the only method to do, care has to be taken at the initial level of preparation of gel, in ensuring the absence of oxygen in the gel that can hinder the polymerization process. Polymer gels with good reproducibility can be achieved when the same protocols are followed with much attention to the concentration of each component in the gel and by maintaining the temperature. Every stage of the process that includes irradiation, storage of the gel, and imaging needs to be monitored to prevent any alterations in the dose response. Readymade gels are also available which can be used as an alternate (MGS, Guildford, New Haven, CT, USA). Advantages of the polymer gel include to be used in various shapes depending upon the need. This technique of extracting dose has been used with various radiation techniques where the conventional dosimeters have failed to do so.

Rapid development is being happened in the area of polymer gel dosimeters. Several aspects in the field of polymer gel as dosimeter have been covered as research. Enormous studies on the gel chemistry and various gel combinations have been carried out. More understanding of the chemical and physical interaction within the gel is required to attain high sensitivity. Different recipes and alternatives for monomers, crosslinkers, antioxidant, and gelling agent are being introduced to fulfill the basic requisite. Furthermore, alternatives can be found which can be less toxic when compared to the existing chemicals used for the manufacture. The different scanning techniques and the gel system scanned have to be optimized for better imaging. Currently, the focus is on less toxic and user-friendly gel dosimeters

and making use of X-ray CT and Optical CT as an alternate for the expensive MRI unit. Optimal gel systems have to be found for different scanning modalities; in MRI, the relaxation rates show significant change, and in X-ray CT the density changes. Using dyes in gel which is radiation sensitive can make it apt for imaging in optical CT.

Focus will also be on investigation on some new ingredients or additives in order to improve the sensitivity of gel and also stability after irradiation. Usage of nanoparticles (high atomic number) as an agent for dose enhancement throws limelight to unexplored paths. So far, only less work has been reported on the application of nanoparticles in gel dosimetry. The most studied nanoparticle among them is gold, though it is not used yet clinically. Research on increasing the efficiency of the treatments based on nanoparticle is underway. Less expensive and alternatives like silver, bismuth, platinum, and hafnium have been produced but not taken to a level as that of gold. Metal or metal oxide nanoparticles can be of scope for dose enhancement which is dependent on the atomic number, electron density, and the energy or irradiation used. Gadolinium and iron nanoparticles can also be used as a favorable for dose enhancement as well as for imaging based on magnetism as they exhibit magnetic properties. Nanoparticles can be prepared by physical, chemical, and biological means and can be introduced into the system. Different sizes, with dopants, can be studied with its effect on sensitivity and factors related to response. Polymer gels thus create a milestone in radiation therapy as carriers of dose distribution which can be identified and evaluated using the readout techniques discussed. New polymer dosimeters that can validate doses below 1 gray are the need of the hour.

References

- Adamovics J, Maryanski M (2003) New 3D radiochromic solid polymer dosimeter from leuco dyes and a transparent polymeric matrix. *Med Phys* 30:1349
- Alexander P, Charlesby A, Ross M (1954) The degradation of solid polymethylmethacrylate by ionizing radiations. *P Roy Soc Lond A Mat* 223:392–404
- Alqathami M, Blencowe A, Yeo UJ, Doran SJ, Qiao G, Geso M (2012) Novel multicompartment 3-dimensional radiochromic radiation dosimeters for nanoparticle-enhanced radiation therapy dosimetry. *Int J Radiat Oncol* 84:e549–e555
- Alqathami M, Blencowe A, Yeo UJ, Franich R, Doran S, Qiao G, Geso M (2013) Enhancement of radiation effects by bismuth oxide nanoparticles for kilovoltage x-ray beams: a dosimetric study using a novel multi-compartment 3D radiochromic dosimeter. *J Phys: Conf Ser* 444:012025
- Andrews HL, Murphy RE, LeBrun EJ (1957) Gel dosimeter for depth dose measurements. *Rev Sci Instrum* 28:329–332
- Atae G, Mahdavi SR, Mohammadi NA, Taheri OM, Khadem AM (2015) Effect of mega voltage energy on dose enhancement in phantom study by using gold nanoparticle polymer gel dosimeter. *Inter J Biomed Sci Engg* 3:1–4
- Audet C, Duzenli C, Kwa W, Tsang V, Mackay A (1996) An example of MRI polymer dosimetry applied to 3D conformal radiotherapy. *Med Phys* 23:803

- Avery S, Kraus J, Lin L, Kassae A, Maryanski M (2015) MO-F-CAMPUS-T02: dosimetric accuracy of the crystalball: new reusable radiochromic polymer gel dosimeter for patient QA in proton therapy. *Med Phys* 42:3581
- Babaei M, Ganjalikhani M (2014) The potential effectiveness of nanoparticles as radiosensitizers for radiotherapy. *Bioimpacts* 4:15–20
- Babic S, Battista J, Jordan K (2009) Radiochromic leuco dye micelle hydrogels: II. Low diffusion rate leuco crystal violet gel. *Phys Med Biol* 54:6791–6808
- Back SA (1998) Implementation of MRI gel dosimetry in radiation therapy. Ph.D. thesis, Department of radiation physics, Malmo Lund University, Sweden
- Baldock C (2006) Historical overview of the development of gel dosimetry. *J Phys: Conf Ser* 56:14–22
- Baldock C, Burford RP, Billingham NC, Cohen D, Keevin SF (1996) Polymer gel composition in MRI dosimetry. *Med Phys* 23:1070
- Baldock C, Burford RP, Billingham NC, Wagner GS, Patval S, Badawi R, Keevil SF (1998a) Experimental procedure for the manufacture and calibration of Polyacrylamide gel (PAG) for magnetic resonance imaging (MRI) radiation dosimetry. *Phys Med Biol* 43:695–702
- Baldock C, Rintoul L, Keevil SF, Pope JM, George GA (1998b) Fourier transform raman spectroscopy of polyacrylamide gels (PAGs) for radiation dosimetry. *Phys Med Biol* 43:3617–3627
- Baldock C, De Deene Y, Doran S, Ibbott G, Jirasek A, Lepage M, McAuley KB, Oldham M, Schreiner LJ (2010) Polymer gel dosimetry. *Phys Med Biol* 55:R1–R63
- Basfar AA, Moftah B, Rabaeh KA, Almousa AA (2015) Novel composition of polymer gel dosimeters based on *N*-(Hydroxymethyl) acrylamide for radiation therapy. *Radiat Phys Chem* 112:117–120
- Bero MA, Gilboy WB, Glover PM, El-masri HM (2000) Tissue-equivalent gel for non-invasive spatial radiation dose measurements. *Nucl Instrum Meth B* 166–167:820–825
- Boni AL (1961) A polyacrylamide gamma dosimeter. *Radiat Res* 14:374–380
- Brun E, Sanche L, Sicard-Roselli C (2009) Parameters governing gold nanoparticle X-ray radiosensitization of DNA in solution. *Colloid Surface B* 72:128–134
- Butterworth KT, McMahan SJ, Currell FJ, Prise KM (2012) Physical basis and biological mechanisms of gold nanoparticle radiosensitization. *Nanoscale* 4:4830–4838
- Chang YJ, Hsieh LL, Liu MH, Liu JS, Hsieh BT (2013) The study of *N*-isopropylacrylamide gel dosimeter doped iodinated contrast agents. *J Phys: Conf Ser* 444:012109
- Cheow WS, Xu R, Hadinoto K (2013) Towards sustainability: new approaches to nano-drug preparation. *Curr Pharm Des* 19:6229–6245
- Cho SH, Jones BL, Krishnan S (2009) The dosimetric feasibility of gold nanoparticle-aided radiation therapy (GNRT) via brachytherapy using low-energy gamma/X-ray sources. *Phys Med Biol* 54:4889–4905
- Cho Y, Lee D, Lee Y, Park J, Kim K, Jung H, Ji Y, Chang U, Kwon S (2014) Dosimetric evaluation of polymer gel dosimeter using saccharide in clinical radiation therapy system. *Int J Radiat Oncol* 90:S936
- Cooper DR, Bekah D, Nadeau JL (2014) Gold nanoparticles and their alternatives for radiation therapy enhancement. *Front Chem* 2:86
- Day MJ, Stein G (1950) Chemical effects of ionizing radiation in some gels. *Nat* 166:146–147
- De Deene Y, Hurley C, Venning A, Vergote K, Mather M, Healy BJ, Baldock C (2002) A basic study of some normoxic polymer gel dosimeters. *Phys Med Biol* 47:3441–3463
- Deyhimahighi N, Mohd Noor N, Soltani N, Jorfi R, Erfani Haghiri M, Adenan MZ, Saion E, Khandaker MU (2014) Contrast enhancement of magnetic resonance imaging (MRI) of polymer gel dosimeter by adding Platinum nano-particles. *J Phys: Conf Ser* 546:012013
- Dong C, Zhang X, Cai H (2014) Green synthesis of monodisperse silver nanoparticles using hydroxyl propyl methyl cellulose. *J Alloy Compd* 583:267–271
- Doran SJ, Koerkamp KK, Bero MA, Jenneson P, Morton EJ, Gilboy WB (2001) A CCD-based optical-CT scanner for high-resolution 3D-imaging of radiation dose distributions: equipment specifications, optical simulations and preliminary results. *Phys Med Biol* 46:3191–3213

- DOSGEL (1999) In: Schreiner LJ, Audet C (eds) Proceeding 1st international workshop on radiation therapy gel dosimetry. Canadian organization of medical physicists, Lexington, KY
- DOSGEL (2001) In: Baldock C, De Deene Y (eds) Proceeding 1st international conference on radiation therapy gel dosimetry. Queensland University of Technology, Brisbane, Australia
- DOSGEL (2004) In: Deene Y De, Baldock C (eds) Proceeding 3rd international conference on radiation therapy gel dosimetry. Ghent University, Ghent, Belgium
- DOSGEL (2006) In: Lepage M, Jirasek A, Schreiner LJ (eds) Proceeding 4th international conference on radiation therapy gel dosimetry. Universit'e de Sherbrooke, Sherbrooke, Canada
- DOSGEL (2008). In: Maris TG, Pappas E (eds) Proceeding 5th international conference on radiation therapy gel dosimetry. University of Crete, Greece
- El- Alaily TM, El- Nimr MK, Saafan SA, Kamel MM, Meaz TM, Assar ST (2015) Construction and calibration of a low cost and fully automated vibrating sample magnetometer. *J Magn Mater* 386:25–30
- Elango G, Roopan SM (2016) Efficacy of SnO₂ nanoparticles toward photocatalytic degradation of methylene blue dye. *J Photochem Photobiol B* 155:34–38
- Elango G, Kumaran SM, Kumar SS, Muthuraja S, Roopan SM (2015) Green synthesis of SnO₂ nanoparticles and its photocatalytic activity of phenolsulfonphthalein dye. *Spectrochim Acta A* 145:176–180
- Farajollahi AR, Bonnett DE, Aukett RJ, Radcliffe AJ (1997) The advantages and limitations of polymer gel dosimetry in brachytherapy. *J Int Fed Med Biol Eng* 35:1012
- Fernandes JP, Pastorello BF, de Araujo DB, Baffa O (2008) Formaldehyde increases MAGIC gel dosimeter melting point and sensitivity. *Phys Med Biol* 53:N53–N58
- Fong PM, Keil DC, Does MD, Gore JC (2001) Polymer gels for magnetic resonance imaging of radiation dose distributions at normal room atmosphere. *Phys Med Biol* 46:3105–3113
- Fricke H, Morse S (1927) The chemical action of Roentgen rays on dilute ferrous sulphate solutions as a measure of radiation dose. *Am J Roentgenol Radium Ther Nucl Med* 18:430–432
- Gafar SM, El-Ahdal MA (2015) Radiochromic fuchsine-gel and its possible use for low dosimetry applications. *Adv Polym Tech*. <https://doi.org/10.1002/adv.21538>
- Gafar SM, El-Kelany MA, El-Ahdal MA, El-Shawadfy SR (2014) Toluidine Blue O-gelatin gel dosimeter for radiation processing. *Open J Polym Chem* 4:56–61
- Gambarini G, Arrigoni S, Bonardi M, Cantone MC, deBartolo D, Desiati S, Facchielli L, Sichirollo AE (1994) A system for 3-D absorbed dose measurements with tissue-equivalence for thermal neutrons. *Nucl Instrum Meth A* 353:406–410
- Gochberg DF, Kennan RP, Maryanski MJ, Gore JC (1998) The role of specific side groups and pH in magnetization transfer in polymers. *J Magn Reson* 131:191–198
- Gore JC, Kang YS, Schulz RJ (1984) Measurement of radiation dose distributions by nuclear magnetic resonance (NMR) imaging. *Phys Med Biol* 29:1189–1197
- Gore JC, Ranade M, Maryanski MJ, Schulz RJ (1996) Radiation dose distributions in three dimensions from tomographic optical density scanning of polymer gels: I. Development of an optical scanner. *Phys Med Biol* 41:2695–2704
- Govi N, Gueye P, Avery S (2013) Application of MAGAT polymer gel dosimetry in breast balloon. *J Phys: Conf Ser* 444:012103
- Hainfeld JF, Slatkin DN, Smilowitz HM (2004) The use of gold nanoparticles to enhance radiotherapy in mice. *Phys Med Biol* 49:N309–N315
- Hainfeld JF, Slatkin DN, Focella TM, Smilowitz HM (2006) Gold nanoparticles: a new x-ray contrast agent. *Br J Radiol* 79:248–253
- Hassani H, Nedaie HA, Zahmatkesh MH, Shirani K (2014) A dosimetric study of small photon fields using polymer gel and Gafchromic EBT films. *Med Dosim* 39:102–107
- Hayashi S, Fujiwara F, Usui S, Tominaga T (2012) Effect of inorganic salt on the dose sensitivity of polymer gel dosimeter. *Radiat Phys Chem* 81:884–888
- Helan V, Prince JJ, Al-Dhabi NA, Arasu MV, Ayeshamariam A (2016) Neem leaves mediated preparation of NiO nanoparticles and its magnetization, coercivity and antibacterial analysis. *Res Phys* 6:712–718

- Hilts M, Duzenli C (2004) Image filtering for improved dose resolution in CT polymer gel dosimetry. *Med Phys* 31:39–49
- Hilts M, Audet C, Duzenli C, Jirasek A (2000) Polymer gel dosimetry using x-ray computed tomography: a feasibility study. *Phys Med Biol* 45:2559–2571
- Hiroki A, Sato Y, Nagasawa N, Ohta A, Seito H, Yamabayashi H, Yamamoto T, Taguchi M, Tamada M, Kojima T (2001) Preparation of polymer gel dosimeters based on less toxic monomers and gellan gum. *J Phys: Conf Ser* 58:7131–7141
- Hiroki A, Yamashita S, Sato Y, Nagasawa N, Taguchi M (2013) New polymer gel dosimeters consisting of less toxic monomers with radiation-crosslinked gel matrix. *J Phys: Conf Ser* 444:012028
- Hoecker FE, Watkins IW (1958) Radiation polymerization dosimetry. *Int J Appl Radiat Is* 3:31–35
- Hsieh B, Chiang C, Hung P, Kao C, Liang J (2011) Preliminary investigation of a new type of propylene based gel dosimeter (DEMBIG). *J Radioanal Nucl Ch* 288:799–803
- Ibbott GS, Bova FJ, Maryanski MJ, Zhang Y, Holcomb S, Avison RG, Meeks SL (1996) Use of BANG polymer gel dosimeter to evaluate repeat-fixation stereotactic radiation therapy. *Med Phys* 23:1070
- Ibbott GS, Maryanski MJ, Eastman P, Holcomb SD, Zhang Y, Avison R, Sanders M, Gore JC (1997) Three dimensional visualization and measurement of conformal dose distributions using magnetic resonance imaging of BANG gel dosimeters. *Int J Radiat Oncol Biol Phys* 38:1097–1103
- Jain S, Hirst DG, O'Sullivan JM (2012) Gold nanoparticles as novel agents for cancer therapy. *Br J Radiol* 85:101–113
- Jelveh S, Chithrani DB (2011) Gold nanostructures as a platform for combinational therapy in future cancer therapeutics. *Cancers* 3:1081–1110
- Jeremic B, Aguerri AR, Filipovic N (2013) Radiosensitization by gold nanoparticles. *Clin Transl Oncol* 15:593–601
- Jirasek A, Hilts M, McAuley KB (2010) Polymer gel dosimeters with enhanced sensitivity for use in x-ray CT polymer gel dosimetry. *Phys Med Biol* 55:5269–5281
- Jordan K (2009) Optical CT scanning of cross-linked radiochromic gel without cylinder wall. *J Phys: Conf Ser* 164:012029
- Jordan K, Avvakumov N (2009) Radiochromic leuco dye micelle hydrogels: I initial investigation. *Phys Med Biol* 54:141–153
- Kakade NR, Sharma SD (2015) Dose enhancement in gold nanoparticle-aided radiotherapy for the therapeutic photon beams using Monte Carlo technique. *J Can Res Ther* 11:94–97
- Kalaiselvi A, Roopan SM, Madhumitha G, Ramalingam C, Elango G (2015) Synthesis and characterization of palladium nanoparticles using Catharanthus roseus leaf extract and its application in the photo-catalytic degradation. *Spectrochim Acta A* 135:116–119
- Kalin IP, Mequanint K (2013) The effect of mixed dopants on the stability of Fricke gel dosimeters. *J Phys: Conf Ser* 444:012105
- Kamiar A, Ghotaslou R, Valizadeh H (2013) Preparation, physicochemical characterization and performance evaluation of gold nanoparticles in radiotherapy. *Adv Pharm Bull* 3:425–428
- Kawamura H, Shinoda K, Miyamoto K, Sakae T, Monma M, Matsumura A (2013) Investigation of polymer gel dosimetry for small circular irradiated fields. *Nihon Hoshasen Gijutsu Gakkai zasshi* 69:933–943
- Kennan RP, Richardson KA, Zhong J, Maryanski MJ, Gore JC (1996) The effects of cross-link density and chemical exchange on magnetization transfer in Polyacrylamide gels. *J Magn Reson* 110:267–277
- Khadem AM, Mahdavi M, Mahdavi SRM, Ataei G (2013) Dose enhancement effect of gold nanoparticles on MAGICA polymer gel in mega voltage radiation therapy. *Int J Radiat Res* 11:55–61
- Khan FM (2003) *The physics of radiation therapy*. Lippincott Williams and Wilkins, Philadelphia
- Khoei S, Mahdavi SR, Fakhimikabir H, Shakeri-Zadeh A, Hashemian A (2014) The role of iron oxide nanoparticles in the radiosensitization of human prostate carcinoma cell line du145 at megavoltage radiation energies. *Int J Radiat Biol* 90:1–6

- Khosravi H, Hashemi B, Mahdavi SR, Hejazi P (2015) Effect of gold nanoparticles on prostate dose distribution under ir-192 internal and 18 mv external radiotherapy procedures using gel dosimetry and monte carlo method. *J Biomed Phys Eng* 5:3–14
- Kobayashi K, Usami N, Porcel E, Lacombe S, LeSech C (2010) Enhancement of radiation effect by heavy elements. *Mutat Res* 704:123–131
- Krstajic N, Doran S (2006) Focusing optics of a parallel beam CCD optical tomography apparatus for 3D radiation gel dosimetry. *Phys Med Biol* 51:2055–2075
- Krstajic N, Doran S (2007) Fast laser scanning optical-CT apparatus for 3D radiation dosimetry. *Phys Med Biol* 52:N257–N263
- Kumar DS, Samuel EJJ (2012) Polymer gel dosimetry for radiation therapy. In: Gopishankar N (ed) *Modern practices in radiation therapy*. Intech, Germany, pp 309–326
- Kumar M, Varshney L, Francis S (2005) Radiolytic formation of Ag clusters in aqueous polyvinyl alcohol solution and hydrogel matrix. *J Radiat Phys Chem* 73:21–27
- Kumar DA, Palanichamy V, Roopan SM (2014) Green synthesis of silver nanoparticles using *Alternanthera dentata* leaf extract at room temperature and their antimicrobial activity. *Spectrochim Acta A* 127:168–171
- Kumar DA, Palanichamy V, Roopan SM (2015) One step production of AgCl nanoparticles and its antioxidant and photo catalytic activity. *Mater Lett* 144:62–64
- Kwatra D, Venugopal A, Anant S (2013) Nanoparticles in radiation therapy: a summary of various approaches to enhance radiosensitization in cancer. *Transl Cancer Res* 2:330–342
- Lai T, Park HG, Choi SH (2007) γ -Irradiation-induced preparation of Ag and Au nanoparticles and their characterizations. *Mater Chem Phys* 105:325–330
- Le Duc G, Miladi I, Alric C, Mowat P, Bräuer-Krisch E, Bouchet A, Khalil E, Billotey C, Janier M, Lux F, Epicier T, Perriat P, Roux S, Tillement O (2011) Toward an image-guided microbeam radiation therapy using gadolinium-based nanoparticles. *ACS Nano* 5:9566–9574
- Le Duc G, Roux S, Paruta-Tuarez A, Dufort S, Brauer E, Marais A, Truillet C, Sancey L, Perriat P, Lux F, Tillement O (2014) Advantages of gadolinium based ultrasmall nanoparticles vs molecular gadolinium chelates for radiotherapy guided by MRI for glioma treatment. *Cancer Nanotechnol* 5:4
- Leung MKK, Chow JCL, Chithrani BD, Lee MJG, Oms B, Jaffray DA (2011) Irradiation of gold nanoparticles by x-rays: monte carlo simulation of dose enhancements and the spatial properties of the secondary electrons production. *Med Phys* 38:624–631
- Low DA, Dempsey JF, Venkatesan R, Mutic S, Markman J, Haacke EM, Purdy JA (1999) Evaluation of polymer gels and MRI as a 3D dosimeter for intensity-modulated radiation therapy. *Int J Radiat Oncol Biol Phys* 26:15
- Maggiorella L, Barouch G, Devaux C, Pottier A, Deutsch E, Bourhis J, Borghi E, Levy L (2012) Nanoscale radiotherapy with hafnium oxide nanoparticles. *Future Oncol* 8:1167–1181
- Mahdavi M, Khadem AM, Mahdavi SRM, Ataei G (2013) Effect of gold nanoparticle on percentage depth dose enhancement on megavoltage energy in MAGICA polymer gel dosimeter. *J Biomed Phys Eng* 3:37–44
- Marill J, Anesary NM, Zhang P, Vivet S, Borghi E, Levy L, Pottier A (2014) Hafnium oxide nanoparticles: toward an in vitro predictive biological effect? *Radiat Oncol* 9:150
- Marques T, Schwarcke M, Garrido C, Zucolotto V, Baffa O, Nicolucci P (2010) Gel dosimetry analysis of gold nanoparticle application in kilovoltage radiation therapy. *J Phys: Conf Ser* 250:012084
- Maryanski MJ, Gore JC, Schulz RJ (1992) 3-D radiation dosimetry by MRI: solvent proton relaxation enhancement by radiation-controlled polymerisation and cross-linking in gels. *Proc Intl Soc Mag Reson Med* (New York)
- Maryanski MJ, Gore JC, Kennan RP, Schulz RJ (1993) NMR relaxation enhancement in gels polymerized and cross-linked by ionizing radiation: a new approach to 3D dosimetry by MRI. *Magn Reson Imaging* 11:253–258
- Maryanski MJ, Gore JC, Schulz R (1994a) Three-dimensional detection, dosimetry and imaging of an energy field by formation of a polymer in a gel. US Patent 5,321,357

- Maryanski MJ, Schulz RJ, Ibbott GS, Gatenby JC, Xie J, Horton D, Gore JC (1994b) Magnetic resonance imaging of radiation dose distributions using a polymer-gel dosimeter. *Phys Med Biol* 39:1437–1455
- Maryanski MJ, Zastavker YZ, Gore JC (1996) Radiation dose distributions in three dimensions from tomographic optical density scanning of polymer gels: 2. Optical properties of the BANG polymer gel. *Phys Med Biol* 41:2705–2717
- Maryanski MJ, Audet C, Gore JC (1997) Effects of crosslinking and temperature on the dose response of a BANG polymer gel dosimeter. *Phys Med Biol* 42:303–311
- Mather ML, Charles PH, Baldock C (2003) Measurement of ultrasonic attenuation coefficient in polymer gel dosimeters. *Phys Med Biol* 48:N269–N275
- Mattea F, Chacón D, Vedelago J, Valente M, Miriam CS (2015) Polymer gel dosimeter based on itaconic acid. *Appl Radiat Isotopes* 105:98–104
- McJury M, Oldham M, Leach MO, Webb S (1999a) Dynamics of polymerization in polyacrylamide gel (PAG) dosimeters: (i) aging and long-term stability. *Phys Med Biol* 44:1863–1873
- McJury M, Tapper PD, Cosgrove VP, Murphy PS, Griffin S, Leach M, Webb S, Oldham M (1999b) Experimental 3D dosimetry around a high dose-rate clinical ¹⁹²Ir source using a polyacrylamide gel (PAG) dosimeter. *Phys Med Biol* 44:2431–2444
- McJury M, Oldham M, Cosgrove VP, Murphy PS, Doran S, Leach MO, Webb S (2000) Radiation dosimetry using polymer gels: methods and applications. *Br J Radiol* 73:919–929
- McMahon SJ, Mendenhall MH, Jain S, Currell F (2008) Radiotherapy in the presence of contrast agents: a general figure of merit and its application to gold nanoparticles. *Phys Med Biol* 53:5635–5651
- Meesat R, Jay-Gerin JP, Khalil A, Lepage M (2009) Evaluation of the dose enhancement of iodinated compounds by polyacrylamide gel dosimetry. *Phys Med Biol* 54:5909–5917
- Miladi I, Le Duc G, Kryza D, Bernard A, Mowat P, Roux S, Taleb J, Bonazza P, Perriat P, Lux F, Tillement O, Billotey C, Janier M (2013) Biodistribution of ultrasmall gadolinium-based nanoparticles as theranostic agent: application to brain. *J Biomater Appl* 28:385–394
- Nagahata T, Yamaguchi H, Monzen H, Nishimura Y (2014) The use of polymer gel dosimetry to measure dose distribution around metallic implants. *Nihon Hoshasen Gijutsu Gakkai Zasshi* 70:1160–1165
- Oldham M, McJury M, Baustert I, Webb S, Leach MO (1998) Improving calibration accuracy in gel dosimetry. *Phys Med Biol* 43:2709–2720
- Oldham M, Siewerdsen JH, Shetty A, Jaffray DA (2001) High resolution gel-dosimetry by optical-CT and MR scanning. *Med Phys* 28:1436–1445
- Olsson LE, Westrin BA, Fransson A, Nordell B (1992) Diffusion of ferric ions in agarose dosimeter gels. *Phys Med Biol* 37:2243–2252
- Ono K, Fujimoto S, Hayashi S, Miyazawa M, Akagi Y, Hirokawa Y (2015) Dosimetric evaluation of ArcCHECK and 3DVH system using customized polymer gel dosimeter. *Med Phys* 42:3406
- Pal SL, Jana U, Manna PK, Mohanta GP, Manavalan R (2011) Nanoparticle: an overview of preparation and characterization. *J Appl Pharm Sci* 1:228–234
- Pilarova (Vavru) K, Kozubikovaá P, Solc J, Spevacek V (2014) Characteristics of polyacrylamide gel with THPC and tumbull blue gel dosimeters evaluated using optical tomography. *Radiat Phys Chem* 104:283–286
- Porcel E, Liehn S, Remita H, Usami N, Kobayashi K, Furusawa Y, Le Sech C, Lacombe S (2010) Platinum nanoparticles: a promising material for future cancer therapy? *Nanotechnol* 21:085103
- Porcel E, Kobayashi K, Usami N, Remita H, Le Sech C, Lacombe S (2011) Photosensitization of plasmid-DNA loaded with platinum nano-particles and irradiated by low energy X-rays. *J Phys: Conf Ser* 261:012004
- Rabin O, Perez JM, Grimm J, Wojtkiewicz G, Weissleder R (2006) An X-ray computed tomography imaging agent based on long-circulating bismuth sulphide nanoparticles. *Nat Mater* 5:118–122

- Rahman WN, Bishara N, Ackerly T, He CF, Jackson P, Wong C, Davidson R, Geso M (2009) Enhancement of radiation effects by gold nanoparticles for superficial radiation therapy. *Nanomed Nanotechnol* 5:136–142
- Rahman WN, Wonga CJ, Yagi N, Davidson R, Geso M (2010) Dosimetry and its enhancement using gold nanoparticles in synchrotron based microbeam and stereotactic radiosurgery. *AIP Conf Proc* 1266:107
- Roopan SM, Bharathi A, Kumar R, Khanna VG, Prabhakarn A (2012) Acaricidal, insecticidal, and larvicidal efficacy of aqueous extract of *Annona squamosa* L peel as biomaterial for the reduction of palladium salts into nanoparticles. *Colloid Surf B* 92:209–212
- Roopan SM, Surendra TV, Elango G, Kumar SHS (2014) Biosynthetic trends and future aspects of bimetallic nanoparticles and its medicinal applications. *Appl Microbiol Biotechnol* 98:5289–5300
- Sakhalkar HS, Oldham M (2008) Fast, high-resolution 3D dosimetry utilizing a novel optical-CT scanner incorporating tertiary telecentric collimation. *Med Phys* 35:101–111
- Samuel EJJ, Sathiyaraj P, Titus D, Kumar DS (2015) Antioxidant effect of green tea on polymer gel dosimeter. *J Phys: Conf Ser* 573:012065
- Schreiner LJ (2004) Review of Fricke gel dosimeters. *J Phys: Conf Ser* 3:9–21
- Sellakumar P, Samuel EJJ, Supe SS (2007) Water equivalence of polymer gel dosimeters. *Radiat Phys Chem* 76:1108–1115
- Senden RJ, De Jean P, McAuley KB, Schreiner LJ (2006) Polymer gel dosimetry with reduced toxicity: a preliminary investigation of the NMR and optical dose–response using different monomers. *Phys Med Biol* 51:3301–3314
- Senkesen O, Tezcanli E, Buyuksarac B, Ozbay I (2014) Comparison of 3D dose distributions for HDR 192Ir brachytherapy sources with normoxic polymer gel dosimetry and treatment planning system. *Med Dosim* 39:266–271
- Solc J, Spevacek V (2009) New radiochromic gel for 3D dosimetry based on Turnbull blue: basic properties. *Phys Med Biol* 54:5095–5101
- Soliman YS (2014) Gamma-radiation induced synthesis of silver nanoparticles in gelatin and its application for radiotherapy dose measurements. *Radiat Phys Chem* 102:60–67
- Su XY, Liu PD, Wu H, Gu N (2014) Enhancement of radiosensitization by metal-based nanoparticles in cancer radiationtherapy. *Cancer Biol Med* 11:86–91
- Subramanian B, Ravindran PB, Baldock C (2006) Optimization of the imaging protocol of an X-ray CT scanner for evaluation of normoxic polymer gel dosimeters. *J Med Phys* 31:72–77
- Surendra TV, Roopan SM, Arasu MV, Al-Dhabi NA, Rayalu GM (2016) RSM optimized *Moringa oleifera* peel extract for green synthesis of *M. oleifera* capped palladium nanoparticles with antibacterial and hemolytic property. *J Photochem Photobiol, B* 162:550–557
- Taupin F, Flaender M, Delorme R, Brochard T, Mayol J, Arnaud J, Perriat P, Sancey L, Lux F, Barth RF, Carrière M, Ravanat J, Elleaume H (2015) Gadolinium nanoparticles and contrast agent as radiation sensitizers. *Phys Med Biol* 60:4449–4464
- Tengire MK, Joshi SS (2004) Optical and structural studies of silver nanoparticles. *J Radiat Phys Chem* 71:1039–1044
- Thakur VK, Kessler MR (2015) Self-healing polymer nanocomposite materials: a review. *Polymer* 69:369–383
- Thakur VK, Thakur MK (2014) Recent trends in hydrogels based on psyllium polysaccharide: a review. *J Clean Prod* 82:1–15
- Thakur VK, Thakur MK (2015) Recent advances in green hydrogels from lignin: a review. *Int J Biol Macromolec* 72:834–847
- Trapp JV, Leach MO, Webb S (2005) Preliminary dose response study of a gel dosimeter using 2-Hydroxyethyl Methacrylate (HEMA). *Australas Phys Eng Sci Med* 28:172–174
- Vachier MC, Rutledge DN (1996) Influence of temperature, pH, water content, gel strength and their interactions on NMR relaxation of gelatins ID analysis of the calculated relaxation times. *J Magn Reson Analysis* 2:311–320
- Van den Heuvel F, Locquet JP, Nuyts S (2010) Beam energy considerations for gold nano-particle enhanced radiation treatment. *Phys Med Biol* 55:4509–4520

- Van Doorn T, Bhat M, Rutten TP, Tran T, Costanzo A (2005) A fast, high spatial resolution optical tomographic scanner for measurement of absorption in gel dosimetry. *Australas Phys Eng Sci Med* 28:76–85
- Vegeera AV, Zimon AD (2006) Synthesis and physicochemical properties of silver nanoparticles stabilized by acid gelatin. *Rus J Appl Chem* 79:1403–1406
- Venning AJ, Hill B, Brindha S, Healy BJ, Baldock C (2005a) Investigation of the PAGAT polymer gel dosimeter using magnetic resonance imaging. *Phys Med Biol* 50:3875–3888
- Venning AJ, Nitschke KN, Keall PJ, Baldock C (2005b) Radiological properties of normoxic polymer gel dosimeters. *Med Phys* 32:1047–1053
- Vergote K, De Deene Y, Claus F, De Gersem W, Van Duyse B, Paelinck L, Achten E, De Neve W, De Wagter C (2003) Application of monomer/polymer gel dosimetry to study the effects of tissue inhomogeneities on intensity-modulated radiation therapy (IMRT) dose distributions. *Radiother Oncol* 67:119–128
- Vergote K, De Deene Y, Bussche EV, De Wagter C (2004) On the relation between the spatial dose integrity and the temporal instability of polymer gel dosimeters. *Phys Med Biol* 49:4507–4522
- Watanabe Y, Nakaguchi Y (2013) 3D evaluation of 3DVH program using BANG3 polymer gel dosimeter. *Med Phys* 40:082101
- Wuu C-S, Schiff P, Maryanski MJ, Liu T, Borzillary S, Weinberger J (2003) Dosimetry study of Re-188 liquid balloon for intravascular brachytherapy using polymer gel dosimeters and laser-beam optical-CT scanner. *Med Phys* 30:132–137
- Yao T, Denkova AG, Warman JM (2014) Polymer-gel formation and reformation on irradiation of tertiary-butyl acrylate. *Radiat Phys Chem* 97:147–152
- Yun Z, Pingqiang W, Bo L, Li Maoshun, Wuxiong F, Rui C (2010) An improvement for polymer gel dosimeter of type PAGAT. *Nucl Electron Detect Technol* 30:935–939
- Zhang XD, Wu D, Shen X, Chen J, Sun YM, Liu PX, Liang XJ (2012) Size-dependent radiosensitization of PEG-coated gold nanoparticles for cancer radiation therapy. *Biomaterials* 33:6408–6419
- Zhu X, Reese TG, Crowley EM, El Fakhri G (2010) Improved MAGIC gel for higher sensitivity and elemental tissue equivalent 3D dosimetry. *Med Phys* 37:183–188

Chapter 9

Polymeric Gels: Vehicles for Enhanced Drug Delivery Across Skin



Rachna Prasad and Veena Koul

Abstract Polymeric gels have emerged as promising vehicles for drug delivery across the skin. Stratum corneum, the topmost layer of the skin, does not allow hydrophilic and high molecular weight drugs to permeate without enhancing techniques. A number of enhancement techniques are being developed to increase the transdermal drug permeation. The transdermal route has many advantages and has therefore evolved as an attractive and convenient alternative to the existing routes of drug delivery that causes many side effects. In the present chapter, we shall be focusing on the physical enhancement techniques of iontophoresis, electroporation and sonophoresis for transport of drug molecules across skin using polymeric gels.

Keywords Polymeric gels · Transdermal drug delivery · Skin Iontophoresis · Electroporation · Sonophoresis

1 Introduction

Polymeric gels have emerged as promising vehicles for drug delivery across the skin. Skin, a complex and heterogeneous biological barrier is the main hurdle for transdermal delivery of drugs. Drug delivery through the skin is an attractive and convenient alternative to the conventional routes. To facilitate drug transport across the skin, polymeric gels have been employed to encapsulate the drug and allow its permeation in a controlled manner. The word 'gel' was coined by a Scottish

R. Prasad
Centre for Biomedical Engineering, Indian Institute of Technology,
New Delhi, India

V. Koul (✉)
Biomedical Engineering Unit, All India Institute of Medical Sciences,
New Delhi, India
e-mail: veenak_iitd@yahoo.com

chemist, Thomas Graham, the Father of Colloid Science in 1861. Additionally, these gels are helpful as drug carriers for high molecular weight hydrophilic drugs.

To overcome the skin barrier function and enhance transdermal drug transport, a wide variety of enhancing methods, including formulations and device-based technologies, have been developed. In the present chapter, we shall be focusing on the device-based (physical enhancement) techniques of iontophoresis, electroporation and sonophoresis.

2 Polymeric Gels

Transdermal drug delivery systems have gained importance over the other modes of delivery both in research and marketable products. However, designing a suitable vehicle for drug delivery through the skin is challenging.

Vehicles (polymeric gels, creams, emulsions, lotions, etc.) have a noticeable effect especially on the skin preparations and play an important role in delivering the drug molecules to the application site/target organ.

Gels are suitable vehicle for transdermal drug delivery systems especially for iontophoresis, electroporation, sonophoresis, and other device-based non-invasive enhancement approaches because they can easily mix with the delivery system and also match the contours of the skin. Thus, these polymeric gels act as an important connector/link between the skin, drug and the device. Being soft and wet material, these gels can withstand huge deformation and form a backbone for the control of drug release (Osada and Gong 1998). They are either semi-solid or cross-linked, three-dimensional polymeric network structure. They comprise small amount of solid particles dispersed in large amount of liquid/water, thus giving them a semi-solid character that has the ability to swell or shrink (Bhojar et al. 2012). Because of their inherent remarkable properties, these gels have wide applications in medicine, biotechnology, food industry and cosmetics (Rehman and Zulfakar 2014). Many polymeric gels possess charges in their network and are important for electrically enhanced drug delivery (Oosawa 1957; Gong et al. 1997).

Gel-forming polymers can be classified as natural, semisynthetic and synthetic. The different polymers that are commonly used for application on skin are derivatives of polyacrylic acid like carbomers, polyvinylpyrrolidone, polyvinylalcohol, carrageenan, chitosan, cellulose derivatives like carboxymethyl cellulose, hydroxypropyl methyl cellulose, hydroxyethyl cellulose and hydroxypropyl cellulose (Fig. 1). They are safe and non-toxic, and they also do not permeate through the skin and do not cause skin irritation (Saroja et al. 2013; Uma et al. 2002). The polymers are used in the concentration range of 1–5% for gel formulations and are responsible for its consistency and viscoelastic property (Valenta and Auner 2004).

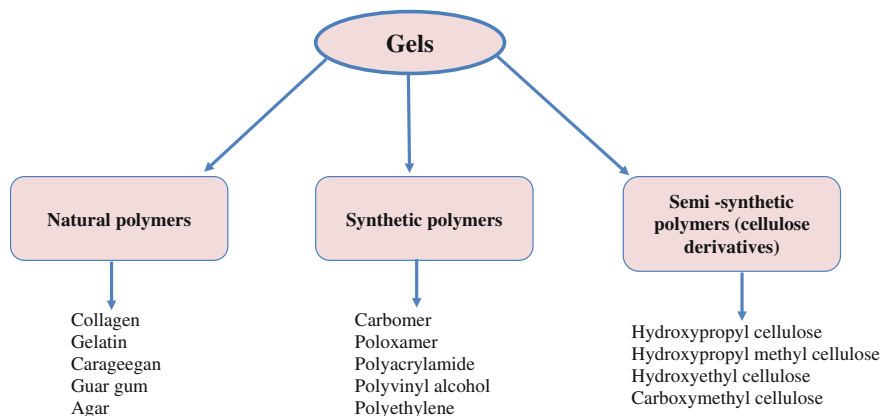


Fig. 1 Classification of the polymers used in transdermal drug delivery

2.1 Classification of Gel

They are classified as physical gels and chemical gels based on their internal structure. As the name suggests, physical gels are the noncovalent gels and are held together by physical bonds, i.e. the crosslinking is due to weak physical forces like hydrogen bonding, ionic interactions, van der Waals, etc., and are thus reversible, whereas chemical gels are the covalently crosslinked gels that are held by chemical bonds and are irreversible and are categorized under hydrogels (Jagur-Grodzinski 2010).

Polymeric gels can be deformed by various external stimuli like temperature, pH, ionic strength, electric field, etc. This ability to withstand swelling and collapsing as a function of their environment is the most significant property of these materials. The gel volume transitions have motivated/impelled the researchers to explore these polymeric gels for many different applications like drug delivery, sensors, actuators, etc. (Osada and Gong 1998).

2.2 Hydrogel

Hydrogels are three-dimensional, cross-linked, hydrophilic polymeric network (can be made of natural or synthetic polymers) and were first synthesized by Wichterle and Lim in 1959 (Wichterle and Lim 1960). They can absorb large quantity of water (can contain 99.9% or more) or biological fluid and swell tremendously, but maintain their three-dimensional structure and do not dissolve in it (Gehrke and Lee 1990). The hydrophilic part of the hydrogel is responsible for interaction with water or biological fluid and promoting swelling. Because of the excellent biocompatibility and hydrophilicity and also due to the soft and elastic nature, the hydrogels

are widely used in many biomedical and pharmaceutical applications including drug delivery (Khademhosseini and Langer 2007; Park et al. 2011).

Hydrogels are divided according to their composition, chemical constituents, physical nature, degradation behaviour and environmental response (Fig. 2).

Hydrogels can be made of homopolymers (single polymer) or copolymers (more than one polymer), and are crosslinked either chemically or physically (Wichterle and Lim 1960; Lee and Mooney 2001; Drury and Mooney 2003). The chemical crosslinked networks are called interpenetrating networks (IPNs). IPNs are further divided into (i) full IPNs and (ii) semi-IPNs. Both the polymeric chains are crosslinked in full IPNs, whereas in semi-IPNs, only one chain is crosslinked.

Hydrogels have further been classified as amorphous, semicrystalline and complexation depending on their physical nature. Environmental responsive hydrogels are sensitive to variables like temperature, pH, ionic strength, electric and magnetic field. These stimuli-sensitive hydrogels undergo significant volume changes with slight changes in environment and thus have a sensor and effector function and are also called intelligent materials (Qiu and Park 2001; Kost and Langer 2001; Tuncel et al. 2002; Jeong et al. 2002; Kikuchi and Okano 2002; Miyata et al. 2002; Hoare and Kohane 2008; Samchenko et al. 2011). Depending on their ionic charge, they have been classified as neutral, anionic and cationic, and play significant role in drug delivery based on the application.

For drug delivery applications, the hydrogel allows sustained release of drug. Diffusion and chemical stimulation are the two mechanisms by which drug release from hydrogels takes place. The swelling behaviour of the hydrogels can be manipulated based on their chemical moiety and interactions employed for their formation.

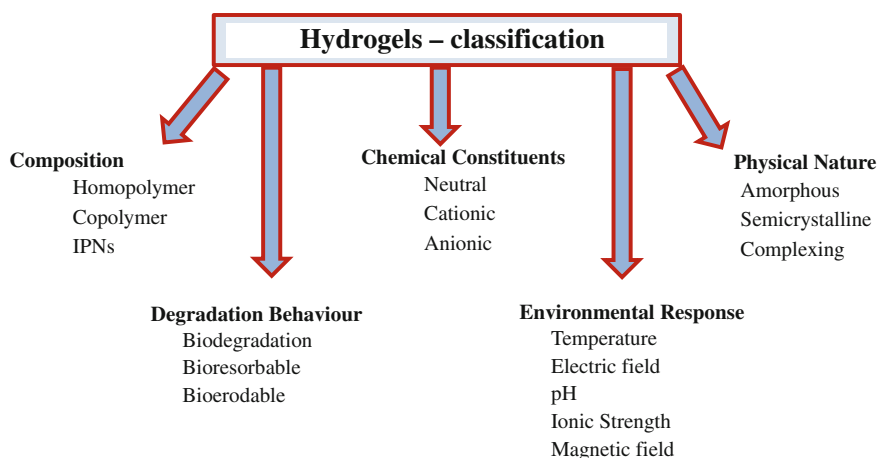


Fig. 2 Classification of hydrogels

The swelling behaviour of the hydrogel is expressed as swelling ratio, degree of swelling, equilibrium swelling and percentage swelling. These are measured by weight or volume changes.

1. Swelling ratio = W_t/W_i ,
2. Degree of swelling at time $t = [W_t/W_i]/W_i$,
3. Equilibrium swelling = $[W_f - W_i]/W_i$,

where W_t is the weight of swollen gel at time 't',

W_i = initial weight of the dry gel,

W_f = final constant weight of the gel after equilibrium.

4. Volume swelling ratio = V_s/V_o ,

where V_o is the initial volume and V_s is the final volume of the hydrogel.

Crosslinking density, chemical structure and ionic strength of the surrounding media (environment) affect the water absorption capacity/swelling behaviour of hydrogels.

Crosslinking ratio is very important, and it controls the swelling behaviour of the hydrogel. It is defined as the ratio of moles of crosslinker to the moles of polymer. With increase in crosslinking, the swelling of hydrogel decreases, because the crosslinking hinders the mobility of the polymer chain, which in turn lowers the swelling ratio.

Peppas et al. (1987) have proposed a mathematical model to evaluate the properties of hydrogel and also to predict the mechanism of drug release.

The transport kinetics can be determined by fitting the swelling curves in the equation given below (Peppas and Ritger 1987a, b):

$$M_t/M_\infty = kt^n$$

where M_t is the solvent uptake at 't', M_∞ is the equilibrium solvent uptake at infinity (∞), k is a constant and t is the time. The numerical value of the exponent 'n' gives an insight into the mode of transport, which can be obtained as a slope of M_t/M_∞ versus t on log/log scale. The transport mechanism is said to be Fickian or Case I type, where the rate of diffusion of solvent is slower than chain stretching and the value of n is between 0 and 0.5. It is non-Fickian or anomalous type, where the rates of solvent diffusion and chain stretching are comparable and the value of n is between 0.5 and 1. The mode of transport is Case II type when the rate of diffusion of solvent is faster than chain stretching and here the values of n will be greater than 1.

2.3 Hydrogels for Transdermal Drug Delivery

The advantages of gel formulation for transdermal drug delivery include ease of application, controlled drug release, greaseless, non-staining, easily removable, emollient and compatible with many drugs. Moreover, these formulations can

increase the skin compliance as they can absorb the skin secretion, which may become irritating under long-term occlusion (Banga and Chein 1993).

Different gels have been tried for transdermal delivery of drugs and a successful product, Testogel for testosterone delivery, is in commercial use. This product is based on polyacrylate (carbomer) (Valenta and Auner 2004).

Many other drugs are also being tested for transdermal delivery with the help of gels, e.g. insulin delivery has been tried with poloxamer gel in rats and promising results were obtained (Pillai and Panchagnula 2003). Transdermal delivery of Ibuprofen loaded in silicone and cellulose polymer gel has been tested across rat skin both in vitro and in vivo (Aliyar et al. 2014). poly (*N*-vinyl caprolactam) [PNVCL]-based polymeric gel and copolymer of chitosan and poly (*N*-vinyl caprolactam) [PNVCL]-based gel were explored for delivery of hydrophilic as well as hydrophobic drug. They showed the feasibility of being used as transdermal drug delivery systems for the management of pain (Indulekha et al. 2016). Release of silver sulfadiazine from hydrogels was examined for antimicrobial topical applications, and the results suggested that these hydrogels can be used topical drug delivery (Jodar et al. 2015). Recently, Kong et al. (2016) studied transdermal delivery of isoliquiritigenin loaded in hyaluronic acid (HA)-hydroxyethyl cellulose (HEC) hydrogels and reported that the hydrogel significantly improved drug permeation (Kong et al. 2016).

The hydrogels which have been studied for the purpose of iontophoresis include polyacrylamide, poly (2-hydroxyethyl methacrylate), cellulose polymers, polyvinylalcohol (PVA), polyvinylpyrrolidone (PVP) and hydrogels from natural source, for example, agar and chitosan. Banga and Chein (1993) investigated the polyacrylamide and poly (2-hydroxyethyl methacrylamide) hydrogels for the iontophoretic delivery of peptide drugs, viz., vasopressin, calcitonin and insulin. Fang et al. (1999; 1998a, b, 1996) investigated several hydrogels belonging to cellulose derivatives like methyl cellulose (MC), hydroxypropyl methyl cellulose (HPMC), hydroxypropyl cellulose (HPC) and carboxymethyl cellulose sodium (SCMC) for iontophoresis application. Studies of Gupta et al. (1994) demonstrated that non-ionic hydrogels provide better iontophoretic flux than ionic polymers.

More recently hydrogels are also being used as microneedles to facilitate drug delivery across the skin (Kearney et al. 2016). It has been reported that when these hydrogel microneedles are inserted into the skin, they absorb body fluids and swell, thus creating porous network and channels for the movement of drug from the patch to the skin dermal circulation. These hydrogel microneedles have unique features and are thus suitable for a wide variety of drug delivery applications. They also overcome the shortcomings of the conventional ones. The commercialization of this technology is in progress (Donnelly et al. 2012, 2013). Kearney et al. (2016) have successfully demonstrated the transdermal delivery of Donepezil for Alzheimer's disease using hydrogel microneedles. Jeong et al. (2008) have reported that this system possesses the convenience of a transdermal patch along with the effectiveness of a needle.

3 Transdermal Drug Delivery

In the broadest sense, transdermal drug delivery includes all topically applied formulations with the purpose of bringing the therapeutic molecules into the systemic circulation. Transdermal drug delivery systems (TDDS) include a number of non-invasive to minimally invasive technologies for the delivery of therapeutic molecules through the skin (Prausnitz and Langer 2008; Schuetz et al. 2005; Barry 2001). The delivery of drugs transdermally has enormous potential as the skin offers a large surface area for the non-invasive administration of drugs. Transdermal application permits localized drug delivery to the site of interest, thus enhancing the therapeutic effect and minimizing the systemic side effects. It totally avoids pain and presystemic metabolism, and the drug pharmacokinetics is more uniform (Quinn et al. 2016; Ita 2014; Barry 1983).

The clinical reality of transdermal drug delivery began with the scopolamine patches that were approved in 1979. However, it was the nicotine patch introduced for smoking cessation in 1991 that revolutionized the transdermal market. In the last four decades, TDD has made significant progress and now represents a successful method of delivering a large number of drugs, namely, scopolamine, nitroglycerine, nicotine, clonidine, lidocaine, estradiol, fentanyl, testosterone and oxybutynin (Lane 2013; Prausnitz et al. 2004; Langer 2004; Kalia et al. 1998). Hence, it is considered to be one of the most successful controlled release technologies in terms of number of approved products that are in the market (Guy 1996; Nair et al. 1999). In the USA, 51 out of the 129 drug delivery candidates under clinical evaluation and 23 out of 77 drug candidates are under preclinical evaluation belong to transdermal/dermal systems. Thus, transdermal drug delivery is the most successful research area in drug delivery. The worldwide market for transdermal patches is approximately \$32 billion, which is based on the abovementioned few drugs.

Table 1 lists the drugs which are clinically used as transdermal systems for patients. These drugs are loaded either in patch, matrix or gel system and do not use any assistive devices for drug release and permeation (Paudel et al. 2010).

Rotigotine patch introduced in 2007 was recalled in 2008 because of delivery problems but was reformulated and the reintroduced in 2012.

Some therapeutic agents are used as topical gel and patch mainly for the local treatment of pain and for local anaesthesia, e.g. Capsaicin patch for pain relief, diclofenac gel for osteoarthritis, lidocaine cream for local anaesthesia, menthol and capsaicin for arthritic pain, trolamine salicylate as cream for muscle and joint pain and salicylic acid patch for acne vulgaris and hyperkeratotic psoriasis (Paudel et al. 2010). Few drug formulations are under different stages of FDA-approved clinical trials and would soon be available for commercial use.

The main advantages of TDDS over conventional dosage forms are as follows:

1. Easy accessibility of skin.
2. Non-invasive mode of drug delivery, thus no trauma or risk of infection.

Table 1 Transdermal products in the market

Year	Drug	Uses
1979	Scopolamine	Motion sickness, postoperative nausea and vomiting
1981	Nitroglycerin	Angina prophylaxis
1984	Clonidine	Hypertension
1986	Estradiol	Menopause, postmenopausal and osteoporosis, in case of lowered oestrogen levels
1990	Fentanyl	Chronic pain
1991	Nicotine	Smoking cessation
2000	Testosterone	Hypogonadism (testosterone deficiency)
2006	Methylphenidate	Attention-deficit hyperactivity disorder
2006	Selegiline	Major depressive disorder
2007	Rotigotine	Parkinson's disease
2007	Rivastigmine	Dementia associated with Alzheimer's disease and Parkinson's disease
2009	Oxybutynin	Bladder muscle dysfunction

3. Avoids the gastrointestinal drug absorption and drug degradation by gastrointestinal enzymes.
4. Avoids the first pass metabolism, thereby increasing bioavailability.
5. Avoids the risk and inconveniences of intravenous therapy.
6. Less proteolytic enzymes.
7. Permits the use of a drug with a very short biological half-life.
8. Sustained and controlled drug administration, and thus, frequent medicine intake is no longer necessary, thereby improving patient compliance.
9. Permits rapid termination of medication, if needed, by removal of drug patch from the surface of skin.
10. Highly patient compliant.
11. Non-invasive, convenient, inexpensive and can be self-administered.

In spite of all the advantages and after nearly four decades of extensive research, only a few transdermal products are available in the market and the route is restricted to the delivery of small, lipophilic drug molecules. Due to the advances in the biotechnological science, a number of products mainly, larger molecules and biomolecules like proteins, oligonucleotides, small interfering RNA, hormones and vaccines are being developed but the main concern lies in the transport across the skin.

Hence, various chemical and physical enhancement approaches are being explored to increase drug permeation across the skin (Langer 2004).

The skin morphology and physiology is very important in determining the drug transport. Hence, we shall discuss the skin structure in detail, i.e. stratum corneum, viable epidermis, dermis and deeper layers and appendages.

4 Skin

Skin is the largest, multifunctional and most complex organ of the body with a surface area of 2 m^2 in human adults. From the very beginning of mankind, skin has played the role of a unique interface and important barrier between the internal organs of the body and external environment. It is also the basis for multi-billion dollar industries of personal care, cosmetics and beauty and fashion business. For pharmaceutical industry, the skin offers a big opportunity due to the large surface area for painless and patient-friendly drug delivery/administration but at the same time also poses a big challenge due of the barrier property of its outermost stratum corneum layer. This layer of the skin serves as the barrier to both the entry and exit of molecules.

The stratum corneum is composed of dead cells, corneocytes that are filled with keratin and are embedded in an extracellular matrix of multilamellar lipid bilayers. For the effective/proper functioning of the skin, it has to be continuously regenerated and hence has a very unique structure to meet this demand. There is a transition from living cells of stratum basale to the dead corneocytes of stratum corneum embedded in skin lipids, thus imparting/offering a high degree of barrier property to it.

The skin has emerged from its classical brick-and-mortar model to a smart, composite and intelligent biopolymer which responds to every external stimulus.

A lot of literature and knowledge have been generated in the last 3–4 decades, still the optimal use/usage of skin as delivery route needs to be established.

4.1 Skin Anatomy

Skin is a complex, multicomponent, dynamic organ and has many functions beyond its role as a barrier to the environment (Mitragotri 2004). It receives about a third of the total blood supply and is a physical and chemical barrier separating the external environment and the internal organs, is a site of thermoregulation (controls and regulates body temperature) and acts as a sensory organ. The skin is also part of our immune system. It is completely renewed every month to maintain its properties (Christophers et al. 1989).

The skin consists of two layers, epidermis and dermis (Williams 2003).

The epidermis is mainly made of keratinocytes (95%). It is 100–150 μm thick and divided into four layers: stratum corneum (SC), the topmost layer, stratum granulosum (SG), stratum spinosum (SS) and stratum basale (SB).

SB is a single layer of oval-shaped cells on the dermal–epidermal junction, nucleated and has intracellular organelles and is metabolically active. In normal skin, only basal cells divide. It also contains a variety of other cells, melanocytes that provide colour (melanin pigment), Langerhans cells that play a critical role in the immunology of skin and Merkel cells functioning as mechanoreceptors to skin.

Stratum spinosum (SS) and stratum granulosum (SG) cells undergo rapid differentiation. During differentiation from basal cells to stratum corneum, the entire cellular make-up changes. During the movement of cells towards SC across the SS and SG, they shrink, flatten and initiate production of keratohyalin granules, lamellar bodies and filaments. At the interface of SG and SC, differentiation of cells ceases and apart from granules and filaments, other intracellular constituents are degraded into protein forming insoluble matrix of keratin. Granules are extruded from cell by exocytosis and form intercellular lipid domain 'mortar', in between keratin-filled cells (corneocytes). Lipids are covalently bound to corneocyte pockets and serve as template for orientation of initially extruded granule contents (Chang et al. 1993; Swartzendruber et al. 1987). This configuration of lipids over corneocytes imparts high degree of barrier property to SC for permeation of drug molecules. The SC consists of cells (corneocytes, 20–40 μm in diameter) that are elongated and flattened, hexagonal in shape, completely devoid of intracellular organelles, organized in columns (Christophers et al. 1974). It is about 15–20 cell layers thick, filled with keratin and embedded in lamellar body secretions which gives the classical brick-and-mortar arrangement. This thin (1–10%), outermost layer of the skin causes around 80% of the resistance in permeation. Lipids between the corneocytes act as 'glue' that helps in sealing the spaces between the cells in the skin. All this causes the tightness and impermeability of the intact skin, and hence efficient permeation of molecules greater than 200–350 Da is restricted in the intact skin. SC and viable epidermis comprise the diffusion resistance in series or two barriers in series.

Dermis is up to 4 mm in depth. Similar to the epidermis, drug diffusion through dermis is also restricted due to the aqueous medium. The dermis forming the bulk of the skin is 10–20 times thicker than the epidermis, made up of connective tissue elements and stabilized by a network of collagen fibres (Cevc et al. 1996). It is mainly composed of fibrous proteins, collagen and elastin produced by the fibroblasts. Collagen protein comprises about three-fourths of the dermal dry weight and is the principle component imparting tensile strength to the dermis. Dermis is highly vascular and also contains different glands. It contains the blood and lymph capillaries and nerve endings. It also contains the hair follicles, sebaceous glands and sweat glands which open directly into the environment at the skin surface. These openings can provide points of entry, the shunt pathways for topically applied materials to enter into the skin. These pathways have varied distribution over the entire skin, for example, hair follicles in humans cover 0.1–0.5% of the total skin surface. Appendages extend up to 500 μm (beyond the depth of epidermal–dermis junction). The glands are located in the lower dermis or hypodermis and are connected to the skin surface by a duct which has a diameter of approx. 100 μm . The skin appendages offer an alternative/attractive pathway for transdermal drug delivery and also avoid the challenges of drug delivery through the SC. Permeation of the drug into the dermis suggests the scope for systemic drug distribution. The vascularized hair follicles and appendageal glands also offer the possibility of systemic drug distribution through these routes.

Despite the extensive research and wealth of experimental studies, the mechanisms which promote drug transport through the glands and hair follicle need/remain to be clearly understood and established.

4.2 Chemical Composition of Skin

The chemical constituents of SC are 15% water, 70% protein and 15% lipids (Law et al. 1995) and of the SC lipids, it is the sphingolipids that are important for the epidermal barrier. In SC, intercellular lipids are arranged as 'mortar' (Fig. 3) and have been the focus of research as it imposes maximum resistance to permeation of drugs. At the interface of SC/SG, lipids extruded from lamellar bodies undergo hydrolysis, resulting in the formation of ceramides and free fatty acids (Elias and Menon 1991). SC lipids are constituted by 50% ceramides, 25% cholesterol and 15% free fatty acids (Law et al. 1995).

4.3 Electrical Property of Skin

The electrical properties of the skin are often characterized by impedance spectra. Skin tissues offer polarized electrical impedance, because cell membrane behaves as tiny capacitors, and the intercellular channels as shunt resistance pathways (Yamamoto and Yamamoto 1976; DeNuzzio and Bemer 1990; Oh et al. 1993).

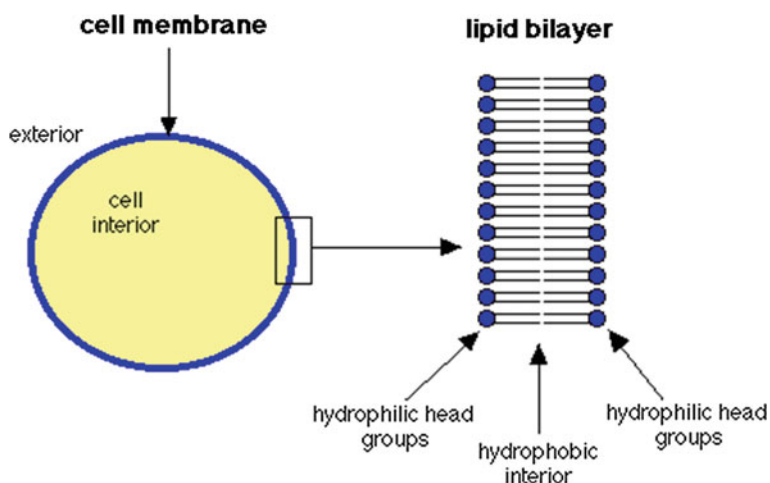


Fig. 3 Schematic representation of arrangement of lipid bilayer in the cell membrane

The skin's electrical properties can be altered by various conditions, like degree of hydration, pH and the presence of chemical additives, electrolyte concentration and valence, thyroid activity, emotional state, temperature, time of year, perspiration and skin disease (Tagami et al. 1980; Allenby et al. 1969; Oh et al. 1993; Yamamoto and Yamamoto 1976). Electrical properties of the skin can also be varied by application of external current, where increased current/voltage/power reduces resistivity (Yamamoto and Yamamoto 1976; Oh et al. 1993; Pikal 1992; Pikal and Shah 1991; Sims et al. 1991; Scott et al. 1993; Rosendal 1943). The electrical properties of skin also depend on the duration of applied electrical current, because the changes occur over time. Moreover, the rate of decrease in resistance depends on the current and voltage applied but the rate of tissue recovery is dependent upon the duration and magnitude of the electrical field (Inada et al. 1994).

Reduction in skin resistance results in increased permeability which can persist even after cessation of electrical exposures (Allenby et al. 1969; Oh et al. 1993; Burnette and Ongpipattanakul 1988; Dinh et al. 1993). Application of current causes local heating of the stratum corneum which could also lead to the changes in skin electrical properties.

4.4 Routes of Penetration Through the Skin

Transappendageal, transcellular and paracellular (Fig. 4) are the three possible pathways for transport of molecules through the skin layers (Scheuplein 1965). The transappendageal pathway is mainly through the hair follicles. The drug permeation through this pathway in humans is limited because of the small surface area available (Scheuplein 1967). The transcellular pathway is the transport of molecules through the corneocytes and the paracellular or intercellular pathway is through the extracellular matrix between the corneocytes. Thus, for intercellular pathway, the hydrophilic molecules are restricted by the lipid environment of the intercellular matrix of the SC (Albery and Hadgraft 1979), whereas the lipophilic molecules can permeate into the intercellular lipids of the SC. Skin permeation also depends on anatomical site, skin care, hydration, age, sex and temperature as well as contact with organic solvents or surfactants (Alexander et al. 2012; Menczel 1985). Moreover, the molecular weight (MW) of the drug molecule also affects skin permeation (Guy and Hadgraft 1991).

For transdermal delivery of low molecular weight lipophilic drugs that are required in low doses, enhancement methods are not needed, whereas for high molecular weight drugs, hydrophilic drugs and also for those requiring higher doses, enhancement methods are required that change the skin's chemical environment (for example, chemical enhancers) or which provide an added driving force (for example, iontophoresis, high-frequency ultrasound). Moreover, for larger

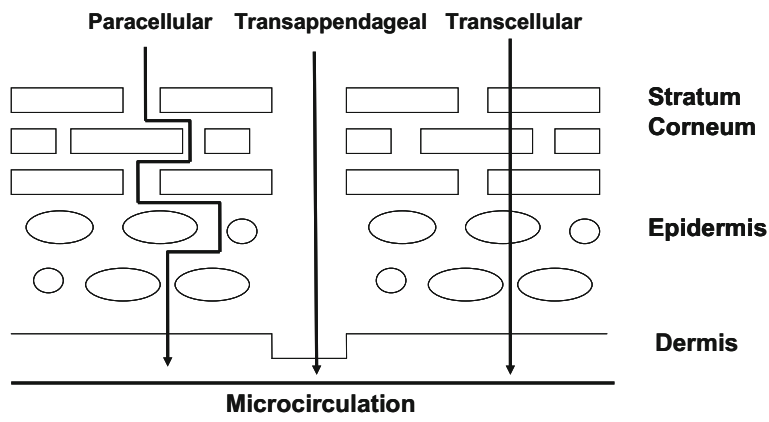


Fig. 4 Schematic representation of the different permeation routes through skin

molecules and drugs requiring large dose, methods that physically disrupt the skin (for example, electroporation, low-frequency ultrasound and microneedles) are employed (Prausnitz 1997).

5 Enhanced Transdermal Drug Delivery

The barrier property of the skin renders difficulty in transdermal delivery of drug molecules, and overcoming the biological barrier in an effective way is a key hurdle for transdermal drug delivery. Several modes of enhancement have been advocated to increase the transdermal delivery of drugs for effective delivery through this route. Technologies used can be divided into chemical or passive and physical or active methods depending on whether an external source of energy is employed for increasing the skin permeation (Wong 2014) (Fig. 5):

1. Chemical or passive methods and
2. Physical or active methods.

The chemical methods are the formulation-based approach, whereas physical methods are device-based approaches. Devices require an external physical unit, which are driven by a power source to deliver the energy required to overcome the barrier and enhance drug delivery (Mitragotri 2013).

These permeation enhancing technologies change the skin's chemical and/or physical environment, thus increasing stratum corneum permeability and allowing the drug molecules to penetrate into the stratum corneum. Additionally, in case of physical methods, an external driving force is applied across the skin, which causes increase in drug transport across the stratum corneum. All these enhancers have

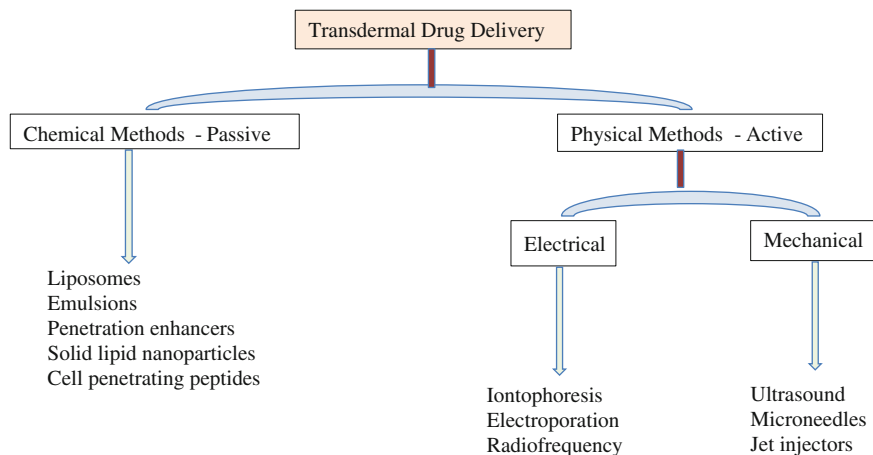


Fig. 5 Enhancement methods for transdermal drug delivery

shown to increase drug permeation across the skin, and their combinations have been shown to be more effective as compared to each of them alone (Mitragotri 2000).

Passive methods use chemical enhancers, emulsions, liposomes and biological methods such as cell penetrating peptides to increase drug permeation across the skin (Schreier and Bouwstra 1994; Karande et al. 2004; Prausnitz et al. 2004; Schuetz et al. 2005; El Maghraby et al. 2006; Kim et al. 2012). FDA-approved GRAS chemicals are employed to enhance the transdermal drug permeation. However, these methods are generally associated with a lag time and thus are not well suited for rapid onset or time-dependent delivery which may be needed for delivery of drugs like insulin.

Active or physical methods of skin permeability enhancement include iontophoresis, electroporation, sonophoresis, microneedles, jet injection, tape stripping, etc. to facilitate the drug permeation across the skin (Prausnitz et al. 1993; Mitragotri et al. 1996; Guy 1998; Bashir et al. 2001; Prausnitz et al. 2004; Kalia et al. 2004; Karande et al. 2004; Arora et al. 2007; Lopez et al. 2011; Prasad and Koul 2012). These methods increase drug transport across the skin with the help of an external driving force or by physically disrupting the skin barrier. These enhancement methods have an advantage over chemical/passive methods as they offer more control over drug delivery and shorter lag time between drug application and drug reaching the systemic circulation. Moreover, the device parameters can be altered to suit individual's skin properties and drug requirement (Tezel et al. 2001; Davis et al. 2004). These devices are particularly useful in targeting the skin and mucosal membranes as they can be placed in direct contact with these membranes. The devices can also be easily designed, modified and tested for skin applications. However, they have the limitation of requiring a power source and can also be expensive (Mitragotri 2013).

6 Iontophoresis (Electrically Enhanced Technology)

Iontophoresis is a mechanism to enhance the permeation of hydrophilic and charged drug molecules across the skin. It is defined as current mediated enhancement of transdermal drug delivery and consists of application of low-intensity current ($<0.5 \text{ mA/cm}^2$) for minutes to hours to increase the permeation of charged drug molecules across the skin (Banga and Chien 1998; Jadoul et al. 1999; Kalia et al. 2004). To deliver the current, an electrode of the same polarity as the charge on the drug is employed to drive ionic molecules into the skin by electrostatic repulsion and to complete the circuit, a return electrode is placed on the skin (Figs. 6 and 7). The passage of current also causes structural and permeability changes in the skin as a secondary phenomenon, which further increases drug permeation. The amount of drug permeated is directly proportional to the quantity of electrical charge passed through the skin. Thus, the drug permeation depends on the intensity of the applied current and also the duration of current application. It also depends on the drug concentration and the skin surface area in contact with the electrode.

The important feature of iontophoresis is the control and ability to individualize the therapies which sets it apart from other technologies. The other advantages include a fast onset and offset time, that is, the drug transport stops when the current is switched off. The current parameters can also be altered to achieve the desired drug permeation. So, the iontophoretic flux can be increased by increasing the applied current; however, at higher current density, a saturation phenomenon is observed and the results start to plateau.

Main drug transport mechanism during iontophoresis is electromigration, which is the movement of charged/ionic drug molecules when the electrical field is applied. Electroosmosis, which is convective solvent flow across the skin due to the applied current, contributes to the permeation of uncharged molecules and peptides

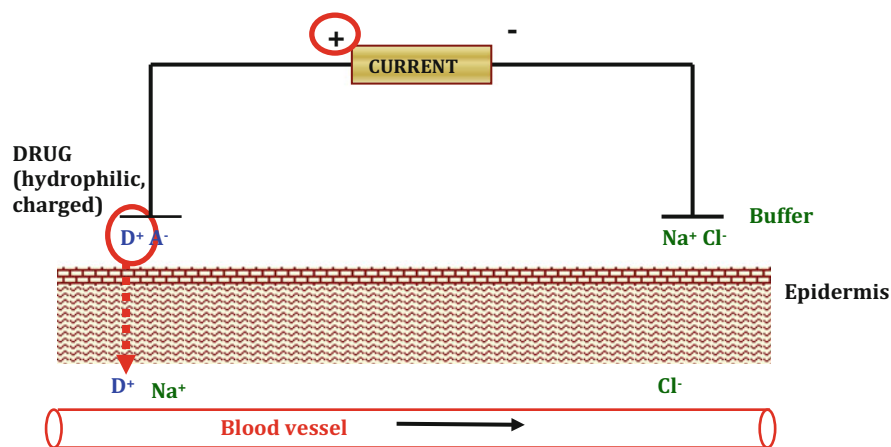
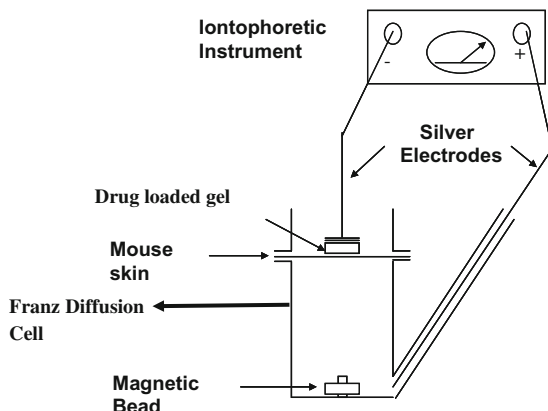


Fig. 6 Schematic diagram showing iontophoresis

Fig. 7 Schematic representation of the iontophoretic setup used for in vitro study



(Kalia et al. 2004). Thus, the iontophoretic enhancement is not only restricted to charged molecules but neutral molecules have also shown enhancement (Sieg et al. 2004). Electroosmotic effect has also led to an interesting development of reverse iontophoresis, in which the molecules present in circulation can be extracted at the surface of the skin and estimated, e.g. glucose and the glucose monitoring system. GlucoWatch Biographer has been developed which monitors the blood glucose level using this method (Naik et al. 2000).

Many different types of electrodes are used for iontophoresis like platinum, gold, silver, carbon, etc. However, Ag/AgCl electrodes are most suited for iontophoresis as its electrolysis occurs at voltages lower than that required for electrolysis of water.

The first scientific experiment using the mechanism of iontophoresis was performed by Leduc in 1900, but the idea of applying electric current to enhance permeation of charged molecules was given by Veratti in 1747 (Leduc 1900).

Iontophoresis increases the hydration of stratum corneum, thus reducing the skin's electrical resistance (Kalia et al. 1996). Changes in skin structure are caused due to the applied electrical field (Prasad et al. 2007). Reorientation of lipid structure could possibly explain these observations. Changes in skin capacitance involve lipids, since the skin's capacitance is generally attributed to the stratum corneum lipids (DeNuzzio and Bemer 1990; Oh et al. 1993).

It has been reported that iontophoresis increases the pore size of the hair follicles, thus providing shunt pathways for drug permeation (Cullander 1992; Prasad et al. 2007). This method of enhancement is generally well tolerated, although mild skin irritation, non-painful sensation and erythema and are sometimes reported.

Iontophoresis (DC) has shown to improve the transdermal delivery of many low molecular (lidocaine, dexamethasone) as well as high molecular (insulin, luteinizing hormone-releasing hormone) weight drugs. However, for delivery of proteins, genes and electrochemotherapy, the scientists are employing the different wave-forms like exponentially decaying pulses (Prausnitz et al. 1993; Pliquett and Weaver 1996) and square-wave pulses (Heller et al. 1999; Denet and Preat 2003)

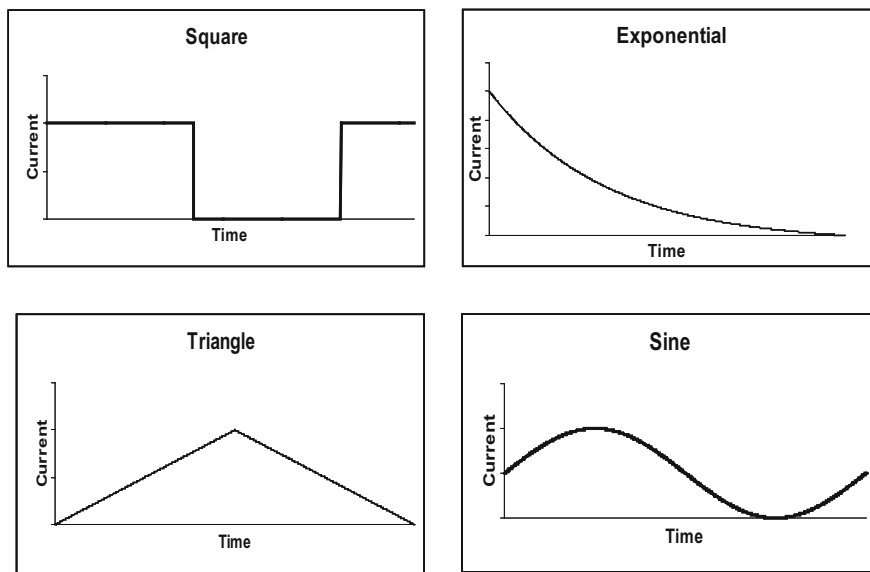


Fig. 8 Different waveforms used for mDC iontophoresis

and have reported that they give more enhancement in drug permeation as compared to constant DC iontophoresis. The effect of the different waveforms like sine, square, exponential and triangle (Fig. 8) on drug permeation and tissue injury have been studied by Prasad et al. (2007) and they have reported it to be safe for skin application.

When direct current electrical field is applied to the skin in a continuous manner, electrochemical polarization develops in the capacitor, C_{sc} . This operates against the applied electric field, thus decreasing the magnitude of effective current across the skin. So, pulsed direct current (pulsed DC) is used to avoid the polarization of SC, (Bagniefski and Burnette 1990). In the pulsed mode, there is an alternating 'on' and 'off' period of the applied voltage. During the 'on' state, the charged molecules are pushed into the skin and the stratum corneum becomes polarized, whereas in the 'off' state, the stratum corneum becomes depolarized as no external stimulation is present. This 'on/off' ratio controls the polarization and depolarization during each cycle.

Thus, the pulsed mode DC or modulated DC (mDC) iontophoresis increases drug permeation by avoiding the polarization of the skin (Odia et al. 1996; Johnson et al. 1998). Moreover, it has been reported by Prasad et al. (2007) that the tissue injury caused by mDC iontophoresis is less as compared to DC, but the flux obtained is higher. They have reasoned that this reverse behaviour is mainly because in mDC iontophoresis the current is given in pulses, which depolarizes the skin and thus reduces skin resistance more effectively. Earlier researchers Denet et al. (2004) and Dujardin et al. (2002) have also reported that square-wave pulses

temporarily impair the barrier function of the skin and the decreased skin resistance causes increase in skin permeability and therefore increased flux.

Our group at IIT Delhi, India has been working on iontophoresis for the last 10 years, and Prasad and coworkers have shown that modulated DC (mDC) iontophoresis significantly increased the permeation of methotrexate across the skin, as compared to DC iontophoresis (Prasad et al. 2007). mDC iontophoresis avoids the polarization effect of skin, thus supporting higher flux. They have also reported that mDC iontophoresis with square-wave pulses showed higher bioavailability, as compared with oral delivery (Prasad et al. 2009). They conducted histopathological studies on mice and found that mDC iontophoresis is well tolerated by the skin tissues and reversal of skin injury takes place within 48 h. They have also reported that the scanning electron micrographs of DC as well as mDC iontophoresis clearly showed increase in the pore size of the hair follicles. This supports the involvement of shunt pathways for drug permeation during iontophoresis (Cullander 1992).

Later, in our lab, Rastogi et al. (2010a, b) have shown the feasibility of using mDC iontophoresis for insulin delivery. They reported higher flux of 0.096 ± 0.040 IU/cm²h with mDC iontophoresis as compared to 0.0244 ± 0.009 IU/cm²h with constant DC iontophoresis. These results are comparable to many reports that state the advantages of pulsed DC iontophoresis over constant DC iontophoresis (Craane-van-Hinsberg et al. 1994; Raiman et al. 2004; Prasad et al. 2007).

A combination of iontophoresis with other physical enhancers or chemical enhancers allows greater drug permeation than either technique employed alone. Mitragotri has also reported that the combinations of enhancers are more efficient than compared to each of them when used alone (Mitragotri 2000, 2004). Combinations of iontophoresis with chemical enhancers, sonophoresis and electroporation have been evaluated to increase the transdermal drug permeation and decrease the possible side effects and tissue injury (Batheja et al. 2006; Choi et al. 1999; Wang et al. 2000).

Prasad et al. (2009) have reported that combination of chemical enhancers (ethyl acetate, ethanol and menthol) and mDC iontophoresis resulted in 161% enhancement in methotrexate loaded in polyacrylamide hydrogel. They showed that the combination of enhancers resulted in synergistic increase in drug permeation, whereas the tissue injury was not the additive of that caused by the individual enhancers, thus resulting in decreased skin injury (Prasad et al. 2009).

Rastogi et al. (2010a, b) have also reported that a combination of chemical enhancers (sodium deoxycholate, oleic acid, 1,8 cineole in ethanol: propylene glycol (3:7) mixture) followed by 1 h mDC iontophoresis significantly increased the transdermal permeation of insulin loaded in PVA hydrogel. They have also showed that in vivo studies in diabetic Wistar rats showed lowering of blood glucose levels by 84%.

Effect of iontophoretic duration on insulin release from polyacrylamide hydrogels has been studied by Banga and Chien (1993). They also evaluated poloxamer P407 gel formulation of insulin for ex vivo and in vivo skin permeation studies in rats, with chemical enhancer and/or iontophoresis.

Alvarez-Figuera and Blanco-Mendez (2001) demonstrated iontophoretic delivery of methotrexate from polyacrylic acid–polyacrylamide hydrogels. Huang et al. (2005) have reported that iontophoresis increased the transdermal delivery of nalbuphine loaded in hydrogel formulation. Patel et al. (2013) have demonstrated that iontophoresis significantly enhanced the transport of macromolecules across buccal mucosa using polymeric hydrogel. Hydroxyethyl cellulose gel has been used for transdermal iontophoretic delivery of diclofenac (Arunkumar et al. 2015). Recently, Chen et al. (2016) have demonstrated the use of carbopol hydrogel for transdermal iontophoresis of acyclovir.

Few iontophoretic products are under different development stages and shall soon be available for clinical use, e.g. delivery system for insulin, antimicrobials, hydromorphone and analgesics (Panchagnula et al. 2000). Furthermore, this method has been clinically approved for the delivery of lidocaine for local anaesthesia and delivery of pilocarpine for cystic fibrosis diagnosis (Spierings et al. 2008; Lark and Gangarosa 1990; Langkjaer et al. 1998; Raiman et al. 2004).

The first drug to be approved by FDA for transdermal iontophoretic delivery was lidocaine, for dermal anaesthesia. The product was called iontocaine and was approved in 1995. The other FDA-approved commercial iontophoretic transdermal patch system was lidosite (2004), which was also used for the local delivery of lidocaine to induce dermal anaesthesia. This system had hydrogel patch loaded with the drug. The second drug to be approved was fentanyl, and the iontophoretic system was called Ionsys (2006) to provide fast relief from pain. However, this product was withdrawn from the market in 2009 due to corrosion of a component of the system in one of the batches of Ionsys. Now, this system is being modified to be permitted for clinical use. A third drug sumatriptan in gel formulation for the treatment of migraine has been developed as transdermal iontophoretic system, Zecuity, and was approved for clinical use in 2013 (Gratieri et al. 2013; Hao 2014).

While considerable research has been carried out on iontophoresis and promising results have been obtained, the main challenge is to develop a portable and cost-effective device, suitable semi-solid formulations that are compatible with the device, drug and the skin and development of protocols that are suited to clinical settings.

7 Electroporation (Electrically Enhanced Technology)

Application of high-voltage pulses (>100 V) for a very short duration of time from microsecond to milliseconds is called electroporation (Prausnitz 1999; Weaver and Chizmadzhev 1996). It is also called electroporabilization as it causes temporary structural disturbance in the skin due to application of large voltages, thereby increasing the permeation many folds. The structural changes lead to the formation of pores or aqueous pathways, thus increasing drug permeation. While iontophoresis acts on the charged drug molecules, electroporation mainly acts on the skin to increase its permeation. It exerts some force on the drug during the pulse,

and hence, the contribution of electroosmosis in drug transport is low because of the very short time of current application in electroporation. Electrophoresis and diffusion are the main modes of drug permeation across the skin (Denet et al. 2004). Many small as well as large molecules have been delivered successfully under experimental conditions. Moreover, a large number of drugs and even macromolecules, vaccines, etc. can be delivered across the skin with the help of electroporation technique either used alone or in combination with other enhancement modes.

Electroporation has been used for gene transfer, DNA vaccination, transdermal delivery of low molecular weight peptide of protein vaccines and transdermal delivery of other drug molecules like fentanyl, insulin and methotrexate (Sardesia and Weiner 2011; Wong et al. 2011; Yarmush et al. 2014).

An important application of electroporation is in electrochemotherapy, where high-voltage pulses are applied to permeabilize the tumour cells to increase the transport of cytotoxic drugs. High-voltage electroporation (Fig. 9) causes structural changes in the stratum corneum's lipid bilayers, thus creating new pathways for drug transport (Fig. 10) and also provides an electrophoretic driving force on the drug molecules during the pulse (Prausnitz 1998; Banga et al. 1999).

This technique was first reported by Sale and Hamilton in 1967, wherein application of electrical pulses for transformation and fusion of cells were shown to cause the death and lysis of cells (Sale and Hamilton 1967). Further studies revealed that the membrane permeability barrier might be weakened temporarily and reversibly, by subjecting cells to well-controlled, high-intensity electric field pulses (Neumann and Rosenheck 1972). Electroporation was first used medically by Neumann and coworkers in 1982 for the delivery of DNA into the cells (Neumann et al. 1982). This technology is now being extensively used for biomedical applications such as electrochemotherapy, electrogene therapy and transdermal drug delivery (Hofmann et al. 1995, 1996). Huang et al. (2005) have reported that iontophoresis and electroporation increased the transdermal delivery of nalbuphine loaded in hydrogel formulation.

Fig. 9 Schematic representation of the mechanism of electroporation

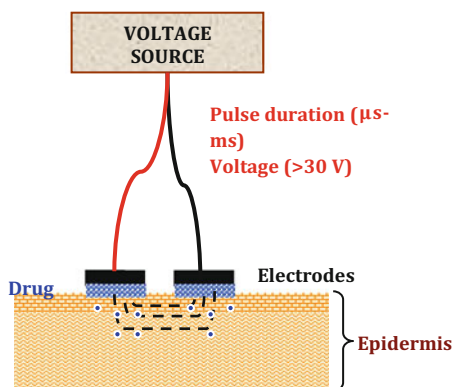
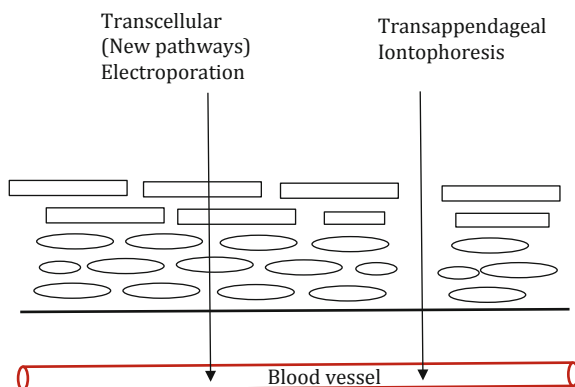


Fig. 10 Different pathways for drug permeation through SC by low-voltage iontophoresis and high-voltage electroporation



Electric field of 60 V or higher transdermal voltage is known to electroporate the lipid bilayers of the stratum corneum, thus creating transcellular pathways. These pathways form local transport regions (LTRs) across the stratum corneum layer, thus enhancing the permeation of macromolecules into the skin.

Many different types of electrodes needle, plate, multi-electrode array and needle-free microelectrode array are used for the delivery of electric pulses to enhance skin permeation. Moreover, the transdermal drug delivery also depends on amplitude of the electric pulses, shorter pulses (μs) are used for delivery of small molecules like drugs, whereas long pulses (ms) are needed for DNA delivery (Denet et al. 2004; Blagus et al. 2013).

Mainly two types of pulses, exponentially decaying and square-wave pulses, have been used in electroporation for transdermal drug delivery (Zorec et al. 2013). Further, Zorec et al. (2015) have shown that pulse amplitude is also important in drug permeation. They demonstrated that calcein delivery with 100 V pulses was negligible, whereas with 200 V pulses, there was significant enhancement in skin permeation.

Electroporation has been used to increase the transdermal transport of insulin across animal skin (Rastogi et al. 2010a, b; Sen et al. 2002). Combination of electroporation and iontophoresis has been reported to further increase the insulin permeation (Murthy et al. 2006). Petchsangsaï et al. (2014) have also reported the use of enhancer combinations of electric pulses, ultrasound and microneedles to increase the transdermal delivery of FITC dextran.

Although the experimental results are promising, electroporation has still not been approved as an enhancement technique for transdermal drug delivery because of muscle contractions and pain associated with this method. Recently, a special electrode design has been proposed for use with electroporation that causes less muscle tremors (Golberg and Rubinsky 2012).

Electroporation has many medical applications and a proper understanding of the mechanisms at the cellular level, and overcoming its limitations will see a tremendous rise in its application in drug delivery systems.

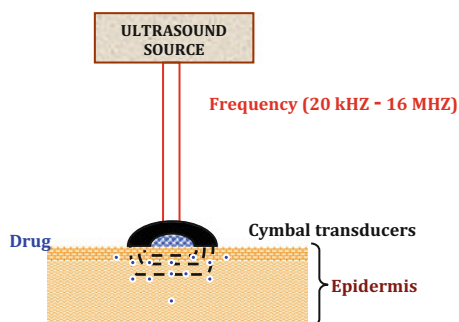
8 Sonophoresis (Ultrasonically Enhanced Technology)

The use of ultrasound (US) as an external physical force to increase the permeation of drug molecules through the skin is called sonophoresis (Fig. 11). The use of sonophoresis was first reported in the 1950s (Mitragotri and Kost 2004). Frequencies in the range of 20 kHz–16 MHz are used to increase skin permeability, and thus sonophoresis has been done using both high-frequency and low-frequency ultrasound. However, in the last two decades, researchers have shown that low-frequency ultrasound (20–100 kHz) is more effective for transdermal drug delivery and has been used to increase transdermal permeation of many drugs like lidocaine, insulin, etc. and also in extraction of interstitial fluid for glucose monitoring (Ogura et al. 2008; Mitragotri and Kost 2004).

For therapy, high-frequency ultrasound (1–3 MHz) is used and the therapeutic ultrasound can be in continuous mode, which has thermal effect, or in pulsed mode, which has mechanical effect like cavitation (Shipton 2012; Wong 2014). High-frequency ultrasound is mainly used for imaging and physiotherapy, and delivery of a few high molecular weight drugs (more than 1000 Da) has also been tried with it (Polat et al. 2011; Azagury et al. 2014). Increase in transdermal permeation of mannitol and physostigmine with ultrasound (1 MHz) across hairless rat in vivo has been reported by Levy et al. (1989). They also demonstrated that the lag time present with transdermal delivery was almost eliminated with ultrasound exposure.

With high-frequency ultrasound, the enhancement is mainly because of a pressure-driven driving force along with the physical disruption of stratum corneum lipids, which causes creation of pathways, but at low-frequency, ultrasound-induced cavitation is the main mechanism that causes physical disruption of stratum corneum and also renders a pressure-driven driving force on the drug (Mitragotri et al.

Fig. 11 Schematic representation of the mechanism of sonophoresis



1996; Mitragotri and Kost 2004; Park et al. 2014). When the ultrasound wave travels through the body, physical changes like local hyperthermia, cavitation and pressure variation occur and these help in transdermal drug delivery as well as in diagnostics (Sirsi and Borden 2014). The skin enhancement induced by ultrasound depends on different parameters like duty cycle, frequency, intensity and application time.

Two different ways of applying low-frequency ultrasound to enhance transdermal drug delivery are the simultaneous method, where the drug and ultrasound are applied simultaneously to the skin, and the pretreatment method, where the skin is first permeabilised with the application of ultrasound followed by drug delivery. The main mechanism responsible for enhanced skin permeation with low-frequency ultrasound is the formation of gaseous cavities and its collapse, acoustic cavitation.

Application of hydrocortisone with ultrasound for the treatment of polyarthritis of hand joints has been successfully reported by Fellingner and Schmidt in 1954. Later in 1960, Coodley demonstrated that hydrocortisone injection along with ultrasound massage gave better results for bursitis treatment as compared to injection alone. Ultrasound has also shown to improve the permeation of local anaesthetics (Cameroy 1966).

Low-frequency sonophoresis (48 kHz) increases the transdermal permeation of lidocaine and insulin as reported by Tachibana and Tachibana (1991, 1993). The effectiveness of low-frequency ultrasound for delivery of proteins was first reported by Mitragotri et al. in 1995 (Mitragotri et al. 1995a, b). They have also reported that ultrasound application using 20 kHz frequency increases the transdermal permeation of many low as well as high molecular weight drugs. They showed that there was an increase in skin permeability with decreasing frequency, and also with increasing the intensity and the time of exposure. They identified collapse cavitation as the main causative mechanism (Mitragotri et al. 1996). It has also been reported that these cavitations create reversible channels in the stratum corneum lipid layers, thus providing pathways of transport for many drug molecules and even macromolecules (Tezel et al. 2002).

Kost et al. (2003) have shown clinically that skin pretreatment with 55 kHz ultrasound gave better level of anaesthesia with EMLA cream as compared to EMLA alone.

Histological studies with rat and pig skin after low-frequency sonophoresis showed no structural changes suggesting its safety.

Low-frequency ultrasound has shown to increase the permeation of large molecular weight molecules across skin and is currently under clinical trials for the delivery of insulin and pain medication (Langer 2003).

Ogura et al. (2008) have reported that application of 20 kHz ultrasound increased the permeation of many proteins across human skin *in vivo*.

Application of ultrasound and iontophoresis has shown synergistic effect on the permeation of heparin with 56-fold enhancement (Le et al. 2000).

Extensive work has been carried out on transducer design to enhance its portability without comprising with the efficiency of the technique. A cymbal transducer design has been used to attain intensities in the range of 12.5–225 mW/

cm². This transducer has been chosen because of its light and compact structure and also low resonance frequency in water (Maione et al. 2002; Smith et al. 2003a; Luis et al. 2007). The efficacy of the technique has been investigated in vivo in various animal models, Sprague Dawley rats, rabbits and large animals, viz., swine (Lee et al. 2004a, b; Smith et al. 2003b; Park et al. 2007). A fall in blood glucose levels was noted for nearly 60 min for all experiments, which continued even after removal of the transducer. In a recent study, Park et al. (2008) have compared the effectiveness of ultrasound-mediated delivery using a cymbal transducer array to that of subcutaneously administered insulin over a 90 min experiment in rat model. The change in blood glucose level with ultrasound treatment was greater, thus suggesting that a higher effective dose of insulin was delivered.

Researchers have reported that low-frequency ultrasound was effective in increasing the delivery of insulin and vasopressin loaded in hydrogel (Zhang et al. 1996; Peppas et al. 1999). This proved that poly (ethylene glycol) containing hydrogel was useful for protein delivery. Meshali et al. (2011) have demonstrated the efficiency of gels over emulsion in the transport of ibuprofen using ultrasound across rabbit skin. Bani et al. (2015) showed that hydrogel formulation of manganese-containing antioxidant drug showed significant transepidermal permeation with the application of ultrasound. Jiang et al. (2016) have recently reported the efficiency of ultrasound for delivery of mimosa from cellulose gel.

Ultrasonic-mediated enhanced delivery of hydrocortisone and lidocaine has been tested clinically. Moreover, ultrasound is also used to extract interstitial fluid for diagnostics, e.g. in blood glucose monitoring system. Preclinical research with ultrasound-enhanced transdermal delivery of insulin (Smith et al. 2003a), low molecular weight heparin, oligonucleotides and vaccines are in progress.

The future of ultrasound-enhanced transdermal drug delivery has a lot of potentials. Ultrasonic skin permeation system, SonoPrep[®] developed by Prof. Robert Langer and Prof. Joseph Kost, Massachusetts Institute of Technology, USA, is the first FDA-approved system based on this technique. The system has been tested for transdermal delivery of proteins, viz., insulin and heparin and local anaesthesia. SonoPrep[®] is also used to induce local dermal anaesthesia using lidocaine prior to cutaneous procedures. Moreover, application of SonoPrep with EMLA cream before any IV cannulation has shown benefits in terms of pain reduction and patient satisfaction (Kim et al. 2012). Furthermore, Gupta and Prausnitz (2009) have reported that SonoPrep showed increased skin permeability for a long time and the skin recovery was also very fast.

The use of low-frequency ultrasound for delivery of local anaesthetics has been approved by FDA (Shipton 2012).

Sonophoresis is expected to be a useful tool for both diagnosis and treatment of diseases, such as diabetes in the near future.

9 Conclusion and Future Perspective

Skin has the natural protective function in the body, and it limits the delivery of drug molecules into the body. Skin represents an important drug delivery route especially for molecules destroyed by the liver after oral intake. Drug delivery through the skin is an attractive and challenging area for research, and optimization of drug delivery is important in modern therapy.

The drug formulations play an important role in transdermal drug delivery and are a critical link between the drug, device and skin.

Transdermal delivery is particularly advantageous for localized effect and hence more appropriate to use for targeting the skin directly.

The acceptance of transdermal products is very high, and this can be clearly seen from the increasing market for such products. Thus, it has made significant contribution to the medicinal world but has still not achieved its goal as an alternative to the conventional modes of drug delivery. Research should be aimed at better designing of the transdermal device, with minimum skin irritation and higher flux for a large number of molecules.

A lot of researches are being done to explore the feasibility of using iontophoresis to increase transdermal drug delivery and to use it as a treatment modality for a number of therapeutic molecules. However, till date only two transdermal iontophoretic patches are available in the market. These assisted delivery devices will expand the scope of transdermal permeation of many macromolecules like proteins, vaccines, hormones, enzymes, genes, etc. An increasing effort and effective collaboration are required between the medical practitioners, research scientists and device manufacturers to develop the devices and achieve the desired goals for assisted transdermal drug delivery.

The ongoing clinical trials for a number of drugs represent a great future for transdermal delivery of drugs. However, the challenge lies in getting useful products out of these discoveries for the benefit of mankind.

References

- Albery WJ, Hadgraft J (1979) Percutaneous absorption: theoretical description. *J Pharm Pharmacol* 31:129–139
- Alexander A, Dwivedi S, Ajazuddin GTK, Saraf S, Saraf S, Tripathi DK (2012) Approaches for breaking the barriers of drug permeation through transdermal drug delivery. *J Control Rel* 164:26–40
- Aliyar H, Huber R, Loubert G, Schalaus G (2014) Efficient ibuprofen delivery from anhydrous semisolid formulation based on a novel cross-linked silicone polymer network: an in vitro and in vivo study. *J Pharm Sci* 103:2005–2011
- Allenby AC, Fletcher J, Schock C, Tees TFS (1969) The effect of heat, pH and organic solvents on the electrical impedance and permeability of excised human skin. *Br J Dermatol* 81:31–39

- Alvarez-Figueroa MJ, Blanco-Méndez J (2001) Transdermal delivery of methotrexate: iontophoretic delivery from hydrogels and passive delivery from microemulsions. *Int J Pharm* 215:57–65
- Arora A, Hakim I, Baxter J, Rathnasingham R, Srinivasan R, Fletcher DA, Mitragotri S (2007) Needle-free delivery of macromolecules across the skin by nanoliter-volume pulsed microjets. *Proc Natl Acad Sci USA* 104:4255–4260
- Arunkumar S, Ashok P, Desai BG, Shivakumar HN (2015) Effect of chemical penetration enhancer on transdermal iontophoretic delivery of diclofenac sodium under constant voltage. *J Drug Del Sci Technol* 30:171–179
- Azagury A, Khoury L, Enden G, Kost J (2014) Ultrasound mediated transdermal drug delivery. *Adv Drug Del Rev* 72:127–143
- Bagniefski T, Burnette RR (1990) A comparison of pulsed and continuous current iontophoresis. *J Control Rel* 11:113–122
- Banga AK, Chien YW (1998) Iontophoretic delivery of drugs: fundamentals, developments and biomedical applications. *J Control Rel* 7:1–24
- Banga AK, Bose S, Ghosh TK (1999) Iontophoresis and electroporation: comparisons and contrasts. *Int J Pharm* 179:1–19
- Banga AK, Chien YW (1993) Hydrogel-based iontotherapeutic delivery devices for transdermal delivery of peptide/protein drugs. *Pharm Res* 10:697–702
- Bani D, Bencini A, Bergonzi MC, Bilia AR, Guccione C, Severi M, Udisti R, Valtancoli B (2015) Enhanced intra-cutaneous delivery of a Mn-containing antioxidant drug by high-frequency ultrasounds. *J Pharm Biomed Anal* 106:197–203
- Barry BW (1983) Properties that influence percutaneous absorption. In: Barry BW (ed) *Dermatological formulations; percutaneous absorption*. Marcel Dekker, New York, pp 127–233
- Barry BW (2001) Novel mechanisms and devices to enable successful transdermal drug delivery. *Eur J Pharm Sci* 14:101–114
- Bashir SJ, Chew AL, Anigbogu A, Dreher F, Maibach HI (2001) Physical and physiological effects of stratum corneum tape stripping. *Skin Res Technol* 7:40–48
- Batheja P, Thakur R, Michniak B (2006) Transdermal iontophoresis. *Expert Opin Drug Deliv* 3:127–138
- Bhojar TKG, Tripathi DK, Alexander A, Ajazuddin (2012) Recent advances in novel drug delivery system through gels: review. *J Pharm Allied Health Sci* 2:21–39
- Blagus T, Markelc B, Cemazar M, Kosjek T, Preat V, Miklavcic D, Sersa G (2013) In vivo real-time monitoring system of electroporation mediated control of transdermal and topical drug delivery. *J Control Rel* 172:862–871
- Burnette RR, Ongpipattanakul B (1988) Characterisation of the pore transport properties and tissue alteration of excised human skin during iontophoresis. *J Pharm Sci* 77:132–137
- Cameroy BM (1966) Ultrasound enhanced local anesthesia. *Am J Orthop* 8:47
- Cevc G, Blumeb G, Schitzlein A, Gebaue D, Paul A (1996) The skin: a pathway for systemic treatment with patches and lipid-based agent carriers. *Adv Drug Deliv Rev* 18:349–378
- Chang F, Swartzendruber DC, Wertz PW, Squier CA (1993) Covalently bound lipids in keratinizing epithelia. *Biochim Biophys Acta* 1150:98–102
- Chen Y, Zahui T, Alberti I, Kalia YN (2016) Cutaneous biodistribution of ionizable, biolabile aciclovir prodrugs after short duration topical iontophoresis: targeted intraepidermal drug delivery. *Eur J Pharm Biopharm* 99:94–102
- Choi EH, Lee SH, Ahn SK, Hwang SM (1999) The pretreatment effect of chemical skin penetration enhancers in transdermal drug delivery using iontophoresis. *Skin Pharmacol Appl Skin Physiol* 12:326–335
- Christophers E, Schubert C, Goes M (1989) The epidermis. In: Greaves MW, Shuster S (eds) *Pharmacology of the skin*, vol I. Springer-Verlag, Berlin, pp 3–30
- Christophers E, Wolff HH, Laurence EB (1974) The formation of epidermal cell columns. *J Invest Dermatol* 62:555–559
- Coodley GL (1960) Bursitis and post-traumatic lesions. *Am Pract* 11:181–187

- Coury AJ, Fogt EJ, Norenberg MS, Untereker DF (1983) Development of a screening system for cystic fibrosis. *Clin Chem* 29:1593–1597
- Craane-van-Hinsberg WHM, Bax L, Flinterman NHM, Verhoef J, Junginger HE, Bodde HE (1994) Iontophoresis of a model peptide across human skin in vitro: effects of iontophoresis protocol, pH, and ionic strength on peptide flux and skin impedance. *Pharm Res* 11:1296–1300
- Cullander C (1992) What are the pathways of iontophoretic current flow through mammalian skin? *Adv Drug Deliv Rev* 9:119–135
- Davis SP, Landis BJ, Adams ZH, Allen MG, Prausnitz MR (2004) Insertion of microneedles into skin: measurement and prediction of insertion force and needle fracture force. *J Biomech* 37:1155–1163
- Denet AR, Preat V (2003) Transdermal delivery of timolol by electroporation through human skin. *J Control Rel* 88:253–262
- Denet A-R, Vanbever R, Preat V (2004) Skin electroporation for transdermal and topical delivery. *Adv Drug Deliv Rev* 56:659–674
- DeNuzzio JD, Bemer B (1990) Electrochemical and iontophoretic studies of human skin. *J Control Rel* 11:105–112
- Dinh SM, Luo C-W, Bemer B (1993) Upper and lower limits of human skin electrical resistance in iontophoresis. *AIChE J* 39:2011–2018
- Donnelly RF, Singh TRR, Garland MJ, Migalska K, Majithiya R, McCrudden CM, Kole PR, Mahmood TMT, McCarthy HO, Woolfson AD (2012) Hydrogel-forming microneedle arrays for enhanced transdermal drug delivery. *Adv Funct Mater* 22:4879–4890
- Donnelly RF, Singh TR, Alkilani AZ, McCrudden MT, O'Neill S, O'Mahony C, Armstrong K, McLoone N, Kole P, Woolfson AD (2013) Hydrogel-forming microneedle arrays exhibit antimicrobial properties: potential for enhanced patient safety. *Int J Pharm* 451:76–91
- Drury JL, Mooney DJ (2003) Hydrogels for tissue engineering: scaffold design variables and applications. *Biomaterials* 24:4337–4351
- Dujardin N, Staes E, Kalia Y, Clarys P, Guy R, Preat V (2002) In vivo assessment of skin electroporation using square wave pulses. *J Control Rel* 79:219–227
- El Maghraby GMM, Williams AC, Barry BW (2006) Can drug-bearing liposomes penetrate intact skin? *J Pharm Pharmacol* 58:415–429
- Elias PM, Menon GK (1991) Structural and lipid biochemical correlates of the epidermal permeability barrier. *Adv Lipid Res* 24:1–26
- Fang J-Y, Huang Y-B, Lin HH, Tsai Y-H (1998a) Transdermal iontophoresis of sodium nonivamide acetate IV: effect of polymer formulations. *Int J Pharm* 173:127–140
- Fang J-Y, Huang Y-B, Wu PC, Tsai Y-H (1996) Transdermal iontophoresis of sodium nonivamide acetate II: optimisation and evaluation of solutions and gels. *Int J Pharm* 145:175–186
- Fang J-Y, Kuo CT, Huang Y-B, Wu PC, Tsai Y-H (1998b) Transdermal iontophoresis of sodium nonivamide propionate by iontophoresis. *Biol Pharm Bull* 21:1117–1120
- Fang J-Y, Sung SC, Lin HH, Fang CL (1999) Transdermal iontophoretic delivery of diclofenac sodium from various polymer formulations: in vitro and in vivo studies. *Int J Pharm* 178:83–92
- Fellinger K, Schmidt J (1954) *Klinik und Therapies des Chronischen Gelenkreumatismus*. Maudrich Vienna, Austria, pp 549–552
- Gehrke SH, Lee PI (1990) Hydrogels for drug delivery. In: Tyle P (ed) *Specialized drug delivery systems, manufacturing and production technology*. Marcel Dekker, New York, pp 333–392
- Golberg A, Rubinsky B (2012) Towards electroporation based treatment planning considering electric field induced muscle contractions. *Technol Cancer Res Treat* 11:189–201
- Gong JP, Komatsu N, Nitta T, Osada Y (1997) Electrical conductance of polyelectrolyte gels. *J Phys Chem B* 101:740–745
- Gratieri T, Alberti I, Lapteva M, Kalia YN (2013) Next generation intra- and transdermal therapeutic systems: using non- and minimally-invasive technologies to increase drug delivery into and across the skin. *Eur J Pharm Sci* 18:609–622
- Gupta J, Prausnitz MR (2009) Recovery of skin barrier properties after sonication in human subjects. *Ultrasound Med Biol* 35:1405–1408

- Gupta SK, Kumar S, Bolton S, Behl CR (1994) Optimization of iontophoretic transdermal delivery of a peptide and a non-peptide drug. *J Control Rel* 30:253–261
- Guy RH (1996) Current status and future prospects of transdermal drug delivery. *Pharm Res* 13:1765–1769
- Guy RH (1998) Iontophoresis—recent developments. *J Pharm Pharmacol* 50:371–374
- Guy RH, Hadgraft J (1991) Principles of skin permeability relevant to chemical exposure. In: Hobson DW (ed) *Dermal and ocular toxicology: fundamentals and methods*. CRC Press, Boca-Raton, FL, pp 221–246
- Hao J (2014) Topical iontophoresis for local therapeutic effects. *J Drug Del Sci Technol* 24:255–258
- Heller R, Gilbert R, Jaroszeski MJ (1999) Clinical applications of electrochemotherapy. *Adv Drug Del Rev* 35:119–129
- Hoare TR, Kohane DS (2008) Hydrogels in drug delivery: progress and challenges. *Polymer* 49:1993–2007
- Hofmann GA, Dev SB, Nanda GS (1996) Electrochemotherapy: transition from laboratory to the clinic. *IEEE Eng Med Biol Mag* 15:124–132
- Hofmann GA, Rustrum WV, Suder KS (1995) Electro-incorporation of microcarriers as a method for the transdermal delivery of large molecules. *Bioelectrochem Bioenerg* 38:209–222
- Huang J-F, Sung KC, Hu OY-P, Wang J-J, Lin Y-H, Fang J-Y (2005) The effects of electrically assisted methods on transdermal delivery of nalbuphine benzoate and sebacyl dinalbuphine ester from solutions and hydrogels. *Int J Pharm* 29:162–171
- Inada H, Ghanem A-H, Higuchi WI (1994) Studies on the effects of applied voltage and duration on human epidermal membrane alteration/recovery and the resultant effects upon iontophoresis. *Pharm Res* 11:687–697
- Indulekha S, Arunkumar P, Bahadur D, Srivastava R (2016) Thermoresponsive polymeric gel as an on-demand transdermal drug delivery system for pain management. *Material Sci Engg: C* 62:113–122
- Ita KB (2014) Transdermal drug delivery: progress and challenges. *J Drug Delivery Sci Technol* 24:245–250
- Jadoul A, Bouwstra J, Preat V (1999) Effects of iontophoresis and electroporation on the stratum corneum: review of the biophysical studies. *Adv Drug Del Rev* 35:89–105
- Jagur-Grodzinski J (2010) Polymeric gels and hydrogels for biomedical and pharmaceutical applications. *Polym Adv Technol* 21:27–47
- Jeong B, Kim SW, Bae YH (2002) Thermosensitive sol-gel reversible hydrogels. *Adv Drug Deliv Rev* 54:37–51
- Jeong WL, Park JH, Prausnitz MR (2008) Dissolving microneedles for transdermal drug delivery. *Biomaterials* 29:2113
- Jepps OG, Dancik Y, Anissimov YG, Roberts MS (2013) Modeling the human skin barrier—towards a better understanding of dermal absorption. *Adv Drug Del Rev* 65:152–168
- Jiang H, Tovar-Carrillo K, Kobayashi T (2016) Ultrasound stimulated release of mimosa medicine from cellulose hydrogel matrix. *Ultrason Sonochem* 32:398–406
- Jodar KSP, Balcao VM, Chaud MV, Tubino M, Yoshida VMH, Oliveira JM Jr, Vila MMDC (2015) Development and characterization of a hydrogel containing silver sulfadiazine for antimicrobial topical applications. *J Pharm Sci* 104:2241–2254
- Johnson PG, Gallo SA, Hui SW, Oseroff AR (1998) A pulsed electric field enhances cutaneous delivery of methylene blue in excised full-thickness porcine skin. *J Invest Dermatol* 111:457–463
- Kalia Y, Nonato LB, Guy RH (1996) The effect of iontophoresis on skin barrier integrity: non-invasive evaluation by impedance spectroscopy and transepidermal water loss. *Pharm Res* 13:957–961
- Kalia YN, Merino V, Guy RH (1998) Transdermal drug delivery: clinical aspects. *Dermatol Clin* 16:289–299
- Kalia YN, Naik A, Garrison J, Guy RH (2004) Iontophoretic drug delivery. *Adv Drug Deliv Rev* 56:619–658

- Karande P, Jain A, Mitragotri S (2004) Discovery of transdermal penetration enhancers by high-throughput screening. *Nat Biotechnol* 22:192–197
- Kearney M-C, Caffarel-Salvador E, Fallows SJ, McCarthy HO, Donnelly RF (2016) Microneedle-mediated delivery of donepezil: potential for improved treatment options in Alzheimer's disease. *Eur J Pharm Biopharm* 103:43–50
- Khademhosseini A, Langer R (2007) Microengineered hydrogels for tissue engineering. *Biomaterials* 28:5087–5092
- Kikuchi A, Okano T (2002) Pulsatile drug release control using hydrogels. *Adv Drug Deliv Rev* 54:53–77
- Kim D, Choi S, Kwak Y (2012) The effect of SonoPrep on EMLA cream application for pain relief prior to intravenous cannulation. *Eur J Pediatr* 171:985–988
- Kong BJ, Kim A, Park SN (2016) Properties and in vitro drug release of hyaluronic acid-hydroxyethyl cellulose hydrogels for transdermal delivery of isoliquiritigenin. *Carbohydr Polym* 147:473–481
- Kopeček J (2007) Hydrogel biomaterials: a smart future? *Biomaterials* 28:5185–5192
- Kost J, Katz N, Shapiro D, Herrmann T, Kellogg S, Warner N, Custer L (2003) Ultrasound skin permeation pretreatment to accelerate the onset of topical anesthesia. *Proc Inter Symp Bioact Mater*
- Kost J, Langer R (2001) Responsive polymeric delivery systems. *Adv Drug Deliv Rev* 53:125–148
- Lane ME (2013) The transdermal delivery of fentanyl. *Eur J Pharm Biopharm* 84:449–455
- Langer R (2003) Where a pill won't go. *Sci Am* 288:50–57
- Langer R (2004) Transdermal drug delivery: past progress, current status and future prospects. *Adv Drug Deliv Rev* 56:557–558
- Langkjaer L, Brange J, Grodsky GM, Guy RH (1998) Iontophoresis of monomeric insulin analogues in vitro: effects of insulin charge and skin pretreatment. *J Control Rel* 51:47–56
- Lark MR, Gangarosa LP Sr (1990) Iontophoresis: an effective modality for the treatment of inflammatory disorders of the temporomandibular joint and myofascial pain. *Cranio* 8:108–119
- Law S, Wertz PW, Swartzendruber DC, Squier CA (1995) Regional variation in content, composition and organization of porcine epithelial barrier lipids revealed by thin-layer chromatography and transmission electron microscopy. *Arch Oral Biol* 40:1085–1091
- Le L, Kost J, Mitragotri S (2000) Combined effect of low-frequency ultrasound and iontophoresis: applications for transdermal heparin delivery. *Pharm Res* 17:1151–1154
- Leduc S (1900) Introduction of medicinal substances into the depth of tissues by electric current. *Ann d' Electrobiol* 3:545–560
- Lee KY, Mooney DJ (2001) Hydrogels for tissue engineering. *Chem Rev* 101:1869–1880
- Lee S, Newnham RE, Smith NB (2004a) Short ultrasound exposure times for noninvasive insulin delivery in rats using the lightweight cymbal array. *IEEE Trans Ultrason Ferroelectr Freq Control* 51:176–180
- Lee S, Snyder B, Newnham RE, Smith NB (2004b) Non-invasive ultrasonic transdermal insulin delivery in rabbits using the light-weight cymbal array. *Diabetes Technol Ther* 6:808–815
- Levy D, Kost J, Meshulam Y, Langer R (1989) Effect of ultrasound on transdermal drug delivery to rats and guinea pigs. *J Clin Invest* 83:2074–2078
- Lopez RFV, Seto JE, Blankschtein D, Langer R (2011) Enhancing the transdermal delivery of rigid nanoparticles using the simultaneous application of ultrasound and sodium lauryl sulfate. *Biomaterials* 32:933–941
- Luis J, Park EJ, Meyer RJ, Smith NB (2007) Rectangular cymbal arrays for improved ultrasonic transdermal insulin delivery. *J Acoust Soc Am* 122:2022–2030
- Maione E, Shung KK, Meyer RJ Jr, Hughes JW, Newnham RE, Smith NB (2002) Transducer design for a portable ultrasound enhanced transdermal drug-delivery system. *IEEE Trans Ultrason Ferroelectr Freq Control* 49:1430–1436
- Menczel E (1985) Skin delipidization and percutaneous absorption. In: Bronaugh RL, Maibach HI (eds) *Percutaneous absorption: mechanisms—methodology—drug delivery*. Marcel Dekker, New York, pp 231–242

- Meshali M, Abdel-Aleem H, Sakr F, Nazzal S, El-Malah Y (2011) Effect of gel composition and phonophoresis on the transdermal delivery of ibuprofen: in vitro and in vivo evaluation. *Pharm Dev Technol* 16:93–101
- Mitragotri S (2000) Synergistic effect of enhancers for transdermal drug delivery. *Pharm Res* 17:1354–1359
- Mitragotri S (2004) Breaking the skin barrier. *Adv Drug Deliv Rev* 56:555–556
- Mitragotri S (2013) Devices for overcoming biological barriers: the use of physical forces to disrupt the barriers. *Adv Drug Deliv Rev* 65:100–103
- Mitragotri S, Blankschtein D, Langer R (1995a) Ultrasound-mediated transdermal protein delivery. *Science* 269:850–853
- Mitragotri S, Blankschtein D, Langer R (1996) Transdermal drug delivery using low-frequency sonophoresis. *Pharm Res* 13:411–420
- Mitragotri S, Edwards DA, Blankschtein D, Langer (1995b) A mechanistic study of ultrasonically-enhanced transdermal drug delivery. *J Pharm Sci* 84:697–706
- Mitragotri S, Kost J (2004) Low-frequency sonophoresis a review. *Adv Drug Deliv Rev* 56:589–601
- Miyata T, Urugami T, Nakamae K (2002) Biomolecule sensitive hydrogels. *Adv Drug Deliv Rev* 54:79–98
- Murthy SN, Zhao YL, Marlan K, Hui SW, Kazim AL, Sen A (2006) Lipid and electroosmosis enhanced transdermal delivery of insulin by electroporation. *J Pharm Sci* 95:2041–2050
- Naik A, Kalia YN, Guy RH (2000) Transdermal drug delivery: overcoming the skin's barrier function. *Pharm Sci Technol Today* 3:318–326
- Nair V, Pillai O, Ramarao P, Panchagnula R (1999) Transdermal iontophoresis. Part I: basic principles and considerations methods find exp. *Clin Pharmacol* 21:139–151
- Neumann E, Rosenheck K (1972) Permeability changes induced by electrical pulses in vesicular membranes. *J Membr Biol* 10:279–290
- Neumann E, Schaefer-Ridder M, Wang Y, Hofschneider PH (1982) Gene transfer into mouse lymphoma cells by electroporation in high electric fields. *EMBO J* 1:841–845
- Odia S, Vocks E, Rakoski J, Ring J (1996) Successful treatment of dyshidrotic hand eczema using tap water iontophoresis with pulsed direct current. *Acta Derm Venereol (Stockh)* 76:472–474
- Ogura M, Paliwal S, Mitragotri S (2008) Low-frequency sonophoresis: current status and future prospects. *Adv Drug Deliv Rev* 60:1218–1223
- Oh SY, Leung L, Bommannan D, Guy RH, Potts RO (1993) Effect of current, ionic strength and temperature on the electrical properties of skin. *J Control Rel* 27:115–125
- Oosawa F (1957) A simple theory of thermodynamic properties of polyelectrolyte solutions. *J Polymer Sci* 23:421–430
- Osada Y, Gong J-P (1998) Soft and wet materials: polymer gels. *Adv Mater* 10:827–837
- Panchagnula R, Pillai I, Nair VB, Ramarao P (2000) Transdermal iontophoresis revisited. *Curr Opin Chem Biol* 4:468–473
- Park D, Park H, Seo J, Lee S (2014) Sonophoresis in transdermal drug delivery. *Ultrasonics* 54:56–65
- Park EJ, Dodds J, Smith NB (2008) Dose comparison of ultrasonic transdermal insulin delivery to subcutaneous insulin injection. *Int J Nanomed* 3:335–341
- Park EJ, Werner J, Smith NB (2007) Ultrasound mediated transdermal insulin delivery in pigs using a lightweight transducer. *Pharm Res* 24:1396–1401
- Park H, Park K, Shalaby WSW (2011) Biodegradable hydrogels for drug delivery. CRC Press
- Park K, Shalaby WSW, Park H (1993) Biodegradable hydrogels for controlled drug delivery. Technomic Publishing Co., Inc., Lancaster, PA Chapter 1
- Patel MP, Churchmana ST, Cruchley AT, Bradena M, Williams DM (2013) Delivery of macromolecules across oral mucosa from polymeric hydrogels is enhanced by electrophoresis (iontophoresis). *Dental Mat* 29:e299–e307
- Paudel KS, Milewski M, Swadley CL, Brogden NK, Ghosh P, Stinchcomb AL (2010) Challenges and opportunities in dermal/transdermal delivery. *Ther Deliv* 1:109–131
- Peppas NA, Keys KB, Torres-Lugo M, Lowman AM (1999) Poly(ethylene glycol)-containing hydrogels in drug delivery. *J Control Rel* 62:81–87

- Peppas NA, Ritger PL (1987a) A simple equation for description of solute release I. Fickian and non-fickian release from non-swollable devices in the form of slabs, spheres, cylinders or discs. *J Control Rel* 5:23–36
- Peppas NA, Ritger PL (1987b) A simple equation for description of solute release II. Fickian and anomalous release from swellable device. *J Control Rel* 5:37–42
- Petchsangai M, Rojanarata T, Opanasopit P, Ngawhirunpat T (2014) The combination of microneedles with electroporation and sonophoresis to enhance hydrophilic macromolecule skin penetration. *Biol Pharm Bull* 37:1373–1382
- Pikal MJ (1992) The role of electroosmotic flow in transdermal iontophoresis. *Adv Drug Deliv Rev* 9:137–176
- Pikal MJ, Shah S (1991) Study of the mechanisms of flux enhancement through hairless mouse skin by pulsed DC iontophoresis. *Pharm Res* 8:365–369
- Pillai O, Panchagnula R (2003) Transdermal delivery of insulin from poloxamer gel: ex vivo and in vivo skin permeation studies in rat using iontophoresis and chemical enhancers. *J Control Rel* 89:127–140
- Pliquett U, Weaver JC (1996) Transport of a charged molecule across the human epidermis due to electroporation. *J Control Rel* 38:1–10
- Polat BE, Hart D, Langer R, Blankschtein D (2011) Ultrasound-mediated transdermal drug delivery: mechanisms, scope, and emerging trends. *J Control Rel* 152:330–348
- Prasad R, Anand S, Khar RK, Dinda AK, Koul V (2009) Studies on in vitro and in vivo transdermal flux enhancement of methotrexate by a combinational approach in comparison to oral delivery. *Drug Dev Ind Pharm* 11:1281–1292
- Prasad R, Koul V (2012) Transdermal delivery of methotrexate: past, present and future prospects. *Ther Del* 3:315–325
- Prasad R, Koul V, Anand S, Khar RK (2007) Effect of DC/mDC iontophoresis and terpenes on transdermal permeation of methotrexate: in vitro study. *Int J Pharm* 333:70–78
- Prausnitz MR (1998) Electroporation. In: Berner B, Dinh SM (eds) Electronically controlled drug delivery. CRC Press, Boca Raton, FL, pp 185–214
- Prausnitz MR (1999) A practical assessment of transdermal drug delivery by skin electroporation. *Adv Drug Deliv Rev* 35:61–76
- Prausnitz MR, Bose VG, Langer R, Weaver JC (1993) Electroporation of mammalian skin: a mechanism to enhance transdermal drug delivery. *Proc Natl Acad Sci USA* 90:10504–10508
- Prausnitz MR, Langer R (2008) Transdermal drug delivery. *Nat Biotech* 26:1261–1268
- Prausnitz MR, Mitragotri S, Langer R (2004) Current status and future potential of transdermal drug delivery. *Nat Rev Drug Discov* 3:115–124
- Prausnitz MR (1997) Reversible skin permeabilization for transdermal delivery of macromolecules. *Crit Rev Ther Drug Carrier Syst* 14:455–483
- Qiu Y, Park K (2001) Environment -sensitive hydrogels for drug delivery. *Adv Drug Deliv Rev* 53:321–339
- Quinn HL, Hughes CM, Donnelly RF (2016) Novel methods of drug administration for the treatment and care of older patients. *Int J Pharm*. In Press
- Raiman J, Koljonen M, Huikko K, Kostianen R, Hirvonen J (2004) Delivery and stability of LHRH and Nafarelin in human skin: the effect of constant/pulsed iontophoresis. *Eur J Pharm Sci* 21:371–377
- Rastogi R, Anand S, Koul V (2010a) Electroporation of polymeric nanoparticles: an alternative technique for transdermal delivery of insulin. *Drug Dev Ind Pharm* 36:1303–1311
- Rastogi R, Anand S, Dinda AK, Koul V (2010b) Investigation on the synergistic effect of a combination of chemical enhancers and modulated iontophoresis for transdermal delivery of insulin. *Drug Dev Ind Pharm* 36:993–1004
- Rehman K, Zulfakar MH (2014) Recent advances in gel technologies for topical and transdermal drug delivery. *Drug Dev Ind Pharm* 40:433–440
- Rosendal T (1943) Studies on the conducting properties of the human skin to direct current. *Acta Physiol Scand* 5:130–151

- Sale AJH, Hamilton WA (1967) Effects of electric fields on microorganisms killing of bacteria and yeasts. *Biochim Biophys Acta* 118:781–788
- Samchenko Y, Ulberg Z, Korotych O (2011) Multipurpose smart hydrogel systems. *Adv Colloid Interface Sci* 168:247–262
- Sardesai NY, Weiner DB (2011) Electroporation delivery of DNA vaccines: prospects for success. *Curr Opin Immunol* 23:421–429
- Saroha K, Singh S, Aggarwal A, Nanda S (2013) Transdermal gels—an alternative vehicle for drug delivery. *Int J Pharm Chem Biol Sci IJPCBS* 3:495–503
- Scheuplein RJ (1965) Mechanism of percutaneous absorption: I. Routes of penetration and the influence of solubility. *J Invest Dermatol* 29:131–149
- Scheuplein RJ (1967) Mechanism of percutaneous absorption: II. Transient diffusion and the relative importance of various routes of skin penetration. *J Invest Dermatol* 48:79–88
- Schreier H, Bouwstra J (1994) Liposomes and niosomes as topical drug carriers—dermal and transdermal drug-delivery. *J Control Rel* 30:1–15
- Schuetz YB, Naik A, Guy RH, Kalia YN (2005) Emerging strategies for the transdermal delivery of peptide and protein drugs. *Expert Opin Drug Deliv* 2:533–548
- Scott ER, Laplaza AI, White HS, Phipps JB (1993) Transport of ionic species in skin: contribution of pores to the overall skin conductance. *Pharm Res* 10:1699–1709
- Sen A, Daly MS, Hui SW (2002) Transdermal insulin delivery using lipid enhanced electroporation. *Biochim Biophys Acta* 1564:5–8
- Shipton EA (2012) Advances in delivery systems and routes for local anaesthetics. *Trends Anaesth Critical Care* 2:228–233
- Sieg A, Guy RH, Delgado-Charro MB (2004) Electroosmosis in transdermal iontophoresis: implications for noninvasive and calibration-free glucose monitoring. *Biophys J* 87:3344–3350
- Sims SM, Higuchi WI, Srinivasan V (1991) Skin alteration and convective solvent flow effects during iontophoresis: I. Neutral solute transport across human skin. *Int J Pharm* 69:109–121
- Sirsi SR, Borden MA (2014) State-of-the-art materials for ultrasound-triggered drug delivery. *Adv Drug Del Rev* 72:3–14
- Smith NB, Lee S, Maione E, Roy RB, McElligott S, Shung KK (2003a) Ultrasound-mediated transdermal transport of insulin in vitro through human skin using novel transducer designs. *Ultrasound Med Biol* 29:311–317
- Smith NB, Lee S, Shung KK (2003b) Ultrasound-mediated transdermal in vivo transport of insulin with low-profile cymbal arrays. *Ultrasound Med Biol* 29:1205–1210
- Spierings EL, Brevard JA, Katz NP (2008) Two-minute skin anesthesia through ultrasound pretreatment and iontophoretic delivery of a topical anesthetic: a feasibility study. *Pain Med* 9:55–59
- Swartzendruber DC, Wertz PW, Madison KC (1987) Evidence that the corneocyte has a chemically bound lipid envelope. *J Invest Dermatol* 88:709–713
- Tachibana K, Tachibana S (1991) Transdermal delivery of insulin by ultrasonic vibration. *J Pharm Pharmacol* 43:270–271
- Tachibana K, Tachibana S (1993) Use of ultrasound to enhance the local anesthetic effect of topically applied aqueous lidocaine. *Anesthesiology* 78:1091–1096
- Tagami H, Ohi M, Iwatsuki K, Kanamaru Y, Yamada M, Ichijo B (1980) Evaluation of the skin surface hydration in vivo by electrical measurement. *J Invest Dermatol* 75:500–507
- Tezel A, Sens A, Mitragotri S (2002) Incorporation of lipophilic pathways into the porous pathway model for describing skin permeabilization during low frequency sonophoresis. *J Control Rel* 83:183–188
- Tezel A, Sens A, Tuchscherer J, Mitragotri S (2001) Frequency dependence of sonophoresis. *Pharm Res* 18:1694–1700
- Tuncel A, Demiroz PS, Piskin E (2002) A novel approach for albumin determination in aqueous media by using temperature and pH sensitive *N*-isopropyl acrylamide-co-*N*-[3-(dimethylamino)-propyl] methacrylamide random co-polymers. *J Appl Polym Sci* 84:2060–2070
- Uma DS, Ganesan M, Mohanta GP, Manavalan R (2002) Design and evaluation of tetracycline hydrochloride gels. *Indian Drugs* 39:552–554

- Valenta C, Auner BG (2004) The use of polymers for dermal and transdermal delivery. *Eur J Pharm Biopharm* 58:279–289
- Wang YM, Allen LV, Li LC (2000) Effect of sodium dodecyl sulphate on iontophoresis of hydrocortisone across hairless mouse skin. *Pharm Dev T* 5:533–542
- Weaver JC, Chizmadzhev YA (1996) Theory of electroporation: a review. *Bioelectrochem Bioenerg* 41:135–160
- Wichterle O, Lim D (1960) Hydrophilic gels for biological use. *Nature* 1185:117–118
- Williams AC (2003) Structure and function of human skin. In: *Transdermal and topical drug delivery—from theory to clinical practice*. Pharmaceutical press, London, pp 1–25
- Wong TW (2014) Electrical, magnetic, photomechanical and cavitational waves to overcome skin barrier for transdermal drug delivery. *J Control Rel* 193:257–269
- Wong TW, Chen TY, Huang CC, Tsai JC, Hui SW (2011) Painless skin electroporation as a novel way for insulin delivery. *Diabetes Technol Ther* 13:929–935
- Yamamoto T, Yamamoto Y (1976) Electrical properties of the epidermal stratum corneum. *Med Biol Eng Comput* 14:151–158
- Yarmush ML, Golberg A, Serša G, Kotnik T, Miklavci D (2014) Electroporation based technologies for medicine: principles, applications, and challenges. *Annu Rev Biomed Eng* 16:295–320
- Zhang I, Shung KK, Edwards DA (1996) Hydrogels with enhanced mass transfer for transdermal drug delivery. *J Pharm Sci* 85:1312–1316
- Zorec B, Becker S, Reberšek M, Miklavci D, Pavšelj N (2013) Skin electroporation for transdermal drug delivery: the influence of the order of different square wave electric pulses. *Int J Pharm* 457:214–223
- Zorec B, Jelenc J, Miklavčič D, Pavšelj N (2015) Ultrasound and electric pulses for transdermal drug delivery enhancement: ex vivo assessment of methods with in vivo oriented experimental protocols. *Int J Pharm* 490:65–73

Chapter 10

Graphene Oxide–Polymer Gels



Abbas Dadkhah Tehrani, Mohsen Adeli, Sh. Sattari
and Kh. Soleimani

Abstract Recently, graphene oxide (GO), as a two-dimensional carbon nanomaterial, has received a surge of attention in the scientific communities due to its unique structure and properties. The GO-based hydrogels have been prepared using different strategies such as acidification or by addition of organic molecules, polymers, or ions as crosslinkers which could crosslink them by covalent and supramolecular interactions such as H-bonding, coordination interactions, and hydrophobic interactions. Similarly, hydrogels based on chemically modified or grafted GO have been also reported. GO-based composites and hydrogels due to their unique features broadly examined for numerous applications such as wastewater treatment, catalysis, biomedical applications, energy storage devices, supercapacitors, and sensors. To meet the demands of such applications, assembling of graphene-based nanolayers into three-dimensional gel-like networks is the main issue that should be considered. This chapter reviews some recent progress on 3D GO-based composites and gels.

Keywords Polymer gels · Graphene oxide · Hydrogel · 3D network structure

1 Introduction

A gel is described as a soft, solid, or liquid-like unique condensed material that has a three-dimensional network composed of several components such as long polymers, species of small molecules, and a large amount of solvent. These 3D network-condensed materials usually form through chemical, physical, or supramolecular crosslinking. The weight and size of gels are more like a liquid, but they are treated like a solid. Two important characteristics of gels are phase state and their rheological properties. In addition to the customary gels, the progress in

A. Dadkhah Tehrani (✉) · M. Adeli · Sh.Sattari · Kh.Soleimani
Department of Chemistry, Faculty of Science, Lorestan University,
Khorramabad, Iran
e-mail: a_dadkhahtehrani@yahoo.com; Dadkhah.a@lu.ac.ir

technology and fabrication has led to the development of a new generation of gels known as smart gels, which are sensitive to different kinds of stimuli agents. In the other words, their network gel structures can alter upon changes in pH, temperature, ionic strength, solvent type, or electrical potential (Lloyd and Steed 2009; Jung et al. 2013; Chaterji et al. 2007; Mao et al. 1998; Rogovina and Vasil'ev 2010; Liu et al. 2016; Jagur-Grodzinski 2010; Can et al. 2003).

Polymeric gels are known as 3D network polymer solvent systems comprised of flexible polymer chains, crosslinking agent, and large amount of solvent (Thakur and Thakur 2014, 2015). An interesting feature of polymeric gels is their ability to swell in liquids without dissolving in them and their capability to retain a large quantity of solvent (from tens to thousands of times larger than the amount of the polymeric matrix weight). The distance between the crosslinking points is an important parameter in the increment of the equilibrium swelling capacity of polymeric gels. The phase state, structure, and rheological properties are also important characteristics of polymer gels. Hydrogels and organogels are two main types of polymeric gels. Hydrogels containing hydrophilic groups in their structures, and consequently can absorb water and swell, while organogels can swell in the liquid organic phases due to their hydrophobic nature. Moreover, polymeric gels in another classification can be classified as covalently crosslinked gels and non-covalent crosslinked networks that are also known as supramolecular polymer gels. Supramolecular polymeric gels usually fabricate through supramolecular interactions such as hydrophobic interactions, electrostatic forces, hydrogen bonds, π - π interactions, and metal-ligand coordination bonding (Chaterji et al. 2007; Liu et al. 2016; Jagur-Grodzinski 2010; Can et al. 2003). Polymer gels due to their specific mechanical characteristics like low elastic moduli and large deformability have attracted considerable attention. The elasticity of polymer gels is mostly due to a large amount of solvent and the flexibility of polymer chains. An important property of polymer gels, versus polymer solutions, is that they maintain their shape under their own weight.

2 The Importance and Application of Polymeric Gels

To further understand the importance and application of polymeric gels and gels, many studies have been conducted on them. Polymeric hydrogels can swell in aqueous solutions and also due to their phase state, structure and rheological properties, have great importance in different industries. Polymer hydrogels especially those prepared from biopolymers are biocompatible and, therefore, are appropriate candidates for biomedical applications. In fact, polymer hydrogels have been widely used as drug delivery systems because of their high solute diffusion rate. On the other hand, these gels due to their high transparency and their ideal soft and wet surface are considered as one of the best choices for contact lenses (Lee et al. 2014; Alam et al. 2016). Polymeric gels usually contain huge number of functional groups and consequently can adsorb a variety of organic and inorganic

materials (Franklin and Guhanathan 2015; Cha et al. 2014; Tai et al. 2013; Zhang et al. 2011; Gan et al. 2015). They exhibited many applications in diverse technologies including templates for biomedical devices, biological scaffolds for tissue engineering (Yamato et al. 2002; Yeo and Kohane 2008; Cong et al. 2013; Luo and Shoichet 2004; Nowak et al. 2002), biosensors (Lee et al. 2008), actuators (Hoffmann et al. 1999; Yu et al. 2015b), catalysis (as supports) (Lloyd and Steed 2009), enzyme immobilization, molecular separation (Shen et al. 2009), energy storage devices, electric fields, and chronobiology. Biocompatible hydrogels are the potential candidates for applications such as drug and gene delivery and tissue engineering (Chaterji et al. 2007; Fan et al. 2013; Ma et al. 2013; Hong et al. 2008). Moreover, porous GO-biopolymer gels can be applied as an adsorbent for removal of cationic dyes and heavy metal ions from wastewater (Deng et al. 2013; Wang et al. 2014a). Polymeric gels have also been used as an electrolyte in rechargeable batteries (Sun et al. 2016).

However, gels have several limitations in their applications due to their poor mechanical properties, but via incorporating with nanoparticles especially graphene and its derivatives, they showed improved new properties, such as large surface areas, very low density, and enhanced mechanical performance (Zhao et al. 2015; Shen et al. 2012).

Graphene, a one-atom-thick two-dimensional crystal with high planar surface, remarkable electronic, mechanical, optical, and thermal properties has attracted tremendous attention in various fields (Mao et al. 2013; Zhu et al. 2010a; Park and Ruoff 2009; Eigler and Hirsch 2014; Zheng and Kim 2015; Miculescu et al. 2016). Large-scale production of graphene and its homogeneous dispersion in the polymer matrices are the main issues in the preparation of graphene-based nanocomposites and hydrogels. In fact, graphene oxide (GO) considered as an excellent precursor for large-scale fabrication of graphene. GO generally provided by oxidation of graphite powder to produce graphite oxide using suitable oxidizing agents and then exfoliation of graphite oxide to form GO sheets by sonication. GO is the most important derivative of graphene because of its two specific characters: (1) due to the existence of polar functional groups on its surface, GO easily can be dispersed in aquatic environment; (2) GO can be functionalized with wide spectrum of compounds through covalent and noncovalent interactions to prepare functionalized GO derivatives (Li et al. 2014; Chen et al. 2012; Su and Loh 2012; Dreyer et al. 2010, 2014).

Meanwhile, GO has a flexible 2D structure and is containing plenty of carboxylic acid groups, which can be the source of repulsive electrostatic forces as well as hydrogen bonding interaction, and consequently considered as a suitable candidate for fabricating 3-dimensional (3D) graphene-based materials. The balance between attractive and repulsive forces due to covalent and noncovalent interactions, by addition of crosslinkers (organic molecules, polymers, or ions) or by adjustment of pH of the solution can lead to the adjustment of interlayer distance and preparation of self-assembled structures and can promote gelation of GO. Compared with the graphene oxide, graphene-based gels exhibit improved structural features such as larger specific surface areas, higher interpenetrated porous

network architecture, and better electronic properties that remark its potential applications in the fields of electrochemical biosensors, energy storage, supercapacitors, biological fuel cells, drug delivery systems, and wastewater treatment (Li and Shi 2014; Bai et al. 2011a; Yuan et al. 2014). The studies on the GO-based polymer gels have been grown because these types of gels benefited from the advantages of both the graphene oxide and the polymer used. Also, grafting of the polymers to the surface of graphene oxide and its derivatives during GO-based polymeric hydrogel fabrication can prevent aggregation of its sheets and could alter the chemical structure of GO (Gan et al. 2015; Zhang et al. 2014).

3 Synthesis of Graphene and Graphene-Related Nanostructures

3.1 *Synthesis of GO*

The present section deals with the history and the most important preparation methods of graphene oxide. GO as an amphiphilic macromolecule, is significantly used in the construction of 3D graphene-based materials. Normally, GO is synthesized by the controlled oxidation of graphite in acidic media. The obtained graphite oxide at the next step undergoes an exfoliation process. Mechanical shaking and ultrasonication are most commonly used approaches for exfoliation of graphite oxide layers. The quality of resulting GO after exfoliation process significantly depends on starting materials, oxidation process, and the method used for exfoliation (Dreyer et al. 2010; Chen et al. 2012; Li et al. 2014). The first study on the chemistry of graphite has been done by Brodie (1859). He succeeded to prepare GO with the net molecular formula of $C_{2.19}H_{0.80}O_{1.00}$ by adding potassium chlorate ($KClO_3$) and nitric acid (HNO_3) to a slurry of graphite, for the first time. Resulting GO showed better dispersion in basic and neutral media than acidic media. Nearly 40 years later, Staudenmaier (1899) made a slight change in Brodie's procedure for the preparation of GO. He used concentrated H_2SO_4 and potassium chlorate solution and successfully synthesized GO nanosheets with higher oxidation level compared with GO that was provided by Brodie. Nearly 60 years after Staudenmaier, Hummers and Offeman (1958) oxidized graphite to graphite oxide using a mixture of oxidizing agents consist of sulfuric acid, sodium nitrate, and potassium permanganate. In general, the strategies used by Brodie and Staudenmaier not only required a longer time to react but also these methods were not safe due to ClO_2 gas that was produced during the reaction. However, Hummers method was usually carried out in a very short time (about 2 h at 45 °C). This method is also more safe due to the absence of hazardous ClO_2 gas. Kovtyukhova et al. (1999), introduced modified Hummers method and improved the efficiency of the oxidation by adding H_2SO_4 , $K_2S_2O_8$, and P_2O_5 to graphite powder. In 2010,

Marcano used different oxidizing agents such as KMnO_4 , H_2SO_4 , and H_3PO_4 . This method is also known as improved Hummers method. Improved Hummers' method has some significant advantages over Hummers' method such as increment in the number of isolated aromatic rings that are produced in this process in comparison with other related processes, easy temperature control, and more regular structure. Moreover, this method avoids the release of NO_x (Marcano et al. 2010). In fact, improved Hummers' method is a more favorable choice than other methods because of its convenient operation, safety, and its better reaction efficiency (Chen et al. 2013a, 2015).

3.2 *Reduced GO (rGO)*

The GO sheets synthesized by chemical oxidation unlike their parents, graphene sheets, have electrical insulating characteristics due to defect formation in the carbon-conjugated system during oxidation process. Fortunately, GO can be easily converted to the reduced GO by chemical, electrochemical, hydrothermal, solvothermal, thermal, and photo-catalyzed reduction. Hydrogels provided by rGO because of their higher electrical conductivities, strong mechanical strengths, wonderful thermal, chemical, and electrochemical stability have attracted a widespread attention in recent years (Mao et al. 2012; Chua and Pumera 2014; Compton and Nguyen 2010; Pei and Cheng 2012). Reduction of graphene oxide using chemical methods has a great advantage compared to other methods of reduction. For example, the chemical reduction process can be carried out at a relatively low temperature and it is applicable under acidic or alkaline conditions, in both solutions and gas phases (Pei and Cheng 2012). Up to now, various reducing agents such as hydrazine (Li et al. 2008a; Chen et al. 2008; Tung et al. 2009), NaBH_4 (Gao et al. 2009; Wang et al. 2011a; Shin et al. 2009), ascorbic acid (Zhang et al. 2010; Fernandez-Merino et al. 2010), hydrogen-rich water (Akhavan et al. 2015), green tea (Wang et al. 2011b), and amino acids (Chen et al. 2011) have been applied to reduce GO. Among them, hydrazine and NaBH_4 are the most efficient reducing reagents, which can be used for large-scale fabrication of GO without the need of stabilizers. However, toxicity, corrosiveness, and existence of traces of heteroatoms in the obtained rGOs by these reducing agents lead to the use of alternative non-toxic reducing agents including ascorbic acid as well as reduction of graphene oxide through alternative strategies, for example, hydrothermal and electrochemical reduction (Pei and Cheng 2012; Thakur and Karak 2015). In hydrothermal approach, the exfoliation of stacked layers is usually performed through a rapid increase of the temperature that leads to generation and increment of the interlayer gas pressure due to the production and evaporation of CO , CO_2 , H_2O , etc. As mentioned, reduction of GO by microwave irradiation also have been reported (Hayes et al. 2015; Jia et al. 2015; Vermisoglou et al. 2015). The microwave irradiation as heating sources in the thermal reduction can generate uniform and rapid heat within a short period of time. This kind of energy source by lowering the

activation energies can promote the chemical reactions compared with traditional thermal methods (Chen et al. 2010; Zhu et al. 2010b; Wang et al. 2015b). Photothermal approach also can be used for reduction of the GO sheets via thermal deoxygenation process (Yeh et al. 2014; Guo et al. 2013; Mukherjee et al. 2012). As an example, organic photocatalysts have been utilized to produce reduced graphene with high electrical conductivity (Zhang et al. 2012).

Inorganic nanomaterials are rarely used to reduce graphene oxide because the remaining metals in the produced rGO dramatically influence the electrical properties of the produced graphene (Wu et al. 2011; Williams and Kamat 2009). Electrochemical reduction is another route for the preparation of rGO. The reduction process is carried out either by exposure of GO films to a negative potential or by electrophoretic and potentiostatic routes. Reduction process by electrophoretic and potentiostatic routes leads to simultaneous assembly and reduction. In these methods, electrons act as reducing agents and effectively eliminate oxygen-containing functional groups of graphene oxide surface and lead to the production of rGO without heteroatom contaminations (Moraes et al. 2015; Low et al. 2013). The hydrothermal or solvothermal process also can be used to reduce GO. However, heteroatoms, various metal oxides, and sulfides can be introduced into graphene under hydrothermal or solvothermal conditions (Moussa et al. 2016; Liu et al. 2015b).

3.3 *Synthesis of Graphene*

In the literature, there are two different types of methods for the synthesis of graphene, top-down and bottom-up approaches that each of these methods include several different ways (Zheng and Kim 2015; Edwards and Coleman 2013; Avouris and Dimitrakopoulos 2012). In top-down approach, single graphene sheets can be achieved from graphite, whereas in bottom-up approaches usually carbon-containing sources have been used for the synthesis of graphene sheets. Top-down methods involve micromechanical cleavage, solvent-based and electrochemical exfoliation, graphite and graphite oxide intercalation compounds exfoliation, and unzipping of carbon nanotubes. In top-down methods, there are several challenges including reaction yields, numerous steps, and production of defect-free graphene sheets (Edwards and Coleman 2013). Bottom-up methods are generally carried out in a simple manner and produce a large area of graphene sheets but require higher temperature and lead to fabrication of sheets which are containing higher levels of defects (Zhu et al. 2010a; Eigler and Hirsch 2014; Edwards and Coleman 2013; Avouris and Dimitrakopoulos 2012; Choi and Jo-won 2013).

Micromechanical cleavage also known as “scotch tape” or “peel-off” method is the first method that is used to experimentally isolate graphene. This method is suitable for the preparation of high-quality graphene. However, high-scale production of graphene using this technique is difficult and requires more time (Edwards and Coleman 2013; Choi and Jo-won 2013). Also, various strategies reported on the preparation of graphene by using electrochemical approaches

(Aqil et al. 2013; Wei et al. 2012). Solvent assisted and thermal exfoliation are two main methods for preparation of graphene from graphite intercalation compounds (GICS). In solvent-assisted strategies, exfoliation is performed by sonicating of graphite intercalation compounds (GICS) in solution. In thermal exfoliation, GICS is exfoliated to a nanoscale level along the *c*-axis of the graphene layer by thermal decomposition of the intercalated species (Vallés et al. 2008; Li et al. 2008b). Moreover, sonication of unmodified graphite flakes in aqueous surfactant solutions and organic solvent like *N*-methylpyrrolidone (NMP 230 °C) is another method to produce graphene. However, exfoliation and reduction of graphite oxide is the most common method to produce graphene. Also, it is worth noting that the reducing of GO to graphene is not complete even if the reduction process is complete (Gounko et al. 2008). Therefore, high levels of defects which are created during the oxidation process will remain in the resulting graphene sheets. As previously mentioned unzipping single or multiwalled carbon nanotubes by chemical and physical treating is an effective technique for preparation of graphene “nanoribbons”. Regular nanoribbons are achieved via unzipping of flattened carbon nanotubes (Edwards and Coleman 2013; Kosynkin et al. 2009).

Sublimation of silicon from the silicon carbide (SiC) surface and graphitization of the excess carbon atoms left behind is a bottom-up method for preparation of graphene (Sutter 2009; Srivastava et al. 2012). Besides, chemical vapor deposition (CVD), using pyrolysis of carbon-containing compounds in gaseous form, as another bottom-up method was first reported in 2008 and 2009 and is known as an effective technique for the synthesis of single- or few-layer graphene (Edwards and Coleman 2013; Avouris and Dimitrakopoulos 2012; Reina and Kong 2012; Miao et al. 2011). Depending on the type of metal that is used as substrate, preparation of graphene through CVD approach can be performed by surface catalyzed or segregation methods. In addition to the methods mentioned above, many other methods have been reported in the literature for synthesizing few-layer graphene (Reina and Kong 2012; Miao et al. 2011).

4 GO-Based Hydrogels

GO-based hydrogels can be constructed through aggregation of GO layers upon addition of crosslinking agents such as polymers, divalent cations or small organic molecules (Li and Shi 2014; Bai et al. 2011a; Zhao et al. 2014). Moreover, additive-free GO pristine hydrogels are another type of GO-based hydrogels which can be produced by tuning physical conditions of the system such as pH, temperature, and ultrasonication of GO aqueous dispersions. The electrostatic repulsion due to the presence of negatively charged carboxylate and other anions along with the bonding force among GO sheets, commonly due to the hydrogen bonding, can control the gelation process. Moreover, the concentration of GO and crosslinking agents has a significant effect on pore density and size of gels (Li and Shi 2014; Bai et al. 2011a; Chabot et al. 2014). In the following sections, we will focus on

graphene oxide gelation by polymers and other approaches which lead to preparation of GO-based hydrogels is partially discussed.

4.1 Gelation of GO Through Complexation with Metal Ions

Up to now, considerable effort has been devoted to develop strategies in order to promote gelation of GO sheets by a variety of metal ions as crosslinkers agent (Li and Shi 2014; Zhao et al. 2014). Researchers found that multivalent ions through coordination with oxygenated moieties on GO sheets could promote gelation of GO sheets. Hydrogels provided by multivalent ions typically exhibit greater formation constants with oxygen-containing surface functional groups of GO sheets than that of monovalent ions (Park et al. 2008). For example, Huang, and co-workers (Huang et al. 2012) prepared a homogenous graphene oxide (GO) hydrogels using the multivalent metal ions (e.g., La^{3+} , Co^{2+} , Ni^{2+}) as a crosslinkers agent. They added glucono- γ -lactone to the obtained hydrogel and found that addition of glucono- γ -lactone (GDL) by adjusting the pH could promote the process of gelatinization GO by metal ions. The results indicated that the reduction of pH value resulting in gradual hydrolysis of GDL and consequently leads to in situ release of multivalent metal ions and aggregation of GO sheets into a gel.

In another example, Chai et al. (2015) investigated the effect of Cu^{2+} ion on the gelatinization of GO in the presence of poly(m-phenyldiamine). They found that gelatinization process of GO was greatly enhanced in the presence of Cu^{2+} ion that is related to the interaction and electron transfer of Cu^{2+} ion between mPD and GO (Fig. 1). Moreover, cooperative effect of Cu^{2+} leads to highly efficient polymerization of m-phenyldiamine (>99%).

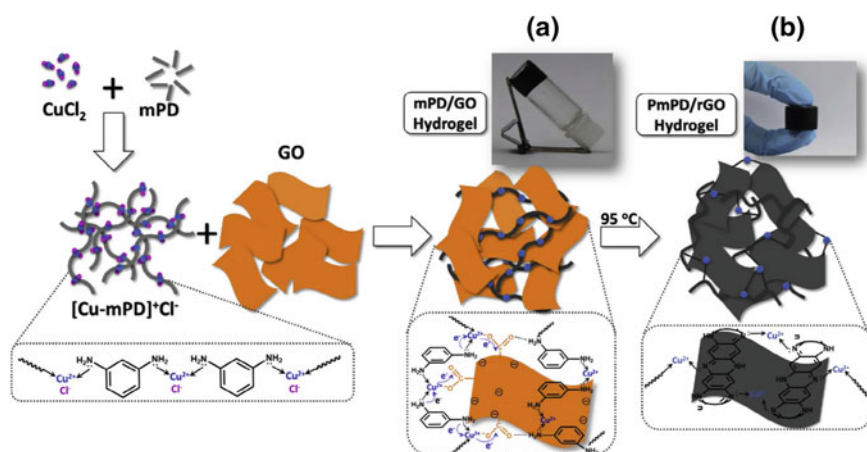


Fig. 1 The mechanism for Cu^{2+} induced the rapid formation of PmPD/rGO hydrogel. Reprinted with permission from Chai et al. (2015), Copyright © 2014 Elsevier Ltd

Cong et al. (2012), reported on the fabrication of a macroscopic graphene/iron oxide hydrogels through simultaneous reduction and decoration of graphene oxide sheets by ferrous ions. At the end of the process, the ferrous ions as α -FeOOH nanorods and magnetic Fe_3O_4 nanoparticles deposited on the surface of reduced GO layers and resulting gel illustrated excellent capability for removal of pollutants from aqueous solutions. ZnO nanorods/rGO hydrogel were also fabricated by Luan et al. (2015), through a two-step process: electrostatic interactions between negatively charged functional groups of GO and positively charged Zn^{2+} ions and then in situ growth of ZnO nanorods under a high temperature between GO nanosheets. ZnO nanorods/graphene-based hydrogels showed excellent electrochemical performances and photocatalyst activity due to effective charge transfer between graphene sheet and ZnO nanorods. Luan et al. reported that 3D-networked ZnO/rGO hydrogel exhibited enhanced photocatalytic activity and excellent dye removal efficiency than that of pristine rGO due to the presence of ZnO nanorods between the rGO layers. Increased surface to volume ratio of ZnO nanorods, improved crystal structures of rGO gel networks and strong electrostatic interactions between positively charged cationic dyes and the negatively charged surface of GO leads to enhanced dye removal efficiency of hydrogel under both UV and visible light illumination.

Interestingly, Zhong et al. (2015) studied the dual crosslinking effects of Fe^{3+} ions within hydrogels based on graphene oxide (GO)-poly(acrylic acid) (PAA). Hydrogels showed excellent mechanical and self-healing properties that may be due to the presence of Fe^{3+} ions into the 3D network. Fe^{3+} ions within the network structure not only attached the polymer chains to each other but also leads to the coordination of GO with polymer chains. In these hydrogels, GO nanosheets and acrylic acid are used as reinforcement agents and polymer matrix, respectively, and Fe^{3+} ions act as the linker that provides excellent mechanical strength, flexibility, and recoverable crosslinking.

As another example, Luan et al. (2015), have employed Ni ions as the linkages to synthesize three-dimensional-reduced graphene oxide hydrogel as a supercapacitor electrode with highly enhanced capacitance. As reported, the capacitance of resulting supercapacitor has remained approximately unchanged even after 1000 charge/discharge cycles. They also reported that the main reason for the GO gelation is an electrostatic force between positively charged Ni^{2+} ions and the negatively charged carboxylic acid and epoxy groups on the GO.

4.2 Gelation Using Small Compounds

As described above, small organic molecules such as amino acids, nucleosides, cetyltrimethyl ammonium bromide, melamine, etc., can also lead to gelation of GO. Adhikari et al. (2011), synthesized GO-Au nanohybrid system. They used amino acids (arginine/tryptophan/histidine) and nucleosides (adenosine/guanosine/cytidine) for the preparation GO-based hydrogels. In these hydrogels, amino

acids or nucleosides can be decorated at the GO surface through hydrogen bonding and acid–base-type electrostatic interactions between hydroxyl or carboxyl groups of GO surface and amino groups of nucleosides/amino acids. Strong interactions between GO sheets and amino acids/nucleosides have been confirmed by AFM, FE-SEM, and XRD techniques. Meanwhile, reduction of Au ions by tryptophan and homogeneous and uniform formation of Au NPs on the surface of the GO nanosheets within the hydrogel were approved by UV/vis spectroscopy, X-XRD, and TEM techniques. Rheological studies of GO-based hydrogel-containing arginine approved that this hydrogel is effective hydrogel with high storage modulus (6.058×10^4 Pa).

In another work, Ma et al. (2012), prepared GO-based hydrogels using doxorubicin hydrochloride. They reported that doxorubicin hydrochloride as an anti-tumor drug also can promote the gelation of graphene oxide nanosheets through various types of interactions such as hydrogen bonding, π – π stacking, and electrostatic interactions. They also found that the gelation time, viscoelasticity, and drug release can be modified by the number of GO nanosheets and the amount of DOX so that, an increase of the GO or DOX amount led to increase and decrease in gel strength and drug release rate, respectively. Moreover, GO/DOX gel showed better mechanical and drug release behavior as well as better inject ability and antitumor efficacy compared to free DOX. Tao et al. (2012), in a similar work, utilized metformin hydrochloride (MFH) as crosslinking agents. MFH as the model drug without the presence of any polymers or other chemical additives under mild conditions can be dispersed within GO layers homogeneously through noncovalent interactions between surface functional groups of GO sheets and its *N*-containing functionalities. These interactions usually are pH dependent. As reported, the weight ratio of MFH to GO can also remarkably affects the gelation process. On the other words, with sufficiently high numbers of crosslinking sites (high content of GO), a GO composite hydrogel will be generated. Inversely, for the composites with high contents of the MFH, a MFH-decorated GO will be generated. Also, evaluation of the obtained results of MFH hydrogel release showed that these samples can be successfully utilized for controlled drug release. Moreover, due to the changes and balance between the repulsive electrostatic forces and attractive forces of hydrogen bonding under different pH conditions, this hydrogel showed pH-dependant release. In this case, the hydrogel exhibited higher release rate in acidic conditions (around 74% during 72 h) than neutral condition (around 50% during 72 h).

4.3 Crosslinker-Free GO Gels

Acidified GO also can be self-assembled into 3D GO network without the influence of any crosslinking agents. The protonation of GO carboxylic groups under acidic conditions in concentrated GO aqueous solutions can form a hydrogel as a result of hydrogen bond formation and reduction of the repulsive forces between GO sheets

(Compton et al. 2012). Lateral dimensions of GO sheets have a significant impact on graphene oxide gelatinization under acidic conditions, so that GO sheets with a thickness smaller than 1 μm could not form gel even in high concentrations of GO and acid. Moreover, the formation of a 3D network with large GO sheets is kinetically favorable. Compton et al. (2012) reported that GO hydrogel can also be prepared by ultrasonication of GO aqueous dispersions even without the addition of any crosslinking agent. They confirmed that ultrasonication as a nonchemical method has no effect on the chemical structure of graphene oxide nanosheets. In this case, the decreasing of lateral dimensions of the nanosheets by ultrasonication and consequently creation of new sheet edges without carboxylate groups, is responsible for the sol–gel transition. They also found that shear modulus of hydrogels increases during ultrasonication (1.6 kPa after 120 min of ultrasonication and 0.3 kPa after 30 min of ultrasonication). Meanwhile, the resulting GO hydrogels exhibited remarkably low critical concentrations for gelation ranging from 0.050 to 0.125 mg mL^{-1} .

4.4 Graphene–Polymer Hydrogels

4.4.1 Gelation Through Covalent Bonding

As a new class of gels, polymer–GO gels due to the combination of both the characteristics of GO and polymers were highly regarded in recent years. Fan et al. (2013), prepared a novel ternary nanocomposite composed of sodium alginate (SA), polyacrylamide (PAM), and GO nanosheets. The composite prepared by free-radical polymerization of acrylamide in the presence of SA and GO and then calcium ions were added to the composite for ionic crosslinking of composite components. In fact, the resulting hydrogel is containing two kinds of crosslinking, ionic crosslinking that acts between alginate chains and covalent crosslinking which forms during polymerization of AM. Also, an enhanced mechanical performance have been reported after the combination of GO into the hydrogels. Ionic crosslinking along with covalent crosslinking leads to the strong interfacial interactions between GO nanosheets and polymer chains and cause the hydrogels illustrate good flexibility.

Zhang et al. (2014) similarly synthesized a novel ternary nanocomposite hydrogel composed of GO, poly acrylamide, and carboxymethylcellulose sodium. They finally used aluminum ions for ionic crosslinking of carboxymethylcellulose sodium (Fig. 2). Moreover, this nanocomposite showed improved mechanical strength due to the formation of homogeneous and strong interactions between the composite components. As the authors stated that the strong interaction between the polymer chains and GO nanosheets plays an important role in improving gel mechanical properties. This hydrogel due to its high level of swelling index and swelling rate constant could be applied in bioengineering and drug delivery system.

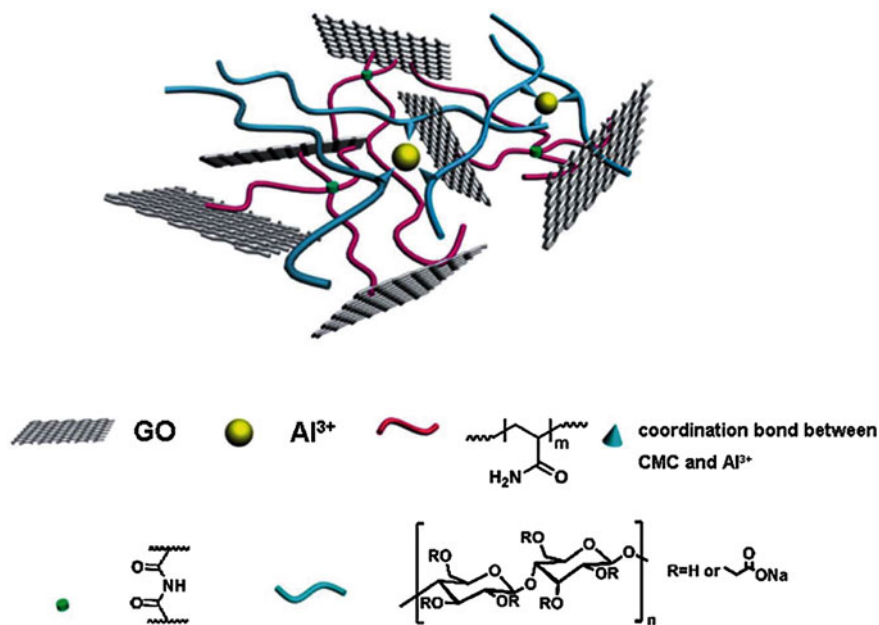


Fig. 2 Diagram of GO/PAM/CMC ternary nanocomposite hydrogel, reprinted with permission from Zhang et al. (2014), Copyright © 2014, Royal Society of Chemistry

Also, the X-ray diffraction studies indicated that GO has been distributed homogeneously in all of the obtained composites.

In addition to polymers, copolymers also have been used as polymer matrices. For example, Yang et al. (2013), prepared an ion gel based on GO using poly(vinylidene fluoride-hexafluoro propylene), [P(VDF-HFP)]. This GO-doped ion gel due to homogeneous distribution of GO can act as ion “highway” to simplify the ion transport. P(VDFHFP)-EMIMBF₄-GO gels due to its excellent compatibility and long-term stability can be applied for the design of energy storage devices in the future. Using a new technique, through a one-step method, Sun and Wu (2011), prepared the GO/PNPIPAM interpenetrating polymer network through covalently bonding of carboxyl groups of GO and PNPIPAM by epichlorohydrin (ECH) (Fig. 3). They reported that this hydrogel network due to its high elasticity can quickly recover to its initial order under the cooling mode. Also, this hydrogel is pH sensitive due to the existence of carboxyl groups and may be able to use for biological applications as a carrier for controlled drug delivery.

In a new research, using ECH, Guo et al. (2015b), prepared chitin/graphene oxide hybrid hydrogels. They stated that this hydrogel due to the layered porous structure has high mechanical properties and can be used to design the criteria for tissue engineering. The resulted hydrogels showed higher compressive strength (260 kPa) in the presence of 35% GO, as compared with pure chitin hydrogel (72.6 kPa).

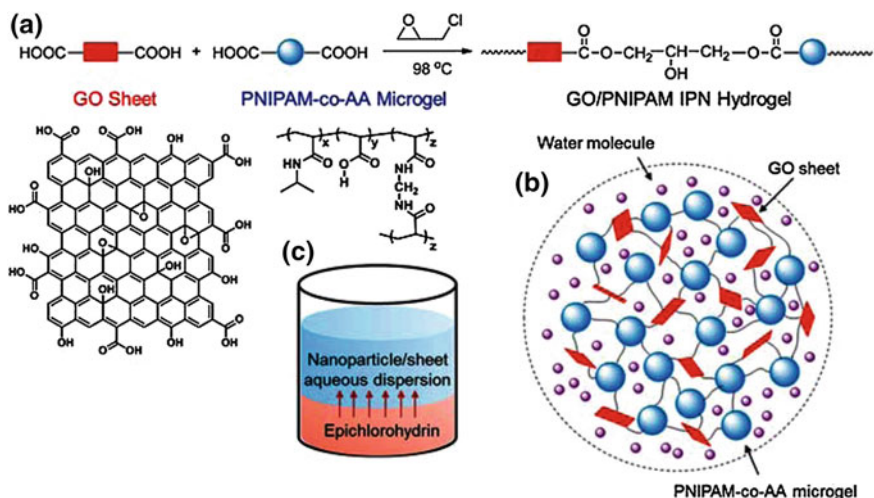


Fig. 3 **a** Synthesis route of GO/PNIPAM, **b** schematic illustration of GO/PNIPAM hydrogel, **c** the schematic sealed reaction tube used for crosslinking by ECH, Reprinted with permission from Sun and Wu (2011), Copyright © 2011, Royal Society of Chemistry

Hyperbranched polymers as highly branched macromolecules with 3D dendritic architectures due to their ease of synthesis on a large scale, unique physical and chemical properties as well as their multiple chain end functionalities represent an important type of soft nanomaterial which has been the focus of modern scientific researches. In this context, recently Yu et al. (2015b), reported a new one-pot, affordable and eco-friendly process for the synthesis of a hydrogel composed of graphene oxide and hyperbranched polyester containing 64 hydroxyl end groups (HB) with high water swelling ratio and appropriate mechanical properties (Fig. 4). These hybrid hydrogels can be employed for heavy metal ion adsorption. Incorporation of hyperbranched polymers and graphene oxide created hydrogels with enhanced mechanical properties.

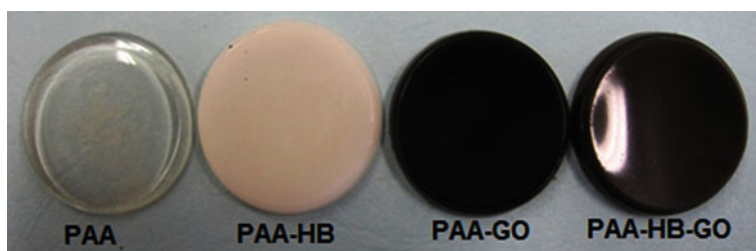


Fig. 4 Photo images of PAA and PAA hybrid samples, reprinted with permission from Yu et al. (2015b), Copyright © 2015, Springer Science + Business Media New York

These days production of eco-friendly materials especially those are based on biopolymers is growing due to the concerns about the limited nature of petroleum-based polymers. Therefore, polysaccharides such as starch, chitin, and cellulose also have been used to fabricate hydrogel composites. For example, Liu et al. reported the synthesis of new economical and eco-friendly hydrogel based on hydroxypropyl cellulose (HPC) and GO through esterification reaction between the composite components. The HPC-GO/HPC hydrogels demonstrated excellent adsorption capacity toward methylene blue and can be applied as economical bio-adsorbent (Fig. 5).

Lin et al. (2015) in a different work used ionic liquids instead of water and other traditional organic solvents to prepare poly(ionic liquid)/ionic liquid/graphene oxide as a polyelectrolyte with high performance, conductivity, and good durability for dye-sensitized solar cells. The maximum efficiency of 4.83% under AM 1.5 solar spectrum irradiation was gained for polyelectrolyte with 2 wt% of GO. They used 1-propyl-3-methylimidazolium iodide and poly(1-butyl-3-vinylimidazolium bis (trifluoromethanesulfonyl) imide) as solvent and polymer respectively.

Acrylamide is one of the most commonly used monomers in hydrogel production, which has been utilized through different strategies and polymerization methods. Graphene oxide/polyacrylamide hydrogels were synthesized by Shen et al. (2012). They used in situ polymerization technique. By using this technique, they could control the polymer architecture as well as the final structure of the hydrogel. This gel showed good mechanical and thermal properties and could be used in various fields such as medical, biological, pharmaceutical, and electronics industry (Fig. 6).

In 2012, Zhu et al. applied γ -irradiation to synthesis photothermally sensitive nanocomposites composed of poly(*N*-isopropylacrylamide) and GO. They used γ -irradiation-assisted polymerization technique for this purpose. The authors found that the GO doping level can effectively control the changes in the colors and phase-transition temperatures of the hydrogels. Resulted nanocomposites with

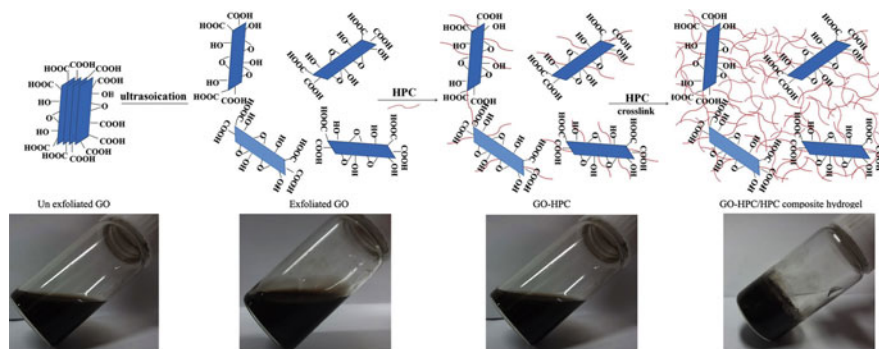


Fig. 5 Scheme of functionalized GO with HPC and HPC-GO/HPC hydrogels, reprinted with permission from Liu et al. (2015a), Copyright © 2015, Springer Science + Business Media New York

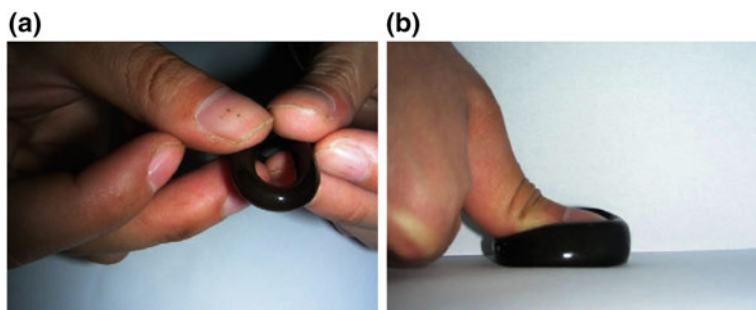


Fig. 6 Mechanical behavior of GO/polyacrylamide gel upon bending (a) and compression (b), reprinted with permission from Shen et al. (2012), Copyright © 2012 Elsevier Ltd

photothermal properties are promising materials for biomedical issues such as drug delivery, microdevices, etc. Zhang et al. (2013) alternatively used free-radical polymerization technique for the polymerization of *N*-isopropyl acrylamide as a vinyl monomer in the presence of an aqueous dispersion of GO. Unfortunately, the composite components did not show appropriate compatibility and do not have strong interaction and therefore they tried to overcome this problem by the addition of hectorite clay as additional nanoparticles to the hydrogels. As the prepared hydrogel exhibited high mechanical strength and can be used as a stimuli-response material. Through the incorporation of graphene oxide (GO) into *N,N*-dimethylaminoethyl methacrylate (DMAEMA), Wang et al. (2014a, b), prepared hybrid hydrogels with excellent adsorption performance. They also used in situ polymerization route and investigated composite sensitivity attribute to alterations in pH and temperature. This hydrogel due to excellent adsorption performance (the maximum Cr(VI) adsorption of 180 mg/g) can be a suitable candidate for water treatment. In another work, via γ -ray pre-irradiation technique, Lee et al. (2014) proposed a controllable route for synthesizing of hydrogels using covalent crosslinking of GO and poly(acrylic acid). The mechanical properties and thermal stability investigations demonstrated that the composite hydrogel containing only 0.05 wt% GO showed enhanced modulus and thermal stability properties (Fig. 7).

4.4.2 Polymer–GO Gels Through Noncovalent Interactions

Preparation of hydrogels through noncovalent interactions is an attractive synthetic method because this method usually preserves the graphene structure and properties. Up to now, a large number of synthetic methods have been reported for preparation of hydrogels through noncovalent interactions between the polymer as crosslinkers and graphene oxide as major nanoscale component (Cui et al. 2015; Baruah and Chowdhury 2016). For example, Cui et al. reported a fully physically crosslinked reusable adsorbent (GHA gel) with superior mechanical strength and high toughness based on the graphene oxide and a copolymer based on

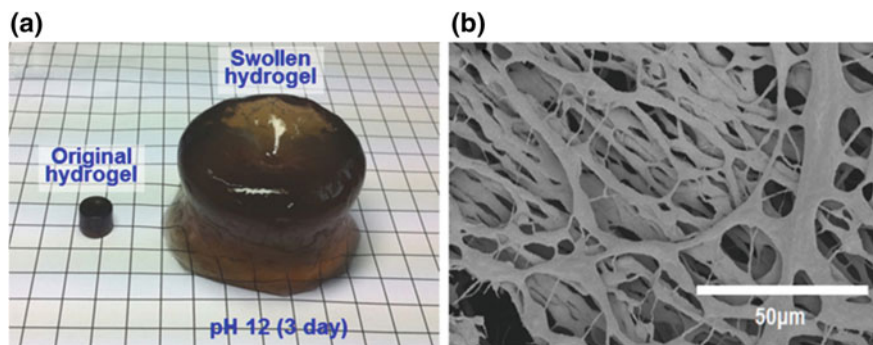


Fig. 7 **a** Digital image and **b** SEM micrograph of hydrogel which stored at pH 12 for 3 days, reprinted with permission from Lee et al. (2014), Copyright © 2014, The Polymer Society of Korea and Springer Science + Business Media Dordrecht

polyacrylamide which contains hydrophobic short chains. This copolymer could interconnect the graphene nanosheets through noncovalent interactions and leads to gelation of the polymer matrix in the presence of GO. This hydrophobic gel was produced by copolymerization of acrylamide as hydrophilic monomer along with stearyl methacrylate as a hydrophobic monomer with a short hydrophobic chain that was designed for noncovalent interaction with GO surface (Fig. 8). GO sheets as physical crosslinking junctions by reversible noncovalent interactions between the functional groups of graphene nanosheets and the amide groups of polyacrylamide as well as stearyl methacrylate chains leads to dramatic enhancement in mechanical strength of GHA gels. GHA gel showed swollen state stability in water for a long period of time and showed desirable mechanical properties even after swelling, because the network structure reorganization of hydrophobically associated polyacrylamide significantly increased self-healing ability and fatigue resistance of GHA gel. GHA gels as recyclable adsorbents showed excellent cyclic dye adsorption capacity towards methylene blue and congo red through electrostatic interaction, π - π interaction, and hydrogen bonding compared with HAPAM (59 mg/g for methylene blue and 13 mg/g for congo red, respectively). In adsorption process, the adsorption kinetic was well simulated with the pseudo-second-order model.

There are many reports on the use of *N,N*-methylenebisacrylamide (BIS) as crosslinking agent for preparation of polyacrylamide (PAM) hydrogels. However, the resulting hydrogels usually exhibit low tensile strength and toughness strength due to formation of short inter crosslinking chains, which form in the PAM network during crosslinking with BIS. Liu et al. (2012) to overcome this limitation, used graphene oxide nanosheets as crosslinkers. Several types of prepared polyacrylamide (PAM)/graphene oxide (GO) nanocomposite hydrogels synthesized using different driving forces such as hydrogen bonding, ionic bonding, and physical adsorption which are shown in Fig. 9. As reported, incorporation of the small amounts of GO can produce PAM hydrogels with enhanced mechanical

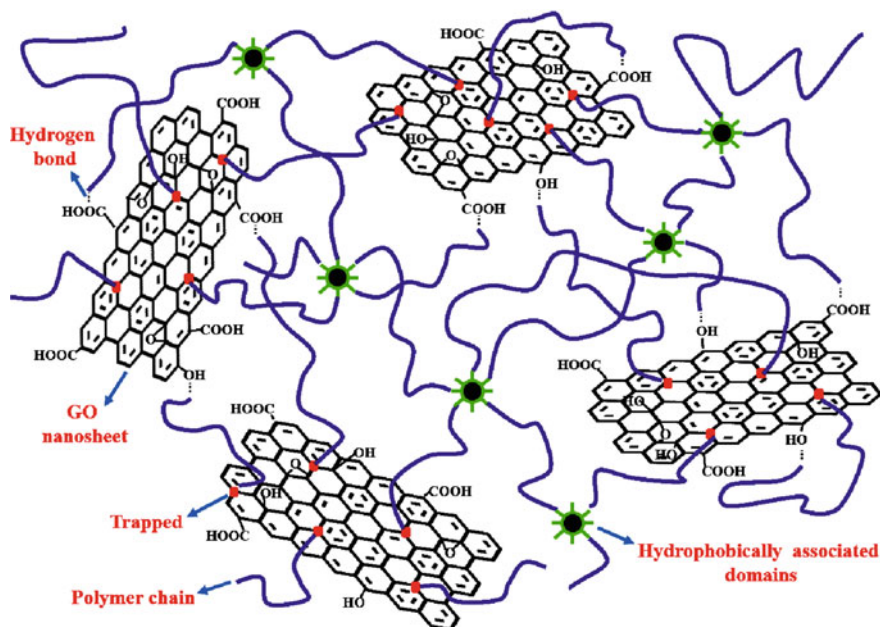


Fig. 8 Illustration of the proposed structure of the GHA gels. Reprinted with permission from Cui et al. (2015), Copyright © 2015, Royal Society of Chemistry

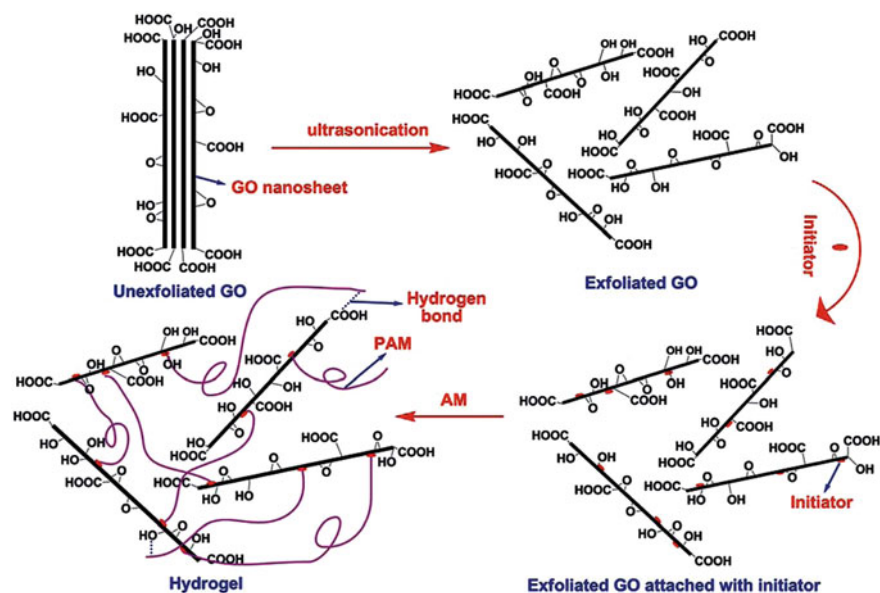


Fig. 9 Schematic of the synthesis of PAM/GO hydrogels. Reprinted with permission from Liu et al. (2012), Copyright © 2012, Royal Society of Chemistry

performance. Moreover, with the same weight percentage of crosslinkers (GO rather than *N,N*-methylenebisacrylamide), hydrogels exhibited lower T_g , higher flexibility and larger deformation that was attributed to the high mobility of crosslinked polymer chains in the GO containing hydrogels.

Polyvinyl alcohol and other hydroxyl containing polymers such as starch and chitosan also have been widely used to fabricate GO-based hydrogels. Hydroxyl-containing polymers, just like polyacrylamide can interact with oxygen-containing groups of GO sheets through hydrogen bonding. Graphene oxide-poly(vinyl alcohol) (PVA) hydrogel with improved mechanical properties has potential application in a variety of fields such as sensors. For instance, Baruah and Chowdhury (2016), used small GO particles known as quantum dot GO for preparation of composites. They prepared different GO-based functionalized graphene oxide quantum dots (GOQDs) through reaction of GO quantum dots by ethylene diamine and PEG and then applied them as crosslinking agents in the preparation of GOQD–PVA hybrid hydrogels. They utilized this hydrogel for easy and simple colorimetric detection of Cu^{2+} , Fe^{2+} , and Co^{2+} with detection limit about 1×10^{-7} M. The results showed that amine-functionalized GOQDs was more stable compared to the GOQDs with $-\text{OH}$, $-\text{COOH}$, and $-\text{COOR}$ functionalities due to increased hydrogen bond sites between polymers and GOQDs-en. Bai et al. (2010), similarly prepared hydrogels using PVA. They systemically investigated gelation process of PVA in the presence of GO and found that the weight ratio of PVA to GO has tremendous effects on gelation process. The results revealed that with increasing the PVA content (more than $0.5\text{--}2.5 \text{ mg mL}^{-1}$) a gel–sol transition can be occurred due to absorption of PVA chains on both surfaces of a GO sheet. In this hydrogel, hydroxyl-rich PVA chains act as a physical crosslinking agent. Hydrogen bond interaction between the hydroxyl-rich PVA chains and oxygen functional groups on GO nanosheets, mentioned as the main driving force in the formation of this hydrogel.

The process of gelatinization in graphene oxide/polyvinyl alcohol composite can be controlled by adjusting the pH of the solution. In acidic conditions, electrostatic repulsion forces within GO layers were declined and as a consequence, the connection between GO sheets and PVA significantly improved. As a result, GO/PVA composite hydrogel can be used for selective drug release at physiological pH. In other similar work, Xue et al. (2015) studied the effect of molecular weight of PVA in the gelation process in PVA/GO composites. They found that mechanical performance and interfacial adhesion of nanocomposites significantly increases during the gelatinization process through hydrogen bond formation and electrostatic interactions between GO and PVA. The mechanical performance of composites is under the influence of the molecular weights of PVA as well as the weight ratio of the PVA/GO. PVA/GO hydrogels with lower concentrations and higher molecular weight of PVA exhibited lower critical gel concentration (CGC) due to the increasing the interactions between GO layers and PVA molecules. The PVA molecules with higher molecular weights lead to increasing the number of bonding force between GO sheets as well as the number of the GO layers linked by the PVA molecules and can effectively promote the gelation of GO. Moreover, hydrogen

bonding between GO and PVA restricts the segmental motion of the PVA chains and leads to gradually increase of the glass transition temperature (T_g). The results also showed that even low concentrations of the graphene sheets can significantly influence the thermal stability and mechanical properties of the nanocomposites. The obtained hydrogels systems have the ability to absorb methylene blue (MB). Besides, desorption studies indicated that electrostatic interaction, hydrogen bonding, π - π conjugation, and chemisorption interaction between MB and PVA/GO nanocomposites are driving forces of absorption.

Rui-Hong et al. (2016) used PVA in combination with regenerated cellulose as a biocompatible polymer in the preparation of PVA/cellulose/GO composites. They prepared graphene oxide-regenerated cellulose/polyvinyl alcohol ternary hydrogel with high pH sensitivity and good mechanical properties via the freeze-thaw method. In fact, the studies revealed that polymers could be intercalated between GO layers and formed a ternary hybrid material with strong interfacial adhesion between GO and polymer matrix (Fig. 10). Swelling behaviors of the ternary hydrogel showed that the GO contents and pH effectively can influence the water uptake rate and swelling ratio. With 0.8wt% GO loading, ternary hydrogel showed maximum swelling ratio under the alkaline conditions (150%; pH = 2 and 310%; pH = 14). It was also found that mechanical properties of GO-RCE/PVA hydrogels have been significantly improved compared with RCE/PVA. The presence of only 1.0 wt% of GO, improved the tensile strength of composite about 40.4% (from 0.52 to 0.73 MPa). Also, elongation at break was increased from 103 to 238%.

Hydrogels with excellent mechanical property and self-healing characteristic simultaneously is an interesting topic in hydrogel science and has attracted much attention in different fields (Liu et al. 2012; Xue et al. 2015). Cong et al. (2013), reported a novel class of graphene oxide (GO)/poly(acryloyl-6-aminocaproic acid) (PAACA) composite hydrogel with both enhanced mechanical behavior and self-healing properties. In the GO/PAACA composite hydrogel, Ca^{2+} introduced as the secondary crosslinker to form a robust and flexible polymer network. The 3D hydrogen bonding network between functional groups of PAACA side chains with both its own functional groups and GO surface functional groups nanosheets as well as coordination interactions between Ca^{2+} and carboxylate groups of GO nanosheets and polar groups of poly(acryloyl-6-aminocaproic acid) side chains, endowed GO/PAACA composite hydrogel with the rapid self-healing properties and higher mechanical strength than that of PAACA hydrogel.

Conducting polymer (CP) hydrogels as another class of hydrogels have been broadly examined for various potential applications. Application of appropriate methods in the preparation of the conducting polymer (CP) hydrogels is essential due to insolubility and low hydrophilicity of CP. This kind of hydrogels generally shows high conductivities and good electrochemical activity (Guiseppi-Elie 2010; Dai et al. 2010). In this context, Bai et al. (2011b), synthesized conducting polymer (CP)/Graphene oxide(GO) composite hydrogels by the growth of pyrrole (Py), 3, 4-ethylenedioxythiophene and aniline on GO sheets in aqueous media through chemical polymerization. GO/PPy composite hydrogels showed higher storage moduli (>10 kPa), stronger electrical conductivity and electrochemical activity

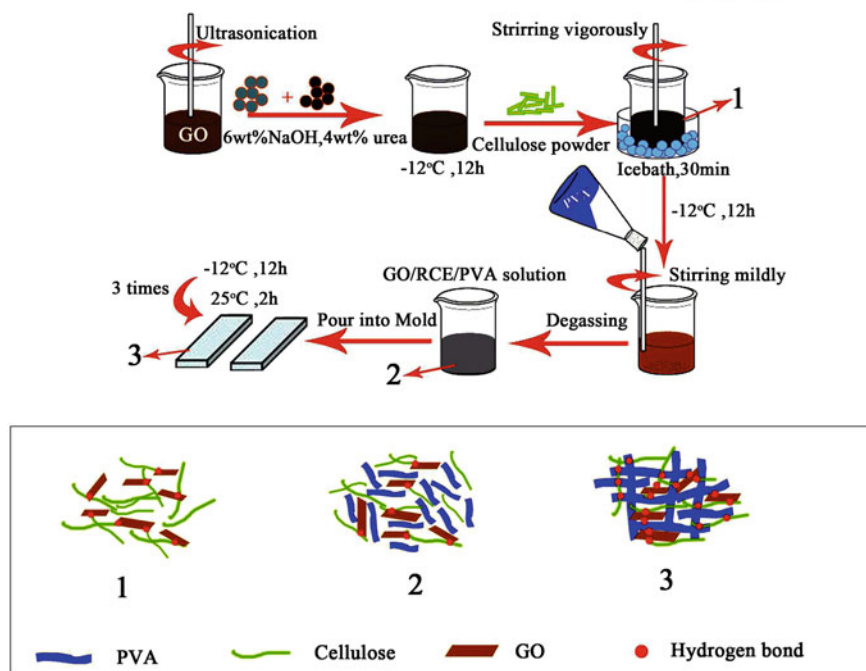


Fig. 10 The schematic illustration of the preparation of the GO-RCE/PVA ternary hydrogels. Reprinted with permission from Rui-Hong et al. (2016), Copyright © 2015 Elsevier Ltd

compared with 3,4-ethylenedioxythiophene (PEDOT) and polyaniline (PANI). The gelation of GO was promoted by increasing the strength of the bonding forces between layers against the repulsive forces through: (1) weakening the electrostatic repulsion force via the neutralization of anionic GO sheets with cationic PPy chains and (2) increasing the bonding force via crosslinking effect of PPy chains due to electrostatic interactions. GO due to its amphiphilic nature prevents quick precipitation of polymer and causes the PPy to preferentially grow on GO sheets via π - π interaction, electrostatic attraction, and hydrogen bonding. Interestingly, this hydrogel also showed high sensitivity to ammonia gas.

Biopolymers/graphene oxide gels by crosslinking of graphene oxide (GO) with biopolymers such as DNA (Xu et al. 2010), chitosan (Chen et al. 2013b; Sayyar et al. 2015), cellulose (Zhang et al. 2014) are highly regarded by researchers due to their good biocompatibility for biomedical applications especially blood-contact applications. In an interesting work, He et al. (2013), fabricated a new hydrogel consists of GO and a mixture of DNA, proteins, and chitosan. Resulting gel exhibited an interconnected 3D porous network, which was examined for various applications such as drug delivery and removal of toxic dyes and metal cations from wastewater. Interestingly, it showed excellent blood compatibility as well as high level of lodging capacity either for drugs or against cationic dyes and heavy metal

ions. These hydrogels were prepared from the crosslinking of GO sheets in the presence of different biopolymers through the noncovalent interactions (Fig. 11). Since negatively charged bovine serum albumin (BSA) and DNA contain the hydroxyl and carboxylic acid groups as well as hydrophobic groups in their polymer chains then, in gelation process hydrogen bonding and hydrophobic interactions are the main crosslinking forces. However, chitosan as cationic polysaccharide can effectively attract the anionic GO sheets through electrostatic interactions and hydrogen bond because of the presence of $-\text{NH}_2$ and $-\text{OH}$ groups in its polymer chains. The studies revealed that biopolymers effectively improved the blood compatibility of GO gels because the biopolymers can effectively mediate the surfactant-like property of GO sheet.

Moreover, GO/biopolymer gels could act as appropriate adsorbents for cationic dyes as well as removal of heavy metal ions such as Pb^{2+} and Cd^{2+} . In fact, these synergistic effects take place because of the static electrical attraction and the complexation ability of the surface functional groups of GO. Furthermore, GO/biopolymer gels showed the higher releasing speed of DOX as an anticancer drug in comparison with pristine GO. GO/biopolymer gels demonstrated the superior releasing speed of DOX in acidic solution due to the increasing hydrophilicity and solubility of DOX in acidic solutions.

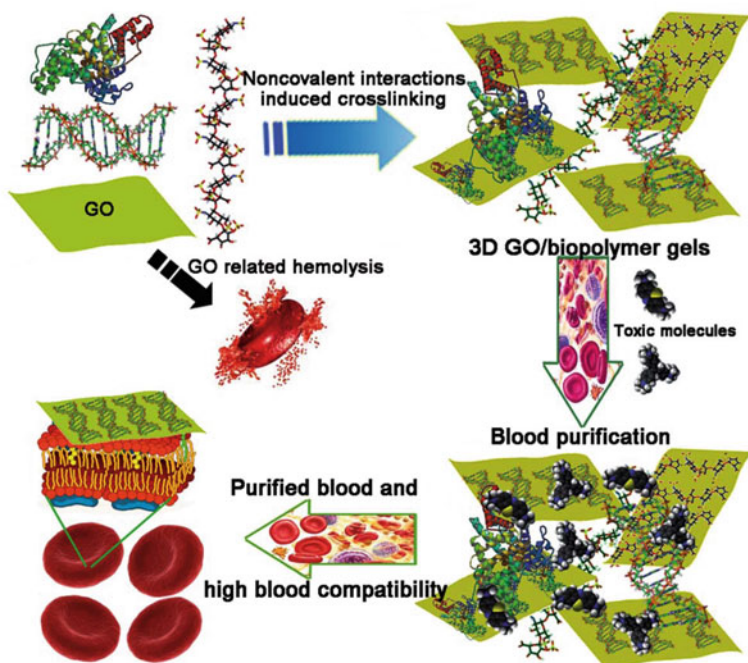


Fig. 11 Schematic illustration of the preparation of 3D GO/biopolymers gels and their application for removal of toxic molecules. Reprinted with permission from He et al. (2013), Copyright © 2013, Royal Society of Chemistry

Yu et al. (2015a) investigated the gelation behavior of welan gum in the presence of GO. Welan gum as a biocompatible and biodegradable microbial polysaccharide could effectively reduce the critical gelation concentration through H-bonding, hydrophobic interaction and electrostatic interaction with graphene oxide sheets. Furthermore, the resulting hydrogels examined for removal of various dyes such as methylene blue, methyl violet, amido black 10B, rhodamine 6G, and chrome Azurol S from wastewater.

GO-based hydrogels with their superior properties have been opened new opportunities for biomimetic researches. Peng et al. (2016) reported a polyvinyl alcohol/graphene oxide (PVA/GO) nanocomposite hydrogel with properties very similar to jellyfish mesogloea collagen. More interestingly, jellyfish-like PVA/GO nanocomposite hydrogels showed anisotropic porous structures consisting of micro-sized fibers and lamellar structure, high tensile and compressive strengths, pH-responsive properties, appropriate mechanical properties, and high water contents (97–99 wt%), which are suitable for design of soft robots, catalyst, carrier, etc. These hydrogels could be fabricated through a simple and effective directional freezing-thawing process as a result of the strong hydrogen bond formation between PVA and GO.

The application of graphene oxide to purify the water contaminant is restricted due to problems related to its separation from the water. GO-based hydrogels could provide a perfect solution to solve these problems. Li et al. have used the polymeric networks of poly(vinyl alcohol) (PVA) with sulfonated graphene (SG) for selective removal of cationic dyes from wastewater. SG/PVA (SP) composite hydrogel formed through physical interactions between the SG and PVA. Investigations showed that pH and ionic strength have minimum effect on the adsorption of methylene blue (MB). Moreover, SG/PVA (SP) composite hydrogel exhibited enhanced mechanical property (maximum tensile strength of 37.34 kPa) than that of pure PVA hydrogel.

NIR light-responsive hydrogels with high tensibility exhibited better performance in many areas such as smart sensors/actuators, controlled release systems, cell scaffolds compared with other stimuli-responsive hydrogels. Recently, Shi et al. (2015), reported new nanocomposite hydrogel by a combination of PNIPAM with GO nanosheets and *N,N'*-methylenebisacrylamide (BIS) molecules as chemical crosslinkers. The as-prepared hydrogel exhibited excellent NIR light-responsive property, ultrahigh tensibility, excellent chemical stability, and extreme stability in both polar solvent and strong acid condition. GO nanosheets can act as a physical crosslinking agent. Formation of hydrogen bonds between GO carboxylic acids and the amide groups of PNIPAM chains can effectively disperse the strain energy in the deformation process of hydrogels. Also, the use of *N,N'*-methylenebisacrylamide (BIS) molecules as chemical crosslinkers leads to strong chemical stability and ultrahigh tensibility of the hydrogels.

Zhao et al. (2015) prepared a composite composed of graphene oxide and chitosan composite through the self-assembly of chitosan molecules and GO. They reduced graphene layers after preparation by an in situ reduction process. Also, they investigated their adsorption capacity for three different dyes, congo red, methylene

blue, and rhodamine b. The results of their study showed that this hydrogel can be a good adsorbent for wastewater remedy as well as the elimination of toxic dyes from wastewater. Polyethylenimine (PEI), just like chitosan is containing many amino groups and, therefore, can be used for the preparation of GO-based hydrogels. In a new work, GO/polyethylenimine (PEI) hydrogels were reported by Guo et al. (2015a). They applied a facile approach to prepare GO/polyethylenimine as the consequence of H-bonding and attractive forces due to the electrostatic forces between PEI amino groups and GO sheets (Fig. 12). This hydrogel can be used in wastewater treatment. They also studied the dye removal ability of the hydrogel by evaluation of both their rates and adsorption capacity toward methylene blue and rhodamine B. For the present hydrogel, adsorption of PEI into the surface of GO significantly altered ordered stacking of GO sheets and leads to better dispersion and exfoliation of GO layers.

Wang et al. (2014b) used a green method to prepare graphene–agarose (AG) multifunctional hydrogels. These hydrogels are formed through strong hydrophobic interactions and hydrogen bonding between surface groups of graphene oxide and agarose (AG) as physical crosslinking sites. Furthermore, AG acts

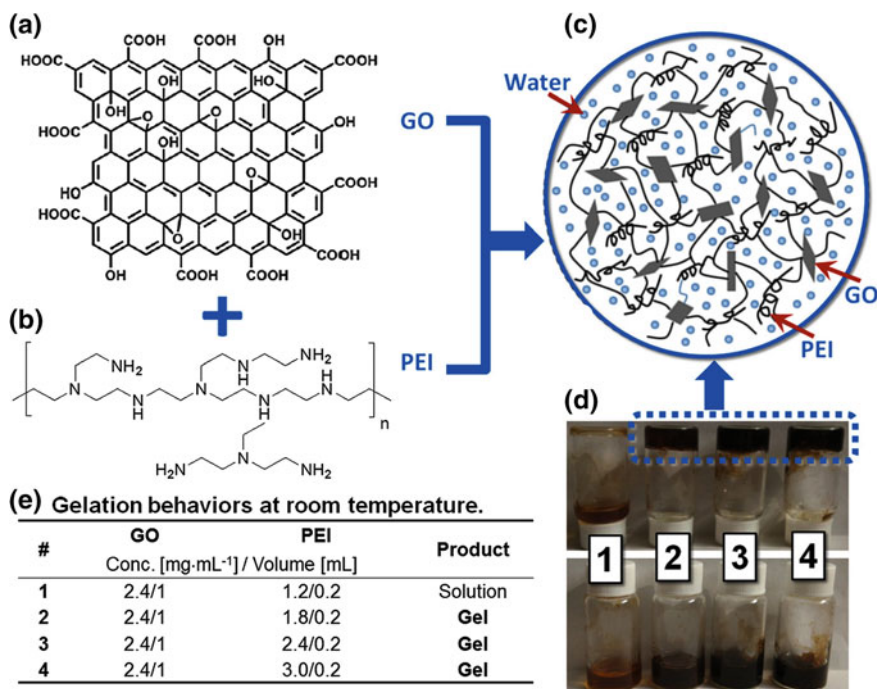


Fig. 12 Schematic depiction of the formation of GO/PEI gels **a** GO and **b** amine-rich PEI were combined to give **(c)** GO/PEI hydrogels gelation pictures **(d)** and Gelation behavior **(e)**, reprinted from Guo et al. (2015a), available under a Creative Commons Attribution License CC-BY 4.0. ©2015 Geo et al.

as stabilizer agent and leads to stability of hydrogels in strong acidic, basic, salty, phosphate buffer aqueous solution, and organic solvents. The adsorption ability of this hydrogel for removal of cationic dyes such as malachite green (MG) and its antibacterial activity against *Escherichia coli* and *Staphylococcus aureus* bacteria make it suitable for miniature-scale water purification.

4.4.3 Graphene-and Reduced Graphene (rGO)-Based Polymer Gels

Graphene- and reduced graphene (rGO)-based polymer gels have better mechanical, electrical, and thermal properties rather than GO-based ones. They also have more chemical and electrochemical stability compared with GO hydrogels (Li et al. 2014).

Zeng et al. (2013), investigated the effect of various amounts of rGO incorporated into two different hydrogels: poly(sodium acrylate) (PSA) and poly(sodium acrylate)-poly(*N*-isopropylacrylamide) (PSA-NIPAM) and realized that composite hydrogels which contained small amounts of rGO sheets showed remarkably enhanced swelling ratios. The resulting composite is a promising material for use as draw agents in the forward osmosis process and can be used in the confectionery industry, water treatment, and food processing. It should be pointed out that polymer hydrogel composites (e.g., 1.2 wt%) exhibited higher flexibility and better swelling behavior rather than the polymer. Synthesis of a catechol-containing organogel in the presence of reduced graphene oxide (RGO) through H-bonding has been reported by Ghavami Nejad et al. (2016). They proposed that *N*-isopropylacrylamide (NIPAM) and dopamine methacrylate (NIDO)/RGO agglomerate through hydrogen bonding and complexation. This pH-sensitive supramolecular hydrogel can be useful in the medical fields especially in drug delivery systems and artificial limbs.

In an interesting work, Yuan et al. (2014), synthesized conducting gel electrolytes from incorporating graphene, graphene oxide, or nanographite dissolved in a liquid electrolyte using freeze-dried poly(acrylic acid)-cetyltrimethyl ammonium bromide (PAA-CTAB). Graphene, graphene oxide, and nanographite by hydrophobic interaction with the 3D framework of PAA-CTAB matrix could create interconnected channels for charge transfer and consequently enhance the ionic conductivity of composites in comparison with pure PAA-CTAB gel electrolyte. Compared with PAA-CTAB gel electrolyte, the nanocomposite gel electrolytes showed higher ionic conductivity and better electrical, electrochemical, and photovoltaic performance.

Nowadays, quantum dot-sensitized solar cells (QDSC), considered as useful compounds, can be used as the third generation of solar cells. Duan et al. (2015) prepared QDSC using conducting polymer gel electrolytes. This conducting polymer gel electrolyte is prepared by incorporating graphene nanosheets into polyacrylamide hydrogel. The gel showed increased photovoltaic performances. Researchers achieved a power conversion efficiency of 2.34% via optimization of the amount of graphene in the composite. The conductive polymer nanocomposites

with 3D framework was also reported by Spasevska et al. (2015). They prepared crosslinked nanocomposites by in situ polymerization of methacrylate monomers in the presence of rGO platelets and polyurethane prepolymer containing isocyanate (Spasevska et al. 2015). Meanwhile, nanocomposites showed enhanced stability, electrical conductivity, and mechanical properties due to a higher degree of crosslinking between polymer chains and graphene platelets.

Huang et al. (2013) prepared a new double-network hydrogel consisting of graphene 3D network as the first network and poly(acrylic acid) as the second. They prepared the double-networks system through adsorption of acrylic acid monomer into the 3D graphene network and then polymerization of AA. This hydrogel showed good flexibility, elasticity, and electrical conductivity. Based on the stress–strain curves, in the first step (below 300% strain) of the deformation process, a quick increase with stress is shown (Fig. 13). But in the second step (up 300% strain), slower increase for Young modulus and tensile strength is showed presumably due to the stretch of PAA.

Using a simple approach, Zu and Han (2009) reported the formation of the stable aqueous copolymer-coated graphene solution via the noncovalent interaction between the hydrophobic PPO segments of a triblock copolymer, poly(ethylene oxide)-*block*-poly(propylene oxide)-*block*-poly-(ethylene oxide), with the hydrophobic graphene surface (Fig. 14). They also by using a simple approach, synthesized the supramolecular hybrid hydrogel by host–guest interaction of cyclodextrin with polyethylene oxide (PEO) of pluronic copolymer containing polypropylene oxide, polyethylene oxide, and graphene. They obtained supramolecular hydrogel which could be useful for drug delivery system. This hydrogel has the shear-thinning property that is the main feature of supramolecular hydrogels.

Graphene as a nanosize flexible-layered structure inorganic material has been used widely to produce organic–inorganic hybrid gel compounds. In an interesting work, hybrid graphene inclusion complex (HGIC) was synthesized through the noncovalent grafting of poly-(*N,N*-dimethylacrylamide)-*b*-poly(*N*-isopropylacrylamide) which was functionalized at the end of its chains by azobenzene groups (AZOPDMA-*b*-PNIPAM). The researchers demonstrated that the GO-graft-block copolymer is thermo- a sensitive polymeric compound and can form supramolecular gels with increasing the temperature. Also, investigation of the thermo-sensitive behavior of the hydrogel composite during gelation revealed that gelation temperature increases with increasing the length of PDMA block rather than PNIPAM block. This hydrogel due to its high biocompatibility can have numerous potential applications in different fields, especially biomedical applications such as drug carriers and tissue engineering (Liu et al. 2011). Hydrogels with enhanced mechanical hardness have been also reported (Cha et al. 2014). Cha et al. in a research study have addressed the successful modification of a GO using methacrylate groups. They used this modified graphene oxide, as active crosslinking agent for the covalent crosslinking of GO into a hydrogel system through radical copolymerization. The results of scanning electron microscopy

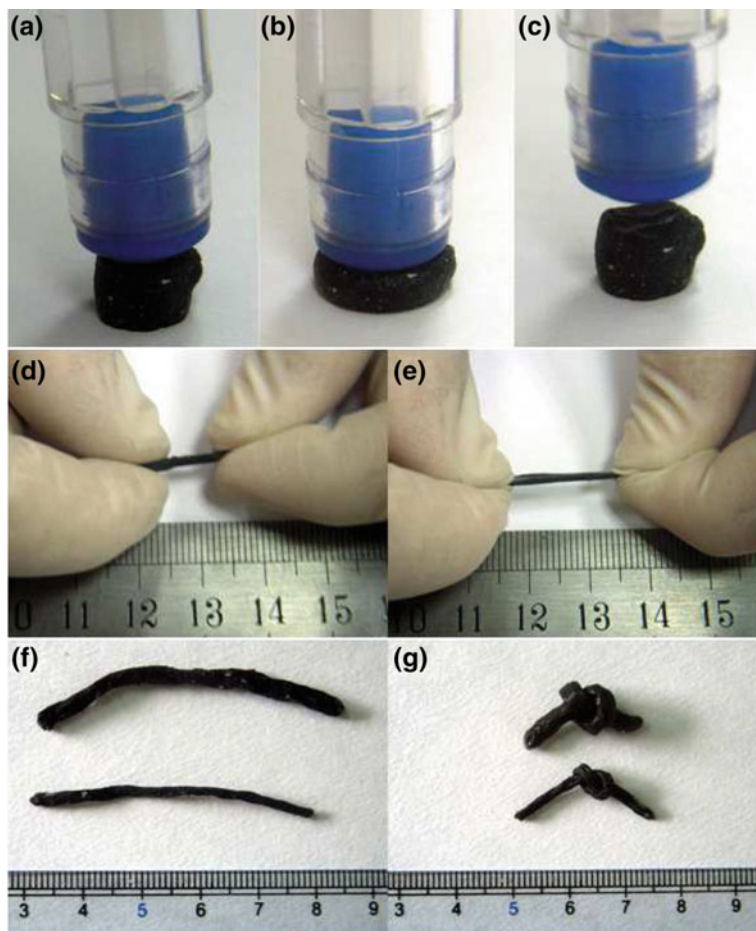


Fig. 13 **a** Mechanical properties of the reduced GO/PAA double networks. (**a–c**) Images of the reduced GO/PAA, under press, and after the press removed; (**d** and **e**) Stretch of the reduced GO/PAA; (**f** and **g**) the reduced GO/PAA DN hydrogel with different thickness and their flexibility, **b** compressive stress–strain curves of the reduced GO/PAA gel with PAA contents of 20, 30, 40, and 50%, reprinted with permission from Huang et al. (2013), Copyright © 2013, Royal Society of Chemistry

(SEM) confirmed that methacrylate monomers have been covalently conjugated to the GO surface (Fig. 15).

Using hydrothermal method, Hou et al. (2012) prepared a 3D network structure of graphene-poly(*N*-isopropylacrylamide) hydrogels. Good electrical conductivity, high mechanical strength, and reversible stimulus-sensitive volume changes have highlighted this hydrogel as artificial muscles (Fig. 16).

Vinyl monomers could be converted to polymeric structures using different approaches and strategies. For instance, using free-radical polymerization,

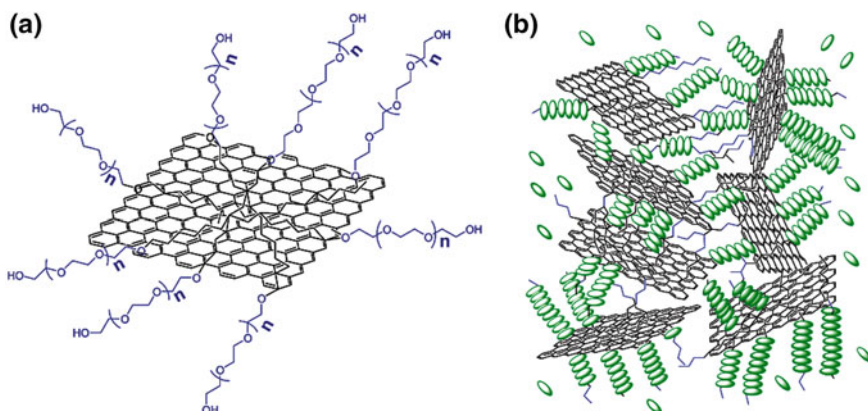


Fig. 14 Proposed structure of the copolymer-coated graphene (a) and supramolecular well-dispersed graphene sheet containing hybrid hydrogel (b), reprinted with permission from Zu and Han (2009), Copyright © 2009, American Chemical Society

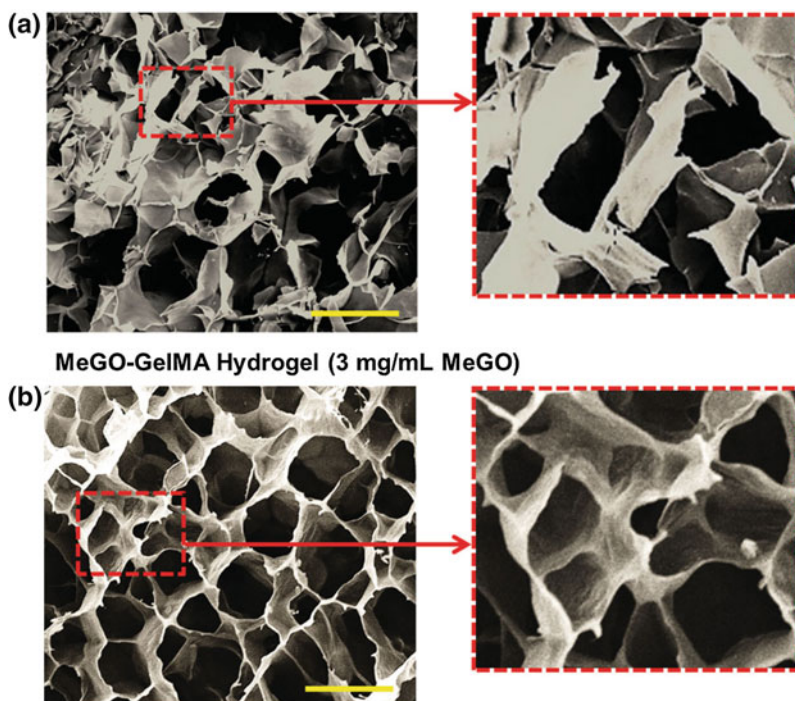


Fig. 15 SEM micrographs of the cross sections of (a) graphene oxide-GelMA (3 mg mL^{-1} GO) hydrogel and (b) Methacrylate graphene oxide-GelMA (3 mg mL^{-1} MeGO) hydrogel. (Scale bar: 200 μm), reprinted with permission from Cha et al. (2014), Copyright © 2013 WILEY-VCH Verlag GmbH & Co. KGaA, Weinheim

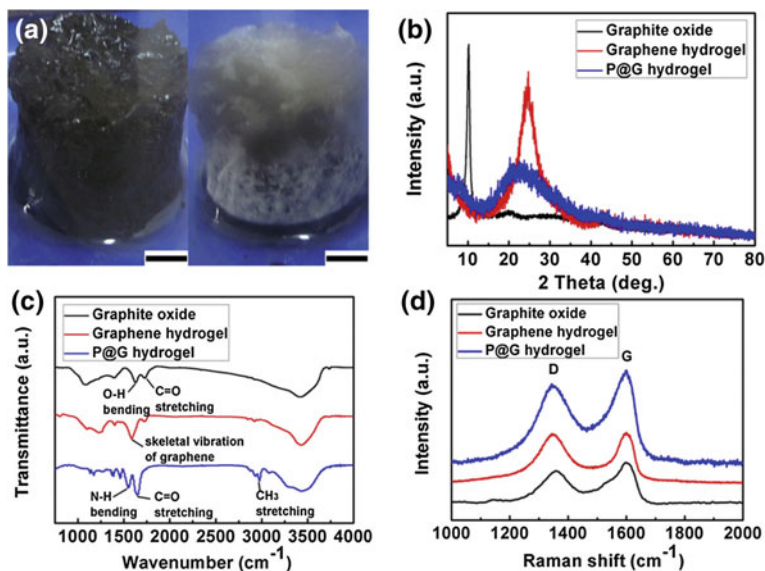


Fig. 16 Digital image of hydrogel (a) X-ray diffraction diagrams (b), FTIR data (c), and Raman spectra (d), reprinted with permission from Hou et al. (2012), Copyright © 2012 Elsevier Ltd

graphene/PAA composite hydrogels were prepared by Alam et al. (2016). As a result of good and strong interaction between graphene sheets and polymer chains as well as appropriate dispersion of graphene sheets into the polymer matrix, the obtained hydrogel illustrated improved electrical conductivity and high mechanical performance. Also, resulting hydrogels showed pH-dependent properties which is a valuable feature for various potential applications such as microswitches to artificial muscles and smart drug release devices. Also, Zhu et al. (2016) utilized γ -ray irradiation as another method for polymerization of acrylamide. They proposed a simple and convenient approach for one-step fabrication of interpenetrating polymer network systems based on graphene and poly acrylamide. Interpenetrating polymer networks due to their specific architecture and their high density of covalent and interlocked crosslinking has outstanding properties. These systems can preserve their macroporous structures even at high temperature (≥ 800 °C) and usually benefited from good mechanical properties.

In addition to the above-mentioned applications, GO-based composites have been used for other applications such as Li-ion batteries and supercapacitors. Studies have shown that 3D graphene/polymer hydrogels could promote the use of silicon (Si) as an anode material for fabrication of the rechargeable lithium-ion batteries. Lin et al. (2014) fabricated a Si/rGO composite with a stable 3D framework through crosslinking reaction between polyacrylamide (PAM) and graphene oxides by hydrogen bond interactions between amide groups in PAM and carboxyl or hydroxyl groups located on the GO sheets in which Si nanoparticles are embedded. This fabricated Si/rGO composite demonstrated excellent

electrochemical performance with a high specific capacity of 1610 mA h g^{-1} . Besides, Wang et al. (2015a) exhibited that 3D graphene/polymer hydrogels have great potential in the development of supercapacitors. They were synthesized iodine-doped polyaniline (PANI)/reduced graphene oxide composite hydrogel with the enhanced specific capacitance as 712.5 F g^{-1} and a good cycling stability of about 77% (from 440 to 340 F g^{-1}) after 1000 charge/discharge cycles. Here, I_2 as a catalyst and dopant leads to the polymerization of aniline also the HI produced from the oxidation can reduce GO to rGO. Electrostatic interactions and hydrogen bonding between GO and amino-group of PANI, were driving forces to form the strong crosslinks within the 3D GO network. Moreover, fabrication of reduced graphene oxide/polypyrrole hydrogels (rGO/PPy) was reported by Ni et al. (2015). They prepared the hydrogel through the self-assembly process in the presence of CuCl_2 as an oxidant agent. This hydrogel showed a compression-tolerant property and a high specific capacitance of 473 F g^{-1} and a good cycling stability of about 82% after 5000 charge/discharge cycles that were suitable for manufacturing energy storage devices.

5 Conclusion Remarks and Future Perspective

In summary, this chapter reviewed the progress made on graphene-based polymeric gels as a series of gels with high capabilities and extensive applications in various fields of application such as biomedical applications, energy storage, wastewater treatments, and environmental restoration. Investigations have shown that graphene oxide with hydrophilic and hydrophobic groups can easily be gelatinized in aqueous and organic solutions using various crosslinking agents. These hydrogels due to their unique structure have the ability to absorb and load various components such as pollutants, hazardous dyes, metal ions, and drugs in their pores. Polymer gels containing nano reinforcement such as graphene oxide usually exhibits higher mechanical properties than normal gels, which is due to the unique performance of graphene oxide. In recent years, the characteristics of graphene oxide polymer gels were widely investigated, however, there are challenges remaining in this area. The main challenge in this area is related to techniques used for the precise evaluation of rheological properties of these hydrogels. Also, GO synthesis methods, require further studies in order to develop methods that produce graphene oxide with less defects, high solubility, and electrical conductivity. On the other hand, graphene-based materials exhibit several advantages such as large surface area, high porosity, and different physical and electronic properties, however preparation of smart hydrogels with high sensitivity to external stimuli still requires more study.

Acknowledgments The authors wish to gratefully acknowledge the support of Lorestan University.

References

- Adhikari B, Biswas A, Banerjee A (2011) Graphene oxide-based supramolecular hydrogels for making nanohybrid systems with Au nanoparticles. *Langmuir* 28(2):1460–1469
- Akhavan O, Azimirad R, Gholizadeh H, Ghorbani F (2015) Hydrogen-rich water for green reduction of graphene oxide suspensions. *Int J Hydrogen Energy* 40(16):5553–5560
- Alam A, Meng Q, Shi G, Arabi S, Ma J, Zhao N, Kuan H-C (2016) Electrically conductive, mechanically robust, pH-sensitive graphene/polymer composite hydrogels. *Compos Sci Technol* 127:119–126
- Aqil A, Ouhib F, Detrembleur C, Vlad A, Melinte S, Jérôme C (2013) High-quality thin graphene films from fast electrochemical exfoliation
- Avouris P, Dimitrakopoulos C (2012) Graphene: synthesis and applications. *Mater Today* 15(3):86–97
- Bai H, Li C, Wang X, Shi G (2010) A pH-sensitive graphene oxide composite hydrogel. *Chem Commun* 46(14):2376–2378
- Bai H, Li C, Wang X, Shi G (2011a) On the gelation of graphene oxide. *J Phys Chem C* 115(13):5545–5551
- Bai H, Sheng K, Zhang P, Li C, Shi G (2011b) Graphene oxide/conducting polymer composite hydrogels. *J Mater Chem* 21(46):18653–18658
- Baruah U, Chowdhury D (2016) Functionalized graphene oxide quantum dot–PVA hydrogel: a colorimetric sensor for Fe^{2+} , Co^{2+} and Cu^{2+} ions. *Nanotechnol* 27(14):145501
- Brodie BC (1859) On the atomic weight of graphite. *Philos Trans R Soc Lond* 149:249–259
- Can HK, Kirci B, Kavlak S, Güner A (2003) Removal of some textile dyes from aqueous solutions by poly (N-vinyl-2-pyrrolidone) and poly (N-vinyl-2-pyrrolidone)/K2S2O8 hydrogels. *Radiat Phys Chem* 68(5):811–818
- Cha C, Shin SR, Gao X, Annabi N, Dokmeci MR, Tang XS, Khademhosseini A (2014) Controlling mechanical properties of cell-laden hydrogels by covalent incorporation of graphene oxide. *Small* 10(3):514–523
- Chabot V, Higgins D, Yu A, Xiao X, Chen Z, Zhang J (2014) A review of graphene and graphene oxide sponge: material synthesis and applications to energy and the environment. *Energy Environ Sci* 7(5):1564–1596
- Chai L, Wang T, Zhang L, Wang H, Yang W, Dai S, Meng Y, Li X (2015) A Cu–m-phenylenediamine complex induced route to fabricate poly (m-phenylenediamine)/reduced graphene oxide hydrogel and its adsorption application. *Carbon* 81:748–757
- Chaterji S, Kwon IK, Park K (2007) Smart polymeric gels: redefining the limits of biomedical devices. *Prog Polym Sci* 32(8):1083–1122
- Chen H, Müller MB, Gilmore KJ, Wallace GG, Li D (2008) Mechanically strong, electrically conductive, and biocompatible graphene paper. *Adv Mater* 20(18):3557–3561
- Chen W, Yan L, Bangal PR (2010) Preparation of graphene by the rapid and mild thermal reduction of graphene oxide induced by microwaves. *Carbon* 48(4):1146–1152
- Chen D, Li L, Guo L (2011) An environment-friendly preparation of reduced graphene oxide nanosheets via amino acid. *Nanotechnol* 22(32):325601
- Chen D, Feng H, Li J (2012) Graphene oxide: preparation, functionalization, and electrochemical applications. *Chem Rev* 112(11):6027–6053
- Chen J, Yao B, Li C, Shi G (2013a) An improved Hummers method for eco-friendly synthesis of graphene oxide. *Carbon* 64:225–229
- Chen Y, Chen L, Bai H, Li L (2013b) Graphene oxide–chitosan composite hydrogels as broad-spectrum adsorbents for water purification. *J Mater Chem A* 1(6):1992–2001
- Chen J, Li Y, Huang L, Li C, Shi G (2015) High-yield preparation of graphene oxide from small graphite flakes via an improved Hummers method with a simple purification process. *Carbon* 81:826–834
- Choi W, Jo-won L (2013) Graphene: synthesis and applications. CRC, Boca Raton

- Chua CK, Pumera M (2014) Chemical reduction of graphene oxide: a synthetic chemistry viewpoint. *Chem Soc Rev* 43(1):291–312
- Compton OC, Nguyen ST (2010) Graphene oxide, highly reduced graphene oxide, and graphene: versatile building blocks for carbon-based materials. *Small* 6(6):711–723
- Compton OC, An Z, Putz KW, Hong BJ, Hauser BG, Brinson LC (2012) Additive-free hydrogelation of graphene oxide by ultrasonication. *Carbon* 50(10):3399–3406
- Cong H-P, Ren X-C, Wang P, Yu S-H (2012) Macroscopic multifunctional graphene-based hydrogels and aerogels by a metal ion induced self-assembly process. *ACS Nano* 6(3):2693–2703
- Cong H-P, Wang P, Yu S-H (2013) Stretchable and self-healing graphene oxide–polymer composite hydrogels: a dual-network design. *Chem Mater* 25(16):3357–3362
- Cui W, Ji J, Cai Y-F, Li H, Ran R (2015) Robust, anti-fatigue, and self-healing graphene oxide/hydrophobically associated composite hydrogels and their use as recyclable adsorbents for dye wastewater treatment. *J Mater Chem A* 3(33):17445–17458
- Dai T, Shi Z, Shen C, Wang J, Lu Y (2010) Self-strengthened conducting polymer hydrogels. *Synth Met* 160(9):1101–1106
- Deng J, Lei B, He A, Zhang X, Ma L, Li S, Zhao C (2013) Toward 3D graphene oxide gels based adsorbents for high-efficient water treatment via the promotion of biopolymers. *J Hazard Mater* 263:467–478
- Dreyer DR, Park S, Bielawski CW, Ruoff RS (2010) The chemistry of grapheme oxide. *Chem Soc Rev* 39(1):228–240
- Dreyer DR, Todd AD, Bielawski CW (2014) Harnessing the chemistry of graphene oxide. *Chem Soc Rev* 43(15):5288–5301
- Duan J, Tang Q, Li R, He B, Yu L, Yang P (2015) Multifunctional graphene incorporated polyacrylamide conducting gel electrolytes for efficient quasi-solid-state quantum dot-sensitized solar cells. *J Power Sour* 284:369–376
- Edwards RS, Coleman KS (2013) Graphene synthesis: relationship to applications. *Nanoscale* 5(1):38–51
- Eigler S, Hirsch A (2014) Chemistry with graphene and graphene oxide—challenges for synthetic chemist. *Angew Chem Int Ed* 53(30):7720–7738
- Fan J, Shi Z, Lian M, Li H, Yin J (2013) Mechanically strong graphene oxide/sodium alginate/polyacrylamide nanocomposite hydrogel with improved dye adsorption capacity. *J Mater Chem A* 1(25):7433–7443
- Fernandez-Merino M, Guardia L, Paredes J, Villar-Rodil S, Solis-Fernandez P, Martinez-Alonso A, Tascon J (2010) Vitamin C is an ideal substitute for hydrazine in the reduction of graphene oxide suspensions. *J Phys Chem C* 114(14):6426–6432
- Franklin D, Guhanathan S (2015) Investigation of citric acid–glycerol based pH-sensitive biopolymeric hydrogels for dye removal applications: a green approach. *Ecotoxicol Environ Saf* 121:80–86
- Gan L, Shang S, Hu E, Yuen CWM, Jiang S-X (2015) Konjac glucomannan/graphene oxide hydrogel with enhanced dyes adsorption capability for methyl blue and methyl orange. *Appl Surf Sci* 357:866–872
- Gao W, Alemany LB, Ci L, Ajayan PM (2009) New insights into the structure and reduction of graphite oxide. *Nat Chem* 1(5):403–408
- GhavamiNejad A, Hashmi S, Vatankhah-Varnoosfaderani M, Stadler FJ (2016) Effect of H₂O and reduced graphene oxide on the structure and rheology of self-healing, stimuli responsive catecholic gels. *Rheol Acta* 1–14
- Gouko I, Nicolosi V, Goodhue R, Scardaci V, Coleman JN, Boland J, Duesberg GS (2008) High-yield production of graphene by liquid-phase exfoliation of graphite
- Guiseppi-Elie A (2010) Electroconductive hydrogels: synthesis, characterization and biomedical applications. *Biomater* 31(10):2701–2716
- Guo H, Peng M, Zhu Z, Sun L (2013) Preparation of reduced graphene oxide by infrared irradiation induced photothermal reduction. *Nanoscale* 5(19):9040–9048

- Guo H, Jiao T, Zhang Q, Guo W, Peng Q, Yan X (2015a) Preparation of graphene oxide-based hydrogels as efficient dye adsorbents for wastewater treatment. *Nanoscale Res Lett* 10(1):1–10
- Guo Y, Duan B, Cui L, Zhu P (2015b) Construction of chitin/graphene oxide hybrid hydrogels. *Cellulose* 22(3):2035–2043
- Hayes WI, Joseph P, Mughal MZ, Papakonstantinou P (2015) Production of reduced graphene oxide via hydrothermal reduction in an aqueous sulphuric acid suspension and its electrochemical behavior. *J Solid State Electrochem* 19(2):361–380
- He A, Lei B, Li S, Ma L, Sun S, Zhao C (2013) Toward safe, efficient and multifunctional 3D blood-contact adsorbents engineered by biopolymers/graphene oxide gels. *RSC Adv* 3(44):22120–22129
- Hoffmann J, Plötner M, Kuckling D, Fischer W-J (1999) Photopatterning of thermally sensitive hydrogels useful for microactuators. *Sens Actuators, A* 77(2):139–144
- Hong W, Zhao X, Zhou J, Suo Z (2008) A theory of coupled diffusion and large deformation in polymeric gels. *J Mech Phys Solids* 56(5):1779–1793
- Hou C, Zhang Q, Li Y, Wang H (2012) Graphene–polymer hydrogels with stimulus-sensitive volume changes. *Carbon* 50(5):1959–1965
- Huang H, Lü S, Zhang X, Shao Z (2012) Glucono- δ -lactone controlled assembly of graphene oxide hydrogels with selectively reversible gel–sol transition. *Soft Matter* 8(17):4609–4615
- Huang P, Chen W, Yan L (2013) An inorganic–organic double network hydrogel of graphene and polymer. *Nanoscale* 5(13):6034–6039
- Hummers WS Jr, Offeman RE (1958) Preparation of graphitic oxide. *J Am Chem Soc* 80(6):1339
- Jagur-Grodzinski J (2010) Polymeric gels and hydrogels for biomedical and pharmaceutical applications. *Polym Adv Technol* 21(1):27–47
- Jia Z, Li C, Liu D, Jiang L (2015) Direct hydrothermal reduction of graphene oxide based papers obtained from tape casting for supercapacitor applications. *Rsc Adv* 5(99):81030–81037
- Jung JH, Lee JH, Silverman JR, John G (2013) Coordination polymer gels with important environmental and biological applications. *Chem Soc Rev* 42(3):924–936
- Kosynkin DV, Higginbotham AL, Sinitskii A, Lomeda JR, Dimiev A, Price BK, Tour JM (2009) Longitudinal unzipping of carbon nanotubes to form graphene nanoribbons. *Nat* 458(7240):872–876
- Kovtyukhova NI, Ollivier PJ, Martin BR, Mallouk TE, Chizhik SA, Buzaneva EV, Gorchinskiy AD (1999) Layer-by-layer assembly of ultrathin composite films from micron-sized graphite oxide sheets and polycations. *Chem Mater* 11(3):771–778
- Lee W, Choi D, Lee Y, Kim D-N, Park J, Koh W-G (2008) Preparation of micropatterned hydrogel substrate via surface graft polymerization combined with photolithography for biosensor application. *Sens Actuators B: Chem* 129(2):841–849
- Lee S, Lee H, Sim JH, Sohn D (2014) Graphene oxide/poly(acrylic acid) hydrogel by γ -ray pre-irradiation on graphene oxide surface. *Macromol Res* 22(2):165–172
- Li C, Shi G (2014) Functional gels based on chemically modified graphenes. *Adv Mater* 26(24):3992–4012
- Li D, Mueller MB, Gilje S, Kaner RB, Wallace GG (2008a) Processable aqueous dispersions of graphene nanosheets. *Nat Nanotechnol* 3(2):101–105
- Li X, Zhang G, Bai X, Sun X, Wang X, Wang E, Dai H (2008b) Highly conducting graphene sheets and Langmuir–Blodgett films. *Nat Nanotechnol* 3(9):538–542
- Li J, Zeng X, Ren T, van der Heide E (2014) The preparation of graphene oxide and its derivatives and their application in bio-tribological systems. *Lubricants* 2(3):137–161
- Lin N, Zhou J, Zhu Y, Qian Y (2014) Embedding silicon nanoparticles in graphene based 3D framework by cross-linking reaction for high performance lithium ion batteries. *J Mater Chem A* 2(46):19604–19608
- Lin B, Feng T, Chu F, Zhang S, Yuan N, Qiao G, Ding J (2015) Poly (ionic liquid)/ionic liquid/graphene oxide composite quasi solid-state electrolytes for dye sensitized solar cells. *RSC Adv* 5(70):57216–57222
- Liu J, Chen G, Jiang M (2011) Supramolecular hybrid hydrogels from noncovalently functionalized graphene with block copolymers. *Macromolecules* 44(19):7682–7691

- Liu R, Liang S, Tang X-Z, Yan D, Li X, Yu Z-Z (2012) Tough and highly stretchable graphene oxide/polyacrylamide nanocomposite hydrogels. *J Mater Chem* 22(28):14160–14167
- Liu X, Zhou Y, Nie W, Song L, Chen P (2015a) Fabrication of hydrogel of hydroxypropyl cellulose (HPC) composited with graphene oxide and its application for methylene blue removal. *J Mater Sci* 50(18):6113–6123
- Liu Y, Yuan G, Jiang Z, Yao Z, Yue M (2015b) Solvothermal synthesis of graphene nanosheets as the electrode materials for supercapacitors. *Ionics* 21(3):801–808
- Liu Y, Genzer J, Dickey MD (2016) “2D or not 2D”: Shape-programming polymer sheets. *Prog Polym Sci* 52:79–106
- Lloyd GO, Steed JW (2009) Anion-tuning of supramolecular gel properties. *Nat Chem* 1(6):437–442
- Low C, Walsh F, Chakrabarti M, Hashim M, Hussain M (2013) Electrochemical approaches to the production of graphene flakes and their potential applications. *Carbon* 54:1–21
- Luan VH, Chung JS, Hur SH (2015) Preparation of a reduced graphene oxide hydrogel by Ni ions and its use in a supercapacitor electrode. *Rsc Adv* 5(29):22753–22758
- Luo Y, Shoichet MS (2004) A photolabile hydrogel for guided three-dimensional cell growth and migration. *Nat mater* 3(4):249–253
- Ma D, Lin J, Chen Y, Xue W, Zhang L-M (2012) In situ gelation and sustained release of an antitumor drug by graphene oxide nanosheets. *Carbon* 50(8):3001–3007
- Ma X, Li Y, Wang W, Ji Q, Xia Y (2013) Temperature-sensitive poly (N-isopropylacrylamide)/graphene oxide nanocomposite hydrogels by in situ polymerization with improved swelling capability and mechanical behavior. *Eur Polymer J* 49(2):389–396
- Mao R, Liu Y, Huglin MB, Holmes PA (1998) Dynamic light scattering from polymer gels: spring-rotor model. *Polym Int* 45(3):321–326
- Mao S, Pu H, Chen J (2012) Graphene oxide and its reduction: modeling and experimental progress. *Rsc Adv* 2(7):2643–2662
- Mao HY, Laurent S, Chen W, Akhavan O, Imani M, Ashkarran AA, Mahmoudi M (2013) Graphene: promises, facts, opportunities, and challenges in nanomedicine. *Chem Rev* 113(5):3407–3424
- Marcano DC, Kosynkin DV, Berlin JM, Sinitiskii A, Sun Z, Slesarev A, Alemany LB, Lu W, Tour JM (2010) Improved synthesis of graphene oxide. *ACS Nano* 4(8):4806–4814
- Miao C, Zheng C, Liang O, Xie YH (2011) Chemical vapor deposition of graphene
- Miculescu M, Thakur VK, Miculescu F, Voicu SI (2016) Graphene-based polymer nanocomposite membranes: a review. *Polym Adv Technol* 27(7):844–859
- Moraes FC, Freitas RG, Pereira R, Gorup LF (2015) Coupled electronic and morphologic changes in graphene oxide upon electrochemical reduction. *Carbon* 91:11–19
- Moussa H, Girod E, Mozet K, Alem H, Medjahdi G, Schneider R (2016) ZnO rods/reduced graphene oxide composites prepared via a solvothermal reaction for efficient sunlight-driven photocatalysis. *Appl Catal B* 185:11–21
- Mukherjee R, Thomas AV, Krishnamurthy A, Koratkar N (2012) Photothermally reduced graphene as high-power anodes for lithium-ion batteries. *ACS Nano* 6(9):7867–7878
- Ni T, Xu L, Sun Y, Yao W, Dai T, Lu Y (2015) Facile fabrication of reduced graphene oxide/polypyrrole composite hydrogels with excellent electrochemical performance and compression capacity. *ACS Sustain Chem Eng* 3(5):862–870
- Nowak AP, Breedveld V, Pakstis L, Ozbas B, Pine DJ, Pochan D, Deming TJ (2002) Rapidly recovering hydrogel scaffolds from self-assembling diblock copolypeptide amphiphiles. *Nature* 417(6887):424–428
- Park S, Ruoff RS (2009) Chemical methods for the production of graphenes. *Nat Nanotechnol* 4(4):217–224
- Park S, Lee K-S, Bozoklu G, Cai W, Nguyen ST, Ruoff RS (2008) The reduction of graphene oxide. *ACS Nano* 2(3):572–578
- Pei S, Cheng H-M (2012) The reduction of graphene oxide. *Carbon* 50(9):3210–3228

- Peng X, He C, Liu J, Wang H (2016) Biomimetic jellyfish-like PVA/graphene oxide nanocomposite hydrogels with anisotropic and pH-responsive mechanical properties. *J Mater Sci* 51(12):5901–5911
- Reina A, Kong J (2012) In: *Graphene nanoelectronics*, Springer, p 167–203
- Rogovina L, Vasil'ev V (2010) Diversity of polymer gels and the main factors determining the properties of gels and related solid polymers. *Polym Sci Ser A* 52(11):1171–1183
- Rui-Hong X, Peng-Gang R, Jian H, Fang R, Lian-Zhen R, Zhen-Feng S (2016) Preparation and properties of graphene oxide-regenerated cellulose/polyvinyl alcohol hydrogel with pH-sensitive behavior. *Carbohydr Polym* 138:222–228
- Sayyar S, Murray E, Thompson B, Chung J, Officer DL, Gambhir S, Spinks GM, Wallace GG (2015) Processable conducting graphene/chitosan hydrogels for tissue engineering. *J Mater Chem B* 3(3):481–490
- Shen J, Hu Y, Li C, Qin C, Ye M (2009) Synthesis of amphiphilic graphene nanoplatelets. *Small* 5(1):82–85
- Shen J, Yan B, Li T, Long Y, Li N, Ye M (2012) Study on graphene-oxide-based polyacrylamide composite hydrogels. *Compos A Appl Sci Manuf* 43(9):1476–1481
- Shi K, Liu Z, Wei Y-Y, Wang W, Ju X-J, Xie R, Chu L-Y (2015) Efficient reduction of graphite oxide by sodium borohydride and its effect on electrical conductance. *ACS Appl Mater Interfaces* 7(49):27289–27298
- Shin HJ, Kim KK, Benayad A, Yoon SM, Park HK, Jung IS, Jin MH, Jeong HK, Kim JM, Choi JY (2009) *Adv Func Mater* 19(12):1987–1992
- Spasevska D, Leal G, Fernández M, Gilev JB, Paulis M, Tomovska R (2015) Crosslinked reduced graphene oxide/polymer composites via in situ synthesis by semicontinuous emulsion polymerization. *RSC Adv* 5(21):16414–16421
- Srivastava N, He G, Mende PC, Feenstra RM, Sun Y (2012) Graphene formed on SiC under various environments: comparison of Si-face and C-face. *J Phys D Appl Phys* 45(15):154001
- Staudenmaier L (1899) Graphite oxide post-synthesis processing protocols. *Ber Dtsch Chem Ges* 32(2):1394–1399
- Su C, Loh KP (2012) Carbocatalysts: graphene oxide and its derivatives. *Acc Chem Res* 46(10):2275–2285
- Sun S, Wu P (2011) A one-step strategy for thermal- and pH-responsive graphene oxide interpenetrating polymer hydrogel networks. *J Mater Chem* 21(12):4095–4097
- Sun X-G, Fang Y, Jiang X, Yoshii K, Tsuda T, Dai S (2016) Polymer gel electrolytes for application in aluminum deposition and rechargeable aluminum ion batteries. *Chem Commun* 52(2):292–295
- Sutter P (2009) Epitaxial graphene: how silicon leaves the scene. *Nat Mater* 8(3):171–172
- Tai Z, Yang J, Qi Y, Yan X, Xue Q (2013) Synthesis of a graphene oxide–polyacrylic acid nanocomposite hydrogel and its swelling and electroresponsive properties. *RSC Adv* 3(31):12751–12757
- Tao C-A, Wang J, Qin S, Lv Y, Long Y, Zhu H, Jiang Z (2012) Fabrication of pH-sensitive graphene oxide–drug supramolecular hydrogels as controlled release systems. *J Mater Chem* 22(47):24856–24861
- Thakur S, Karak N (2015) Alternative methods and nature-based reagents for the reduction of graphene oxide: a review. *Carbon* 94:224–242
- Thakur VK, Thakur MK (2014) Recent trends in hydrogels based on psyllium polysaccharide: a review. *J Clean Prod* 82:1–15
- Thakur VK, Thakur MK (2015) Recent advances in green hydrogels from lignin: a review. *Int J Biol Macromol* 72:834–847
- Tung VC, Allen MJ, Yang Y, Kaner RB (2009) High-throughput solution processing of large-scale graphene. *Nat Nanotechnol* 4(1):25–29
- Vallés C, Drummond C, Saadaoui H, Furtado CA, He M, Roubeau O, Ortolani L, Monthieux M, Pénicaud A (2008) Solutions of negatively charged graphene sheets and ribbons. *J Am Chem Soc* 130(47):15802–15804

- Vermisoglou E, Giannakopoulou T, Romanos G, Giannouri M, Boukos N, Lei C, Lekakou C, Trapalis C (2015) Effect of hydrothermal reaction time and alkaline conditions on the electrochemical properties of reduced graphene oxide. *Appl Surf Sci* 358:100–109
- Wang R, Sun J, Gao L, Xu C, Zhang J, Liu Y (2011a) Effective post treatment for preparing highly conductive carbon nanotube/reduced graphene oxide hybrid films. *Nanoscale* 3(3):904–906
- Wang Y, Shi Z, Yin J (2011b) Facile synthesis of soluble graphene via a green reduction of graphene oxide in tea solution and its biocomposites. *ACS Appl Mater Interfaces* 3(4):1127–1133
- Wang J, Song D, Jia S, Shao Z (2014a) Poly (N, N-dimethylaminoethyl methacrylate)/graphene oxide hybrid hydrogels: pH and temperature sensitivities and Cr (VI) adsorption. *React Funct Polym* 81:8–13
- Wang X, Liu Z, Ye X, Hu K, Zhong H, Yu J, Jin M, Guo Z (2014b) A facile one-step approach to functionalized graphene oxide-based hydrogels used as effective adsorbents toward anionic dyes. *Appl Surf Sci* 308:82–90
- Wang J, Li B, Ni T, Dai T, Lu Y (2015a) One-step synthesis of iodine doped polyaniline-reduced graphene oxide composite hydrogel with high capacitive properties. *Compos Sci Technol* 109:12–17
- Wang Z, Guo H, Yan P (2015b) In-situ synthesis of reduced graphene oxide modified lithium vanadium phosphate for high-rate lithium-ion batteries via microwave irradiation. *Electrochim Acta* 174:26–32
- Wei D, Grande L, Chundi V, White R, Bower C, Andrew P, Ryhänen T (2012) Graphene from electrochemical exfoliation and its direct applications in enhanced energy storage devices. *Chem Commun* 48(9):1239–1241
- Williams G, Kamat PV (2009) Graphene–semiconductor nanocomposites: excited-state interactions between ZnO nanoparticles and graphene oxide. *Langmuir* 25(24):13869–13873
- Wu T, Liu S, Luo Y, Lu W, Wang L, Sun X (2011) Surface plasmon resonance-induced visible light photocatalytic reduction of graphene oxide: using Ag nanoparticles as a plasmonic photocatalyst. *Nanoscale* 3(5):2142–2144
- Xu Y, Wu Q, Sun Y, Bai H, Shi G (2010) Three-dimensional self-assembly of graphene oxide and DNA into multifunctional hydrogels. *ACS Nano* 4(12):7358–7362
- Xue R, Xin X, Wang L, Shen J, Ji F, Li W, Jia C, Xu G (2015) A systematic study of the effect of molecular weights of polyvinyl alcohol on polyvinyl alcohol–graphene oxide composite hydrogels. *Phys Chem Chem Phys* 17(7):5431–5440
- Yamato M, Konno C, Utsumi M, Kikuchi A, Okano T (2002) Thermally responsive polymer-grafted surfaces facilitate patterned cell seeding and co-culture. *Biomater* 23(2):561–567
- Yang X, Zhang F, Zhang L, Zhang T, Huang Y, Chen Y (2013) A high-performance graphene oxide-doped ion gel as gel polymer electrolyte for all-solid-state supercapacitor applications. *Adv Func Mater* 23(26):3353–3360
- Yeh MH, Lin LY, Chang LY, Leu YA, Cheng WY, Lin JJ, Ho KC (2014) Dye-sensitized solar cells with reduced graphene oxide as the counter electrode prepared by a green photothermal reduction process. *Chem Phys Chem* 15(6):1175–1181
- Yeo Y, Kohane DS (2008) Polymers in the prevention of peritoneal adhesions. *Eur J Pharm Biopharm* 68(1):57–66
- Yu M, Song A, Xu G, Xin X, Shen J, Zhang H, Song Z (2015a) Review on synthesis of 3D graphene-based configurations and their adsorption performance for hazardous water pollutants. *RSC Adv* 5(92):75589–75599
- Yu Y, De Andrade LCX, Fang L, Ma J, Zhang W, Tang Y (2015b) Graphene oxide and hyperbranched polymer-toughened hydrogels with improved absorption properties and durability. *J Mater Sci* 50(9):3457–3466
- Yuan S, Tang Q, He B, Zhao Y (2014) Multifunctional graphene incorporated conducting gel electrolytes in enhancing photovoltaic performances of quasi-solid-state dye-sensitized solar cells. *J Power Sour* 260:225–232

- Zeng Y, Qiu L, Wang K, Yao J, Li D, Simon GP, Wang R, Wang H (2013) Significantly enhanced water flux in forward osmosis desalination with polymer-graphene composite hydrogels as a draw agent. *Rsc Adv* 3(3):887–894
- Zhang E, Wang T, Lian C, Sun W, Liu X, Tong Z (2013) Robust and thermo-response graphene–PNIPAm hybrid hydrogels reinforced by hectorite clay. *Carbon* 62:117–126
- Zhang J, Yang H, Shen G, Cheng P, Zhang J, Guo S (2010) Low swelling hyperbranched poly (amine-ester) hydrogels for pH-modulated differential release of anticancer drugs. *Chem Commun* 46(7):1112–1114
- Zhang H, Dong Y, Wang L, Wang G, Wu J, Zheng Y, Yang H, Zhu S (2011) *J Mater Chem* 21 (35):13530–13537
- Zhang H-H, Liu Q, Feng K, Chen B, Tung C-H, Wu L-Z (2012) Facile photoreduction of graphene oxide by an NAD (P) H model: Hantzsch 1, 4-dihydropyridine. *Langmuir* 28 (21):8224–8229
- Zhang H, Zhai D, He Y (2014) Graphene oxide/polyacrylamide/carboxymethyl cellulose sodium nanocomposite hydrogel with enhanced mechanical strength: preparation, characterization and the and the swelling behavior. *RSC Adv* 4(84):44600–44609
- Zhao Z, Wang X, Qiu J, Lin J, Xu D, Zhang CA, Lv M, Yang X (2014) Three-dimensional graphene-based hydrogel/aerogel materials. *Rev Adv Mater Sci* 36:137–151
- Zhao H, Jiao T, Zhang L, Zhou J, Zhang Q, Peng Q, Yan X (2015) Preparation and adsorption capacity evaluation of graphene oxide-chitosan composite hydrogels. *Sci China Mater* 58 (10):811–818
- Zheng Q, Kim JK (2015) In: *Graphene for transparent conductors*, Springer, 29–94
- Zhong M, Liu Y-T, Xie X-M (2015) Self-healable, super tough graphene oxide–poly (acrylic acid) nanocomposite hydrogels facilitated by dual cross-linking effects through dynamic ionic interactions. *J Mater Chem B* 3(19):4001–4008
- Zhu Y, Murali S, Cai W, Li X, Suk JW, Potts JR, Ruoff RS (2010a) Graphene and graphene oxide: synthesis, properties, and applications. *Adv Mater* 22(35):3906–3924
- Zhu Y, Murali S, Stoller MD, Velamakanni A, Piner RD, Ruoff RS (2010b) Microwave assisted exfoliation and reduction of graphite oxide for ultracapacitors. *Carbon* 48(7):2118–2122
- Zhu T, Teng K, Shi J, Chen L, Xu Z (2016) A facile assembly of 3D robust double network graphene/polyacrylamide architectures via γ -ray irradiation. *Compos Sci Technol* 123:276–285
- Zu S-Z, Han B-H (2009) Aqueous dispersion of graphene sheets stabilized by pluronic copolymers: formation of supramolecular hydrogel. *J Phys Chem C* 113(31):13651–13657

Chapter 11

Transport in and Through Gel



Masayuki Tokita

Abstract Gel is a state of matter that classified into the solid because it consists of the three-dimensional cross-linked polymer network. It, however, shows some liquid-like properties since it also contains a considerable amount of fluid. According to such a characteristic structure, many substances can pass the gel. In many separation technologies, therefore, gel is used as a molecular sieve. Although the gel plays many important roles in the separation technologies, the detailed roles played by the gel in the transport phenomena is not well understood yet. The transport phenomena in the gel are necessary to be clarified. In this chapter, we discuss two transport phenomena that is related to the gel. The one is the friction of the gel against the liquid that flows through the gel, and the other is the resistance of the gel for the diffusional translation of the substances in the gel.

Keywords Stokes–Einstein law · Diffusion coefficient · Darcy’s law
Gel-solvent friction · Scaling law

1 Frictional Properties of Polymer Network of Gel

1.1 Introduction

Gel is a complex system of the polymer network and a huge amount of fluid. Today, gel is familiar not only in science but also in our daily life as the food, the medicine, and many commodities. Gels are known to show many unique behaviors. The unique properties of gels are deeply related to the characteristic structure of the gel (Tanaka 1981). In earlier studies of the science of gels, the elastic properties of gel are studied extensively because the formation of the gel is thought to be similar phenomenon to the solidification except a lot of solvent. The phenomenon is simply

M. Tokita (✉)

Department of Physics, Faculty of Science, Kyushu University, 744 Motooka, Fukuoka, Fukuoka 819-0395, Japan
e-mail: tokita@phys.kyushu-u.ac.jp

called as the gelation or the sol-gel transition. The elastic property of the gel is believed to reflect directly the transition of the state from the solution to the gel. Therefore, the critical elasticity of the gel is studied extensively (Tokita 1982, 1985, 1987; Tokita et al. 1985). The scientific knowledge on the sol-gel transition is gained and the phenomenon is believed to belong the class of the percolation transition (De Gennes 1976, 1979).

A new insight into the viscoelasticity of gel is developed theoretically, later that is called as THB theory, with the pioneering experimental studies (Tanaka et al. 1973). In THB theory, the viscoelastic property of gel is explained in terms of the competition between two forces. The one is the entropy elasticity of the polymer network, and the other is the frictional resistance due to the polymer chain and the gel fluid (hereafter, it will be called as friction, frictional property, and/or hydrodynamic friction for the sake of simplicity). It should be emphasized here that the friction that will be discussed in this review do not mean the friction between two surfaces of solids. In the similar ages from 70s to 80s, a new transition phenomenon is discovered in the gel where the gel changes its volume more than thousand times against the infinitesimal change of, say, the solvent composition reversibly (Tanaka 1978). Then the kinetic studies are made to solve the transition phenomena, which also help the use of gels in many applications (Tanaka and Fillmore 1979). In these kinetic studies of the gel, the important roles played by the friction of the gel are revealed eventually. Although the importance, detailed study of the frictional property of gel is postponed because of the reason that the accurate and the reliable determination of the friction in the gel is considerably difficult. However, the situation changes drastically in 1991 by the discovery of the critical slowing down of the friction in a gel (Tokita and Tanaka 1991a, b). The finding opens a new insight into the transport phenomena of the gel. Then, the frictional property of gel draws attention eventually as one of important transport properties of the soft matters. It is well known that the viscoelasticity is a common property of the soft matter from the dilute solution to the gel including the semi-dilute solution. In contrast, the friction is, by its definition, only defined for the porous solid. Today, we believe that the friction between the gel and the gel fluid is most characteristic property that reflects the state of the gel.

It has been well established by the THB theory that the viscoelasticity of gel is uniquely determined by the longitudinal elastic modulus, $E = K + 4\mu/3$, and the friction of the gel, f , as follows.

$$D_c = \frac{E}{f} = \frac{K + 4\mu/3}{f} \quad (1)$$

Here, D_c is the collective diffusion coefficient of the gel, which can be determined from the decay rate, τ_c , of the dynamic light scattering measurement from the gel as follows.

$$\tau_c = \frac{\lambda^2}{4\pi D_c} \quad (2)$$

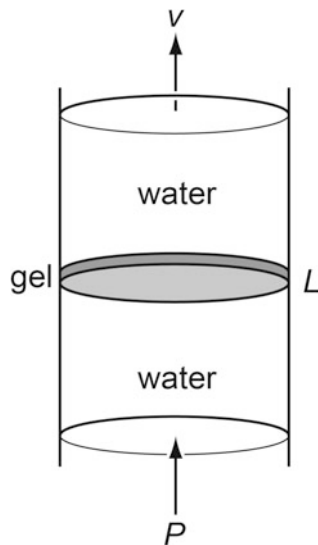
It is clear from Eqs. (1) and (2) that the viscoelasticity of a gel can be determined two of three physical quantities, that is, E , f , and D_c , are experimentally determined. Since the experimental determination of D_c and E are rather easy, the measurements of these physical quantities are extensively made so far to determine the viscoelastic properties of gels (Tanaka et al. 1977; Munch et al. 1977a, b; Takebe et al. 1989). In contrast, systematic studies of the frictional properties of gel have not been made extensively.

In Fig. 1, we show the principle of the friction experiments schematically. The measurement is mechanical as shown in this figure. A slab shaped gel with the thickness, L , is fixed in a space of glass tube with the peripheral portion is attached to the wall of the tube. As shown in Fig. 1, the pressure, P , is applied to the fluid to generate the flow of fluid in gel. The velocity of water flowing in gel, v_s , is determined in a stationary state of the flow. The friction coefficient of the gel, f , is expressed as follows.

$$f = \frac{P}{Lv_s} \quad (3)$$

Here, P/L is the pressure gradient applied to gel. Since P and L are given as the experimental conditions, only v_s is necessary to be determined to obtain the friction coefficient of the gel. The principle of the friction measurement itself is quite simple. The Eq. (3) is sometime called as ‘‘Darcy’s law’’ that also holds for the fluid flow in the porous materials. Darcy’s law is firstly applied to study the transport

Fig. 1 The concept of the friction measurement is schematic illustrated. The peripheral portion of the gel at a thickness of L is fixed to the wall. The small pressure P is applied to water that covers the one side of the gel. The velocity of water that flows in the gel v is measured at the stationary state. Then, the friction coefficient of the gel is calculated by the Darcy’s law, Eq. (3)



phenomena in the hard material systems such as the fluid flow through the sintered glass filter and the flow of groundwater through the bedrock.

Since the principle of friction is simple, as described above, many pioneering studies have been reported (Tanaka et al. 1973; Weiss et al. 1979; Hecht and Geissler 1980; Geissler and Hecht 1982). It becomes, however, clear that the friction measurement is not trivial because of the reason that the gel is soft, elastic, and fragile. Most experimental studies on the frictional properties of the gel so far reported have been made not under ideal conditions. Hence, the frictional properties of the gel thus obtained are less accurate and also less reliable from today's knowledge. Such uncertainty of the friction arises from the fact that the frictional resistance of the polymer network is considerably huge. For instance, the amount of water that flows out of the gel in a unit time is usually very small indicating that the larger gel has the advantage to increase the amount of water that flows out of the gel. If one use a large gel sample, it is required to apply a large pressure to the gel since the flow rate is determined by the pressure gradient, P/L , rather than the pressure itself, P as shown in Eq. (3). However, the relaxation time of the mechanical deformation, which is caused by the applied pressure and the flow of the gel fluid, becomes longer if the size of the gel becomes larger. The THB theory indicates that the relaxation time of deformation of a typical gel with a characteristic size of about 1 cm becomes about 10 days. The THB theory, therefore, indicates that more than 10 days is required to obtain the stationary flow of the fluid in sample gel. Of course, such long-time measurement is not realistic and has never been made so far. In addition to this, the other additional effects become pronounced under the conditions of larger applied pressure. Namely, the structure of the gel would be damaged by the extensive flow of water. The nonlinear effects of water flow and the pressure would be also taking into account. Finally, the shrink of the gel due to the frictional force also occurs at higher applied pressures. All these additional effects occur because of the reason that the gel is soft, elastic, and fragile, those are also the unique characters of the gel. Therefore, there are many complicated problems to be solved when the Darcy's law is applied to study the gel-solvent friction in gel. It may be of importance to solve the problems raised above to construct a newly designed apparatus to study the frictional properties of the gel. This point is described in the following section in detail.

1.2 *Experimental*

1.2.1 Apparatus for Uniform Gel

It may be natural to begin with the description about the apparatus of the friction measurement because the concept of the friction in the gel is not very much familiar even for the researchers who are working with the gel (Tokita and Tanaka 1991a, b). Here, we describe the difficult points of the friction measurements in the gel, and then, how the difficulties are solved. The difficulties we find are ranging from the

simple mechanical problem to the one that is arisen from the characteristic features of the gel. Therefore, the description of analysis and the classification of the difficulties we should solve will assure the reliability of the experimental results. We believe that one can discuss the experimental results on secure ground after these difficulties are solved properly.

First of all, the pressure that is applied to the gel in the measurement of the friction is required to be small enough not to alter the network structure of the gel since the gel is fragile. To avoid the substantial shrink of the gel, the smaller applied pressure is advantageous. Since the osmotic compressibility of the gel is of the order of about 10^3 – 10^4 N/m², the pressure applied to the gel should be comparable with these values. We designed the apparatus to fix the gel volume by choosing the condition at which the gel has a positive osmotic pressure. It also prohibits the gel to swell. A simple calculation using the THB theory yields that the friction coefficient of poly(acrylamide) gel is the order of 10^{14} – 10^{15} Ns/m⁴ (Tanaka et al. 1977). According to the Eq. (3), the velocity of the fluid flow in the gel with $L = 1$ cm becomes of the order of 10^{-8} – 10^{-9} m/s when the applied pressure is 10^3 N/m². In order to determine such a slow velocity, the velocity of the flow in the gel should be amplified. The total volume of water, which flows out of the gel in a measurement, is found to be about 10 μ l or less under present conditions. Therefore, it is possible to determine the velocity of water inside the gel if all the water that flows out of the gel is lead in a thin micropipette. We, therefore, set a micropipette having a capacity of 10 μ l at the out-flow side of the apparatus. It is also clear from above conditions that the leakage around the gel sample deteriorates the final accuracy of the friction measurement of gel because the total amount of water that flows through the gel is only few micro-little. Generally, this is the crucial point in designing the friction apparatus. This point is avoided completely by using a plastic film that has the functional groups, which forms the chemical bond with the sample gel, on the surface. The plastic film used here is called as “Gel Bond Film” (BioRad) and is used in the gel electrophoresis to chemically fix the gel on the surface of the film. By using the gel bonding film, we avoid the leakage of water completely.

Water begins to flow in the gel immediately after pressure is applied to the gel. The apparent velocity of water flow is fast in the initial state. Then it slows down with the time, and finally, it reaches to a steady state velocity. Two effects are responsible for the apparent fast initial velocity of the flow. The first one is the bending of the gel-gel holder system, and the second one is the collapse of the gel that is arisen from the friction between the gel and the flowing water. The effects of the bending of the gel-gel holder system occurs from the structure of the measuring cell. Even though the gel holder is tightly fixed between the thick plastic plate, it can deform slightly. The displacement of the gel-gel holder system causes the volume change of the elution side as a whole. Since the volume change is enhanced by the micropipette, the change of the volume is enhanced. The relaxation time of the bending deformation in gel and gel holder system is found to be about 30 min. The relaxation time for the bending deformation is estimated from the control experiments where the gel is molded between two bonding films while the gel bond film has no openings to prevent water flows out of the gel. The movement of water

in the micropipette, which is observed in the initial state of the friction experiment, is mostly due to the bending of the gel-gel holder system. It is also important to use a stiff material, such as the stainless steel, as the gel holder to decrease the amplitude of the bending deformation. We find that the deformation of the stainless steel gel holder is ten times less deformation than the plastic gel holder. In our experiments, most measurements are made using the stainless steel gel holder. Secondary, the retardation effects of the velocity of the flowing water arise from the relaxation of the deformed polymer network that caused by the flowing water. Because the gel is elastic, the polymer network of the gel deforms at lower applied pressure. The velocity of the flow inside the gel, therefore, generally depends on time. The relaxation time where the flow of the fluid in the gel reaches a stationary state is estimated by the kinetic theory of the volume change of the gel. It is found that the relaxation time of the volume change of a gel is proportional to the square of a typical linear size of the gel (Tanaka and Fillmore 1979). The relaxation time for the present case of the gel with the thickness of L is written as (relaxation time) $= L^2/\pi^2 D_c$. The relaxation time with a gel of thickness $L = 10^{-3}$ m is the order of 10^4 s ~ 3 h. Here, the typical collective diffusion coefficient of $D_c = 10^{-11}$ m²/s is employed. It also indicates that the relaxation time becomes shorter as the thickness of the gel becomes thinner. There is further advantage to use a thinner gel as the sample. According to Eq. (3), the velocity of fluid becomes larger if the thickness of gel becomes thinner. Therefore, the accuracy of the resultant friction coefficient increases in a thinner gel. The steady state flow of water is observed after all these relaxation phenomena are diminished.

All the aspects described above are taking into account to construct the apparatus. The outline of the apparatus is schematically shown in Fig. 2. The cell is made of Plexiglass plates. In other part of the apparatus, we employed the stainless steel pipes and stainless steel valves to prevent the volume change of total system that is caused by the pressure applied to the sample gel. As a reservoir for water, the chromatography column of about 50 cm in length is used that also behaves the pressure generator. By changing the volume of water that is contained in the chromatography column, the height of water column is changed from about 20 to 60 cm. The pressure is, thus, changed from about 2×10^3 to 6×10^3 N/m². The temperature of the water bath is controlled by a circulating bath system within an accuracy better than 0.1°. The apparatus is set on an optical table by which any external mechanical disturbances are avoided.

The gel holder, that is used in this study is made of stainless steel, is shown in Fig. 3 schematically. The gel bonding films, to which the sample gel is fixed chemically, are glued on both sides of the mold. The final thickness of the gel mold with the gel bond films is found to be from about 1 to 2 mm that is measured after the gel is cast. Since the gel is chemically attached to the gel bonding film, the leakage of water from the gel mold is completely prohibited.

After the polymerization of the gel, the glass plates are removed from the gel mold carefully under water to avoid the destruction at the surface portion. Then, the gel mold is tightly fixed between two cells made of plexi-plates of about 1 cm in

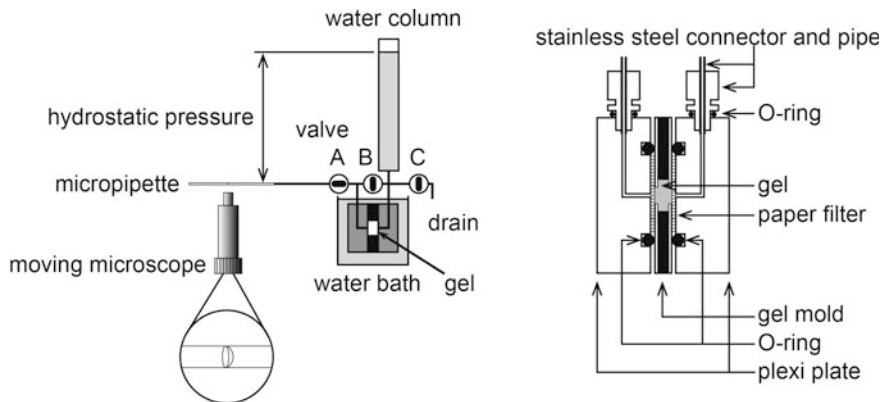
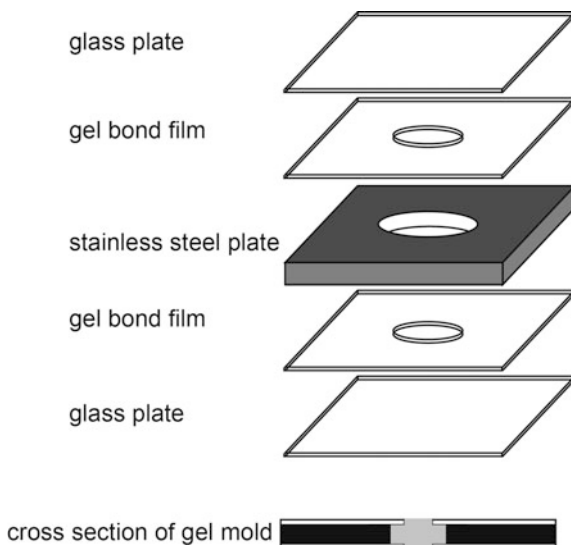


Fig. 2 The apparatus used to determine the friction coefficients of uniform poly(acrylamide) gel and the critical behavior of poly(*N*-isopropylacrylamide) gel is schematically shown in the left figure. The apparatus is set on a vibration free optical table to avoid the mechanical disturbances. The cross section of the sample cell is also illustrated in the right figure. Both plexi-plates in this figure are tightly fixed to avoid the swelling of gel

Fig. 3 The structure of the gel holder. Two gel bond films are glued on the stainless steel plate by the silicone glue. Then the gel mold is soaked into the pre-gel solution with both sides are covered by glass plates. After the reaction is finished, both glass plates are removed carefully under water. Finally, the gel mold is fixed in the sample cell that is shown in Fig. 2



thickness. We embed the most part of O-rings in the plexi-plates to avoid the bending of gel mold. At the end of the stainless steel pipe, a calibrated micropipette of inner diameter ranging from 0.34 to 0.50 mm is attached to measure the flow rate. Different micropipettes are used depending on the applied pressure and the friction coefficient of gel. The micropipettes are commercially available and indicated as 5 and 10 μl .

Before the measurement of the friction coefficient, the gel is left in the cell for overnight to reach equilibrium state under certain temperature. During this time interval, the valve A in Fig. 2 is closed while the valve B is opened not to exert the pressure on the gel. When we measure the friction of gel, firstly the valve B is closed. Then, the valve A is opened immediately to exert the pressure upon the gel. After the pressure is applied, the position of the meniscus of water in the micropipette is measured with the elapsed time by a microscope. The valve A is closed and the valve B is opened to release the applied pressure when the measurement of the friction is done. The gel is left at least overnight to recover the initial equilibrium state. This apparatus is employed to study the frictional properties of poly(acrylamide) gel and poly(*N*-isopropylacrylamide) gel.

1.2.2 Apparatus for Heterogeneous Gel

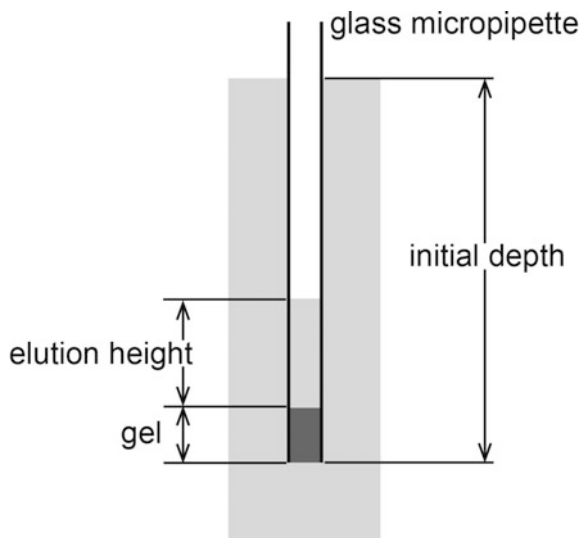
It is easily expected that the friction of polymer network is structure-dependent property. As we will see in the following sections, the friction of uniform poly(acrylamide) gel, which is prepared under optimal polymerization conditions, is very large. On the other hand, it has been found that poly(acrylamide) gel becomes considerably heterogeneous under certain polymerization conditions, which will be described in detail later. The previous studies suggest that the heterogeneous structure is static and the correlation length of the gel increases up to the same order with the wavelength of light. The friction of such heterogeneous poly(acrylamide) gel should also be studied in detail to obtain the full information on the structure-property relationship in poly(acrylamide)gel. We expect that the friction of such heterogeneous gels become smaller due to the long-range structure that is comparable to the wavelength of light. In such heterogeneous gels, much simpler method is preferable for the determination of the friction. In Fig. 4, we show the simple method which is used to determine the friction of the heterogeneous poly(acrylamide) gels (Doi and Tokita 2005a, b). In this case, the gel is prepared in one end of the micropipette of known inner diameter. Then the micropipette is soaked into water at a desired depth, h_0 . The water eventually passing through the gel due to the pressure gradient. The height of the water column in the micropipette, therefore, increases with time by water eluted out of the gel. The time course of the height of water column in the micropipette, which corresponds to the eluted volume of water from the gel, $h(t)$, is related to the friction coefficient of gel as follows.

$$\frac{h_0 - h(t)}{h_0} = \exp(-t/\tau_e) \quad (4)$$

$$\tau_e = \frac{Lf}{\rho g} \quad (5)$$

Here, g , ρ , and L are the acceleration of gravity, the density of fluid, and thickness of the sample gel, respectively. The friction coefficient of the gel f is

Fig. 4 The schematic illustration of the apparatus used in the measurements of the friction coefficient of the tenuous gels. The gel is prepared in one end of a micropipette at a thickness of L . Then the micropipette is soaked into water at a desired depth h_0 to impose the pressure P . The elution height, $h(t)$, is then measured as a function of time. The friction coefficient of the gel is determined by analyzing the elution time course by the Eqs. (4) and (5)



calculated from the characteristic time, τ_e . This apparatus is suitable for the measurement of the friction coefficient less than about 10^{13} Ns/m⁴.

1.2.3 Sample

Poly(acrylamide) gel is mainly used as the sample in this study. The gel is prepared by free radical polymerization method. All reagents used here are the electrophoresis grade (BioRad) and used as obtained. The calculated amount of acrylamide (main chain component) and N,N' -methylenebisacrylamide (cross-linker) are dissolved into distilled and de-ionized water (purified using Milli-Q system). The pre-gel solution, thus prepared, is de-gassed in a decompression chamber for 30–40 min after adding N,N,N',N' -tetramethylethylenediamine (accelerator, added 240 μ l–100 ml of pre-gel solution). Ammoniumpersulfate solution (initiator solution, added 1 ml of 4 wt% solution to 100 ml of pre-gel solution) is added to the pre-gel solution to initiate the polymerization reaction. During the reaction, the solution is kept at the desired temperature. The solution is also kept undisturbed until the reaction is completed. In the preparation of the opaque poly(acrylamide) gel, ammoniumpersulfate is changed to the non-ionic light sensitive initiator, VA-086 (Wako, Tokyo). The pre-gel solution is introduced into the micropipette of known inner diameter after the solution is de-gassed, and then polymerization reaction is initiated by irradiating UV light of about 360 nm for 20 min.

In the case of poly(N -isopropylacrylamide) gel, the monomer is re-crystallized before polymerization. The polymerization is made mostly in the same manner with that of poly(acrylamide) gel. The reaction temperature is, however, controlled

carefully since the gel becomes opaque by the reaction heat if the temperature is not controlled. The polymerization reaction is made at a temperature of 20 °C.

1.2.4 Calibration of Apparatus

First of all, the accuracy of the apparatus described in the previous section of 1.2.1 is checked. Typical experimental results of the elution time course from the poly (acrylamide) gels are shown in Fig. 5. The sample gel used here is poly(acrylamide) gel that is prepared at a total concentration of about 8 g/100 ml with a cross-linking density of about 1 mol%. The time course of the elution of water from the gel is determined by measuring the position of the meniscus of water in the micropipette of 10 μl in capacity. The results are, then, plotted in Fig. 6. The curves given in this figure represent the results gained at different applied pressures. We find that the position of the meniscus moves rapidly in the beginning of the measurements.

The velocity of the movement of meniscus in the micropipette changes with time, then it approaches to the stationary state after about 1×10^4 s. The velocity of water in the micropipette at the stationary state, v_{sc} , is calculated from the slope of the elution time course in Fig. 6. The rapid movement of meniscus in the very initial stage of the measurement can be considerably decreased in the case of the improved friction apparatus. The friction measurement using such an improved cell is reported elsewhere. In such a case, the elution time course from gel can be fitted to the theoretical one (Suzuki et al. 2009).

The values of v_{sc} thus determined are plotted against the applied pressure in Fig. 6.

Fig. 5 The time course of the position of meniscus in the micropipette of 10 μl . The applied pressures are 5.88, 4.90, 3.92, 2.94, and 1.96 (in a unit of 10^3 N/m^2) from top to bottom. The thickness of the gel is 1.95 mm. In this figure, the rapid movement of meniscus in the very initial state is not shown for the simplicity and only the results near the steady state regions are shown. Lines are drawn only guide to the eye

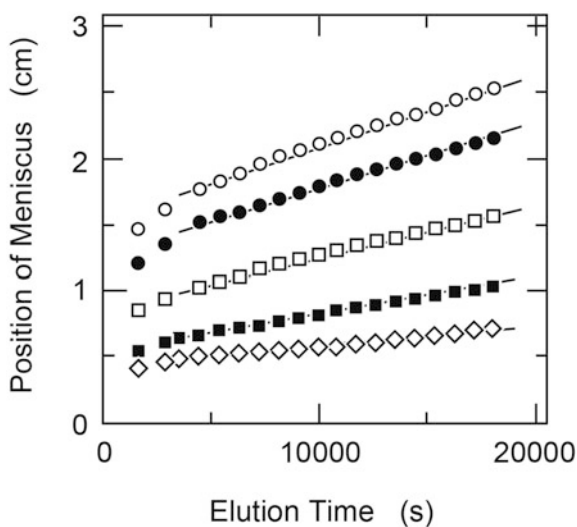
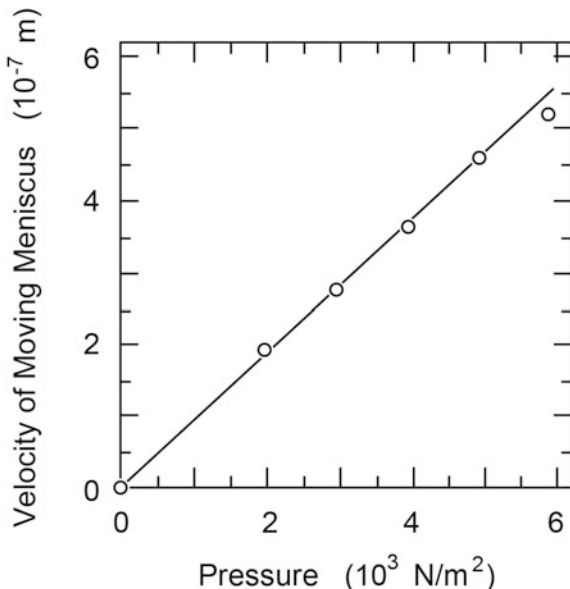


Fig. 6 The relationship between the velocity of the fluid in the micropipette and the applied pressure. The line in this figure is drawn for the guide to the eye



The velocity of water flow, v_{sc} , is proportional to the applied pressure as predicted from Eq. (3). The friction coefficient, $f = 1.0 \times 10^{15} \text{ Ns/m}^4$, is obtained from the results given in Fig. 6 using the following equation.

$$f = \left(\frac{dv_{sc}}{dP} \right)^{-1} \frac{1}{L} \left(\frac{R}{r} \right)^2 \tag{6}$$

Here, $(dv_{sc}/dP) = 8.95 \times 10^{-11} \text{ m}^3/\text{Ns}$ represents the slope of the straight line in Fig. 6. The gel has the thickness of $L = 1.9 \times 10^{-3} \text{ m}$. The factor $(R/r)^2$ represents the ratio of the areas of the cross section of the micropipette and the opening on the gel bonding film. The radii of the micropipette and the hole are measured to be $r = 2.5 \times 10^{-4} \text{ m}$ and $R = 3.3 \times 10^{-3} \text{ m}$, respectively. This factor is necessary to convert v_{sc} to the actual velocity of water flow in the gel v_s . The friction coefficient of gel thus obtained agrees well with the one expected from the THB theory. These results confirm that the friction coefficient of the gel can be determined accurately by our apparatus.

1.3 Gel-Solvent Friction

1.3.1 Friction of Poly(Acrylamide) Gel

The frictional properties of poly(acrylamide) gel are summarized in this section. It is well known that poly(acrylamide) gel has many advantages to study the state of gel: the monomer, acrylamide, is highly soluble in water, the synthesise of gel is

easy, and the gel prepared from acrylamide is usually transparent, and so forth. In this study, therefore, poly(acrylamide) gels are prepared at various conditions, then the friction of the gel is measured.

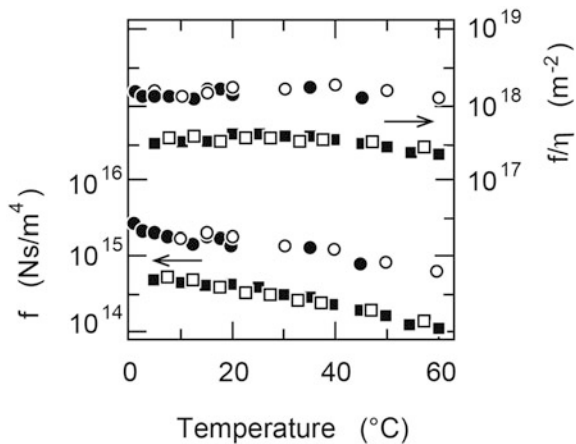
First, we study the relationship between the friction and the temperature. In Fig. 7, we show the results. The concentrations of the two sample gels used in this measurement are 5 and 8 g/100 ml, respectively. We find that the law value of the friction coefficient decreases upon increasing temperature (open symbols in Fig. 7). Then, it increases with decreasing the temperature (closed symbols in Fig. 7). The friction coefficient of poly(acrylamide) gel changes monotonously with the temperature. Besides, it is also clear that the temperature change is entirely reversible. Any singular behavior could not be observed in the temperature dependence of the friction coefficient of poly(acrylamide) gel.

As long as the law value of the friction coefficient is concerned, it decreases with the temperature monotonously as shown in Fig. 7. It can be expected easily that the viscosity of the fluid effects the flow rate of fluid, and hence it also effects the observed values of the friction coefficient of gel. Since the viscosity of the fluid depends on the temperature, $\eta(T)$, the temperature variation in the friction observed here includes the effects of the temperature variation of the viscosity of fluid. On the other hand, the pore size of polymer network also depend on the temperature since the gel may swell or shrink in response to the temperature change. The frictional pore size of the gel, therefore, depends both on the concentration of the gel and the temperature as $\xi^2(C, T)$. Therefore, the friction coefficient of the polymer network of the gel, $f(C, T)$, can be expressed as follows in general.

$$f(C, T) \propto \frac{\eta(T)}{\xi^2(C, T)} \tag{7}$$

Here, $\xi^2(C, T)$ represents the cross section of the frictional pore in the polymer network that expressed by the correlation length of the gel. We, thus, plot the

Fig. 7 The temperature dependence of the friction coefficient of poly (acrylamide) gels, f . The circles are the results of the gel at a concentration of 8 g/100 ml and the squares are the results of 5 g/100 ml gel. The friction coefficient of the gel that is normalized by the viscosity of water, f/η , is also given in this figure. The open symbols are the data obtained with increasing temperature and the closed symbols are the results of cooling process



normalized friction coefficient of poly(acrylamide) gel by the viscosity of water, $f(C, T)/\eta(T)$, in Fig. 7. It is found that the friction of the gel is constant when the friction coefficient is normalized by the viscosity of water. The results suggest strongly that the correlation length of poly(acrylamide) gel is constant in this temperature range. The frictional pore size of the gel thus estimated is smaller in 8 g/100 ml gel than that of 5 g/100 ml gel. The correlation length of the gel primarily depends only on the concentration in the case of acrylamide system. Such a feature is considerably suitable for the medium of the electrophoresis since one can control the mesh size of the molecular sieve only by the concentration of the gel.

In Fig. 8, we show the concentration dependence of the friction coefficient of poly(acrylamide) gel. These results indicate that the existence of the power law between the friction and the total concentration of the gel. A least-squares analysis, which is given in Fig. 8, yields the following relationship between the concentration and the friction coefficient of gel.

$$f \propto C_{total}^{1.5} \tag{8}$$

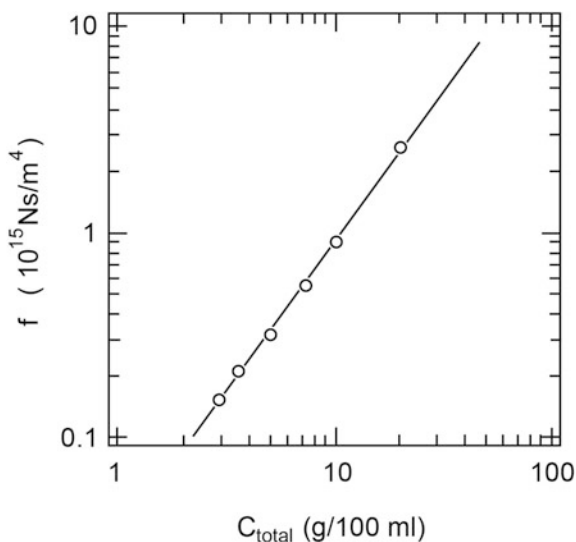
The scaling indicates that the relationship between the correlation length and the concentration in the gel system is expressed by the following equation (De Gennes 1979).

$$\xi \propto C_{total}^{-3/4} \tag{9}$$

We, therefore, find following relationship by substituting the Eq. (9) into (7).

$$f \propto C_{total}^{3/2} \tag{10}$$

Fig. 8 The total concentration dependence of the friction coefficient of poly (acrylamide) gel. The temperature is fixed at 20.0 ° C. The gels are prepared at a constant mole fraction of the cross-linker at 1 mol%. The straight line in this figure is the result of the least-squares analysis. The slope of the straight line is 1.5



Hence, the exponent of the power law relationship that is obtained experimentally agrees well with the one expected from the scaling theory (Fig. 9).

The concentration dependence of the friction on the cross-linking density, C_{CL} , is also studied. In these measurements, the gels are synthesized at various mole fractions of the cross-linking agent. The mole fraction is changed from 0.002 to 0.5 at a fixed total concentration of the gel of 700 mM (Tokita and Tanaka 1991a; Doi and Tokita 2005b). The results are summarized in Fig. 10. The inset figure shows the expanded view of the lower cross-linking density region, which is obtained in earlier study. On the other hand, the results in the concentration region above 20% are obtained in recent studies. The friction of the gel slightly decreases in the cross-linking density region from 0.003 to 0.1 as seen in the inset figure. The friction, however, decreases suddenly at the cross-linking density of about 0.2. The friction becomes smaller more than four orders of magnitude above this cross-linking density. The friction coefficient in this region is measured by the simple method that is described in the Experimental section in this concentration region. It is also found by the naked eye inspection that the gel gets opaque at the higher regions of the cross-linking density. We also find that the opaque gel lost the high elasticity and becomes brittle. In contrast, the gel becomes considerably sticky as the concentration of the cross-linker is decreased to 0.002 at which the friction decreases suddenly. The results suggest that the solution is close to the sol-gel transition point. The sudden decrease of the friction coefficient at this concentration may reflect that the system get closer to the sol-gel transition.

The appearance of the gel varies from transparent, translucent, and then to opaque when the cross-linking density is increased. It suggests that the structure of the polymer network becomes heterogeneous with the cross-linking density. The phenomenon observed here is already reported so far, and the phase diagram and the structure of the opaque gel have been discussed (Richards and Temple 1971;

Fig. 9 The relationship between the friction coefficient of the gel and the concentration of the cross-linker, C_{CL} . The concentration of the cross-linker is changed at a constant total concentration of the gel at 700 mM. The inset shows the expanded view of the lower concentration region of the figure

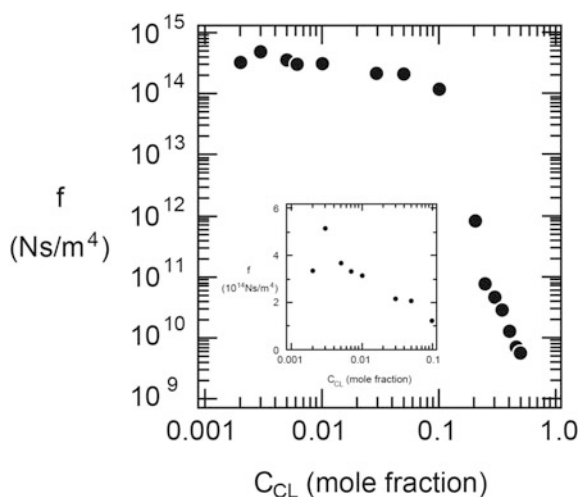
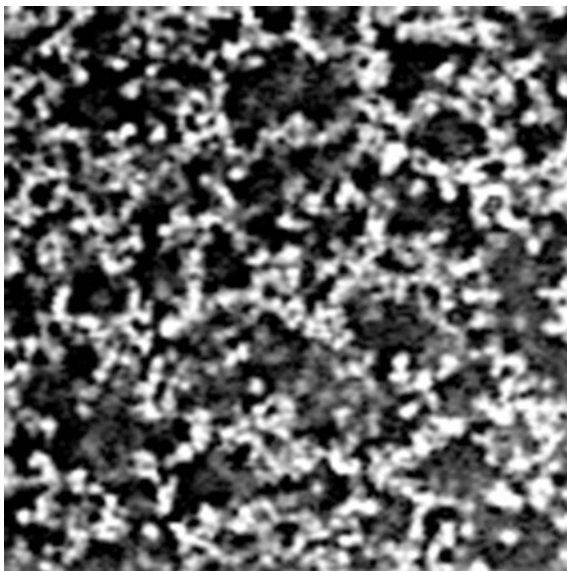


Fig. 10 The confocal laser scanning microscope image of opaque poly(acrylamide) gel. The gel is prepared at a mole fraction of the cross-linker at 350 mM at a total concentration of 700 mM. The one side of the image corresponds to 40 μ m. The image is gained at a magnification of 40 \times . The brighter region represents the dense region of substances while the darker regions are the vacant portions



Bansil and Gupta 1980). However, it is only recently that we obtain the information on the real space structure of opaque gel. The recent advancement of the optical microscope technology enables us to observe the structure of the inside of the materials invasively by using the confocal laser scanning microscope (CLSM) (Hirokawa et al. 1999). Therefore, we use the CLSM imaging to reveal the structure of opaque poly(acrylamide) gel in real space. Such a real space structural analysis of the gel yields that the opaque poly(acrylamide) gels consist of the aggregate of spherical particles. The diameter of the particle grows up to about sub-micrometer in diameter (Doi and Tokita 2005a, b).

The detailed real space structural analysis of the opaque gel suggests that the spherical particles, which forms the aggregate, has almost the same density with that of acrylamide and/or *N,N'*-methylenebisacrylamide in the solid state. The results strongly suggest that all reagents in feed are tightly polymerized into spherical particles. The particles observed in the CLSM image of opaque gels are, therefore, reasonably assumed to be a colloid particle of the hard sphere. As a result of this, the opaque poly(acrylamide) gels do not contain the long chain molecule, which is deformable under the flow of the gel fluid. The opaque gel is, therefore, simply regarded as an aggregated colloidal gel rather than a percolated network gel.

It may be easily expected that the friction of a porous material is mainly governed by the largest pore in the system. The CLSM images of opaque gel indicate that there are many large pores in the opaque gel that is represented by the darker regions of the image. Water, therefore, mainly flows choosing the darker region, which serves as an open space for water flow, avoiding the spherical particles that behave as an obstacle for the flow. Since the size of darker regions are more than few micrometers, water can flow in the gel easily. This is reason why the opaque

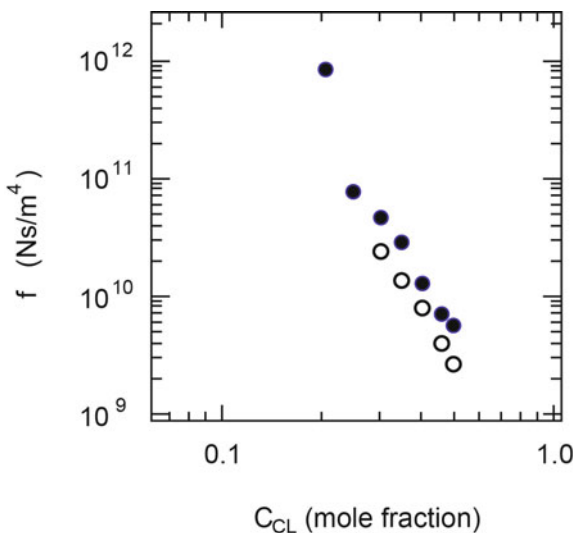
gels show the smaller friction. Because the colloidal particle is found to be regarded as a hard sphere, we expect that the friction of opaque gel can be explained in terms of the hydrodynamic friction of obstacle that made of the spherical particles. It is well established in the hydrodynamic theory that the resistance of the sphere against the fluid flow, f_{obstacle} , can be expressed by the Stokes law that is written as $f_{\text{obstacle}} = 6\pi\eta R$ where R represents the diameter of the particle. In opaque gel, the friction of gel is simply regarded as the superposition of the friction of each particle that consists the aggregate. Therefore, the friction of the gel is reasonably assumed to be expressed as follows:

$$f_{\text{obstacle}} = N6\pi\eta R \quad (11)$$

Here, N represents the number of the particle in a unit volume of the gel. Fortunately, we can determine the parameter N by analyzing the CLSM image. Because the colloidal particles are located in the brighter region in the CLSM image. Hence, the total area of the brighter region in the CLSM image, σ , is proportional to the number of the particle in the observation volume. The number of the particle in the observation volume can be calculated from σ if the average radius of the particle, R , is determined. Both the total area of the brighter region and the average radius of the colloidal particle are easily determined by the image analyses of the CLSM image. Then, the number of the particle in the observation volume is calculated as, $N = \sigma/\pi R^2$. The result of the calculation of f_{obstacle} is shown in the Fig. 11 (Doi and Tokita 2005a, b).

Although the experimental values of friction are about twice of the calculated values, the calculated values well reflect the experimental tendency of the concentration dependence. Since the model used here is crude, several reasons can be

Fig. 11 The expanded view of the higher concentration region in the Fig. 10. The open symbols indicate the calculated values of the friction coefficient from the structural parameters that determined from the confocal laser scanning microscope images of the opaque gels. The closed symbols are the friction coefficient of the gel determined experimentally



considered for the discrepancy. One and the most conceivable reason of the discrepancy may be follows. Generally, the microscope image is the projection of the three-dimensional into the two-dimensional plane. The thickness of the observation volume is usually determined by the performance of the microscope. In the case of the CLSM imaging, the thickness is thinner than the simple optical microscopes, which is the characteristic feature of the CLSM imaging. Even though the thickness is thin, the observation volume of the CLSM image also have a definite thickness. Therefore, this effect should be taking into account when we evaluate the friction of gel from the analyzed results of the CLSM imaging. In our CLSM apparatus, the thickness of the focal plane is about 1 μm according to the manufacturer. On the other hand, the radius of the spherical particle obtained by the analysis of the CLSM images is the order of around 1 μm . Taking into account this fact, the overlap of the particles in two-dimensional image is unavoidable. The calculated value of the number of the particle is obviously under estimated because of the overlapping. The maximum number of the particles in the observation volume, however, does not exceeds twice of the calculated value, which corresponds the case that the *same structure is hidden* behind the observed image. We believe that the calculated values of the friction are, therefore, within the expected maximum error. The results obtained here indicate that the structural of the polymer network of poly(acrylamide) gel changes from the percolated network to the aggregated colloid particle with the increase of cross-linking density.

1.3.2 Poly(*N*-Isopropylacrylamide) Gel

When a system is brought near the phase transition point, many physical quantities show the critical behaviors (Stanley 1971; Papon et al. 2002). It has been shown that the spatial density fluctuation that emerges in the critical region is time dependent and reversible against the temperature change. The distance over which the density fluctuations correlates, ξ , diverges in the critical region that causes many singular behaviors to the physical quantities. When the gel is brought near the transition point, the polymer network is regarded as an assembly of the pores of the typical size of about ξ . It is intuitively expected that the friction of the gel diminishes and eventually disappears as the transition point is approached because of the divergence of the correlation length. The gel fluid, therefore, can pass through the gel without experiencing the frictional resistance of the polymer network in the critical region.

The critical behaviors of the gel are studied extensively after the discovery of thermos-reversible volume phase transition of poly(*N*-isopropylacrylamide) gel. The critical behaviors of gel are studied using poly(*N*-isopropylacrylamide) gel in detail and the results so far obtained indicate following behaviors in the critical region of the gel (Hirokawa and Tanaka 1984; Tanaka et al. 1985).

$$E \rightarrow 0 \quad (12)$$

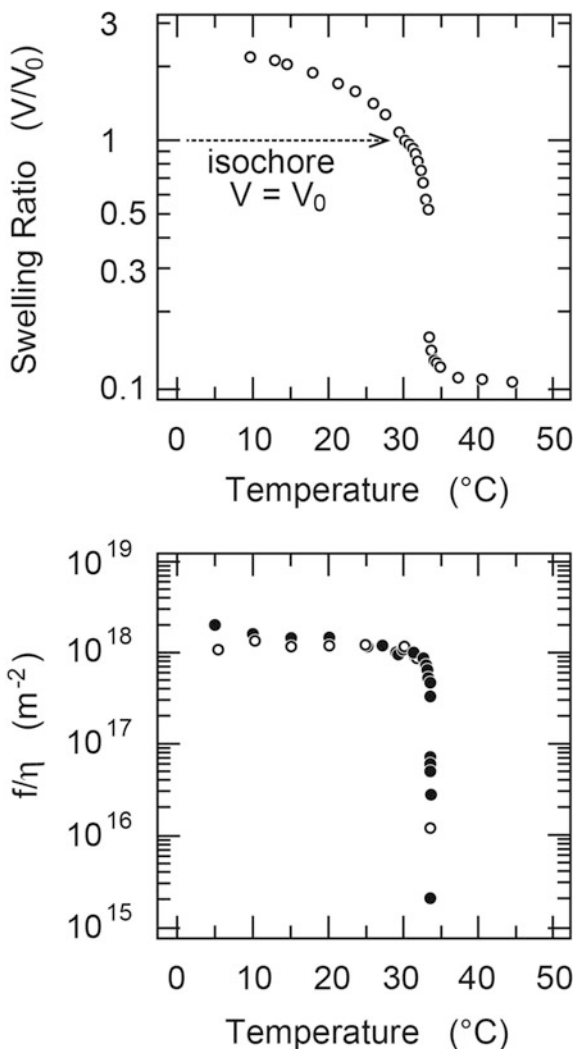
$$D_c = E/f \rightarrow 0 \quad (13)$$

The Eq. (12) indicates that the polymer network becomes infinitely compressible in the critical region of the gel. Besides, the Eq. (13) indicates that the collective motion of the polymer network slows down at the critical point. The critical behaviors of E and D_c are observed and confirmed by experimental studies extensively. The critical behavior of f is not clarified at these days. Although our intuition strongly suggest that the friction of gel diminishes near the volume phase transition point, such a critical behavior is not confirmed by above Eqs. (12) and (13) because the Eq. (13) is sorely confirmed by the Eq. (12). The critical behavior of f is indefinite only from these results. Therefore, the critical behavior of the friction is one of the open question in the physics of the phase transition in gels, and hence, it should be determined experimentally. This is the reason why we study the friction of poly(*N*-isopropylacrylamide) gel.

The sample gel used here is free from the frozen-in density fluctuations and the gel looks completely transparent at a temperature of 20 °C. As is shown in Fig. 12, poly(*N*-isopropylacrylamide) gel shows the discrete volume change at about 33.6 °C. The volume phase transition of poly(*N*-isopropylacrylamide) gel is believed to be caused by the hydrophobic interaction between bulky side chains that promotes a lower critical solution temperature. The swelling curve shown in Fig. 12 corresponds to the isobaric behavior. In contrast the friction experiment is, in the case of our apparatus, carried out under the constant volume conditions of $V/V_0 = 1$. Such an experimental path is called as the isochoric conditions and is also shown in Fig. 12.

When the gel is changed along the isochoric line, the gel may firstly bring into the negative osmotic pressure region, and then, it proceeds into the coexistence regime. Since the volume of the gel changes with the temperature, many effects, which prevent the accurate determination of the friction, can be occur. Hence, the swelling behaviors of the gel should be checked before friction experiments. This is made on a gel that is prepared in the same gel mold for the friction experiments. The open portion of the gel slightly swells at lower temperatures since the sample gel is not clumped into the friction cell. It is confirmed that visible shrinkage of the gel does not occur within the highest temperature of the friction experiment. It is also find that the attachment between the gel and the gel bonding film remains intact within the whole temperature range of the friction measurement. The decrease of the linear size of monitor gel from that of the isochoric gel is found to be less than 10% even at the maximum temperature of our experiment. By these preliminary experiments, we confirm that the swelling or shrinking of the gel do not affect the frictional measurement in the present experimental conditions. A gel, which is freely suspended in water, is soaked in the water bath for the friction measurement to continuously monitor the swelling behavior of the gel. We find that the gel shows a slight opacity near the temperature where the friction diminishes. The increase in

Fig. 12 The swelling curve of poly(*N*-isopropylacrylamide) gel (up) and the temperature dependence of the normalized friction coefficient of poly(*N*-isopropylacrylamide) gel, $f(T)/\eta(T)$ (down). Solid symbols in the down figure indicate that data are taken with increasing temperature and open symbols are the results of decreasing temperature. The reversible decrease of the friction occurs near the volume phase transition temperature



the opaqueness may be due to the emergence of the dynamic density fluctuations. The emergence of the fluctuations seems to be responsible for the decrease of the gel-solvent friction.

The friction coefficient of poly(*N*-isopropylacrylamide) gel is measured as a function of temperature, $f(T)$. The friction coefficients thus obtained are normalized by the viscosity of water, $\eta(T)$, that is taken from a table. The normalized friction coefficient of poly(*N*-isopropylacrylamide) gel, $f(T)/\eta(T)$, is plotted as a function of the temperature in the lower figure of Fig. 12. It is clear that the friction of poly(*N*-isopropylacrylamide) gel is independent of the temperature in the lower temperature regions. The friction, however, abruptly decreases about three orders of

magnitude around 33.6 °C, which is close to the volume phase transition temperature of poly(*N*-isopropylacrylamide) gel. This drastic change of the friction is entirely reversible. Since the viscosity of water does not show any singularity in the temperature region of this friction experiments, the results primarily reflect the temperature dependence of the frictional pore size in poly(*N*-isopropylacrylamide) gel. It is found that the values of normalized friction of poly(*N*-isopropylacrylamide) gel in the lower temperature regions is almost the same with that of poly(acrylamide) gel that is shown in Fig. 7. The results suggest strongly that the frictional pore size of poly(*N*-isopropylacrylamide) gel and that of poly(acrylamide) gel is almost the same with each other when the temperature is far below the volume phase transition temperature of poly(*N*-isopropylacrylamide) gel. Since the frictional pore size of poly(acrylamide) gel is determined by the distance between the nearest neighbor contact points of polymers, that is the correlation length of the polymer network ξ , in the case of poly(acrylamide) gel, it may be reasonably concluded that the frictional pore size of poly(*N*-isopropylacrylamide) gel is also governed by the correlation length of the polymer network of gel at the lower temperature regions. When the temperature is raised near the phase transition point, however, the polymer network undergoes substantial density fluctuations in time and space. According to the dynamic density fluctuations, some portions of the gel swell while the other portions shrink to maintain the constant volume of gel. The effective pore size of such a fluctuated polymer network is determined by the correlation length of the density fluctuations rather than the distance between the nearest neighbor contact points of polymers. Water, thus, passes through the swollen portion of the polymer network of the gel which serve as the open space for water flow. On the other hand, the densely shrunken regions behave as the obstacles for water flow. The pore size of the gel diverges when the gel is brought into the two-phase region. One of the following two reasons are probably possible for the divergence of the pore size of polymer network.

- (1) The gel may remain in the metastable single phase as a superheated gel. The fluctuations are dynamic and should diverge at the spinodal point in this case. Such a metastable state of the gel is actually observed in the phase transition point of many gels as the hysteresis in the swelling curve. Poly(*N*-isopropylacrylamide) gel is also the case. The temperature gap at a hysteresis can become several degrees.
- (2) The gel may undergo phase separation. The domains of swollen and shrunken phases are created within the polymer network in this case. The density fluctuations are static in this case. It, hence, would diverge near the coexistence curve.

Unfortunately, it is difficult to decide which process occurs in the present study. In each case, however, the effective pore size of the gel diverges, and hence, the friction becomes smaller. Clearly, the pore structure is not fixed because the phase transition is reversible. It is, thus, reversibly enlarged or reduced against the temperature change near the phase transition point. Therefore, the friction of the gel

changes reversibly against the temperature change. It is found that the friction of thermos-sensitive gel shows the critical behavior of $f(T) \rightarrow 0$ as the phase transition temperature is approached. The results obtained here indicate that the critical behavior of the collective diffusion coefficient becomes indefinite since $D_c = E/f \rightarrow 0/0$. On the other hand, the behavior $D_c \rightarrow 0$ is actually observed experimentally. The results obtained here, therefore, further suggest that the longitudinal elasticity of gel diminishes faster than the friction of gel as the critical point is attained. As the volume phase transition is a universal behavior of the gel, the reversible decrease of the gel-solvent friction is also a universal phenomenon. Under an optimal combination of solvent and temperature, the reversible decrease of the gel-solvent friction should be observed in any gel.

2 Diffusion of Molecules in Gel

2.1 Introduction

In the previous section, we have discussed about the transport of the gel fluid by the macroscopic flow, which is caused by the mechanical pressure that is applied to the gel fluid. In this section, we discuss another transport phenomenon that is related with the gel, namely, the diffusion of substances in the gel. When a substance molecule is dissolved into the fluid, it moves in the fluid randomly due to the thermal agitation of the surrounding fluid molecules. Such a random motion of the molecule is studied in detail in the statistical physics. One of the characteristic parameters that reflects the random motion of the substance molecule suspended in the fluid is the diffusion coefficient of a molecule in attention. The diffusion coefficient of a substance, D_0 , in a simple fluid of the viscosity, η , is written as follows (Einstein 1956):

$$D_0 = \frac{kT}{6\pi\eta R} \quad (14)$$

Here, k , T , and R are the Boltzmann's constant, the temperature, and the radius of the substance, respectively. Equation (14) is called as the Stokes-Einstein equation for the diffusion coefficient. The Stokes-Einstein relation for the diffusion coefficient indicates that the diffusion of a substance is uniquely determined by the temperature of the system, the characteristics of the fluid, and the size of the substance. However, the diffusional motion of the substance is altered when it is introduced into the gel. Since the polymer network coexists in the system, the substance experiences the additional resistance from the polymer network of the gel (Muhr and Blanshard 1982; Park et al. 1990; Gibbs and Johnson 1991). The resistance of the polymer network is caused by the interactions between the substance and the polymer network. The interaction that causes the resistance on the motion of the substance can be classified into four classes in the case of hydrogel and the substance systems as follows:

- (i) van der Waals interaction
- (ii) hydrophobic interaction
- (iii) hydrogen bonding
- (iv) electrostatic interactions between negatively and/or positively charged groups.

Therefore, as is well known, the interaction among the substances and the polymer network of the gel depends strongly on the chemical structure of both the substance and the gel. In addition to this, it is also well known that these interactions more or less occur between any substances. Therefore, the simple system should be constructed by careful choice of the gel and the substances to avoid the complication in the first step of the study. Then, it may be better to proceed into the complex systems where the interactions between the substance and the polymer network of the gel play essential rolls (Matsukawa et al. 1999; Zhao and Matsukawa 2012). This point has not been taken into account seriously in the previous studies on the diffusion of the substances in the gel. Among others, it is simplest to start with the system in which both the gel and the substance are soluble to a solvent of water since water is common fluid in a wide variety of the system from chemistry to biology. The main interaction we firstly focus our attention is, therefore, the van der Waals interactions. In other words, we firstly study the system that is constructed by the non-ionic poly(acrylamide) gel and the non-ionic hydrophilic substance (highly water-soluble non-ionic molecules) where any strong interactions from (ii) to (iv) raised above do not exist between the polymer network of the gel and the substance. In such a system, the polymer network is regarded just as an obstacle for the diffusional motion of the substance. The substance, which is introduced into the polymer network of gel, diffuses experiencing the resistance from the polymer network. The purpose of the study here is to reveal the effects of the polymer network on the diffusion of the substance and to deduce the physical picture of the diffusion of the substance in the maze of polymer network (Tokita et al. 1996).

2.2 Experimental

The nuclear magnetic resonance technology is considerably advanced during this decade. The useful technique in studying the transport phenomena is the pulsed field gradient nuclear magnetic resonance method (PFG-NMR) (Hahn 1950; Carr and Purcell 1954; Stejskal and Tanner 1965). This NMR technique is used in studying the diffusion of substances in the simple solution. Then, it is expanded to study the diffusion in the complex systems of the semi-dilute polymer solution and the polymer gel systems. Here, we also applied the PGF-NMR method to study the diffusion of substances within the gel. Here after, the substance, which is the target for NMR measurement, will be called as the *probe molecule* for the sake of

simplicity because the circumstances around the substance is searched from the diffusive motion of the substance molecules.

The spectrum of the probe molecules is required to be observed separately in the high-resolution spectrum of entire system when the diffusion coefficient is determined by PFG-NMR method. In the case of high-resolution NMR measurements, the motional narrowing conditions are required to obtain the spectrum. This condition is generally satisfied in the simple solution of substances. We have made the preliminary experiments before the measurements of the diffusion coefficient of the probe molecules. The high-resolution NMR spectra of the gel-probe molecule systems are gained. It is found the probe molecules are observable in the NMR spectrum of gel-probe molecule systems. It indicates that the motional narrowing conditions are also satisfied in our system of poly(acrylamide) gel and the water-soluble probe molecules. It further suggests strongly that the microscopic motion of the probe molecule is rather fast even they are introduced into the gel. In contrast, high-resolution NMR spectrum of acrylamide segment is not observed in the NMR spectrum at a frequency of 60 MHz in proton resonance. It indicates that the collective motion of the polymer network is much slower than the motion of the probe molecules as is expected from the collective diffusion coefficient of gel. The results coincide with the THB theory. The results also indicate that the interaction of the gel and the probe molecules is not very strong in the present system. The polymer network of gel, therefore, can be regarded as a fixed obstacle for the diffusive motions of the probe molecules under the present experimental conditions. Finally, the diffusion coefficient of the probe molecules can be determined by PFG-NMR.

In this study, five substances with different molecular weights are chosen from highly water-soluble non-ionic molecules as the probe molecules, namely, water (solvent), ethanol, glycerin, poly(ethylene glycol), and sucrose, and the gel used in this study is poly(acrylamide) gel. The molecular weights of these probe molecules are, 18, 46, 92, 200, and 342, respectively. The sample gel of poly(acrylamide) is polymerized in an NMR tube of 10 mm in diameter. First of all, water and the heavy water is mixed at a ratio of 9:1. Then, the predetermined amount of the probe molecule is dissolved in this mixture of water and the heavy water. The concentration of the probe molecule is fixed at 10 wt%. Then, the calculated amount of the reagents, acrylamide, *N,N'*-methylenebisacrylamide, and ammonium persulfate (initiator), are dissolved into water that contains the probe molecule. The pre-gel solution thus obtained is de-gassed for 20 min, and then, the reaction is initiated by heating the pre-gel solution at a temperature to 60 °C for 1 h. The total concentration of the gel is charged from 2 to 50 g/100 ml under a constant concentration of the cross-linker at 2 mol%.

The diffusion coefficients of probe molecules are determined by a JEOL FX-60Q spectrometer (60 MHz, JEOL, Japan). The field gradient component NMPL-502 (JEOL, Japan) is also equipped to the spectrometer. The temperature is fixed at 30.0 ± 0.5 °C. Details of the experimental procedure have been reported previously.

2.3 Probe Diffusion in Gel

The diffusion coefficients of all probe molecules are measured in the gels having various concentrations, and then plotted in Fig. 13. First of all, it is clearly seen from this figure that the diffusion coefficients of the probe molecules decrease upon increasing the concentration of the gel, C_{total} gradually and monotonously. The diffusion coefficient of water molecule in the gel, for instance, becomes about 40% of that in the simple solution in the highest concentration of the gel, $C_{\text{total}} = 50 \text{ g}/100 \text{ ml}$. The similar tendency is observed in all probe molecules studied here. Secondly, the diffusion coefficients of the probe molecules also decrease as the molecular weight of the probe molecule is increased. These results indicate that the resistance due to the polymer network of the gel against the diffusional motion of the probe molecule is not very strong, and is a smooth function of the total concentration of the gel. In other words, the interactions that exist between the polymer network and probe molecules are rather weak. These results are what we expected when choosing the present system of poly(acrylamide) gel and the water-soluble non-ionic probe molecules. The diffusion coefficient of the probe molecules does not show any singular behaviors in poly(acrylamide) gel.

The diffusion coefficient of the probe molecule is essentially determined by the ratio of the thermal fluctuation and the hydrodynamic friction applied to the probe molecule, Eq. (14). Since the probe molecules used here are rather compact, it is natural to assume that the radius of the probe molecule increases with the molecular weight. Thus, the diffusion coefficient decreases with the molecular weight of the probe molecule. This is quite simple view of diffusion in the simple fluid. When the probe molecules are introduced into the gel, however, the probe molecules are enforced to move through the mesh of the polymer network. The resistance due to the polymer network increases when the concentration of gel is increased. This is because the size of the maze created by the polymer network becomes narrower when the concentration of gel is increased. The diffusion coefficient of the probe molecule, thus, decreases as the concentration of the gel is increased. It is easily expected, however, whenever the size of the probe molecule is small it can diffuse in the gel rather easily. In contrast, the diffusion of larger probe molecule is considerably decreased when the concentration of gel is increased. However, the larger probe molecule also can diffuse rather easily in the gel when the mesh size of the polymer network of is large enough than the size of the probe molecule. This is the idea of the scaling. Namely, it may be of useful to discuss the diffusion result in terms of the normalized values by the diffusion coefficient of probe molecules in simple fluid of water, D/D_0 , rather than the law values of the diffusion coefficients in the gel to deduce the physical picture of the diffusion phenomenon in the gel. It is worth noting here that such a simple scaling idea is only applicable to the system that the series of the probe molecules studied interact with the polymer network of gel through the same interaction. We, therefore, assume that the normalized diffusion coefficient of the probe molecules, D/D_0 , is the relevant parameter to discuss the diffusion of probe molecules in the gel.

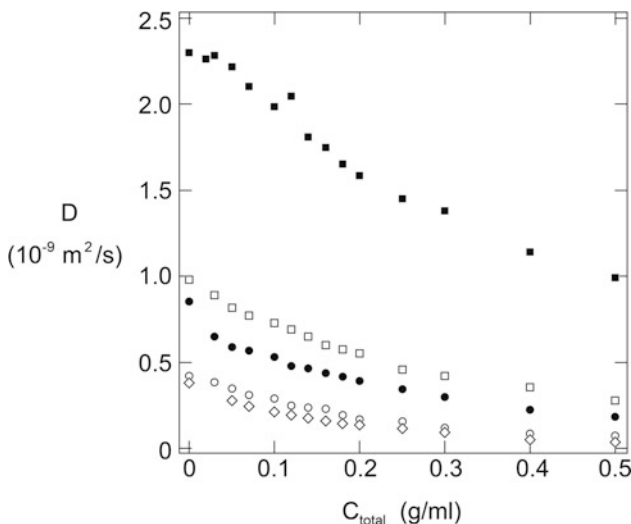


Fig. 13 The total concentration dependence of the diffusion coefficient of the probe molecules. The probe molecule is, water, ethanol, glycerin, poly(ethylene glycol), and sucrose, from top to bottom. The data points shown at the zero concentration of the horizontal axis represent the diffusion coefficient of probe molecules in the solution that is obtained by the same experimental setup

It has been clarified eventually that many physical quantities of the polymer systems follow the scaling law (De Gennes 1979). The gel is also a system where the idea of the scaling law plays important roles. We, therefore, expect that the scaling law is capable of describing the probe diffusion in the gel as intuitively explained in the previous section. The scaling suggests that the normalized diffusion coefficient of the probe molecule, D/D_0 , is expressed by a non-dimensional universal function, $f(x)$.

$$\frac{D(x)}{D_0} = f(x) \quad (15)$$

Here, the scaling variable x is written by the concentration of the gel and the size of the probe molecule as $x = x(C_{\text{total}}, R)$. The scaling variable itself should be a non-dimensional parameter though it is a function of C_{total} and R . Taking into account the previous intuitive discussion, an appropriate the scaling variable in this system is the ratio of two length scales of the problem, $x = R/\xi$, where R and ξ are the radius of the probe molecule and the correlation length of the polymer network of the gel, respectively. The probe molecules studied here is compact that is chosen from the hydrophilic non-ionic substances. We, therefore, expect that the radius of the probe molecule R is written as follows by using the molecular weight of probe molecules, M , as follows:

$$R \propto M^{1/3} \quad (16)$$

On the other hand, the correlation length of the gel, ζ , is written as, $\zeta \propto C_{\text{total}}^{-3/4}$, which is already given as Eq. (9). The combination of the Eqs. (9) and (16) yields that the scaling variable, $x = R/\zeta$, is expressed as follows:

$$x = \frac{R}{\zeta} \propto M^{1/3} C_{\text{total}}^{3/4} \quad (17)$$

Therefore, we plot the normalized diffusion coefficients of all probe molecules, D/D_0 , against the scaling variable, x , in the semi-logarithmic manner in Fig. 14. It is clear that all data of the diffusion coefficient gained at various concentrations of poly(acrylamide) gel falls onto a single master curve. Besides, the scaling function itself is expressed by a single exponential function as follows:

$$f(x) = \exp(-x) \quad (18)$$

The scaling function thus obtained here is similar with the one expected for the semi-dilute solutions (Langevin and Rondelez 1978; Cukier 1984).

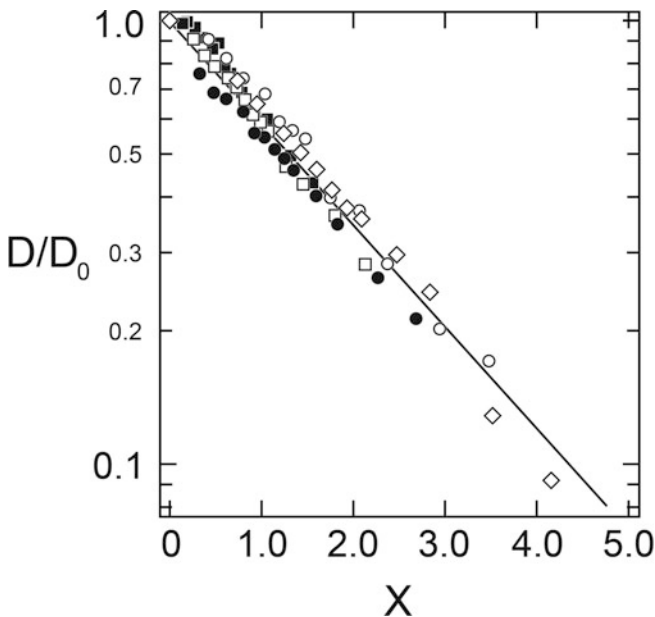


Fig. 14 The diffusion coefficient of the probe molecules in the gel are normalized by its diffusion coefficient in water, D/D_0 , and plotted as a function of the scaling variable, x , in a semi-logarithmic manner. The straight line is the result of the least-squares analysis

The results obtained here indicates that the diffusion coefficient of a substance in the gel becomes smaller than that in a simple fluid. The rate of the decrease in the diffusion coefficient is, however, determined only by a parameter $x = R/\zeta$, that is, the ratio of the radius of the probe molecule and the correlation length of the gel. Although the size of the probe molecule is increased, the relative diffusion coefficient of the probe molecule, D/D_0 , becomes the same if one change the value R/ζ becomes the same. These conditions are usually realized by decreasing the concentration of the gel. The results of the scaling are schematically illustrated in Fig. 15.

3 Concluding Remarks

The transport phenomena that is related to the gel are reviewed. The frictional properties of the gels, poly(acrylamide) gel and poly(*N*-isoprpylacrylamide) gel, are described and many features that characterizes the state of the gel are clarified. We find that why the frictional properties of the gel play important roles in the dynamics of the swelling and shrinking of the gel. The friction of the gel also plays the essential roles in the pattern formation of gel and the large deformation processes of the (Tanaka et al. 1987; Matsuo and Tanaka 1992; Tokita et al. 1999, 2000; Nakamura et al. 2001). The information on the frictional property of gel is, therefore, of useful in many applications such as the medicine, food, chemical engineering, and biotechnology.

The knowledge gained so far is, however, still limited. For instance, we do not have any information on the numerical constant of Eq. (7). In the case of well-defined flow of the fluid, the equation can be written definitively including the numerical constant. The Hagen–Poiseuille law for the capillary flow, which is used

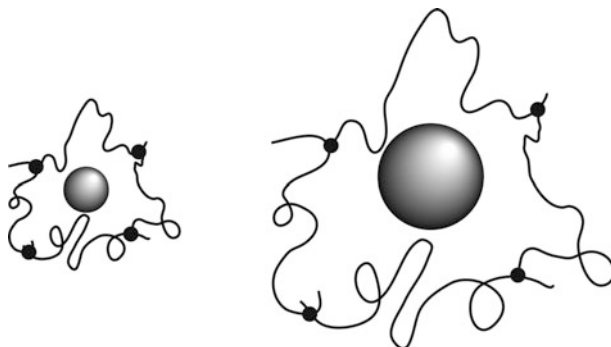


Fig. 15 The schematic illustration of the scaling results. The smaller probe molecule in the dense gel (left) and the larger probe molecule in the tenuous gel (right). The relative size of the probe molecule and the mesh size of the gel are similar in both cases. The relative rate of the diffusion is similar in these two conditions

in determining the viscosity of the fluid, is such a case. In many literatures of the hydrodynamics, the Hagen–Poiseuille law is expressed as follows:

$$\frac{P}{L} = \frac{8\eta}{r^2}v = fv$$

Here, P/L , r , η , and v are the pressure gradient in a capillary of length L , the radius of the capillary, the viscosity of the fluid, and the velocity of the flowing fluid in the capillary. The friction of the capillary of the radius r is, therefore, written as follows.

$$f = \frac{8\eta}{r^2}$$

The above equation agrees with the Eq. (7) since the radius is the typical length scale that describes the cylindrical capillary. Furthermore, the proportional constant is exactly written in the case of the Hagen–Poiseuille flow, which is a numerical constant of 8. Therefore, Eq. (7) should generally be written as follows:

$$f = Q_{\text{shape}} \frac{\eta}{\zeta^2}$$

The constant, Q_{shape} , is determined by the structure of the pore, and hence it may be regarded as the structure factor of porous material. Clearly, $Q_{\text{shape}} = 8$ in the case of Hagen–Poiseuille flow in a capillary of rod shape. If we can determine the structure factor of the porous material experimentally and/or theoretically, it will be possible to design a material with the desired frictional properties. Recently, the frictional property of a well-defined polymer network of the gel is studied in detail (Fujiki et al. 2016). The continuous accumulation of such information will promote the better understanding of the frictional properties of the gel.

The experimental results on the friction of the gel and diffusion within the gel are mostly discussed in terms of the scaling theory in this review. Therefore, it is worth noting here about another scaling analysis of the total concentration dependence of the friction coefficient that is given in Eq. (8). It is shown that the Eq. (8) can be explained by assuming the scaling law for the correlation length, Eq. (9). However, Eq. (8) is also explainable in terms of the scaling results of the longitudinal modulus, E , and the collective diffusion coefficient of the gel, D_c . Both the scaling form of the longitudinal modulus of the gel and the collective diffusion coefficient of the gel are given as follows.

$$E \propto C_{\text{total}}^{9/4}$$

$$D_c \propto C_{\text{total}}^{3/4}$$

Substitution of these equations into Eq. (1) yields the following result:

$$f = \frac{E}{D_c} \propto C_{\text{total}}^{6/4}$$

The scaling of the longitudinal modulus and the collective diffusion coefficient also well describe the experimental results on the friction of the gel. Above result is the experimental confirmation of the relationship between the collective diffusion coefficient of the gel, the elastic modulus of the gel, and the friction coefficient of the gel, that is the Eq. (1). This is a complete confirmation of the THB theory.

The relationship between phase transition and the frictional property is another topic to be studied in future. The friction coefficient of poly(*N*-isopropylacrylamide) gel disappears at the volume phase transition point of the gel due to the critical slowing down. The critical slowing down is a universal behavior that is observed in the system near the phase transition point. Since the critical behavior of the friction is also believed to be a universal phenomenon in the gel, we are interested in the critical transport in the biopolymer gel systems. Recently, we find similar phenomena in the biopolymer gel systems that the gel becomes opaque by the frozen-in density fluctuation due to the phase separation of the system. In such systems, the gelation and the phase separation occur simultaneously (Morita et al. 2013; Yamashita et al. 2014). The frictional properties of such heterogeneous biopolymer gels will contribute to the understanding of the biological transport phenomena.

The probe diffusion in the gel also requires the further detailed studies. We only described on the system of the hydrophilic gel and the hydrophilic probe molecules here. Since this system is an idealized system, we obtain a quite simple scaling results for the probe diffusion phenomena. There are, however, many candidates for the probe molecules that have many chemical structures, and hence, it interacts with the polymer network of the gel in various way. Various diffusional behaviors of the probe molecules can be observed by the carefully designed studies of the diffusion in the gel. The classification of such diffusion results in terms of the four fundamental interactions in water will be of importance in designing the separation systems and the studying the biological transport phenomena. It is reported recently that the Liesegang pattern is formed in the one-dimensional diffusion-reaction system. In such a system, the gelation and the phase separation is coupled, and hence, it suggests strongly that the diffusion of the substances plays the essential roles in pattern formation in the gel (Narita and Tokita 2006, 2010). Further detailed study of the transport phenomena in the gel is, therefore, clearly required not only for the applications but also for the better understanding of the physics of the gel because the gel is a universal state of matter.

References

- Bansil R, Gupta MK (1980) Effects of varying crosslinking density on polyacrylamide gels. *Ferroelectrics* 30:63–71

- Carr HY, Purcell EM (1954) Effects of diffusion on free precession in nuclear magnetic resonance. *Phys Rev* 94:630–638
- Cukier RI (1984) Diffusion of Brownian spheres in semidilute polymer-solutions. *Macromolecules* 17:252–255
- De Gennes PG (1976) On a relation between percolation theory and the elasticity of gels. *J Phys Lett (Paris)* 37:L1–L2
- De Gennes PG (1979) *Scaling concepts in polymer physics*. Cornell University Press. Ithaca, pp 128–162
- Doi Y, Tokita M (2005a) Real space structure of opaque gel. *Langmuir* 21:5285–5289
- Doi Y, Tokita M (2005b) Friction coefficient and structural transition in a poly(acrylamide) gel. *Langmuir* 21:9420–9425
- Einstein A (1956) In: Furth R (ed) *Investigations on the theory of the Brownian Movement*. Dover Publications Inc.
- Fujiki M, Ito M, Kell M, Yashima S, Tokita M, Annaka M (2016) Friction coefficient of well-defined hydrogel network. *Macromolecules* 49:634–642
- Geissler E, Hecht AM (1982) Gel deswelling under reverse osmosis-II. *J Chem Phys* 77:1548–1553
- Gibbs SJ, Johnson CS Jr (1991) Pulsed field gradient NMR-study of probe motion in polyacrylamide gels. *Macromolecules* 24:6110–6113
- Hahn EL (1950) Spin echoes. *Phys Rev* 80:580–594
- Hecht AM, Geissler E (1980) Gel deswelling under reverse osmosis. *J Chem Phys* 73:4077–4080
- Hirokawa Y, Tanaka T (1984) Volume phase transition in a nonionic gel. *J Chem Phys* 81:6379–6380
- Hirokawa Y, Jinnai H, Nishikawa Y, Okamoto T, Hashimoto T (1999) Direct observation of internal structures in poly(*N*-isopropylacrylamide) chemical gels. *Macromolecules* 32:7093–7099
- Langevin D, Rondelez F (1978) Sedimentation of large colloidal particles through semidilute polymer-solutions. *Polymer* 19:875–882
- Matsukawa S, Yasunaga H, Zhao C, Kuroki S, Ando I (1999) Diffusion processes in polymer gels as studied by pulsed field-gradient spin-echo NMR spectroscopy. *Prog Polym Sci* 24:995–1044
- Matsuo ES, Tanaka T (1992) Patterns in shrinking gel. *Nature* 358:482–485
- Morita T, Narita T, Mukai S, Yanagisawa M, Tokita M (2013) Phase behaviors of agarose gel. *AIP Adv* 3:42128
- Muhr AH, Blanshard JMV (1982) Diffusion in gels. *Polymer* 23:1012–1026
- Munch JP, Candau S, Herz J, Hild G (1977a) Inelastic light-scattering by gel modes in semi-dilute polymer solutions and permanent network at equilibrium swollen state. *J Phys (Paris)* 38:971–976
- Munch JP, Lemarchal P, Candau S (1977b) Light-scattering spectroscopy polydimethylsiloxane-toluene gel. *J Phys (Paris)* 38:1499–1509
- Nakamura K, Shinoda E, Tokita M (2001) The influence of compression velocity on strength and structure of gellan gels. *Food Hydrocolloids* 15:247–252
- Narita T, Tokita M (2006) Liesegang pattern formation in k-carrageenan gel. *Langmuir* 22:349–352
- Narita T, Tokita M (2010) Spatial pattern induced by gelation of polysaccharide solutions. In: Lagzi I (ed) *Precipitation patterns in reaction-diffusion systems*. Research Signpost, Kerala
- Papon P, Leblond J, Meijer PHE (2002) *The physics of phase transitions. Concepts and applications*. Springer, Berlin, Heidelberg
- Park IH, Johnson CS Jr, Gablriel DA (1990) Probe diffusion in polyacrylamide gels as observed by means of holographic relaxation methods—search for a universal equation. *Macromolecules* 23:1548–1553
- Richards EG, Temple CJ (1971) Some properties of polyacrylamide gels. *Nature (Phys Sci)* 230:92

- Stanley HE (1971) Introduction to phase transition and critical phenomena. Oxford University Press Inc.
- Stejskal EO, Tanner JE (1965) Spin diffusion measurements: spin echoes in the presence of a time-dependent field gradient. *J Chem Phys* 42:288–292
- Suzuki YY, Tokita M, Mukai S (2009) Kinetics of water flow through a polymer gel. *Eur J Phys E29*:415–422
- Takebe T, Nawa K, Suehiro S, Hashimoto T (1989) Quasielastic light-scattering studies of swollen and stretched polymer gels. *J Chem Phys* 59:4360–4368
- Tanaka T (1978) Collapse of gels and the critical endpoint. *Phys Rev Lett* 40:820–823
- Tanaka T (1981) Gels. *Acc Chem Res* 14:124–136
- Tanaka T, Fillmore DJ (1979) Kinetics of swelling of gels. *J Chem Phys* 70:1214–1218
- Tanaka T, Hocker LO, Benedek GB (1973) Spectrum of light scattered from a viscoelastic gel. *J Chem Phys* 59:5151–5159
- Tanaka T, Ishiwata S, Ishimoto C (1977) Critical behavior of density fluctuations in gels. *Phys Rev Lett* 38:771–774
- Tanaka T, Sato E, Hirokawa Y, Hirotsu S (1985) Critical kinetics of volume phase transition of gels. *Phys Rev Lett* 55:2455–2458
- Tanaka T, Sun S-T, Hirokawa Y, Katayama S, Kucera J, Hirose Y, Amiya T (1987) Mechanical instability of gels at the phase transition. *Nature* 325:796–798
- Tokita M, Hikichi K (1987) Mechanical studies of sol-gel transition: universal behavior of elastic modulus. *Phys Rev A* 35:4329–4333
- Tokita M, Tanaka T (1991a) Friction coefficient of polymer networks of gels. *J Chem Phys* 95:4613–4619
- Tokita M, Tanaka T (1991b) Reversible decrease of gel-solvent friction. *Science* 253:1121–1123
- Tokita M, Hikichi K, Niki R, Arima S (1982) Dynamic viscoelastic studies on the mechanism of milk clotting process. *Biorheology* 19:209–219
- Tokita M, Niki R, Hikichi K (1985) Critical behavior of modulus of gel. *J Chem Phys* 83:2583–2586
- Tokita M, Miyoshi T, Takegoshi K, Hikichi K (1996) Probe diffusion in gels. *Phys Rev E* 53:1823–1827
- Tokita M, Suzuki S, Miyamoto K, Komai T (1999) Confocal laser scanning microscope imaging of a pattern in shrinking gel. *J Phys Soc Jpn* 68:330–333
- Tokita M, Miyamoto K, Komai T (2000) Polymer network dynamics in shrinking patterns of gels. *J Chem Phys* 113:1647–1650
- Weiss N, van Vilet T, Silberberg A (1979) Permeability of heterogeneous gels. *J Polym Sci Polym Phys Eds* 17:2229–2240
- Yamashita Y, Yanagisawa M, Tokita M (2014) Sol-gel transition and phase separation in ternary system of gelatin-water-poly(ethylene glycol) oligomer. *J Mol Liq* 200:47–51
- Zhao QH, Matsukawa S (2012) Estimation of the hydrodynamic screening length in kappa-carrageenan solutions using NMR diffusion measurements. *Polymer J* 44:901–906

Chapter 12

Incorporation of Filler/Additives in Polymer Gel for Advanced Application



**Ida Idayu Muhamad, Eraricar Salleh, Shahruzaman Shaharuddin,
Norhayatie Pa'e, Suguna Selvakumaran and Mohd. Harfiz Salehudin**

Abstract This chapter is aimed to review the literature concerning the filler and additive effect on polymer gel for various advanced applications including food, agriculture, pharmaceutical, and others. To date, polymer gel utilization is important due to its superior properties. Moreover, polymer gel is very responsiveness toward small environmental changes and significantly altered the gel behavior. Currently, incorporation of filler into polymer gel matrices is beneficial to enhance the characteristics of the gel such as mechanical, chemical, physical, and biological properties. Metallic compound, cellulosic material, and crosslinker are the various categories of filler that broadly used based on application and processing. Therefore, filler-loaded polymer gel could be a potential tool or vehicle for different advanced applications.

Keywords Polymer gel · Filler · Metallic compound · Cellulosic material
Crosslinker · Advanced application

1 Introduction

1.1 Gel Polymers

Polymer gel, in general term, often designates as soft and wet material (Osada and Gong 1998). In specific definition, a polymer gel is a solid structure that composed of at least two components. One component which is polymer forms a

I. I. Muhamad (✉) · E. Salleh · S. Shaharuddin · N. Pa'e · S. Selvakumaran ·
Mohd.H. Salehudin
Department of Bioprocess Engineering, Faculty of Chemical Engineering,
Universiti Teknologi Malaysia, 81310 Johor Bahru, Malaysia
e-mail: idayu@cheme.utm.my

I. I. Muhamad
COE—Cardiac Biomaterials Cluster, IJN-UTM Cardiovascular Engineering Center
Level 2, Block B, Building V01/FBME, UTM, 81310 Johor Bahru, Johor, Malaysia

© Springer Nature Singapore Pte Ltd. 2018
V. K. Thakur and M. K. Thakur (eds.), *Polymer Gels*, Gels Horizons: From Science
to Smart Materials, https://doi.org/10.1007/978-981-10-6086-1_12

three-dimensional network by existence of covalent (Chemical gels) or non-covalent bonding (Physical gels). The polymer component on the other hand is located in the medium of liquid which ranged tens to hundreds of times the amount of the polymer. The liquid amount shall be sufficient to ensure the elastic properties of the gel. Polymer gel behaved as an energy transducer as it is capable of undergoing large deformation, turning its chemical and physical potentials. It also shows respond to various external environmental changes such as thermal and chemical.

A polymer gel is a three-dimensionally crosslinked polymer network by virtue of covalent or non-covalent bonding (chemical and physical gels, respectively) swollen by a solvent, most typically water (Rogovina et al. 2008; Thakur and Thakur 2014a, b, 2015). It is also well known as hydrogel. The water retention properties of polymer gel are because of the existence of hydrophilic groups, for example, hydroxyl, carboxyl, amino, and other chemicals in the polymer-forming polymer gel structures (Peppas et al. 2000). In spite of their high water-absorbing ability, polymer gel show good swelling properties which able to retain more than 20% of water within its structure without being dissolved when it is in contact with the aqueous surrounding environment (Peppas et al. 2000).

The nature of polymer gel such as biocompatible, non-toxic and biodegradable, controlled release properties of entrapped molecules, tissue-like properties, higher absorbency to small-sized molecules, and lower interfacial tension makes them an excellent carrier for drugs, protein, peptides, and other biological compound (Muhamad et al. 2011; Peppas 1987; Ratner and Williams 1981; Ratner et al. 1976). In general, polymer gel very responsive to physiological and environmental stimuli including pH, ionic, temperature, and electromagnetic radiation. Besides that, polymer gel is also widely explored in diverse biomedical fields, including biosensor, tissue engineering, wound dressing, biomolecule separation, and the contact lenses (Slaughter et al. 2009; Yaszemski et al. 2004).

1.2 Filler/Additive

In general, understanding filler is an additive that is commonly used to inexpensively increase volume or fill gaps within the material. Fillers are used not only to cut cost of the composites but not only to reduce the cost of composites, but also aided the improvements of composite that might not be achieved by the reinforcement and resin ingredients only (Trache et al. 2017; Corobea et al. 2016; Voicu et al. 2016; Miculescu et al. 2016). Usually, fillers are referred as extenders. In comparison to resins and reinforcements, fillers have minimal cost as the major ingredients (Pappu et al. 2015, 2016). Mechanical properties can be improved including fire and smoke performance by reducing organic content in composite laminates. On the other hand, the dimensional control of molded parts can be achieved as filled resin will undergo less shrinkage that unfilled resin. Proper use of filler can significantly control important properties, including stiffness, water

resistance, surface smoothness, weathering, dimensional stability, and temperature resistance, and can be improved through the proper use of fillers. Increase of inorganic fillers used in composites is also reported. Inorganic fillers can account from 40 to 65% by weight when used in composite laminates. Fillers in polymers show a remarkable variety of chemical natures, sizes, and shapes (Singha and Thakur 2008; Singha et al. 2008). Spheres or plaques (flakes, disks, and lamellas) or rods (needles, fibers) are three common shapes that are mostly known as shown in Fig. 1. Incorporation such basic shapes can result in complex geometrical objects with association of specific reinforcing properties (Leblanc 2009).

An additive on the other hand is a substance that modifies the properties of the plastic, such as a pigment that gives a color and a plasticiser that changes the flexibility. An additive is more of a broader classification, which is used to modify a material's characteristics and encompasses anything from fillers, stabilizers, pigments, and plasticisers.

1.3 Composite

When two or more materials are combined and created a new mixed material, it is described as a composite material (Thakur and Kessler 2014, 2015). This material could improve the material's characteristics and properties compared to those of the individual materials used alone (Affatato et al. 2015; Bernardo et al. 2016; Cevallos et al. 2016; Guilherme et al. 2015). The general structure of these biomaterial composites is divided into two main structures:

1. "Matrix" which always in the form of continuous phase.
2. "Reinforcement" which could be in the form of continuous or discontinuous

In polymer composite, various polymer applications have been explored due to their availability in various forms, properties, and compositions that allow the fabrication of different shapes and structures (Thakur et al. 2013a, b). Polymer composite material could provide significant impact on the final element such as

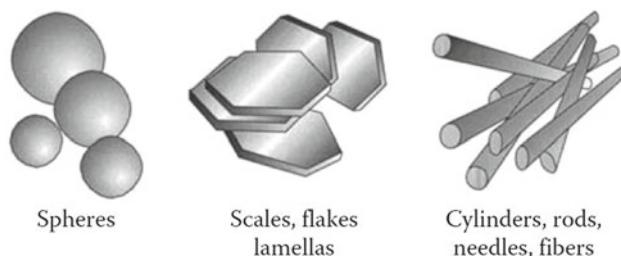


Fig. 1 Basic shape and structure of filler

enhancing their specific characteristics and properties, and creating a flexible structure for specific applications (Affatato et al. 2015). For instance, hydrogel produced using polysaccharides in their native form has low stability condition and affects their controlled release system in an application. This problem could be encountered with the incorporation of filler or crosslinking approach or both (Guilherme et al. 2015).

1.4 Market Trend

Hydrogel demonstrates many advantages such as enhanced water retention ability of the products, improved controlled release of drugs, and protected encapsulated material. These properties have fostered their use as everyday products such as contact lenses, diapers, and wound dressing. The ability to be used in many applications creates huge demand for hydrogel market. However, higher end or commercial hydrogel products especially in medical field is still limited due to their high production costs (Caló and Khutoryanskiy 2015). These include the products for tissue engineering and drug delivery where many products been designed, studied, and in some cases even patented, however, not many have reached the market.

In 2022, market for hydrogel product was projected to be increased up to \$27.2 billion with annual growth rate of 6.3% from 2016 to 2022 (Singh 2016). This phenomenon occurs because of several factors including growing interest for hydrogel-based products, increasing adoption of hydrogel products for various applications, the benefits of the hydrogel itself over conventional substitutes, and rapid research and development activities by large company. Some of the key players that monopoly the market include 3M Company, ConvaTec, Inc and Johnson & Johnson. The market for hydrogel was divided into five categories as listed in Table 1.

Table 1 Categories in hydrogel market

Categories	Type
Raw materials	Natural, synthetic, and hybrid
Composition	Polyacrylate, polyacrylamide, silicone-modified hydrogels, agar-based, and others
Form	Amorphous hydrogels Semi-crystalline hydrogels
Product	Hydrogel sheets, impregnated gauze, amorphous gels, semi-crystalline buttons, and others
End-user	Wound care, contact lenses, drug delivery, tissue engineering, hygiene products, and others

2 Various Polymer Gels

2.1 Carrageenan

Carrageenan is a term to name a group of polysaccharides that occur as intracellular matrix material in red seaweeds or marine algae of the class *Rhodophyta* (Van De Velde et al. 2002). To date, carrageenan is extensively used in food industry, pharmaceutical application, cosmetic industry, and others. Carrageenan is extracted from different genera *Chondrus*, *Euheuma*, *Gigartina*, *Euheuma*, and *Rhodophyceae* (Gupta and Raghava 2008; Stanley 1987). Carrageenan is linear polysaccharides made up of alternating repeating disaccharides unit of β -1,3- and α -1,4-linked galactose residue (D-enantiomer). General structure of the repeating unit is known as carrabiose—4- β -D-pyranosyl 3, 6-anhydro- α -D-galactopyranose (Campo et al. 2009; Norman and Harris 1990). According to the position of sulfate group in the 1,3- and 1,4-linked galactose residue, carrageenan is divided into three families, which is kappa (κ), iota (*I*), and lambda (λ) corresponding to one, two, and three sulfate groups per disaccharides (Michel et al. 2006).

In natural environment, carrageenan exists in algae as a form of gel. It is separated from algae through extraction with water at temperatures above the gel melting point. The most commonly used processes to obtain carrageenan from the seaweeds are alcohol precipitation, freeze–thaw, and gel press method. Carrageenan has shown several potential biological activities such as antiviral, antitumor, antithrombotic, immunomodulatory, and anticoagulant (Zhou et al. 2004; Morris 2003; Panlasigui et al. 2003; Caceres et al. 2000). Their biological activities are due to the presence of sulfate groups in carrageenan. The negatively charged sulfate polysaccharides exert inhibitory effect by interacting with the positive charges on the viruses or on the cell surface and thereby prevent the penetration of virus into the host cells (Necas and Bartosikova 2013). Since carrageenan is used in food and pharmaceutical application, its safety and toxicity levels are very important. Toxicological properties of carrageenan are as follows: LD50 (rat, oral) > 5 g/kg; LD50 (rabbit, skin) > 2 g/kg; and 4 h LC50 (rat, inhalation) > 0.93 mg/L (Weiner 1991). Th carrageenan is relatively a non-toxic material that is safe to use (Rowe et al. 2009).

2.1.1 Chemical Structure of Carrageenan

The *I*- (iota-), κ - (kappa), and λ - (lambda) carrageenan are the most fundamental commercial carrageenan (Steinbuchel and Rhee 2005) which consists of many naturally occurring arrangements of components that will manipulate gel strength, texture, solubility, synergisms, and melting temperature of the carrageenan (Imeson 1997). These three types of carrageenan differ essentially in their degree of sulphation (Necas and Bartosikova 2013; Williams and Philips 2000). Typical *k*- carrageenan contains sulfate (22% w/w), *i*-carrageenan (32% w/w), and

λ - carrageenan (38% w/w), respectively (Campo et al. 2009). According to Barbeyron et al. (2000), higher level of ester sulfate means lower solubility and lower gel strength. Thus, kappa and iota carrageenans have higher gel strength and solubility compared to lambda carrageenan. The chemical structure of kappa carrageenan, iota carrageenan, and lambda carrageenan is shown in Fig. 2.

2.1.2 Physical Properties of Carrageenan

The gelling and thickening behavior of *l*-, κ -, and λ -carrageenan is different. Table 2 briefly describes the properties of *l*-, κ -, and λ - carrageenan:

2.1.3 Food Application

Carrageenan is widely used especially in the production of processed foods including dairy products, meat products, pet foods, water-based foods, and beverages. Figure 3 illustrates the image for application of carrageenan in food industries summarizes the function of carrageenan in food and dairy products.

Fig. 2 Chemical structure of **a** Kappa carrageenan, **b** Iota carrageenan, and **c** Lambda carrageenan (Gupta and Raghava 2008)

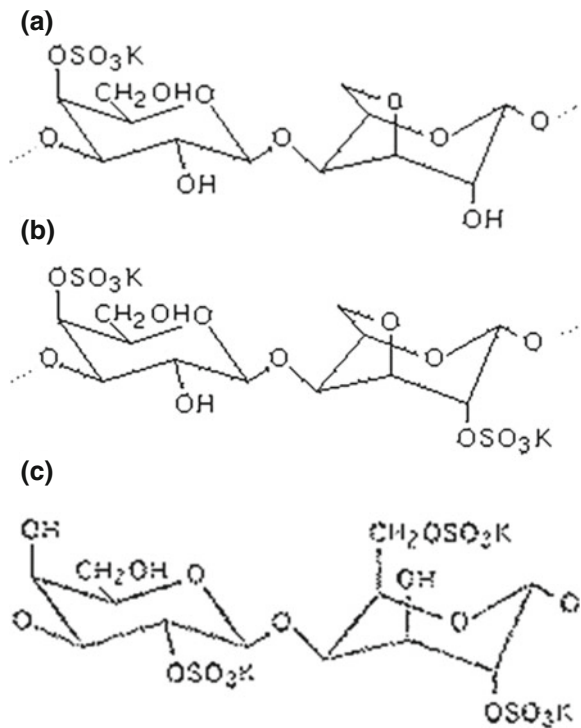
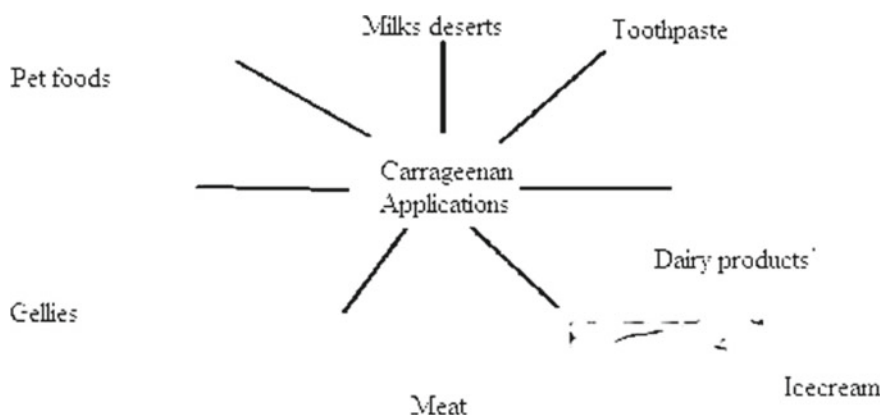


Table 2 Properties of different carrageenans (Shetty et al. 2006)

Carrageenan	Properties
Iota carrageenan	Elastic gels formed with calcium salts Clear gel with no bleeding of liquid Gels freeze/thaw stable
Kappa carrageenan	Strong, rigid gel, formed with potassium salts Brittle gel forms with calcium salts
Lambda carrageenan	No gel formation, forms high viscosity solutions

**Fig. 3** Illustrative image for application of carrageenan in food industries (Prajapati et al. 2014)

2.1.4 Pharmaceutical Application

In pharmaceutical application, carrageenan is mostly used in drug delivery system, wound dressing, bacterial inactivation, and immobilization of cells or enzymes. Asanza-Teruel et al. (1997) had successfully used novel method to improve the production of tetracycline and chlortetracycline (antibiotics) by immobilized *Streptomyces aureofaciens* in kappa carrageenan. Normally, these antibiotics are produced by conventional fermentation approach. Carrageenan-based wound dressing becomes an alternative approach to medical care because it is stable, biodegradable, able to absorb body fluids, delivers medications effectively, and able to keep wounds clean and healthy. It was also found that carrageenan provides a better performance compared to alginates fibers for these functions. Boateng et al. (2013) used polyethylene oxide (Polyox) and carrageenan solvent cast films as a drug delivery system for wound dressing. Drug-loaded POL-CAR films display excellent properties such as smooth, high transparency structure, and neat appearance, which is better in terms of observing the healing process, high elasticity, and high water absorption properties. These attributes make this film an ideal wound dressing material.

Jayaramudu et al. (2013) synthesized biodegradable iota carrageenan-based silver nanocomposite hydrogels to investigate hydrogels function as bacterial inactivation applications. They used iota carrageenan due to its biocompatibility, biodegradability, highly available, and cheap. From their study, the developed silver nanocomposite hydrogels can be promising candidates for antimicrobial applications. Based on their results, there was an inhibition of bacterial zones after 48 h of incubation but no inhibition zone in plain hydrogels. Therefore, Ag⁰-loaded iota carrageenan nanocomposite hydrogels exhibited excellent antibacterial activity. They concluded that iota carrageenan in combination with Ag⁺ nanocomposites hydrogels can be used in medical devices as antimicrobial agents.

Among the three carrageenans, kappa carrageenan-based hydrogels have been widely studied as a carrier for controlling drug release application. Good compatibility, biodegradability, easy gel-forming nature, high robustness, high physical and chemical properties, non-toxic, and high availability make kappa carrageenan suitable excipients for controlled release formulation (Trindade and Daniel-da-Silva 2011). Kappa carrageenan has ability to entrap bioactive agents within hydrocolloid matrix and release the bioactive agents in an extended and controlled manner (Daniel-da-Silva et al. 2012; Hezaveh and Muhamad 2012a, b). Additionally, the presence of pores within kappa carrageenan hydrogels of the matrix lead to controlled drug release.

Leong et al. (2011) formulated carboxymethylation of kappa carrageenan as hydrophilic macromolecules carrier for intestinal-targeted delivery. The encapsulated macromolecules showed high drug release (90%) in simulated intestinal fluid and low release (20%) in simulated gastric fluid in 2 h. Thus, they suggested that carboxymethylated kappa carrageenan can offer targeted release in the intestine and protect encapsulated compounds such as gene fragments or hormones and peptides from being degraded in the stomach condition.

Muhamad et al. (2011) synthesized kappa carrageenan/sodium carboxymethyl-cellulose hydrogels using genipin as a crosslinker to control beta-carotene release. The results showed that as the genipin amount increased, the swelling was decreased due to higher degree of chemical crosslinking and hinders the movement of water into hydrogels networks. In addition, it was also found that the drug release became slower after further crosslinking. This is because drug release depended on genipin concentration and swelling ratio.

Kappa carrageenan-based floating tablets containing sodium salicylate was developed using sodium bicarbonates as gas-forming agents to investigate its sustained release (Onyishi et al. 2013). The physical properties such as floating lag time, total floating time, mechanical properties, and in vitro release were examined. The tablets displayed good mechanical properties. The results showed that in the prepared tablets floating lag time was in the range of 50–55 s and floats over 12 h. Meanwhile, sustained drug release was found where the increase of sodium bicarbonates and kappa carrageenan concentration also increase the drug release rate and floating lag time. Thus, they proposed that kappa carrageenan could be an excellent matrix for sustained sodium salicylate release from floating tablets.

Previous literature survey has shown that research on kappa carrageenan-based floating hydrogels was very few and it is worth to further investigate kappa carrageenan-based floating drug delivery system.

2.2 Alginate

Various algae species were used in the alginate production that involves extraction of polysaccharide. Naturally, it consists of *b*-D-mannuronic and *a*-L-guluronic acids and structure sequential distribution arrangement could be either in blockwise fashion as homopolymer blocks (*MM*, *GG*) or alternating blocks of *M* and *G* with different *M/G* ratios as illustrated in Fig. 4 (Burgain et al. 2011; Dragan 2014). It is widely available in the market molecular weights from tens to hundreds of kilo Daltons (Cook et al. 2012).

The advantages of using alginate for producing hydrogel are because of its simplicity, GRAS (generally recognized as safe) status, non-toxicity, biocompatibility, and low cost (Krasaekoopt et al. 2003; Burgain et al. 2011; Cook et al. 2012). However, several aspects could be considered such as the process is difficult to scale-up and the hydrogel is very porous. Different approaches have been performed previously in reducing the porous effect such as mixing or coating the alginate hydrogel with other polymer compounds or incorporate different additives to modify the alginate structure (Burgain et al. 2011; Krasaekoopt et al. 2003). This characteristic allows alginate to be widely applied in agriculture, food, and pharmaceutical industries (Dragan 2014).

In the alginate transformation, the presence of divalent ions such as Ca^{2+} is crucial to bind to guluronic residues and subsequently crosslinking the alginate structure. This is due to negative charge present in the alginate which attributed to

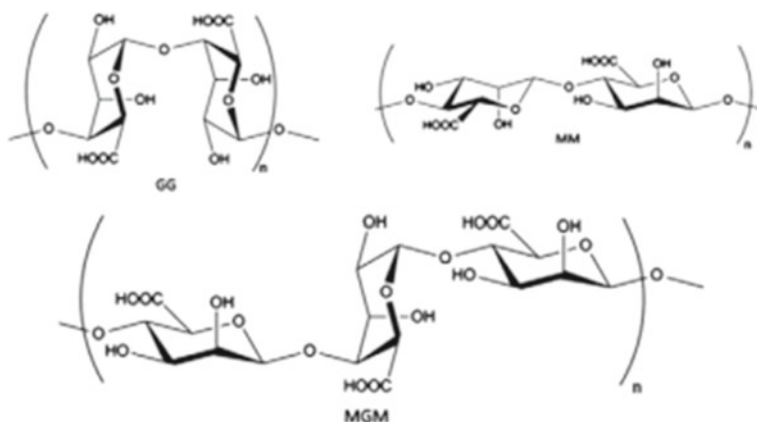


Fig. 4 Arrangement of *b*-D-mannuronic and *a*-L-guluronic acids in alginate structure

the structure of carboxylic acid groups (Cook et al. 2012; Dragan 2014). The size of alginate hydrogel formed depends on the methodology used in producing the hydrogel. For example, the hydrogel size approximately of ten microns could be produced using spray technology; however, the extrusion method produces up to millimeter size of hydrogel (Cook et al. 2012).

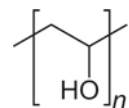
2.3 Polyvinyl Alcohol (PVA)

Polyvinyl alcohol is a non-ionic synthetic polymer that has the linear formula $[-\text{CH}_2\text{CHOH}-]_n$ (Fig. 5). It is derived from polyvinyl acetate through partial or full hydroxylation to remove acetate group. PVA is non-toxic, odorless, and water-soluble that has a melting point of 230 °C (for fully hydrolyzed grade) and 180–190 °C (partially hydrolyzed grade). The degree of hydroxylation can influence the chemical, physical, and mechanical properties of the PVA (Baker et al. 2012). The higher the degree of hydroxylation and polymerization of the PVA, the lower the solubility in water and the more difficult it is to crystallize (Jones 1973). At high temperature above 200 °C, PVA decomposes rapidly as it can undergo pyrolysis within that temperature range.

PVA has outstanding properties in terms of film-forming, emulsifying, and adhesiveness. Because of its properties which is highly soluble, some modifications have been done by addition of filler/additives such as crosslinker for use in several applications. It provides the structural stability of the hydrogel during swelling in the presence of water or biological fluids. Over the years, there are various applications of PVA-based polymer gel that has been developed.

For instance, phosphorylated PVA can be used for the immobilization of bacterial and yeast cells or activated for bioremediation and water filtration systems (Myoga et al. 1991; Wise 2000). In his finding, a PVA that in is spherical-bead form was produced by crosslinked with saturated boric acid solution. The reaction time was minimized to reduce the damage to the immobilized microorganisms. It was then followed by esterification of the PVA with phosphate to harden it. Other researcher also reported the development of PVA-based gel polymer composite by mixing it with other polymer such as alginate (Dave and Madamwar 2006; Vogelsang et al. 1997). The addition of alginate in PVA was expected to give functional stability of temperature-compensated polymer and also change the poor gas permeability of PVA gels (Jegal and Lee 1996). Different concentrations of dimethyl sulfoxide (DMSO) aqueous solutions are dissolved in PVA to obtain 16.7

Fig. 5 Polyvinyl alcohol



wt% PVA hydrogels followed by several freeze–thaw cycles in order to produce high transparency hydrogel (Hou et al. 2015).

2.4 Chitosan

There were extensive researches about chitosan in recent year. Chitosan is a biopolymer that has unique characteristics which are cationic, abundant, low toxicity, biodegradable, and non-immunogenic. Chitosan has the reinforcement capability as it was reported by Ban et al. (2006) that chitosan can enhance starch-based material. Unpublished original data are presented and discussed where chitosan acts as an emulsifier and flocculant. In other word, it shows that highly acetylated chitosans can act both as an emulsifier and as a flocculant.

Chitosan–thioglycolic acid conjugates appear to be very promising new excipients for liquid or semisolid formulations based on their in situ gelling properties. As a result, it should stabilize themselves once applied on the site of drug delivery (Hornof et al. 2003). The relative presence of the two monomeric building units (*N*-acetyl-glucosamine and *D*-glucosamine) is crucial to whether chitosan is predominantly an ampholyte or predominantly a polyelectrolyte at acidic pH values. The chemical composition is not only crucial to its surface activity properties but also to whether and why chitosan can undergo a sol–gel transition (Nilsen-Nygaard et al. 2015). Obtained from crustaceans such as crabs, prawns, shrimps, lobsters, and cell wall of some fungi such as *aspergillus* and *mucor*.

It is a natural cationic polysaccharide that is a weak base and is insoluble in water and organic solvent. However, it is soluble in dilute aqueous acidic solution (pH < 6.5), which can convert glucosamine units into soluble form $R-NH_3^+$ (Kumar et al. 2004). It gets precipitated in alkaline solution or with polyanions and forms gel at lower pH. In economic view, chitosan appears to be fascinating because chitin, the source of chitosan, is the second most abundant biopolymer in the nature (Avadi et al. 2004).

Chitosan has very good gelling properties to form hydrogels that are suitable for biomedical applications, e.g., in tissue engineering and drug delivery, as well as the chitosan's surface activity and its role in emulsion formation, stabilization, and destabilization. The chemical structures of chitin and chitosan are described in Fig. 6.

An important property of chitosan is its positive charge in acidic solution. It carries a positive charge at pH below 6.5. This is due to the presence of primary amines on the molecule that binds protons according to the equation:



The pKa value of the equation is approximately 6.3. Chitosan solubilizes when more than 50% of the amino groups are protonated (Rinaudo 1999), so the solubility of most chitosan preparations decreases sharply at the solution pH rises above

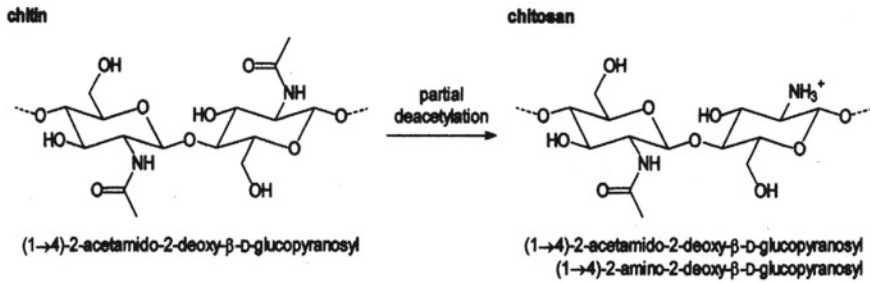
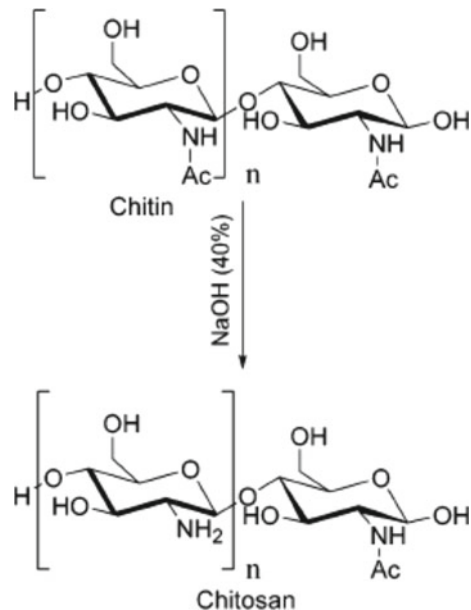


Fig. 6 Structure of chitin and chitosan

6.0–6.5. Many uses of chitosan are based on its positive charge, which is attracted to negatively charged materials. Chitosan is inexpensive, biodegradable, biocompatible (Koide 1998; Shahidi et al. 1999), as a hydrating agent in cosmetics, and more recently as a pharmaceutical agent in biomedicine (Dodane and Vilivalam 1998; Illum 2003; Khor and Lim 2003). Furthermore, it provides films with good mechanical and oxygen barrier properties (Chen et al. 1996; Caner et al. 1998; Sangsuwan et al. 2008). The functional properties of chitosan films are improved when chitosan is combined with other film-forming materials (Xu et al. 2005).

Chitosan is a polycationic polymer with a specific structure and properties. It contains more than 5000 glucosamine units and is obtained commercially from shrimp and crab shell chitin (a *N*-acetylglucosamine polymer) by alkaline deacetylation 2–4 (NaOH, 40–50%) (Fig. 7). Recent advances in fermentation technology

Fig. 7 Preparation of chitosan from chitin (Rabea et al. 2003)



suggest that the cultivation of fungi (*Aspergillus niger*) can provide an alternative source of chitosan (Rabea et al. 2003).

2.5 Starch

Starch is originated from variety of crops such as potato, wheat, rice, and corn. The source is abundant and readily available at low cost (Chang et al. 2010). Starches in chemical term are known as polysaccharides. It consists of a number of monosaccharides or glucose molecules joined together with a α -D-(1-4) and/or a α -D-(1-6) linkages. Main structural components of the starch include amylose and amylopectin (Tester et al. 2004).

Figure 8 shows the structure of starch. However, the relative amount of these components is varied as a function of the starch source (e.g., corn, potato, tapioca, and wheat) and affects the molecular order and crystallinity of the polysaccharide (Ellis et al. 1998). Amylose is linear or slightly branched, while amylopectin is highly branched. About 70% of the mass of starch granule is considered as amorphous and about 30% as crystalline and less than 1% lipids and protein from

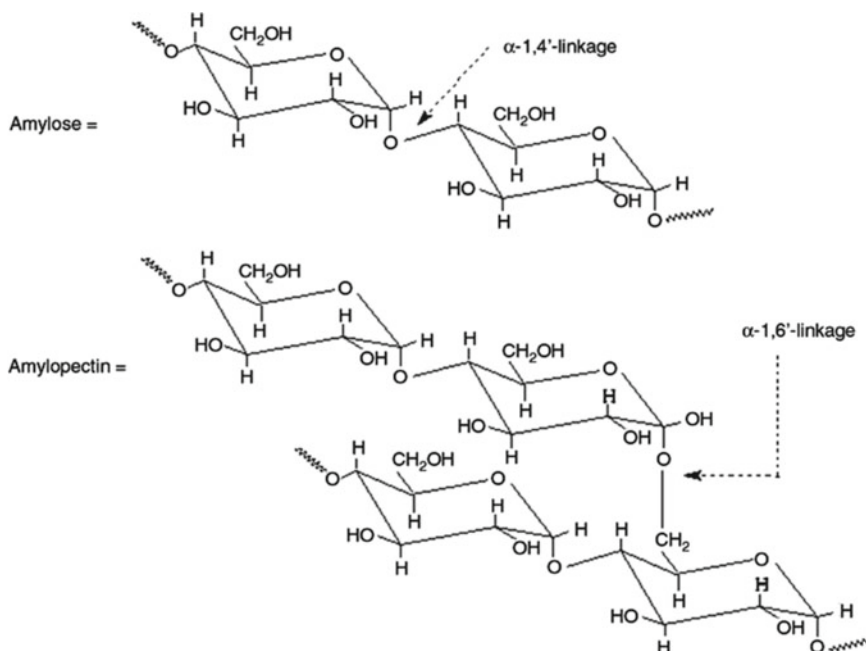


Fig. 8 Structure of amylopectin and amylose in starch. Adapted from Lu et al. (2009)

plant (Zhai et al. 2003). Starch can be converted into gel in a thermally three-step assisted, hydration–plasticization of the polymeric network (Ismail et al. 2013). Initially, adsorption of water in hydrophilic starch granules makes it swell.

Next, gelatinization process will occur after starch is dissolved by heating, resulting in leaching of the amylose component, irreversible physical changes, and the destruction of the granule structure. Finally, retrogradation step will continue where the starch hydrogel network is created upon cooling and aging, resulting in partial recrystallization and reorganization of the polysaccharide structure. Here, the amount of amylase and gelatinization temperature are the two main process parameters affecting the gel formation (White et al. 2008; García-González et al. 2011).

Synthesis of hydrogel is achievable via various pathways. There are also studies that have been conducted on hydrogel synthesis. Preparation of the polysaccharide-based hydrogels via reaction can be classified into two main groups: (1) graft copolymerization of vinyl monomers on polysaccharide in the presence of a crosslinker and (2) direct crosslinking of polysaccharide. For example, previous study reported the preparation of starch-based hydrogel through graft copolymerization of acrylic acid onto maize starch (Athawale and Lele 1998).

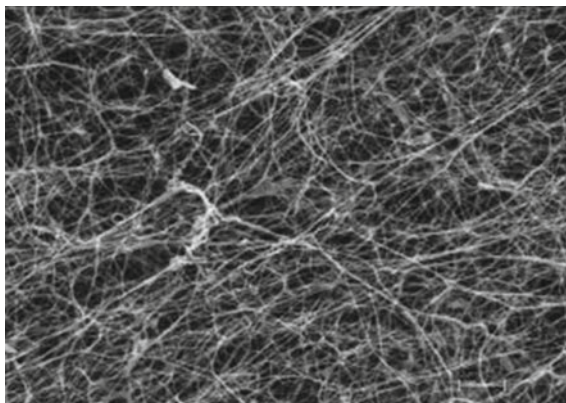
As different from graft copolymerization, direct crosslinking of polysaccharides uses polyfunctional compounds (e.g., glycerol, glyoxal, and epichlorohydrin) or polyvinyl compounds (e.g., divinyl sulphone, DVS) (Zohuriaan-Mehr and Kabiri 2008). An example for direct crosslinking was reported by Demitri et al. (2008) where the preparation of superabsorbent hydrogels is derived from cellulose and crosslinked with citric acid (CA). (Demitri et al. 2008)

2.6 *Bacterial Cellulose*

Bacterial cellulose as a hydrogel is a form of cellulose from bacteria. It is produced by bacteria from many genera such as *Acetobacter*, *Achromobacter*, *Agrobacterium*, and *Sarcina*. Basically, plant cellulose and bacterial cellulose are chemically the same, B-1, 4-glucans, but the degree of polymerization differs from about 13,000 to 14,000 for plant and 2000–6000 for bacterial cellulose.

Cellulose produced by microbes is uniquely different compared to cellulose acquired from plant with many points of interest that can be commercially valuable. Bacterial cellulose is well known for its purity. It is devoid of lignin and hemicellulose, extremely hydrophilic, and has excellent shape and strength retention. This is due to longer fiber length of bacterial cellulose. Cellulose made from trees must undergo many stages of pulping process to remove lignin and other compounds. This step is costly but necessary to obtain pure cellulosic materials. Since bacterial cellulose is pure, fewer steps are required for processing which makes the cost cheaper. Still, the main advantage is that the cellulose stays in place due to the less complex processing, and thus the cellulose remains intact and holds its

Fig. 9 SEM micrograph of the bacterial cellulose



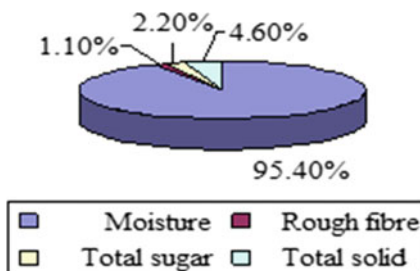
appealing properties. These characteristics of bacterial cellulose open many rooms for new applications in various fields. Figure 9 shows SEM of bacterial cellulose.

Previous researchers found that cellulose layer produced by *Acetobacter xylinum* contains water and cellulose as its main component (Yeoh et al. 1985). Figure 10 shows the compositions of bacterial cellulose which demonstrates high water content of bacterial cellulose.

Acetobacter xylinum (*A. xylinum*) which is acetic acid-producing bacterium is widely used as the model system to study the enzymes and genes involved in cellulose biosynthesis. This species of gram-negative bacteria has high capability to produce cellulose by converting carbon source like glucose to cellulose. It is well known that *A. xylinum* is an obligate aerobe and forms its cellulose at the air/liquid interface in undisturbed cultures.

A. xylinum produces cellulose from glucan chains. The chains extrude into the fermentation medium from *A. xylinum* pores. Each single cell of the bacteria continuously secretes nanofibers that scattered randomly and woven into fibrous layers of segmented nanofibers. These processes repeated until a bundle of microfibrils gathered and form bacterial cellulose. Figure 11 demonstrates the formation of microfibrils by *A. xylinum*. The cellulose synthesis will continue until

Fig. 10 Bacterial cellulose compositions



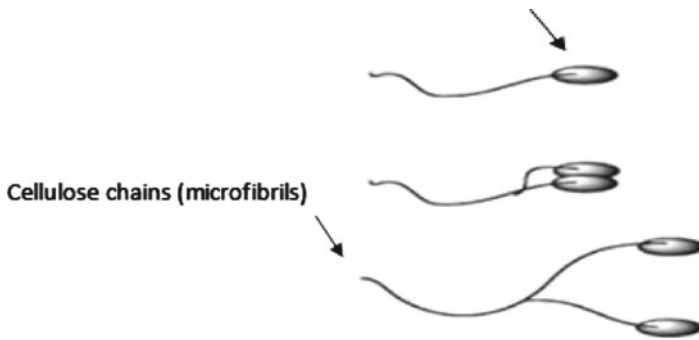


Fig. 11 Secretion of microfibrils by *Acetobacter* cells

a limited condition such as when not enough carbon sources, change of pH (Zahan et al. 2014), or when the bacterial cellulose fills the disks in fermentation using rotary disk reactor (Pa'e et al. 2011).

Bacterial cellulose pellicle is extremely hydrophilic, absorbing 60–700 times its weight in water. The nanofibers present in a structure of multiple cellulose layers in bacterial cellulose which is capable to hold an extensive amount of liquid between the fibrous layers to form a hydrogel (Gao et al. 2016). Wood or cotton must be physically disintegrated to make them hydrophilic (Brown 1991), compromising strength in the process. Since bacterial cellulose is formed in a hydrophilic matrix and needs no treatment, it will retain its long fibrils and exceptional strength. These properties open the doors to new applications in aqueous systems, such as exchanging chemicals and dyes with the water while retaining the native form and properties of the pellicle.

Modification of bacterial cellulose had been done to enhance properties of native BC and impart some additional properties for certain specific application. Microfibrils of BC become denser with time and produce a web-shaped structure (Horii et al. 1997; Tang et al. 2010) that can trap various materials added to the medium (Ul-Islam et al. 2012). The encaged materials become part of the bacterial cellulose fibril network, resulting in bacterial cellulose composites (Buyanov et al. 2010; Wang et al. 2010; Shi et al. 2014). A variety of additives materials had been used as a filler resulted in the development of many new composites materials design for application in different fields. By adding certain substrates as filler, it is possible to change the properties of the cellulose.

3 Various Types of Filler

In polymer technology, there are fundamentally two main filler classes, either extracted or fabricated. Minerals such as clays and talc (Al_2O_3 , 2SiO_2 , and $2\text{H}_2\text{O}$) are grinded, extracted, and probably treated and thus categorized in the first class. Calcite (CaCO_3) on the other hand fits both classes, as it can be either extracted and

grinded or obtained through a chemical process that involves precipitation. Obtained through more or less complex chemical pathways, carbon black is an outcome from the incomplete combustion of hydrocarbon sources and is consequently fabricated fillers, as well as synthetic silica. Short fibers made either of carbon or of glass are fabricated products and arbitrarily include cellulose fibers also in the second class, because quite complex treatments are required before they can be used as a polymer-reinforcing material.

3.1 *Metallic Compound*

The addition and innovative combination of metal compound especially metallic nanoparticle into hydrogel were generated not limited to structural diversity but also a multiplicity of property enhancements (Thoniyot et al. 2015). Such property enhancements were the key focus of research on hydrogel–nanoparticle composite materials that resulted in improved mechanical strength and stimuli response. As reported by Marcelo et al. (2014), when gold nanoparticles incorporated in poly *N*-isopropyl amide hydrogels, there are some significant changes in mechanical property and thermal response observed. There are numbers of metal particle, especially nanoform, which were studied in the past decades such as silver (SNP), aluminum oxide (ANP), zinc oxide, iron (Fe), nickel (Ni), cuprum (Cu), magnesium (Mg), and titanium dioxide nanoparticles (Goswami et al. 2010).

The metal particles are unique when incorporated into polymer gel. In preparation of metal nanoparticle from metal ion, the functional group in the hydrogel structure can act as both chelating and capping agents to stabilize it. At this point, the metal particles are protected from the atmosphere and obstructed the oxidation/deactivation and aggregation, thus increasing its stability and durability (Sahiner 2013). The ability of functional group in hydrogel to bind with certain compound allows metal ions such as Ag which have different oxidation states to be incorporated into the hydrogel matrices. The pioneer investigations of such metal (nanoparticles) into polymer gel were reported by the Willner group in which gold nanoparticles (Au-NPs) were immobilized in polyacrylamide (PAAm) hydrogel by swelling the dehydrated gel in the presence of Au-NP solution, resulting in uniform distribution of the Au-NPs in the gel matrix (Pardo-Yissar et al. 2001).

Consequently, various approaches for realizing these structurally unique dispersions have been reported by researchers investigating potential applications in different fields. Metal filler (nanoparticle) has antimicrobial properties that are significantly valuable for other applications such as food packaging, agricultural, and biomedical sector. Inclusion of silver nanoparticles in cellulose- and collagen-based film that applied as sausage casing was done by Fedotova et al. (2010). As a result, the film has strong antibacterial and antifungal effects, thus extending the food shelf life of the sausage. Antimicrobial activity and efficacy of different metal nanoparticles, particularly copper and silver nanoparticles in nanocomposite polymer, have been investigated by some researchers against the

plant pathogens (Cioffi et al. 2004; Park et al. 2006). For advance biomedical application, Ag-NPs are incorporated into pH-responsive hydrogels with the enzyme glucose oxidase function as glucose concentration sensors (Endo et al. 2008). In other findings, electrical-conducting hydrogel was also been developed by incorporating metal into hydrogel. It highlights the important relation between initial precursor Ag^+ ions concentration and swelling ratio of the hydrogel that has a direct impact toward conductivity of the hydrogel. Better conductivity reached when a higher concentration of Ag^+ ions added with reduced swelling ratios, and vice versa (Saravanan et al. 2007). In muscle-like application, a soft magnetic field-driven actuators for muscle-like was prepared by incorporation of magnetic NPs of cobalt (Co) or nickel (Ni) (Fuhrer et al. 2009). Magnesium oxide has been incorporated into carrageenan-based hydrogel to control the delivery of drug (Hezaveh and Muhamad 2012a, b).

3.2 Cellulosic Material

Cellulosic materials are exclusively renewable resources available abundantly that need to be well utilized to meet our needs. Extracted from natural fibers, the multilevel organization and hierarchical structure allows different kinds of cellulosic structure. Natural fibers are basically built of cellulose, lignin, and hemicellulose. A minimal trace of pectin, extractives, and pigments may also be found in cellulosic body. For this reason, natural fibers are also called as cellulosic or lignocellulosic fibers which have complex cell structure and chemical composition. Each fiber is essentially a composite in which rigid cellulose microfibrils are embedded in a soft matrix mainly composed of lignin and hemicellulose as illustrated in Fig. 12. Furthermore, the structure of the plant could be breaking down into high crystallinity at the same time reducing the amount of amorphous material present (Azeredo et al. 2010).

Cellulose is the renewable and abundant fiber that exists in nature. It gives structural rigidity to most plant. Additionally, agricultural waste offers economically feasible cellulose sources than any other source of fibers currently in use. Those ample sources not only renewable but also marketing appeal that in fact, it already penetrates into Asian marketplace since long time ago (Muhamad et al. 2015). Yet, there are thousands of tons of agricultural waste produced without proper utilization, which found to be useful in preparing polymer composite for commercial purposes, for example, EFB, sisal fiber, wheat straw, and others (Abdul Khalil et al. 2012). Numbers of natural cellulose fibers have been used to reinforce starch-based biocomposites. In fact, various types of natural fibers were investigated for incorporation gel polymer.

Other form of cellulosic material other than plant source is bacterial cellulose. Unlike plant-based cellulose that is extracted from plants or their wastes, this bacterial cellulose (BC) is produced by aerobic bacteria *Acetobacter* sp. with

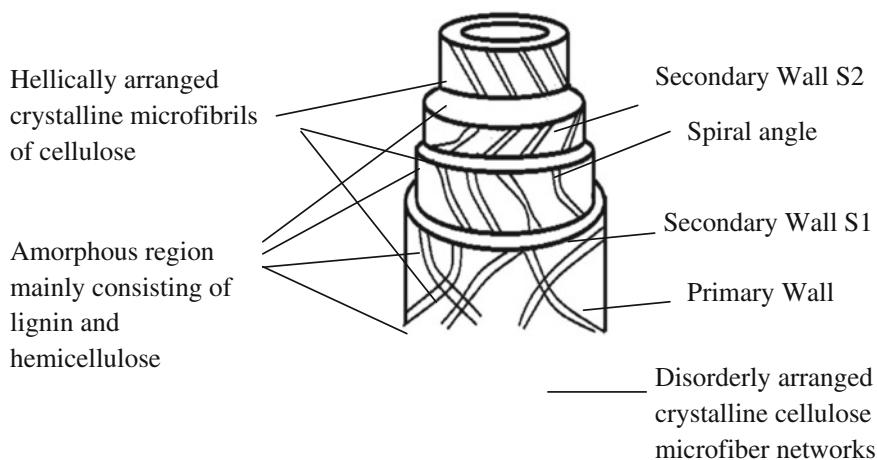


Fig. 12 Structure and contents of biofiber (John and Thomas 2008)

low-cost preparation and high cellulose production (Xie et al. 2013). It also produces high purity of cellulose content that can be used as biomaterial filler for medical field, electrical instrument, and food ingredient (Backdahl et al. 2008; Chin et al. 2014). Basically, cellulose from plant derivation except cellulose bacteria can exist as macro- or nanoscale form. Both can be used as reinforcement in composite materials because of enhanced mechanical, thermal, and biodegradation properties of composites that will be explained in next subchapters.

3.2.1 Microcrystalline Cellulose (MCC)

In general term, cellulose is a natural polymer made and determined as $(C_6H_{10}O_5)_n$ of sugar monomers and is therefore known as a polysaccharide. It consists of a linear chain with thousands of β (1-4) linked D-glucose units, known as cellobiose. Figure 13 shows the molecular structure of cellulose. Micro-cellulose, on the other hand, is a single cellulose chain arranged in bundle to form elementary fibril. The elementary fibril is then arranged heterogeneously in parallel to form parallel elementary fibrils. It called as micro-cellulose fibrils (Ma et al. 2008).

In nature, micro-cellulose fibers are hydrophilic so it is required to increase their surface roughness for the development of composites with enhanced properties. It also called in layman language as refined wood pulp and commonly used as emulsifier, texturizer, an anti-caking agent, a fat substituter, an extender, and a bulking agent in food production. The closest and relatable form of micro-cellulose application is in the making of vitamin supplements or tablets.

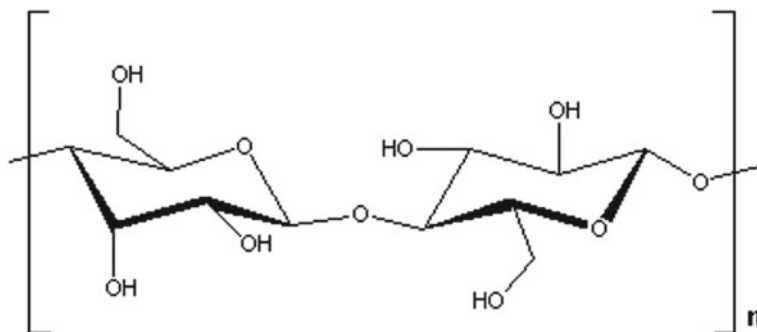


Fig. 13 Illustration of the molecular structure of cellulose

3.2.2 Cellulose Nanocrystal/Cellulose Nanowhisker

Various definitions of these nanofibers are often referred in previous and current works which include “nanowhiskers” (or just simply “whiskers”), “nanocrystals”, or even “monocrystals”. Regardless of their nanoscale dimensions, these crystallites have also often been referred to in literature as “microfibrils”, “microcrystals”, or “microcrystallites”. “Whiskers” is a term that is used to designate elongated crystalline rod-like nanoparticles (Abdul Khalil et al. 2012). The diameters of whisker range from 2 to 20 nm and their lengths can reach several tens of microns depending on its sources.

Understanding the structural hierarchy of cellulose is crucial. It enables the production of finer individualized cellulose in finer form (nanoscale) with high crystallinity (Siqueira et al. 2010). Previous study shows that the crystalline parts such as in whiskers, also known as nanocrystal, nanorods, or rod-like cellulose microcrystal or cellulose crystal can be isolated by several treatments. Cellulose nanofiber in the form of nanofibrils or whiskers is produced by hydrolyzing plant-based fiber with sulfuric acid and through other chemical and physical process. Cellulose whiskers have become an utmost interest as a source of nanometer size filler because of its great mechanical properties.

It started two decades ago when cellulosic nanofibers were studied as a reinforcing phase in nanocomposites (Dufresne 2012; Eichhorn et al. 2010). High-crystalline cellulose nanofibers, which abundantly present in natural plant bodies, naturally have unique properties and sizes. These scientists believe that cellulose nanofibers can potentially be used as transparent and very strong composite/nanocomposite in many different areas. This could lead to environmentally compatible and high-performance polymer gel components

3.2.3 Cellulose Nanofibril/Microfibrillated Cellulose

Different from nanowhisker/crystalline nanocellulose, “nanofibrils” in definition should be used to refer long flexible nanoparticles consisting of alternating crystalline and amorphous strings. It has a diameter range of 10–100 nm, but with a web-like structure (Lavoine et al. 2012). For that reason, they have a very high aspect ratio and a significant load-carrying capability (Phiriyawirut and Maniaw 2012). The CNF/MFC was reported to be added into polymer material. Most of the composites formed significantly show improved properties.

The reinforcement of poly(styrene-co-butyl acrylate) latex was previously compared between cellulose and NFC. It was revealed that both fillers led to an increment in tensile modulus and tensile strength. However, higher value of mechanical strength was resulted in NFC due to the entanglements between the fibrils leading to a rigid network of NFC. In addition, DMA analysis showed a higher thermal stability (higher storage modulus) in the rubbery state of the polymer latex when reinforced with NFC, compared to whiskers (Saïd Azizi Samir et al. 2004).

3.2.4 Lignocellulose

Within the agricultural and forestry sectors, large amount of lignocellulosics were produced as it became most abundant and inexhaustible or renewable natural resource. Furthermore, Kuhad et al. (2007) also stated that this potential “waste” is burnt, instead of producing beneficial products, which can cause the pollution of the environment. They elaborated that, however, many processes involving lignocellulosics biotechnology have received numerous attentions from researchers and have encouraged its improvement over the past few years.

Many advantages could be obtained by using natural fibers as they are eco-friendly, grown abundantly, and have a high stiffness level and great thermal stability (Laksono et al. 2014). Some of the characteristics of lignocellulosic fibers include high length–thickness relation and low density which makes them easily biodegradable and as a cheap resource, respectively (Mulinari et al. 2010; Silva et al. 2012). These fibers generally have a high hygroscopicity and moisture adsorption properties (Mulinari et al. 2010). Consequently, high interest in reutilizing these by-products in various applications was shown. Proven studies of its various applications have been previously conducted such as in animal feed, bio-transformation, bioremediation, production of chemical, stabilization of food and beverages, fillers, paper manufacture, furniture, architectural materials, and automotive sector (Kuhad et al. 2007; Mulinari et al. 2010; Shaharuddin et al. 2014a).

In general, cellulose is the main structure of a lignocellulosic by-product followed by hemicelluloses, cellulose, and lignin (Fig. 14) (Musatto and Teixeira 2010). According to Sun and Cheng (2002), the fraction of these three major components varies depending on the type of lignocellulosic in which cellulose, hemicelluloses, and lignin were ranged from 35–50%, 20–35%, and 10–25%,

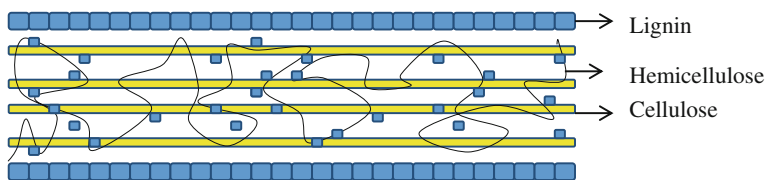


Fig. 14 The general structure of lignocellulosic residues comprises cellulose, hemicellulose, and lignin (adapted from Musatto and Teixeira 2010)

respectively. The remaining fractions were completed by proteins, essential oils, and ash. Non-covalent crosslinkages are their binders as they were strongly bonded (Kuhad et al. 2007). The macromolecules of hemicelluloses and cellulose were fabricated from different sugars. In addition, lignin is known as an aromatic polymer and formed from phenylpropanoid precursors.

3.3 Crosslinker

Crosslinking is a stabilization process in polymer chemistry which leads to multi-dimensional extension of polymeric chain resulting in network structure. Crosslinking is a bond that links one polymer chain to another. Crosslinked polymers are important because they are mechanically strong, resistant to heat and to avoid hydrophilic polymer chain or segment to dissolve aqueous phase (Maitra and Shukla 2014). Figure 15 shows the schematic diagram of polymeric chain before and after crosslinks. Crosslinks within polymeric gels can be made by chemically and physically.

Chemical crosslinking techniques have permanent junctions such as covalent bonds, present between different polymers chain (Maitra and Shukla 2014). Chemical crosslinking mechanisms are shown in Fig. 16. By using chemical crosslinking method, polymeric hydrogels are in a permanent and irreversible condition, which makes them difficult to change the shape of network (Omidian and

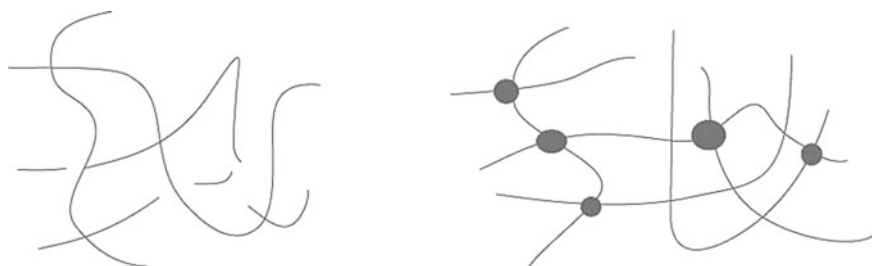


Fig. 15 Schematic diagram of polymeric chain before and after crosslinks (Mendes et al. 2012)

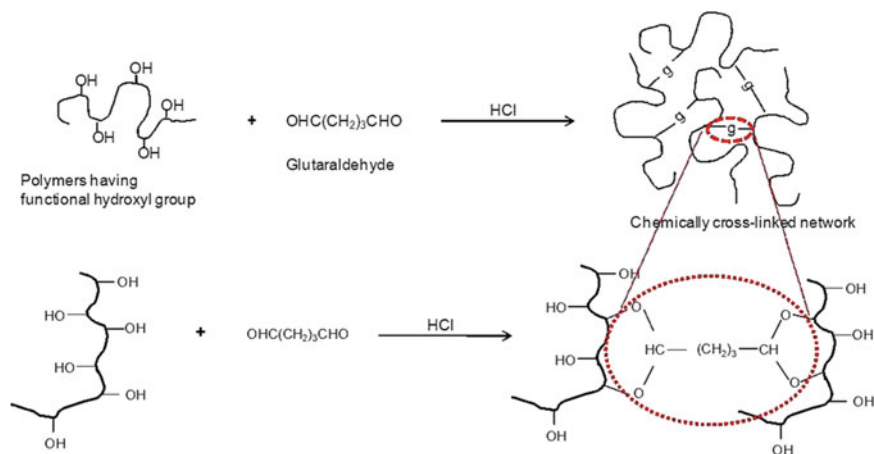


Fig. 16 Chemical crosslinking mechanisms (Gulrez et al. 2011)

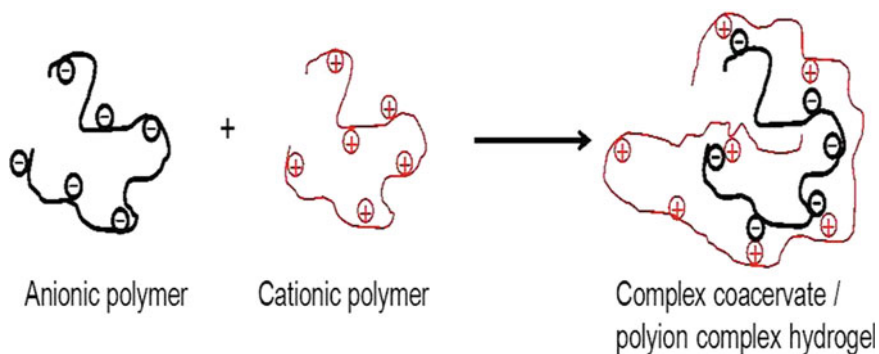


Fig. 17 Physical crosslinking mechanisms (Gulrez et al. 2011)

Park 2012). Chemical crosslinking is a commonly used technique to improve the mechanical property of the polymeric hydrogels. Formaldehyde, glutaraldehyde, polyepoxy compounds, and tannic acids are some of the examples of chemical crosslinkers. However, these agents are toxic compounds and not environmental friendly. They give unwanted reactions with the bioactive substances present in the hydrogel matrix. Besides that, these chemical crosslinking reagents showed high temperature requirement and low productivity (Maitra and Shukla 2014).

Physical crosslinking is a process where polymer chains are interconnected by ionic or polyelectrolyte interaction. Physical crosslinking mechanisms are shown in Fig. 17. These physical crosslinks methods may not be permanent in nature but they are sufficient to make polymeric hydrogels insoluble in an aqueous media. In addition, physical crosslinking gives reversible polymeric hydrogels due to the conformational changes (Omidian and Park 2012). Gamma or ultraviolet radiation,

heating or exposure, and drying are examples of the physical crosslinking approaches. Although physical methods are safe to use, to gain the preferred amount of crosslinking from this method is very hard.

Glutaraldehyde, ethylene glycol, tripolyphosphate, diglycidyl ether, diisocyanate, and genipin are examples of crosslinking reagents that are widely used for crosslinking purposes.

3.3.1 Genipin

Genipin (Fig. 18) is a non-toxic and natural crosslinker. It is obtained from its parent compound, geniposide, via enzymatic hydrolysis with β -glucosidase. Geniposide is isolated from the fruits of *Gardenia jasminoides* Ellis and *Genipa Americana* and it composes about 4–6% of dried fruits (Cui et al. 2014; Butler et al. 2003). Gardenia is an evergreen shrub native to southeastern China. Although it has been adapted to gardens around the world, it prefers warm, humid weather. Gardenia grows up to ten feet tall and produces white flowers in the spring. Genipin has been broadly used in herbal medicine including for diuretic, laxative, choleric, and hemostatic in the treatment of traumatosis by external application. Genipin itself is colorless. It will form blue pigment when it reacts with amino acid (Butler et al. 2003; Mi et al. 2001). The edible blue pigments are currently being used as a blue food colorant in East Asia. Genipin's naturally occurring properties and biodegradable material with low cytotoxicity have recently been investigated as a crosslinking material in many applications especially in pharmaceutical industry such as bioadhesive, wound dressing, bone substitutes, and drug delivery system. The characteristics of genipin are shown in Table 3, and Fig. 19 shows the mechanisms of genipin crosslinking.

Fig. 18 Chemical structure of genipin (Moffat and Marra 2004)

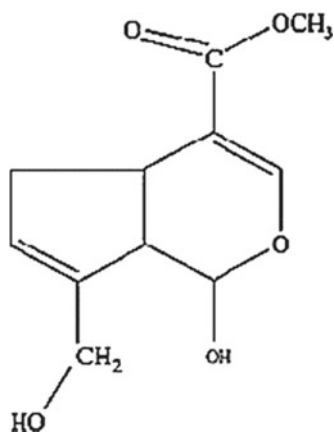
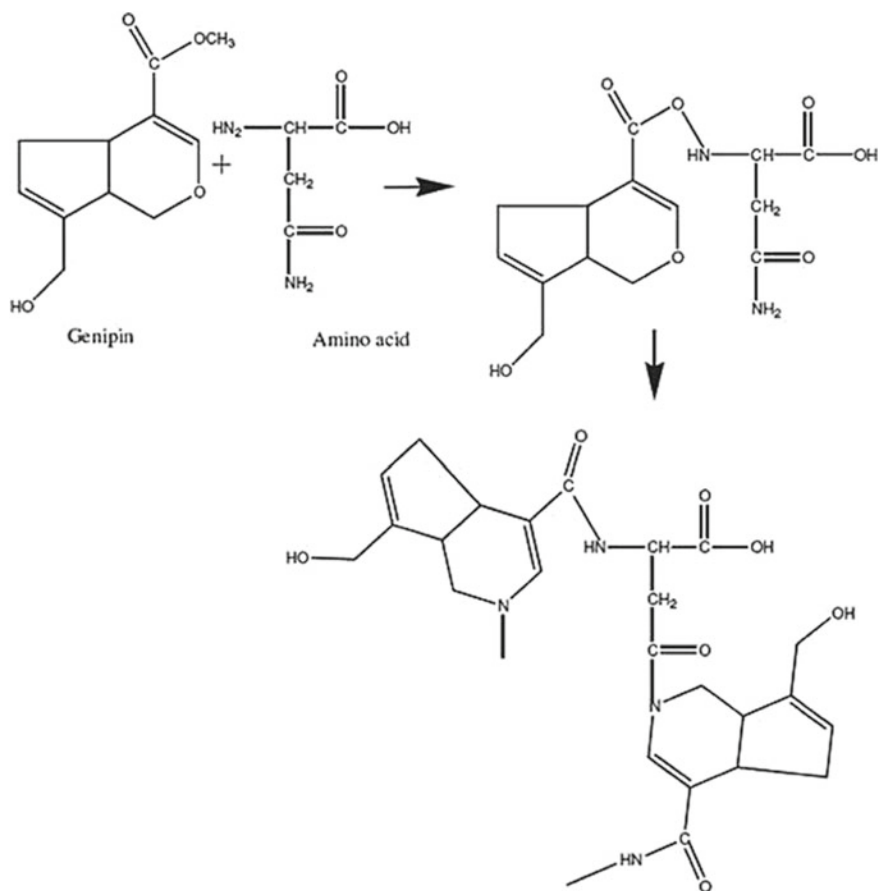


Table 3 Characteristics of genipin

Properties	Description
Molecular formula	C ₁₁ H ₁₄ O ₅
Molecular weight (g/mol)	226.227
Melting point (°C)	120–121
IUPAC name	Methyl (1 R, 2 R, 6 S)-2-hydroxyl-9-(hydroxymethyl)-3-oxabicyclo [4.3.0] nona-4,8-diene- 5- carboxylate
Toxicity	Non-toxic

**Fig. 19** Mechanisms of genipin crosslinking (Meena et al. 2009)

3.3.2 Glutaraldehyde

Glutaraldehyde (Fig. 20) is another most frequently used crosslinker. Glutaraldehyde is an organic compound ($C_5H_8O_2$). Glutaraldehyde is a colorless oily liquid which undergoes typical aldehydes chemical reactions. In the vapor state, glutaraldehyde has a pungent odor, with an odor threshold of 0.04 ppm. Glutaraldehyde is less expensive, easily available, and highly soluble in aqueous solution (Jayakrishnan and Jameela 1996). The characteristics of glutaraldehyde are shown in Table 4, and Fig. 21 shows the mechanisms glutaraldehyde by crosslinking.

4 Application of Filler Contained Gel Polymer in Various Applications

4.1 Agriculture

4.1.1 Probiotic Animal Feed

There have been rising concerns on the usage of antibiotic residues as they may affect the meat products to the point of being harmful for human consumption (Nousiainen et al. 2004; Riddell et al. 2010). Therefore, alternative applications have been considered to decrease the use of antibiotic, and consequently, the introduction of probiotic is one of them. Beneficial additive of these probiotics into the animal feed could provide improvement in health and growth of animal (Fuller 1989; Shaharuddin et al. 2014b).

Seo et al. (2010) stated that many researchers were previously interested in direct-fed microbial (DFM) using probiotic as one of the methodologies in animal feeding. The base of DFM is the presence of probiotic and has been defined as “microbial-based feed additive”. It was explained by Seo et al. (2010) that the maintenance of probiotics viability is an important aspect of DFM in order to ensure

Fig. 20 Chemical structure of glutaraldehyde

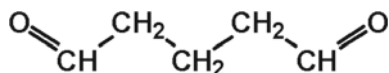


Table 4 Characteristics of glutaraldehyde

Properties	Description
Molecular formula	$C_5H_8O_2$
Molecular weight (g/mol)	100.117
Melting point ($^{\circ}C$)	-14
IUPAC name	Pentane-1,5-dial
Toxicity	Toxic

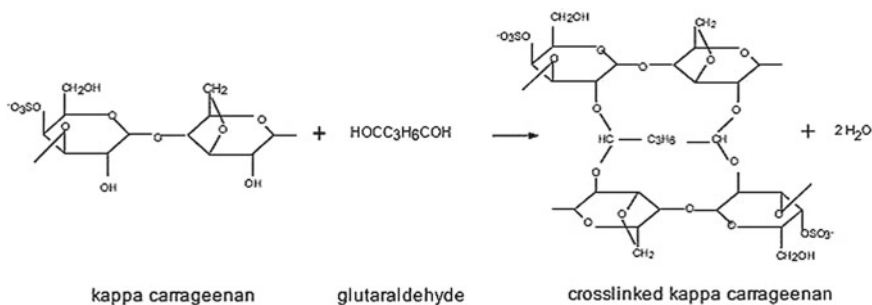


Fig. 21 Mechanisms of glutaraldehyde crosslinking (Distantina et al. 2013)

the maximum delivery of its benefits to host health or growth. They also elaborated on the fact that the dosages of probiotics, timing, strains of DFM, and animal condition are some of the other factors which contribute to the efficiency of DFM. Many studies on direct-fed microbial in animal feeding have been performed over the years (Wallace and Newbold 1993; Keady and Steen 1996; Malik and Sharma 1998; Khuntia and Chaudhary 2002). However, the efficiency of DFM was low due to adverse environments during processing, storage, and in a gastrointestinal system.

One alternative approach in addressing this issue is the introduction of immobilization and microencapsulation technology using hydrogel in animal feed. In animal feed industry, immobilization technique has been used extensively which offers better protection for the probiotic in their survival and could be delivered at the desirable target (Nimrat et al. 2011; Rosas-Ledesma et al. 2012; Ross et al. 2008; Soto et al. 2011; Voo et al. 2011; Woraharn et al. 2010).

In practice, the probiotic hydrogel would be incorporated into pelleted animal feeds as the pellet was used in most animal feeding for easier and better feeding and distribution (Chitprasert et al. 2012; Shaharuddin and Muhamad 2015). However, major stress may be suffered by probiotic from the heat exposure during pelleting and storage that could decrease its viability (De Angelis et al. 2006). The heat-sensitive probiotic could not withstand the high stress from high temperature and caused low viability after the pelleting process (Kosin and Rakshit 2010; Seo et al. 2010). The incorporation of reinforcement (filler) in a matrix would enhance the thermotolerance of probiotic due to improved thermal protection wall. For example, this could be achieved using lignocellulosic materials such as rice bran (Chitprasert et al. 2012) and sugarcane bagasse (Shaharuddin and Muhamad 2015).

Chitprasert et al. (2012) studied the effects of aluminum carboxymethyl cellulose–rice bran (AICMC–RB) composites at weight ratios of 1:0, 1:1, and 1:1.5. They found that both free cells and microencapsulated cells were almost fully destroyed after heat treatment. However, a significant effect could be seen as the higher amount of microencapsulated cells survived compared to the free cells. Thus, composite of AICMC–RB showed high potentials as wall materials in protection against heat (Chitprasert et al. 2012).

The similar effect of filler incorporation on hydrogel could be observed in Shaharuddin and Muhamad (2015). The research synthesized the hydrogel using different alginate concentrations of 1, 2, and 3% and NaA:SB ratio of 1:0, 1:1, and 1:1.5. Microencapsulation efficiency and probiotic survivability after heat exposure of 90 °C for 30 s were significantly enhanced after the incorporation of sugarcane bagasse in alginate microcapsule. The synthesis of heat resistant hydrogels was obtained in both findings which showed potential solution in protecting probiotic during pelleting process.

4.1.2 Pesticide Delivery

In general, pesticide can be defined as a compound used to prevent, destroy, or repel pests. It has been an essential part of agricultural processes by reducing losses from weeds, diseases, and insect pests that can substantially damage harvestable produce or stored food commodities. Clearly, pesticides represent a vital role in optimizing crop yields. By their very nature, most pesticides show a high degree of toxicity, intended to kill those pests, but unintendedly evoked potential harm to non-target organisms and ecosystem. For an example, conventional application of pesticide such as spraying and fumigation gives a high initial dose which rapidly falls below the effective level. In addition, it is highly toxic in gaseous state and is difficult to manage. As in soil treatment using pesticide, a conventional can contaminate surface water through runoff from treated plants and soil which results in incomplete release of the molecules and short residence time at the required sites (Hari et al. 2015). Thus, recent progress in controlled release technology might be used in order to reduce the adverse effect as well.

Through advancement in agricultural technology, numbers of novel smart delivery techniques are available for the growth of precision farming practices that will considerably allow close control of pesticide release to their targets/pests. Application of polymer gel in pesticide management that implied controlled release (CR) mechanism can maintain an effective level for a longer and controllable time. Some of pesticide delivery technology advantages are constant level of active agent over an extended period, phytotoxicity, dose reduction, reduction in environmental pollution, and handling purposes (Hekmat et al. 2009).

Hydrogel has the ability to swell in the presence of fluid regulates the release of encapsulated bioactive agents. PAAm–MC hydrogels as a potential delivery vehicle for the controlled release of paraquat pesticide were investigated. It can sustain release of paraquat pesticide up to 45 days (Aouada et al. 2010). Other gel has also been studied, e.g., Alginate. Gel polymeric delivery system is an innovative technique in which the active ingredient present in the form of solution gets converted into a gel upon application to the site of action. The formation of gel depends on factors like temperature modulation, pH change, presence of ions, and ultraviolet irradiation; the in situ gel formulation can sustain the release and also decrease the frequency of administration.

As an example, pesticide carbaryl (carb) is prepared by the ionotropic crosslinking of sodium alginate (NaAlg) with calcium and nickel ions to form beads (Işıklan 2007). Some of gel polymer modification also been developed by addition of nanomaterial to form nanocomposite. It is reported that silver Ag nanoparticles and gelatin Ag nanoparticles are incorporated into the biocomposites to impart optical absorptivity for SERS detection of pesticide (Fateixa et al. 2015). Other than pesticide release, polymer gel is also used as superabsorbent in agriculture. It was first developed by U.S. Department of Agriculture in 1970s. They prepared starch/acrylonitrile/acrylamide-based polymers, which were originally used in agricultural/horticultural markets as hydrogels in order to retain moisture in soil during the growing and shipping of crops and other plants. It is also reported that starch graft copolymers are prepared by graft copolymerizing acrylonitrile onto a starch substrate.

4.2 *Pharmaceutical*

4.2.1 *Drug Delivery System*

Genipin is widely used in pharmaceutical application, especially in drug delivery system as a crosslinking agent due to its biocompatibility. Genipin is a relevant tool to improve the control of drug delivery. Genipin is relatively less toxic than glutaraldehyde. Sung et al. (1999) reported that when comparing the cytotoxicity of genipin to glutaraldehyde through in vitro using 3T3 fibroblasts via MTT assay, they found that genipin was 10,000 times less cytotoxic than glutaraldehyde. According to Mi et al. (2002), genipin crosslinked chitosan microspheres showed better biocompatibility and slower degradation rate than glutaraldehyde crosslinked microspheres. Thus, they concluded that the compatibility of genipin is better than glutaraldehyde.

Genipin also has been utilized to control swelling ratio and mechanical properties (Hezaveh and Muhamad 2012a, b; Mi et al. 2005; Chen et al. 2004; Mi et al. 2001). Besides that, genipin was also used to control drug release rate. A study conducted by Muhamad et al. (2011) incorporated the use of kappa carrageenan beads that were crosslinked with genipin for delivery of β -carotene. It was also found that the beads released beta-carotene in a controlled manner. Figure 22 shows the accumulate release profile of β -carotene under in vitro release condition (pH 1.2, followed by pH 6.6 and pH 7.4 medium).

According to Meena et al. (2007), crosslinking mechanisms had improved the properties of polysaccharide as compared to non-modified ones. The presence of genipin in polymer matrix helps to control the drug release rate. This was described by Hezaveh and Muhamad (2013), where in vitro release of β -carotene was

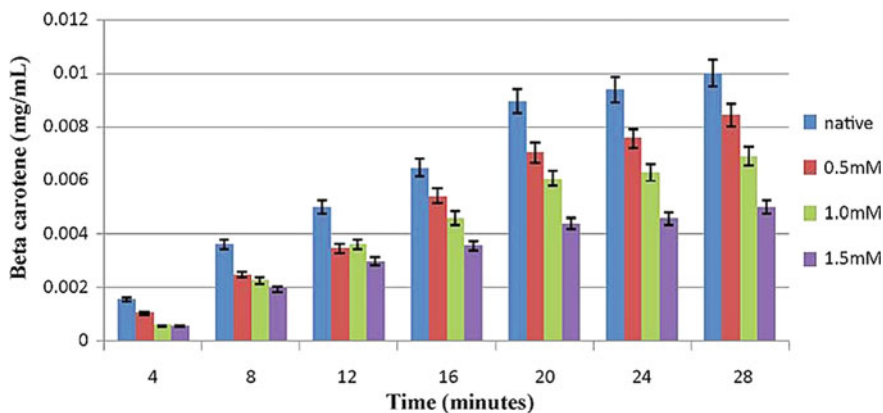


Fig. 22 Accumulate release profile of β -carotene under in vitro release condition (pH 1.2, followed by pH 6.6 and pH 7.4 medium) (Muhamad et al. 2012)

changed by the addition of genipin. The results indicated that suitable amount of genipin causes a decrease in the release rate in acidic, neutral, and alkaline medium. In neutral medium, the genipin has been proven to be useful for a controlled release of β -carotene delivery.

Yuan et al. (2007) showed the effect of genipin crosslinked chitosan microspheres on protein (albumin) release. Ninhydrin assay was carried out to determine the degree of crosslinking. Based on their study, the degree of chitosan crosslinking microsphere was increased with increasing amount of genipin and crosslinking time. The swelling ratio was decreased as genipin concentration and crosslinking time increased. The albumin released from crosslinked chitosan microspheres was slower than non-crosslinked microspheres.

Distantina et al. (2013) prepared crosslinked kappa carrageenan hydrogels using glutaraldehyde as crosslinking agent. They found that the crosslinking treatment enhances the thermal stability of carrageenan film, and this might be due to acetal bridges formed during crosslinking mechanisms in crosslinked kappa carrageenan film.

In another study, glutaraldehyde and potassium sulfate were used as crosslinkers to stabilize kappa carrageenan film to be used as a controlled drug delivery system (Distantina et al. 2014). Crosslinked kappa carrageenan showed swelling ability of pH sensitive, wherein distilled water (pH \sim 7) and phosphate buffer (pH \sim 7.4) potassium sulfate crosslinked films exhibited a higher swelling degree compared to glutaraldehyde. While in NaOH solution (pH \sim 13), the films that were crosslinked with glutaraldehyde exhibited a higher swelling degree than potassium sulfate. This study suggested that both glutaraldehyde and potassium sulfate crosslinking agents can be used for controlled drug delivery system.

4.2.2 Tissue Engineering

Bi et al. (2011) used genipin as crosslinking agent to increase mechanical strength and degradation properties of biopolymers for tissue engineering. In this study, genipin crosslinked chitosan/collagen scaffolds were developed using different genipin concentrations, crosslinking temperatures, and crosslinking times. The results showed that the properties of the genipin crosslinked chitosan/collagen can be greatly affected by different genipin concentrations, crosslinking temperatures, and crosslinking times. The compressive strength increased with the increase of genipin concentration and temperature from 4 to 20 °C. Additionally, the swelling ratio, degradation rate, and pore size changed significantly with different crosslinking conditions. Based on their study, they recommended that 1.0% genipin concentration, 20 °C crosslinking temperature, and longer crosslinking time are suitable for genipin crosslinked chitosan/collagen scaffolds for tissue engineering.

Zhang et al. (2016) prepared genipin crosslinked chitosan/gelatin scaffolds and evaluated their biocompatibility properties for liver tissue engineering. The result showed that the genipin crosslinked chitosan/gelatin scaffolds with 1 and 2% possess ideal porosity and showed the good biocompatibility and maintained liver-specific functions when HepG2 cells seeded on scaffolds. Therefore, genipin crosslinked chitosan/gelatin scaffolds could be a promising biomaterial used in liver tissue engineering.

Glutaraldehyde (GA) crosslinked chitosan:collagen blends were prepared and their microarchitecture and water-binding capacity were investigated for adipose tissue engineering (Wu et al. 2006). The water-binding capacity tends to decrease as the GA concentration increases. In vitro cytocompatibility of pre-adipocytes (PAs) confirm that the viability of PAs on GA-crosslinked collagen:chitosan scaffolds and animal tests proved that PA-seeded scaffolds were biocompatible, could induce vascularization, and form adipose tissue (Liu et al. 2012).

4.2.3 Wound Healing

The genipin crosslinked silk sericin/poly(vinyl alcohol) (PVA) films were developed as two-dimensional wound dressings for the treatment of superficial wounds (Siritientong et al. 2013). The effects of genipin crosslinking concentration on the physical and biological properties of the films were investigated. It was found that genipin crosslinked silk sericin/PVA films showed the increased surface density, tensile strength, and percentage of elongation. Meanwhile, the percentage of light transmission, water vapor transmission rate, and water swelling decreased due to the mobility of molecular chains reduce within the films and become more rigid molecular structure because of crosslinked process. It was found that silk sericin was released in a sustained manner from the genipin crosslinked films. The in vivo test (ISO 10993-6) confirmed that the genipin crosslinked silk sericin/PVA films were safe for the medical usages. The results show that genipin crosslinked silk sericin/PVA films would be promising wound dressings for superficial wounds.

This study was conducted to investigate the *in vitro* characteristics of the genipin crosslinked gelatin membrane for wound dressing purpose and was compared with glutaraldehyde crosslinked gelatin membrane (Chang et al. 2003). A rat model was used to study an *in vivo* experiment and it was found that the degree of inflammatory reaction for the wound treated with the genipin crosslinked dressing was significantly less severe than that covered with the glutaraldehyde crosslinked dressing throughout the entire course of the study. Additionally, the healing rate for the wound treated with the genipin crosslinked dressing was notably faster than its glutaraldehyde crosslinked counterpart.

In another study, bio-polymeric films were prepared for wound healing application by varying the proportion of chitosan and PVA and it was crosslinked with glutaraldehyde to improve the stability using solvent casting method (Panchal et al. 2014). Results suggest that the crosslinked films being compact influence swelling than the uncrosslinked film and water uptake properties of the composites indicate that the films could be tuned for wound healing management.

4.3 Waste Water Treatment

A previous study has proved that hydrogel with filler can be used as a promising material in many applications. In wastewater treatment, hydrogel such as bacterial cellulose provides properties that make it suitable to be used in wastewater treatment to remove heavy metal (Wang et al. 2015; Lu et al. 2010). Those properties include great mechanical strength, porous structure, and high water-holding capacity. Besides that, bacterial cellulose has large surface area with many hydroxyl groups in the chain that makes it effective for separation of heavy metals ions (Lu et al. 2013). Most importantly, bacterial cellulose is simple to produce and the modification can be done using various materials and methods. Furthermore, the physiochemical properties of this bacterial cellulose can be controlled by modifying the fermentation condition or by physical or chemical treatment in order to attain preferred functionality (Pa'e et al. 2011; Sokolnicki et al. 2006; Serafica et al. 2002). These features along with its biocompatibility and low production render this type of hydrogel ideal for use as eco-friendly biosorbent for heavy metal removal.

However, bacterial cellulose itself as biosorbent had several disadvantages such as low adsorption capacity, high hydrophilicity which leads it to swell easily in water and poor selectivity. Therefore, new functional group is added to bacterial cellulose to modified its properties and improve activity of bacterial cellulose on adsorption of heavy metal ions. Table 5 listed previous works on the use of bacterial cellulose for heavy metal removal.

Table 5 Bacterial cellulose as biosorbent for heavy metal removal in wastewater treatment

Adsorbent	Adsorbate	Reference
Bacterial cellulose coated with polyethylenimine	Copper Lead	Wang et al. (2015)
Amino—bacterial cellulose	Lead Cadmium Copper	Lu et al. (2014)
Ammonium sulfamate—bacterial cellulose	Chromium	Lu et al. (2013)
Spherical iron oxide—bacterial cellulose composite	Lead Manganese Chromium	Zhu et al. (2011)
Carboxymethylated—bacterial cellulose	Copper Lead	Chen et al. (2009)

5 Polymer Gel and Development: Case Studies

5.1 Thermotolerance of Probiotic Encapsulated in Bagasse Alginate Microcapsule

Incorporation of beneficial additive during pelleting may enhance the value of an animal feed. Biomaterials such as probiotic, prebiotic, and enzyme are commonly used. However, detrimental effects of high thermal exposure are capable of destroying the biomaterial as they cannot withstand the exposed condition (De Angelis et al. 2006; Slominski et al. 2007; Kosin and Rakshit 2010). This research was embarked in order to design a thermotolerant microcapsule (hydrogel) of immobilized probiotic *Lactobacillus rhamnosus* NRRL 442 using sugarcane bagasse–alginate composite as encapsulant agent. The microcapsule was produced by the combination of immobilization and microencapsulation techniques via adsorption and extrusion, respectively. In this study, alginate was applied as the matrix of composite polymer. Meanwhile, pretreated sugarcane bagasse (SB) was used as the reinforcement (filler and probiotic carrier). First, *L. rhamnosus* (*Lr*) was immobilized with the SB. Then, the microcapsules of immobilized probiotic on bagasse–alginate (NaA-SB) composite (Fig. 23) were synthesized using extrusion method to provide double protection effect to the probiotic.

Hydrogel prepared using ratio of NaA:SB of 1:1.5 and 1:1 showed the highest efficiency ($89.35\% \pm 0.49$ and $89.35\% \pm 0.21$, respectively) (as shown in Table 6). Meanwhile, the highest cell survivability after the heat exposure ($81.30 \pm 0.30\%$) was obtained from the sample synthesized using 3% of NaA and NaA:SB ratio of 1:1.5. The step of filler (SB) incorporation provided better protection toward heat exposure of 90 °C for 30 s and subsequently obtained high probiotic survivability. Inclusion of SB has offered an extra thermal barrier besides alginate matrix and creates a double heat protection for the probiotic as SB has a low thermal conductivity (Britton et al. 2005; Manohar et al. 2006).

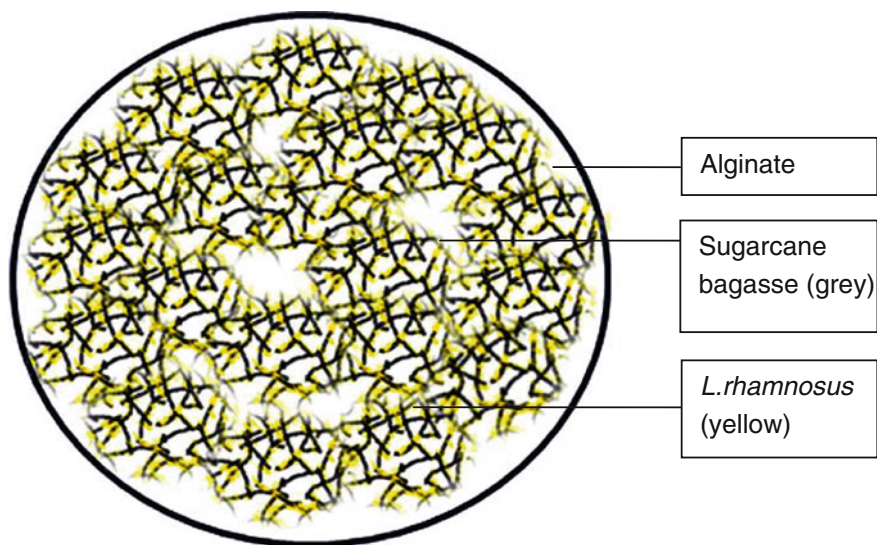


Fig. 23 Schematic diagram. **a** Hydrogel of immobilized *L.rhamnosus* NRRL 442 in NaA-SB composite (Shaharuddin and Muhamad 2015)

Table 6 Cell survival of free and microencapsulated *L.rhamnosus* NRRL 442 under different conditions of synthesis after heat exposure at 90° for 30 s

NaA concentration (%)	NaA: SC ratio	Initial cells concentration (log CFU/g microcapsule)	Final cells concentration (log CFU/g microcapsule)	Cell survivability (%)
Free cells	–	8.62 ± 0.30	3.00 ± 0.19	34.51 ± 2.15*
Microencapsulated cells				
1	1:0	7.90 ± 0.16	3.34 ± 0.12	42.39 ± 1.54*
	1:1.1	7.93 ± 0.07	5.68 ± 0.11	71.67 ± 1.44*
	1:1.5	8.13 ± 0.09	6.50 ± 0.17	80.02 ± 2.13*
2	1:0	7.93 ± 0.07	4.88 ± 0.32	61.57 ± 4.01*
	1:1.1	8.13 ± 0.04	6.21 ± 0.14	76.33 ± 1.73*
	1:1.5	8.13 ± 0.03	6.25 ± 0.06	76.87 ± 0.75*
3	1:0	7.75 ± 0.08	5.94 ± 0.04	77.67 ± 0.54*
	1:1.1	7.98 ± 0.10	5.96 ± 0.11	74.78 ± 1.40*
	1:1.5	8.04 ± 0.08	6.53 ± 0.06	81.30 ± 0.30*

*Means with different superscripts within a column were significantly different [$P < 0.05$, $n = 3$]

The survived probiotic in bagasse–alginate microcapsule after the heat exposure was evident in SEM images as illustrated in Fig. 24. In addition, a synergical presence of sugarcane bagasse, probiotic, and alginate had changed the functional bonding that could be observed in Fourier transform infrared spectroscopy spectra

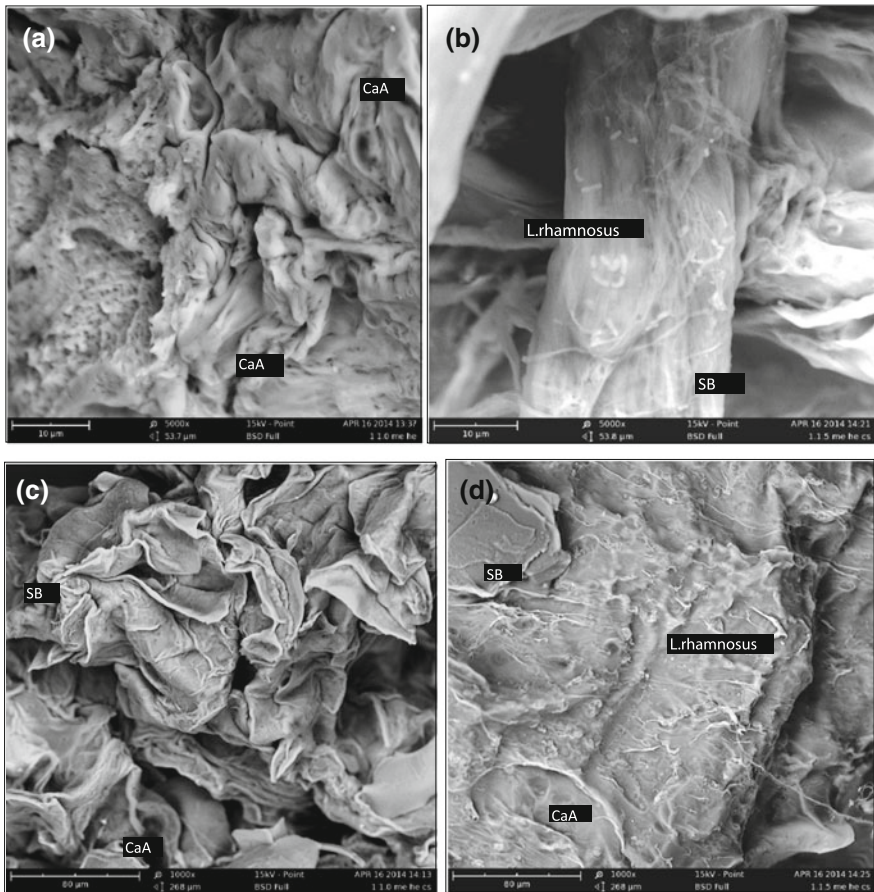


Fig. 24 SEM of NaA and NaA-SB microcapsule areas. Outer surface of heated NaA-SB (1:0) and NaA:SB (1:1.5) microcapsules loaded with *L. rhamnosus* NRRL 442 (a and b, respectively). Inner surface of heated NaA-SB (1:0) and NaA:SB (1:1.5) microcapsules loaded with *L. rhamnosus* NRRL 442 (c and d, respectively)

(Fig. 25). Therefore, the probiotic survivability after heat exposure was improved with the incorporation of SB in alginate hydrogel via double heat protection. As a conclusion, this study demonstrated the advantage of filler incorporation in polymer gel with higher thermotolerance for probiotic and a great potential for inclusion in the pelleted feed as probiotic additive.

The recommended parameters for immobilization and microencapsulation process were 1:8 of the SB:*L.rhamnosus* ratio and 3% of NaA concentration with NaA:SB ratio of 1:1.5, respectively. As a conclusion, the incorporation of filler could significantly improve the probiotic survival up to approximately 47% after the immobilization process and simulated heat treatment.

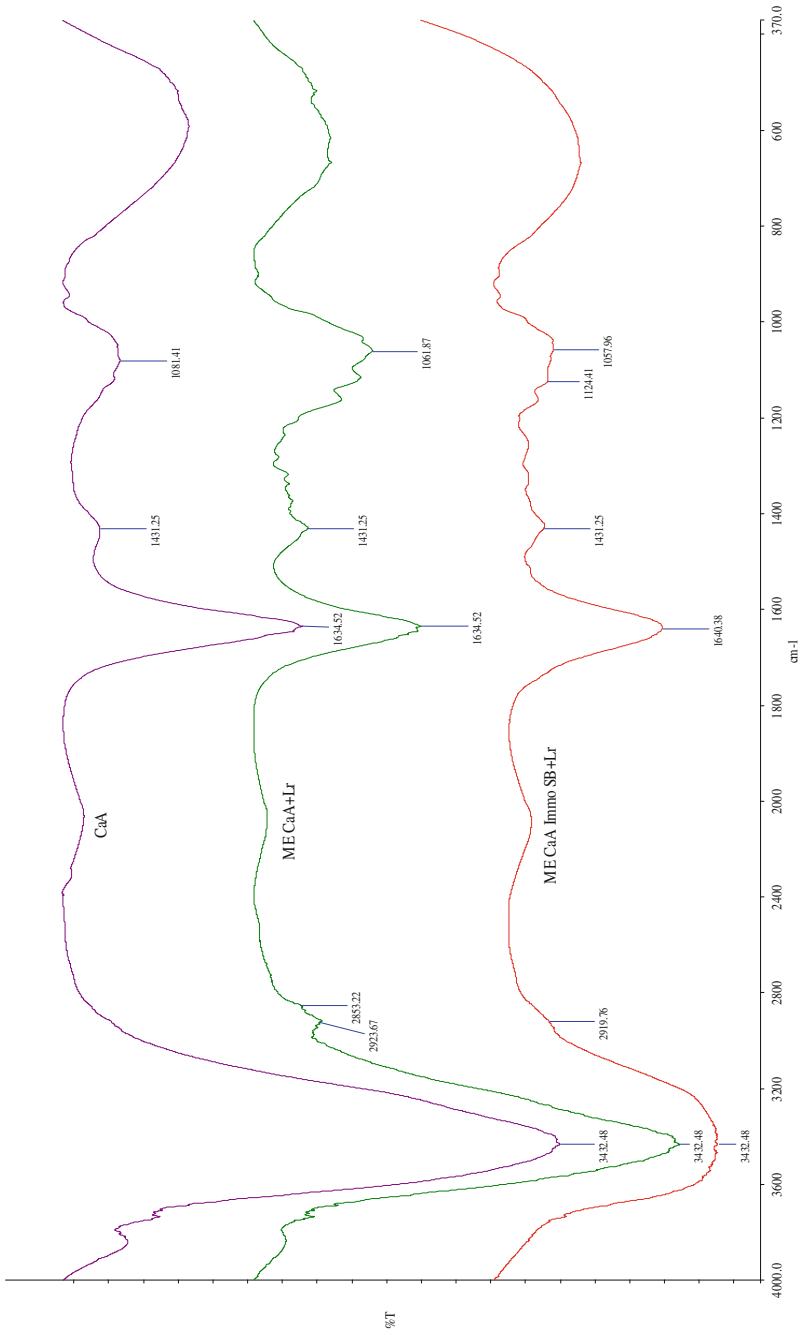


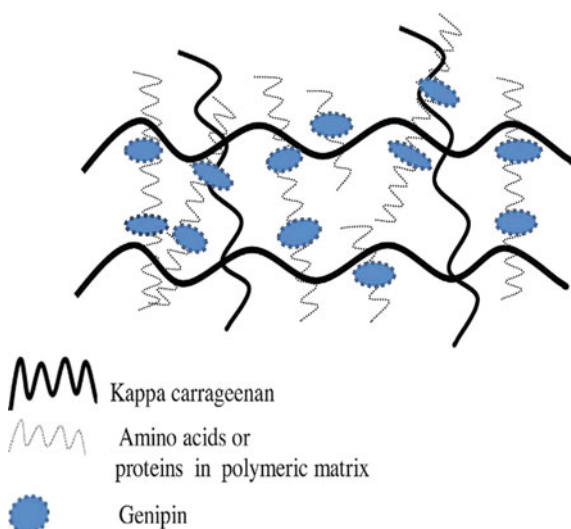
Fig. 25 FTIR spectra of calcium alginate (CaA), microencapsulated microcapsule without Lr (ME CaA + Lr), and microencapsulated microcapsule loaded with L.rhannosus (ME CaA Immo SB + Lr)

5.1.1 Evaluation of Kappa Carrageenan as Potential Carrier for Floating Drug Delivery System: Effect of Crosslinker

In this study genipin, a natural and non-toxic crosslinker was used to prepare crosslinked floating kappa carrageenan/sodium carboxymethyl cellulose hydrogels and the effect of genipin on hydrogels characterization was investigated. Figure 26 shows the mechanisms of genipin in kappa carrageenan hydrogel networks. Fourier transform infrared spectroscopy (FTIR), X-ray diffraction, and thermogravimetric analysis (TGA) were carried out to study the changes in the characteristics of hydrogels. FTIR analysis confirmed the mechanisms of genipin crosslinking in kappa carrageenan hydrogel network. Figure displayed the mechanisms of genipin.

On the other hand, incorporation of genipin enhances the crystallinity properties of kappa carrageenan hydrogels. It is believed that the mechanical properties of hydrogels will be improved with high crystallinity properties. A clear variation has been observed in TGA experiments that crosslinked kC/NaCMC floating hydrogels exhibit excellent thermal stability than kC/NaCMC floating hydrogels. The crosslinking mechanisms between kappa carrageenan and genipin confine the polymeric network which will slow down the degradation. In vitro floating properties showed that all formulated hydrogels had excellent floating behavior. Genipin as crosslinker affected the overall structure of hydrogels where gel strength was improved as genipin amount increased. It was discovered that the crosslinking reaction showed significant effect on swelling ratio compared to non-crosslinked hydrogels where the swelling ratio decreased as crosslinked with genipin. This may be due to the presence of a high amount of genipin that could result to a great extent of chemical crosslinking of the kC/NaCMC/CaCO₃ chains. This confines the movement and hydration of the macromolecular chain in the beads and leads to less

Fig. 26 Mechanisms of genipin in kappa carrageenan hydrogel networks



swelling in diameter (Muhamad et al. 2011). Besides that, compared to acidic medium, crosslinked hydrogels showed highest swelling in neutral medium. At higher pH, the ionization of carboxylic acid group occurs. Electrostatic repulsion force caused by the breakdown of hydrogen bonds leads to more water penetrating into the network. Figure 27 displays swelling ratio of non-crosslinked and genipin crosslinked floating kappa carrageenan hydrogels in acidic (pH 1.2) and alkaline (pH 7.4) medium (Selvakumaran and Muhamad 2015).

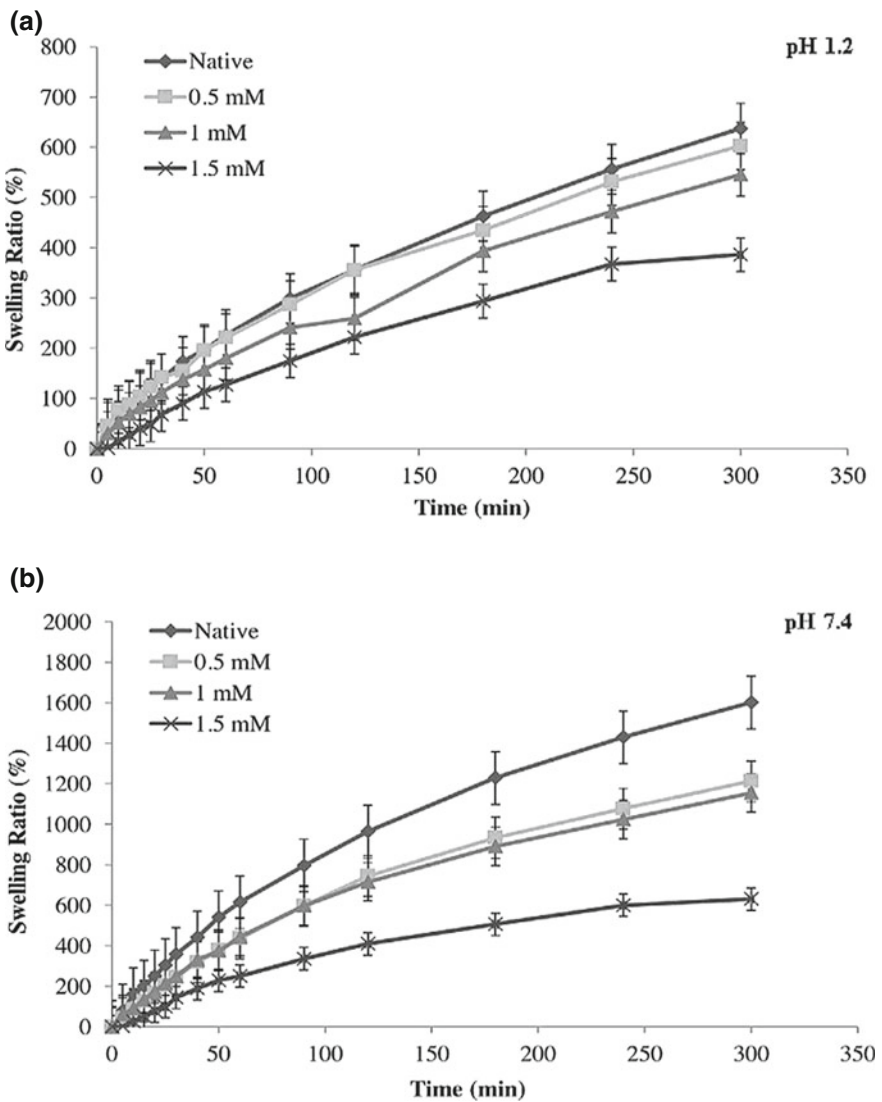


Fig. 27 Swelling ratio of non-crosslinked and genipin crosslinked floating kappa carrageenan hydrogels in acidic (pH 1.2) and alkaline (pH 7.4) medium

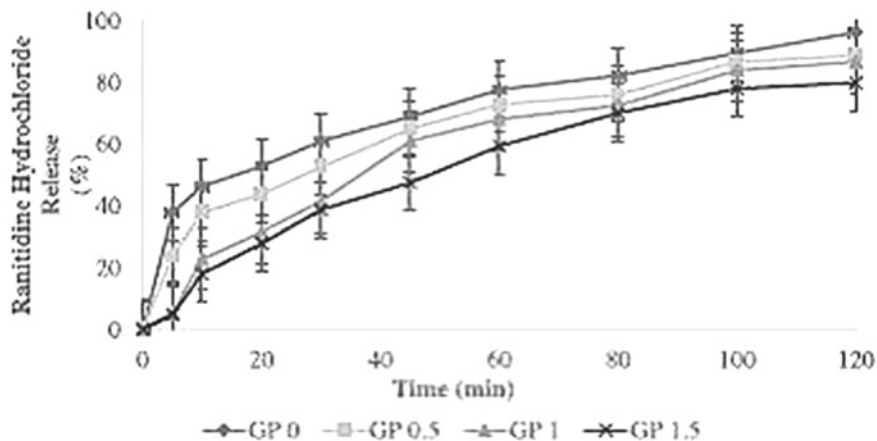


Fig. 28 Ranitidine hydrochloride drug release of non-crosslinked and crosslinked floating hydrogel

Figure 28 shows the ranitidine hydrochloride drug release of non-crosslinked and crosslinked floating hydrogel. It was found that the drug release was slower and lesser after being crosslinked. This is because an increase of the degree of polymer crosslinking increases the polymer density and therefore decreases the available free space for drug diffusion which results in a decrease in drug release rates (Selvakumaran and Muhamad 2015). Therefore, genipin can be an interesting crosslinking agent for controlled drug delivery in gastrointestinal tract.

6 Conclusion

According to the text reported above, it showed the importance of filler incorporation in polymer gels in various applications and this enforcement step has caught much attention from researchers. As mentioned earlier, the filler could bring beneficial and positive impacts on the polymeric gel characteristics and properties. Therefore, this step is crucial and should be highly considered in the development of advanced polymer gel functionality. The development of such should be emphasized and further improved for more global applications.

References

Abdul Khalil HPS, Bhat AH, Ireana Yusra AF (2012) Green composites from sustainable cellulose nanofibrils: a review. *Carbohydr Polym* 87:963–979

- Affatato S, Ruggiero A, Merola M (2015) Advanced biomaterials in hip joint arthroplasty. A review on polymer and ceramics composites as alternative bearings. *Compos Part B* 83:276–283
- Aouada F, de Moura M, Orts W, Mattoso LC (2010) Polyacrylamide and methylcellulose hydrogel as delivery vehicle for the controlled release of paraquat pesticide. *J Mater Sci* 45:4977–4985
- Asanza-Teruel ML, Gontier E, Bienaime C, Nava-Saucedo JE, Barbotin JN (1997) Response surface analysis of chlortetracycline and tetracycline production with K-carrageenan immobilized streptomyces aureofaciens. *Enzyme Microb Technol* 21:314–320
- Athawale VD, Lele V (1998) Graft copolymerization onto starch. II. Grafting of acrylic acid and preparation of its hydrogels. *Carbohydr Polym* 35:21–27
- Avadi MR, Sadeghi AMM, Tahzibi A, Bayati K, Pouladzadeh M, Zohuriaan-Mehr MJ, Rafiee-Tehrani M (2004) Dithymethyl chitosan as an antimicrobial agent: synthesis, characterization and antibacterial effects. *Eur Polym J* 40:1355–1361
- Azeredo HM, Mattoso LH, Avena-Bustillos RJ, Filho GC, Munford ML, Wood D, McHugh TH (2010) Nanocellulose reinforced chitosan composite films as affected by nanofiller loading and plasticizer content. *J Food Sci* 75:N1–N7
- Backdahl H, Esguerra M, Delbro D, Risberg B, Gatenholm P (2008) Engineering microporosity in bacterial cellulose scaffolds. *J Tissue Eng Regen Med* 2:320–330
- Baker MI, Walsh SP, Schwartz Z, Boyan BD (2012) A review of polyvinyl alcohol and its uses in cartilage and orthopedic applications. *J Biomed Mater Res B Appl Biomater* 100B:1451–1457
- Ban W, Song J, Argyropoulos DS, Lucia LA (2006) Improved the physical and chemical functionality of starch-derived films with biopolymers. *J Appl Poly Sci* 100(3):2542–2548
- Barbeyron T, Michel G, Potin P, Henrissat B, Kloareg B (2000) I-Carrageenases constitute a novel family of glycoside hydrolases, unrelated to that of K-carrageenases. *J Biol Chem* 275:35499–35505
- Bernardo LFA, Amaro APBM, Pinto DG, Lopes SMR (2016) Modeling and simulation techniques for polymer nanoparticle composites—a review. *Comput Mater Sci* 118:32–46
- Bi L, Cao Z, Hu Y, Song Y, Yu L, Yang B, Mu J, Huang Z, Han Y (2011) Effects of different cross-linking conditions on the properties of genipin cross-linked chitosan/collagen scaffolds for cartilage tissue engineering. *J Mater Sci Mater Med* 461(22):51–62
- Boateng JS, Pawar HV, Tetteh J (2013) Polyox and carrageenan based composite film dressing containing anti-microbial and anti-inflammatory drugs for effective wound healing. *Int J Pharm* 441:181–191
- Britton P, Teh E, Close D (2005) Investigation of the efficiency of bagasse as a thermal insulator. *Proc Aust Soc Sugar Cane Technol* 27:462–471
- Brown RM Jr (1991) Advances in cellulose biosynthesis. In: Chum HL (ed) *Polymers from biobased materials*. Doyes Data Corp, New Jersey
- Burgain J, Gaiani C, Linder M, Scher J (2011) Encapsulation of probiotic living cells: from laboratory scale to industrial applications. *J Food Eng* 104:467–483
- Butler MF, Ng YF, Pudney PDA (2003) Mechanism and kinetics of the crosslinking reaction between biopolymers containing primary amine groups and genipin. *J Polym Sci Part A Polym Chem* 41:3941–3953
- Buyanov AL, Gofman IV, Revel'skayaa LG, Khripunova AK, Tkachenkob AA (2010) Anisotropic swelling and mechanical behavior of composite bacterial cellulose–poly(acrylamide or acrylamide–sodium acrylate) hydrogels. *J Mech Behav Biomed Mater* 3:102–111
- Caceres PJ, Carlucci MJ, Damonte EB, Matsuhira B, Zuniga EA (2000) Carrageenans from Chilean samples of *Stenogramme interrupta* (Phyllophoraceae): structural analysis and biological activity. *Phytochemistry* 53:81–86
- Caló E, Khutoryanskiy VV (2015) Biomedical applications of hydrogels: a review of patents and commercial products. *Eur Polym J* 65:252–267
- Campo VL, Kawano DF, Silva DB Jr, Carvalho DI (2009) Carrageenans: biological properties, chemical modifications and structural analysis—a review. *Carbohydr Polym* 77:167–180
- Caner C, Vergano P, Wiles J (1998) Chitosan film mechanical and permeation properties as affected by acid, plasticizer and storage. *J Food Sci* 63:1049–1053

- Cevallos J, Bar-cohen A, Deisenroth DC (2016) Thermal performance of a polymer composite webbed-tube heat exchanger. *Int J Heat Mass Transf* 98:845–856
- Chang WH, Chang Y, Lai PH, Sung HW (2003) A genipin-crosslinked gelatin membrane as wound-dressing material: in vitro and in vivo studies. *J Biomater Sci Polym Ed* 14(5):481–495
- Chang PR, Jian R, Yu J, Ma X (2010) Starch-based composites reinforced with novel chitin nanoparticles. *Carbohydr Polym* 80:420–425
- Chen MC, Yeh GHC, Chiang BH (1996) Antimicrobial and physicochemical properties of methyl cellulose and chitosan films containing a preservative. *J Food Process Preserv* 20:279–390
- Chen SC, Wu YC, Mi FL, Lin YH, Yu LC, Sung HW (2004) A novel pH-sensitive hydrogel composed of N, O-carboxymethyl chitosan and alginate cross-linked by genipin for protein drug delivery. *J Control Release* 96:285–300
- Chen S, Zou Y, Yan Z, Shen W, Shi S, Zhang X, Wang H (2009) Carboxymethylated-bacterial cellulose for copper and lead ion removal. *J Hazard Mater* 161:1355–1359
- Chin NL, Che Man HA, Talib R, Esa F, Tasirin SM, Rahman NA (2014) 2nd international conference on agricultural and food engineering (CAFEi 2014)—new trends forward overview of bacterial cellulose production and application. *Agric Agric Sci Procedia* 2:113–119
- Chitprasert P, Sudsai P, Rodklongtan A (2012) Aluminum carboxymethyl cellulose–rice bran microcapsules: enhancing survival of *Lactobacillus reuteri* KUB-AC5. *Carbohydr Polym* 90:78–86
- Cioffi N, Torsi L, Ditaranto N, Sabbatini L, Zamboni PG, Tantillo G, Ghibelli L, D'Alessio M, Bleve-Zacheo T, Traversa E (2004) Antifungal activity of polymer-based copper nanocomposite coatings. *Appl Phys Lett* 85:2417–2419
- Corobea MC, Muhulet O, Miculescu F, Antoniac IV, Vuluga Z, Florea D et al (2016) Novel nanocomposite membranes from cellulose acetate and clay-silica nanowires. *Polym Adv Technol* 27(12):1586–1595
- Cook MT, Tzortzis G, Charalampopoulos D, Khutoryanskiy VV (2012) Microencapsulation of probiotics for gastrointestinal delivery. *J Control Release Official J Control Release Soc* 162:56–67
- Cui L, Jia J, Guo Y, Liu Y, Zhu P (2014) Preparation and characterization of IPN hydrogels composed of chitosan and gelatin cross-linked by genipin. *Carbohydr Polym* 99:31–38
- Daniel-Da-Silva AL, Moreira J, Neto R, Estrada AC, Gil AM, Trindade T (2012) Impact of magnetic nanofillers in the swelling and release properties of K-carrageenan hydrogel nanocomposites. *Carbohydr Polym* 87:328–335
- Dave R, Madamwar D (2006) Esterification in organic solvents by lipase immobilized in polymer of PVA–alginate–boric acid. *Process Biochem* 41:951–955
- De Angelis M, Siragusa S, Berloco M, Caputo L, Settanni L, Alfonsi G, Gobetti M (2006) Selection of potential probiotic lactobacilli from pig feces to be used as additives in pelleted feeding. *Res Microbiol* 157:792–801
- Demetri C, Del Sole R, Scalera F, Sannino A, Vasapollo G, Maffezzoli A, Ambrosio L, Nicolais L (2008) Novel superabsorbent cellulose-based hydrogels crosslinked with citric acid. *J Appl Polym Sci* 110:2453–2460
- Distantina S, Rochmadi, Fahrurrozi M, Wiratni (2013) Preparation and characterization of glutaraldehyde-crosslinked kappa carrageenan hydrogel. *Eng J* 17:3
- Distantina S, Rochmadi, Fahrurrozi M, Wiratni (2014) Stabilization of kappa carrageenan film by crosslinking: comparison of glutaraldehyde and potassium sulphate as the crosslinker. In: 5th international conference on chemical engineering and applications 74
- Dodane V, Vilivalam VD (1998) Pharmaceutical applications of chitosan. *Pharm Sci Tech Today* 1(6):246–253
- Dragan ES (2014) Design and applications of interpenetrating polymer network hydrogels: a review. *Chem Eng J* 243:572–590
- Dufresne A (2012) TEMPO-mediated oxidation. In: Dufresne A (ed) *Nanocellulose*. Walter de Gruyter, Berlin/Boston, pp 162–164
- Eichhorn SJ, Dufresne A, Aranguren M, Marcovich NE, Capadona JR, Rowan S (2010) Review: current international research into cellulose nanofibres and nanocomposites. *J Mat Sci* 45:1–33

- Ellis RP, Cochrane MP, Dale MFB, Duffus CM, Lynn A, Morrison IM, Prentice RDM, Swanston JS, Tiller SA (1998) Starch production and industrial use. *J Sci Food Agric* 77:289–311
- Endo T, Ikeda R, Yanagida Y, Hatsuzawa T (2008) Stimuli-responsive hydrogel–silver nanoparticles composite for development of localized surface plasmon resonance-based optical biosensor. *Anal Chim Acta* 611:205–211
- Fateixa S, Soares SF, Daniel-da-Silva AL, Nogueira HIS, Trindade T (2015) Silver-gelatine bionanocomposites for qualitative detection of a pesticide by SERS. *Analyst* 140:1693–1701
- Fedotova AV, Snezhko AG, Sdobnikova OA, Samoilova LG, Smurova TA, Revina AA, Khailova EB (2010) Packaging materials manufactured from natural polymers modified with silver nanoparticles. *Int Polym Sci Technol* 37:59
- Fuhrer R, Athanassiou EK, Luechinger NA, Stark WJ (2009) Crosslinking metal nanoparticles into the polymer backbone of hydrogels enables preparation of soft, magnetic field-driven actuators with muscle-like flexibility. *Small* 5:383–388
- Fuller R (1989) Probiotics in man and animals. *J Appl Bacteriol* 66:365–378
- Gao X, Shi Z, Lau A, Liu C, Yang G, Silberschmidt VV (2016) Effect of microstructure on anomalous strain-rate-dependent behavior of bacterial cellulose hydrogel. *Mater Sci Eng C* 62:130–136
- García-González CA, Alnaief M, Smirnova I (2011) Polysaccharide-based aerogels—promising biodegradable carriers for drug delivery systems. *Carbohydr Polym* 86:1425–1438
- Goswami A, Roy I, Sengupta S, Debnath N (2010) Novel applications of solid and liquid formulations of nanoparticles against insect pests and pathogens. *Thin Solid Films* 519:1252–1257
- Guilherme MR, Aouada FA, Fajardo AR, Martins AF, Paulino AT, Davi MFT, Muniz EC (2015) Superabsorbent hydrogels based on polysaccharides for application in agriculture as soil conditioner and nutrient carrier: a review. *Eur Polymer J* 72:365–385
- Gulrez SKH, Al-Assaf S, Phillips GO (2011) Hydrogels: methods of preparation, characterisation and applications. *Progress in molecular and environmental bioengineering—from analysis and modelling to technology applications*
- Gupta MN, Raghava S (2008) Natural based polymers for biomedical application. *T J International Limited, Cornwall*, pp 129–130
- Hari BNV, Lobo FJ, Devi DR (2015) Polymeric in-situ gels as smart carriers for pesticide delivery in agricultural practice. *Int J Pharm Clin Res* 7:113–118
- Hekmat A, Barati A, Frahani EV, Afraz A (2009) Synthesis and analysis of swelling and controlled release behaviour of anionic sIPN acrylamide based hydrogels. *World Acad Sci Eng Technol* 56:96–100
- Hezaveh H, Muhamad II (2012a) Effect of natural cross-linker on swelling and structural stability of kappa-carrageenan/hydroxyethyl cellulose pH-sensitive hydrogels. *Korean J Chem Eng* 29 (11):1647–1655
- Hezaveh H, Muhamad II (2012b) Impact of metal oxide nanoparticles on oral release properties of pH-sensitive hydrogel nanocomposites. *Int J Biol Macromol* 50:1334–1340
- Hezaveh H, Muhamad II (2013) Controlled drug release via minimization of burst release in pH-response kappa-carrageenan/polyvinyl alcohol hydrogels. *Chem Eng Res Des* 9(1):508–519
- Horii F, Yamamoto H, Hirai A (1997) Microstructural analysis of microfibrils of bacterial cellulose. *Macromol Symp* 120:197–205
- Hornof MD, Kast CE, Bernkop-Schnürch A (2003) In vitro evaluation of the viscoelastic properties of chitosan–thioglycolic acid conjugates. *Eur J Pharm Biopharm* 55:185–190
- Hou Y, Chen C, Liu K, Tu Y, Zhang L, Li Y (2015) Preparation of PVA hydrogel with high-transparency and investigations of its transparent mechanism. *RSC Adv* 5:24023–24030
- Illum L (2003) Nasal drug delivery—possibilities, problems and solutions. *J Control Release* 87(1–3):187–198
- Imeson A (1997) Thickening and gelling agents for food, 2nd edn. Blackie Academic & Professional, London, pp 45–83

- İşiklan N (2007) Controlled release study of carbaryl insecticide from calcium alginate and nickel alginate hydrogel beads. *J Appl Polym Sci* 105:718–725
- Ismail H, Irani M, Ahmad Z (2013) Starch-based hydrogels: present status and applications. *Int J Polym Mater Polym Biomater* 62:411–420
- Jayakrishnan A, Jameela SR (1996) Glutaraldehyde as a fixative in bioprostheses and drug delivery matrices. *Biomaterids* 17:471–484
- Jayaramudu T, Raghavendra GM, Varaprasad K, Sadiku R, Ramamc K, Raju KM (2013) Iota-carrageenan-based biodegradable Ag₀ nanocomposite hydrogels for the inactivation of bacteria. *Carbohydr Polym* 95:188–194
- Jegal J, Lee KH (1996) Pervaporation separation of water-ethanol mixtures through PVA-Sodium alginate blend membranes. *J Appl Polym Sci* 61:389–392
- John M, Thomas S (2008) Biofibres and biocomposites. *Carbohydr Polym* 71:343–364
- Jones JI (1973) Polyvinyl alcohol. Properties and applications. *Br Polym J* 5:493–494 (Finch CA (ed), Wiley, Chichester, pp xviii + 622)
- Keady TWJ, Steen WJ (1996) Effect of applying a bacterial inoculants to silage immediately before feeding on silage intake, degradability and rumen volatile fatty acid concentrations in growing beef cattle. *Grass Forage Sci* 51:155–162
- Khuntia A, Chaundhary LC (2002) Performance of male cross-bred calves as influenced by substitution of grain by wheat bran and the addition of lactic acid bacteria to diet. *Asian Aust J Anim Sci* 15:188–194
- Khor E, Lim LY (2003) Implantable applications of chitin and chitosan. *Biomaterials* 24 (13):2339–2349
- Koide SS (1998) Chitin–chitosan: properties, benefits and risks. *Nutr Res* 18:1091–1101
- Kosin B, Rakshit SK (2010) Induction of heat tolerance in autochthonous and allochthonous thermotolerant probiotics for application to white shrimp feed. *Aquaculture* 306:302–309
- Krasaekoopt W, Bhandari B, Deeth H (2003) Evaluation of encapsulation techniques of probiotics for yoghurt. *Int Dairy J* 13:3–13
- Kuhad RC, Kuhar S, Kapoor M, Sharma KK, Singh A (2007) Lignocellulolytic microorganisms, their enzymes and possible biotechnologies based on lignocellulolytic microorganisms and their enzymes. In: Kuhad RC, Singh A (eds) *Lignocellulose biotechnology: future prospects*. New Delhi, I.K. International
- Kumar MNVR, Muzzarelli RAA, Muzzarelli C, Sashiwa H, Domb AJ (2004) Chitosan chemistry and pharmaceutical perspectives. *Chem Rev* 104:6017–6084
- Laksono PW, Rochman T, Setyanto H, Pujiyanto E, Diharjo K (2014) Design and manufacturing bio composite (sugarcane bagasse—polyvinyl acetate) panel that characterized thermal conductivity. *Adv Mater Res* 893:504–507
- Lavoine N, Desloges I, Dufresne A, Bras J (2012) Microfibrillated cellulose—its barrier properties and applications in cellulosic materials: a review. *Carbohydr Polym* 90:735–764
- Leblanc JL (2009) Types of fillers. In: *Filled polymers*. CRC Press, Boca Raton, pp 11–14
- Leong KH, Chung LY, Noordin MI, Mohamad K, Nishikawa M, Onuki Y, Morishitab M, Takayamabet K (2011) Carboxymethylation of kappa carrageenan for intestinal-targeted delivery of bioactive macromolecules. *Carbohydr Polym* 83:1507–1515
- Liu Y, Ma L, Gao C (2012) Facile fabrication of the glutaraldehyde cross-linked collagen/chitosan porous scaffold for skin tissue engineering. *Mater Sci Eng C* 32:2361–2366
- Lu M, Li YY, Guan XH, Wei DZ (2010) Preparation of bacterial cellulose and its adsorption of Cd²⁺. *J Northeast Univ* 31(8):1196–1199
- Lu M, Guan XH, Xu X, Wei DZ (2013) Characteristic and mechanism of Cr(VI) adsorption by ammonium sulfamate-bacterial cellulose in aqueous solutions. *Chin Chem Lett* 24:253–256
- Lu M, Zhang YM, Guan XH, Xu X, Gao T (2014) Thermodynamics and kinetics of adsorption for heavy metal ions from aqueous solutions onto surface amino-bacterial cellulose. *Trans Nonferrous Met Soc China* 24:1912–1917
- Ma XF, Chang PR, Yu JG (2008) Properties of biodegradable thermoplastic pea starch/carboxymethyl cellulose and pea starch/microcrystalline cellulose composites. *Carbohydr Polym* 72:369–375

- Maitra J, Shukla VK (2014) Cross-linking in hydrogels—a review. *Am J Polym Sci* 4(2):25–31
- Malik R, Sharma DD (1998) In vitro evaluation of different probiotics as feed supplement. *Indian J Dairy Sci* 51:357–362
- Manohar K, Ramlakhan D, Kochhar G, Halder S (2006) Biodegradable fibrous thermal insulation. *J Braz Soc Mech Sci Eng* 28:45–47
- Marcelo G, López-González M, Mendicuti F, Tarazona MP, Valiente M (2014) Poly (N-isopropylacrylamide)/gold hybrid hydrogels prepared by catechol redox chemistry. Characterization and smart tunable catalytic activity. *Macromolecules* 47:6028–6036
- Meena R, Prasad K, Siddhanta AK (2007) Effect of genipin, a naturally occurring crosslinker on the properties of kappa-carrageenan. *Int J Biol Macromol* 41:94–101
- Meena R, Prasad K, Siddhanta AK (2009) Development of a stable hydrogel network based on agar–kappa-carrageenan blend cross-linked with genipin. *Food Hydrocolloids*, pp 497–509
- Mendes DF, Nascimento JE, Facholli AFDL, Casa MDA, Carvalho LDS, Sato K (2012) Evaluation of plasticity and radiopacity of elastic separators by means of traction tests and radiography. *Dent Press J Orthod* 17:6
- Mi FL, Tan YC, Liang HC, Huang RN, Sung HW (2001) In vitro evaluation of a chitosan membrane cross-linked with genipin. *J Biomater Sci Polym Ed* 12(8):835–850
- Mi FL, Tan YC, Liang HF, Sung HW (2002) In vivo biocompatibility and degradability of a novel injectable-chitosan based implant. *Biomaterials* 23:181–191
- Mi FL, Shyu SS, Peng CK (2005) Characterization of ring opening polymerization of genipin and pH-dependent cross-linking reactions between chitosan and genipin. *J Polym Sci Part A Polym Chem* 43:1985–2000
- Miculescu M, Thakur VK, Miculescu F, Voicu SI (2016) Graphene-based polymer nanocomposite membranes: a review. *Polym Adv Technol* 27(7):844–859
- Michel G, Nyval-Collen P, Barbeyron T, Czjzek M, Helbert W (2006) Bioconversion of red seaweed galactans: a focus on bacterial agarases and car-rageenases. *Appl Microbiol Biotechnol* 71:23–33
- Moffat KL, Marra KG (2004) Biodegradable poly (ethylene glycol) hydrogel crosslinked with genipin for tissue engineering application. *J Biomed Mater Res Part B Appl Biomater* 71:181–187
- Morris CJ (2003) Carrageenan-induced paw edema in the rat and mouse. *Methods Mol Biol* 225:115–121
- Muhamad II, Fen LS, Hui HN, Mustapha NA (2011) Genipin-cross-linked kappa carrageenan/carboxymethyl cellulose beads and effects on beta-carotene release. *Carbohydr Polym* 83:1207–1212
- Muhamad I, Salehudin M, Salleh E (2015) Cellulose nanofiber for eco-friendly polymer nanocomposites. In: Thakur VK, Thakur MK (eds) *Eco-friendly polymer nanocomposites*, vol 75, pp 323–365. Springer India, New Delhi
- Mulinari DR, Voorwald HJC, Cioffi MOH, Rocha GJ, Lucia CPM (2010) Surface modification of sugarcane bagasse cellulose and its effect on mechanical and water absorption properties of sugarcane bagasse cellulose/HDPE composites. *BioResources* 5:661–671
- Musatto SI, Teixeira, JA (2010) Lignocellulose as raw material in fermentation processes. In: Mendez-Vilas (ed) *Current research, technology and education topics in applied microbiology and microbial biotechnology*. Braga, Portugal
- Myoga H, Asano H, Nomura Y, Yoshida H (1991) Effects of immobilization conditions on the nitrification treatability of entrapped cell reactors using the PVA freezing method. *Water Sci Technol* 23:1117–1124
- Necas J, Bartosikova L (2013) Carrageenan: a review. *Vet Med* 58:187–205
- Nilsen-Nygaard J, Strand S, Vårum K, Draget K, Nordgård C (2015) Chitosan: gels and interfacial properties. *Polymers* 7:552
- Nimrat S, Boonthai T, Vuthiphandchai V (2011) Effects of probiotic forms, compositions of and mode of probiotic administration on rearing of Pacific white shrimp (*Litopenaeus vannamei*) larvae and postlarvae. *Anim Feed Sci Technol* 169:244–258

- Norman FS, Harris P (1990) Carrageenans. Food Gel. Galliard (Printers) Ltd., Great Britain, pp 79–111
- Nousiainen J, Javanainen P, Setälä J (2004) Lactic acid bacteria: microbiology and functional concepts, 3rd edn. Valio Ltd, Helsinki, pp 547–588
- Omidian H, Park KJ (2012) Hydrogels. In: Siepmann et al. (eds) Fundamentals and applications of controlled release drug delivery. Adv Deliv Sci Technol, 75–106
- Onyishi IV, Chime SA, Egwu E (2013) Application of k-carrageenan as a sustained release matrix in floating tablets containing sodium salicylate. Afr J Pharm Pharmacol 7(39):2667–2673
- Osada Y, Gong JP (1998) Soft and wet materials: polymer gels. Adv Mater 10:827–837
- Pa'e N, Zahan KA, Muhamad II (2011) Production of biopolymer from acetobacter xylinum using different fermentation methods. Int J Eng Technol (IJET-IJENS) 11(5):90–98
- Panchal R, Thakur G (2014) Glutaraldehyde cross-linked chitosan-PVA composite films: a promising candidate for wound healing management. In: MUSRF-SRPC-2014, pp 11–12
- Panlasigui LN, Baello OQ, Dimatangal JM, Dumelod BD (2003) Blood cholesterol and lipid-lowering effects of carrageenan on human volunteers. Asia Pac J Clin Nutr 12:209–214
- Pardo-Yissar V, Gabai R, Shipway AN, Bourenko T, Willner I (2001) Gold nanoparticle/hydrogel composites with solvent-switchable electronic properties. Adv Mater 13:1320–1323
- Park HJ, Kim SH, Kim HJ, Choi SH (2006) A new composition of nanosized silica-silver for control of various plant diseases. Plant Pathol J 22(3):295–302
- Pappu A, Patil V, Jain S, Mahindrakar A, Haque R, Thakur VK (2015) Advances in industrial prospective of cellulosic macromolecules enriched banana biofibre resources: a review. Int J Biol Macromol 79:449–458
- Pappu A, Saxena M, Thakur VK, Sharma A, Haque R (2016) Facile extraction, processing and characterization of biorenewable sisal fibers for multifunctional applications. J Macromol Sci Part A 53(7):424–432
- Peppas NA (1987) Hydrogels in medicine and pharmacy, vols I–III. CRC, Boca Raton
- Peppas NA, Bures P, Leobandung W, Ichikawa H (2000) Hydrogels in pharmaceutical formulations. Eur J Pharm Biopharm 50:27–46
- Phiriyawirut M, Maniaw P (2012) Cellulose microfibril from banana peels as a nanoreinforcing fillers for zein films. Open J Polym Chem 02:56–62
- Prajapati VD, Maheriya PM, Jani GK, Solanki HK (2014) Carrageenan: a natural seaweed polysaccharide and its applications. Carbohydr Polym 105:97–112
- Rabea EI, Badawy MET, Stevens CV, Smagghe G, Steurbaut W (2003) Chitosan as antimicrobial agent: applications and mode of action. Biomacromolecules 4:1457–1465
- Ratner BD, Williams DF (1981) Biocompatibility of clinical implant materials. CRC, Boca Raton
- Ratner BD, Hoffman AS, Andrade JD (1976) Hydrogels for medical and related applications. American Chemical Society, Washington, p 1
- Rowe RC, Sheskey PJ, Quinn ME (2009) Handbook of pharmaceutical excipients. Pharmaceutical Press, London
- Riddell JB, Gallegos AJ, Harmon DL, McLeod KR (2010) Addition of a Bacillus based probiotic to the diet of preruminant calves: influence on growth, health, and blood parameters. Int J Appl Res Vet Med 8:78–85
- Rinaudo M (1999) Influence of acetic acid concentration on the solubilization of chitosan. Polymer 40:7029–7032
- Rogovina LZ, Vasil'ev VG, Braudo EE (2008) Definition of the concept of polymer gel. Polym Sci Ser C 50(1):85–92
- Rosas-Ledesma P, Leon-Rubio JM, Alarcon FJ, Morinigo MA, Balebona MC (2012) Calcium alginate capsules for oral administration of fish probiotic bacteria: assessment of optimal conditions for encapsulation. Aquac Res 43:106–116
- Ross GR, Gusils C, Gonzalez SN (2008) Microencapsulation of probiotic strains for swine feeding. Biol Pharm Bull 31:2121–2125
- Sahiner N (2013) Soft and flexible hydrogel templates of different sizes and various functionalities for metal nanoparticle preparation and their use in catalysis. Prog Polym Sci 38:1329–1356

- Saïd Azizi Samir MA, Alloin F, Paillet M, Dufresne A (2004) Tangling effect in fibrillated cellulose reinforced nanocomposites. *Macromolecules* 37:4313–4316
- Sangsuwan J, Rattanapanone N, Rachtanapun P (2008) Effect of chitosan/methyl cellulose films on microbial and quality characteristics of fresh-cut cantaloupe and pineapple. *Postharvest Bio Tech* 49:403–410
- Saravanan P, Padmanabha Raju M, Alam S (2007) A study on synthesis and properties of Ag nanoparticles immobilized polyacrylamide hydrogel composites. *Mater Chem Phys* 103:278–282
- Selvakumaran S, Muhamad II (2015) Evaluation of kappa carrageenan as potential carrier for floating drug delivery system: effect of cross linker. *Int J Pharm* 496:323–331
- Seo JK, Kim S, Kim MH, Upadhaya SD, Kam DK, Ha JK (2010) Direct-fed microbials for ruminant animals. *Asian Aust J Anim Sci* 23:1657–1667
- Serafica G, Mormino R, Bungay H (2002) Inclusion of solid particles in bacterial cellulose. *Appl Microbiol Biotechnol* 58:756–760
- Shaharuddin S, Muhamad II (2015) Microencapsulation of alginate-immobilized bagasse with *Lactobacillus rhamnosus* NRRL: enhancement of survivability and thermotolerance. *Carbohydr Polym* 119:173–181
- Shaharuddin S, Muhamad II, Seng KF, Zahan KA, Khairuddin N (2014a) Potential use of biofibers for functional immobilization of *Lactobacillus rhamnosus* NRRL 442. *Key Eng Mater* 595:231–235
- Shaharuddin S, Saiful IAR, Muhamad II (2014b) Sugarcane bagasse as the potential agro-waste resource for the immobilization of *Lactobacillus rhamnosus* NRRL 442. *Adv Mater Res* 1043:214–218
- Shahidi F, Arachchi JKV, Jeon YJ (1999) Food applications of chitin and chitosans. *Trends Food Sci Tech* 10:37–51
- Shetty K, Paliyath G, Pometto A, Levin RE (2006) *Food biotechnology*, 2nd edn. CRC Press, Boca Raton, pp 512–514
- Shi Z, Zhang Y, Phillips GO, Yang G (2014) Utilization of bacterial cellulose in food. *Food Hydrocoll* 35:539–545
- Silva AJPS, Lahr FAR, Christofor AL, Panzera TH (2012) Properties of sugar cane bagasse to use in OSB. *Int J Mater Eng* 2:50–56
- Singh V (2016) World hydrogel market- opportunities and forecasts, 2015–2022. Allied market research report
- Siqueira G, Bras J, Dufresne A (2010) Cellulosic bionanocomposites: a review of preparation, properties and applications. *Polymers* 2:728–765
- Siritientong T, Ratanavaraporn J, Srichana T, Aramwit P (2013) Preliminary characterization of genipin-cross-linked silk sericin/poly (vinyl alcohol) films as two-dimensional wound dressings for the healing of superficial wounds. *BioMed Res Int*, 1–13
- Singha AS, Shama A, Thakur VK (2008) X-ray diffraction, morphological, and thermal studies on methylmethacrylate graft copolymerized *Saccharum ciliare* fiber. *Int J Polym Anal Charact* 13 (6):447–462
- Singha AS, Thakur VK (2008) Fabrication and study of lignocellulosic hibiscus sabdariffa fiber reinforced polymer composites. *BioResources* 3(4):1173–1186
- Slaughter BV, Khurshid SS, Fisher OZ, Khademhosseini A, Peppas NA (2009) Hydrogels in regenerative medicine. *Adv Mater* 21:3307–3329
- Slominski BA, Davie T, Nyachoti MC, Jones O (2007) Heat stability of endogenous and microbial phytase during feed pelleting. *Livestock Sci* 109:244–246
- Sokolnicki AM, Fisher RJ, Harrah TP, Kaplan DL (2006) Permeability of bacterial cellulose membranes. *J Membr Sci* 272(1–2):15–27
- Soto LP, Frizzo LS, Avataneo E, Zbrun MV, Bertozzi E, Sequeira G, Rosmini MR (2011) Design of macrocapsules to improve bacterial viability and supplementation with a probiotic for young calves. *Anim Feed Sci Technol* 165:176–183
- Stanley N (1987) Production and utilization of products from commercial seaweeds. In: Mchugh DJ (ed) *FAO fisheries technical paper* (vol 288, pp 116–146). FAO, Rome

- Steinbuechel A, Rhee SK (2005) Polysaccharides and polyamides in food industry (vol 1). Wiley-VCH, Germany, pp 85–166
- Sun Y, Cheng J (2002) Hydrolysis of lignocellulosic material from ethanol production: a review. *Biores Technol* 83:1–11
- Sung HW, Huang RN, Huang LLH, Tsai CC (1999) In vitro evaluation of cytotoxicity of a naturally occurring cross-linking reagent for biological tissue fixation. *J Biomater Sci Polym Ed* 10(1):63–78
- Tang W, Jia S, Jia Y, Yang H (2010) The influence of fermentation conditions and post-treatment methods on porosity of bacterial cellulose membrane. *World J Microbiol Biotechnol* 26:125–131
- Tester RF, Karkalas J, Qi X (2004) Starch—composition, fine structure and architecture. *J Cereal Sci* 39:151–165
- Thoniyot P, Tan MJ, Karim AA, Young DJ, Loh XJ (2015) Nanoparticle–hydrogel composites: concept, design, and applications of these promising, multi-functional materials. *Adv Sci* 2:1–2
- Thakur VK, Thakur MK (2014a) Recent trends in hydrogels based on psyllium polysaccharide: a review. *J Clean Prod* 82:1–15
- Thakur VK, Thakur MK (2014b) Recent advances in graft copolymerization and applications of chitosan: a review. *ACS Sustain Chem Eng* 2(12):2637–2652
- Thakur VK, Kessler MR (2014) Synthesis and characterization of AN-g-SOY for sustainable polymer composites. *ACS Sustain Chem Eng* 2(10):2454–2460
- Thakur VK, Kessler MR (2015) Self-healing polymer nanocomposite materials: a review. *Polymer* 69:369–383
- Thakur VK, Thakur MK (2015) Recent advances in green hydrogels from lignin: a review. *Int J Biol Macromol* 72:834–847
- Thakur VK, Thakur MK, Gupta RK (2013a) Development of functionalized cellulosic biopolymers by graft copolymerization. *Int J Biol Macromol* 62:44–51
- Thakur VK, Thakur MK, Gupta RK (2013b) Rapid synthesis of graft copolymers from natural cellulose fibers. *Carbohydr Polym* 98(1):820–828
- Trindade T, Daniel-Da-Silva AL (2011) Nanocomposite particles for bioapplications, materials and bio-interfaces. Pan Stanford Publishing Pte Ltd, Singapore
- Trache D, Hazwan Hussin M, Mohamad Haafiz MK, Kumar Thakur V (2017) Recent progress in cellulose nanocrystals: sources and production. *Nanoscale* 9(5):1763–1786
- UI-Islam M, Khan T, Park JK (2012) Water holding and release properties of bacterial cellulose obtained by in situ and ex situ modification. *Carbohydr Polym* 88(2):596–603
- Van De Velde F, Knutsen SH, Usov AL, Rollema HS, Cerezo AS (2002) ¹H and ¹³C high resolution NMR spectroscopy of carrageenans: application in research and industry. *Trends Food Sci Technol* 13:73–92
- Vogelsang C, Husby A, Østgaard K (1997) Functional stability of temperature-compensated nitrification in domestic wastewater treatment obtained with PVA-SbQ/alginate gel entrapment. *Water Res* 31:1659–1664
- Voo WP, Ravindra P, Tey BT, Chan ES (2011) Comparison of alginate and pectin based beads for production of poultry probiotic cells. *J Biosci Bioeng* 111:294–299
- Voicu SI, Condruz RM, Mitran V, Cimpean A, Miculescu F, Andronesu C, Thakur VK (2016) Sericin covalent immobilization onto cellulose acetate membrane for biomedical applications. *ACS Sustain Chem Eng* 4(3):1765–1774
- Wallace RJ, Newbold CJ (1993) Rumen fermentation and its manipulation: the development of yeast cultures as feed additives. In: Lyons TP (ed) *Biotechnology in the feed industry*. Alltech Technical Publications, Kentucky, pp 173–192
- Wang J, Gao C, Zhang Y, Wan Y (2010) Preparation and in vitro characterization of BC//PVA hydrogel composite for its potential use as artificial cornea biomaterial. *Mater Sci Eng C* 30:214–218
- Wang J, Lu X, Ng PF, Lee K, Fei B, Xin JH, Wu J (2015) Polyethylenimine coated bacterial cellulose nanofiber membrane and application as adsorbent and catalyst. *J Colloid Interface Sci* 440:32–38

- Weiner ML (1991) Toxicological properties of carrageenan. *Agents Actions* 32(1-2):46–51
- White RJ, Budarin VL, Clark JH (2008) Tuneable mesoporous materials from α -D-polysaccharides. *ChemSuschem* 1:408–411
- Williams PA, Phillips GO (2000) Gum Arabic. In: Philips GO, Williams PA (eds) *Handbook of hydrocolloids*, Woodhead Publishing Limited, New York, pp 155–168
- Wise DL (2000) Bioremediation of contaminated soils. Taylor & Francis, UK
- Woraham S, Chaiyasut C, Sirithunyalug B (2010) Survival enhancement of probiotic *Lactobacillus plantarum* CMU-FP002 by granulation and encapsulation techniques. *Afr J Microbiol Res* 4:2086–2093
- Wu X, Black L, Santacana-Laffitte G, Patrick CW Jr (2006) Preparation and assessment of glutaraldehyde-crosslinked collagen–chitosan hydrogels for adipose tissue engineering. *Wiley InterScience*, New Jersey, pp 59–65
- Xie F, Pollet E, Halley PJ, Avérous L (2013) Starch-based nano-biocomposites. *Prog Polym Sci* 38:1590–1628
- Xu YX, Kim KM, Hanna MA, Nag D (2005) Chitosan-starch composite film: preparation and characterization. *Ind Crops Prod* 21:185–192
- Yaszemski M, Trntolo D, Lewandrowski KU, Hasirci V, Altobelli D, Wise D (eds) (2004) *Tissue engineering and novel delivery systems*. CRC Press, Boca Raton
- Yeoh QL, Lee GL, Fatimah H (1985) Teknologi pengeluaran Nata. *J Teknologi Makanan* 4(1): 36–39
- Yuan Y, Chesnutt BM, Utturkar G, Haggard WO, Yang Y, Ong JL, Bumgardner JD (2007) The effect of cross-linking of chitosan microspheres with genipin on protein release. *Carbohydr Polym* 68(3):561–567
- Zahan KA, Pa'e N, Muhamad II (2014) Process parameter for fermentation in rotary discs reactor for optimum bacterial cellulose production using response surface methodology. *Bioresources* 9(2):1858–1872
- Zhai M, Yoshii F, Kume T (2003) Radiation modification of starch-based plastic sheets. *Carbohydr Polym* 52:311–317
- Zhang Y, Wang QS, Yan K, Qi Y, Wang GF, Cui YL (2016) Preparation, characterization, and evaluation of genipin crosslinked chitosan/gelatin three-dimensional scaffolds for liver tissue engineering applications. *J Biomed Mater Res Part A*, 1–8
- Zhou G, Sun Y, Xin H, Zhang Y, Li Z, Xu Z (2004) In vivo antitumor and immunomodulation activities of different molecular weight lambda-carrageenans from *chondrus ocellatus*. *Pharmacol Res* 50:47–53
- Zhu H, Jia S, Wan T, Jia Y, Yang H, Li J, Yan L, Zhong C (2011) Biosynthesis of spherical Fe_3O_4 /bacterial cellulose nanocomposites as adsorbents for heavy metal ions. *Carbohydr Polym* 86:1558–1564
- Zohuriaan-Mehr MJ, Kabiri K (2008) Superabsorbent polymer materials: a review. *Iran Polym J* 17:451–477 (English Edition)